

ANALYTICA CHIMICA ACTA

International journal devoted to all branches of analytical chemistry

EDITORS

A. M. G. MACDONALD (Birmingham, Great Britain)

HARRY L. PARDUE (West Lafayette, IN, U.S.A.)

ALAN TOWNSHEND (Hull, Great Britain)

J. T. CLERC (Bern, Switzerland)

Editorial Advisers

F. C. Adams, Antwerp
H. Bergamin F^o, Piracicaba
G. den Boef, Amsterdam
A. M. Bond, Waurin Ponds
D. Dyrssen, Göteborg
J. W. Frazer, Livermore, CA
S. Gomisček, Ljubljana
S. R. Heller, Washington, DC
G. M. Hieftje, Bloomington, IN
J. Hoste, Ghent
A. Hulanicki, Warsaw
G. Johansson, Lund
D. C. Johnson, Ames, IA
P. C. Jurs, University Park, PA
D. E. Leyden, Fort Collins, CO
F. E. Lytle, West Lafayette, IN
H. Malissa, Vienna
D. L. Massart, Brussels
A. Mizuike, Nagoya
E. Pungor, Budapest

W. C. Purdy, Montreal
J. P. Riley, Liverpool
J. Růžicka, Copenhagen
D. E. Ryan, Halifax, N.S.
S. Sasaki, Toyohashi
J. Savory, Charlottesville, VA
W. D. Shults, Oak Ridge, TN
H. C. Smit, Amsterdam
W. I. Stephen, Birmingham
G. Tölg, Schwäbisch Gmünd, B.R.D.
B. Trémillon, Paris
W. E. van der Linden, Enschede
A. Walsh, Melbourne
H. Weisz, Freiburg i. Br.
P. W. West, Baton Rouge, LA
T. S. West, Aberdeen
J. B. Willis, Melbourne
E. Ziegler, Mühlheim
Yu. A. Zolotarev, Moscow

ANALYTICA CHIMICA ACTA

*International journal devoted to all branches of analytical chemistry
Revue internationale consacrée à tous les domaines de la chimie analytique
Internationale Zeitschrift für alle Gebiete der analytischen Chemie*

PUBLICATION SCHEDULE FOR 1983

	J	F	M	A	M	J	J	A	S	O	N	D
Analytica Chimica Acta	145	146	147	148	149	150/1 150/2	151	152	153/1	153/2	154	155

Scope. *Analytica Chimica Acta* publishes original papers, short communications, and reviews dealing with every aspect of modern chemical analysis, both fundamental and applied.

Submission of Papers. Manuscripts (three copies) should be submitted as designated below for rapid and efficient handling:

Papers from the Americas to: Professor Harry L. Pardue, Department of Chemistry, Purdue University, West Lafayette IN 47907, U.S.A.

Papers from all other countries to: Dr. A. M. G. Macdonald, Department of Chemistry, The University, P.O. Box 363 Birmingham B15 2TT, England. Papers dealing particularly with computer techniques to: Professor J. T. Cleverly, Universität Bern, Pharmazeutisches Institut, Baltzerstrasse 5, CH-3012 Bern, Switzerland.

Submission of an article is understood to imply that the article is original and unpublished and is not being considered for publication elsewhere. Upon acceptance of an article by the journal, authors resident in the U.S.A. will be asked to transfer the copyright of the article to the publisher. This transfer will ensure the widest dissemination of information under the U.S. Copyright Law.

Information for Authors. Papers in English, French and German are published. There are no page charges. Manuscripts should conform in layout and style to the papers published in this Volume. Authors should consult Vol. 132, p. 239 for detailed information. Reprints of this information are available from the Editors or from: Elsevier Editorial Services Ltd., Mayfield House, 256 Banbury Road, Oxford OX2 7DH (Great Britain).

Reprints. Fifty reprints will be supplied free of charge. Additional reprints (minimum 100) can be ordered. An order form containing price quotations will be sent to the authors together with the proofs of their article.

Advertisements. Advertisement rates are available from the publisher.

Subscriptions. Subscriptions should be sent to: Elsevier Science Publishers B.V., P.O. Box 211, 1000 AA Amsterdam, The Netherlands.

Publication. *Analytica Chimica Acta* appears in 11 volumes in 1983. The subscription for 1983 (Vols. 145–155) costs Dfl. 1980.00 plus Dfl. 220.00 (postage) (total approx. U.S. \$880.00). Journals are sent automatically by airmail to the U.S.A. and Canada at no extra cost and to Japan, Australia and New Zealand for a small additional postal charge. Earlier volumes (Vols. 1–144) except Vols. 23 and 28 are available at Dfl. 182.00 (U.S. \$72.80), plus Dfl. 14.00 (U.S. \$5.60) postage and handling, per volume.

Claims for issues not received should be made within three months of publication of the issue, otherwise they cannot be honoured free of charge.

Customers in the U.S.A. and Canada who wish to obtain additional bibliographic information on this and other Elsevier journals should contact Elsevier Science Publishing Company Inc., Journal Information Center, 52 Vanderbilt Avenue, New York, NY 10017. Tel: (212) 867-9040.

Reagents

MERCK

Reagents for Instrumental Analysis

Uvasol® solvents for spectroscopy
Preparations for atomic absorption
Preparations for X-ray fluorescence
Scintillation chemicals

Please send for our special leaflets

E. Merck, Darmstadt, Federal Republic of Germany

**IF YOU DON'T SUBSCRIBE YET,
YOU WILL HAVE MISSED THESE....**

TRAC

trends in analytical chemistry

From the March issue:

The capillary column carousel

by R. P. W. Scott

Spectroscopic data banks

by J. T. Clerc and G. Székely

Polarography: a classical method with a new lease of life

by S. K. Vohra

Biomedical applications of derivative spectroscopy

by A. F. Fell

Proton and carbon-13 high resolution NMR spectroscopy
of high polymers

by Q. T. Pham

From the April issue:

Affinity chromatography in biotechnology -

not just a pious thought?

by P. D. G. Dean

Differential scanning calorimetry and fibre analysis

by C. Taylor

Monitoring of environmental water using continuous flow

by M. Goto

NMR examination of fossil fuels Part I: solid samples

by D. W. Jones

A comprehensive critical collection of electrochemical data

by L. Meites and P. Zuman

**TrAC publishes jargon-free articles and reviews dealing with
advances over the whole range of analytical methods.**

If you want to subscribe or receive a **FREE SAMPLE COPY** call or write to:
Elsevier Science Publishers,

P.O. Box 211, 1000 AE Amsterdam, The Netherlands tel. no. (20) 580 39 11

52 Vanderbilt Avenue, New York, N.Y. 10017 tel. no. (212) 867-9040

3-28-1, Yushima, Bunkyo-ku, Tokyo 113 tel. no. (03) 836-0810

ANALYTICA CHIMICA ACTA

International journal devoted to all branches of analytical chemistry

EDITORS

A. M. G. MACDONALD (Birmingham, Great Britain)

HARRY L. PARDUE (West Lafayette, IN, U.S.A.)

ALAN TOWNSHEND (Hull, Great Britain)

J. T. CLERC (Bern, Switzerland)

Editorial Advisers

F. C. Adams, Antwerp
H. Bergamin F^o, Piracicaba
G. den Boef, Amsterdam
A. M. Bond, Waurin Ponds
D. Dyrssen, Göteborg
J. W. Frazer, Livermore, CA
S. Gomisček, Ljubljana
S. R. Heller, Washington, DC
G. M. Hieftje, Bloomington, IN
J. Hoste, Ghent
A. Hulanicki, Warsaw
G. Johansson, Lund
D. C. Johnson, Ames, IA
P. C. Jurs, University Park, PA
D. E. Leyden, Fort Collins, CO
F. E. Lytle, West Lafayette, IN
H. Malissa, Vienna
D. L. Massart, Brussels
A. Mizuike, Nagoya
E. Pungor, Budapest

W. C. Purdy, Montreal
J. P. Riley, Liverpool
J. Růžicka, Copenhagen
D. E. Ryan, Halifax, N.S.
S. Sasaki, Toyohashi
J. Savory, Charlottesville, VA
W. D. Shults, Oak Ridge, TN
H. C. Smit, Amsterdam
W. I. Stephen, Birmingham
G. Tölg, Schwäbisch Gmünd, B.R.D.
B. Trémillon, Paris
W. E. van der Linden, Enschede
A. Walsh, Melbourne
H. Weisz, Freiburg i. Br.
P. W. West, Baton Rouge, LA
T. S. West, Aberdeen
J. B. Willis, Melbourne
E. Ziegler, Mülheim
Yu. A. Zolotov, Moscow



ELSEVIER Amsterdam—Oxford—New York

Anal. Chim. Acta, Vol. 149 (1983)

All rights reserved. No part of this publication may be reproduced, stored in a retrieval system or transmitted in any form or by any means, electronic, mechanical, photocopying, recording or otherwise, without the prior written permission of the publisher, Elsevier Science Publishers B.V., P.O. Box 330, 1000 AH Amsterdam, The Netherlands.

Submission of an article for publication implies the transfer of the copyright from the author(s) to the publisher and entails the author(s) irrevocable and exclusive authorization of the publisher to collect any sums or considerations for copying or reproduction payable by third parties (as mentioned in article 17 paragraph 2 of the Dutch Copyright Act of 1912 and in the Royal Decree of June 20, 1974 (S. 351) pursuant to article 16b of the Dutch Copyright Act of 1912) and/or to act in or out of Court in connection therewith.

Special regulations for readers in the U.S.A. — This journal has been registered with the Copyright Clearance Center, Inc. Consent is given for copying of articles for personal or internal use, or for the personal or internal use of specific clients.

This consent is given on the condition that the copier pay through the Center the per-copy fee stated in the code on the first page of each article for copying beyond that permitted by Sections 107 or 108 of the U.S. Copyright Law. If an appropriate fee should be forwarded with a copy of the first page of the article to the Copyright Clearance Center, Inc., 21 Congress Street, Salem, MA 01970, U.S.A. If no code appears in an article, the author has not given broad consent to copy and permission to copy must be obtained directly from the author. All articles published prior to 1980 may be copied for a per-copy fee of US \$2.25, also payable through the Center. This consent does not extend to other kinds of copying, such as for general distribution, resale, advertising and promotion purposes, or for creating new collective works. Special written permission must be obtained from the publisher for such copying.

Special regulations for authors in the U.S.A. — Upon acceptance of an article by the journal, the author(s) will be asked to transfer copyright of the article to the publisher. This transfer will ensure the widest possible dissemination of information under the U.S. Copyright Law.

Printed in The Netherlands.

TRIPLE-PULSE AMPEROMETRIC DETECTION OF CARBOHYDRATES AFTER CHROMATOGRAPHIC SEPARATION

SCOTT HUGHES^a and DENNIS C. JOHNSON*

Department of Chemistry, Iowa State University, Ames, IA 50011 (U.S.A.)

(Received 2nd August 1982)

SUMMARY

Triple pulse amperometry at a platinum wire electrode is demonstrated for chromatographic separations of carbohydrate mixtures on two commercially available "carbohydrate columns" and the performances of the columns are compared. The effect of detector temperature is described; an increase from 35 to 85°C resulted in an increase of sensitivity by a factor of 1.5–2.1. A consideration of errors is presented and dilution is recommended for samples of high concentration to minimize relative error. Results are given for determination of dextrose, fructose, glycerol, and ethanol in three wines with relative uncertainties of approximately 10% or better, calculated at the 90% confidence level.

Moderately efficient columns have been developed for the liquid chromatographic separation of complex mixtures of carbohydrates [1]. Because of the low molar absorptivities of carbohydrates in the ultraviolet–visible region of the spectrum, the measurement of refractive index has been the standard method of chromatographic detection. Conventional refractive index detection is sometimes characterized by a poor detection limit [2], however, a value of 0.04 mg ml⁻¹ has been reported [3].

Recently, we described the development of a very sensitive method for the amperometric detection of organic compounds containing the C–OH moiety at platinum electrodes in alkaline media [4, 5]. The technique is based on the application of a triple-pulse potential waveform which achieves detection of the organic analyte as well as reactivation of the platinum electrode within each waveform executed in a time period of 0.5–2 s. Application of triple pulse amperometry (t.p.a.) is especially promising for detection of simple alcohols, polyols, and simple carbohydrates in flow-through detectors applied for liquid chromatography as well as for flow-injection determinations [4–6]. A detection limit of about 5 µg ml⁻¹ was obtained for dextrose in a 100-µl sample by t.p.a. in 0.1 M NaOH.

The mechanism for oxidation of alcohols and carbohydrates on a platinum electrode is concluded to involve adsorption of the analyte on the electrode

^aPresent address: Utopia Instrument Co., P.O. Box 863, Joliet, IL 60434, U.S.A.

surface followed by the surface-catalyzed anodic dehydrogenation of the adsorbed molecule [4, 5]. The hydrocarbon products of the surface-controlled reaction remain adsorbed on the electrode surface, thereby inhibiting adsorption of unreacted molecules, and the anodic current observed at the detection potential quickly decays to zero. If the electrode potential is made sufficiently large and positive, corresponding approximately to the anodic breakdown of the aqueous solvent, the adsorbed hydrocarbons are oxidatively removed from the electrode, perhaps as CO_2 , with concomitant formation of platinum oxide, PtO . Oxidation of the organic analyte in the solution will not occur on the oxide-covered surface. The PtO is reduced by the subsequent application of a negative potential, corresponding approximately to the cathodic breakdown of the solvent, resulting in "reactivation" of the electrode surface, and analyte molecules are again adsorbed. The waveform for t.p.a. corresponds to the sequential application of three electrode potentials corresponding to anodic detection (E_1), anodic cleaning (E_2), and cathodic reactivation (E_3). The current is sampled near the end of the period for application of E_1 and a proportional voltage is retained in analog or digital memory until updated during the succeeding application of the waveform.

Because the mechanism of the anodic detection of alcohols and carbohydrates involves prior adsorption, the shape of the response curve is strongly influenced by the adsorption isotherm for the analyte. Under conditions for which the extent of adsorption is at an equilibrium value prior to application of E_1 , the absolute value of faradaic signal (I) can be related satisfactorily to the concentration of the electroactive species (C) by

$$I = C/(b + aC) \quad (1)$$

Equation (1) has the form of the Langmuir isotherm and is expected to be valid for relatively low surface coverages, for which the lateral interaction of adsorbed molecules is minimal. The constants a and b for the detection of alcohols and carbohydrates are determined experimentally by linear regression analysis of the linear plot of $1/I$ vs. $1/C$ [7]: $I^{-1} = a + b(C)^{-1}$. Furthermore, a and b are concluded to correspond to fundamental chemical and electrochemical constants according to the equations

$$a = (nFAk\Gamma_{\max})^{-1} \text{ and } b = (nFAkK\Gamma_{\max})^{-1} \quad (2)$$

where K is the equilibrium constant for adsorption, k is the heterogeneous rate constant (s^{-1}) for the faradaic reaction, Γ_{\max} is the maximum surface coverage (mol cm^{-2}) of adsorbed analyte at high concentration in the solution, and n , F , and A have their usual electrochemical significance.

There is virtually no selectivity afforded by the triple pulse technique and application of t.p.a. to mixtures of carbohydrates and alcohols is predicated on successful a priori separation. Use of h.p.l.c. for separation of carbohydrates has numerous advantages over other types of chromatography [8–12]. Two classes of column materials are used primarily for separation of carbo-

hydrates by h.p.l.c.: silica-based materials and ion-exchange. For the former, some workers have used pure silica columns with a small amount of an amine added to the eluent which then coats the silica by simple adsorption [2, 13]. More commonly, commercially available, chemically modified columns with alkylamine or octadecylamine functional groups are utilized. The mobile phase in the case of the silica columns is usually a mixture of water and acetonitrile with the water content between 10% and 40%. A retention mechanism based on hydrogen bonding between the sugar hydroxyl groups and the amine groups of the stationary phase can satisfactorily explain the observed retention orders, with longer retention times observed for sugars having a greater number of hydroxyl groups [14, 15].

Anion-exchange columns in the sulfate form have been utilized with excellent resolution of complex mixtures of carbohydrates [16–21]. The weakly acidic hydroxyl groups of the sugar are considered to play a part in the separation; however, steric influences are probably also important [20]. Reports of long separation times, ranging from 4 h [21] to 15 h [17], have hindered the acceptance of anion-exchange columns for routine use. The separation of sugars with cation-exchange resins is steadily gaining in acceptance [9, 20, 22–24]. Separations have the advantage that pure water can be used as the eluent and separation times are well under an hour. Several factors are considered to be responsible for the separation; however, the most important is thought to be the partitioning of the carbohydrate between the mobile phase and the stagnant water phase within the resin matrix. Increased resolution is obtained when the column is operated at elevated temperature, because of the increased diffusion of the analyte between the mobile and stagnant phases [9]. Size exclusion also plays a role in the separation, with the larger saccharides having the shorter retention times [24]. The degree of cross-linking of the resin can be altered to optimize this effect, with less cross-linking (i.e. larger pore size) being used for the separation of oligosaccharides. Results are included here for two commercially available cation-exchange columns in the Ca(II) form operated at 80°C with water as eluent.

EXPERIMENTAL

Instrumentation

Potentiostatic control was achieved with a Model 173 potentiostat, with a Model 176 current-to-voltage converter (EG & G Princeton Applied Research, Princeton, NJ). Generation of the triple-pulse waveform was by a device built in this laboratory from timing modules [4]. Values of potential and their duration were as follows: $E_1 = -0.40$ V (182 ms) with the faradaic signal sampled for 1 ms after 173 ms, $E_2 = +0.80$ V (185 ms), and $E_3 = -1.00$ V (223 ms). All electrode potentials were measured vs. the SCE reference. All chromatographic data were obtained with a data system [25] based on the HP-85 computer (Hewlett-Packard, Corvallis, OR).

Separations were achieved with calcium(II)-loaded, cation-exchange

columns from Hamilton (Model HC-75, Rainin Instrument Co., Woburn, MA; 10–15 μm particle size, 7.5% cross-linked, 30-cm length) and Dionex Corp. (Sunnyvale, CA; 7.5 μm size, 7% cross-linked, 25-cm length). The chromatographic columns were maintained at 80°C during separations by means of a thermostated water jacket. The eluent was water, pumped at a flow rate of 0.50 ml min⁻¹ by a Milton Roy Model CK miniPump with a Model 709 pulse dampener (Laboratory Data Control, Riviera Beach, FL). The sample-injection valve was a Rheodyne Model 7125 (Larry Bell and Assoc., Minneapolis, MN) with a sample loop of 100 μl .

Detection of carbohydrates by triple pulse amperometry (t.p.a.) is most sensitive at high pH. Hence a stream of 6.1 M NaOH pumped at 0.01 ml min⁻¹ by a Gilson Minipuls-2 peristaltic pump (Middleton, WI) equipped with 0.25-mm i.d. polyvinyl chloride manifold tubing (Rainin Instrument Co.) was mixed with the effluent stream in a tee-connexion of low dead volume (Unimetrics, Anaheim, CA). The mixing tee was maintained at 60°C (except for the temperature study) by circulating thermostated water through a surrounding water jacket. The net concentration of sodium hydroxide in the detector was 0.1 M. All tubing was stainless-steel with compression fittings used for all connections. An adjustable needle valve constructed locally from Kel-F was connected in the flow system after the detector to generate sufficient back-pressure (about 15 psi) to eliminate bubble formation in the detector. The platinum, wire-tip, flow-through detector has been described [6].

Chemicals and procedures

All chemicals were reagent grade. All water had been distilled, demineralized, passed through a 12-in. \times 1.5-in. o.d. column of activated carbon, and filtered through a 0.45- μm membrane. Dissolved oxygen was removed from the eluent by saturation with nitrogen.

To extend the life of the chromatographic columns, all samples were passed through a mixed bed of ion-exchange resin (Amberlite MB-3; Mallinckrodt).

RESULTS AND DISCUSSION

Chromatography

The resolutions of the Hamilton and Dionex columns were compared. Synthetic samples containing 0.40 mg ml⁻¹ each of eight carbohydrates were injected onto each column and typical chromatograms are shown in Fig. 1. The retention times (t_r), number of theoretical plates (N), and heights equivalent to theoretical plates (H) are listed for each compound in Table 1. Even though the Dionex column is 5 cm shorter than the Hamilton column, it exhibited much better resolution. The smaller size of the resin particles in the Dionex column undoubtedly is a factor contributing to the higher resolution.

To illustrate the applicability of the technique for a complex matrix, a

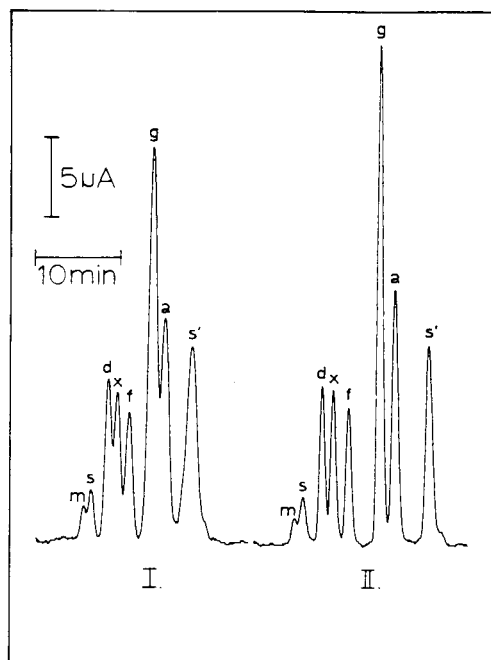


Fig. 1. Comparison of separations for eight carbohydrates (each at 0.40 mg ml^{-1}) by Hamilton (I) and Dionex (II) h.p.l.c. columns: m, maltotriose; s, sucrose; d, dextrose; x, xylose; f, fructose; g, glycerol; a, arabinol; s', sorbitol. Sample volume, $100 \mu\text{l}$.

TABLE 1

Comparison of performance of Hamilton^a and Dionex^b h.p.l.c. columns

Carbohydrate ^c	Hamilton			Dionex		
	t_r (min:s)	N^d	H^e	t_r	N	H
Maltotriose	10:52	1600	0.19	10:06	1000	0.25
Sucrose	11:42	1100	0.27	10:56	600	0.42
Dextrose	13:42	1000	0.30	13:08	1400	0.179
Xylose	14:47	1100	0.27	14:24	1900	0.132
Fructose	16:12	1400	0.21	16:11	2100	0.119
Glycerol	18:58	1400	0.21	19:50	3200	0.078
Arabinol	20:32	1200	0.25	21:35	3100	0.081
Sorbitol	23:37	1600	0.19	25:33	3900	0.064

^aHamilton column: $10\text{--}15 \mu\text{m}$ particle size, 7.5% cross-linking, 30 cm long. ^bDionex column: $7.5 \mu\text{m}$ particle size, 7% cross-linking, 25 cm long. ^c 0.40 mg ml^{-1} . ^d $N = 16 (t_r/W)^2$ where W is the peak width. ^e $H = L/N$ where L is the column length (mm).

chromatogram of a human urine sample is shown in Fig. 2. Peaks were identified by comparison of retention times to standards. Peaks corresponding to dextrose, xylose, arabinose, glycerol, and urea were identified. No attempt was made to quantify the carbohydrates in this sample.

The application of t.p.a. detection for quantitative purposes was demonstrated for three varieties of wine. Chromatograms are shown in Fig. 3 for 1:12.5 dilutions of the three wines, a "sweet" white, a "dry" red, and a "light" burgundy. Peaks were observed for dextrose, fructose, glycerol and ethanol. A calibration curve was made for each of these compounds. The concentrations of the compounds in the wine varieties are given in Table 2. Even though many other carbohydrates than detected here are found in grapes, they are broken down in the fermentation process and, therefore, are not observed in the final product [26]. The absence of a peak for sorbitol is consistent with the fact that this carbohydrate, though commonly found in many fruits, is not observed in grapes. The presence of sorbitol in wines

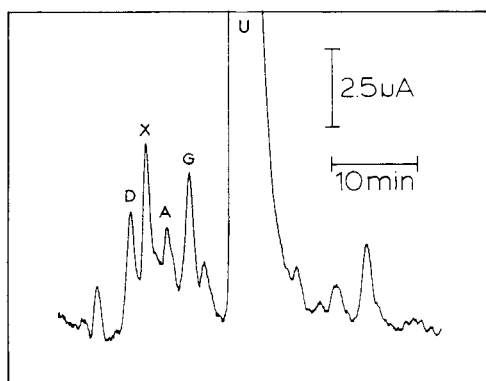


Fig. 2. Chromatographic separation of human urine components. Separation achieved with the Dionex column. Peaks: D, dextrose; X, xylose; A, arabinose; G, glycerol; U, urea.

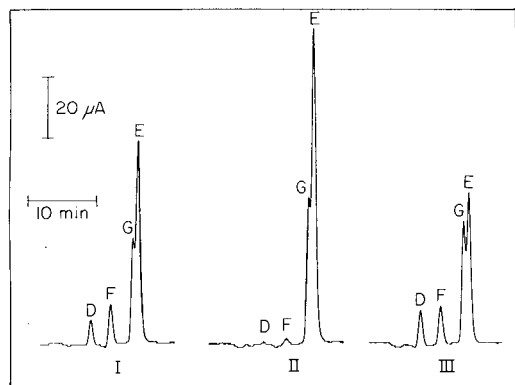


Fig. 3. Chromatographic data for wine on the Dionex column. Wines: I, sweet white; II, dry red; III, light burgundy. Peaks: D, dextrose; F, fructose; G, glycerol; E, ethanol.

TABLE 2

Results of the wine analysis

Type	Carbohydrate content (mg ml ⁻¹)			Ethanol (% by vol)
	Dextrose	Fructose	Glycerol	
Liebfraumilch, "sweet" white	5.67 ± 0.12	15.4 ± 1.5	5.2 ± 0.3	7.4 ± 0.4
Premium red, "dry" red	0.049 ± 0.005	1.30 ± 0.03	7.6 ± 0.6	9.7 ± 0.4
Light burgundy, "sweet" red	7.7 ± 0.2	9.5 ± 0.7	6.2 ± 0.4	4.60 ± 0.14

has been used to indicate adulteration of the grape wine with fermentation products of other fruits [26].

The sweetness of a wine is a function of the carbohydrate concentration. This is readily observed by an examination of Table 2 with the dry red wine having very low dextrose and fructose concentrations compared to the sweet white. The light Burgundy is marketed as a "diet wine", lower in calories than regular wines. The results indicate that the caloric savings are due not to the lowering of carbohydrates but to the reduction of the ethanol content of the product.

Detector temperature

Because the chromatographic column in this work is operated at an elevated temperature, it is convenient to operate the detector at an elevated temperature. Chromatograms obtained with the Dionex column at 80°C were recorded as a function of detector temperature in the range 35–85°C for a synthetic mixture of six carbohydrates, which included two sugar alcohols, three aldoses and a disaccharide. The results are shown in Fig. 4 plotted as $\log(I_p)$ vs. T^{-1} where I_p is the absolute value of the anodic detection peak corresponding to detector temperature T (K). Increasing the temperature over the range 35–85°C resulted in higher detector sensitivity by a factor of from 1.5 for arabitol and sorbitol to 2.1 for lactose. Without thermostatic control of the detector, the average temperature of the solution entering the detector was approximately 60°C and this temperature was chosen for all qualitative and quantitative work.

Plots of the type shown in Fig. 4 are useful in estimating the overall energy of activation for kinetically controlled processes. For the range of concentrations used to obtain the data in Fig. 4, plots of I_p vs. C were nearly linear, i.e., $b \gg a$ for Eqn. (1) and I_p was proportional to C/b . On the basis of the substitution for b from Eqns. (2) we can write

$$\begin{aligned} d \ln(I_p)/d(T^{-1}) = & [d \ln(\Gamma_{\max})/d(T^{-1})] + [d \ln(k)/d(T^{-1})] \\ & + [d \ln(K)/d(T^{-1})] \end{aligned} \quad (3)$$

It is assumed that $\ln(\Gamma_{\max})$ varies insignificantly. The substitution for an irreversible electron-transfer reaction is made so that

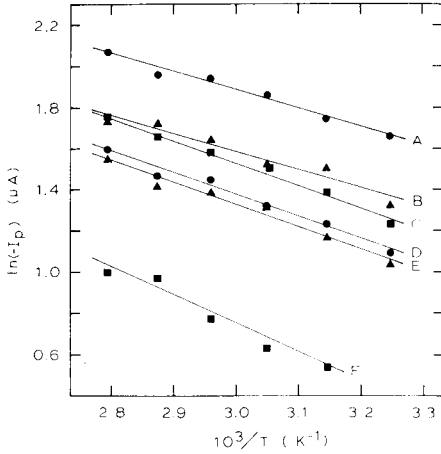


Fig. 4. Results of temperature study. A, Arabitol (0.12 mg ml^{-1}); B, sorbitol (0.12 mg ml^{-1}); C, arabinose (0.12 mg ml^{-1}); D, xylose (0.12 mg ml^{-1}); E, glucose (0.12 mg ml^{-1}); F, lactose (0.14 mg ml^{-1}).

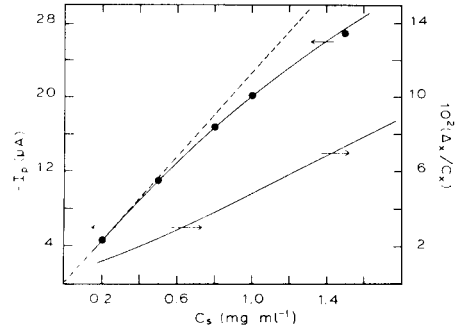


Fig. 5. Calibration curve and estimated relative error. (---) extrapolation of linear portion of I_p - C_s plot; (—) calculated on the basis of data in Table 3.

$$\begin{aligned} d \ln(k)/d(T^{-1}) &= [d \ln(A_{\text{anod}})/d(T^{-1})] - [\Delta G_{\text{anod}}^*/R] \\ &+ [\alpha_{\text{anod}} F(E - E^0)/R] \end{aligned} \quad (4)$$

where A_{anod} is the preexponential term in the Arrhenius rate equation and ΔG_{anod}^* is the activation energy for the anodic process at $E = E^0$. The number of electrons, n , for the anodic reaction is included in the coefficient α_{anod} ; the value of n is not known for these reactions. Following the formulation of an expression for K based on the Arrhenius equations for the adsorption and desorption processes, $K = k_{\text{ads}}/k_{\text{des}}$,

$$d \ln(K)/d(T^{-1}) = [d \ln(A_{\text{ads}}/A_{\text{des}})/d(T^{-1})] - [\Delta G_{\text{ads}}^*/R] + [\Delta G_{\text{des}}^*/R] \quad (5)$$

where A_{ads} and A_{des} are the Arrhenius preexponential terms for adsorption and desorption, respectively, and ΔG_{ads}^* and ΔG_{des}^* are the respective activation energies with $\Delta G_{\text{ads}}^0 = \Delta G_{\text{ads}}^* - \Delta G_{\text{des}}^*$. The preexponential terms are assumed to be independent of temperature, so that

$$d \ln(I_p)/d(T^{-1}) = [-\Delta G_{\text{anod}}^*/R] - [\Delta G_{\text{ads}}^0/R] + [\alpha_{\text{anod}} F(E - E^0)/R] \quad (6)$$

In Eqn. (6), the first term must be negative because, for a reaction of finite rate, ΔG_{anod}^* is taken to have a positive value. The second and third terms, however, are probably positive because ΔG_{ads}^0 is negative for spontaneous adsorption and $E \gg E^0$ for an irreversible anodic reaction. Hence, depending on the relative values of the three terms in Eqn. (6), the slope of the plot of $\ln(I_p)$ vs. T^{-1} can be expected to be negative, zero, or positive. The slopes of the six plots in Fig. 4 are consistently negative and of similar value. We

TABLE 3

Linear regression statistics for the calibration curve for dextrose plotted in Fig. 5 ($N = 5$)

Parameter	Symbol	Value
Slope	b	$(4.048 \pm 0.049) \times 10^{-2} \text{ mg ml}^{-1} \mu\text{A}^{-1}$
Intercept	a	$(9.3 \pm 1.2) \times 10^{-3} \mu\text{A}^{-1}$
Standard error of estimate	$s_{y,x}$	$5.4 \times 10^{-4} \mu\text{A}^{-1}$
Correlation coefficient	r	0.99998

conclude that the term, $\Delta G_{\text{anod}}^*/R$, in Eqn. (6) dominates and, furthermore, that the compounds studied react by a similar electrochemical mechanism, i.e., similar values of ΔG_{anod}^* .

Variation of results

The slope of the nonlinear plot of I vs. C for carbohydrates detected by t.p.a. decreases with increasing C . Hence, it is expected that the relative error for determination of an unknown concentration will be inversely proportional to C . Calibration data for the measurement of dextrose was obtained for standard samples of concentration, C_s , in the range 0.2–1.5 mg ml^{-1} and the plot of I_p vs. C_s is shown in Fig. 5. The regression statistics for the linear plot of $1/I_p$ vs. $1/C_s$ are summarized in Table 3 with uncertainties computed at the 90% confidence level. The fit of the I_p vs. C_s data shown in Fig. 5 was made based on Eqn. (1) using values of a and b from Table 3.

Of primary concern is the minimization of the relative uncertainty for determination of an unknown concentration C_x , Δ_x/C_x . In Fig. 5 is shown the estimated value of Δ_x/C_x computed on the basis of single values for measured anodic currents over the range of values of $C_x = C_s$ included in the figure. It is quite apparent that unknown samples of high concentration should be diluted to minimize relative error of the results.

The support of this research by Dionex Corp., Sunnyvale, CA, is gratefully acknowledged.

REFERENCES

- 1 K. Aitzetmüller, *J. Chromatogr.*, 156 (1978) 354.
- 2 S. I. M. Johncock and P. J. Wagstaffe, *Analyst*, 105 (1980) 581.
- 3 K. Brunt, Potato Processing Research Institute, Groningen, personal communication, 1982.
- 4 S. Hughes, P. L. Meschi and D. C. Johnson, *Anal. Chim. Acta*, 132 (1981) 1.
- 5 S. Hughes and D. C. Johnson, *Anal. Chim. Acta*, 132 (1981) 11.
- 6 S. Hughes and D. C. Johnson, *J. Agric. Food Chem.*, 30 (1982) 712.
- 7 M. G. Natrella, *Experimental Statistics*, Nat. Bur. Stds. Handbook 91, U.S. Dept. Commerce, Washington, 1963, Ch. 5.
- 8 J. A. Elvidge and P. G. Sammes, *A Course in Modern Techniques of Organic Chemistry*, 2nd edn., Butterworths, London, 1966.

- 9 J. K. Palmer and W. B. Brandes, *J. Agric. Food Chem.*, 22 (1974) 709.
- 10 P. E. Shaw, C. W. Wilson III and R. J. Knight, Jr., *J. Agric. Food Chem.*, 28 (1980) 379.
- 11 G. J. Dickes and P. V. Nicholas, *Gas Chromatography in Food Analysis*, Butterworths, London, 1976, Ch. 8 and 15.
- 12 J. C. Linden and C. L. Lawhead, *J. Chromatogr.*, 105 (1975) 125.
- 13 K. Aitzetmuller, *J. Chromatogr.*, 156 (1978) 354.
- 14 H. Binder, *J. Chromatogr.*, 189 (1980) 414.
- 15 M. D'Amboise, D. Noel and T. Hanai, *Carbohydr. Res.*, 79 (1980) 1.
- 16 S. Katz, S. R. Dinsmore and W. W. Pitt, Jr., *Clin. Chem.*, 17 (1971) 731.
- 17 R. L. Jolley and M. L. Freeman, *Clin. Chem.*, 14 (1968) 538.
- 18 K. Mopper, *Anal. Biochem.*, 87 (1978) 162.
- 19 E. Martinson and O. Samuelson, *J. Chromatogr.*, 50 (1970) 429.
- 20 P. Jondera and J. Churacek, *J. Chromatogr.*, 98 (1974) 55.
- 21 J. Havlicek and O. Samuelson, *J. Inst. Brew.*, 81 (1975) 466.
- 22 J. C. Kuo and E. S. Yeung, *J. Chromatogr.*, 223 (1981) 321.
- 23 J. S. Hobbs and J. G. Lawrence, *J. Chromatogr.*, 72 (1978) 311.
- 24 H. D. Scobell, K. M. Brobst and E. M. Steele, *Cereal Chem.*, 54 (1977) 905.
- 25 S. Hughes, Ph.D. Thesis, Iowa State University, Ames, IA, 1982.
- 26 J. F. Gallander, in A. D. Webb (Ed.), *Chemistry of Winemaking*, American Chemical Society, Washington DC, 1974, Ch. 2.

SEPARATION OF SELECTED POLYNUCLEAR AROMATIC HYDROCARBONS IN MINERAL OIL BY LIQUID–SOLID CHROMATOGRAPHY ON AMBERLITE XAD-2

JACK L. ROBINSON*, PAUL E. GRIFFITH, DAVID S. SALAS and G. EMMA SAM

Physical Sciences Department, Southeastern Oklahoma State University, Durant, OK 74701 (U.S.A.)

(Received 4th October 1982)

SUMMARY

Representative polynuclear aromatic hydrocarbons are separated from mineral oil by using step-wise gradient elution chromatography on Amberlite XAD-2. The aliphatic hydrocarbon sample matrix elutes in the column void volume under normal phase conditions with 2,2,4-trimethylpentane used as the eluent. Lower-molecular-weight aromatics are eluted with isohexanes or heptane, and higher-molecular-weight aromatics are eluted under size-exclusion conditions after changing to tetrahydrofuran or dichloromethane as the eluent. Linear elution adsorption chromatography theory is used to interpret the retention behavior of the polynuclear compounds.

White mineral oil is used as a multipurpose additive in products intended for human consumption, and technical white mineral oil is used in other applications in which there is the possibility of incidental contact with food. Even though these oils are highly refined liquids, obtained from the distillation of petroleum or oil shale, there remains the possibility that they may contain trace quantities of carcinogenic polynuclear aromatic hydrocarbons (PAH). Consequently, the U.S. Federal Government has established specifications and procedures for monitoring the PAH content of mineral oils [1].

The F.D.A. method for determining the PAH content of mineral oils produced for non-food applications involves both liquid–liquid extractions and column chromatography [1, 2]. The method involves 28 extraction steps for one sample and blank, and requires in excess of 24 man-hours for both reagent preparation and sample processing [2]. As an alternative, Skinner and Smith [2] have developed a linear elution adsorption chromatographic (l.e.a.c.) method which utilizes PAH class separation on partially deactivated alumina, followed by resolution of the PAH on magnesium oxide-Celite, and u.v. measurement of the individual PAH.

Previous work in this laboratory has demonstrated that Amberlite XAD-2 (a macroporous styrene–divinylbenzene copolymer adsorbent) is effective for separating the PAH class from cigarette smoke condensate [3]. While the

chromatographic properties of XAD-2 were investigated, it was observed that PAH are highly adsorbed from branched-chain aliphatic solvents, particularly 2,2,4-trimethylpentane (TMP) [4]. This observation indicated that PAH might be separated from oils having a high aliphatic hydrocarbon content. This paper describes the class separation of PAH from mineral oil and subsequent class fractionation using step-wise gradient elution chromatography on XAD-2. The solvent sequence of TMP, heptane, and tetrahydrofuran (THF) or dichloromethane is used to change the separation mode from normal phase to size-exclusion mode.

EXPERIMENTAL

Apparatus, reagents, and samples

A chromatography column (2 × 30 cm, Glenco Scientific Co.) was dry-packed with approximately 40 g of Amberlite XAD-2 (Rohm and Haas). A flow rate of 1.5–2.0 ml min⁻¹ was maintained with a mini-pump (Milton Roy Co.). The column effluent was monitored with a u.v. absorption detector (Perkin Elmer, Model 250) at 254 nm. Solvents were distilled-in-glass products (Burdick and Jackson), except for ethanol (U.S. Industrial Chemical Co.) and methanol (Fisher Scientific). Unlabeled PAH (Aldrich Chemical Co.) were recrystallized from ethanol if necessary. Stock solutions of ¹⁴C-PAH (Amersham Corp.) were made by dissolving 50 μCi of PAH in 25.00 ml of ethanol. Initial samples were food-grade mineral oils such as Hospital Brand Heavy (Dixie Laboratories), Squibb, and McKesson Heavy Liquid Petrolatum (USP Grade). Two mineral seal oils used were Cotton Valley 600 Solvent and Kermac 600 (both obtained from Kerr-McGee Corp.). The former sample historically has met the requirements of FDA § 178.3620(C), but was not specifically tested for PAH. The latter sample was a base stock that was not expected to meet the requirements of FDA § 178.3620(C).

All experimental work was done in a room equipped with low u.v. yellow fluorescent lights (Westinghouse F40G0).

Procedures

Fractionation of PAH. Model samples were prepared by mixing 2–5 g of mineral oil with 100 μl of the appropriate ¹⁴C-labeled compound (hexadecane, naphthalene, phenanthrene, or benz[a]pyrene) and diluting to 10 ml with TMP. A portion of the sample was injected without flow onto an XAD-2 column that had been preconditioned with TMP. After 10 min of equilibration, the pump was started and 25-ml fractions were collected.

Liquid scintillation counting. When ¹⁴C-compounds were used, 2.00 ml of each fraction was placed in a 20-ml glass scintillation vial with 13.0 ml of scintillation solution (Beckman EP) and disintegrations were counted for 50 min in a Beckman LS-100C liquid scintillation spectrometer, using the external standard channels ratio mode to correct for quenching. A quench calibration curve was prepared with the Beckman and Amersham Standard Quench Sets.

Subsequent processing. The mineral oil mass distribution in selected fractions was determined by evaporating the solvent from a 20-ml aliquot in a tared vial, and weighing the oil residue. Fractions collected from fractionations of unspiked oil were scanned from 400 to 200 nm with a u.v. spectrophotometer (Varian 634S). High-performance reversed-phase liquid chromatography was used to examine selected fractions of mineral oil eluate. The original solvent was evaporated from an aliquot of the fraction in order to permit redilution with methanol. Gradient elution with methanol–water (80–100% at 2% per min) on a reversed-phase column (4 × 250 mm, Bio-Sil ODS-10, Bio-Rad Laboratories) was accomplished with a modular chromatograph consisting of dual pumps (Beckman Model 110), a programmable controller (Beckman Model 420), an injection valve (Rheodyne Model 70-10), and a variable wavelength u.v. detector (Perkin Elmer Model LC-55) operated at 254 nm.

RESULTS AND DISCUSSION

General column characteristics

In preliminary investigations, ^{14}C -hexadecane and ^{14}C -benz[a]pyrene were used as model compounds for aliphatic hydrocarbons and PAH, respectively. Figure 1 illustrates a separation of 0.22 μg (5.2×10^{-2} μCi) of hexadecane and 0.85 μg (7.3×10^{-2} μCi) of benz[a]pyrene from 2.0 g of medicinal-grade mineral oil. Here 99.1% of the hexadecane activity was eluted in fractions 1–5 with 125 ml of TMP, and less than 1% of the activity tailed over into fractions 6 and 7. Fraction 3 (elution interval 50–75 ml), which contains 81.5% of the activity, corresponds to the void volume (57.5 ± 0.3 ml) of the column, and that fraction containing the largest mass of mineral oil, which was measured in subsequent mineral oil mass distribution experiments. The benz[a]pyrene is highly retained by XAD-2 when TMP is the eluent, because the distribution constant (K_D) is over 200 [4]; however, by judiciously changing eluents the K_D can be decreased to zero and the separation mode changes from the normal-phase to the size-exclusion mode. Solvents such as tetrahydrofuran (THF), dichloromethane, or toluene readily elute benz[a]pyrene. In triplicate experiments, $101.4 \pm 2.8\%$ of the benz[a]pyrene was recovered in fractions 12–24, with 2% or less of the activity tailing over into the last four fractions.

The alternative of using a semipreparative-scale alkyl reversed-phase column for the aliphatic/PAH class fractionation was examined. The column (Li-Chroprep RP-8, 2.5 × 31 cm, EM Laboratories) was used for an attempted fractional separation of hexadecane and benz[a]pyrene in a medicinal oil sample, with TMP as eluent. The result was that 99.0% of the total activity emerged in fractions 2–10, suggesting that these two compounds could not be separated under normal-phase elution conditions with this column.

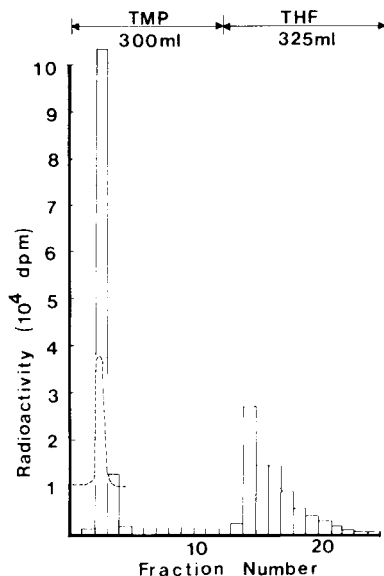


Fig. 1. Separation of ^{14}C -hexadecane (fractions 1–5) and benz[a]pyrene (fractions 14–25) from medicinal mineral oil. The elution profile of an unretained solute (NaNO_3) is shown by the dashed line (---).

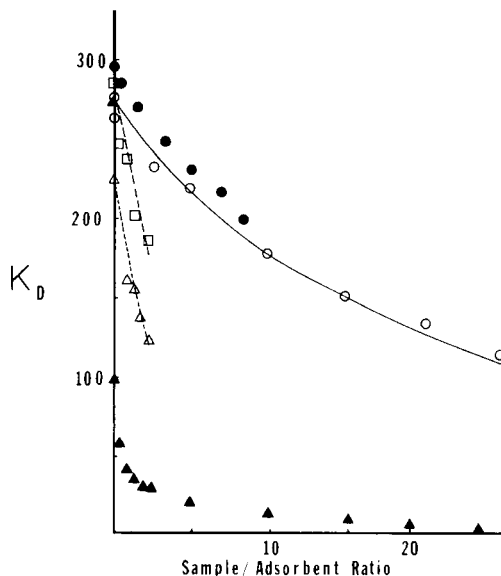


Fig. 2. Effect of the sample matrix type and sample/adsorbent ratio (W_O) on the distribution constant (K_D) of benz[a]pyrene in 2,2,4-trimethylpentane. Oil samples include: (\circ , \bullet) medicinal mineral oil; (\blacktriangle) technical oil; (\triangle) vaseline; (\square) paraffin wax. The solid line is the variation in elutropic value of a binary solution containing TMP and a hypothetical stronger solvent whose ϵ^0 is 0.045.

Sample matrix effects

The influence of mineral oil and selected other matrices on the retention of benz[a]pyrene by XAD-2 is shown in Fig. 2. The K_D value was measured by an equilibrium tracer method [4], in which $2.03\ \mu\text{g}$ of benz[a]pyrene was spiked into TMP solutions containing approximately 0.5 g of XAD-2, and increasing quantities of sample. The mass of oil sample per gram of XAD-2 in the system, W_O , was varied over a range many times larger than the typical sample loading used for column operations. Linear elution conditions specify a sample/adsorbent ratio that causes no more than 10% decrease in K_D [5]. Hence, a ratio of about 0.1 g of sample per g of adsorbent could be used for oils such as the Cotton Valley type. The significant retention of benz[a]pyrene at W_O values of 5–10 suggests that XAD-2 may be useful for the concentration of trace quantities of 4–5-ring PAH from oils by frontal elution chromatography.

The dramatic differences in the K_D versus W_O trends for the Cotton Valley Mineral Seal Oil and the medicinal oil samples was somewhat unexpected. The gradual decrease in K_D for the medicinal oil sample is similar to a solvent

eluotropic effect that would be observed for binary solutions where the oil matrix emulates a solvent stronger than TMP. The abrupt decrease in K_D for vaseline, paraffin wax, and the Cotton Valley sample illustrates a matrix effect where presumably there are components that compete with benz[a]-pyrene for adsorption sites on XAD-2.

Application of linear elution adsorption chromatographic theory to the fractionation of model PAH mixtures

The K_D values of PAH on XAD-2 can be calculated for various eluents from the theory of linear elution adsorption chromatography. The general equation is:

$$\log K_D = \log V_a + \alpha S^0 - \alpha A_s \epsilon^0$$

where α is the adsorbent activity (assumed to be unity for clean XAD-2), V_a is the volume of an adsorbed monolayer ($V_a = \text{adsorbent surface area} \times 0.00035$ for XAD-2), S^0 is the solute adsorption energy, A_s is the area covered on the adsorbent surface by an adsorbed sample molecule, and ϵ^0 is the solvent eluotropic value [5]. In the case of PAH adsorbed onto XAD-2 it has been demonstrated that $S^0 = 0.252 \times A_s$, $\log V_a = -1.021$, and the A_s value of unsubstituted PAH, C_cH_h , can be calculated by the formula $A_s = 6 + 0.8(h - 6) + 0.25(c - h)$ [4]. Consequently, the K_D values of PAH on XAD-2 are readily calculated by using the equation

$$\log K_D = -1.021 + 0.252 A_s - A_s \epsilon^0$$

The K_D values for four representative PAH with several eluents are shown in Table 1. The retention volume (R') of each PAH can be predicted by the equation: $R' = K_D \times W + V^0$, where W is the dry weight of XAD-2 packed into the column (39.8 g for Fig. 3), and V^0 is the column void volume (60.9 ml for Fig. 3). The solvent sequence shown in Fig. 3 was selected to demonstrate the separation of a hydrocarbon mixture (benzene, naphthalene, and benz[a]pyrene) from a mineral oil matrix. The sample contained 7.04 mg of benzene, 2.30 μg of naphthalene, 0.80 μg of benz[a]pyrene, and 1.62 g of medicinal mineral oil. As expected, the bulk of the mineral oil sample matrix eluted in fractions 1–5, with 84.5% in fraction 3 alone. Fraction 6, which contained 60% of the unlabeled benzene spike, corresponds to the peak maximum and an elution interval of 125–150 ml. This value is significantly less than the predicted retention volume of 220 ml. In three other runs in which mineral oil was present, the benzene peak consistently occurred in fraction 6, and was totally eluted in fractions 3–10. The u.v. absorption spectra of medicinal mineral oils indicate the presence of chromophores with peaks near 270 and 278 nm and a valley near 245 nm. Presumably the absorption represents some unsaturation or aromatic character in the oil matrix that can compete with benzene for adsorption sites on XAD-2 and effectively lower its K_D value to approximately 1.9 in the matrix environment.

Naphthalene, which was chosen as a model for di-aromatic fused PAH,

TABLE 1

Calculated distribution constants and retention volumes for representative PAH

Compound	A_s	Eluents (elutropic value) ^a					
		TMP (-0.018)		Isohexanes (0.062)		Heptane (0.078)	
		K_D	R'	K_D	R'	K_D	R'
Benzene	6.0	4.0	220	1.3	113	1.1	103
Naphthalene	8.1	14.7	650	3.3	190	2.4	160
Phenanthrene	10.2	54.1	2210	8.3	390	5.7	290
Benz[a]anthracene	12.3	200	8020	20.7	890	13.2	580
Benz[a]pyrene	12.8	275	11000	25.8	1090	16.1	700

^aFor elutropic values, see [4].

was eluted with heptane. After switching to heptane, the seventh heptane fraction (collected in the interval of 150–175 ml after switching to heptane) coincides with the naphthalene peak. This interval is in excellent agreement with the predicted retention volume of 158 ml for elution with heptane. Two repeat experiments gave identical results for the elution of naphthalene with heptane. Thus it can be concluded that the first eluent, TMP, is very ineffective in moving naphthalene down the column, and secondly, the u.v. absorbing chromophores in the oil matrix exert minimal influence on di-aromatics in the environment of the column. In general, the naphthalene activity would be distributed through ten fractions of heptane eluent. It would be helpful if a minor eluent component could be identified that could be added to heptane in order to reduce the tailing of the naphthalene distribution profile and effectively sharpen its peak. Benz[a]pyrene which was chosen as a model for penta-aromatic fused PAH, was eluted with THF. Several fractionations revealed that the benz[a]pyrene fraction of maximum activity always appeared in fraction 2 or 3 after switching to THF eluent and would

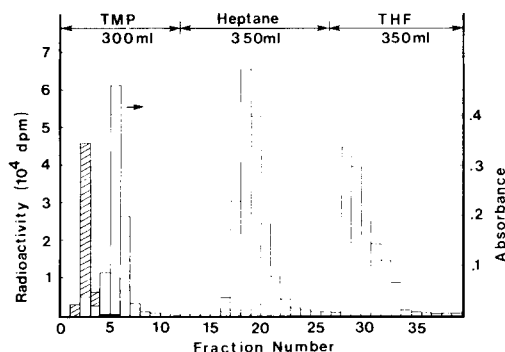


Fig. 3. Separation of a three-component aromatic hydrocarbon mixture from medicinal mineral oil. Collected fractions include the oil matrix (2–6), benzene (3–10), naphthalene (17–28), and benz[a]pyrene (29–40). Mineral oil mass (g) = 4.00 × benzene absorbance.

be distributed throughout 10–12 fractions. The fraction of maximum benz[a]pyrene activity again is very close to the column void volume, which implies that the K_D value drops to zero in THF.

The fractionation of a mineral oil sample (5.01 g) spiked with a four-component mixture of benzene (17.6 mg), naphthalene (5.60 μ g), phenanthrene (6.20 μ g), and benz[a]pyrene (2.02 μ g) was accomplished with a sequence of four solvents which included TMP (250 ml), heptane (650 ml), cyclopentane (100 ml), and dichloromethane (475 ml). The elution of the oil matrix, benzene, and naphthalene was consistent with previous results. A small amount of 14 C-activity in fractions 3–10 was equivalent to 0.18% of the total activity, or no more than 48 ng of PAH. The phenanthrene peak at fraction 13 (collected in the interval 300–325 ml) after switching to heptane was in good agreement with its predicted retention value. The estimated resolution of 0.7 for the separation of naphthalene and phenanthrene was in good agreement with an expected resolution of 0.85, which is based on 58 theoretical plates in the column. Even though the 14 C-activity did not reach the baseline between phenanthrene and benz[a]pyrene, the activity of each fraction in the region of fractions 31–36 was only about 2.5% of the total phenanthrene activity. With the particular solvent sequence used in the fractionation, one would expect the di- and tri-aromatics to be eluted together in the heptane fractions, and the tetra- and penta-aromatics would be collected in the dichloromethane fractions.

Figure 4 shows that the resolution between naphthalene and phenanthrene can be increased to about one by changing the eluent sequence. In this particular case the mineral oil sample (2.51 g) was spiked with the previously described four-component hydrocarbon mixture.

Fractionation of mineral oil samples

The PAH fractionation method was applied to mineral oil samples that had not been refined to meet the standards for human consumption. Figure

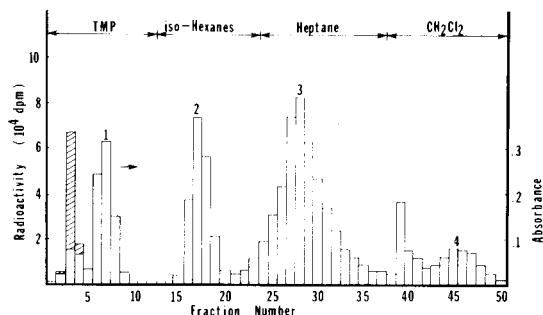


Fig. 4. Separation of a four-component PAH mixture from medicinal mineral oil. Collected fractions include the oil matrix (2–5), benzene (3–9), naphthalene (15–21), phenanthrene (22–37), and benz[a]pyrene (38–50). Mineral oil mass (g) = 5.00 \times benzene absorbance.

5, which is typical of the fractionation of two different samples, shows the fractionation of 5.01 g of Kermac 600 mineral seal oil. Here 90.04% of the oil matrix was recovered in fractions 1–6. A u.v. spectrum (400–200 nm) was obtained for each fraction after making dilutions as needed. The absorbances at 300, 275, and 250 nm were very high through fraction 20, and decreased to 0.1 or less by fraction 30. These results suggest that there were large quantities of mono-, di-, and tri-aromatics in the oil sample. The inset for a different oil sample (Cotton Valley 600) suggest some differences in the higher aromatic region for the fractions eluted with dichloromethane.

High-performance reversed-phase chromatography with the system described in a previous section was applied to fractions 14, 37, and 41 of Fig. 5. The results in Fig. 6 suggest that each fraction contained more than one PAH, presumably similar PAH derivatives.

Re-use of XAD-2 columns

Three different XAD-2 columns were used for 13 different fractionations, and the third one was used for the last eight runs. After several model PAH fractionation experiments with ^{14}C -labeled PAH had been completed, a blank run was conducted by pumping solvents only through the column, using the sequence of TMP (375 ml), heptane (375 ml), THF (375 ml), and dichloromethane (250 ml). The ^{14}C -activity of most fractions was at the background level; however, four of the THF and dichloromethane fractions gave a residual activity of 250 dpm per fraction. This would be equivalent to 5 ng of benz[a]pyrene (if the activity represented this compound), or 0.05 ppb contamination from re-use of the column. The net u.v. absorbance of the fractions at 250 nm was as follows for the eluents: TMP (0.001 or less), heptane (0.008 or less), THF (0.067 or less), and dichloromethane (0.040 or less). The solvents were not checked with standard evaporation

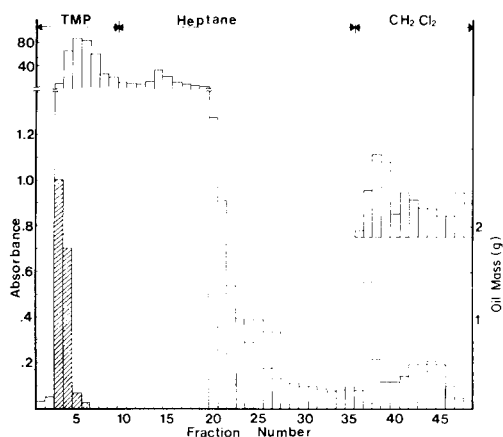


Fig. 5. Fractionation of Kermac 600 mineral seal oil. The inset shows differences obtained for a Cotton Valley 600 sample. Fractions 2–6 contain the oil matrix.

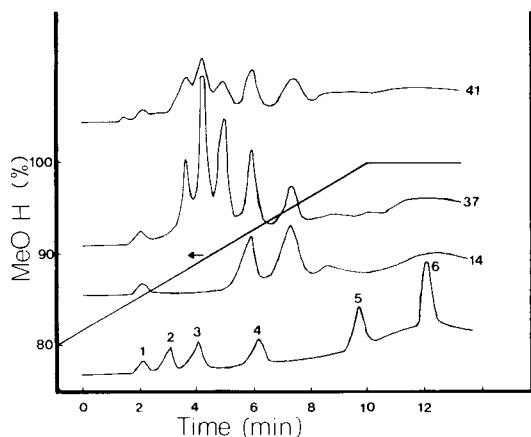


Fig. 6. Reversed-phase l.c. examination of fractions 14, 37, and 41 obtained from the fractionation of Kermac oil shown in Fig. 5. Standards in the lowest chromatogram are: (1) solvent artifact, (2) benzene, (3) naphthalene, (4) phenanthrene, (5) benz[a]anthracene and (6) benz[a]pyrene.

tests for trace u.v. impurities. After each separation, the column was reconditioned with TMP.

Fractionation of a 20-g sample of medicinal mineral oil with the above solvent sequence gave similar results for residual ^{14}C -activity and u.v. absorbance, except that fractions 2–5 showed characteristic absorbance at 250 and 275 nm.

Conclusions

The applicability of linear elution normal-phase chromatography on Amberlite XAD-2 (and presumably other styrene divinylbenzene copolymer adsorbents) for the fractionation of PAH from mineral oil has been demonstrated. Although this technique will not provide complete resolution of each individual PAH from complex oil samples, it does provide a means for separating the aliphatic oil matrix from the PAH fraction and offers the possibility of dividing the PAH fraction into aromatics of lower and higher molecular weight. The isolation of PAH by XAD-2 under normal-phase conditions could find application in other situations where PAH are to be isolated from an aliphatic matrix.

The XAD-2 column size and packing mesh (20–50) used in this work were selected as a matter of convenience. Future efforts will focus on the use of smaller semi-preparative columns (Hamilton PRP-1, 0.70×30.5 cm, 8–12 μm particle diameter) to reduce the total fractionation time and improve the resolution between aromatics of lower and higher molecular weight.

This work was presented in part at the combined Southwest—Southeast Regional Meeting of the American Chemical Society, New Orleans, LA, December 1980, and the 10th Annual MBS Symposium, Albuquerque, NM, April 1982. It was supported by the National Institutes of Health, Division of Research Resources, under Grant RR-08003. The authors thank Gordon R. Skinner and the Kerr-McGee Corporation for supplying two of the mineral oil samples.

REFERENCES

- 1 Code of Federal Regulations, Title 21 (Food and Drugs), § 172.878 and § 178.3620 (1981).
- 2 G. R. Skinner and R. E. Smith, *J. Chromatogr. Sci.*, 15 (1977) 75.
- 3 J. L. Robinson, M. A. Marshall, M. E. Draganjac and L. C. Noggle, *Anal. Chim. Acta*, 115 (1980) 229.
- 4 J. L. Robinson, W. J. Robinson, M. A. Marshall, A. D. Barnes, K. J. Johnson and D. S. Salas, *J. Chromatogr.*, 189 (1980) 145.
- 5 L. R. Snyder, *Principles of Adsorption Chromatography*, Marcel Dekker, New York, 1968.

THE DETERMINATION OF LIGHT STABILISERS IN PLASTICS BY HIGH-PERFORMANCE LIQUID CHROMATOGRAPHY

P. PERLSTEIN

Organic Materials Division, National Building Research Institute, CSIR, P.O. Box 395, Pretoria 0001 (Republic of South Africa)

(Received 2nd November 1982)

SUMMARY

High-performance liquid chromatography is used to determine light stabilisers in plastic materials. Most of the light stabilisers in commercial use can be separated on a reversed-phase column. Stabilisers which elute together on this column are successfully separated on a silica column. For quantitative analysis of PVC and its blends, different extraction methods were compared for the light stabilisers. The best results were obtained by using Soxhlet extraction of finely milled material.

Most plastic materials intended for outdoor use contain one or more light stabilisers for protection against photo-degradation. Thin-layer chromatography has been used to separate light stabilisers, but quantitative analysis was not attempted [1]. Gas chromatography was used with greater success in the separation and measurement of the benzophenone and benzotriazole types of light stabiliser [2]. A disadvantage of this method is the very high column temperature (270°C) which is required. More recently, light stabilisers of the benzophenone and benzotriazole type have been determined by acetylation and high-performance liquid chromatography (h.p.l.c.) on a silica column [3]. However, acetylation is possible only if an active hydrogen atom is present in the molecule, and some of the important light stabilisers, such as the cyanacrylates, do not contain these.

Research into the long-term resistance of different plastics to sunlight is currently conducted in this Institute. A method was required for the rapid identification and determination of the widest possible range of light stabilisers before or after exposure. Most commonly used light stabilisers could be separated and identified by means of h.p.l.c. on a reversed-phase column. Certain stabilisers which eluted together on this column could be separated on a normal-phase silica column.

EXPERIMENTAL

Materials and instrumentation

The light stabilisers were commercially available materials of the following types: Cyasorb (Cyanamid), Tinuvin (Ciba-Geigy), and Uvinul (General Aniline & Film Corporation). Other materials used were methyl and phenyl salicylates (BDH), 2,4-dihydroxybenzophenone and resorcinol monobenzoate (Eastman Kodak), and tetrahydrofuran (THF; u.v.-grade; Waters Associates, Milford, MA). Diethyl ether, chloroform (stabilised with ethanol) and n-hexane were of analytical-reagent grade.

The Waters liquid chromatograph used was equipped with two pumps (a model 6000A and a model M-45), a model 720 system controller with gradient-programming capability, a model 450 variable-wavelength detector, a model U6K injector and a plotter-printer-integrator data module. The reversed-phase column was μ Bondapak- C_{18} (Waters, 7.8 mm i.d., 30 cm long). The silica column was μ Porasil (Waters, 7.8 mm i.d., 30 cm long, 10- μ m particle size).

Procedures

Sample preparation. The polyvinyl chloride (PVC) and the PVC-vinyl chloride/vinyl acetate copolymer blend were both formulated with one light stabiliser on normal compounding equipment. In certain experiments, a second light stabiliser was added as follows: 6 g of the polymer and 15–20 mg of the light stabiliser were dissolved in 100 ml of THF (the pigment remained in suspension) and then reprecipitated by being poured into 1 l of water (light stabilisers are insoluble in water). After filtration and drying overnight in a vacuum oven at 60°C, the plastic material was ground to particles less than 0.5 mm in diameter in a Wiley mill (Arthur Thomas Co.).

Soxhlet extraction. The material (1 g), in the form of a film, or unground or finely ground particles, was extracted in a Soxhlet apparatus with diethyl ether for 16 h. The ether was evaporated, the precipitate was redissolved in 10 ml of THF, the solution was filtered for column protection through a Millipore teflon filter (0.5- μ m pore size), and 10 μ l of this solution was injected into the reversed-phase column.

Solution/precipitation method. The plastic (1 g) was dissolved in 20 ml of THF and precipitated by pouring the solution into 300 ml of well stirred n-hexane. The polymer was filtered off and discarded, and the hexane was evaporated. The precipitate was redissolved in 10 ml of THF and 10 μ l of this solution was injected into the reversed-phase column.

RESULTS AND DISCUSSION

The separation of light stabilisers

The h.p.l.c. conditions are listed in Table 1. The results of the isocratic separation of light stabilisers on the reversed-phase C_{18} column and on the normal-phase silica column are given in Table 2.

TABLE 1

Conditions for h.p.l.c.

Eluent No.	Eluent	Composition (by volume)	Flow rate (ml min ⁻¹)	Column	U.v.-detector λ (nm)
1	THF + water	60 + 40	1	μ Bondapak C ₁₈	225
2	n-hexane + chloroform	90 + 10	1.5	μ Porasil	254
3	Chloroform	100	3.5	μ Porasil	254

Figure 1 shows the h.p.l.c. of a mixture of all the light stabilisers mentioned in Table 2; a gradient programme was used in which both the eluent composition and the flow rate were changed. For the first 15 min, the flow rate was kept at 0.8 ml min⁻¹ and the eluent composition was THF/water in the volume ratio 55:45. The ratio was then changed to 65:35 and the flow rate to 1.2 ml min⁻¹ during 9 min, by using the steepest concave curve available on the programmer (curve no. 2). In this way, most light stabilisers could be separated. Two groups of stabilisers still eluted together: the two benzophenones, Uvinul 400 and Cyasorb UV-24, with resorcinol monobenzoate at 4.5 min, and Tinuvin 320 with Cyasorb 531 and the nickel chelate Cyasorb 1084 at 14 min.

As shown in Fig. 2, on a silica column with n-hexane/chloroform (90 + 10) as eluent, one of the groups eluting together on the reversed-phase column, namely that containing Cyasorb UV-1084, Tinuvin 320 and Cyasorb UV-531 (peak 7), separated well, the first two exhibiting particularly sharp peaks. The benzophenones, Uvinul-400 and Cyasorb UV-24, were strongly retained on the silica column because of the presence of two hydroxyl groups in their molecules; the retention times were extremely long with the above solvents. This also applied to resorcinol monobenzoate. When the solvent strength was increased to n-hexane/chloroform (50 + 50), the resorcinol monobenzoate appeared as a very sharp peak at a retention volume of 11 ml. The two benzophenones also appeared, but showed very strong tailing. When only chloroform was used at a flow rate of 3.5 ml min⁻¹, the tailing of these benzophenones was substantially reduced. They were well separated, and resorcinol monobenzoate showed no tailing at all (Fig. 3). Under these conditions, all the other light stabilisers eluted together, at the solvent front, with a retention volume of 3.3 ml.

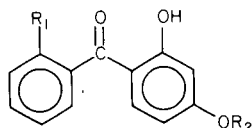
Determination of light stabilisers in PVC and PVC blends

In order to attempt the quantitative h.p.l.c. of light stabilisers by extraction from a plastic material, PVC or PVC blended with a vinyl chloride/vinyl acetate copolymer was prepared in admixture with one or more light stabilisers. In practice, these stabilisers are often used together because of their synergic effects. A typical formulation is shown in Table 3. In a number of experiments, a second light stabiliser, either Uvinul N-539 or Cyasorb UV-9, was solvent-blended into the formulation.

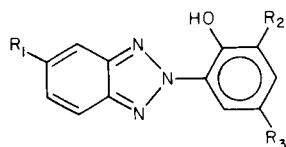
TABLE 2

Retention times (t_R) of light stabilisers^a

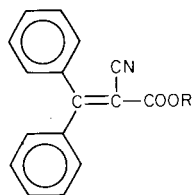
Light stabiliser	Trade name	Reversed-phase column	Silica column	
		t_R (min)	t_R (min)	Eluent No.

Benzophenones

$R_1 = H$	$R_2 = H$	Uvinul-400	4.5	1.9	3
$R_1 = OH$	$R_2 = CH_3$	Cyasorb UV-24	4.6	1.1	3
$R_1 = H$	$R_2 = CH_3$	Cyasorb UV-9	5.5	4.7	2
$R_1 = H$	$R_2 = C_8H_{17}$	Cyasorb UV-531	14.1	3.2	2
$R_1 = H$	$R_2 = C_{10}H_{21}$	Uvinul M-410	18.8	3.2	2

Benzotriazoles

$R_1 = H$	$R_2 = H$	$R_3 = CH_3$	Tinuvin P	6.6	2.7	2
$R_1 = H$	$R_2 = t\text{-butyl}$	$R_3 = t\text{-butyl}$	Tinuvin 320	14.2	2.3	2
$R_1 = Cl$	$R_2 = t\text{-butyl}$	$R_3 = CH_3$	Tinuvin 326	15.4	2.3	2
$R_1 = Cl$	$R_2 = t\text{-butyl}$	$R_3 = t\text{-butyl}$	Tinuvin 327	20.1	2.3	2

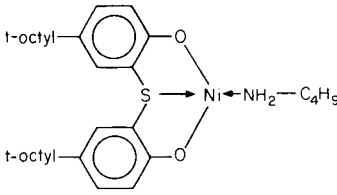
Cyanacrylates

$R = C_2H_5$	Uvinul N35	5.4	8.8	2
$R = CH_2-\underset{\substack{ \\ C_2H_5}}{CH}-C_4H_9$	Uvinul N539	10.4	4.9	2

Salicylates

Methyl salicylate	Sunkem MS	4.9	2.85	2
Phenyl salicylate	Salol (Bayer)	6.3	2.85	2
Resorcinol monobenzoate	Eastman RMB	4.5	1.6	3

TABLE 2 (continued)

Light stabiliser	Trade name	Reversed-phase column	Silica column	
		t_R (min)	t_R (min)	Eluent No.
	Cyasorb UV-1084	13.8	2.0	2

^aRefer to Table 1 for h.p.l.c. conditions. The C₁₈ column was always used with eluent No. 1.

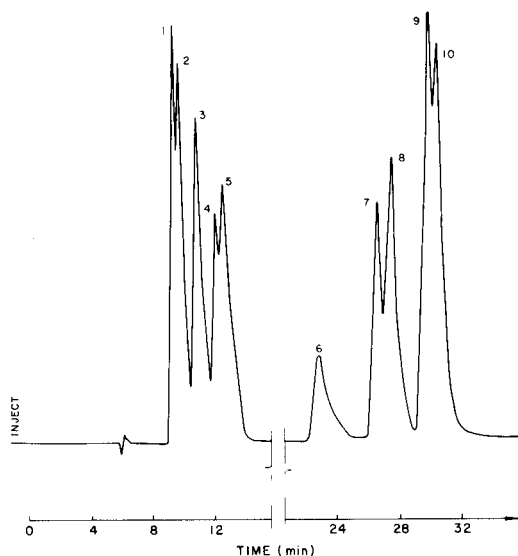


Fig. 1. Separation by h.p.l.c. with gradient elution of light stabilisers on a μ Bondapak C₁₈ column. Peaks: (1) Uvinul-400, Cyasorb UV-24, resorcinol monobenzoate; (2) methyl salicylate; (3) Uvinul N-35, Cyasorb UV-9; (4) phenyl salicylate; (5) Tinuvin P; (6) Uvinul N-539; (7) Tinuvin 320, Cyasorb 1084, Cyasorb 531; (8) Tinuvin 326; (9) Uvinul M-410; (10) Tinuvin 327. Detection at 225 nm; for gradient conditions, see text.

Two methods were used for the extraction of the light stabilisers from the formulations, namely extraction with diethyl ether in a Soxhlet apparatus, and dissolution in THF followed by reprecipitation. The influences of the extraction method and the physical form of the PVC blend on the yield are summarised in Table 4. The results given are averages of at least

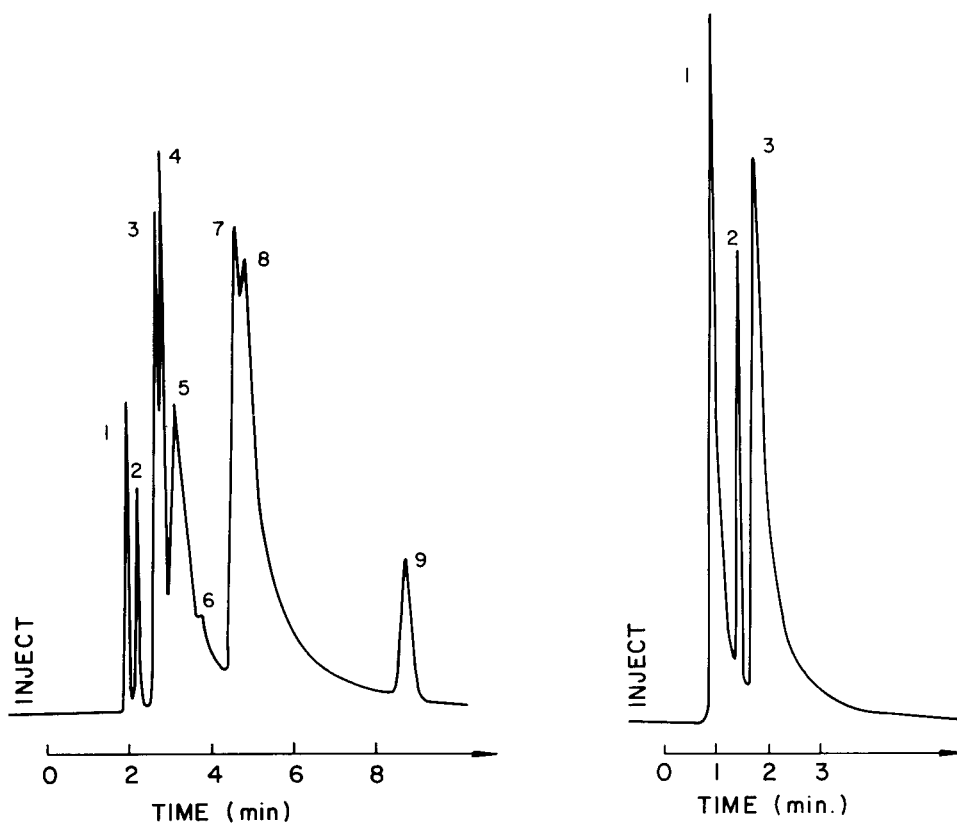


Fig. 2. Separation of light stabilisers on a μ Porasil column. Peaks: (1) Cyasorb 1084; (2) Tinuvin 320, 326, 327; (3) Tinuvin P; (4) methyl and phenyl salicylates; (5) Cyasorb UV 531, Uvinul M-410; (6) impurity in Uvinul M-410; (7) Cyasorb UV-9; (8) Uvinul N-539; (9) Uvinul N-35. Mobile phase, *n*-hexane/chloroform (90 + 10); detection at 254 nm, 0.4 a.f.s.; injected sample volume 5 μ l; 0.2% solution in chloroform; flow rate 1.5 ml min⁻¹.

Fig. 3. Separation of light stabilisers on a μ Porasil column with chloroform (containing 0.6% ethanol) as eluent. Peaks: (1) Cyasorb UV-24; (2) resorcinol monobenzoate; (3) Uvinul-400. Detection at 254 nm, 1.0 a.f.s.; injected sample volume 4 μ l, 1% solution in chloroform; flow rate 3.5 ml min⁻¹.

TABLE 3

Composition of a typical blend

Component	Parts by mass	Component	Parts by mass
PVC	43.3	Epoxidised soya bean oil	2
Vinyl chloride—vinyl acetate copolymer	43.3	Titanium dioxide	5
Cadmium, barium stabiliser	2	Acrylic impact modifier	1
Dibasic lead phosphate	3	Wax	0.2
		Tinuvin 320	0.2

TABLE 4

Recovery of light stabiliser from PVC blends by different extraction methods

Method	Physical form of PVC blend	Recovery (%)		
		Tinuvin 320	Cyasorb UV-9	Uvinul N-539
Solution/precipitation	—	88	81	99
Diethyl ether (Soxhlet)	film ^a	86	78	89
Diethyl ether (Soxhlet)	unground ^b	65	59	92
Diethyl ether (Soxhlet)	ground particles ^c	94	97	95

^aThickness 150 μ m. ^bDiameter 2–10 mm. ^cDiameter <0.5 mm.

five determinations. Good recoveries were obtained for all three types of stabiliser only when the material was finely ground. For the last extraction, in order to obtain the recoveries shown in the table, a period of 30 min was sufficient; further extraction did not alter the results.

The author expresses his thanks to Dr. H. M. Saayman for helpful discussions and to Messrs. A. Jurriaanse and B. Zahradnik for kindly providing the samples.

REFERENCES

- 1 D. Simpson and B. R. Currell, *Analyst*, 96 (1971) 515.
- 2 J. Horaček, *Plasty Kauč.*, 13 (1976) 274.
- 3 D. K. C. Hodgeman, *J. Chromatogr.*, 214 (1981) 237.

A LIQUID CHROMATOGRAPHIC METHOD FOR CHLORAMPHENICOL AND ITS NITRO DEGRADATION PRODUCTS WITH REDUCTIVE AMPEROMETRIC DETECTION AT A MERCURY ELECTRODE

J. J. VAN DER LEE*^a, H. B. J. VAN DER LEE-RIJSBERGEN, U. R. TJADEN and W. P. VAN BENNEKOM

Department of Pharmaceutical Analysis and Analytical Chemistry, Subfaculty of Pharmacy, State University, Gorlaeus Laboratories, P.O. Box 9502, 2300 RA Leiden (The Netherlands)

(Received 9th July 1982)

SUMMARY

A liquid chromatographic system for the separation of chloramphenicol and some of its nitro degradation products is described. The substances were detected electrochemically at a mercury drop electrode. Continuous effort was needed to obtain and maintain the necessary low oxygen level in the eluent and the samples. Under the optimized conditions, with a hanging mercury drop electrode and d.c. amperometry at -0.5 V vs. Ag/AgCl (saturated KCl), the detection limit was 1 ng of chloramphenicol, the sensitivity was 0.3 nA ng⁻¹ and the linear dynamic range was 2 ng to 20 µg of chloramphenicol. Application to extracts of bovine blood is reported.

The polarographic determination of chloramphenicol at low concentrations has been described [1]. This method also proved to be suitable for the determination of metabolites and other degradation products of chloramphenicol, provided that these substances still possessed the nitro group. However, direct polarographic analysis of a mixture of chloramphenicol and its nitro degradation products is not possible without prior separation, because all these substances have approximately the same half-wave potential. Therefore, a combination of the low detection limit of polarography with the high selectivity of high-performance liquid chromatography (h.p.l.c.) appeared attractive.

In the present study, a commercially available polarographic detector was used to detect and quantify chloramphenicol and some of its nitro degradation products after a liquid chromatographic separation. This detector has already been used by several investigators [2–5].

^aPresent address: Department of Soil Science and Plant Nutrition, Agricultural University, De Dreijen 3, 6703 BC Wageningen, The Netherlands.

EXPERIMENTAL

Reagents and standard solutions

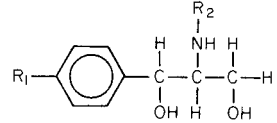
All reagents were of analytical grade and were used as received. Demineralized water was further purified by leading it through a Millipore Milli-Q Water Purification System. Measurements were done on solutions of (mixtures of) chloramphenicol (CAP), CAP-alcohol, desacetyl-CAP (see Table 1), *p*-nitrobenzoic acid and *p*-nitrobenzaldehyde. All substances were purchased commercially, except for CAP-alcohol which was kindly donated by Dr. M. L. Black (Warner-Lambert Company, Ann Arbor, MI). For each substance, 3×10^{-4} M stock solutions in purified water were prepared every two months and kept at room temperature ($18 \pm 2^\circ\text{C}$) in the dark. From these solutions, the required mixtures were made by appropriate dilution with the eluent used.

Conditions for h.p.l.c.

The system used is outlined in Fig. 1. The liquid chromatograph was constructed from commercially available and custom-made parts. It consisted of a glass eluent reservoir, a reciprocating plunger-membrane pump (DMP 1515, Orlita, Giessen, G.F.R.), a flow-through Bourdon-type manometer acting as damping device, a 20- μl sample injection valve (Model 70-10, Rheodyne) and a stainless steel column (2.8 mm i.d., 6.35 mm o.d., 100 mm long). For detection, either a polarographic detector (E.G. and G. Princeton Applied Research Corp., model 310) or a multi-wavelength u.v. detector (LC-3-UV, Pye-Unicam) operating at 280 nm, was used. Columns were packed by a pressurized slurry technique with an air amplifier booster, as described elsewhere [6]. The first stationary phase examined was LiChrosorb RP-8 (5 μm ; Merck); later, the packing used was (methyloctylsilica)-Hypersil C-8 (5 μm , spherical; Merck), henceforth referred to as Hypersil. The mobile

TABLE 1

Chloramphenicol and some metabolites and degradation products

	R ₁	R ₂
Substance, Chemical Abstracts name and Chemical Abstracts registry number	R ₁	R ₂
Chloramphenicol	NO ₂	COCHCl ₂
"Hydroxyamphenicol" (CAP-alcohol), [R-(R*, R*)]-N-[β -hydroxy- α -(hydroxymethyl)- <i>p</i> -nitrophenethyl]glycolamide, [23885-72-5]	NO ₂	COCH ₂ OH
"Nitroaminopropanediol" (desacetyl-CAP), [R-(R*, R*)]-2-amino-1-(4-nitrophenyl)-1,3-propanediol, [716-61-0]	NO ₂	H

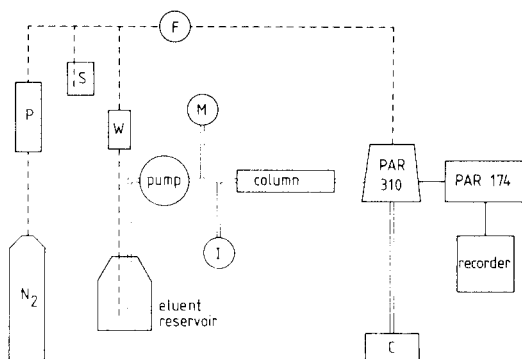


Fig. 1. Block diagram of the h.p.l.c.-PAR-310 system: P, pyrogallol nitrogen purifying device; S, sample being out-gassed just prior to injection; W, wash bottle filled with methanol; F, nitrogen flow meter; M, manometer; I, injection loop; C, waste collector.

phases were mixtures of methanol and solutions of sodium 1-pentane-sulphonate (5×10^{-4} M) and perchloric acid (0.01 M) in water.

Electrochemical detection

The PAR-310 detector consists of a mercury drop electrode assembly in a flow-through cell fitted with an Ag/AgCl reference electrode, a platinum auxiliary electrode and a nitrogen inlet. A delivery tip directs the column upwards toward the mercury drop. The PAR-310 was installed and interfaced to a PAR Model 174 Polarographic Analyzer as recommended by the manufacturer.

Measurements were done on standard mixtures of chloramphenicol and some of its nitro degradation products at room temperature by several potentiostatic techniques. Mercury drop sizes were "large", "medium" or "small", using either the hanging mercury drop electrode (HMDE) or the static mercury drop electrode (SMDE) mode, along with an Ag/AgCl reference electrode in saturated potassium chloride solution and an auxiliary platinum electrode.

Continuous vigilance was required to obtain and maintain the necessary low oxygen level in the eluent. The eluent was vacuum-degassed directly after preparation and was purged day and night thoroughly with pre-purified nitrogen. The nitrogen used was passed through an oxygen-scavenging system containing 7% pyrogallol in aqueous 14 M potassium hydroxide, and subsequently through a gas-washing bottle filled with methanol. Chromatograms were recorded on a strip-chart recorder (BD 8; Kipp & Zonen, Delft, The Netherlands).

Recommended conditions for use. The best stationary phase was found to be MOS-Hypersil C-8 ($5 \mu\text{m}$) with a mobile phase of $(85 + 15)$ 0.01 M perchloric acid-methanol, made 5×10^{-4} M in sodium 1-pentanesulphonate, at a flow rate of 2.2 ml min^{-1} . The PAR-310 was best used in the d.c. mode (low pass filter 3 s) with the HMDE ("large" drop size) held at -500 mV vs. Ag/AgCl (sat. KCl).

RESULTS AND DISCUSSION

Optimization of h.p.l.c. conditions

The combination of LiChrosorb RP-8 ($5\ \mu\text{m}$) as the stationary phase with methanol -10^{-2} M perchloric acid (20 + 80) as the mobile phase and u.v. detection had proved to be suitable for the determination of chloramphenicol after extraction from biological material [7]. For the studies with the PAR-310, the same phase system was applied but with another batch of LiChrosorb. It then appeared that the peak resolution was no longer adequate; in particular, the signals of CAP-alcohol and desacetyl-CAP coincided and overlapped with the preceding oxygen peak (Table 2, line 1). No reasonable explanation is apparent for this change in behaviour. The phase system had therefore to be re-optimized for the separation of oxygen, CAP-alcohol and desacetyl-CAP, while the already sufficient separation of *p*-nitrobenzaldehyde, CAP and *p*-nitrobenzoic acid was to be maintained.

The first step in optimization was to lower the methanol content of the eluent; the oxygen peak was then separated but the CAP-alcohol and desacetyl-CAP peaks still virtually coincided (Table 2, line 2). Moreover, the capacity ratio (*k*) of *p*-nitrobenzoic acid increased to >100 . The LiChrosorb stationary phase was then replaced by Hypersil. The separation between CAP-alcohol and desacetyl-CAP was then improved, although their capacity ratios had diminished to values near that of oxygen (Table 2, line 3). Therefore, Hypersil was adopted as the stationary phase in order to optimize the composition of the mobile phase. A u.v. detector was used in these tests.

Of the five compounds concerned, CAP-alcohol and desacetyl-CAP have a distinct polar character, as indicated by their low capacity ratios in a reversed-phase system. The other three components are less polar, and have satisfactory *k* values. Thus, the mobile phase can be optimized by means of ion-pair formation to improve the selective retention of the more polar components. The compounds in question possess an aliphatic amino group which is protonated in acidic medium, so that an ion-pair can be formed, e.g., with an

TABLE 2

Optimization of the phase system with respect to oxygen, CAP-alcohol and desacetyl-CAP

Detector	Stationary phase	Mobile phase		Capacity ratio <i>k</i>		
		Methanol + HClO ₄	Counter-ion	O ₂	CAP-alcohol	Desacetyl-CAP
PAR 310	LiChrosorb	20 + 80	—	1.2	1.8	1.8
PAR 310	LiChrosorb	15 + 85	—	1.3	2.6	2.4
PAR 310	Hypersil	15 + 85	—	1.3	1.8	1.5
U.v.	Hypersil	15 + 85	SDS, 10^{-3} M	n.d. ^a	0.9	$\gg 100$
U.v.	Hypersil	15 + 85	SPS, 10^{-3} M	n.d.	1.9	>100
PAR 310	Hypersil	15 + 85	SPS, 5×10^{-4} M	1.3	2.6	4.5

^aNot detected.

alkylsulphonate as counter-ion. Because the polarity of the ion-pair is lower than that of the parent compound, the ion-pair will be retained more in a reversed-phase system.

In order to investigate this effect, sodium dodecylsulphate (SDS) was added to the mobile phase to give a concentration of 1×10^{-3} M. With this eluent, CAP-alcohol and the three less polar components were retained slightly less, but the retention time for desacetyl-CAP was > 2 h (Table 2, line 4); the desired effect was therefore too strong, possibly because of the long aliphatic chain of SDS and the relatively high concentration of SDS in the mobile phase. Therefore, the system was cleaned out with 2 l of purified water, and sodium 1-pentanesulphonate (SPS) was added to the (15 + 85) eluent to give a concentration of 1×10^{-3} M. Under these conditions, desacetyl-CAP was retained for 88 min, whereas CAP-alcohol was retained slightly more (Table 2, line 5).

A satisfactory separation of the three compounds was finally obtained by halving the SPS concentration to 5×10^{-4} M (Table 2, line 6). The time for chromatography was 14 min at a flow rate of 1.16 ml min^{-1} ; this time could be halved by increasing the flow rate while the resolution R_{ji} was maintained at values suitable for quantitative work (Table 3). The separating power of the system, especially at lower flow rates, was large enough to separate oxygen from CAP-alcohol, and separation of the five compounds under test was good (Fig. 2).

Under these optimum conditions, the chromatographic system functioned satisfactorily for several months and many separations were done, both with u.v. and polarographic detection [9]. With another column and a new batch of Hypersil, however, the results could not be reproduced immediately.

TABLE 3

Composition of test mixtures and conditions of test measurements (Hypersil column; (15 + 85) methanol- 10^{-2} M HClO_4 , 5×10^{-4} M in SPS as eluent; HMDE, drop size "large"; d.c. amperometry at an applied potential of -500 mV vs. Ag/AgCl)

Compound	Test mixture 1 ^a				Test mixture 2 ^b				<i>R</i> _{ji}
	Concentration		Amount injected (ng)	<i>t</i> _R (min)	Concentration		Amount injected (ng)	<i>t</i> _R (min)	
	10 ⁻⁵ M	ppm			10 ⁻⁵ M	ppm			
CAP-alcohol	1.5	4	80	1.6	3.0	8	160	0.7	—
Desacetyl-CAP	2.4	5	100	2.5	4.8	10	200	1.1	20
<i>p</i> -Nitrobenzaldehyde	5.0	7.5	150	5.8	13	20	400	2.5	7.2
CAP	4.6	15	300	9.0	9.2	30	600	3.8	3.4
<i>p</i> -Nitrobenzoic acid	9.0	15	300	11.6	18	30	600	4.8	4.5

^aFlow rate 1.16 ml min^{-1} . ^bFlow rate 2.73 ml min^{-1} .

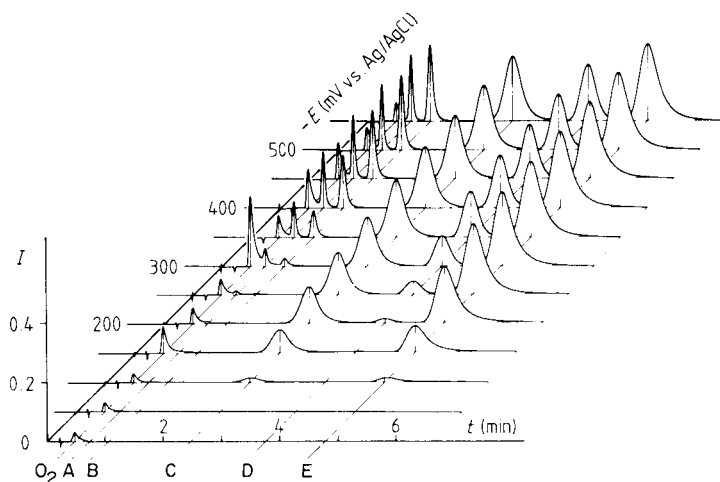


Fig. 2. Chromatograms of test mixture 2 under the optimum conditions, recorded at different potentials. Flow rate 2.73 ml min^{-1} ; PAR-310. Peaks: A, CAP-alcohol; B, desacetyl-CAP; C, *p*-nitrobenzaldehyde; D, CAP; E, *p*-nitrobenzoic acid.

Although selective retention was obtained with SPS, it appeared that the system was not stable. The desired stability was obtained by loading the stationary phase with SDS after packing the column and then using the eluent containing SPS [8].

The polarographic detection system

Oxygen removal. Before the PAR-310 polarographic detector could be used and evaluated, the oxygen problem had to be controlled. The removal of dissolved oxygen to the desired trace level, and the maintenance of that level, required rigorous measures. Because of the low pH of the eluent, the method of sulphite addition could not be applied and outgassing with nitrogen was necessary. The following measures were found essential in obtaining the desired low oxygen level. The eluent in the reservoir was purged day and night with a constant flow (200 ml min^{-1}) of nitrogen, which had been deoxygenated by bubbling through alkaline pyrogallol solution and pre-saturated with methanol to avoid preferential evaporation of methanol from the eluent. (Later work showed that better scavenging of oxygen was obtained with an all-glass purification tube filled with finely divided copper (BTS-catalyst, BASF, Ludwigshafen, G.F.R.); a low but noticeable background from oxygen was observed even under the best conditions.) Further, samples were deoxygenated just prior to injection, via a side-line of the main nitrogen supply (Fig. 1). Stainless steel tubing and connections were used where possible; at places where flexibility was required, teflon tubing was used, jacketed by a second teflon tubing with nitrogen pumped through the spacing.

Measurements on chloramphenicol and nitro degradation products.

Measurements were done with test mixtures of chloramphenicol and nitro degradation products under the optimum separating conditions. In order to find the optimum potential for maximum response, a series of chromatograms were run with increasingly negative potential of the mercury electrode (Fig. 2). In these experiments, the HMDE mode was used with a 'large' drop size and d.c. amperometry. The results indicated that an applied potential of -500 mV (vs. Ag/AgCl) was required for maximum response of a mixture of the five compounds (Fig. 3). The $E_{1/2}$ values of the five compounds can be determined from the voltammograms in Fig. 3. The half-wave potentials in the eluent used differ from those determined polarographically in acetate buffer pH 4.7 [1], even after correction for the different reference electrodes and the different pH; the deviation might be due to the presence of SPS. The current-potential curve for *p*-nitrobenzaldehyde shows two points of inflection, which may be ascribed to reduction of the nitro and aldehyde groups.

Analytical evaluation. Blood extracts of cows treated with chloramphenicol can be determined polarographically [9]. The applicability of the present h.p.l.c.-PAR-310 combination to extracts from biological material was examined by injections of some of these blood extracts. Figure 4 indicates that the present system is well suited for the examination of such extracts.

Comparison of the HMDE and SMDE. Although usage of the SMDE is assumed in h.p.l.c. detection, operation of the PAR-310 in the HMDE mode was more practical. Measurements with the HMDE provided less noise and slightly greater sensitivity compared to the SMDE; moreover, smooth peaks were obtained instead of stepped ones. A chromatographic run could be completed on a single drop without noticeable baseline offset; electrode ageing effects were also not observed. This may be ascribed to the low concentrations of electroactive compounds and to the absence of adsorption effects in the solutions used. The HMDE offers the advantages of both mercury and solid electrodes.

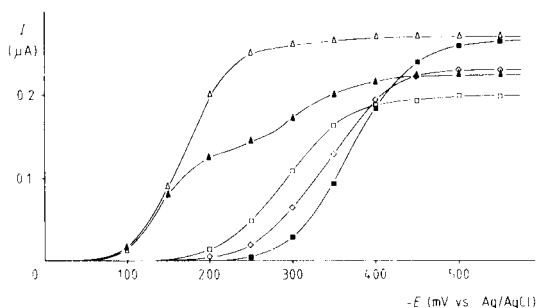


Fig. 3. Current-potential relationships for CAP and four nitro degradation products, taken from Fig. 2: (Δ) *p*-nitrobenzoic acid; (\blacktriangle) *p*-nitrobenzaldehyde; (\square) CAP; (\diamond) CAP-alcohol; (\blacksquare) desacetyl-CAP.

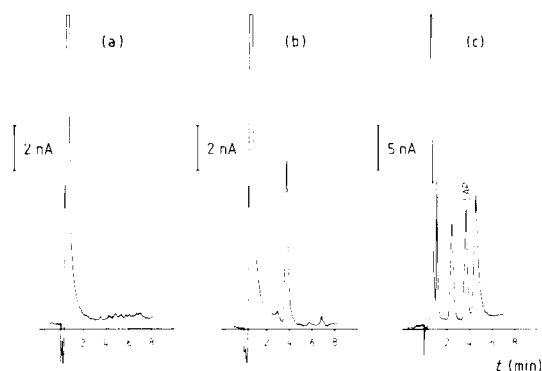


Fig. 4. Chromatograms of an extract of blood from a dairy cow treated intramammarily with CAP: (a) before treatment; (b) 5.25 h after administration of a single dose of CAP (9.4 mg kg^{-1} body weight giving a calculated blood concentration $1.84 \mu\text{g ml}^{-1}$); (c) test mixture 1, diluted 10 times, not extracted. All three chromatograms were recorded under optimum conditions, flow rate 2.73 ml min^{-1} , PAR-310 detector.

Sensitivity and detection limit by different voltammetric techniques. Measurements were done on test mixture 1 with the HMDE at various drop sizes by the different modes available on the PAR-174 analyzer. From the results, the sensitivity and detection limits for chloramphenicol were calculated (Table 4). For d.c. and sampled d.c. amperometry, the potential was fixed at -500 mV ; for normal pulse amperometry the initial potential was -100 mV and the final potential -500 mV ; for the differential pulse mode, the potential window was -300 to -400 mV (all vs. Ag/AgCl). The cycle period was set at 0.5 s , except for the d.c. mode; a baseline offset was applied when necessary by means of the "output offset". Measurements were done at time constants (low pass filter) of 0 , 0.3 , 1 and 3 s . For a 3-s time constant, sensitivities were 20% lower than for a zero time constant, but the noise level was 15-fold lower. The detection limit was calculated by taking 3 times the recorded peak-to-peak noise and dividing by the sensitivity. All values of Table 4 were measured twice, except for the sensitivity in d.c. amperometry,

TABLE 4

Sensitivity and detection limits for chloramphenicol measured with the PAR-310 detector under optimum conditions and the PAR-174 analyzer in different modes^a

	HMDE ^b				SMDE	
	D.c.	S.d.c.	N.p.	D.p.	S.d.c.	N.p.
Sensitivity (nA ng^{-1})	0.29	0.25	0.65	0.25	0.55	0.85
Noise (nA)	0.07	0.7	0.3	1.2	2.5	0.7
Detection limit (ng)	0.7	8	1	15	15	2.5

^aThe modes used were d.c., sampled d.c., normal pulse and differential pulse amperometry.

^b"Large" drop.

which is the average value of 13 measurements and has a standard deviation of 0.03. Detection limits were not calculated to more than one decimal place because the noise was so low that measuring errors were large.

Table 4 shows, as expected, that the d.c. and sampled d.c. modes have the same sensitivity; with the differential pulse mode, the numerical value was similar, but the true sensitivity is 10 times less because the internal gain of the PAR Model 174 is ten times greater in the d.p. mode than in the other modes. The sensitivity is only slightly enhanced in the normal pulse mode. The noise level is by far the lowest in the d.c. mode, which results in the lowest limit of detection. When the SMDE was used, the noise level was always larger than with the HMDE. With all three drop sizes, equal signal-to-noise ratios were obtained.

The calculated detection limit for chloramphenicol by d.c. amperometry was verified experimentally by spiking: injection of 20 μ l of a 1.0×10^{-7} M solution (0.67 ng of chloramphenicol) gave a signal of 0.2 nA, which was just 3 times the noise level. This value is similar to that calculated for u.v. detection.

Repeatability. The repeatability was checked by doing 5 successive d.c. measurements on a 3×10^{-5} M chloramphenicol solution with the same mercury drop; the average signal height was 111.3 (± 0.3) mm (s.d.). Under the same conditions, five similar measurements on five successive drops gave an average signal of 111.5 (± 0.1) mm. Both results may be judged as very good; the standard deviation for the successive drops is surprisingly good.

Linear dynamic range. A series of nine chloramphenicol solutions in water was prepared, ranging from 3×10^{-3} M (1 mg ml $^{-1}$) to 3×10^{-7} M (0.1 μ g ml $^{-1}$), corresponding to amounts injected of 20 μ g to 2 ng; every solution was made from the preceding one by (1 + 2) dilution. Measurements were done under the optimum conditions (see Experimental). The log-log plot of the results had a slope of 1.002, which does not deviate significantly from 1 at the 0.05 probability level; the correlation coefficient was 0.9999 and the relative standard deviation was better than 2%. Threefold dilution of the lowest standard to 1×10^{-7} M (33 ng ml $^{-1}$, or 0.67 ng injected) resulted in a significant upward deviation from linearity; the upper limit is set by the solubility (2.5 mg ml $^{-1}$). Thus the linear dynamic range covers four decades, viz., 3×10^{-7} M to 3×10^{-3} M (2 ng to 20 μ g).

Conclusions

The PAR Model 310 Detector is suitable for the detection of chloramphenicol and its nitro degradation products, either directly or after extraction from biological material. For h.p.l.c. detection, the HMDE offers better results than the SMDE with respect to detection limit, sensitivity, noise and smoothness of peaks. Under optimum conditions, the detection limit for chloramphenicol is similar to that obtained with u.v. detection. Of the different modes available, differential pulse amperometry offers no advantage over d.c. amperometry in the flow system used. For trace level determinations in acidic media, the main drawback of the PAR-310 is its sensitivity to oxygen.

REFERENCES

- 1 J. J. van der Lee, W. P. van Bennekom and H. J. de Jong, *Anal. Chim. Acta*, 117 (1980) 171.
- 2 M. R. Hackman and M. A. Brooks, *J. Chromatogr. (Biomed. Appl.)*, 222 (1981) 179.
- 3 R. Samuelsson and J. Osteryoung, *Anal. Chim. Acta*, 123 (1981) 97.
- 4 H. B. Hanekamp, W. H. Voogt, P. Bos and R. W. Frei, *Anal. Chim. Acta*, 118 (1980) 81.
- 5 B. Persson and L. Rosén, *Anal. Chim. Acta*, 123 (1981) 115.
- 6 U. R. Tjaden, M. Th. H. A. Meeles, C. P. Thys and M. van der Kaay, *J. Chromatogr. (Biomed. Appl.)*, 181 (1980) 227.
- 7 J. J. van der Lee, Thesis, Leiden (1981).
- 8 M. van der Kaay and U. R. Tjaden, *J. Chromatogr.*, in press.
- 9 J. J. van der Lee, J. F. M. Nouws and F. W. R. Bloemendal, *J. Vet. Pharmacol. Ther.*, 5 (1982) 161.

A DITHIZONE POST-COLUMN DETECTOR FOR THE HIGH-PERFORMANCE LIQUID CHROMATOGRAPHIC DETERMINATION OF TRACE METALS

P. JONES, P. J. HOBBS and L. EBDON*

Department of Environmental Sciences, Plymouth Polytechnic, Drake Circus, Plymouth, Devon PL4 8AA (Great Britain)

(Received 4th November 1982)

SUMMARY

A multi-element post-column high-performance liquid chromatographic detector based on dithizone as a complex-forming reagent is described. The separation was achieved in aqueous media on a sulphonated 10% cross-linked polystyrene resin. Cadmium(II), cobalt(II), copper(II), lead(II), nickel(II) and zinc(II) ions were detected down to nanogram levels. Working ranges up to the microgram level were possible. The use of this heavy metal detector which may be tuned by pH control is discussed. An advantage of the system for multi-element determinations is that the decrease in the dithizone absorbance at 590 nm is measured rather than increased absorbances at different wavelengths particular to each metal dithizonate.

Considerable attention has been directed in recent years towards the detection and determination of trace metals. Perhaps the most popular technique for quantifying trace metals is atomic absorption spectrometry. Yet, when several elements have to be determined separately in many samples, essentially single-element techniques such as atomic absorption spectrometry may become very time-consuming and may use excessive sample. Rapid multi-element techniques for quantifying trace metals have become of increasing interest, but several of these multi-element approaches, e.g., inductively-coupled plasma emission spectrometry, are very capital-intensive. The multi-element technique discussed in this paper requires only equipment now available in many laboratories, i.e., high-performance liquid chromatography (h.p.l.c.).

The aim of this study was to separate trace metals by h.p.l.c. followed by sequential spectrophotometric detection at a single wavelength by using a simple post-column reactor system. Such an investigation is timely because of the availability of novel separation materials, particularly small particle size resins. Many previous h.p.l.c. separations of trace metals have involved the formation of metal complexes prior to injection onto the column. This may prevent some species from being eluted and normally involves using quantities of organic solvents. Liska et al. [1] separated nine metals as their

diethyldithiocarbamates, using LiChrosorb Si-60 (10 μm) and 10% chloroform in cyclohexane as the eluent. Similarly, strong complexing reagents such as dithizone [2] and 8-mercaptoquinoline [3] have been used with pre-column preparation. Further examples of this approach have been discussed in a comprehensive review by Schwedt [4] of inorganic trace analysis by chromatography. Many environmental samples are dynamic in nature and injection without sample pretreatment has obvious advantages.

Takata and Muto [5] separated six metals on a cation-exchange resin column with tartaric acid as the eluting agent. The effluent was passed through a coulometric detector with the addition of electrolytes to stabilize the detector signal. While few laboratories have access to coulometric detectors, most h.p.l.c. systems incorporate a spectrophotometric detector. Thus the systems employing separation and then reaction with a colour-forming reagent perhaps offer more ready applicability. Careful choice of the reagent and wavelength should allow either selective or general detection with acceptable sensitivity. Other advantages of post-column derivatisation are that it is readily automated and that defined products and completed reactions are not essential. Significantly for environmental applications, the separation is now based upon the parent species.

Fritz and Story [6] found that arsenazo-I formed coloured species in a post-column reactor with calcium, magnesium and several other ions. Arsenazo-III gave coloured species with eleven metals and the lanthanides, whereas 4-(2-pyridylazo)-resorcinol (PAR) formed coloured species with sixteen metals [6]; PAR has also been used by Cassidy and Elchuk [7]. Kawazu [8] separated ten metals with a macroreticular resin (Amberlite 200) and again PAR was used to detect these species after a 35-min separation. Polystyrene cross-linked resins are increasingly being used because of their stability between pH 1 and 13. Kawazu and Fritz [9] separated cadmium and zinc on a macroreticular resin, using 1-(2-pyridylazo)-2-naphthol as a post-column reactant.

Beckett and Nelson [10] described a detector that offered improved sensitivity based on derivatisation with an ethylenediaminetetraacetic acid (EDTA) analogue; the EDTA molecule had an aniline moiety attached and the separated metal-ligand species reacted with fluorecamine in the post-column reactor to give fluorescent detection in the sub-picomolar range. However, pre-column derivatisation was necessary and the column separation was effected in acetate media.

Chromatographic systems also offer considerable potential for the investigation of metal speciation. Interest in differentiating inorganic and organic mercury in environmental samples led Gast and Kraak [11] to develop a method whereby the mercury species were separated on a reversed-phase column with acetonitrile and 0.1 M sodium bromide as the mobile phase and then detected with a dithizone post-column reaction system set at 480 nm.

In the work described here, a general detector was based on monitoring the decrease of absorbance of unreacted dithizone. This report is concerned

with the separation of cadmium, cobalt, copper, lead, nickel and zinc and their detection by a post-column reaction. The current limits of detection and linear working ranges are reported and the possibilities of the method are discussed. The most successful approach was to separate the analyte species on a polystyrene-based cation-exchange resin with an aqueous tartaric acid eluent. Dithizone dissolved in acetone was added to the column effluent which then proceeded into a reactor coil prior to the detector. The decrease in absorbance at 590 nm was used to quantify the trace metal levels.

EXPERIMENTAL

Apparatus

A schematic diagram of the main components is shown in Fig. 1. A double-beam u.v./visible spectrophotometric flow monitor (SF 770; Schoeffel Instrument Corporation, Westwood, NJ) was equipped with a tungsten lamp and the wavelength was set to 590 nm. A 1-cm cell was used with a 10- μ l volume. The pumps (Constametric III; Laboratory Data Control, Riviera Beach, FL 33404) were operated from a central microprocessor control unit (Control Command Module, L.D.C.). Samples were injected on to the cation-exchange resin (Aminex A9, $11.0 \pm 0.5 \mu\text{m}$, Bio-Rad) in a 90 mm \times 5 mm column, with an injection valve (Rheodyne Model 7125; Rheodyne, Cotati, CA 94928) and a 100- μ l sampling loop.

The cation-exchange column was prepared by degassing the beads in a vacuum whilst in a beaker containing the eluent at the highest concentration to be used to separate the metal species. The eluent has also to be at the lowest pH at which it will be required to function. A standard packing pro-

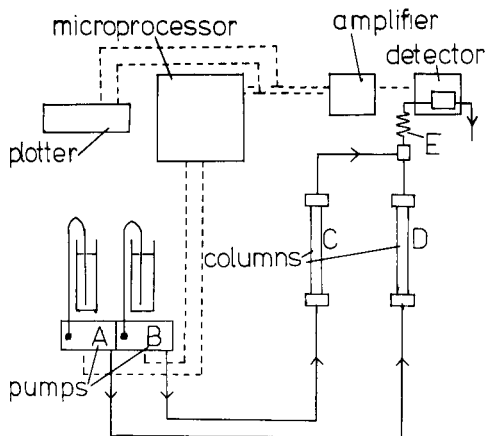


Fig. 1. Schematic diagram of the apparatus. Solid lines represent liquid flows; dashed lines represent electrical connections. The ions are separated on column D (Aminex A9 cation-exchange resin) with the tartrate eluent pumped by pump A. The post-column reactant (dithizone) is pumped by pump B to meet the effluent in reactor coil E. Column C packed with silica gel is inserted into the dithizone line to provide back-pressure.

cedure was used except that the initial pressure was 500 psi which was raised to 5000 psi after 5 min, until 150 ml of eluent had passed through. In this instance the eluent was 0.4 M tartaric acid at its natural pH of approximately 2.4.

The eluent was met by a flow of dithizone as post-column reactant in a T-junction. A back-pressure was induced in the dithizone flow by a 100 mm \times 4 mm column packed with 5- μ m silica gel prior to the T-junction. A reactor coil (1.5 m \times 0.3 mm) was connected to the detector which incorporated a heat sink.

Reagents

Glass-distilled water was used throughout and all the chemicals were of analytical-reagent grade (BDH Chemicals). Stock solutions of 1000 ppm cadmium, copper, cobalt, lead, nickel and zinc were diluted as necessary for working standards. A typical standard solution of 10 ppm copper, 20 ppm cadmium and zinc, 30 ppm cobalt and 30 ppm nickel was prepared and dilutions of this mixture were injected. A separate solution was prepared for the separation of lead and nickel.

A stock solution of 0.4 M tartaric acid was diluted to 0.2 M with distilled water and an alkaline solution was added to give the required pH. The alkaline solution contained a 40:60 mixture of 2 M sodium hydroxide and 2 M ammonia solution, respectively. The post-column reagents were made up as needed for each experiment, but in all instances the dithizone, sufficient to give a required absorbance, was dissolved in acetone (80 ml) and diluted with 20 ml of distilled water. Solutions were degassed with helium.

RESULTS AND DISCUSSION

Preliminary considerations

Most h.p.l.c. methods have been concerned with the separation of organic species, and it is only in the last few years with the production of the necessary materials that h.p.l.c. has become an important area of study for inorganic species. Thus some of the more recent papers have been concerned with metal ions, which have been separated in several ways. Some of these involved separations on silica or reversed-phase systems, and the use of organic solvents and precolumn derivatisation was often necessary. The aqueous ion-exchange systems were preferred here.

Separations could potentially be performed on either a cation- or an anion-exchange resin normally in conjunction with a low-molecular-weight polycarboxylic acid. A cation-exchange column was chosen, as high-quality resins of small particle size are easily obtainable and adequate separations had already been demonstrated [5, 12]. Of the polycarboxylic acids considered, tartaric acid gave the best chromatographic performance with the Aminex A9 resin, producing relatively fast elution times with sharp peaks of good symmetry for all metals investigated, except for copper which always showed significant tailing.

To obtain optimum separation, pH adjustment was required. Initially this was achieved with sodium hydroxide solution, but subsequent work showed ammonia to be a better base because nickel gave an increased response. Further investigations showed this to be a kinetic problem and that the reaction went to completion after a period of time. Unfortunately, however, after the addition of this post-column reactant, precipitation occurred and it was necessary to reduce the dilute ammonia solution to 60% of the neutralizing agent, the other 40% being sodium hydroxide. This compromise mixture of bases was sufficient to prevent precipitation up to a maximum eluent concentration of 0.2 M tartrate.

As dithizone is more soluble in acetone, which is easily miscible with water, it was decided to use this as the solvent for dithizone. The optimum conditions for the reactions with dithizone involved the following variables. At low percentage additions of the acetonetic dithizone solution to the post-column reactor, the high water content of the cation-exchange column effluent caused precipitation of the metal dithizonates. At high additions of the reagent solution to the column effluent, the greater dilution resulted in a lower detection signal. Maximum response was found when, after the post-column addition, the absorbance at 590 nm was between 0.15 and 1.0 absorbance units in a 1-cm path length cell. At high absorbance, the noise contributed a large part of the signal when set to detect low quantities of metal ions. At low absorbance, the sensitivity was less. The pH also had an effect on the sensitivity and the greatest response was achieved when the final pH of the mixed reactant and column effluent was between 4.85 and 5.0, except for lead and nickel where the maximum response occurred at pH 5.2. Noise came from many sources and was high with dithizone solution additions less than 25% of the total flow. To reduce the noise from pump pulsing, a back-pressure was introduced by placing a column before the T-junction in the post-column reactant system. The addition of 20% water reduced the compressibility of the acetone and increased the back-pressure, PTFE tubing also aided the buffering of the pulses from the pumps. Figure 2 shows the maximum sensitivity for four metals obtained by optimising the response in terms of pH, elution time, dithizone concentration and ratio of post-column reactant to column effluent.

Selection of working pH

Dithizone dissolved in aqueous acetone gradually changes from light blue through blue-grey to grey-brown from pH 4.0 to 5.3. This is accompanied by a decrease in the molar absorptivity of dithizone at 590 nm especially above pH 4.5. The colour changes to pink with the addition of a metal. A different pH is optimal for different metal complexes and three pH levels were therefore studied, each at high and low absorbances (about 0.8 and 0.25, respectively) of dithizone. The linearity of response, the working range and detection limits were then calculated. The usual chromatographic problem of a decrease in sensitivity by peak broadening with increasing

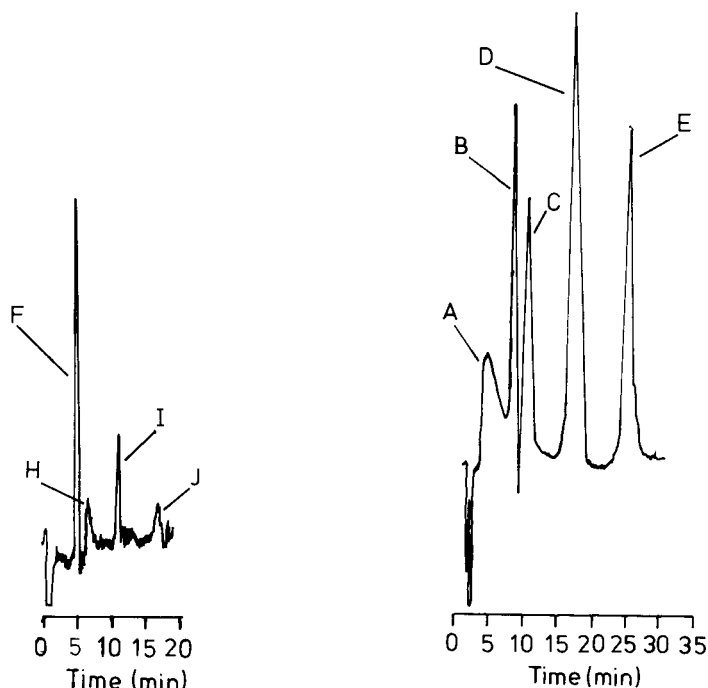


Fig. 2. Chromatogram showing the detection of low quantities at pH 5.2: F, 0.02 μg of zinc; H, 0.03 μg of nickel; I, 0.03 μg of cobalt; J, 0.02 μg of cadmium; no peak was obtained from 0.01 μg of copper.

Fig. 3. Chromatogram showing the separation of: A, 0.5 μg of copper; B, 1.0 μg of zinc; C, 1.5 μg of nickel; D, 1.5 μg of cobalt; E, 1.0 μg of cadmium. Sample (100 μl) injected on Aminex A9 (90 mm \times 50 mm) at 60°C; 0.2 M tartrate eluent at pH 4.25; post-column eluent pH 4.8, with absorbance 0.613.

retention time being opposed by the need to retain resolution, was further complicated in this case, because the sensitivity of the detector and the retention times depended on the pH of the eluate. It was difficult to lower the pH by post-column addition, as metals were extracted by acid from the surfaces of the pumps and tubing. The dithizone also decomposed in the polythene container and therefore pH manipulation via the post-column reactant solution was considered too difficult. The variability of response for individual metals may offer the possibility of selective detection and a greater sensitivity for a required species but the concern here was for multi-element determinations. Therefore three pH values, 4.3, 4.8 and 5.2, were chosen for study in the post-column detector. At pH 4.3, only a 20% addition of the dithizone solution could be made to the analytical column eluate; more caused precipitation of the ammonium tartrate, which is less soluble in acetone than in water, and thus blocked the post-column reactor. Also the rhythmic pulsing of the pumps at this low percentage addition prevented the detection of smaller quantities of the metals. Consequently, the linear ranges possible when the post-column mixture gave an unreacted absorbance

of 0.25 at 590 nm were from 200 ng to 3 μg for cobalt, copper and zinc, and from 200 ng to 1 μg for cadmium. At this low pH the sensitivity to nickel is poor and lead does not respond.

The post-column reactor was at its most sensitive at pH 4.8–5.0. By adjustment of the dithizone concentration in the post-column reactant mixture, the working range could be extended. When the analytical column effluent was mixed in a 3:2 ratio with the dithizone solution in the post-column reactor and when this ratio was varied so that the absorbance of the final unreacted effluent at 590 nm was 0.2 at one extreme and 0.6 at the other, a working range for the five metals of 10 ng–20 μg was obtained. The limits of detection (2σ) in the order of their elution were 1 ng of copper, 6 ng of zinc, 8 ng of nickel, 4 ng of cobalt and 5 ng of cadmium.

Analytical performance

A comparison of the responses at pH 4.8 and 5.2 is shown in Figs. 3 and 4, where the absence of a copper peak and the generally decreased response at

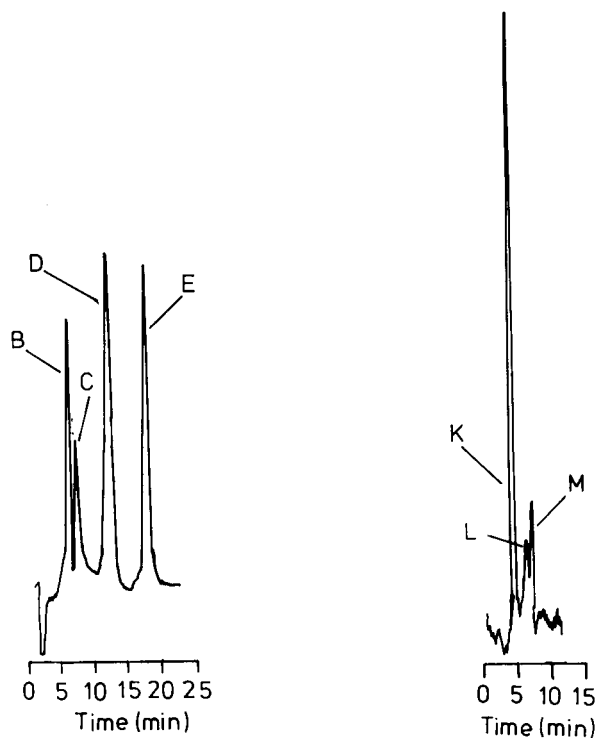


Fig. 4. Chromatogram of the same solution as in Fig. 3 under the same conditions except that the 0.2 M tartrate eluent was at pH 4.55 and the post-column pH was 5.2, with absorbance of 0.49. Response to copper is negligible.

Fig. 5. Chromatogram under the same conditions as Fig. 3: K, 0.06 μg of zinc; L, 0.093 μg of nickel; M, 0.5 μg of lead.

pH 5.2 can be noted (Fig. 4). At the higher pH, the linear working range was from 20 ng to 2 μ g for all metals except lead, with a lower limit of 100 ng and zinc with an upper limit of 1 μ g. Figure 5 shows the difficult yet quantifiable separation of lead from nickel. In contrast to the other metals, the response for lead and nickel was at an optimum at a post-column pH of 5.2.

An anomaly that occurred throughout the pH range was the slight negative curvature of the cobalt calibration graphs irrespective of the quantity injected. Copper gives a broad peak although it emerges first and this is more pronounced when the column is not heated, suggesting a kinetic interaction with the cross-linked sulphonated resin.

The ability of dithizone to react with many metals is well known and investigation into the detection of other metals is in progress. Bismuth, gold, indium, mercury, palladium, platinum, silver and tin react with dithizone, as do some of their organic derivatives [13]. Bismuth and indium were eluted on the solvent front from the column used at all pH values in the present study. Manganese and iron species reacted but with little sensitivity. In the case of iron(III), the response was probably due to loss of dithizone by oxidation. While manganese(II) may form a complex of low stability, the complex is susceptible to oxidation and decomposition at the pH used. The loss of dithizone by oxidation or by the formation of unstable complexes may be exploited by monitoring the decreased dithizone absorption as in this detector. The instability of some metal complexes may also be countered by the rapid air-free detection system reported here. The detector may also be adapted to the specific requirements of an operator, by pH adjustment or by altering the dithizone absorbance in the final eluted mixture.

Work is continuing on this promising approach to the h.p.l.c. of metal ions with a view to both improving the separation by studying other chromatographic systems and to exploiting the utility of this versatile dithizone post-column detector.

We thank the S.E.R.C. for the award of a grant towards equipment used in this work.

REFERENCES

- 1 O. Liška, J. Lehotay, E. Brandšteterová, G. Guiochon and H. Colin, *J. Chromatogr.*, 172 (1979) 384.
- 2 J. O'Laughlin and T. P. O'Brien, *Anal. Lett.*, A11 (1978) 829.
- 3 K.-H. König, H.-U. Ehmcke, G. Schneeweis and B. Steinbrech, *Fresenius Z. Anal. Chem.*, 297 (1979) 411.
- 4 G. Schwedt, *Top. Curr. Chem.*, 85 (1979) 160.
- 5 Y. Takata and G. Muto, *Anal. Chem.*, 45 (1973) 1864.
- 6 J. S. Fritz and J. N. Story, *Anal. Chem.*, 46 (1974) 825.
- 7 R. M. Cassidy and S. L. Elchuk, *J. Chromatogr. Sci.*, 18 (1980) 217.
- 8 K. Kawazu, *J. Chromatogr.*, 137 (1977) 381.
- 9 K. Kawazu and J. S. Fritz, *J. Chromatogr.*, 77 (1973) 397.
- 10 J. R. Beckett and D. A. Nelson, *Anal. Chem.*, 53 (1981) 909.
- 11 C. H. Gast and J. C. Kraak, *Int. J. Environ. Anal. Chem.*, 6 (1979) 297.
- 12 Y. Takata and K. Fusita, *J. Chromatogr.*, 108 (1975) 255.
- 13 H. M. N. H. Irving, *Dithizone*, The Chemical Society, London, 1977.

APPLICATION OF CONTINUOUS-FLOW ULTRAFILTRATION AND COMPETING LIGAND/DIFFERENTIAL SPECTROPHOTOMETRY FOR MEASUREMENT OF HEAVY METAL COMPLEXATION BY DISSOLVED ORGANIC MATTER

J. R. TUSCHALL, Jr.*

Illinois State Water Survey, P.O. Box 5050, Station A, Champaign, IL 61820 (U.S.A.)

P. L. BREZONIK

Department of Civil and Mineral Engineering, University of Minnesota, Minneapolis, MN 55455 (U.S.A.)

(Received 30th September 1982)

SUMMARY

Continuous ultrafiltration and competing ligand/differential spectrophotometric methods were developed to quantify metal complexation by naturally occurring aquatic organic matter. Results for copper(II) ion complexation by organic matter in two swamp waters and by a model compound (polyaspartic acid) were compared to values obtained by the established ion-selective electrode method. Copper(II) solution was added, and the parameters used to quantify complexation were the metal-binding capacity of the organic matter and conditional stability constant (β') of the metal–organic complexes. Copper complexed strongly with the organic material at pH 6.25; β' values ranged from $10^{5.3}$ to $10^{8.5}$. Values obtained with the three procedures compared well.

Heavy metal complexation by naturally occurring organic matter has been studied by many methods which have been discussed in recent reviews [1, 2]. Unfortunately, all existing methods suffer from at least one of the following drawbacks: (1) poor sensitivity, (2) adsorption of metal or organic matter to working surfaces, (3) lengthy, repetitive procedures, (4) inclusion of complexed metal in results for uncomplexed metal, (5) lengthy and frequent calibration procedures, (6) disruption of equilibrium conditions, (7) restriction to only a few metals, or (8) restriction of working pH. Consequently, incomplete and incorrect data often are obtained with these methods [3–10]. Because of the problems associated with existing procedures, we developed two new methods to measure metal complexation by dissolved organic matter; descriptive names for these methods are continuous flow ultrafiltration and competing ligand with differential spectrophotometric detection.

The commonest use of ultrafiltration in natural water studies has involved the determination of metal distribution by filtering a sample at fixed values of metal and ligand concentrations [11–15]. For this approach, filtrations

must be repeated if different concentrations of metal are to be evaluated. The tedium of performing individual experiments for each addition of metal has made ultrafiltration unappealing for extensive metal-binding studies. Ultrafiltration also has been used simply to fractionate organic matter into different size ranges, followed by use of other techniques to investigate interactions of heavy metals with fractionated organic matter [15–17].

A continuous ultrafiltration procedure that obviates the necessity of repeating the experiment for each concentration of binding component has been reported for binding of organic compounds (e.g., steroids) to large proteins [18]. This method uses a pressurized reservoir to feed a solution of the binding component continuously into a stirred ultrafiltration cell that contains high-molecular-weight organic matter (initially with no binding component). By collecting discrete fractions of effluent, the bound and unbound concentrations of the added component can be evaluated for various total concentrations. Until now, the continuous ultrafiltration method has not been used for metal-binding studies with macromolecular ligands.

Competitive equilibria have been used extensively to establish stability constants of metals with pure organic compounds [6]. Frequently, the concentration of metal complexed with the competing (auxiliary) ligand is determined spectrophotometrically by measuring the charge-transfer absorption band of the metal–ligand complex. Interfering background absorbance is subtracted by differential spectrophotometry. Competing equilibrium methods with EDTA as the competing ligand have been used to determine conditional stability constants for iron(III) with microbially produced siderophores [19, 20]. However, for most systems, EDTA complexes metal ions much more strongly than naturally occurring organic matter does; thus only a small amount of metal remains complexed with the organic matter. A useful competing ligand should allow a nearly equal distribution of metal ion between the ligand and the organic matter of interest. Selecting an appropriate competing ligand is not a simple task because strong absorption bands for many metal–organic complexes with suitable β' values are between 200 and 300 nm, a range in which the organic matter of interest also absorbs strongly.

This report describes the development of two methods for quantifying metal–organic interactions, namely, continuous-flow ultrafiltration and competing ligand (salicylate) using differential spectrophotometry. Results obtained for copper using the two methods for two humic-rich waters in Florida and a homopolyamino acid are compared to results obtained with an ion-selective electrode.

EXPERIMENTAL

Sample preparation

Surface water samples were collected from two hardwood swamps in northern Florida, Basin Swamp (BS), near Jasper, FL, and Waldo Swamp

(WS) in Waldo, FL. Samples were collected in 5-l polypropylene carboys and returned to the laboratory, where each sample was filtered through a 1.0- μ m polycarbonate (Nuclepore) filter and stored at 4°C. Polyaspartic acid (m.w. 5400; Miles Biochem.) was dissolved in distilled, deionized water (Milli-Q-II) at 3.7×10^{-5} M. Prior to use, all samples were adjusted to pH 6.25 with sodium hydroxide, and to ionic strength of 0.1 M with potassium nitrate which had been purified by electrolysis before use.

Ultrafiltration

Samples (70 ml) were placed above an Amicon UM10 or UM02 ultrafiltration membrane in a 70-ml capacity ultrafiltration cell (Amicon model 52). Each sample was rinsed with 250 ml of 0.1 M KNO_3 at pH 6.25 to remove filterable compounds. The sample volume was maintained at 70 ml during the rinsing process. To ensure that the sample was not contaminated with copper from a previous experiment, several membranes were dedicated to rinsing samples and were replaced prior to determinations of binding capacity and stability constant. The cell and tubing were flushed with 0.1 M HNO_3 prior to adding samples. After rinsing, each sample was transferred from the cell to an acid-washed bottle. A fresh membrane was inserted and equilibrated with a 1.5×10^{-6} M copper(II) solution (Fisher Certified) for 1 h. Subsequently, the membrane was rinsed with 15 ml of 0.1 M KNO_3 (pH 6.25) and then the prerinsed sample was returned to the cell. A reservoir containing a solution of copper(II) (and 0.1 M KNO_3 at pH 6.25) was connected to the ultrafiltration cell, and nitrogen was applied at a pressure of 2 atm. The sample was stirred continuously, and effluent was collected in 3–8-ml fractions with a Gilson GME automatic collector. After collection, samples were acidified to pH 2 with nitric acid and the copper content was measured by atomic absorption spectrometry (Perkin-Elmer Model 5000), in either the flame or flameless mode.

Competing ligand/differential spectrophotometry

Samples (50 ml) were pipeted into each of several 125-ml flasks containing 0.50 ml of 0.10 M salicylate (anionic form of *o*-hydroxybenzoic acid; J. T. Baker). The ionic strength of samples was made 0.1 M (KNO_3), and copper(II) was added in various quantities (10^{-7} – 7×10^{-4} M) to each flask. The pH was adjusted to 6.25 ± 0.05 with sodium hydroxide or hydrochloric acid. A sample with no added Cu(II) was placed in the reference cell (1, 4, or 10 cm pathlength) of a Perkin-Elmer Model 552 spectrophotometer, and samples with added copper were placed in the sample cell. Absorbance was recorded at 320 nm. Standard curves were prepared by processing distilled, deionized water.

Calculation of stability constants

The parameters used to quantify metal–organic interactions were binding capacity (C_L), which is the maximum amount of metal ion that can be

complexed by the ligands in a water sample [8, 21], and conditional stability constant (β'), which was defined by Ringbom [22] as

$$\beta' = [M_a L_b] / [M']^a [L']^b \quad (1)$$

where $M_a L_b$ is the complex of interest, M' represents metal not complexed with L , L' is ligand not complexed with M , and brackets denote concentrations.

Values of β' were estimated with the method of Scatchard [11, 23, 24]. The basic Scatchard equation is

$$\bar{\nu} / [M]_f = \beta' (n - \bar{\nu}) \quad (2)$$

where $\bar{\nu}$ is the ratio of metal bound to total ligand, $[M]_f$ is the concentration of unbound metal, and n is the number of binding sites per ligand molecule. Thus a plot of $\bar{\nu} / [M]_f$ versus $\bar{\nu}$ (called a Scatchard plot) is expected to produce a line with a slope of $-\beta'$. Values of L_T for the two swamp waters were estimated from the concentrations of dissolved organic carbon in the two waters (50 and 25 mg l⁻¹ for WS and BS, respectively), assuming that the organic matter was 50% carbon and that it had an average molecular weight of 1000. The estimated values of L_T were 10⁻⁴ M (WS) and 5 × 10⁻⁵ M (BS). It should be mentioned that the value used for L_T in the Scatchard method does not affect the value of the calculated β' .

Although Scatchard plots of pure compounds containing one distinct binding site ideally will produce a straight line with slope $-\beta'$, typical plots for environmental samples yield curved Scatchard plots that imply variable strength metal binding. Many research workers who use Scatchard plots to determine β' for metals with naturally occurring organics classify the sites into two categories (a "strong" site and a "weak" site). However, this approach is too simplistic to characterize metal binding in many environmental samples. For the data presented here, subtraction of the "strong" site from the "weak" site produced plots that remained curved. Therefore, the conditional stability constant data generated here were treated as a continuum, and the method commonly used to correct the plots for contributions from the "strong" and "weak" sites was not performed. Instead, the curves were divided into sections of $\bar{\nu}$, and the data in each section were fitted to a straight line. Ranges of $\bar{\nu}$ were selected by visually sectioning Scatchard plots into linear segments. Three segments were used to fit the experimental data. Nonetheless, the data are nonlinear and the only intent of fitting segments of the data to straight lines was to obtain comparisons among the three procedures used to determine the levels of complexed and uncomplexed metal ion.

RESULTS AND DISCUSSION

Ultrafiltration

Several experimental parameters affected the results of the continuous flow ultrafiltration procedure for metal-binding studies. First, the type of

filtration membrane was important. Filters with small pores have more ionic character than those with large pores, and copper interaction with ionic membranes produced erratic results. Yet, with increasing porosity, retention of organic matter diminished. The Amicon UM10 membrane produced optimum results for the two surface waters, retaining over 95% of the soluble organic carbon in each sample. Polyaspartic acid was not retained by UM10 membranes, but smaller porosity UM02 membranes retained 92% of polyaspartic acid.

A second parameter that controls the success of this procedure is the flow rate through the membrane. At fast flow rates ($0.5\text{--}1.0\text{ ml min}^{-1}$) and a purely inorganic matrix, the concentration of metal ion in the retained solution eventually exceeded the concentration of metal ion in the feed solution, apparently because of partial rejection of metal ions by the membrane. A flow rate of 0.2 ml min^{-1} alleviated this problem, but metal concentrations in the filtrate of inorganic solutions still were lower than those in the retained solution, apparently because metal ions were binding to the membrane. It was found that ionic strength influenced the extent to which metal ions were retained on the filters, and subsequently, all solutions were adjusted with potassium nitrate to 0.1 M, the lowest level found to prevent metal loss to the membrane.

After choices of membrane, flow rate, and ionic strength had been optimized, copper(II) was added to a solution containing only 0.1 M KNO_3 at pH 6.25 to ensure that the system followed predicted behavior (based on simple mixing and dilution). For continuous filtration with no binding component in the cell, the following equation relates effluent concentrations of metal ion $[\text{M}]_e$, to influent metal ion concentrations $[\text{M}]_i$ [18]:

$$[\text{M}]_e = [\text{M}]_i [1 - (1 - \alpha)^n] \quad (3)$$

where n is the fraction number, and α is the ratio of the fraction volume to cell volume. Results for copper (Fig. 1A) were nearly identical to predicted values, indicating that metal rejection or binding by the membrane was not occurring. Plots of M_e vs. n (or V_{out}) are inherently nonlinear, however, and deviations from ideal behavior are not easily detected graphically. After rearranging and taking logarithms, Eqn. (3) becomes:

$$\log \{[\text{M}]_i / ([\text{M}]_i - [\text{M}]_e)\} = -n \log (1 - \alpha) \quad (4)$$

A plot of the left side of Eqn. (4) vs. n (or V_{out}) thus is linear for the simple dilution experiment, and the results (Fig. 1A) clearly show that the experiment followed predicted behavior.

The addition of copper to Waldo Swamp water (Fig. 1A) indicates that copper was retained by the high-molecular-weight organics in the sample. However, neither the amount of metal bound, M_b , nor C_L can be quantified graphically from such plots, and the following mass-balance equation was used to determine M_b :

$$M_b = V_{\text{out}} [\text{M}]_i - V_{\text{cell}} [\text{M}]_e - [\text{M}]_{\text{out}} \quad (5)$$

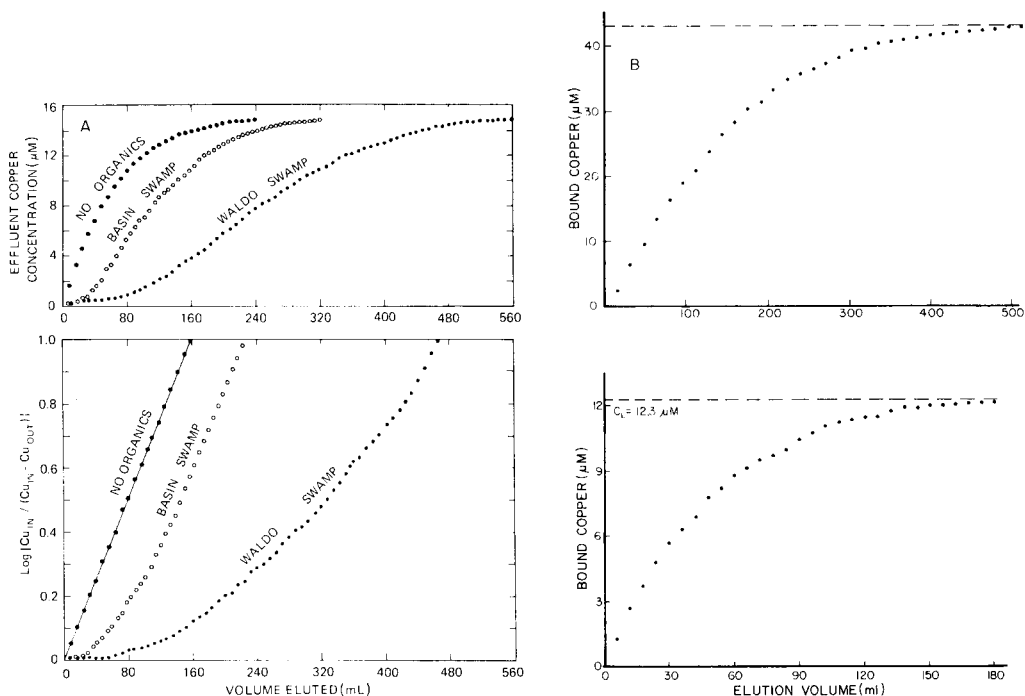


Fig. 1. Binding curves of Waldo Swamp and Basin Swamp water samples and organic-free solutions with copper(II) using continuous ultrafiltration. (A) Plots of Eqns. (3) and (4); solid line represents theoretical dilution. (B) Binding curves for Waldo Swamp water with $C_L = 43 \mu\text{M}$ (upper) and Basin Swamp water with $C_L = 12.3 \mu\text{M}$ (lower).

where V_{out} is the total volume of effluent collected, V_{cell} is the cell volume, and M_{out} is the total amount of metal ion collected in the effluent. For the j^{th} fraction, $M_{\text{out}} = \sum_{n=1}^j V_n [M_{e,n}]$, where V_n is the volume of each fraction and $[M_{e,n}]$ is the effluent metal ion concentration in each fraction.

The calculated values of M_b for each fraction collected during addition of copper were plotted against V_{out} (Fig. 1B), resulting in an asymptotic curve that was extrapolated to obtain C_L . Calculated values of C_L for the two water samples and polyaspartic acid compare well with concentrations of copper in the retained solution after the experiment was complete (Table 1).

Values for β' were determined by inserting calculated values of M_b into Eqn. (5) and constructing Scatchard plots for each sample as described earlier (Fig. 2). For the continuous-flow ultrafiltration method, no data were obtained in the lowest region of the Scatchard plot because precise results were not obtainable below 10^{-7} M Cu(II) . Data for the other ranges are presented in Table 2. In all cases, the strength of Cu(II) binding decreased as more Cu(II) was added. The curvature of the Scatchard plots suggests either that there is more than one class of binding sites (each characterized

TABLE 1

Summary of copper(II) binding capacities (C_L) determined by three separate techniques

	Binding capacity (mol l ⁻¹)		Competing ligand method	I.s.e.
	Ultrafiltration			
	Calculated ^a	Measured ^b		
Waldo Swamp	4.3 × 10 ⁻⁵	4.1 × 10 ⁻⁵	6.8 × 10 ⁻⁵	7.9 × 10 ⁻⁵
Basin Swamp	1.23 × 10 ⁻⁵	1.17 × 10 ⁻⁵	1.3 × 10 ⁻⁵	1.4 × 10 ⁻⁵
Polyaspartic acid (3.7 × 10 ⁻⁵ M)	3.0 × 10 ⁻⁴	3.0 × 10 ⁻⁴	4.2 × 10 ⁻⁴	5.0 × 10 ⁻⁴

^aCalculated using Eqn. (5) and Fig. 1B. ^bDetermined in retained solution at conclusion of experiment.

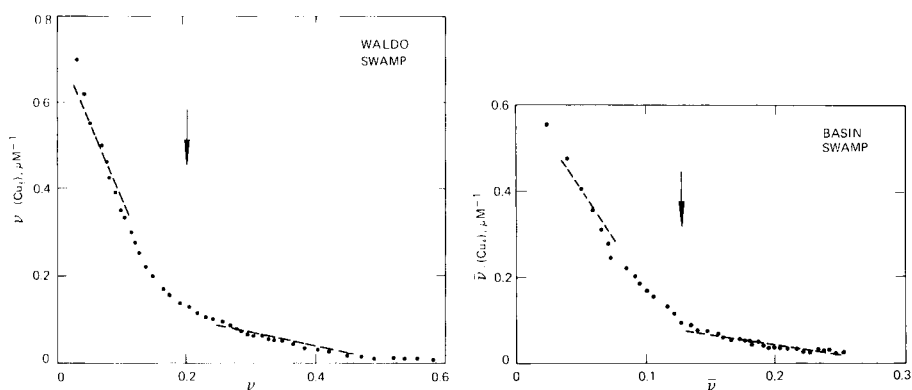


Fig. 2. Scatchard plots of Waldo Swamp and Basin Swamp samples with copper(II) using continuous ultrafiltration. Arrows delimit linear segments (dashed lines).

by a different intrinsic stability constant), or that binding of each successive Cu(II) alters the β' for the next molecule of Cu(II) bound [25].

Competing ligand and differential spectrophotometry

Several organic compounds were examined for use as competing ligands. Most absorbed radiant energy in the region below 300 nm, a region in which naturally occurring organics absorb strongly. Salicylate was found to absorb strongly at 296 nm, and the addition of copper caused a bathochromic shift in the absorption spectrum. The shift resulted from absorption at 320 nm (maximal intensity) of the copper salicylate. Because salicylate absorbed appreciably at 320 nm, the difference between samples with and without Cu(II) added was used. The molar absorptivity (ϵ) of salicylate at 296 nm was found to be identical to reported values ($\epsilon = 3200$) [26].

TABLE 2

Summary of log β' values for surface waters and polyaspartic acid with copper

$\bar{\nu}$ range	Method		
	Ultrafiltration	Competing ligand	I.s.e.
<i>Waldo Swamp</i>			
0—0.02	ND ^a	ND	8.11
0.021—0.2	6.54	6.61	6.72
0.21—0.8	5.50	5.48	5.34
<i>Basin Swamp</i>			
0—0.025	ND	ND	7.82
0.026—0.125	6.67	6.72	6.85
0.126—0.4	5.56	5.54	5.26
<i>Polyaspartic acid</i>			
0—0.25	ND	ND	8.50
0.26—4	7.50	7.31	7.04
4.1—15	5.36	5.18	5.44

^aND = not detected.

Absorbance values were standardized by adding copper to a solution of 10^{-3} M salicylate. The concentration of the copper salicylate formed at each level of total copper concentration was calculated by a computer program (MINEQL), and a plot of absorbance vs. copper salicylate concentration was linear (Fig. 3). The lower limit of detection using a 4-cm cell was 10^{-7} M copper salicylate. Measurement of lower concentrations was attempted with a 10-cm cell, but total absorbance of the initial sample solution was beyond the maximum measurable with the instrument.

The absorbance values obtained for samples were converted to concentrations of copper salicylate using the standard curve. The competing equilibria are $\text{Cu}^{2+} + \text{L} \rightleftharpoons \text{CuL}$ and $\text{Cu}^{2+} + \text{Sal} \rightleftharpoons \text{CuSal}$, where L is the ligand of interest, Cu^{2+} is uncomplexed copper ion, and Sal is salicylate. Equilibrium concentrations of Cu^{2+} , CuL, and L were calculated by using the mass balance of each component, the value of β' (CuSal) and the empirically derived concentration of copper salicylate. The mass balance equations are

$$\text{Cu}_T = (\text{Cu}^{2+}) + (\text{CuL}) + (\text{CuSal}); \text{Sal}_T = (\text{Sal}) + (\text{CuSal}); \text{L}_T = (\text{CuL}) + (\text{L})$$

where the parentheses indicate aqueous concentrations and the subscript T indicates the total concentration of each species. The conditional stability constant, β' , for copper salicylate was calculated from the thermodynamic stability constant [27] by the method of Ringbom [22]; at pH 6.25, from Eqn. (1), $\beta' = 10^{3.5} = (\text{CuSal})/(\text{Cu}^{2+})(\text{Sal})$. The empirical concentration of copper salicylate for each addition of copper(II) ions was inserted into

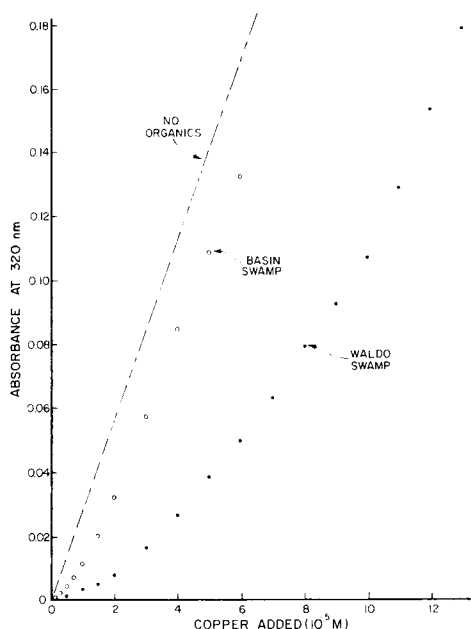


Fig. 3. Absorbance values for swamp waters and copper(II) using the competing ligand/differential spectrophotometric method. Dashed line is the standard plot for copper salicylate formation in the background electrolyte solution.

the equations for Sal_T and β' , and Cu^{2+} was calculated by solving the two equations simultaneously. Subsequently, (CuL) was determined from the equation for Cu_T . These data were treated in the same manner as the ultrafiltration data for determining C_L and β' .

Several assumptions about the competing ligand/spectrophotometric procedure were examined to ensure its validity. To produce accurate results, salicylate ion must remain available (to complex copper) at the same effective concentration in both sample and standard. Adsorption of salicylate to organic matter in water samples would reduce its effective concentration. The possible occurrence of adsorption was investigated by continuous ultrafiltration using an eluant solution of salicylate (which permeated the membrane) in a manner analogous to that described for metal-binding studies. The organic matter in each sample was retained by an ultrafiltration membrane (UM10 for surface waters; UM02 for polyaspartic acid), and therefore any retention of salicylate by the organics would be detected as a deficiency of salicylate in the effluent fractions. Spectrophotometric measurements of salicylate in the fractions indicated that salicylate followed ideal dilution and that there was no binding of salicylate by the retained organic matter.

The possible formation of mixed ligand complexes, Cu(L)(Sal) , was examined by ultrafiltration using solutions containing copper(II) ions, salicylate and the ligands from each sample. A small fraction (<2%) of the cell

contents was filtered to minimize changes in equilibrium concentrations of CuL in the retained solution. Spectrophotometric studies of the ultrafiltrate showed that equivalent amounts of copper salicylate were present in both filtrate and unfiltered sample, from which it was concluded that mixed complexes were not present in substantial amounts. Further evidence for this is provided by the close agreement of β' and C_L among the three procedures.

Another possible discrepancy could occur if the absorbance at 320 nm were changed by interaction of salicylate or copper with solutes in the samples. Absorption spectra of each swamp sample containing salicylate (10^{-3} M) were indistinguishable from scans for the salicylate standards. However, the spectrum of Waldo Swamp water (in the absence of salicylate) with additional copper showed a slight increase in absorbance, apparently because of absorbance of a copper—organic complex. No absorbance occurred for copper solutions alone in the region 280–400 nm. Therefore, the increase in absorbance was subtracted from the readings taken for this sample containing salicylate at corresponding levels of copper, although the correction was small (<15%). No correction was necessary for the other swamp sample or for polyaspartic acid.

Addition of copper(II) ions to surface water samples (by the competing ligand/spectrophotometric method) resulted in curved plots that departed from the standard curve for solutions containing only salicylate (Fig. 3). The horizontal difference between the dashed line (standard curve) and the curve for a sample represents copper bound to natural organics in each sample. A plot of (Cu_b) (calculated from the above equations for Cu_T , Sal_T , L_T and β') vs. the concentrations of copper added was used to determine C_L (Table 1). Subsequently, a Scatchard plot was constructed (Fig. 4), and values of β' for each $\bar{\nu}$ range were determined (Table 2). Agreement of both C_L and β' values from the ultrafiltration and competing ligand methods was good.

The competing ligand method described here is restricted in some cases by its limit of detection (10^{-7} M Cu^{2+}). For samples producing (Cu^{2+}) below 10^{-7} M, an auxiliary competing ligand could be used to speciate copper. The auxiliary competing ligand should have a larger β' for copper than that of salicylate in order to compete more effectively with organic ligands that produce such low concentrations of uncomplexed copper. The most formidable obstacle in selecting an alternative ligand is the difficulty of measuring the concentration of metal complexed to the competing ligand in the sample matrix. An acceptable alternative ligand has not been found yet.

Ion-selective electrode method

Values of C_L and β' determined by the i.s.e. method compare well with values produced by the ultrafiltration and competing ligand methods (Tables 1 and 2). For the lowest ranges of $\bar{\nu}$, only the i.s.e. method was sensitive enough to allow calculation of β' . Consequently, the Scatchard plots in Fig. 5 most clearly illustrate the hyperbolic nature of the present results. It is noteworthy

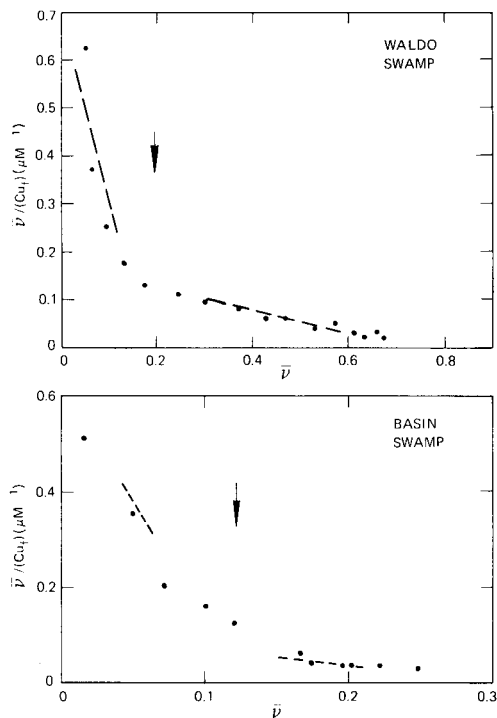


Fig. 4. (Left) Scatchard plots for addition of copper to swamp waters using the competing ligand—differential spectrophotometric method. Arrows delimit linear segments (dashed lines).

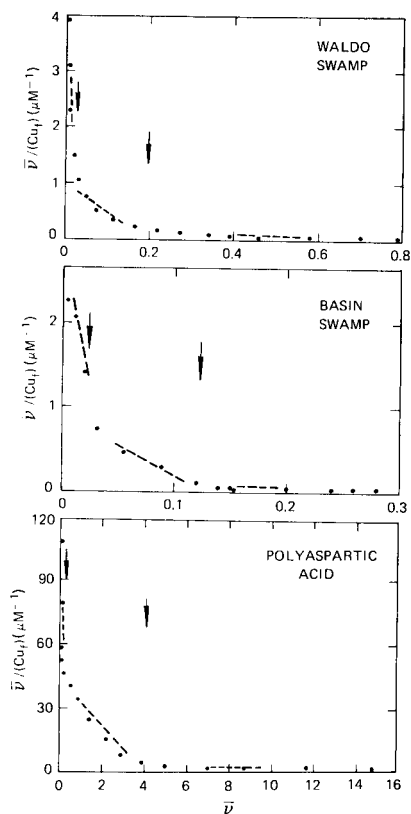


Fig. 5. (Right) Scatchard plots for addition of copper(II) ion to samples with the i.s.e. method. Arrows delimit linear segments (dashed lines).

that the plot for polyaspartic acid is nonlinear, even though $Cu(II)$ is most likely complexed to a single type of binding site (COO^-) [28]. The phenomenon observed here may reflect electrostatic effects, such that the tendency of a metal ion to interact with a ligand group on a macromolecule varies with the electrostatic free energy needed to change the electric charge of the macromolecule. This free energy is related to all the ionic equilibria in which the functional groups on the macromolecule participate [29]. In the case of polyaspartic acid, the shape of the Scatchard plot suggests that complexation of one copper ion to the polymer decreased the tendency of a neighboring functional group to complex another copper ion, which in turn decreased the affinity for the next copper ion. The same effect may cause the curvature of Scatchard plots of the swamp water samples. However, more research in this area is necessary before sound conclusions can be reached.

It should be mentioned that the three methods used here will not produce comparable results with some solution conditions because different species of metal are measured by the methods. The i.s.e. method quantifies Cu^{2+} , whereas the other two methods include inorganic metal complexes as well as some small metal-organic species. In the present experiments, solution conditions were selected so that nearly all of the copper not bound to organic matter was present as the free aquated ion, Cu^{2+} . However, at higher pH and carbonate concentrations, such would not be the case and direct comparisons must account for the different species measured.

Support for this research was provided, in part, by grants from the National Science Foundation (PFR-78-19199) and the U.S. Environmental Protection Agency (EPA-R-806286020) to the Center for Wetlands at the University of Florida.

REFERENCES

- 1 T. M. Florence, *Talanta*, 29 (1982) 345.
- 2 R. A. Saar and J. H. Weber, *Environ. Sci. Technol.*, 16 (1982) 510A.
- 3 J. R. Tuschall, Jr. and P. L. Brezonik, *Anal. Chem.*, 53 (1981) 1986.
- 4 F. L. Greter, J. Buffle and W. Haerdi, *J. Electroanal. Chem.*, 101 (1979) 211.
- 5 P. L. Brezonik, P. A. Brauner and W. Stumm, *Water Res.*, 10 (1976) 605.
- 6 F. J. C. Rossotti and H. Rossotti, *The Determination of Stability Constants*, McGraw-Hill, New York, 1961.
- 7 T. M. Florence and G. E. Batley, *Talanta*, 24 (1977) 151.
- 8 K. W. Hanck and J. W. Dillard, *Anal. Chim. Acta*, 89 (1977) 329.
- 9 P. L. Brezonik and J. R. Tuschall, Jr., *Anal. Chem.*, 54 (1982) 1000.
- 10 J. R. Tuschall, Jr. and P. L. Brezonik, *Anal. Chem.*, 54 (1982) 2116.
- 11 R. D. Guy and C. L. Chakrabarti, *Can. J. Chem.*, 54 (1976) 2600.
- 12 E. T. Gjessing, *Environ. Sci. Technol.*, 4 (1970) 437.
- 13 J. E. Schindler, J. J. Alberts and K. R. Honick, *Limnol. Oceanogr.*, 17 (1972) 952.
- 14 P. Benes, E. T. Gjessing and E. Steinnes, *Water Res.*, 10 (1976) 711.
- 15 M. R. Hoffman, E. C. Yost, S. J. Eisenreich and W. J. Maier, *Environ. Sci. Technol.*, 15 (1981) 655.
- 16 H. L. Allen, *Oikos*, 27 (1976) 64.
- 17 R. G. Smith, Jr., *Anal. Chem.*, 48 (1976) 74.
- 18 M. T. Ryan and N. S. Hanna, *Anal. Biochem.*, 40 (1971) 364.
- 19 G. Anderegg, F. L'Eplattenier and G. Schwarzenbach, *Helv. Chim. Acta*, 46 (1963) 1409.
- 20 W. R. Harris, C. J. Carrano, S. R. Cooper, S. R. Sofen, A. E. Avdeef, J. F. McArdle and K. N. Raymond, *J. Am. Chem. Soc.*, 101 (1979) 6097.
- 21 Y. K. Chau, *J. Chromatogr. Sci.*, 11 (1973) 579.
- 22 A. J. Ringbom, *Complexation in Analytical Chemistry*, Wiley-Interscience, New York, 1963, p. 38.
- 23 R. F. C. Mantoura and J. P. Riley, *Anal. Chim. Acta*, 78 (1975) 193.
- 24 G. Scatchard, *Ann. N.Y. Acad. Sci.*, 51 (1949) 660.
- 25 G. Scatchard, I. H. Scheinberg and S. H. Armstrong, Jr., *J. Am. Chem. Soc.*, 72 (1950) 535, 540.
- 26 P. Csokan, *Z. Physik. Chem., Teil A*, 191 (1942) 164.
- 27 A. E. Martell and R. M. Smith, *Critical Stability Constants*, Plenum Press, New York, 1977, p. 186.
- 28 V. V. Korshak, S. V. Rogozhin, V. A. Davankov, Yu. A. Davidovich and T. A. Makarova, *Russ. Chem. Rev.*, 34 (1963) 329.
- 29 W. Stumm and J. J. Morgan, *Aquatic Chemistry*, Wiley, New York, 1981, p. 382.

COMPARISON OF 8-QUINOLINOL-BONDED POLYMER SUPPORTS FOR THE PRECONCENTRATION OF TRACE METALS FROM SEA WATER

S. N. WILLIE, R. E. STURGEON* and S. S. BERMAN

Division of Chemistry, National Research Council of Canada, Ottawa, Ontario K1A 0R6 (Canada)

(Received 29th November 1982)

SUMMARY

8-Quinolinol, immobilized on cross-linked polyvinyl pyrrolidone, a macroreticular styrene–divinylbenzene (XE-305) or methylated polystyrene (Merrifield resin) substrates, was used for the preconcentration of ions of Cd, Zn, Pb, Cu, Fe, Mn, Ni, Co, and Cr from sea water prior to their measurement by electrothermal atomic absorption spectrometry. Optimal results were obtained when the XE-305 substrate was used. Except for chromium, recoveries of the above elements from sea water with this material averaged 100% (range 88–109%) with absolute blanks ranging between 0.1 ng (Cd) and 7 ng (Zn). Performance is demonstrated by quantitation of metal ions in open ocean water.

Analytical literature is replete with articles attesting to the widespread use of polymer matrices for the immobilization of chelates and their subsequent use in the separation of trace metals from aqueous and organic media [1]. Whereas chelates immobilized on silica supports suffer from cleavage of the bonded phase and characteristic “bleeding” of the chelating group by hydrolysis [2], polymer substrates offer the inherent advantage of greater stability at pH > 8. Furthermore, because of their relatively inert nature, polymer substrates should result in lower quantitative blanks [2].

Styrene–divinylbenzene copolymers are the most widely used substrates for immobilization of 8-quinolinol, the synthesis most often used being nitration of the polystyrene followed by its reduction to aminopolystyrene and diazotization. The 8-quinolinol is then coupled to the support via this linkage [3–5]. Condensation resins [5–7], represented by the resorcinol–formaldehyde–8-quinolinol type, are less stable than the latter resins. Although silica-immobilized 8-quinolinol was demonstrated to be useful for the concentration of trace metals from sea water [2], it suffers from hydrolysis (at pH > 5) and, as a consequence of some dissolution of the substrate, a high iron blank results. Attempts to prepare immobilized 8-quinolinol on a high-purity silica substrate were unsuccessful.

Despite widespread interest in the preparation and characterization of 8-quinolinol containing polymers [1] and their use in chromatographic separa-

tions of cationic mixtures [5, 8–11], no systematic investigation of their application to the preconcentration of trace metals from sea water has been made. This work was undertaken to study this facet of resin performance.

8-Quinolinol was immobilized onto a polystyrene via a methylene linkage and also onto a cross-linked polyvinyl pyrrolidone and a divinylbenzene–styrene copolymer (XE-305) via a phenylazo linkage. Comparison of the performance of these three resins for the preconcentration of ions of Cd, Zn, Pb, Cu, Fe, Mn, Ni, Co, and Cr from sea water showed the XE-305-based resin to be superior in terms of spike recovery, stability, and ease of preparation. Use of this resin provides a simple, fast, accurate, and precise technique for the separation and concentration of these metal ions from sea water and can be recommended as an alternative to use of the more difficult to prepare silica-immobilized 8-quinolinol.

EXPERIMENTAL

Instrumentation and reagents

The Perkin-Elmer model 5000 atomic absorption spectrometer used was fitted with an HGA-500 furnace with Zeeman background correction and an AS-40 autosampling device. Tubes coated with pyrolytic graphite were used exclusively.

Amberlite XE-305 (a 4% divinylbenzene–styrene macroreticular copolymer), chloromethylated polystyrene (Merrifield resin, $2.63 \text{ meq Cl g}^{-1}$) and cross-linked polyvinyl pyrrolidone (PVP) were obtained from Polysciences (Warrington, PA). The chloromethylated polystyrene was used as supplied (200–400 mesh) whereas the PVP and XE-305 were ground in a mortar and pestle and dry-sieved. A 60–150 mesh fraction was retained for use.

All reagents were purified prior to use. Concentrated nitric and hydrochloric acids as well as fuming nitric acid were prepared by sub-boiling distillation in a quartz still using reagent-grade acids for nitric and hydrochloric acids and a $\text{HNO}_3/\text{H}_2\text{SO}_4$ mixture for fuming nitric acid. A saturated ammonia solution (28%) was prepared by isothermal distillation of reagent-grade ammonia liquor.

Standard solutions of the elements of interest were prepared by dissolution of the pure metals or their salts. Serial dilutions were made with high-purity deionized–distilled water (called pure water below) in order to prepare working standards.

8-Quinolinol was purified by vacuum sublimation at 390 K onto a cold finger.

Two samples of open ocean water were used in this study. The salinity of each was $35.0^\circ/\text{‰}$. Both samples were obtained from approximately the same site 13 km SE of Bermuda from a depth of 1300 m by using modified GO-FLO samplers. One of these samples was subsequently used in the preparation of the trace metal reference material for sea water, NASS-1 [12].

Procedures

All samples were prepared in a clean laboratory equipped with laminar flow benches and fume cupboards providing a class 100 working environment.

Preparation of resins. 8-Quinolinol was immobilized onto PVP via azo coupling after silanization of the surface by the procedure outlined by Hill [13] for silica surfaces. The reddish product was washed with methanol and then cleaned with (1 + 1) hydrochloric acid and pure water and allowed to air-dry.

8-Quinolinol was bonded to the Merrifield resin by a Friedel-Crafts acylation. Resin (10 g) was placed in a mixture containing 75 ml of nitrobenzene, 5 g of 8-quinolinol, and 20 g of tin(IV) chloride and heated for about 60 h at 330 K. The greenish-yellow product was isolated by frequent washing by decantation from methanol and cleaned by washing with (1 + 1) hydrochloric acid. Following a final wash with ether, the product was air-dried.

The XE-305-bonded 8-quinolinol was prepared in two different ways. In one, XE-305 (5 g) was nitrated with a 9:1 mixture of HNO_3 /fuming HNO_3 by heating for 12 h at 350 K. The product was washed with pure water and the nitrate was reduced to the amine by heating for 24 h at 350 K in 100 ml of a solution of tin(IV) chloride (14 g) in (1 + 1) hydrochloric acid. The brownish product was washed with pure water by decantation and air-dried. This aminopolystyrene was then either (a) directly diazotized by reaction with sodium nitrite in 1% acetic acid at 273 K, washed with cold pure water, and coupled to 8-quinolinol in ethanolic solution [13] or (b) benzoylated by reaction with *p*-nitrobenzoylchloride in chloroform, reduced with sodium dithionite, diazotized with sodium nitrite, and then coupled to 8-quinolinol as above [13]. The difference in the two magenta products is that, with the latter synthesis, 8-quinolinol is attached to the polymer support through a phenylazo linkage.

After several washings in 1.0 M hydrochloric acid, 600 mg of each product was slurry-loaded into glass columns supported by coarse sintered-glass frits. The column assembly and polypropylene sample reservoir were described earlier [2]. Prior to use, the entire assembly was carefully precleaned by gravity feed of 200 ml of a solution of 1 M HCl/0.1 M HNO_3 through the column. The system was then washed free of excessive acid with pure water.

Preconcentration. Spiked or unspiked aliquots of sea water, previously acidified with nitric acid to pH 1.6 for storage, were adjusted to $\text{pH } 8.0 \pm 0.2$ with high-purity ammonia solution and drawn through the column (under water pump suction) at a nominal flow rate of 5 ml min^{-1} . After the passage of the sample, the column was washed free of sea water with two 10-ml aliquots of pure water, each being allowed to drain by gravity. The trace metal ions were then eluted from the column by using 10.0 ml of a 1 M HCl/0.1 M HNO_3 solution. This concentrate was stored in a 30-ml screw-capped polypropylene bottle prior to analysis. The column was then further

cleaned by passage of an additional 25 ml of the acidic eluent. After a wash with pure water to remove excess of acid, the column was ready for the next sample aliquot.

With XE-305, it was found necessary initially to wash the column at pH 10 with pure water and allow it to drain to the meniscus before the pH 8 sea-water sample was loaded. Without the pH 10 wash, passage of the sea water resulted in an immediate drop in effluent pH to about 7 with slow recovery to pH 8. With the pH 10 prewash, passage of the sea water resulted in a very rapid drop in effluent pH to a stable value of 8 over the course of only several milliliters of sample.

Blanks involving acid elution of the column were found to be identical to blank runs consisting of aliquots of sea water which had been stripped free of trace metal ions by prior passage through the column.

Ion contents of blanks and concentrates were obtained by calibration against a spiked aliquot of concentrate, thereby effecting an identical matrix match. Furnace conditions used for the atomization of samples were those recommended by the manufacturer.

RESULTS AND DISCUSSION

PVP-8-quinolinol

The manner in which 8-quinolinol becomes immobilized onto the PVP substrate is open to speculation. Presumably, it is ultimately attached through a silanol linkage (as in the case of silica-immobilized 8-quinolinol [2]). The material exhibited good stability at low pH (<1) but suffered hydrolysis and visible "bleeding" at pH ≥ 9 . The exchange capacity, as measured by batch equilibration with copper(II) at pH 8.0, was 1 mg g^{-1} ($0.015 \text{ mmol g}^{-1}$), somewhat lower than its silica-immobilized counterpart (0.06 mmol g^{-1} [2]).

Recoveries of trace metal spikes added to 300-ml aliquots of sea water are given in Table 1. Except for the ions of cadmium and chromium, all metal ions of interest could be quantitatively recovered. The behavior of cadmium(II) is highly unusual in view of its stability constant for chelation with 8-quinolinol relative to the other metals. The chlorocadmium complex is less stable than that of several others of these elements. Steric hindrance to chelation, noted for tetravalent metal ions [6], cannot account for this observation because the ionic radius of Cd(II) is smaller than that of lead(II), which was quantitatively recovered. Thus, no consistent explanation can be offered for the non-quantitative recovery of cadmium.

Blanks for the PVP-8-quinolinol resin are given in Table 2. As expected, the inertness of the PVP substrate toward hydrolysis and dissolution results in a significant lowering of the iron blank over that obtained with a silica substrate [2] at pH 8.

Results for a sample of open ocean water are shown in Table 3, wherein the mean and standard deviation of triplicate determinations on 300-ml aliquots are given. "Accepted" values for these samples were obtained by

TABLE 1

Recovery of trace metals from sea water with 8-quinolinol immobilized on various substrates

Element	Recovery ^c (%)			
	PVP ^a	Merrifield resin ^b	XE-305 ^d	Silica ^e
Cd	50 ± 7	25 ± 6	105 ± 7	94 ± 5
Pb	100 ± 8	69 ± 10	88 ± 7	92 ± 10
Zn	95 ± 5	101 ± 10	110 ± 4	94 ± 9
Cu	90 ± 10	94 ± 2	93 ± 5	96 ± 12
Fe	100 ± 3	97 ± 14	109 ± 5	96 ± 10
Mn	100 ± 4	<7	91 ± 10	115 ± 5
Ni	100 ± 4	106 ± 6	99 ± 2	96 ± 8
Co	100 ± 5	81 ± 3	107 ± 10	74 ± 1
Cr	<10	62 ± 6	43 ± 8	—

^aCross-linked polyvinylpyrrolidone; 8-quinolinol immobilized via phenylazo linkage on silica chain. ^bChloromethylated polystyrene; 8-quinolinol immobilized via methylene linkage. ^cMean and standard deviation of 3 determinations; 30-fold concentration. ^dStyrene divinylbenzene copolymer; 8-quinolinol immobilized via phenylazo linkage. ^ePorasil B (Waters Scientific, 200–400 mesh); 8-quinolinol immobilized via phenylazo linkage [2].

extensive examination based on several different quantitative techniques [14] including isotope-dilution spark-source mass spectrometry [15].

Good agreement with accepted values is apparent for all elements but cadmium. Results for this element fall into line if account is made for its 50% recovery efficiency. Determination of cobalt was not attempted because of

TABLE 2

Blanks for different supports

Element	Blanks (ng)			
	PVP	Merrifield resin	XE-305	Silica ^a
Cd	0.3 ± 0.1	<0.8	0.10 ± 0.05	<0.1
Pb	<1.8	<1.5	<0.4	<0.8
Zn	3 ± 1	<1.5	7 ± 3	2 ± 1
Cu	0.7 ± 0.03	<1	0.5 ± 0.1	<0.2
Fe	4 ± 1	5 ± 1	7 ± 1	>75
Mn	<0.4	<0.4	<0.4	<1
Ni	<2	<2	<2	<3
Co	<0.5	<0.5	<0.5	<1
Cr	<1	<1	<1	—

^aReproduced from [2].

TABLE 3

Results for open ocean water after trace metal concentration onto PVP-8-quinolinol

Element	Concentration (ng ml ⁻¹)	
	PVP-8-quinolinol ^a	Accepted value
Cd	0.014 ± 0.001	0.030 ± 0.002
Pb	0.12 ± 0.01	0.09 ± 0.01
Zn	0.19 ± 0.01	0.20 ± 0.02
Cu	0.09 ± 0.01	0.12 ± 0.01
Fe	0.170 ± 0.005	0.18 ± 0.04
Mn	0.025 ± 0.001	0.023 ± 0.003
Ni	0.28 ± 0.01	0.27 ± 0.01
Co	ND	0.004 ± 0.001
Cr	ND	0.16 ± 0.03

^aMean and standard deviation of three determinations with a 30-fold preconcentration.

its low concentration, and recovery of chromium was too poor (Table 1) to permit quantitative measurement of this element.

The PVP substrate thus provides an alternative medium to silica on which to immobilize 8-quinolinol for the preconcentration of trace metals. However, the resin is as time and labor-consuming to prepare as its silica counterpart and, although the substrate does not hydrolyze at high pH, the 8-quinolinol bleeds from the polymer because of hydrolysis of the silanol linkages.

Merrifield resin-8-quinolinol

Attachment of 8-quinolinol onto chloromethylated polystyrene (Merrifield resin) via a Friedel-Crafts acylation results in a resin which is stable at all pH values studied (0-12) and the lifetime of which under normal operating conditions, should be indefinite.

The exchange capacity of this material, determined by batch equilibration with copper(II) at pH 8, was 0.13 mg g⁻¹ (0.002 mmol g⁻¹). Sugii et al. [16] have suggested that when this resin is prepared by Friedel-Crafts acylation of the chloromethylated polystyrene, only a small amount of the desired product is formed. However, about 60% substitution of the chloromethyl groups can be obtained by treating the resin with zinc 8-quinolate in nitrobenzene [16]. Use of the former reaction for preparation of the resin has, no doubt, resulted in low exchange capacity observed here.

Despite the low absolute blank obtained with this resin (Table 2), non-quantitative recoveries of several elements from sea water (Table 1) precluded further investigations.

XE-305-8-quinolinol

The immobilized 8-quinolinol resin prepared by simple nitration, reduction, diazotization and coupling was found to give nonquantitative recovery of several elements (Cd, Cr, Co, Pb) from sea water. It has been postulated

that the hydrophobic nature of the polystyrene matrix may act to prevent interaction of the aqueous ions with the 8-quinolinol groups [17]. That this appeared plausible was substantiated by subsequent studies of an XE-305 resin in which the 8-quinolinol was attached to the polymer by a phenylazo linkage [13]. Quantitative recoveries of all trace metal ions but chromium could be obtained by using this synthesis modification (cf. Table 1).

Although Parrish [17] has commented on the problem of slow exchange kinetics for 8-quinolinol resins utilizing cross-linked polystyrene substrates, this was not apparent in these studies. In fact, recoveries of trace metals from sea water remained quantitative at flow rates up to 16 ml min⁻¹ (the highest studied) for all elements but manganese. Nonquantitative recovery of Mn(II) at higher flow rates was also noted for 8-quinolinol immobilized on silica gel [2]. This is the first element to be lost, as it forms the least stable 8-quinolate of the elements studied.

An exchange capacity of 0.02 mmol g⁻¹ was obtained for this resin, substantially lower than that for similar resins reported in other studies [4, 5, 16]. The low capacity may be attributed to poor yields in the nitration-reduction steps because numerous, apparently unreacted, styrene particles were still visible after these reactions. More severe or lengthy nitration procedures increased the exchange capacity. Preparation of a subsequent batch of this material under the more stringent nitration conditions suggested by Davies et al. [18] resulted in a resin with an exchange capacity of 0.92 mmol g⁻¹, comparable to that reported by other workers for this material [4, 5, 16].

Blanks obtained with this material (Table 2) are comparable to those given with silica-immobilized 8-quinolinol [2], with the significant advantage that all elements can be collected at pH 8.

Results for 750-ml aliquots of the NASS-1 reference material are given in

TABLE 4

Results for NASS-1 after trace metal concentration onto XE-305-8-quinolinol

Element	Concentration (ng ml ⁻¹)	
	XE-305-8-quinolinol ^a	Accepted value ^b
Cd	0.032 ± 0.001	0.029 ± 0.004
Pb	0.042 ± 0.001	0.039 ± 0.006
Zn	0.175 ± 0.007	0.159 ± 0.028
Cu	0.102 ± 0.006	0.099 ± 0.010
Fe	0.21 ± 0.04	0.192 ± 0.036
Mn	0.010 ± 0.001	0.022 ± 0.007
Ni	0.29 ± 0.01	0.257 ± 0.027
Co	0.008 ^c	0.004 ± 0.001
Cr	—	0.184 ± 0.016

^aMean and standard deviation of triplicate determinations on 750-ml aliquots. ^bReference values from [12] giving mean and 95% confidence limits. ^cSingle determination, 375-fold preconcentration.

Table 4. Agreement with accepted values is apparent for all ions but manganese, for which low results were obtained. No attempt was made to determine chromium because of the poor recovery efficiency (Table 1). Non-quantitative recovery of manganese is related to the sample volume processed. No problems were encountered when 300-ml volumes of sea water were used. Despite apparently adequate exchange capacity, manganese is perhaps displaced from the column by the overwhelming excess of magnesium and calcium in samples of large volume.

Of the substrates selected for study, the lightly cross-linked styrene divinylbenzene XE-305 polymer performs most satisfactorily when the 8-quinolinol is immobilized via a phenylazo linkage. Use of this resin provides a simple, fast, accurate and precise technique for the separation and concentration of trace metals from sea water and can be recommended as an alternative to use of silica-immobilized 8-quinolinol, which is more difficult to prepare.

REFERENCES

- 1 G. V. Myasoedova and S. B. Savvin, *Zh. Anal. Khim.*, 37 (1982) 499.
- 2 R. E. Sturgeon, S. S. Berman, S. N. Willie and J. A. H. Desaulniers, *Anal. Chem.*, 53 (1981) 2337.
- 3 J. R. Parrish, *Chem. Ind. (London)*, (1956) 137.
- 4 M. Griesbach and K. H. Lieser, *Angew. Makromol. Chem.*, 90 (1980) 143.
- 5 F. Vernon and H. Eccles, *Anal. Chim. Acta*, 63 (1973) 403.
- 6 R. D. Degeiso, L. G. Donamura and E. A. Tomic, *J. Appl. Polymer Sci.*, 9 (1965) 411.
- 7 J. R. Parrish, *Chem. Ind. (London)*, (1955) 386.
- 8 Z. Slovak and J. Toman, *Fresenius Z. Anal. Chem.*, 278 (1976) 115.
- 9 J. R. Parrish and R. Stevenson, *Anal. Chim. Acta*, 70 (1974) 189.
- 10 Z. Slovak, S. Slovakova and M. Smir, *Anal. Chim. Acta*, 75 (1975) 127.
- 11 M. Griesbach and K. H. Lieser, *Fresenius Z. Anal. Chem.*, 302 (1980) 181.
- 12 S. S. Berman, R. E. Sturgeon, J. A. H. Desaulniers and A. P. Mykytiuk, *J. Mar. Pollut. Bull.*, 14 (1983) 69.
- 13 J. M. Hill, *J. Chromatogr.*, 76 (1973) 455.
- 14 R. E. Sturgeon, S. S. Berman, J. A. H. Desaulniers, A. P. Mykytiuk, J. W. McLaren and D. S. Russell, *Anal. Chem.*, 52 (1980) 1585.
- 15 A. P. Mykytiuk, D. S. Russell and R. E. Sturgeon, *Anal. Chem.*, 52 (1980) 1281.
- 16 A. Sugii, N. Ogawa and M. Hisamitsu, *Chem. Pharm. Bull.*, 26 (1978) 798.
- 17 J. R. Parrish, *Anal. Chem.*, 54 (1982) 1890.
- 18 R. V. Davies, J. Kennedy, E. S. Lane and J. L. Willans, *J. Appl. Chem.*, 8 (1958) 368.

COLLECTION OF TRACE METALS FROM SEA WATER BY COLUMN ELECTROLYSIS FOR NEUTRON ACTIVATION— γ -SPECTROMETRY

RYUJI NAKATA^{a*}, SATOSHI OKAZAKI, TOSHITAKA HORI and
TAITIRO FUJINAGA

*Department of Chemistry, Faculty of Science, Kyoto University, Sakyo-ku, Kyoto 606
(Japan)*

(Received 25th September 1982)

SUMMARY

Electrolysis on a carbon-fiber column electrode is evaluated for the collection of trace metals from sea water, as a preliminary step to the simultaneous determination of the metals by neutron activation/ γ -spectrometry. The sea-water sample is passed through the carbon-fiber column to which is applied a suitable negative potential. After the electrolysis, the carbon fiber electrode is removed and irradiated in a nuclear reactor, and the induced radioactivity is measured. The effects of the pH of the sample solution on electrolysis are described. Results are reported for gold, cadmium, copper, molybdenum, uranium and zinc. The collection efficiency for uranium and chromium by electrolysis is improved by increasing the pH of the sea-water sample.

In environmental chemistry and in geochemistry, increasing attention is being given to clarifying not only the concentration levels but also the chemical behavior of trace elements in the hydrosphere. Yet, despite the significant developments of modern instrumental methods of analysis, determinations of trace metals in sea water generally require preliminary separation or concentration steps because of their extremely low concentration levels and because of the interferences of major electrolytes or organic components. Accordingly, the procedures tend to be tedious.

Neutron activation/ γ -spectrometry is excellent in terms of its sensitivity and the possibility of determining many elements simultaneously in small samples. However, in the case of sea waters, this method has the disadvantage that the irradiated sample must be desalinated and solidified. Thus far, the application of neutron activation techniques to sea water has been studied after various preconcentration processes, e.g., liquid–liquid extraction or chelating ion-exchange resin [1–3].

The use of electrodeposition techniques for the concentration of radioisotopes is common in radiochemistry [4, 5]. But, there have been only a few reports concerning the application to sea water of controlled-potential

^aPresent address: Department of Chemistry, Faculty of Education, Fukui University, Fukui 910, Japan.

electrolytic separation prior to neutron activation: trace gold and indium have been electrodeposited from sea water [6] and electrolytic separation of trace elements on a mercury pool has been used after irradiation of freeze-dried sea water [7].

Methods of rapid electrolytic separation based on flow coulometry with a glassy carbon column electrode have been developed [8–10]. This method, termed “coulopotentiography”, has been successfully utilized for the automatic determination of copper and lead in sea water at sub- $\mu\text{g l}^{-1}$ levels [11]. The present paper is concerned with a simple, highly sensitive and simultaneous determination of trace metals in sea water; column electrolysis is used for separation and concentration before neutron activation and γ -spectrometry.

EXPERIMENTAL

Apparatus

Controlled-potential flow electrolysis was achieved with a column electrode (Fig. 1) and a potentiostat (Shibata Kagaku Co.); a three-electrode configuration was used. The working electrode (a) of carbon fiber (Torayca M40, Toray Co., Tokyo) was tightly packed in a porcelain tube (d) and carbon tubes (e), and connected to the potentiostat by leads attached to the carbon tubes. A counter electrode (b) of platinum wire was wound around the outside of the porcelain tube. To avoid any contamination by metals, a quinhydrone electrode was used as the reference electrode (c); it was connected to the column by a salt bridge filled with the supporting electrolyte. This reference electrode was prepared as follows: equimolar amounts of *p*-benzoquinone and *p*-dihydroxybenzene purified by sublimation were added to weakly acidified redistilled water, and a platinum wire cleaned by washing with hot nitric acid solution was immersed in this solution. As the potential of this electrode was not very stable, the applied potential was corrected vs. a silver/silver chloride electrode before and after use. So that as many elements as possible could be deposited on the electrode, the applied potential was chosen as -1.5 V vs. Ag/AgCl. Sample solutions and counter electrolyte were propelled with Mini-micro pumps (Kyowa Seimitsu Co.). A schematic diagram of the flow electrolysis system is shown in Fig. 2. Coulopotentiography was examined by scanning the electrode potential in this system.

For neutron activation, the loaded carbon fiber (see below) was irradiated for 60 min in the pneumatic tube of KUR (Research Reactor Institute, Kyoto University) at a neutron flux of 10^{12} n cm $^{-2}$ s $^{-1}$; it was then cooled for a week. The γ -ray spectra were measured with a Ge(Li) detector (active volume 46 cm 3) coupled to a NAIG 4096-channel analyzer which was equipped with open magnetic tapes. All data were treated on a Okitac 50 mini-computer.

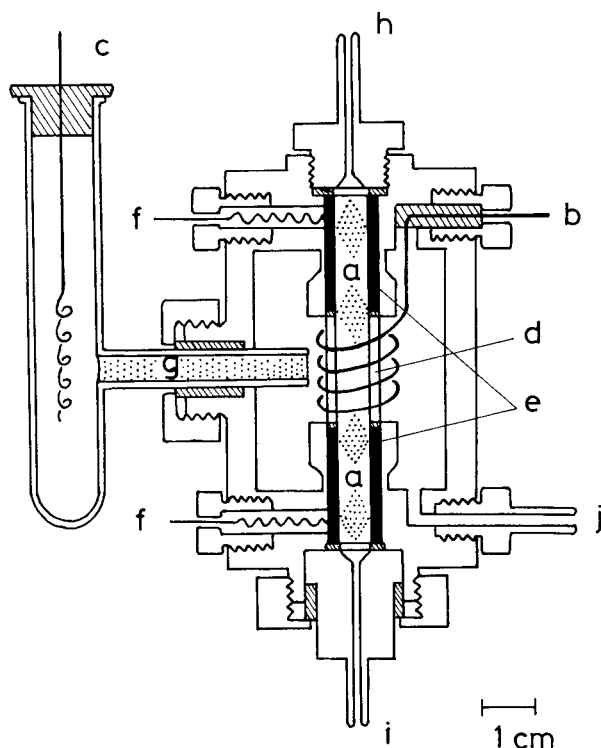


Fig. 1. Column electrode system: (a) carbon fibers; (b) platinum wire; (c) quinhydrone electrode; (d) porcelain tube; (e) carbon tubes; (f) leads; (g) agar bridge; (h) sample outlet; (i) sample inlet; (j) counter electrolyte inlet.

Reagents

An ammonium acetate solution for cleaning electrodes was prepared as follows: 68 ml of 14.7 M ammonia solution (reagent for the determination of toxic metals, Wako Pure Chemical Industries) and 57 ml of anhydrous acetic acid (Suprapur, Merck) were diluted with purified water to 1 l. Unless otherwise noted, all chemicals were of analytical-reagent grade. Standard solutions of the metals of interest were prepared by dissolving the pure metal or their salts in appropriate acids. Water purified by distillation and ion-exchange resin was used throughout the work.

Procedure

The sea-water samples, taken from the Pacific Ocean 7 km off-shore from Shirahama, were filtered through clean 0.4- μ m Nuclepore membrane filters. The pH of the samples was adjusted with acetic acid or ammonia solution. The sample solutions were poured into the polyethylene reservoirs, which had been washed with 6 M hydrochloric acid and rinsed several times with distilled water, and deaerated by bubbling nitrogen. During electrolysis,

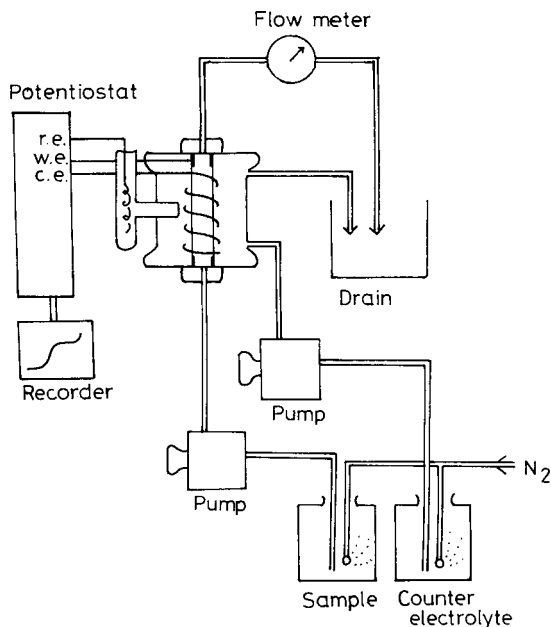


Fig. 2. Schematic diagram of the flow electrolysis system.

the sample solution was supplied to the column at a flow rate of 4 ml min^{-1} . The carbon fiber working electrode was pretreated electrochemically by applying $+0.4 \text{ V}$ and then scanned to -1.0 V in the flowing electrolyte solution. This procedure was repeated several times before use. The counter electrolyte, 0.7 M sodium chloride solution, was also pumped into the counter electrode chamber. After the electrolysis, the working electrode was rinsed by introducing 1 M ammonium acetate solution in order to exclude sodium ion, chloride, etc. Then the carbon fiber was pushed out of the column and air-dried. The carbon fiber was wrapped in clean polyethylene bags in order to avoid contamination during handling and irradiation. The metal standards for irradiation were made by spotting $50\text{-}\mu\text{l}$ aliquots of standard solutions containing Co, Cr, Sb and U on a Millipore filter paper. The air-dried filter paper was also wrapped in polyethylene bags. Both carbon fiber and filter paper were placed in the central part of the capsules so as to minimize errors caused by the neutron flux gradient within the irradiation capsules. The capsules were irradiated for 60 min (see above). The error caused by the flux gradient is estimated to be $\pm 5\%$ at most with this arrangement.

RESULTS AND DISCUSSION

In coulopotentiography with a column electrode, the depolarizer pumped into the column is electrolyzed rapidly and quantitatively, if the electrode

potential is selected properly on the limiting current plateaux. The following equation is derived from differentiation of the Faraday law:

$$I_l = dQ/dt = d(FnCv)/dt = FnC \, dV/dt = FnCf \quad (1)$$

where I_l is the limiting current, Q is the quantity of electricity, F is the Faraday constant, n is the number of electrons gained or lost per molecule in the electrode reaction, V is the volume of the electrolysis solution, and f is the volume flow rate. The limiting currents were measured from current–potential curves (coulopotentiograms) obtained in the same manner as in polarography. Thus, the concentration of the depolarizer could be directly calculated from the observed values of the limiting current and the flow rate by Eqn. (1). As an example, the coulopotentiogram recorded for a solution which was 40 μM in Cu^{2+} , Pb^{2+} , and Cd^{2+} in sea water (pH 4) is shown in Fig. 3. From the flow rate and the limiting currents measured in Fig. 3, the concentrations of these ions could be estimated by Eqn. (1). These calculated values agreed well with the true values.

The number of elements determined in this way was limited in terms of reversibility or reduction potential in the electrode reaction. For example, the direct determination of traces of zinc ions by coulopotentiography was difficult, owing to the very negative reduction potential of zinc and the high background current, but zinc can be quantified by application of neutron activation to the electrode, provided that it has been electrodeposited quantitatively on the carbon fiber electrode. The preconcentration method with

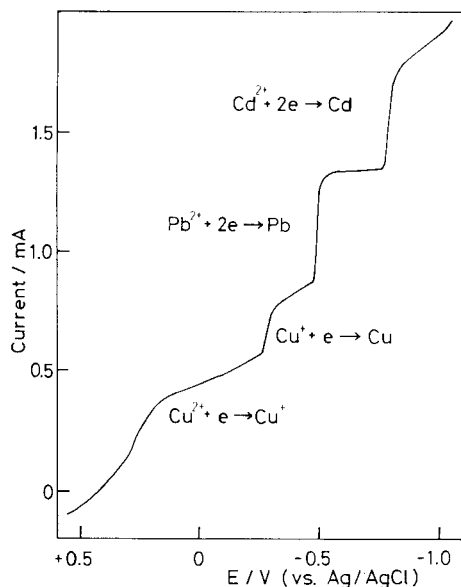


Fig. 3. Coulopotentiogram of a mixture of Cu^{2+} , Pb^{2+} and Cd^{2+} (40 μM each) in acidified sea water (pH 4.0). Scan rate 1 mV s^{-1} ; flow rate 3.16 ml min^{-1} .

The results obtained for several trace metals in sea water, estimated on the assumption of quantitative electrolytic collection are listed in Table 1. The concentrations estimated for copper, zinc and uranium are in reasonably good agreement with values reported in the literature [12]. Though a comparison with values obtained by application of another method to the same sample would be desirable to validate these values, the utility of the proposed method in sea-water analysis is evident. The electrode reactions of metal ions such as Cu^{2+} , Cd^{2+} and Zn^{2+} , are simple electrochemical reduction steps to their metallic states. However, more complicated deposition processes would be expected to occur during the collection of U, Cr and Mo.

The coulopotentiographic behavior of uranyl and chromate ions at the carbon fiber column electrode is shown in Fig. 5. Uranyl ion gave a two-electrode irreversible reduction wave at $E_{1/2} = -0.62$ V vs. Ag/AgCl. The electrolysis efficiency for uranyl ion was estimated absolutely as 108% at pH 8.4, according to Eqn. (1), and an anodic stripping peak was observed at -0.23 V in the anodic potential scan after electrolysis at -1.0 V. This reduction wave probably corresponds to the reduction of U(VI) to U(IV),

TABLE 1

Results obtained for a sea-water sample

Element	Isotope	γ -Energy used for determination (keV)	Concentration ($\mu\text{g l}^{-1}$)	
			This work	Literature data [12]
Au	^{198}Au	411.8	0.0009	0.004
Cd	$^{115\text{m}}\text{In}$	336.3	1.1	0.11
Cu	^{64}Cu	511.0	1.6	3.0
Mo	$^{99\text{m}}\text{Tc}$	140.3	1.5	10.0
U	^{239}Np	106.1, 228.2, 277.6	Ave. 1.2	3.0
Zn	^{65}Zn	1115.4	5.8	10.0

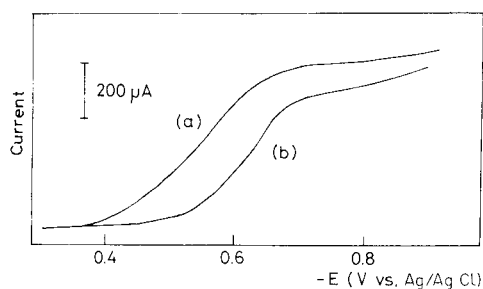


Fig. 5. Coulopotentiograms of chromate and uranyl ions: (a) $50 \mu\text{M}$ chromate in sea water (pH 9.2); (b) $50 \mu\text{M}$ uranyl in sea water (pH 8.4).

the U(IV) then being collected as hydroxide or oxide similarly to other actinides [4]. Chromate ion gave a three-electron irreversible wave at $E_{1/2} = -0.54$ V with an efficiency of 98%, but under the conditions used no anodic stripping peak was observed in the anodic scan. In alkaline solution, chromium(VI) was reduced to Cr(III) and collected as the hydroxide, $\text{Cr}(\text{OH})_3$ [13, 14]. In case of molybdenum, neither reduction waves nor anodic stripping peaks could be observed in cyclic coulopotentiograms with the carbon column electrode. The formation of a surface film of either $\text{MoO}_2 \cdot 2\text{H}_2\text{O}$ [15, 16] or a $\text{HMo}(\text{VI})$ species [17] at a mercury electrode has been reported, but the electrochemical behavior of molybdenum is not well established in alkaline solution.

The relationships between the electrolysis-collection efficiency and the pH of sea-water samples, to which small amounts of Cr, Mo, U and Au were added, were investigated. The γ -spectra of the spiked acidic and alkaline sea water are shown in Fig. 6. There are some distinct differences between these two spectra; in particular, the peaks from chromium and uranium are small or insignificant in the spectrum of acidic sea water. Figure 7 illustrates the relationships between the electrolysis-collection efficiency of these metals and the pH of the samples. The collection efficiency for chromium and especially uranium increases significantly at $\text{pH} > 8$; these results could be explained by the formation of hydroxides of chromium or uranium at the surface of the electrode in alkaline solution. From spectrophotometric determinations on sea water which was $10 \mu\text{M}$ in uranyl ion and was concentrated by column electrolysis, the collection efficiency was estimated as 93–99% for untreated sea water and as 95–99% for alkaline sea water at pH 9.0. However, for the deposition of molybdenum and gold reproducible recoveries could not be obtained even under the same electrolysis conditions.

Though a more detailed study is required to clarify the collection behavior of these metals, it is apparent that many elements can be collected at the surface of the electrode by flow column electrolysis with deposition or adsorption. The method has attractive features for the preconcentration of trace metals in the hydrosphere, particularly for highly saline samples such as sea water.

The authors thank the Research Reactor Institute, Kyoto University, for the neutron activation facilities. Thanks are also due to Professor Mutsuo Koyama and Rokuji Matsushita for their continuing interest and encouragement.

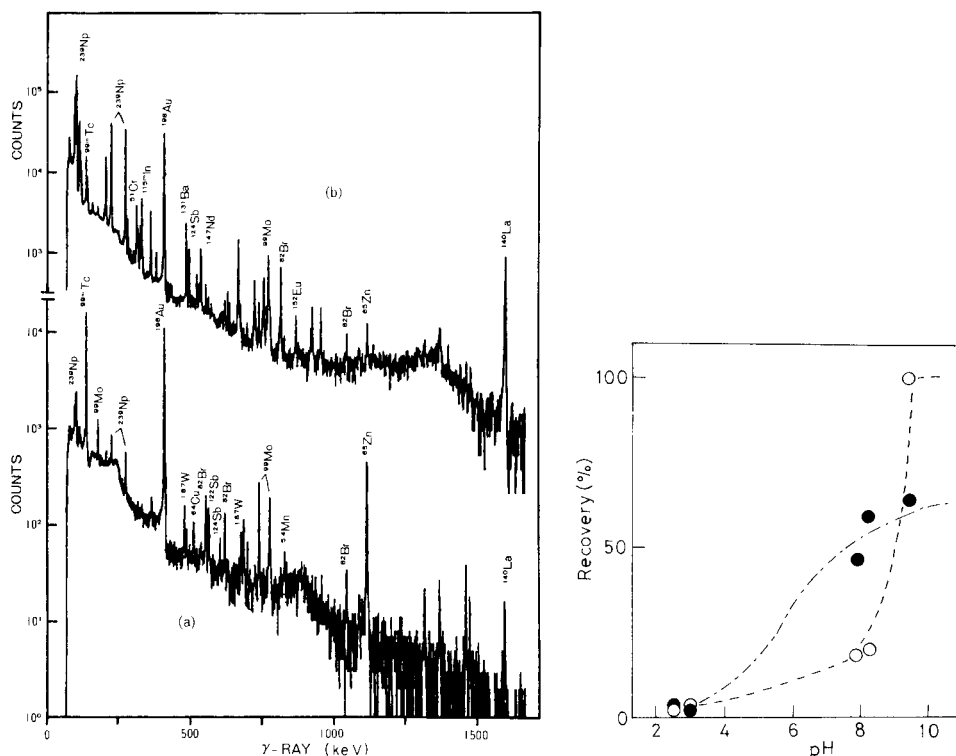


Fig. 6. γ -Spectra of a sea-water sample preconcentrated on carbon fiber: (a) 1 l of sea water acidified to pH 3.0; (b) 1 l of sea water made alkaline to pH 9.4. Counting time 5000 s; concentration potential -1.5 V vs. Ag/AgCl; internal standards added were $0.5 \mu\text{g l}^{-1}$ Au, $138 \mu\text{g l}^{-1}$ Mo, $10.6 \mu\text{g l}^{-1}$ Cr, $33 \mu\text{g l}^{-1}$ U.

Fig. 7. Effect of pH on the recovery of (○) uranium and (●) chromium with column electrolysis.

REFERENCES

- 1 J. M. Rottschäfer, R. J. Boczkowski and H. B. Mark, Jr., *Talanta*, 19 (1972) 163.
- 2 Y. Kusaka, H. Tsuji, S. Imai and S. Ohmori, *Radioisotopes*, 28 (1979) 139.
- 3 C. Bergerioux, J. P. Blanc and W. Haerdi, *J. Radioanal. Chem.*, 37 (1977) 823.
- 4 R. F. Mitchell, *Anal. Chem.*, 32 (1960) 326.
- 5 N. A. Talvitie, *Anal. Chem.*, 44 (1972) 280.
- 6 Y. Tateno and N. Ohta, *Bunseki Kagaku*, 28 (1979) 666.
- 7 K. Jørstad and B. Salbu, *Anal. Chem.*, 52 (1980) 672.
- 8 T. Fujinaga, S. Okazaki and T. Yamada, *Chem. Lett.*, (1972) 863.
- 9 T. Yamada, S. Okazaki and T. Fujinaga, *Bull. Inst. Chem. Res., Kyoto Univ.*, 56 (1978) 151.
- 10 T. Fujinaga and S. Kihara, *CRC Crit. Rev. Anal. Chem.*, 6 (1977) 223.
- 11 R. Nakata, S. Okazaki and T. Fujinaga, *Nippon Kagaku Kaishi*, (1980) 1615.
- 12 E. D. Goldberg, in J. P. Riley and G. Skirrow (Eds.), *Chemical Oceanography*, 1st edn., Academic Press, London, 1965, p. 164.
- 13 Kh. Z. Brainina, *Talanta*, 18 (1971) 513.
- 14 G. E. Batley and J. P. Matousek, *Anal. Chem.*, 52 (1980) 1570.
- 15 P. Lagrange and J. P. Schwing, *C. R. Acad. Sci., Ser. C*, 263 (1966) 848.
- 16 P. Lagrange and J. P. Schwing, *Bull. Soc. Chim. Fr.*, (1968) 536.
- 17 K. Ogura and Y. Enaka, *J. Electroanal. Chem.*, 95 (1979) 169.

BESTIMMUNG VON REFRAKTÄRMETALLEN IN PFLANZLICHEM MATERIAL DURCH RÖNTGENFLUORESZENZANALYSE NACH ANREICHERUNG

H. F. HAAS und V. KRIVAN*

Sektion Analytik und Höchstreinigung, Universität Ulm, D-7900 Ulm-Donau (B.R.D.)

H. M. ORTNER

Metallwerk Plansee GmbH., A-6600 Reutte/Tirol (Österreich)

(Eingegangen den 15. September 1982)

SUMMARY

(Determination of refractory metals in plant material by x-ray fluorescence spectrometry after preconcentration.)

An x-ray fluorescence spectrometric method is described for determining molybdenum, tungsten, niobium and tantalum in plant material. The sample is decomposed with nitric acid, hydrogen peroxide and hydrofluoric acid, and the refractory metals are collected on an anion-exchange paper and quantified by wavelength-dispersive x-ray fluorescence spectrometry. The decomposition of the sample and the enrichment of the elements on the ion-exchange paper including the mutual interference of the elements were investigated by using the radiotracer technique. In all cases, recoveries exceeded 95%. For about 1 g of sample material, limits of detection between $0.3 \mu\text{g g}^{-1}$ (Mo) and $0.6 \mu\text{g g}^{-1}$ (Ta) are achieved. After the same decomposition procedure, molybdenum was also determined by flame atomic absorption spectrometry; the sensitivity was $0.7 \mu\text{g ml}^{-1}$ for 1% absorption. The results for molybdenum and tungsten obtained on different grass samples are discussed in detail. The accuracy of the technique was checked for molybdenum and tungsten by instrumental neutron activation analysis; the results agreed within 5–11%.

ZUSAMMENFASSUNG

Es wurde ein röntgenfluoreszenzspektrometrisches Verbundverfahren zur Bestimmung von Molybdän, Wolfram, Niob und Tantal in Gras und anderem pflanzlichen Material entwickelt. Das Verfahren beruht auf dem Aufschluß der Probe unter Verwendung von HNO_3 , H_2O_2 und HF, der Anreicherung der interessierenden Elemente an stark basischen Anionenaustauscherpapieren und ihre Bestimmung durch wellenlängendispersive Röntgenfluoreszenzspektrometrie. Sowohl der Aufschluß als auch die Anreicherung wurden mit Hilfe der Radiotracertechnik überprüft. Bei der Anreicherung wurde auch die gegenseitige Beeinflussung der Elemente bezüglich ihrer Ausbeuten untersucht. In allen Fällen lagen die Ausbeuten über 95%. Bei einer Einwaage von etwa 1 g liegen die Nachweisgrenzen zwischen $0,3 \mu\text{g g}^{-1}$ (Mo) und $0,6 \mu\text{g g}^{-1}$ (Ta). Nach dem Aufschluß wurde Molybdän auch mit der Atomoabsorptions-Spektrometrie (Flamme) bestimmt, wobei eine Empfindlichkeit von $0,7 \mu\text{g ml}^{-1}$ (1% Absorption) erreicht wurde. Ergebnisse von mit Molybdän und Wolfram belasteten Mischgrasproben werden diskutiert. Eine Kontamination mit Niob und Tantal wurde nicht festgestellt. Die Richtigkeit für Molybdän und Wolfram wurde mit der instrumentellen Neutronenaktivierungsanalyse überprüft. Dabei wurde eine Übereinstimmung der Ergebnisse innerhalb von 5 bzw. 11% erzielt.

Als Bestandteil der Enzyme Xanthinoxidase und Aldehydoxidase ist Molybdän eines der essentiellen Spurenelemente für Menschen und Säugetiere [1, 2]. Aus diesem Grunde ist die Zufuhr geringer und dem Bedarf entsprechender Mengen an Molybdän über die Nahrung notwendig. Andererseits treten bei der Zufuhr von sehr viel höheren Molybdänmengen toxische Wirkungen auf.

Die Herstellung sowie die Anwendung von Molybdän in weiten Bereichen der Industrie kann erhebliche lokale Belastungen der Umwelt durch dieses Element zur Folge haben. Zur Belastung von pflanzlichen und tierischen Organismen können bisweilen auch molybdänreiche Böden beitragen. Unter den verschiedenen Tierarten wurde bei Wiederkäuern eine besonders starke toxische Wirkung von Molybdän festgestellt [1, 3, 4]. Allgemeine Symptome einer Molybdänintoxikation bei Wiederkäuern sind Gewichtsverlust, verminderte Milchleistung, Anämie, Infertilität, Osteoporose, Gelenkveränderungen, schwere Gastroenteritis, Koma und Tod durch Herzversagen. Schwere Molybdänose bei Rindern kommt unter speziellen Umweltbedingungen in vielen Teilen der Welt vor, wobei vor allem Milchrassen und Kälber am anfälligsten sind. Sie tritt bei einem Molybdängehalt des Futters von 20 bis 100 $\mu\text{g g}^{-1}$ (bezogen auf Trockenbasis) auf, während mit 3–5 $\mu\text{g g}^{-1}$ noch nahezu gesundes Futter vorliegt [5]. Eine Vergiftung mit Molybdän hängt außerdem noch von dessen chemischer Form ab und wird beeinflusst durch Sulfat, Cu^{2+} , Zn^{2+} , Pb^{2+} und die Proteinaufnahme [6]. Wichtig ist vor allem die Form und Menge von Kupfer und der organisch gebundene Schwefel, z. B. im Cystin und Methionin im Körper. In der Literatur wird eingehend ein Molybdän–Kupfer Antagonismus beschrieben [4, 6, 7].

Ähnlich wie bei Molybdän ist auch eine toxische Wirkung von Wolfram für Wiederkäuer bekannt [4, 6]. Eine akute Wolframvergiftung äußert sich bei diesen Tieren durch nervöse Erschöpfung, Durchfälle, Atemlähmung und schließlich Tod. Insgesamt ist Wolfram jedoch weit weniger toxisch als Molybdän [6].

Für Niob und Tantal konnte keine essentielle Wirkung auf den tierischen und menschlichen Organismus, bzw. eine Beteiligung an spezifischen enzymatischen Systemen nachgewiesen werden. Insgesamt sind Studien über den Metabolismus dieser beiden Elemente selten [6, 8].

Die Bestimmung dieser Elemente in Futter, besonders von Molybdän und Wolfram in Gras, ist für Refraktärmetallbetriebe und Umweltschutzbehörden wichtig. Jedoch stehen kaum verlässliche Analysenverfahren zur Verfügung, die genügend nachweisstark und für den routinemäßigen Einsatz geeignet wären. Für die Bestimmung von Refraktärmetallen in biologischem Material hat sich in bezug auf Empfindlichkeit und Richtigkeit die Neutronenaktivierungsanalyse sehr gut bewährt [9–11]. Der industriellen Anwendbarkeit dieser Methode sind aber durch die Notwendigkeit eines Kernreaktors und eines radiochemischen Labors Grenzen gesetzt.

Am häufigsten wurde bisher zur Molybdän- und Wolframbestimmung in biologischem Material die Lösungsabsorptionspektrometrie [12] ange-

wendet. Zur Bestimmung von Molybdän wird außerdem auch die Flammen-Atomabsorptions-Spektrometrie (AAS) [13, 14] benutzt. In Verbindung mit einer spezifischen Abtrennung, bzw. Anreicherung können damit Nachweisgrenzen in der Größenordnung von $0,1\text{--}1\text{ }\mu\text{g g}^{-1}$ Probenmaterial erreicht werden. Für Wolfram-, Niob- und Tantal-Spuren unter $100\text{ }\mu\text{g g}^{-1}$ ist die Flammen-Atomabsorptions-Spektrometrie zu unempfindlich. Von großer Bedeutung ist auch die Wahl eines geeigneten Aufschlußverfahrens.

In der vorliegenden Arbeit wird ein röntgenfluoreszenzspektrometrisches (RFS) Verfahren beschrieben, das die Bestimmung der Refraktärmetalle in Gras und anderen pflanzlichen Materialien noch im $0,1\text{ }\mu\text{g g}^{-1}$ -Bereich erlaubt. Zur Bestimmung von Molybdän wurde auch die Flammen-Atomabsorptions-Spektrometrie eingesetzt.

EXPERIMENTELLER TEIL

Reagenzien

Es wurden HNO_3 (65%, Suprapur) und HF (40%, Suprapur), H_2O_2 (30%, pro analysi), alle bezogen von Merck (Darmstadt) sowie in Quarz bidestilliertes Wasser verwendet. Lösungen von Molybdän, Wolfram, Niob und Tantal wurden durch Auflösen des reinen Metalls (Max-Planck-Institut für Metallforschung, Stuttgart) in HF/HNO_3 (9:1) erhalten.

Geräte

Probenhomogenisierung. Mikrodismembrator II (Braun, Melsungen) mit zylindrischem Teflongefäß (20 ml) und einer teflummantelten Homogenisationskugel.

Anreicherung von Refraktärmetallspuren am Ionenaustauscherpapier. Swinnex-Filtrationsaufsatz (Millipore, Molsheim, Frankreich) mit zugehöriger 50-ml Polyethylen-Spritze.

Röntgenfluoreszenzspektrometrie. Siemens-Sequenz-Röntgenspektrometer SRS 1. Meßparameter: Rhodium-Anode, Arbeitsbereich bei 45 kV und 30 mA; LiF (200) Kristall; Szintillationszähler mit NaI (Tl)-Kristall, Arbeitsbereich bei 1250 V; Impulshöhenanalysator durch Differentialeinstellung mit Fensterbreite bei $1,5 \times$ Halbwertsbreite; 40 s Meßzeit. Verwendete Analysenlinien: $K_{\alpha 1,2}$ für Mo und Nb; $L_{\alpha 1}$ für W und Ta.

Atomabsorptionsspektrometrie. Perkin Elmer Modell 400. Meßparameter für Molybdän: 313,3 nm; 0,7 nm Spalt; Einzelhohlkathodenlampe für Molybdän; $\text{N}_2\text{O/C}_2\text{H}_2$ Flamme; 2-s Integrationszeit; Messung mit Deuteriumkompensation und Schreiberaufzeichnung.

Aktivitätsmessungen. Ein Meßplatz (Berthold, Wildbad) bestehend aus einem 77×77 mm NaI(Tl) -Detektor, einem Einkanalanalysator und einem automatischen Probenwechsler. Ein Gammaskpektrometer bestehend aus einem Ge(Li) -Detektor und einem Multikanalanalysator (Canberra, Frankfurt) mit den folgenden Parametern für die 1,332-MeV Linie: Energieauflösung = 1,9 keV, Peak/Compton-Verhältnis = 40:1, relative Effizienz bezüglich eines 77×77 mm NaI -Detektors = 20%.

Probennahme und -vorbehandlung

Es wurden sowohl Grasproben aus einem Reinstgebiet als auch aus einem mit hochschmelzenden Metallen belasteten Gebiet entnommen. Das Gras wurde jeweils etwa 1 cm oberhalb des Erdreiches mit einem Plastikmesser abgeschnitten. Die Grasproben wurden 4 Stunden bei 110°C im Trockenschrank getrocknet. Zur kontaminationsfreien Homogenisierung der Proben wurde ein Mikrodismembrator II verwendet. Die Proben wurden dabei zuerst im Homogenisationsgefäß in flüssigem Stickstoff vorgekühlt und über 4 min bei maximaler Amplitude (1,5 cm) homogenisiert.

Traceruntersuchungen

Die Aufschluß- und Anreicherungsverfahren wurden in bezug auf Ausbeute mit Hilfe der Tracertechnik überprüft und optimiert. Die Radiotracer ^{99}Mo , ^{182}Ta und ^{187}W wurden durch eine 4-tägige Bestrahlung von eingedampften Lösungen reiner Metalle mit Neutronen eines thermischen Flusses von $8 \times 10^{13} \text{ n cm}^{-2} \text{ s}^{-1}$ im FR-2 Reaktor des Kernforschungszentrums Karlsruhe hergestellt. Die spezifischen Aktivitäten am Bestrahlungsende betrugen für ^{99}Mo $0,5 \mu\text{Ci } \mu\text{g}^{-1}$, für ^{182}Ta $6 \mu\text{Ci } \mu\text{g}^{-1}$ und für ^{187}W $100 \mu\text{Ci } \mu\text{g}^{-1}$. Sie wurden durch Zugabe von inaktivem Träger nach Bedarf verdünnt. Bei den Tracerexperimenten wurden immer zu 1 g homogenisierter Probe vor dem Aufschluß die entsprechenden Tracer- und Trägermengen zugesetzt. Die Ausbeuten wurden durch Messung der Radioaktivität der Aufschlußlösung (Überprüfung der Anreicherung der Elemente am Ionenaustauscherpapier) ermittelt. Die Aktivitätsmessungen wurden mit dem NaI(Tl)-Bohrlochdetektor in Verbindung mit dem Einkanalanalysator ausgeführt. Der statistische Fehler der Aktivitätsmessung war dabei kleiner als 3%. Bei Gras wurde zusätzlich auch die in situ Markierung durch Bestrahlung durchgeführt und die Aktivität mit dem hochauflösenden Gammaspektrometer gemessen.

Probenaufschluß

Die homogenisierte Grasprobe (1 g) wurde in einem 100-ml Erlenmeyerkolben zusammen mit 20 ml HNO_3 (65%) vorsichtig erhitzt (starkes Schäumen). Nach Abklingen der Schaumbildung erfolgte tropfenweise Zugabe von 7 ml H_2O_2 (30%). Nach Eindampfen bis fast zur Trockene wurde dieses in 7 ml HNO_3 (65%) und 2 ml H_2O_2 (30%) aufgenommen und bis zum Sieden erhitzt. Nach 3 min wurde die Lösung in einen 100-ml Teflonbecher gegossen. Um ein quantitatives Lösen des Rückstandes zu erreichen, wurde anschließend noch zweimal mit neuen Mischungen aus 7 ml HNO_3 und 2 ml H_2O_2 wie oben erhitzt und jeweils im Teflonbecher gesammelt. Die 27 ml der HNO_3 - H_2O_2 -Lösung wurden unter weiterer Zugabe von wenigen Milliliter H_2O_2 eingedampft. Der Rückstand wurde in 10 ml HF (40%)/ HNO_3 (65%) (1:1) und 3 ml H_2O_2 (30%) aufgenommen und eingedampft. Nach Aufnahme des verbleibenden Rückstandes in 10 ml HF (40%) erfolgte erneutes Eindampfen. Diese Trockene wurde nun in 30 ml 2%-iger HF unter leichtem Erhitzen und Umrühren aufgelöst. Ein kleiner möglicher Rückstand wurde durch

Filtrieren oder Dekantieren von der Probenlösung abgetrennt. Die erhaltene Probenlösung konnte zur Bestimmung von Molybdän, Wolfram, Niob und Tantal durch RFS oder von Molybdän durch AAS verwendet werden.

Bestimmung von Mo, W, Nb und Ta mit RFS nach Anreicherung am Anionenaustauscherpapier

Es wurden kreisrunde Scheiben von 25 mm Durchmesser aus einem Bogen des Anionenaustauscherpapiers SB-2 (Serva, Heidelberg) ausgeschnitten. Zur Überführung der Chlorid- in die Fluoridform wurden die ausgeschnittenen Scheiben in 4% HF solange vorbehandelt, bis mit 1% AgNO_3 -Lösung im Waschwasser kein Chlorid mehr nachgewiesen werden konnte. Schließlich wurden die Ionenaustauscherpapiere mit bidestilliertem Wasser ausgewaschen und in 2% HF-Lösung aufbewahrt. Zur Ausführung des Ionenaustausches wurde eine Filtrationsapparatur verwendet, die sich schon in ähnlicher Form bewährte [15]. Es wurden jeweils zwei Ionenaustauscherpapiere eingelegt. Nach der Anreicherung wurden die Ionenaustauscherpapiere langsam unter einer IR-Lampe getrocknet.

Aufgrund eines etwaigen Konzentrationsgefälles der angereicherten Elemente senkrecht zu den Ionenaustauscherschichten, wurden die Ionenaustauscherpapiere sämtlicher Proben auf beiden Seiten gemessen und aus beiden Messungen der Mittelwert gebildet. Die Eichung für die zu bestimmenden Elemente Molybdän, Wolfram, Niob und Tantal erfolgte über Eichlösungen verschiedener Konzentrationen, die, wie die Lösungen der Grasproben, an Anionenaustauscherpapieren angereichert und gemessen wurden. Die Eichfunktion ist für alle untersuchten Elemente über den Bereich von 0–150 μg eine Gerade. Zur Ermittlung der Blindwerte wurden die Aufschluß- und Anreicherungsprozeduren nur mit den Reagenzien durchgeführt. Dieselben Blindwerte ergaben sich für das reine Filterpapier nach Überführung in die Fluoridform.

Bei der Bestimmung von Molybdän in Gras durch AAS konnte die vom Hersteller angegebene reziproke Empfindlichkeit von $0,5 \mu\text{g ml}^{-1}$ (1% Absorption) nicht ganz erreicht werden; sie lag bei $0,7\text{--}0,8 \mu\text{g ml}^{-1}$ (1% Absorption). Dies ist offenbar auf den Einfluß von in der Probenlösung anwesenden Begleitkomponenten zurückzuführen. Die Empfindlichkeit ist überdies sehr vom Verhältnis $\text{N}_2\text{O}:\text{C}_2\text{H}_2$ abhängig. Um ein zu schnelles Zuwachsen des Brenners zu vermeiden, wurde mit einer eher lachgasreichen Flamme gearbeitet.

ERGEBNISSE UND DISKUSSION

Das Analyseverfahren

Die Traceruntersuchungen zur Überprüfung des Aufschlusses wurden an 1 g Gras, das etwa $50 \mu\text{g g}^{-1}$ von jedem der Elemente Molybdän, Wolfram und Tantal enthielt, durchgeführt. Aus Tabelle 1 ist ersichtlich, daß die Ausbeuten und ihre Streuung den Anforderungen der quantitativen Spurenanalyse völlig genügen, und daß bei den einzelnen Elementen praktisch keine Unterschiede bezüglich der Ausbeute festzustellen sind.

TABELLE 1

Ausbeuten für Mo, Ta und W beim Aufschluß

Element	Mo	Ta	W
Ausbeute (%) ^a	95,5 ± 1,8	95,1 ± 1,2	95,6 ± 1,4

^aMittelwert und mittlere Abweichung aus 3 Experimenten.

Die auf der in situ Markierung basierenden Tracerexperimente zeigten, daß der geringe nicht aufgeschlossene Probenrest lediglich einen vernachlässigbar kleinen Anteil der fraglichen Elemente von weniger als 3% der Gesamtmenge enthält. Diese zusätzlichen in situ Experimente waren erforderlich, da die herkömmliche Markierung mit Tracerlösungen keine eindeutige Aussage über die im Probenrest eventuell verbleibenden Elementanteile zuläßt. Die Ergebnisse der Untersuchung des Anreicherungs-schrittes am Ionenaustauscherpapier sind in Tabelle 2 zusammengestellt. Für Molybdän und Wolfram wurde die Anreicherung am Ionenaustauscherpapier bei zwei unterschiedlichen Mengen untersucht: 1 µg und 100 µg. Es ist ersichtlich, daß die Ausbeute bei der Anreicherung in dem untersuchten Bereich von der Elementmenge unabhängig ist. Die etwas niedrigeren Ausbeuten für Molybdän im Vergleich mit Tantal und Wolfram sind dadurch zu erklären, daß die Verteilungskoeffizienten für Dowex 1-X8 und verdünnte HF-Lösungen in der Reihenfolge $D_{\text{Mo}} < D_{\text{W}} < D_{\text{Nb}} < D_{\text{Ta}}$ ansteigen [16]. Aus dem gleichen Grunde kann man auch annehmen, daß der Einfluß der Elementmenge bei Niob und Tantal noch geringer sein müßte als bei Molybdän und Wolfram. Diesbezüglich erfolgten deshalb mit der Tracertechnik keine weiteren Untersuchungen. Darüberhinaus wurde für Molybdän, Tantal und Wolfram die gegenseitige Beeinflussung der Anreicherung der Elemente untersucht. Hierfür wurde die Anreicherung von 50 µg eines Elements in Anwesenheit jeweils gleicher Mengen der übrigen Elemente durchgeführt. Dabei wurde, wie die Überprüfung mit Hilfe des *t*-Tests ergab, kein meßbarer Einfluß festgestellt (siehe Tabelle 2).

TABELLE 2

Ausbeuten für Mo, Ta und W bei der Anreicherung am Ionenaustauscherpapier

Element	Ausbeute (%) ^a		
	1 ^b	2 ^b	3 ^b
Mo	98 ± 1,2	97,8 ± 1,2	96,6 ± 2,0
W	>99,5	>99,5	>99,5
Ta	—	—	>99,5

^aMittelwert und mittlere Abweichung aus 3 Experimenten. ^b(1) Menge von Mo und W = 100 µg; (2) Menge von Mo und W < 1 µg; (3) Menge von Mo, W und Ta = 50 µg.

Bei der Röntgenfluoreszenzanalyse muß generell mit Matrixeffekten gerechnet werden. Dabei wird einerseits durch Absorption in der Probe die emittierte Strahlung eines Elements geschwächt. Die Schwächung hängt dabei von der Zusammensetzung der Probe ab. Andererseits kann durch Interelementanregung eine Verstärkung der Intensität auftreten. Hierbei wird die Fluoreszenzstrahlung eines Elements neben der Anregung durch die primäre Röhrenstrahlung auch durch Fluoreszenzstrahlung anderer Elemente in der Probe zusätzlich angeregt (Sekundärfluoreszenz). Bei Anreicherung von Elementen an dünnen Schichten (z.B. Filtern, Membranen usw.) treten jedoch solche Matrixeffekte in den Hintergrund [17]. In einer anderen Arbeit [15] wurden Interelementeffekte bei der Bestimmung von Zr, Mo, Hf und W in Niob und Tantal genauer untersucht. Diese zeigen in dem für die vorliegende Problemstellung relevanten Konzentrationsbereich jedoch keinen meßbaren Einfluß. Außerdem bietet die Filtertechnik den Vorteil einer einfachen Standardisierung, da sie die Herstellung probenanaloger Standards ermöglicht. Dadurch bleiben komplizierte Matrixkorrekturen [18, 19] erspart.

Nachweisgrenzen und Empfindlichkeiten für die Bestimmung der vier Refraktärmetalle sind in Tabelle 3 aufgeführt. Wie vorausszusehen, sind die Nachweisgrenzen und Empfindlichkeiten für die Elemente Molybdän und Niob etwas besser als die für Wolfram und Tantal. Dies ist darauf zurückzuführen, daß die Messung für Molybdän und Niob über die K_{α} -Linien und für Tantal und Wolfram über die $L_{\alpha 1}$ -Linien erfolgte. Der für Molybdän und Niob höhere Untergrund spielt eine nur untergeordnete Rolle.

Analyse von Grasproben

Abbildung 1 zeigt als Beispiel ein Röntgenfluoreszenz-Spektrum einer mit Molybdän und Wolfram belasteten Probe. Die in dem Spektrum auftretenden Cu- und Au-Röntgenlinien sind dem Untergrund zuzuschreiben.

In Tabelle 4 sind die Ergebnisse für Molybdän und Wolfram einer Reihe von belasteten Grasproben zusammengestellt. Dabei handelt es sich durchweg um Grasmischproben ohne Pflanzenvorsortierung und um ungewaschenes Probenmaterial. Alle Werte beziehen sich auf die Trockensubstanz der jeweiligen Grasprobe, welche großen Schwankungen unterlag: für Altgras betrug der Anteil an Trockensubstanz zwischen 70 und 85%, für das im Mai

TABELLE 3

Nachweisgrenzen und Empfindlichkeiten von Mo, W, Nb und Ta

Element	Mo	W	Nb	Ta
Nachweisgrenze ^a (μg)	0,3	0,4	0,3	0,6
Empfindlichkeit ($\text{Imp. s}^{-1} \mu\text{g}^{-1}$)	12,7	7,6	15	4,3

^aDreifache Standardabweichung des Untergrunds beim Blindwertversuch.

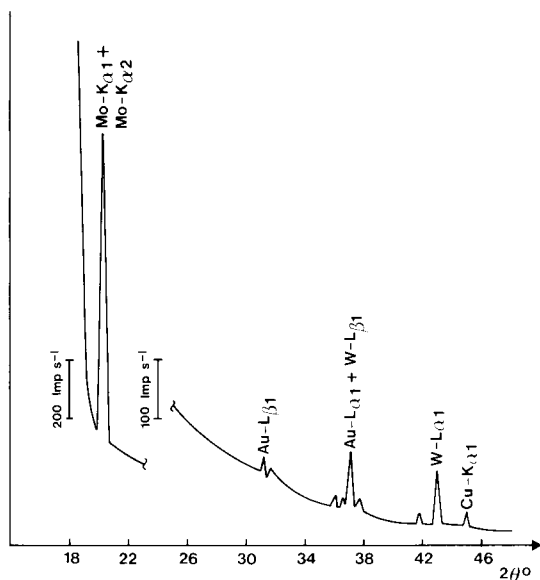


Abb. 1. Röntgenfluoreszenz-Spektrum einer mit Molybdän ($\approx 100 \mu\text{g g}^{-1}$) und Wolfram ($\approx 50 \mu\text{g g}^{-1}$) belasteten Grasprobe.

gesammelte Gras wurden Trockensubstanzgehalte zwischen 20 und 30% festgestellt. Die erhaltenen Ergebnisse weisen eine zum Teil beträchtliche Belastung vor allem durch Molybdän auf. Niob und Tantal konnte in keiner der untersuchten Proben nachgewiesen werden ($\text{Nb} \leq 0,3 \mu\text{g g}^{-1}$, $\text{Ta} \leq 0,6 \mu\text{g g}^{-1}$). Der Molybdän- und Wolframgehalt schwankt mit der Jahreszeit, bzw. den Witterungsbedingungen. Die niedrigsten Werte wurden für Ende April

TABELLE 4

Gehalte von Molybdän und Wolfram in belasteten Grasproben

Probenstelle Nr.	1	2	3	4	5	6	7
Molybdän Gehalt ^a ($\mu\text{g g}^{-1}$)							
24.4 ^b	60	58	53	73	114	81	61
20.5	67	60	48	110	125	75	63
5.8	82	70	62	113	130	103	72
31.8	105	75	115	180	175	185	75
Wolfram Gehalt ($\mu\text{g g}^{-1}$)							
24.4	5	12	12	15	10	5	7
20.5	8	15	17	15	21	14	17
5.8	20	7	13	11	13	15	17
31.8	28	21	25	27	35	36	25

^aMittelwerte aus 4 Einzelbestimmungen. ^bProbensammeldatum, 1981.

erhalten, wo das Altgras durch die vorangegangene Schneeschmelze offensichtlich von anhaftenden Molybdän- und Wolframspuren weitgehend befreit wurde. Relativ niedrige Werte wurden auch noch Ende Mai erhalten, was vermutlich auf eine sehr niederschlagsreiche Witterung zurückzuführen ist. Der relativ schnelle Pflanzenwuchs bewirkt ebenfalls eine entsprechende "Verdünnung" der Schadstoffe. Die höchsten Werte wurden für Molybdän und Wolfram ohne Ausnahme zu Ende der Vegetationsperiode sowie nach einer längeren Schönwetterperiode erhalten. Hier addieren sich die Effekte der Anreicherung von Flugstaub auf den Pflanzen sowie das stagnierende Pflanzenwachstum.

An vier Proben wurde sowohl die RFS als auch die AAS als Endbestimmungsmethode verwendet. Die diesbezüglichen Ergebnisse sind in Tabelle 5 aufgeführt. Da die AAS ohne Voranreicherung an Filterpapier auskommt, ist sie für ein Schnellverfahren geeignet, wenn es darum geht, nur den Molybdängehalt in den belasteten Grasproben zu ermitteln. Nachdem Molybdän der Hauptkontaminant unter den gegebenen Bedingungen ist, kommt dieser Methode im speziellen Fall große praktische Bedeutung zu. Beide Methoden arbeiten mit etwa vergleichbarer Reproduzierbarkeit. Bei der besonders guten Übereinstimmung der RFS- und AAS-Ergebnisse ist allerdings zu berücksichtigen, daß die Endbestimmung durch beide Verfahren jeweils an derselben aufgeschlossenen Probe vorgenommen wurde.

An einer weiteren Grasprobe wurden vergleichende Untersuchungen mittels RFS und instrumenteller Neutronen-Aktivierungsanalyse (INAA) durchgeführt. Dabei wurde für Molybdän ein Gehalt von $92,5 \pm 1,9 \mu\text{g g}^{-1}$ mit RFS und $97,3 \pm 3,8 \mu\text{g g}^{-1}$ mit INAA erhalten. Für Wolfram ergab die Bestimmung mit RFS $40,1 \pm 1,8 \mu\text{g g}^{-1}$ und mit INAA $45,2 \pm 1,8 \mu\text{g g}^{-1}$. Für Tantal lag der mit RFS ermittelte Wert unterhalb der Nachweisgrenze ($<0,6 \mu\text{g g}^{-1}$), während sich mit INAA $0,57 \pm 0,04 \mu\text{g g}^{-1}$ ergaben. Die gute Übereinstimmung der Ergebnisse dieser beiden Verfahren zeigt, daß mit dem entwickelten RFS-Verbundverfahren ein hoher Grad an Richtigkeit erreicht werden kann.

Der Deutschen Forschungsgemeinschaft danken wir (H. F. H. und V. K.) für die Bereitstellung des Atomabsorptions-Spektrometers.

TABELLE 5

Vergleich der durch RFS und AAS erhaltenen Ergebnisse bei der Bestimmung von Molybdän in vier verschiedenen Grasproben

Probe Nr.	1	2	3	4
Gehalt ($\mu\text{g g}^{-1}$) ^a				
RFS	$41 \pm 3,2$	$89 \pm 4,0$	$106 \pm 4,6$	$185 \pm 5,9$
AAS	$42 \pm 2,4$	$86 \pm 3,5$	$110 \pm 3,1$	$185 \pm 3,8$

^aMittelwerte aus 4 Einzelbestimmungen.

LITERATUR

- 1 E. J. Underwood, Trace Elements in Human and Animal Nutrition, 4th edn., Academic Press, New York, 1977.
- 2 E. I. Stiefel, The Coordination and Bio-inorganic Chemistry of Molybdenum, in S. J. Lippard, Ed., Progress in Inorganic Chemistry, Vol. 22, Wiley, New York, 1977.
- 3 J. K. Miller, B. R. Moss, M. C. Bell und N. N. Sneed, J. Anim. Sci., 34 (1972) 846.
- 4 G. Rosenberger, Krankheiten des Rindes, Paul Parey Verlag, Berlin, 1970.
- 5 A. H. Lewis, J. Agric. Sci., 33 (1943) 58.
- 6 T. D. Luckey, B. Venugopal und D. Hutcheson, Heavy Metal Toxicity, Safety and Hormonology, Vol. 1, EQS Environmental Quality and Safety, Georg Thieme Verlag Stuttgart, 1975.
- 7 W. J. Clawson, A. L. Lesperance, V. R. Bohman und D. C. Layhee, J. Anim. Sci., 34 (1972) 516.
- 8 B. Venugopal und T. D. Luckey, Metal Toxicity in Mammals, Vol. 2, Chemical Toxicity of Metals and Metalloids, Plenum Press, New York, 1978.
- 9 L. E. Morales de Flores, A. Faanhof, H. A. Das und H. A. van der Sloot, Radiochem. Radioanal. Lett., 42 (1980) 107.
- 10 J. Kucera, Radiochem. Radioanal. Lett., 38 (1979) 229.
- 11 N. V. Bagdavadze und L. M. Mosulishvili, J. Radioanal. Chem., 24 (1975) 65.
- 12 O. G. Koch und G. A. Koch-Dedic, Handbuch der Spurenanalyse, 2. Auflage, Springer Verlag, Berlin, 1974.
- 13 S. U. Khan, O. R. Cloutier und M. Hidioglou, J. Assoc. Off. Anal. Chem., 62 (1979) 1062.
- 14 R. C. Daniel, E. Haenni und H. Shariatmadari, Mitt. Geb. Lebensmittelunters. Hyg., 70 (1979) 49.
- 15 H. Knote und V. Krivan, Anal. Chem., 54 (1982) 1858.
- 16 W. G. Faix, R. Caletka und V. Krivan, Anal. Chem., 53 (1981) 1719.
- 17 R. Plesch, Siemens-Z., 51 (1977) 108.
- 18 L. Beitz, Mitt. Geb. Lebensmittelunters. Hyg., 68 (1977) 451.
- 19 L. Beitz, R. Plesch und H. Rethfeld, Landwirtsch. Forschung, 33 (1980) 30.

IDENTIFICATION OF METHACRYLATES AND ACRYLATES IN DENTAL MATERIALS BY MASS SPECTROMETRY

NINA GJØS* and KJELL URDAL

Central Institute for Industrial Research, P.O. Box 350, Blindern, Oslo 3 (Norway)

IVAR EYSTEIN RUYTER and INGER JULIE SJØVIK

NIOM, Scandinavian Institute of Dental Materials, Blindern, Oslo 3 (Norway)

(Received 7th October 1982)

SUMMARY

The electron-impact and methane chemical-ionization mass spectra of selected methacrylate and acrylate monomers commonly used in dental materials are reported and discussed. The two ionization modes complement each other, and together the mass spectra offer adequate information for identification purposes. The application of the mass spectral methods is demonstrated on resin-based dental materials with identification of the monomer content.

Esters of methacrylic acid and acrylic acid are commonly used monomers in dental resin and composite materials [1, 2]. The structure and quantity of the monomers will influence the properties of the polymerized materials [3, 4]. The composition of commercial dental composite and resin systems varies. Thus there is a need for suitable methods for characterizing the products.

Proprietary restorative resin materials have been analyzed by various techniques, e.g., high-performance liquid chromatography, infrared spectroscopy, nuclear magnetic resonance spectroscopy, gas chromatography and mass spectrometry [1, 5]. The electron-impact mass (e.i.m.) spectra of the methacrylate monomers often show ions of low abundance in the molecular weight region so that spectral interpretation becomes difficult. Chemical-ionization mass spectrometry (c.i.m.s.) may offer additional structural information [6, 7]; such spectra are known to be simple with pronounced molecular ions or ions which differ by one mass unit. Use of different reactant gases makes the technique flexible.

This paper is concerned with the possibility of using mass spectrometry for the identification of methacrylate and acrylate monomers in dental materials. The electron-impact and chemical ionization techniques are applied to a series of 26 selected monomers and three resin-based dental materials.

EXPERIMENTAL

Samples

The selected samples comprised 26 standard compounds of acrylates, methacrylates and dimethacrylates and three different resin-based dental materials (Table 1). The dimethacrylate derivatives of bisphenol-A and the "urethane dimethacrylate" were used as received from the manufacturer and introduced via the direct probe inlet system. The other standard compounds, 10 μ l of each, were dissolved in 100 ml of dichloromethane. Dental materials consisting of monomers and filler particles were dissolved in dichloromethane and the particles were separated by centrifugation. The solutions were injected into the gas chromatograph.

Instrumentation

The instrument was a Finnigan 4021 quadrupole mass spectrometer equipped with a Finnigan 9610 gas chromatograph and a dual electron-impact/chemical-ionization ion source. Data acquisition and mass spectrometer control were done by an Incos 2300 data system. The mass spectra were recorded with an electron energy of 70 eV and a source temperature of 250°C. In the c.i. mode, methane was used as the reagent gas with a source pressure of 0.15 torr and a manifold pressure of 3×10^{-5} torr. The spectra were recorded every other second for g.c./m.s. and every fourth second for the direct probe; the spectra covered the ranges 35–550 mass units (e.i.) and 45–600 mass units (c.i.). The direct insertion probe was heated from 30 to 300°C at a rate of 80 K min⁻¹. The gas chromatograph was supplied with a 30 m \times 0.25 mm glass capillary column coated with 0.30- μ m SE-54, (Supelco); 2- μ l samples were injected splitless into a Grob type injector with helium as carrier gas. The injector was kept at 250°C and the oven heated from 30 to 250°C at a rate of 4 K min⁻¹.

Synthesis of dimethyltricyclo[5.2.1.0^{2,6}]decane dimethacrylate

Bis(hydroxymethyl)tricyclo[5.2.1.0^{2,6}]decane (9.8 g; Aldrich-Europe), 12.9 g of methacrylic acid and 0.7 g of *p*-toluenesulphonic acid in 20 ml of cyclohexane were heated at 90°C for 24 h [8]. To prevent polymerization, 0.04 g of hydroquinone and 0.04 g of copper(I) chloride were added, and air was drawn through the solution [9]. The reaction mixture was treated repeatedly with 0.2 M sodium hydroxide. The decanted cyclohexane solution was decolorized by treatment with alumina. The solvent was evaporated in vacuum.

RESULTS AND DISCUSSION

The compounds investigated were grouped into four classes, and the mass spectral data are given in Tables 2–5. The most prominent ions of each spectrum are given together with their intensity relative to the base peak. The compound numbers follow Table 1.

TABLE 1

Selected monomers and resin systems investigated

Compound	Source	Compound	Source
1 Methyl acrylate	Fluka ^a	13 <i>N,N</i> -dimethylaminoethyl methacrylate	Koch-Light ^c
2 Ethyl acrylate	Fluka ^a	14 Ethylene dimethacrylate	Merck
3 Butyl acrylate	Fluka ^a	15 Trimethylene dimethacrylate	Polysciences
4 Tetramethylene diacrylate	Merck ^b	16 Tetramethylene dimethacrylate	Merck ^b
5 Methyl methacrylate	Fluka ^a	17 Hexamethylene dimethacrylate	Esschem
6 Ethyl methacrylate	Koch-Light ^c	18 Diethyleneglycol dimethacrylate	Sci-Pharm
7 Propyl methacrylate	ICN, K & K	19 Triethyleneglycol dimethacrylate	Koch-Light ^c
8 Butyl methacrylate	Fluka ^a	20 Tetraethyleneglycol dimethacrylate	Aldrich
9 Phenyl methacrylate	ICN, Pharmaceutical	21 Trimethylolpropan trimethacrylate	Sartomer Monomer SR 350
10 2-Ethoxyethyl methacrylate	Koch-Light ^c	22 2,2-Bis(4-methacryloyloxy-phenyl)-propane	Aldrich-Europe
11 2,3-Epoxypropyl methacrylate	Merck ^b	23 2,2-Bis[4-(2-methacryloyloxyethoxy)-phenyl]propane	Ancomer
12 Tetrahydrofurfuryl methacrylate	Polysciences	24 2,2-Bis[4-(3-methacryloyloxypropoxy)phenyl]propane	ESPE
		25 2,2-Bis[4-(2-hydroxy-3-methacryloyloxypropoxy)phenyl]propane	Sci-Pharm
		26 "Urethane dimethacrylate"	Ivoclar
<i>Dental materials</i>			
Caulk Vytol	Batch No. 012180, L.D. Caulk Co.		
Heliobond	Batch No. 651080, Vivadent		
Visio-Dispers	Batch No. G 14976, ESPE		

^aPurum grade. ^bZur Synthese. ^cPure grade.

Acrylates

The electron-impact and methane chemical-ionization mass spectral data of three alkyl acrylates and one diacrylate are given in Table 2. The e.i.m. spectra all showed a prominent cleavage of the -OR group from the molecular ion thus giving the acryloyl ion, m/z 55, as the base peak. In the spectra of methyl acrylate and ethyl acrylate the molecular ions were present, and in addition the $(M - H)^+$ ions were quite abundant. The two spectra were in accordance with the data earlier reported by Bowles et al. [10]. Butyl acrylate showed no ions in the molecular weight region. An intense fragment ion at m/z 73 was observed. This corresponded to loss of the butyl group and formation of a protonated acrylic acid ion [11]. Tetramethylene diacrylate showed scarcely no ions beyond the acryloyl ion. A small peak was observed at m/z 126, and this corresponded to loss of acrylic acid from the molecular ion.

The molecular ions or protonated molecular ions were more pronounced in the c.i.m. spectra. These ions made the base peaks in the spectra of methyl and ethyl acrylate. Ethyl acrylate also showed an abundant m/z 73 ion. This ion was probably the $C_2H_5OCO^+$ ion formed by loss of the vinyl group [10], or the protonated acrylic acid ion. The latter turned out to be the base peak in the spectrum of butyl acrylate. The present results were consistent with the data on *n*-propyl acrylate reported by Rapp and Dielmann [12], whose equivalent mass spectrum contained m/z 73 as the base peak and a $(M + H)^+$ ion of about 50% relative abundance. It thus turned out that the ions in the molecular weight region were most pronounced in the spectra of the less substituted acrylates. Tetramethylene diacrylate gave m/z 127 as the base peak, which corresponded to loss of one of the acrylate groups. The protonated molecular ion was not observed. This is in contrast to the data reported on hexamethylene diacrylate [12] which gave a $(M + H)^+$ ion of about 30% relative abundance.

A comparison of the two types of mass spectra for the monoacrylates showed that the c.i.m. spectra were the most informative as they showed both the molecular weight and the compound type. For the diacrylate both modes gave very simple spectra. The prominent acryloyl ion easily showed the compound class, but further structure identification based on this type of spectrum would be difficult.

Methacrylates

The mass spectral data of nine different methacrylates are given in Table 3. The e.i.m. spectra showed abundant ions at m/z 69, the methacryloyl ion $C_4H_5O^+$, and at m/z 41, the $C_3H_5^+$ ion. Thus the cleavage of the -OR group was a prominent fragmentation just as observed for the acrylates. The molecular ions were of moderate intensity in the spectra of the methyl-, ethyl- and phenyl-substituted compounds, but were not visible at all for the others. Propyl and butyl methacrylate both gave abundant m/z 87 ions. Parallel to the m/z 73 ion in the butyl acrylate spectrum this was most

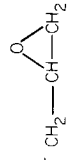
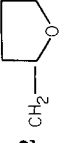
TABLE 2

Electron-impact and chemical-ionization mass spectral data of acrylates, $\text{CH}_2=\text{CH}-\overset{\text{O}}{\parallel}\text{C}-\text{O}-\text{R}$

Compound	Electron impact		Chemical ionization (CH_4)		
	M^+	($\text{M}-\text{H}$) $^+$	($\text{M}-\text{OR}$) $^+$ m/z 55	($\text{M}+\text{H}$) $^+$	M^+ Other fragments m/z 55
1 CH_3	86(4%)	85(36%)	(100%)	87(100%)	86(14%) (9%)
2 C_2H_5	100(0.5)	99(7)	(100)	101(100)	100(33) (12)
3 n- C_4H_9	128(-)	127(-)	(100)	73(5), 85(4)	73(81)
4 $(\text{CH}_2)_4\text{OCOCH}=\text{CH}_2$	198(-)	197(-)	(100)	73(39), 85(5)	73(100), 101(8)
				71(8), 126(3)	127(100)
				199(-)	198(-) (31)

TABLE 3

Electron-impact and chemical-ionization mass spectral data of methacrylates, $\text{CH}_2=\overset{\text{CH}_3}{\underset{\text{O}}{\parallel}}\text{C}-\text{O}-\text{R}$

Compound	Electron impact		Chemical ionization (CH_4)			
	M^+	($\text{M}-\text{OR}$) $^+$ m/z 69	C_3H_5^+ m/z 41	($\text{M}-\text{C}_4\text{H}_6\text{O}_2$) $^+$ Other fragments	($\text{M}+\text{H}$) $^+$ ($\text{M}-\text{OR}$) $^+$ m/z 69	Other fragments
5 CH_3	100(15%)	(54%)	(100%)	39(55%)	101(100%)	(2%)
6 C_2H_5	114(7)	(100)	(89)	99(11)	115(100)	(4)
7 C_3H_7	128(-)	(100)	(95)	87(81)	129(31)	(11)
8 C_4H_9	142(-)	(96)	(100)	87(83)	143(28)	(12)
9 C_6H_5	162(16)	(100)	(76)	76(0.1)	163(100)	57(-)
10 $(\text{CH}_2)_4\text{OC}_2\text{H}_5$	158(-)	(100)	(89)	59(51)	159(5)	77(-)
11 	142(-)	(100)	(63)	56(6)	143(24)	73(11)
					(100)	57(31)
12 	170(-)	(13)	(28)	84(18)	171(41)	85(100)
13 $(\text{CH}_2)_2-\text{N}(\text{CH}_3)_2$	157(-)	(9)	(12)	71(13)	158(100)	72(78)
				58(100)	(-)	156(17)

probably the protonated methacrylic acid ion. Cleavage of the same bond, but opposite charge retention, occurred for the compounds with substituted alkyl chains, compounds 10–13; the ions m/z 72, m/z 56, m/z 84 and m/z 71, respectively, were consistent with loss of methacrylic acid. In contrast to the other methacrylates, m/z 69 was of quite low abundance in the spectra of tetrahydrofurfuryl methacrylate and *N,N*-dimethylaminoethyl methacrylate. For these compounds, the base peaks were likely produced by bond cleavage in the alkyl chain to give m/z 71 (tetrahydrofurfuryl ion) and m/z 58 (trimethylamino ion).

All the c.i.m. spectra showed protonated molecular ions, the base peaks for some of the compounds. The methacryloyl ion, m/z 69, varied in intensity; it was the base peak for the epoxy compound 11 but not visible for the amino compound 13. The protonated methacrylic acid ion, m/z 87, in the spectra of the alkyl methacrylates was more pronounced than in the e.i.m. spectra. The same trend was also noticed for the acrylates where the c.i.m. spectra showed more of the protonated acrylic acid ion (m/z 73) than the e.i.m. spectra. The loss of the methacrylate group was distinct in compounds 10–13, and gave abundant ions at m/z 73, 57, 85 and 72, respectively. This was one mass unit higher than in the corresponding e.i.m. spectra where cleavage of methacrylic acid occurred. Ethoxyethyl methacrylate showed a characteristic cleavage of the ethoxy group which produced the base peak, m/z 113. This fragmentation was also observed in the e.i.m. spectrum but was less important. *N,N*-Dimethylaminoethyl methacrylate gave in addition to the $(M + H)^+$ ion also a quite abundant $(M - H)^+$ ion.

In total, the c.i.m. spectra were mainly more informative than the e.i.m. spectra. They all gave information about the molecular weight, which is of great value for interpretation. Though the ions originating from the methacrylate group were not as pronounced as in the e.i.m. spectra, they were of sufficient abundance to identify the compound as a methacrylate. The exception was *N,N*-dimethylaminoethyl methacrylate which gave no m/z 69 ion, but showed loss of the methacrylate group as the main fragmentation reaction. Methyl, ethyl and phenyl methacrylates gave very characteristic spectra with molecular ions also in the e.i.m. mode, and for these compounds the e.i. ionization technique seemed preferable.

Dimethacrylates

Table 4 shows the mass spectral data of seven alkane and ethyleneglycol dimethacrylates and one trimethacrylate. Ions originating from the methacrylate group, m/z 69 and m/z 41, were the most abundant in the e.i.m. spectra. In addition, the ethyleneglycol dimethacrylates showed characteristic intensive m/z 113 ions, likely formed by cleavage of the C—O ether bond. Few ions were observed in the high mass region. Molecular ions could not be detected except for the spectrum of the trimethacrylate which showed a diminutive peak (0.1% relative abundance) corresponding to the molecular weight. Fragment ions of low abundance corresponding to the loss

TABLE 4

Electron-impact and chemical-ionization mass spectral data of dimethacrylates, $\text{CH}_2=\text{C}(\text{CH}_3)\text{COO}-\text{CH}_2-\text{CH}_2-\text{R}-\text{O}-\text{C}(\text{CH}_3)=\text{CH}_2$, and the trimethacrylate $\text{C}_3\text{H}_5-\text{C}-[\text{CH}_2\text{OCOC}(\text{CH}_3)=\text{CH}_2]_3$

Compound	Electron impact		Chemical ionization (CH_4)				
R	($\text{M}-\text{CO}$) ⁺	($\text{M}-\text{C}_4\text{H}_5\text{O}_2$) ⁺ and ($\text{M}-\text{C}_4\text{H}_6\text{O}_2$) ⁺	m/z 113	m/z 69	m/z 41	Other fragments	($\text{M} + \text{H}$) ⁺ m/z 113 m/z 69 (M-C ₄ H ₅ O ₂) ⁺
14 —	170(4%)	113(16%), 112(14%)	(16%)	(100%)	(47%)		199(—) (100%) 113(100%)
15 CH_2	184(3)	127(18), 126(18)	(0.3)	(100)	(51)		213(—) (—) 127(100)
16 $(\text{CH}_2)_2$	198(0.1)	141(8), 140(10)	(—)	(100)	(51)	54(18)	227(—) (—) 141(100)
17 $(\text{CH}_2)_4$	226(1)	169(—), 168(0.1)	(—)	(100)	(66)	82(25)	255(100) (—) 169(24)
18 OCH_2CH_2	214(—)	157(—), 156(—)	(99)	(100)	(58)	86(36)	243(—) (100) 157(—)
19 $(\text{OCH}_2\text{CH}_2)_2$	258(—)	201(—), 200(4)	(100)	(77)	(39)	86(11)	287(—) (100) 201(—)
20 $(\text{OCH}_2\text{CH}_2)_3$	302(—)	245(—), 244(0.1)	(100)	(46)	(24)	86(8)	331(—) (100) 245(—)
21 Trimethacrylate	310(6)	253(13), 252(5)	(—)	(100)	(34)		339(—) (—) 253(100)

of a carbonyl group were noted in the spectra of the alkane dimethacrylates and the trimethacrylate. These compounds also lost the methacrylate group and methacrylic acid and gave fairly distinct ions. This was in contrast to the alkane methacrylates (Table 3) where the charge retention occurred on the methacrylate group. In addition, the spectra of the tetramethylene and hexamethylene dimethacrylates showed quite abundant ions (m/z 54 and m/z 82) that corresponded to loss of two methacrylic acid groups. Compound 14, ethylene dimethacrylate, may be considered as the first compound both in the alkane dimethacrylate series and in the oligo-ethyleneglycol dimethacrylate series. The fragmentation mainly followed the alkane series. The spectra of the dimethacrylates of all the ethyleneglycols were quite similar in that the high masses were of very low abundance. The methacrylic acid ion, m/z 86, differed between the individual compounds. This ion was not detected in the spectrum of ethylene dimethylacrylate, but it had a relative abundance of 36% for diethyleneglycol dimethacrylate and about 10% for tri- and tetra-ethyleneglycol dimethacrylate.

The c.i.m. spectra were quite simple, and some of the compounds gave mainly one ion. The structure information obtained was therefore very limited. An exception was hexamethylene dimethacrylate which showed the protonated molecular ion as the base peak and abundant fragment ions corresponding to the methacryloyl ion and to loss of the methacrylate group. No other protonated molecular ions or ions in the high mass region were observed. The ion m/z 113 was the base peak for the ethyleneglycol dimethacrylates, while the main fragmentation for the alkane dimethacrylates was loss of the methacrylate group.

Bisphenol-A dimethacrylates and "urethane" dimethacrylate

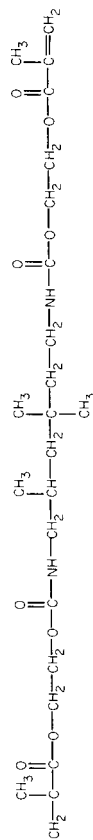
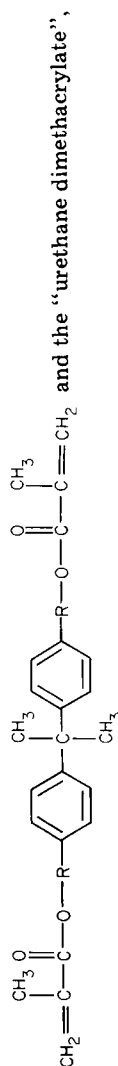
Table 5 shows the mass spectral data of four dimethacrylate derivatives of bisphenol-A and one aliphatic dimethacrylate containing urethane groups. The aromatic compounds gave very informative and characteristic spectra. In the e.i.m. mode both the molecular ion and cleavage of a methyl group gave pronounced peaks which readily showed the molecular weights. The methacrylate group was obvious, as the m/z 41 and m/z 69 peaks were intense. The base peaks in the spectra of compounds 23, 24 and 25 corresponded to cleavage of an ether bond with retention of the charge on the methacrylate part of the molecule.

The c.i.m. spectra were also excellent. The protonated molecular ions were intense, and cleavage at the quaternary carbon atom gave rise to characteristic abundant fragment ions. A weak point, however, was that the m/z 69 ion representing the methacrylate group was of low abundance.

For the urethane compound the two ionization modes led to greater differences between the mass spectra. The e.i.m. spectrum showed mainly the methacrylate group (m/z 41 and 69) with a following ethoxy group (m/z 113). The c.i.m. spectrum was more informative. The protonated molecular ion was abundant, and fragment ions that corresponded to cleav-

TABLE 5

Electron-impact and chemical-ionization mass spectral data of dimethacrylate derivatives of bisphenol-A,



Compound	Electron impact			Chemical ionization (CH ₃)		
	M ⁺	(M-CH ₃) ⁺	Other fragments	(M+H) ⁺	(M-CH ₃) ⁺	Other fragments
R						
22 —	364(33%)	349(78%)	(100%)	365(100%)	349(6%)	203(59%)
23 CH ₃ CH ₂ O	452(12)	437(5)	(75%)	453(100)	437(6)	247(80)
24 CH ₃ CH ₂ CH ₂ O	480(36)	465(52)	(40)	481(38)	465(7)	261(100)
25 CH ₃ CH(OH)CH ₂ O	512(25)	497(37)	(30)	513(52)	497(7) ^a	277(78), 427(58)
26 "Urethane di-methacrylate"	470(0.04)	455(-)	(34)	471(31)	455(0.2)	113(100), 385(37), 341(18)

^aThe value is corrected for the isotopic contribution from the *m/z* 495 ion. The observed relative abundance of *m/z* 497 is 15%.

age of the methacrylate group (m/z 385) and the ethoxy methacrylate group (m/z 341) were easily recognized.

All the compounds in Table 5 showed peaks at 29 and 41 mass units above the molecular weight. This was due to addition of $C_2H_5^+$ ions and $C_3H_5^+$ ions and is often observed in c.i.m. spectra when methane is used as the reagent [6, 7].

Applications

Three different resin-based dental materials of unknown composition were analyzed. The usefulness of recording both the e.i.m. and c.i.m. spectra was clearly demonstrated. The information obtained in the two modes complemented each other very well. The e.i.m. spectra covered the low mass region with information on the compound class, while the c.i.m. spectra showed the molecular weight and characteristic fragment ions.

The materials were analyzed by combined g.c./m.s., thus the identified compounds were limited to those amenable to gas chromatography. For complete characterization of the dental materials, additional techniques, e.g., liquid chromatography, would be needed.

Caulk Vytol. This material was found to contain three main components. Based on the mass spectra, the two most prominent peaks in the total ion current chromatogram were methacrylate monomers. By comparison with the mass spectral data of the standard compounds, these were identified as triethyleneglycol dimethacrylate and 2,2-bis(4-methacryloyloxyphenyl)propane. The third component was identified as phenyl salicylate, a commonly used photostabilizer in polymer materials.

Heliobond. Heliobond gave a simple total ion current chromatogram with only one main component. The e.i.m. and c.i.m. spectra of this compound are given in Fig. 1. The e.i.m. spectrum evidently showed a methacrylate compound (m/z 41 and m/z 69) and the m/z 87 ion implied an alkane mono- or di-methacrylate. The ion m/z 310 could be the molecular ion, and in that case m/z 224 corresponded to loss of methacrylic acid. The c.i.m. spectra confirmed the molecular weight, as an intense ion was observed at m/z 311, most probably the $(M + H)^+$ ion. The ions m/z 225 and m/z 139 corresponded to loss of the methacrylate group and further loss of methacrylic acid. This was the same fragmentation path that was observed for hexamethylene dimethacrylate. In total, both the e.i.m. and c.i.m. spectra resembled the spectra of hexamethylene dimethacrylate. The interpretation implied that the unknown compound was decamethylene dimethacrylate. The identification were confirmed by analyzing an authentic sample of decamethylene dimethacrylate (Polysciences) and comparing the data.

Visio-Dispers. The total ion current chromatogram in the c.i.m. mode is given in Fig. 2. Five main components can be observed in the chromatogram. The mass spectra of components 1 and 2 were almost identical and showed acrylate groups. Components 3, 4 and 5 also had very similar spectra, but these were methacrylates. Figure 3 shows the e.i.m. and c.i.m. spectra of

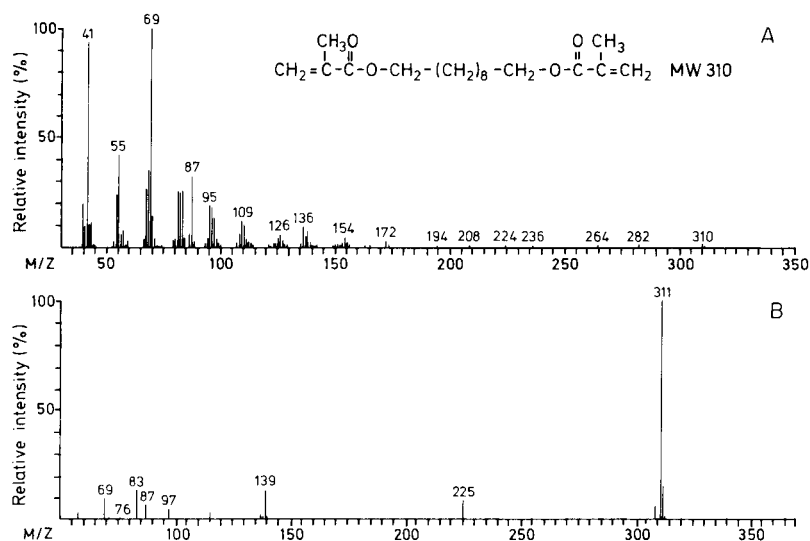


Fig. 1. The e.i.m. (A) and c.i.m. (B) spectra of the main component found in the dental material Heliobond by g.c./m.s.

component 1. A diminutive peak could be observed at m/z 304 in the e.i.m. spectrum. A corresponding ion one mass unit higher, m/z 305, was observed in the c.i.m. spectrum. This indicated that m/z 305 could be the $(M + H)^+$ ion, and the fragment ions m/z 233 and m/z 161 (base peak) would then correspond to loss of one and two acrylic acid groups, respectively. In the e.i.m. spectrum, the ion m/z 160 was also consistent with loss of two acrylic

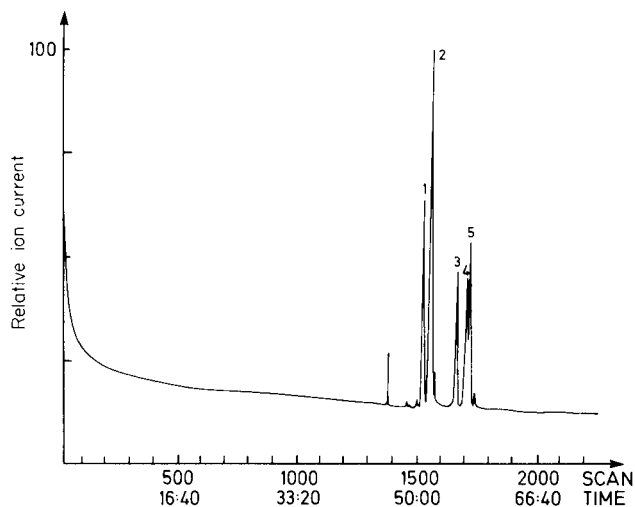


Fig. 2. The total ion current chromatogram in the c.i. mode of the dental material Visio-Dispers.

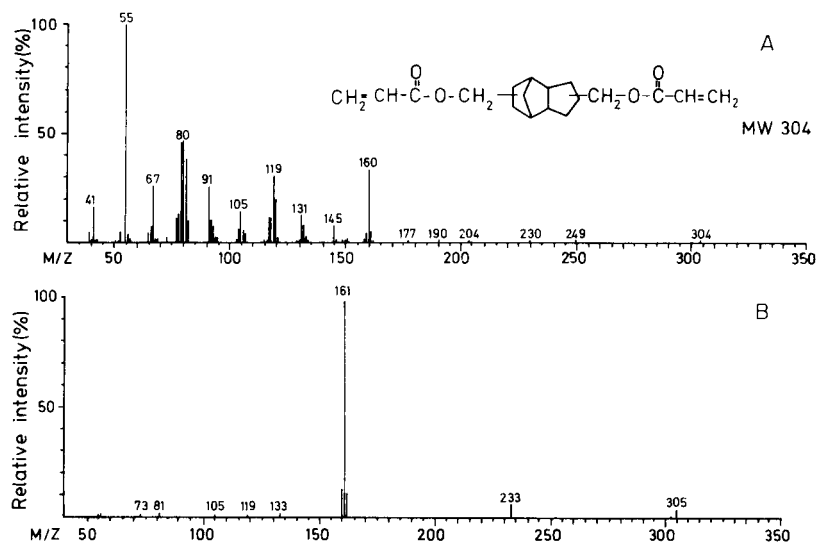


Fig. 3. The e.i.m. (A) and c.i.m. (B) spectra of component 1 found in the dental material Visio-Dispers.

acid groups. Components 3, 4 and 5 showed the same type of mass spectra except for methacrylate groups instead of acrylate groups. The molecular weights were assumed to be 332, as the m/z 332 ion was barely observable in the e.i.m. spectra, whereas the m/z 333 ion was clearly noted (about 8% relative abundance) in the c.i.m. spectra. Abundant fragment ions consistent with loss of one and two methacrylic acid groups were present in both the e.i.m. and c.i.m. spectra. The mass spectral data showed close resemblance to the spectra of alkane dimethacrylates. A saturated alkane was not consistent with the assumed molecular weights, but a hydrocarbon with an unsaturation index of three would correspond. The interpretation resulted in the following conclusion. The dental material contained diacrylates of m.w. 304 (two isomers detected) and the corresponding dimethacrylates of m.w. 332 (three isomers detected). The structure proposed was dimethyltricyclo[5.2.1.0^{2,6}]decane diacrylate and dimethyltricyclo[5.2.1.0^{2,6}]decane dimethacrylate. Monomers of these esters have recently been utilized in dental materials [8]. The identification was confirmed by comparing the mass spectral data with those of an authentic sample of the dimethacrylate prepared by reaction of bis(hydroxymethyl)tricyclo[5.2.1.0^{2,6}]decane with methacrylic acid [8, 9].

This work was supported by the Norwegian Council for Scientific and Industrial Research under contract No. 0106.08147.

REFERENCES

- 1 I. E. Ruyter and I. J. Sjøvik, *Acta Odontol. Scand.*, 39 (1981) 133.
- 2 I. E. Ruyter and H. Øysæd, *J. Biomed. Mater. Res.*, 16 (1982) 741.
- 3 I. E. Ruyter and P.-P. Gyørøsi, *Scand. J. Dent. Res.*, 84 (1976) 396.
- 4 I. E. Ruyter and S. A. Svendsen, *Acta Odontol. Scand.*, 36 (1978) 75.
- 5 E. Asmussen, *Acta Odontol. Scand.*, 33 (1975) 129.
- 6 M. S. B. Munson and F. H. Field, *J. Am. Chem. Soc.*, 88 (1966) 2621.
- 7 B. Munson, *Anal. Chem.*, 43 (1971) 28A; 49 (1977) 772A.
- 8 W. Schmitt, R. Purrmann, P. Jochum and W.-D. Zahler, U.S. Patent 4,131,729, Dec. 26, 1978.
- 9 G. V. Moikin, E. N. Gumenchuk, E. N. Krom and V. R. Kartashov, *Zh. Prikl. Khim.*, 52 (1979) 1136.
- 10 A. J. Bowles, E. F. H. Brittain and W. O. George, *Org. Mass. Spectrom.*, 2 (1969) 809.
- 11 T. J. Mead and D. H. Williams, *J. Chem. Soc. B*, 8 (1971) 1654.
- 12 U. Rapp and G. Dielmann, Varian MAT GmbH, Bremen, Application note No. 31, 10/78 (1978).

A MICROCOMPUTER SYSTEM FOR PROCESSING DATA FROM A THREE-CHANNEL ATOMIC ABSORPTION SPECTROMETER^a

M. J. ADAMS*, M. C. MITCHELL and G. J. EWEN

*Department of Spectrochemistry, The Macaulay Institute for Soil Research,
Craigiebuckler, Aberdeen AB9 2QJ (Gt. Britain)*

(Received 22nd November 1982)

SUMMARY

A microcomputer system is interfaced to a three-channel atomic absorption spectrometer, to eliminate the manual recording and tedious processing of data. The microcomputer and spectrometer are connected via a multichannel, analog-to-digital convertor, enabling the computer to monitor the status of the spectrometer as well as record automatically the analytical data. Operator control of the system is achieved with the aid of a microterminal linked to the computer. The system is presently employed for the routine determination of calcium and magnesium in soil extracts.

The use of microprocessors has produced dramatic changes in the design and construction of modern commercial analytical instruments. In such equipment, a microprocessor unit can improve the data handling capabilities and the "intelligence" of the instrument. For the single, one-off instrument, usually designed in-house, the application of microprocessor engineering has been more limited. The expertise and time required to implement the early microprocessor and single-board microcomputer systems could seldom be justified. A development which has brought about a change in this situation is the introduction of the personal microcomputer. The scope for applying these computers in instrumental chemistry is now being recognised by instrument manufacturers and laboratory staff. Unlike the single-chip microprocessor alone, such computers can provide powerful control and data-processing facilities with a minimum of interface engineering. The microcomputers contain the microprocessor, standard input–output facilities, read/write memory (RAM) for data storage and permanent memory (ROM) containing at least one high-level language. The language is usually BASIC but PASCAL and FORTRAN are rapidly becoming more widely available. Programming in these languages considerably reduces software development time and most microcomputers permit direct access to the microprocessor for time-dependent, machine-coded routines. Hence, many useful programs can be developed by a user without recourse to specialist assistance.

^aCopyright reserved to the Macaulay Institute for Soil Research.

The microprocessor can serve as a controlling element in optimising an instrument and can provide an intelligent base for data collection and processing [1]. In the present application, the microcomputer is used to digitise analog signals from a three-channel atomic absorption spectrometer and to analyse mathematically the resulting data.

The three-channel atomic absorption spectrometer has been described in an earlier paper by Ure et al. [2]. The instrument employs a novel burner for use with a nitrous oxide/air/acetylene flame and two nebulisers, allowing continuous nebulisation of an ionization suppressant with the sample and buffer solutions. The system is successfully employed for the routine determination of calcium and magnesium in soil extract solutions. The use of this instrument obviates the need for time-consuming additions of buffering materials to sample and standard solutions. Also, the need for dilution of samples is minimised by making use of burner rotation to reduce the absorbing path-length and by employing two channels, with different flame path-length, for one element, calcium. Although the measurement time is reduced by such an arrangement, the manual recording and processing of data can create a serious obstacle to efficient use of the system. To eliminate this problem, the instrument was interfaced to a microcomputer unit for data recording and evaluation.

INSTRUMENTATION

The instrumental arrangement employed is illustrated schematically in Fig. 1. Only minor changes to the original spectrometer were necessary to allow the use of a microcomputer for logging the transmittance signals from the three detectors. As well as the signal voltage lines from the detectors, the reset control and the rotating chopper output reference signals were also monitored by the computer. These five analog input lines to the computer were digitised with the aid of an eight-bit, medium speed (5 kHz bandwidth), analog-to-digital converter (type AI-02; Interactive Structures Inc., Bala Ave., PA). The microcomputer employed was an Apple II system with 48 K RAM and a single 5.25-in. floppy disk unit for program and temporary data storage. A thermal printer was also connected in the system for output of the final results. To prevent accidental damage to the computer from chemical spillage, it was installed remotely (about 25 m) from the spectrometer. The operator communicates with the computer via a microterminal and a second video unit installed adjacent to the spectrometer. The microterminal (Model TM25, Burr-Brown, Watford, U.K.) provides a sealed hexadecimal keyboard and is capable of transmitting and receiving ASCII characters at 300 baud. A simple keypad can be interfaced directly to the microcomputer keyboard decoder unit but it was found that this was reliable only for relatively short distances between the computer and the keypad (up to 5 m). Once the program is initiated, all communication between the operator and computer is via the remote terminal and monitor.

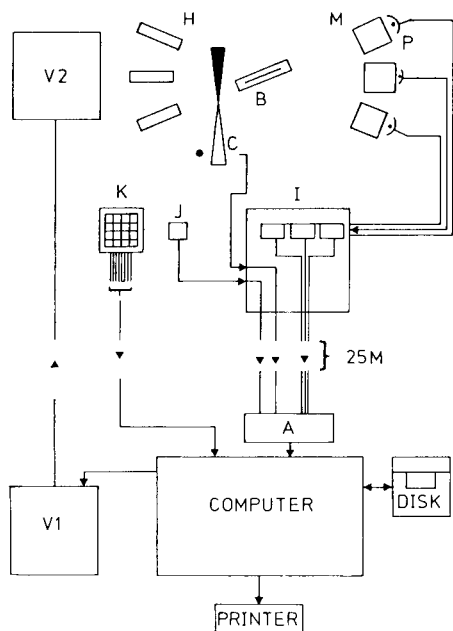


Fig. 1. The microcomputer/spectrometer system. Radiation from the hollow-cathode sources (H) after passing through the rotating sector (C) and the burner (B) is focussed at the entrance slit of each monochromator unit (M). The signals from the detectors (P), the beam chopper and the start/reset unit (J) are fed to the spectrometer control panel (I). The condition of each signal is displayed on the panel and is also transmitted to the analog/digital converter (A) of the microcomputer. Operator communication with the computer is via the remote terminal (K). Data and results are displayed on the video monitors (V1 and V2).

OPERATING PRINCIPLES AND PROCEDURE

A detailed procedure for the use of the three-channel atomic absorption instrument has been described elsewhere [2]. During warm-up of the spectrometer, the burner is aligned and the wavelengths of the three monochromators are checked and set as required. The background and 100% transmittance levels of the three channels, with the flame ignited, are set on the spectrometer control panel to provide a working range of about 4.0–4.5 V for digitising.

The computer program consists of three main routines. The first (DATA ENTRY) is a status input routine which enables the user to enter details and comments concerning the analysis for later printout. Concentration data for the highest standard sample to be used for each of the spectrometer channels and the number of samples per set are also entered. The second routine (MEASUREMENT) provides for the data logging and evaluation, and on completion, passes control to the third routine (PRINT-OUT) for formatting the data and printing out the results.

The principles and procedure may be appreciated with the aid of the simplified flow charts illustrated in Fig. 2, and the spectrometer timing diagram in Fig. 3. Figure 2(a) presents the general scheme. Following an initial blank, the calibration graph for each channel is constructed from the range of standard solutions. The curve-fitting procedure employed is a standard least-squares routine, fitting the measurement data, expressed as absorbance, to a quadratic function of solution concentration. Linear plots are not assumed. Each plot for the three channels is displayed on the video monitors throughout the run of measurements. The sample solutions are examined in sets (typically of seven samples) followed by a repeat of the top standards

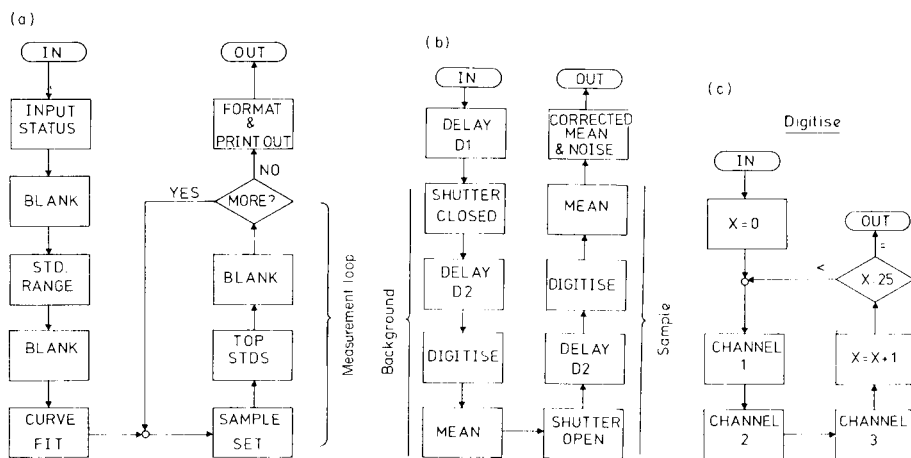


Fig. 2. (a) Flow diagram showing the sequence of operations involved in the use of the microcomputer/atomic absorption spectrometer system. (b, c). The digitising scheme and signal sampling procedures used to evaluate the spectrometric data.

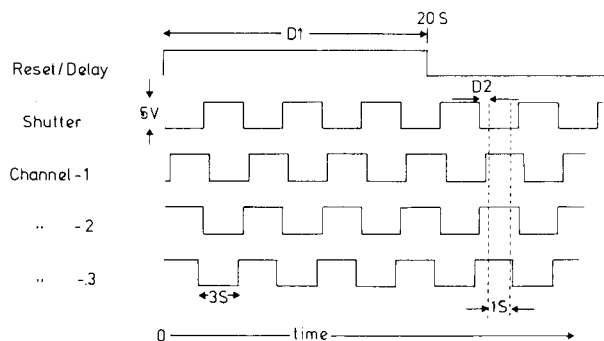


Fig. 3. The voltage/time signals from the spectrometer used by the microcomputer for sampling the data signals. D1 is a 20-s initialising delay before any sample measurement is made. D2 is a short delay (about 0.5 s) to ensure that measurements are made only when all channels are simultaneously open, or closed.

and the blank solution. The arithmetic means of the transmittance values of these solutions, taken at the beginning and end of each sample set, are used to correct the sample results for any slow drift occurring in the spectrometer during lengthy sample preparation procedures. As the transmittance data from each solution are digitised, an approximate point on each standard plot is displayed on the monitors along with the percentage relative standard deviation for the data points collected. The result may be accepted or rejected by the user as required, via the terminal. Thus the operator has the final decision in rejecting a result, perhaps because of excessive instrumental noise, nebuliser blockage or other instrument failure. The measurement procedure can be terminated at the end of any sample set and the results, expressed in pre-selected concentration units, passed to the final routine for output.

The digitising procedure is illustrated in Fig. 2 (b, c). Immediately a solution is nebulised into the spectrometer flame, the operator sets a reset delay switch that provides a 5-V pulse of 20-s duration (D1) before the instrument panel display operates (Fig. 3). This delay allows the nebulising system to stabilise before any readings are recorded. The computer awaits this delay pulse which serves as a trigger to initiate a new solution measurement.

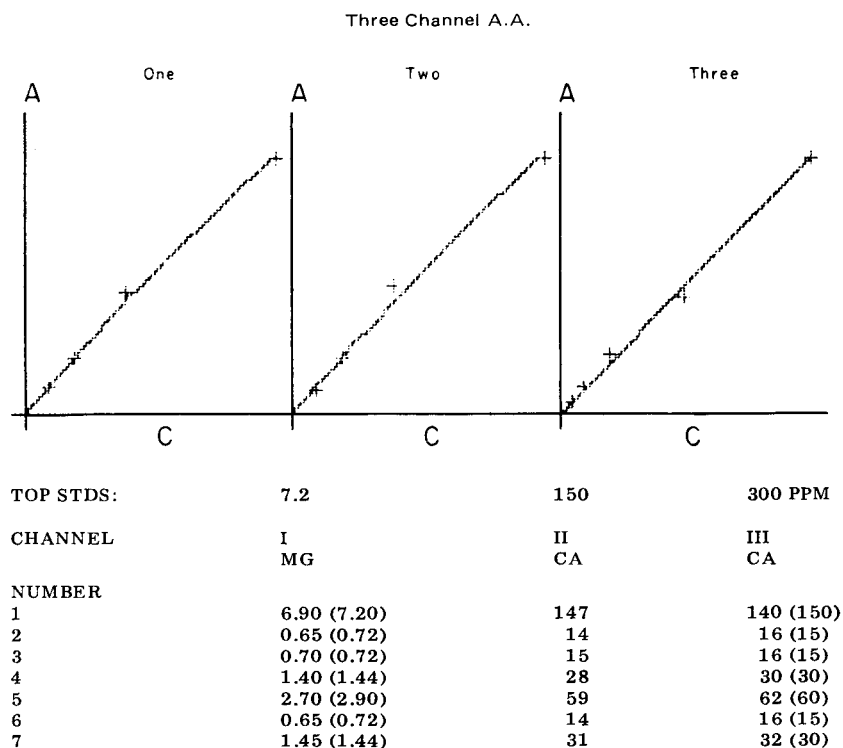


Fig. 4. A typical format for the PRINT-OUT procedure displaying the calibration graphs and computed sample results. In this example, the known magnesium and calcium concentrations of the samples are given, in parentheses, for comparison purposes only. All results are expressed as ppm (solution).

When the delay voltage has returned to its low value (0 V), the computer monitors the condition of the shutter. Background readings are recorded from each channel, with the shutter closed, followed by the sample transmittance data with the shutter open. Because the rotating shutter is not at the intersection of the radiation from the three hollow-cathode sources, only the central channel signal is in-phase with the shutter signal. To compensate for this, a short delay (D2) is introduced between monitoring the shutter open/closed conditions and sampling the channel signals. During the period in which all three channels are open or closed (about 1 s), the signal for each channel is digitised twenty-five times. With an analog-to-digital conversion and data storage rate of approximately 100 μ s per reading, a delay of about 30 ms between each sample point is employed to ensure that data are recorded throughout the available time-window. This digitising routine is machine-coded into the program to enable advantage to be taken of the high sampling rates. The sample transmittance data are corrected for background emission, and the arithmetic mean and percentage relative standard deviation of the data calculated are displayed for the operator to examine.

The output of the results can take one of several forms, but usually a thermal printer is employed which enables the graphics image on the video monitors to be printed along with the computed sample solution results. A typical printout of this type is illustrated in Fig. 4. As well as the results and the computed analytical curves, the output also includes the status information regarding the operation, date of analysis and operator's comments.

The sample results shown in Fig. 4 were produced from a repetitive analysis of standard solutions to test the curve-fit procedure employed. There is reasonably good agreement between the computed results and the known concentration of the samples, and similar good agreement between the two calcium channels.

Conclusion

A major use for a microcomputer in an analytical laboratory is to reduce the time devoted to tedious data processing. The microcomputer system described here is not only capable of evaluating the data from an atomic absorption spectrometer but can also automatically digitise and record the original transmittance data from the instrument. The system is always under the control of the operator, who can accept or reject a result during the spectrometric measurements.

REFERENCES

- 1 D. Betteridge and T. B. Good, *Analyst*, 106 (1981) 257.
- 2 A. M. Ure, G. J. Ewen and M. C. Mitchell, *Anal. Chim. Acta*, 118 (1980) 1.

INTERFERENCES DES ELEMENTS MAJEURS SUR LA DETERMINATION DE Pb, Cu, Cd, Cr ET Ni DANS LES SEDIMENTS DE COURS D'EAU ET LES BOUES DE STATIONS D'EPURATION PAR SPECTROMETRIE D'ABSORPTION ATOMIQUE SANS FLAMME

M. LEGRET*, D. DEMARE, P. MARCHANDISE et D. ROBBE

Laboratoire Central des Ponts et Chaussées, BP 19, 44340 Bouguenais (France)

(Reçu le 7 septembre 1982)

SUMMARY

(Interferences of major elements in the determination of lead, copper, cadmium, chromium and nickel in river sediments and sewage sludges by electrothermal atomic absorption spectrometry.)

The interferences of major elements of river sediments and sewage sludges (Fe, Al, Mg, Ca, Na, K, Ti and P) in the determination of Pb, Cu, Cd, Cr and Ni by electrothermal atomic absorption spectrometry are studied and the concentration ranges found in these environments are specified. Lead, cadmium and chromium were subject to the most interferences.

RESUME

Les interférences des éléments majeurs des sédiments de cours d'eau et des boues de stations d'épuration (Fe, Al, Mg, Ca, Na, K, Ti et P) sur la détermination de Pb, Cu, Cd, Cr et Ni par spectrométrie d'absorption atomique sans flamme ont été étudiées et les domaines de concentrations des milieux naturels ont été précisés. Les éléments les plus sensibles aux interférences sont Pb, Cd et Cr.

L'intérêt de l'étude des pollutions métalliques du milieu naturel à partir des sédiments a été démontré [1, 2]. Du fait de la capacité des sédiments à piéger les polluants, il est possible de déterminer la provenance et l'étendue d'une contamination métallique, mais également l'évolution de l'intensité de celle-ci au cours du temps. En ce qui concerne les boues de stations d'épuration, l'épandage dans le domaine agricole est un moyen intéressant pour leur élimination, mais la présence de métaux lourds reste une des plus grandes contraintes qui s'oppose à cette utilisation [3]. La connaissance de la concentration des métaux dans les boues est donc indispensable.

La méthode analytique la plus employée pour le dosage des métaux lourds dans les milieux naturels est actuellement la spectrométrie d'absorption atomique et notamment la méthode d'atomisation électrothermique. Les échantillons de sédiment ou de boue sont mis en solution par attaque à l'aide d'un mélange d'acides, précédée ou non d'une calcination. La solution à

doser contient donc, outre les métaux lourds à l'état de traces, tous les éléments majeurs qui constituent les minéraux, et en particulier Fe, Al, Mg, Ca, Na, K, Ti et P. Le silicium est en général éliminé soit par insolubilisation en milieu acide, soit par volatilisation en présence d'acide fluorhydrique.

L'ensemble des interférences chimiques dues à la présence des éléments majeurs du milieu analysé et qui accompagnent l'élément trace à doser constituent l'effet de matrice. Des études générales ont montré que certains éléments pouvaient provoquer des interactions très importantes lors des dosages et cela malgré l'optimisation des programmes thermiques [4, 5].

Des études récentes [6–8] ont mis en évidence les difficultés rencontrées lors du dosage des éléments traces dans les milieux naturels, en particulier les eaux, les végétaux ou les tissus animaux.

On s'est donc proposé dans ce travail d'étudier systématiquement l'influence des éléments majeurs sur la détermination des métaux lourds par absorption atomique sans flamme, en se plaçant dans les conditions habituelles de dosage de ces éléments et en précisant les domaines de concentrations rencontrés dans les sédiments et les boues de stations d'épuration.

METHODE EXPERIMENTALE

Tous les essais ont été réalisés à l'aide d'un spectrophotomètre Perkin-Elmer, modèle 272, équipé d'un four graphite HGA-76 et d'un passeur d'échantillons automatique AS-1 effectuant des injections de 20 μ l de solution. Dans tous les cas les absorptions non spécifiques ont été corrigées automatiquement par une lampe au deutérium. Les programmes de température du four ainsi que les longueurs d'ondes utilisées sont indiqués dans le Tableau 1.

L'eau utilisée est purifiée sur une installation de déminéralisation Maxy comportant deux colonnes de résines échangeuses d'ions (Modèle Recherche). Les solutions contenant les métaux à l'état de traces sur lesquels nous avons étudié les interférences ont été préparées à partir de Titrisol Merck (chlorures

TABLEAU 1

Programmes de températures du four graphite et longueurs d'ondes utilisées pour le dosage des métaux lourds, et concentrations en métaux lourds dans les solutions étudiées

	Décomposition ^a	Atomisation	Raie (nm)	Conc. étudiées (μ g l ⁻¹)
Pb	550°C, 35 s	2200°C, 10 s	283,3	40
Cu	850°C, 35 s	2700°C, 8 s	324,7	80
Cd	250°C, 35 s	1950°C, 10 s	228,8	5
Cr	1100°C, 25 s	2600°C, 10 s	357,9	40
Ni	1000°C, 20 s	2700°C, 10 s	232,0	200

^aSéchage à 100°C pendant 30 s.

de Cu, Cr, Cd, Ni et nitrate de Pb). Les concentrations en métaux lourds ont été choisies afin d'obtenir en absorption atomique un signal voisin de 0,200 d'absorbance, suffisamment important pour pouvoir bien observer les variations et de manière à se situer dans la partie linéaire des courbes d'étalonnage, ce qui correspond aux valeurs du Tableau 1.

Les solutions contenant les éléments majeurs interférents ont été obtenues à partir des nitrates correspondants pour Ca, K, Mg, Na (Merck, Suprapur), de même que Al et Fe (Merck, pro analysi). Les solutions de Ti ont été obtenues à partir de TiCl_4 (Titrisol, Merck) et celles de P à partir de H_3PO_4 (Prolabo, R.P. Normapur). Les mélanges métaux lourds—éléments interférents ont été préparés en milieu HNO_3 0,2%(v/v) (Merck, Suprapur) sauf pour Ti où on a utilisé HCl 0,2% (v/v) (Merck, Suprapur), la concentration en interférent étant pour chaque élément successivement de 10, 50, 100 et 500 mg l^{-1} . Les concentrations en Ti et P ont été limitées à 100 mg l^{-1} , ces éléments apparaissant généralement en moindre quantité que les autres dans les échantillons.

Pour chaque élément nous avons effectué les essais suivants: (1) mise à zéro de l'appareillage sur une solution d'eau déminéralisée en milieu acide à 0,2% (v/v) (HNO_3 ou HCl); (2) détermination du blanc pour chaque concentration d'élément interférent (10, 50, 100 et 500 mg l^{-1}); (3) détermination du signal non perturbé à partir d'une solution simple de métal en milieu acide; (4) détermination du signal en présence de l'élément interférent pour chaque concentration. Chaque détermination est la moyenne de deux mesures. Les résultats ont été calculés en % de variation du signal mesuré en absence d'élément interférent.

RESULTATS

Les résultats des essais sont présentés sur la Fig. 1 en % de variation du signal.

Plomb. Les effets les plus importants sont dus à K et Na qui provoquent une inhibition importante de l'absorption, de 10 à 30% environ dans le domaine considéré ainsi que Fe à 500 mg l^{-1} (18%). Les interférences provoquées par les autres éléments restent inférieures à 11%; Ca et Al entraînant une légère dépression du signal. Les perturbations dues à Mg, Ti et P sont inférieures à 5%.

Cuivre. D'une manière générale le cuivre est assez peu perturbé par les éléments majeurs. Seul le fer provoque une inhibition notable du signal et pour des concentrations supérieures à 100 mg l^{-1} .

Cadmium. La présence des éléments majeurs provoque d'importantes perturbations de l'absorption de Cd; Al et surtout P entraînent une exaltation du signal pouvant dépasser 100% (P au dessus de 50 mg l^{-1}); Mg, Ca, Na, K provoquent une inhibition de l'absorption comprise entre 10 et 20% sur tout le domaine considéré; Fe et Ti entraînent également une diminution du signal, 9% à 500 mg l^{-1} .

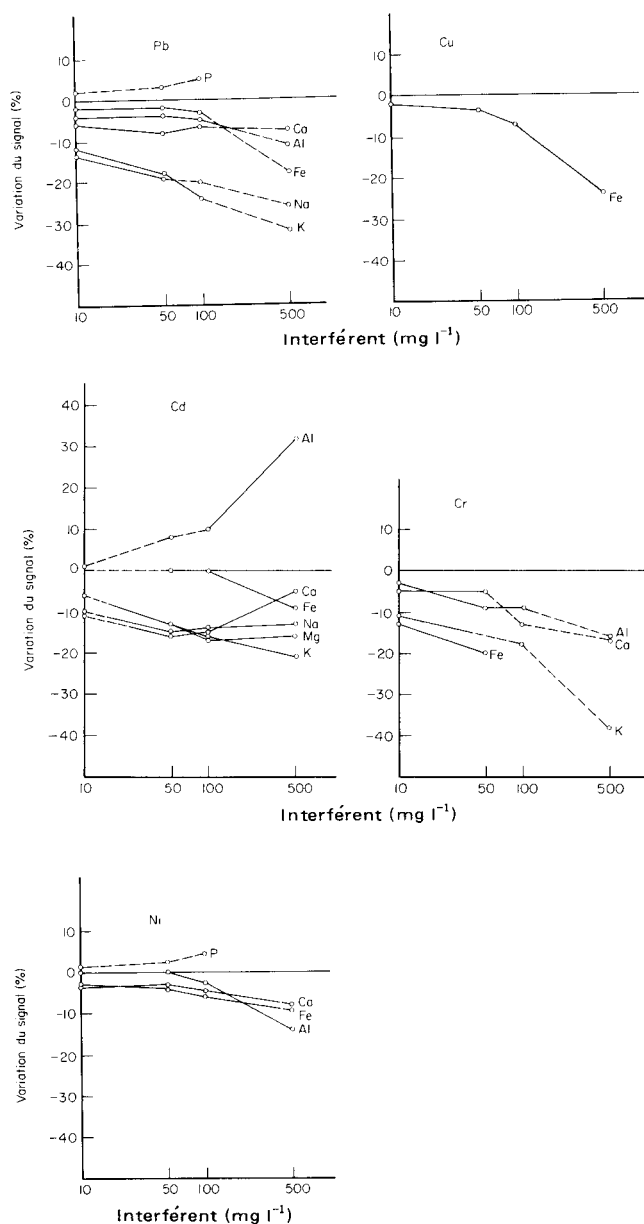


Fig. 1. Interférences lors du dosage de Pb (40 μg l⁻¹), Cu (80 μg l⁻¹), Cd (5 μg l⁻¹), Cr (40 μg l⁻¹) et Ni (200 μg l⁻¹). Les parties renforcées des courbes représentent les gammes de concentrations rencontrées dans les sédiments.

Chrome. La présence de Mg, Na et P ne perturbe pas le dosage du chrome de manière notable, par contre, celle des autres éléments entraîne une inhibition de l'absorption. La solution de Fe contenant une concentration trop importante de Cr, les essais ont été limités à 50 mg l⁻¹ d'interfèrent; Fe et K provoquent une inhibition très importante du signal, supérieure à 10% dès la concentration de 10 mg l⁻¹; Al, Ca et Ti entraînent également une inhibition de l'absorption de l'ordre de 10% à partir de 100 mg l⁻¹ d'interfèrent.

Nickel. L'absorption du nickel est assez peu perturbée par la présence de Mg, Na, K, Ti et P. Seuls Fe, Al et Ca provoquent une dépression du signal, de l'ordre de 10% à partir de 500 mg l⁻¹.

DISCUSSION

Etude des binaires métaux lourds-majeurs

Les teneurs en éléments majeurs des sédiments sont très variables. Le Tableau 2 présente les valeurs moyennes des teneurs dans les matières en suspension des cours d'eau non pollués, extraites de Martin et Meybeck [9], ainsi que les valeurs minimales et maximales que nous avons estimées. De même, les teneurs en éléments traces des matières en suspension, citées par Martin et Meybeck, sont présentées dans le Tableau 3 ainsi que les teneurs généralement rencontrées dans les sédiments non pollués. A partir de ces données, nous avons pu établir les rapports des teneurs minimales et maximales en éléments majeurs sur les teneurs en éléments traces. Ces couples de rapports vont donc nous permettre de préciser l'importance des

TABLEAU 2

Teneurs moyennes [9], maximales et minimales d'éléments majeurs dans les sédiments (en g kg⁻¹ de matière sèche)

	Fe	Al	Mg	Ca	Na	K	Ti	P
Valeur moyenne	48	94	13,5	21,5	7,1	20	5,6	1,2
Valeur minimale	10	20	3,0	5,0	3,0	5,0	1,0	0,05
Valeur maximale	60	120	30	60	30	50	12	2,0

TABLEAU 3

Teneurs moyennes [9] en éléments traces et teneurs des sédiments non pollués (en mg kg⁻¹ de matière sèche)

	Pb	Cu	Cd	Cr	Ni
Teneurs moyennes	150	100	1	100	90
Teneurs des sédiments non pollués	20	10	0,3	50	30

perturbations auxquelles il faut s'attendre lors du dosage des traces dans les sédiments. Les gammes de concentrations rencontrées dans les sédiments sont représentées en traits renforcés sur la Fig. 1. Les rapports éléments majeurs sur éléments traces étant variables d'un métal à l'autre et les métaux lourds testés se trouvant à des concentrations différentes, ces domaines seront donc également différents d'une figure à l'autre.

D'après la teneur moyenne en Pb des sédiments citée par Martin et Meybeck [9] (150 mg kg^{-1}), l'absorption de cet élément devrait être peu perturbée par Fe, Al, Mg, Ti et P. Si Ca ne provoquera qu'une légère diminution du signal, K et Na pourront provoquer une inhibition du signal supérieure à 10%. Néanmoins, les teneurs en Pb qui sont généralement rencontrées dans les sédiments peuvent descendre jusqu'à 20 mg kg^{-1} . Dans ces conditions, les interférences dues à Fe et Al seront plus importantes mais inférieures à 10%, et surtout celles dues à Na et K pourront dépasser 20% du signal.

Le dosage de Cu sera peu perturbé par la présence des éléments majeurs. Dans certains sédiments non pollués les teneurs en Cu pouvant atteindre 10 à 20 mg kg^{-1} , l'inhibition de l'absorption due à Fe pourra alors dépasser 20% du signal si le sédiment contient beaucoup de Fe (plus de 60 g kg^{-1}). Par contre, Cd est un élément sensible à de nombreuses perturbations, notamment par Al susceptible d'augmenter le signal de 10 à 30% et P de plus de 50%, alors que Na, Ca et Mg pourront le réduire de 10 à 15% et K de 10 à 20%. La présence de Fe et K peut provoquer une inhibition de l'absorption de Cr de l'ordre de 10 à 20%. La dépression du signal due aux autres éléments, notamment Al, n'excèdera pas 10%.

Le nickel ne sera pas perturbé par la présence de Na, K, Mg, Ti et P; Ca et Fe pourront introduire une diminution du signal de l'ordre de 10% et Al une diminution comprise entre 10 et 20%, notamment pour des sédiments peu pollués, contenant 30 mg kg^{-1} de Ni par exemple.

En ce qui concerne les boues de stations d'épuration, les niveaux de concentrations des métaux lourds sont en général beaucoup plus élevés que dans les sédiments (Tableau 4 [3]). Nous trouvons dans les boues d'épuration les mêmes éléments majeurs que dans les sédiments, mais avec des quantités de Ca et P beaucoup plus importantes, particulièrement dans les boues issues de traitements physico-chimiques tels que le traitement à la chaux: la concentration de Ca peut varier de 5 à 250 g kg^{-1} de matière sèche, celle de P de 12 à 35 g kg^{-1} .

TABLEAU 4

Teneurs moyennes de métaux lourds dans les boues de stations d'épuration des eaux usées urbaines en France (en mg kg^{-1} de matière sèche) [3]

	Pb	Cu	Cd	Cr	Ni
Valeur moyenne	800	900	59	150	140

De la même manière que pour les sédiments, nous pouvons établir les rapports entre éléments majeurs et éléments traces dans les boues pour Ca et P. Les autres éléments apparaissant généralement en moindre quantité que dans les sédiments et les métaux traces se trouvant à des teneurs plus élevées, ces rapports seront inférieurs à ceux des sédiments sauf pour Ca en présence de Cr et Ni, et pour P vis-à-vis de tous les métaux sauf Cd. Le dosage de Pb et Cu sera donc peu affecté par les éléments majeurs, par contre, l'absorption de Cr, Ni et Cd pourra être diminuée de plus de 10% dans les boues contenant beaucoup de Ca, alors que celle de Cd sera augmentée par P.

Les boues provenant de stations d'épuration qui traitent des effluents strictement urbains ont des teneurs en métaux lourds nettement plus faibles que celles issues d'effluents mixtes ou industriels. Les teneurs minimales en métaux peuvent être de l'ordre de 100 mg kg⁻¹ pour Pb, 200 pour Cu, 5 pour Cd, 50 pour Cr et 25 pour Ni. Pour ces boues nous pourrions donc constater les mêmes interférences que dans le cas des sédiments avec en plus l'interférence de Ca sur Cr, Ni et Cd pour les boues traitées à la chaux.

Etude des matrices complexes

Afin de compléter l'étude des effets séparés des éléments majeurs sur chaque métal, trois matrices réelles représentatives de sédiments différents ont été reconstituées. Les compositions de ces matrices sont indiquées dans le Tableau 5. Chacune des trois solutions testées correspondait à la mise en solution de 1 g de sédiment sec dans 100 ml contenant 20 µg de Pb, 10 µg de Cu, 0,3 µg de Cd, 50 µg de Cr et 30 µg de Ni. Les résultats obtenus (Tableau

TABLEAU 5

Composition des matrices complexes étudiées en % d'oxydes

Matrice	Composition					
	Fe ₂ O ₃	Al ₂ O ₃	MgO	CaO	Na ₂ O	K ₂ O
A	8	20	8	7	3	3
B	5	4	8	30	3	3
C	2	3	32	7	2	2

TABLEAU 6

Interférences lors du dosage des métaux lourds dans les matrices complexes en % de variation du signal

Matrice	Elément				
	Pb	Cu	Cd	Cr	Ni
A	-50	0	-18	+10	+14
B	-31	+3	-26	+2	+6
C	-25	-8	-30	-8	-1

6) sont exprimés en % de variation du signal mesuré sur la solution contenant les cinq métaux lourds seuls en milieu HNO_3 0,2% (v/v). Les éléments qui subissent les perturbations les plus importantes sont Pb et Cd. Le signal de Pb est diminué de 25 à 50%, celui de Cd de 18 à 30% suivant les matrices. Les interférences sont inférieures à 15% pour le dosage de Ni, et inférieures à 10% pour celui de Cu et Cr.

Comme lors des études des effets séparés des éléments majeurs, l'absorption de Cu et Ni est peu perturbée en présence des matrices complexes. Par contre, les effets inhibiteurs semblent s'annuler pour le dosage de Cr. Enfin, en ce qui concerne Pb et Cd, la résultante des effets des éléments majeurs conduit à une importante inhibition du signal notamment pour Pb, et pour les trois matrices considérées.

Conclusion

La présence des éléments majeurs dans les solutions de dosage de certains métaux traces dans les sédiments, notamment le plomb, le cadmium et le chrome, peut provoquer d'importantes interférences. La détermination précise de ces éléments nécessite donc l'utilisation d'une méthode d'étalonnage complexe ou de la méthode des ajouts dosés, bien que cette dernière entraîne généralement une plus grande variabilité des résultats [10]. Par contre, le dosage du cuivre et du nickel est en général peu perturbé (sauf Cu en présence de Fe où l'inhibition du signal peut dépasser 20%, et Ni en présence de Al où elle peut dépasser 14%). Ces conclusions demeurent valables pour le dosage des métaux dans les boues de stations d'épuration notamment pour les boues issues du traitement d'effluents urbains à teneurs plus faibles en micropolluants.

D'autre part, l'interférence du phosphore sur le cadmium sera plus importante et, dans le cas de boues traitées à la chaux ou de boues issues d'un traitement physico-chimique des eaux usées à la chaux, l'interférence du calcium sur le chrome, le nickel et le cadmium sera à prévoir. Enfin, les perturbations constatées en présence de matrices de sédiments reconstituées ne correspondent pas entièrement aux effets cumulés des interférents pris séparément, notamment lors du dosage du chrome.

BIBLIOGRAPHIE

- 1 D. Robbe, Ministère de l'Urbanisme et du Logement, Rapport de recherche LPC 104, 1981, p. 88.
- 2 U. Förstner et W. Salomons, Environ. Technol. Lett., 1 (1980) 494.
- 3 C. Juste, La Tribune du Cebedoc, 432 (1979) 461.
- 4 M. Pinta, Spectrométrie d'absorption atomique, Tome 1, Masson, O.R.S.T.O.M., Paris, 1979, p. 262.
- 5 M. Pinta et C. Riandey, Analisis, 3 (1975) 86.
- 6 M. Hoenig, S. Dupire et R. Wollast, L'atomisation électrothermique en spectrométrie d'absorption atomique et son application dans les études de l'environnement, Cebedoc, Liège, Technique et Documentation, Paris, 1981, p. 218.
- 7 A. Montiel, B. Welte et J. Carre, Analisis, 9 (1981) 1.
- 8 M. Hoenig, C. Lima et S. Dupire, Analisis, 10 (1982) 132.
- 9 J. M. Martin et M. Meybeck, Mar. Chem., 7 (1979) 173.
- 10 P. Marchandise, J. L. Olié, D. Robbe et M. Legret, Environ. Technol. Lett., 3 (1982) 157.

DETERMINATION OF TRACE CONCENTRATIONS OF LEAD AND NICKEL IN FREEZE-DRIED HUMAN MILK BY ATOMIC ABSORPTION SPECTROMETRY AND INDUCTIVELY-COUPLED PLASMA EMISSION SPECTROMETRY

N. W. BARNETT, L. S. CHEN and G. F. KIRKBRIGHT*

Department of Instrumentation and Analytical Science, UMIST, P.O. Box 88, Manchester M60 1QD (Gt. Britain)

(Received 29th October 1982)

SUMMARY

The lead and nickel contents of freeze-dried samples of human milk were determined. Lead was quantified by electrothermal atomic absorption spectrometry and nickel was measured by inductively-coupled plasma emission spectrometry with electrothermal vapourisation. Sample pretreatment consisted of acid digestion and dithizone extraction.

In a recent publication [1], trace level concentrations of lead and nickel were determined in freeze-dried samples of human milk. The procedure for sample pretreatment consisted of heating the milk samples with aqueous tetramethylammonium hydroxide to dryness and then re-suspending the solid residue in a known volume of deionised water. The resulting suspensions were then analysed for lead and nickel by using instrumentation similar to that described herein. The samples analysed in both the previous [1] and present studies were collected under the auspices of the International Atomic Energy Agency and the World Health Organisation from differing socio-economic groups in various countries.

The literature [2–6] contains numerous papers concerned with the determination of lead and various other trace and non-trace elements in cow milk. Koops and Westerbeek [5] cited more than fifty papers on the determination of lead in milk by u.v./visible spectrophotometry, atomic absorption spectrometry and neutron activation techniques. There have been relatively few studies concerning the determination of lead [7, 8] and nickel [9] in human milk.

The work described here was an attempt to improve on the analytical methodology previously reported [1] by acid digestion and preconcentration using liquid–liquid extraction with dithizone; this procedure reduces the high background emission observed in the nickel determination and increases the precision of the results for both elements.

EXPERIMENTAL

Instrumentation and apparatus

For atomic absorption spectrometry (a.a.s.) with electrothermal atomisation, a Perkin-Elmer Model 305B atomic absorption spectrometer fitted with a deuterium arc background corrector was used with a Model HGA-2000 graphite furnace atomiser and a Tarkan 600 chart recorder (W & W Electronics, Switzerland).

For inductively-coupled plasma emission spectrometry (i.c.p.e.s.) with electrothermal vaporisation, a Plasma-Therm Model HFP-2500D, 27.12-MHz plasma source, 2.5-kW generator matching unit and torch box were used with a demountable torch as described by Bombelka [10] and an electrothermal vaporisation sample introduction system as described by Gunn et al. [11]. Other equipment included a Rank-Hilger Monospek 1000, 1-m-focal length monochromator with 1200 lines mm^{-1} plane grating blazed at 300 nm, an E.M.I. Electronics Model 6256B photomultiplier tube, a Brandenburg Model 476R photomultiplier power supply and an Oxford Instruments Series 3000 chart recorder.

Mini-Kjeldahl digestion flasks (5 ml; bulb diameter 25 mm, neck diameter 12 mm, neck length 80 mm) and long-handled glass spoons were produced in the laboratory. The flasks were heated in an Isopad digestion bank (6 × 25—50 ml mantles; Nelson Scientific). Sample solutions were injected from microsyringe/pipettes (0—15 μl) with disposable PTFE tips (Model 15A-SV Scientific Glass Engineering Pty.). The eight-position flask shaker had variable speed and timing (Stuart Scientific Co.).

All the samples analysed and solid reagents were transferred by means of the glass spoons to avoid any contact with metal surfaces and thereby to minimise the risk of contamination.

Cleaning of apparatus. All glassware, plastic ware and anti-bumping granules used were soaked in Decon-90 solution (5% v/v) for 24 h, thoroughly rinsed in distilled water, and soaked in dilute nitric acid (1 + 9). When required, the equipment was removed from the dilute nitric acid, rinsed thoroughly with distilled water, and used immediately. The anti-bumping granules were rinsed with distilled water, carefully dried in an oven at 150°C, and then transferred to a dried acid-washed container.

Reagents and solution preparation

Sulphuric acid (1.835—1.840 g ml^{-1}), nitric acid (1.412—1.417 g ml^{-1}), ammonia solution (0.88) and chloroform were of Aristar grade (BDH Chemicals). Ethanol, diphenylthiocarbazone (dithizone; 99.0% pure), ammonium chloride (99.5% pure), and lead nitrate (99.5% pure) were of AnalaR grade (BDH Chemicals). Nickel wire (99.9% pure; laboratory reagent) provided the nickel standard solution. Singly-distilled water was used.

Dithizone/chloroform solution. A 1.0% (w/v) solution of dithizone in chloroform was stored in a dark bottle. The working reagent (0.01% w/v)

was prepared fresh daily by diluting the stock solution (1 + 99) with chloroform in a polypropylene volumetric flask.

Nickel and lead working solutions. Stock solutions (1000 mg l^{-1}) of nickel and lead were prepared as outlined by Dean and Rains [12] from nickel wire and lead nitrate, respectively. From those stock solutions, a series of combined working standards was prepared daily by serial dilution. The working standards contained both lead and nickel at concentrations of 5.0, 2.0 and 1.0 mg l^{-1} .

Procedures

Sample pretreatment. Portions (0.1 g) of the freeze-dried milk samples were weighed ($\pm 0.1 \text{ mg}$) into mini-Kjeldahl flasks, each containing two anti-bumping granules. The milk was transferred from the polyethylene sample containers to the flasks with a glass spoon. The spoon was designed to hold approximately 0.1 g of milk powder and to fit down the neck of the Kjeldahl flask without touching the inner walls, so that the sample could be placed directly in the bottom of the flask. From Pasteur pipettes, sulphuric acid (5 drops) and nitric acid (10 drops) were added to each flask and the flasks were placed in the digestion bank. At this stage, standard additions were made at 0.1, 0.2 and $0.5 \mu\text{g g}^{-1}$ nickel and lead. The milk was then decomposed by the conventional digestion procedure. At the completion of digestion, the flasks were removed from the heat and allowed to cool to ambient temperature. To each of the cooled digests, distilled water (1 ml) was added and the flask was swirled gently. Then 10 drops of ammonia/ammonium chloride buffer solution ($\approx 1 \text{ M}$, pH 9), and 1 drop of phenolphthalein solution (0.5% w/w in aqueous 50% ethanol) were added to each flask with careful mixing. Ammonia solution was then added to the diluted digests to the first permanent pink colour of the phenolphthalein, thereby adjusting the solutions to pH 8.5–9.0. Within the pH range 8.5–10.5, both nickel(II) and lead(II) can be efficiently extracted with dithizone in chloroform [13, 14]. Immediately after the pH adjustment, the treated digests were extracted with the dithizone/chloroform solution (0.5 ml, 0.01% w/v). The aliquots of the dithizone solution were delivered from a bulb pipette directly into the digestion flasks. The flasks were then shaken for 15 min. The dithizone extracts were then injected for spectrometric measurement of lead and nickel as quickly as was practicable. Experiments showed, however, that the extracts suffered no significant degradation up to 3 h after extraction, i.e., there was no significant change in the signal intensity of the standards or standard additions compared to their initial values.

Instrumental parameters. The instrumental parameters used on both instruments are summarised in Table 1.

Calibration. During the development of the method, it was necessary to obtain a relatively larger amount of freeze-dried human milk than those supplied as individual samples by the International Atomic Energy Agency (about 250 mg). It was decided to pool the residues of freeze-dried human

TABLE 1

Instrumental parameters

I.c.p.e.s. for nickel		A.a.s. for lead	
Wavelength (nm)	352.45	Wavelength (nm) ^b	283.31
Slits (μm)	40	Slits (bandpass nm)	0.3
PMT (kV)	1.4	<i>Furnace programme</i>	
Plasma gas flow rate (l min^{-1})	13.0	Argon flow rate (l min^{-1})	3
Carrier gas flow rate (l min^{-1})	1.8	Drying ($^{\circ}\text{C}$; s)	100; 30
Forward power (kW)	0.85	Ashing ($^{\circ}\text{C}$; s)	400; 30
Reflected power (W)	< 2	Atomisation ($^{\circ}\text{C}$; s) ^c	2000; 4
Viewing height ^a (mm)	33	Sample volume (μl)	15
<i>Electrothermal vaporisation programme</i>			
Drying (V; s)	5.5; 30		
Ashing (V; s)	6.0; 30		
Vaporisation (V; s)	9.0; 3.5		
Sample volume (μl)	15		

^aMeasured from the top of the load coil.

^bLead hollow-cathode lamp operated at manufacturers' specifications, D_2 arc background correction employed.

^c60 s cooling time allowed between end of atomisation and injection of next sample.

milk samples from the previous study [1]. These residues had been resealed and stored at 5°C after analysis. Each of the small plastic containers was emptied into a dried acid-washed beaker (200 ml). The total contents (about 5 g) were then thoroughly mixed with a glass spatula. At this stage, portions of about 1 g were homogenised in a dry acid-washed agate mortar and pestle. These 1-g portions were collected in a dried acid-washed beaker and thoroughly mixed. To ensure homogeneity, this process was repeated again; great care was taken to avoid contamination.

This homogenised pooled sample was utilised for calibration by the method of standard additions. Calibration was also done by using normal

TABLE 2

Equations of the calibration graphs obtained from direct standards and from standard additions

Element	Calibration procedure	Equation of the line ^a	Correlation coefficient
Lead	Standard additions	$y = 117x + 24.6$	0.99995
Lead	Direct standards	$y = 116x + 0.5$	0.99997
Nickel	Standard additions	$y = 46.7x + 30.0$	1.000000
Nickel	Direct standards	$y = 49x - 0.6$	0.99998

^a y is the absorption/emission signal (i.e., peak heights in mm); x is standard concentration ($\mu\text{g g}^{-1}$).

aqueous standards added to reagent blanks which were subjected to exactly the same heating cycle and dithizone extraction as the digested milk samples. Both these methods were found to be satisfactory for lead and nickel. There was no significant difference between the sensitivities of either technique. As the direct standards method was slightly faster, and did not consume the limited supply of pooled milk sample, this means of calibration was used routinely for each set of samples. The method of standard additions was used periodically during the study in conjunction with the direct standardisation as a means of checking the method. Table 2 gives the equations for the typical calibration graphs for both lead and nickel using standard additions and direct standards. Peak height measurements were found to be satisfactory for both elements.

RESULTS

The samples of freeze-dried human milk from different countries were classified into three socio-economic groups; (1) urban elite, (2) urban poor, (3) traditional rural. A summary of the results obtained from the analysis (in duplicate) of 133 samples by the present procedure is presented in Table 3 together with the mean results obtained earlier for the same socio-economic groups [1]. These results do not provide any evidence for the effect of environmental and/or socio-economic conditions on the concentrations of lead and nickel in human milk.

The precision of the present method was measured by calculating the relative standard deviation (RSD) for both lead and nickel in sample solutions without standard addition. The least-squares method of Levitt [15] was used to evaluate the standard deviation of the y intercept and so the RSD. On each of six occasions when the method of standard additions was used, the RSD for the solution without standard additions of lead and nickel was computed. The average of these RSD values appears in Table 4 together with the detec-

TABLE 3

Statistical summary of results for lead and nickel in human milk

Country	Group	No. of samples	Lead ($\mu\text{g g}^{-1}$)			Earlier mean ^a	Nickel ($\mu\text{g g}^{-1}$)			Earlier mean ^a
			Range	Mean	σ		Range	Mean	σ	
A	1	12	<0.01–0.06	0.02	0.02	0.13	0.03–0.43	0.17	0.12	0.11
	2	14	<0.01–0.08	0.03	0.02	0.11	<0.01–0.40	0.11	0.11	0.16
	3	36	<0.01–0.12	0.04	0.04	0.15	<0.01–0.28	0.11	0.07	0.14
B	1	34	<0.01–0.30	0.05	0.07	0.14	<0.01–0.37	0.09	0.09	0.12
	3	25	<0.01–0.16	0.04	0.04	0.12	<0.01–0.30	0.07	0.09	0.11
C	1	5	0.02–0.16	0.08	0.05	0.14	0.04–0.28	0.12	0.09	0.10
	3	7	<0.01–0.17	0.05	0.05	—	0.02–0.24	0.11	0.07	—

^aMean results obtained by the earlier procedures [1] for the same socio-economic groups 1–3 but from countries other than A–C.

TABLE 4

Precision and detection limits

Element	Average RSD	Detection limit ^a (pg)	RSD [1]
Lead	0.05 ^b	12	0.40 ^d
Nickel	0.02 ^c	14	0.07 ^e

^aCalculated assuming 100% extraction into dithizone/chloroform, from 2σ (blank).^bMeasured at $0.07 \mu\text{g g}^{-1}$. ^cMeasured at $0.21 \mu\text{g g}^{-1}$. ^dMeasured at $<0.1 \mu\text{g g}^{-1}$. ^eMeasured at $>0.2 \mu\text{g g}^{-1}$.

tion limits obtained when this method is used, and the RSD values at similar concentrations obtained by the earlier method [1].

DISCUSSION

During the initial stages of the analytical method development, experiments were conducted to establish whether the acid digests could be analysed directly, without dithizone extraction. This approach was found to be satisfactory for quantifying lead; however, when the acid digests were injected to quantify nickel, there was an extremely high background emission at 341.48 nm. Some improvement in the signal-to-background ratio was achieved at 352.45 nm, the improvement being due to an increase in sensitivity rather than a lowering of the background level. As the line at 352.45 nm was approximately twice as sensitive as the 341.48-nm line, the former was used throughout the present study. The intense background emission, which was also observed by Camara-Rica and Kirkbright [1], was virtually eliminated when the dithizone/chloroform extracts of acid digests were injected.

Clearly it would have been expedient to use the same instrumental technique for both lead and nickel. The determination of nickel by electrothermal a.a.s. was discounted on the basis of the work of Batoreu [16] who, using the instrumentation described herein, obtained a detection limit for nickel of 200 pg which is an order of magnitude greater than the present results (see Table 3). Some work was also undertaken with a view to quantifying lead by i.c.p.e.s. with electrothermal vaporisation. Results were obtained at 283.31 and 405.78 nm; those at the latter wavelength were the more promising. However, the day-to-day resetting of the major instrumental parameters proved to be extremely critical with respect to attaining the desired sensitivity. As a consequence, it was often impossible to attain the required sensitivity and thus the measurements were impracticable. The technique favoured was therefore electrothermal a.a.s. which provided a reliable means of quantifying lead at the concentration required.

The mini-Kjeldahl flasks were used throughout the entire procedure for digestion, extraction and sample containment. Only two sample transfers

were required during the entire procedure, thus minimising the possibility of either loss or contamination.

The authors thank the International Atomic Energy Agency for partial support of this work and Mr. Eric Wiggett for technical assistance.

REFERENCES

- 1 C. Camara Rica and G. F. Kirkbright, *Sci. Total Environ.*, 22 (1982) 193.
- 2 D. C. Manning, *Am. Lab.*, August (1973) 37.
- 3 H. L. Huffman and J. A. Caruso, *Talanta*, 22 (1975) 871.
- 4 P. J. Barlow, *J. Dairy Res.*, 44 (1977) 377.
- 5 J. Koops and D. Westerbeek, *Neth. Milk Dairy J.*, 32 (1978) 149.
- 6 J. Koops and D. Westerbeek, *Neth. Milk Dairy J.*, 34 (1980) 31.
- 7 G. K. Murthy and U. S. Rhea, *J. Dairy Sci.*, 54 (1971) 1001.
- 8 W. Bailus, *J. Food Prot.*, 43 (1980) 178.
- 9 G. D. O'Dell, W. J. Miller, W. A. King, J. C. Eller and H. J. Juracek, *J. Dairy Sci.*, 53 (1970) 53.
- 10 R. M. Bombelka, Ph. D. Thesis, University of London, 1978.
- 11 A. M. Gunn, D. L. Millard and G. F. Kirkbright, *Analyst*, 103 (1978) 1066.
- 12 J. A. Dean and T. C. Rains, in R. Mavrodineanu (Ed.), *Procedures Used at the National Bureau of Standards to Determine Selected Trace Elements in Biological and Botanical Materials*, NBS Spec. Publ. 492, Washington, 1977.
- 13 G. F. Morrison and H. Freiser, *Solvent Extraction in Analytical Chemistry*, Wiley, New York, 1962.
- 14 J. Stary, *Solvent Extraction of Metal Chelates*, Pergamon, London, 1964.
- 15 B. P. Levitt (Ed.), *Findlay's Practical Physical Chemistry*, 9th edn., Longman, London, 1973.
- 16 M. C. C. Batoreu, Ph. D. Thesis, University of Manchester, 1982.

THE DETERMINATION OF ARSENIC BY ELECTROTHERMAL ATOMIC ABSORPTION SPECTROMETRY AFTER LIQUID–LIQUID EXTRACTION

F. PUTTEMANS, P. VAN DEN WINKEL and D. L. MASSART*

Pharmaceutical Institute, Vrije Universiteit Brussel, Laarbeeklaan 103, B-1090 Brussels (Belgium)

(Received 10th May 1982)

SUMMARY

Two extraction procedures are described for determinations of total arsenic in biological materials. In the first, organic matter is wet-ashed, followed by an extraction with ammonium pyrrolidinedithiocarbamate and chloroform; back-extraction is done with a solution of copper(II) chloride. The second procedure is based on an oxygen-flask combustion with absorption of the products in concentrated hydrochloric acid, followed by reduction of arsenic(V) with potassium iodide; extraction with benzene and back-extraction into 0.1 M hydrochloric acid precede the final measurement by graphite-furnace atomic absorption spectrometry. The accuracy of both methods was proved by analyzing a standard reference material. Because the oxygen-flask combustion takes only a few minutes, this procedure is preferred for routine applications, although it is restricted to biological materials with arsenic contents of at least $0.3 \mu\text{g g}^{-1}$ (dry weight).

Liquid–liquid extraction offers many possibilities for separating the element of interest from interfering matrix compounds and for preconcentrating the element prior to its measurement by atomic absorption spectrometry (a.a.s.), for example [1]. Usually chelating agents are applied to achieve this. In the first part of this study [2], a liquid–liquid extraction procedure was proposed in which ammonium pyrrolidinedithiocarbamate (APDC) or diethyldithiophosphoric acid (HDEDTP) was used for the quantitative extraction of arsenic(III) from strongly acidic media. A preliminary reduction step permitted the differential determination of arsenic(III) and arsenic(V) in water. In this article, the same method is used to determine the total arsenic content of biological material after wet-ashing of the organic matter.

A second possibility is the direct extraction of the halides of arsenic(III) [3]. A neutron activation method for the determination of arsenic in biological material, based on extraction of the iodide from sulfuric acid–potassium iodide medium with toluene, was described by Byrne [4]. In other procedures, 2 g of biological material [5] or 2 ml of blood [6] was dry-ashed at 550°C after the addition of the same amount of 50% (w/v) magnesium nitrate solution; the ash was dissolved in hydrochloric acid,

potassium iodide was added, and arsenic was extracted with chloroform and back-extracted with a 0.26% (w/v) magnesium nitrate hexahydrate solution. Ishizaki et al. [7] also described a method in which 1 ml of urine was added to absorbent cotton, which was dried for 3 days at room temperature and then burned in an oxygen flask [8, 9]; the same chloroform extraction from potassium iodide-hydrochloric acid medium was then applied. The methods of Ishizaki and co-workers [5-7] show that extraction of arsenic halides may be used prior to a.a.s. However, the methods are rather time-consuming and the suitability of a dry-ashing procedure is somewhat uncertain with regard to quantitative recovery of arsenic [10]. A method more suitable for routine purposes is proposed below.

EXPERIMENTAL

Equipment and reagents

The apparatus was a Perkin-Elmer 460 atomic absorption spectrometer, equipped with a HGA-76B graphite furnace unit. Operating and instrumental conditions were as described previously [2]. The oxygen-flask combustions were done with a Heraeus Model K Schöniger combustion unit, using suitable 500-ml pyrex Erlenmeyer flasks. Most reagents used were described earlier [2]. The hydrochloric acid (Carlo Erba, RSE quality) and benzene (Merck) were of the highest analytical purity. Freshly prepared twice-distilled water was used for all experiments. All glassware was acid-washed before use. All extractions were done in cylindrical 50-ml separating funnels.

Tracer solution

Arsenic-76 was obtained by irradiation of arsenic(III) oxide in the Thetis reactor at Gent (Instituut Nucleaire Wetenschappen, Belgium) at a flux of $4 \times 10^{11} \text{ n cm}^{-2} \text{ s}^{-1}$ for about 6 h. When the irradiated target material was dissolved in 12 M hydrochloric acid and the solution was diluted, appropriate specific activities were obtained for evaluating the extraction yields. The 559- and 657-keV γ -radiation of ^{76}As was measured by means of a 3×3 -in. well-type NaI (Tl) detector (Bicron) coupled to a multichannel analyzer (Canberra Series 40) provided with peak area and peak integral functions.

Oxygen-flask combustion and extraction for the determination of total arsenic

The dried biological material (ca. 40 mg) is accurately weighed and burned in a 500-ml Schöniger flask containing 10 ml of 12 M hydrochloric acid. The stopper is rinsed with 5 ml of 12 M hydrochloric acid, and the flask with another 5-ml portion of the same acid, the acid washes being collected in a 25-ml volumetric flask containing 2 ml of 20% (w/v) potassium iodide solution. The solution is diluted to the mark with 12 M hydrochloric acid.

A 10-ml portion of this solution is shaken vigorously for 1 min with 5 ml

of benzene, previously saturated with concentrated hydrochloric acid. After phase separation, the upper benzene layer is pipetted off and the extraction is repeated with another 5-ml portion of benzene. Then 8 ml of the collected benzene fractions is back-extracted with 4 ml of 0.1 M hydrochloric acid, previously saturated with benzene. A 50- μ l fraction of the acid layer is injected into the graphite furnace followed by an injection of 50 μ l of a 2500 ppm nickel(II) solution as stabilizing agent. The arsenic content of the acid fractions is determined by interpolation of the a.a.s. signals on a calibration graph of the appropriate arsenic(III) standard solutions, made up in 0.1 M hydrochloric acid.

Acid digestion and extraction for the determination of total arsenic

The lyophilized material is transferred to a Kjeldahl flask, and 5 ml of concentrated nitric acid is added. After moderate heating, 3 ml of a (1 + 2) mixture of perchloric acid and nitric acid is added, and the mixture is digested with evaporation until a 0.5-ml residue remains. This residue is dissolved in 10 ml of twice-distilled water and the solution is transferred to a 25-ml volumetric flask with two 5-ml portions of water; the flask is previously charged with 0.5 ml of 20% (w/v) potassium iodide solution. A few drops of 0.1 N sodium thiosulfate are added before dilution to the mark with water.

For the extraction, 5 ml of 0.1% (w/v) APDC is added to a 20-ml portion of the solution with 20 ml of chloroform. After vigorous shaking for 2 min and phase separation, 10 ml of the chloroform layer is back-extracted with 5 ml of 200 ppm copper(II) chloride solution. Aliquots (50 μ l) of the aqueous phase are injected into the graphite furnace followed by the nickel(II) solution as described above. The a.a.s. signals are interpolated on a calibration graph obtained from the extraction of a blank and three standard solutions, containing 10, 15 and 20 ng As(III) ml⁻¹, respectively, made up in 2% (v/v) perchloric acid and 0.4% (w/v) potassium iodide.

RESULTS AND DISCUSSION

Of the generally applied methods for the decomposition of organic materials prior to the determination of arsenic, the most effective are probably those in which mixtures with perchloric acid are used [10]. The vital point seems to be that the sample must be heated moderately in the presence of an excess of nitric acid, so as to avoid charring. Under these conditions, losses of arsenic through volatilization are likely to be minimized. This cannot be said of the dry-ashing methods, the suitability of which for quantitative recovery of arsenic is uncertain.

The optimum conditions for the extraction procedure with APDC and chloroform were described earlier [2]. The accuracy of the combined digestion and extraction procedure was investigated by determining the total arsenic content of the N.B.S. standard reference material, orchard leaves (SRM 1571), which has a certified arsenic content of $10.0 \pm 2 \mu\text{g g}^{-1}$.

For seven determinations, done on four different days, arsenic contents between 9.3 and 10.5 $\mu\text{g g}^{-1}$ were calculated, with a mean content of $10.1 \pm 0.4 \mu\text{g g}^{-1}$ and a relative standard deviation of 4.4%. Nearly 1.0 g of biological material can be digested adequately, so that the limit of detection for arsenic is 0.015 $\mu\text{g g}^{-1}$ of dried material. However, only five samples and a blank can be processed in a day, because complete destruction takes at least 5 h.

To establish the optimum conditions for the extraction of arsenic with benzene from hydrochloric acid medium, a 20-ml portion of a tracer solution of arsenic(III) made up in 12 M hydrochloric acid was extracted with two 10-ml portions of benzene. These fractions were collected and counted, as well as the residual activity of the hydrochloric acid phase. An identical experiment was done with a tracer solution made up in 10 M hydrochloric acid. The results, summarized in Table 1, indicate that quantitative extraction is achieved only when 12 M hydrochloric acid is used. These results do agree with those reported previously [11]. A maximum recovery of 90% was obtained for a single extraction of arsenic from 12 M hydrochloric acid with an equal volume of benzene.

Because 12 M hydrochloric acid cannot be used in a wet-ashing procedure, the Schöniger oxygen-flask combustion technique [8, 9] was preferred. In this technique, the organic material to be ashed is wrapped in a piece of Whatman paper no. 44 (3 × 3 cm), which is placed in a platinum gauze holder and inserted into a flask (ca. 500 ml) filled with pure oxygen, with electrical ignition of the paper. Much larger samples have been burned in larger flasks for the determination of traces of arsenic [12] but samples of about 40 mg sufficed for the present purpose.

Under the above conditions, arsenic(V) is not extracted at all, so that any arsenic(V) in the solution resulting from the combustion must first be reduced. Attempts to use hydrazinium chloride or cold hydroxylammonium chloride as reducing agents failed; the extraction recovery was only about 80%. Potassium iodide yields better results, as was concluded from the following experiments. In the first tests, 1 ml of 20% (w/v) potassium iodide was added to a 20-ml portion of arsenic(III) tracer solution in 12 M hydrochloric acid, which was then extracted with 10 ml of benzene. The results, summarized in Table 2, show that the addition of iodide does not interfere with the

TABLE 1

Extraction recoveries for arsenic(III) from 12 M and 10 M hydrochloric acid into benzene

	Recovery (%)	
	12 M HCl	10 M HCl
HCl phase	1.4	12.9
Benzene phase	100.4	88.2

TABLE 2

Extraction recoveries for arsenic in the presence of iodide and after oxygen-flask combustion

	Recovery (%)	
	From KI solution	Recovery after combustion
HCl phase	<0.1	<0.1
Benzene phase	101.3	101.6

quantitative extraction of arsenic(III). Secondly, 100 μl of the same tracer solution was spotted on a Whatman paper which was burned and the solution obtained was extracted, following the procedure described under Experimental, but without the back-extraction into 0.1 M hydrochloric acid. The activities of both phases were counted. The results (Table 2) prove that the extraction is still complete. Potassium iodide can thus be used successfully to reduce any arsenic(V) resulting from the combustion to arsenic(III) prior to the extraction. In the extremely acidic medium used, iodide is spontaneously oxidized to iodine; although co-extracted, the iodine does not affect the extraction of arsenic(III) with benzene.

The procedure is completed with back-extraction into 0.1 M hydrochloric acid, which greatly simplifies the final measurement by electrothermal atomic absorption spectrometry. The precision and accuracy of the entire procedure were evaluated by analyzing the same N.B.S. standard reference material (orchard leaves) 23 times over a period of almost 5 weeks. The samples taken ranged in size from 30 to 53 mg and an average arsenic content of $10.3 \pm 0.6 \mu\text{g g}^{-1}$ was calculated. The precision of the procedure is characterized by a relative standard deviation of 5.6%.

The N.B.S. certificate states that a minimum sample of 250 mg of the dried material should be used for any determination to be related to the certified values. In the Schöniger oxygen-flask procedure used (500-ml flask), however, 50 mg was the maximal amount of material that could be completely burned. The above results show that even with these small samples the accuracy is good, which means that the homogeneity of the reference material is excellent. The detection limit is about 1 ng As ml^{-1} in the final solution, thus the limit of detection for arsenic in biological material is about $0.3 \mu\text{g g}^{-1}$ of dried material.

It can be concluded that the combination of liquid-liquid extraction with the oxygen-flask combustion yields a reproducible and accurate method for the determination of arsenic in biological materials. The method has the advantage that it is much faster than the wet-ashing procedure and therefore suited to routine work. The combustion takes only a few minutes, and an experienced worker can complete twelve determinations within the course of a normal working day instead of the five determinations possible with

TABLE 3

Comparative study of the arsenic content of feces and some organs of mice fed with arsenic for 2–8 weeks

Sample ^a	Arsenic content of the organs ($\mu\text{g g}^{-1}$, dry weight)							
	2 weeks		4 weeks		6 weeks		8 weeks	
	A.a.s.	N.a.a.	A.a.s.	N.a.a.	A.a.s.	N.a.a.	A.a.s.	N.a.a.
Feces	124.3	105.3	184.3	155.5	125.5	127.6	164.3	146.0
Kidney	12.9	11.3	21.0	14.1	21.5	16.8	22.7	41.3
Liver	6.6	4.6	5.2	5.2	5.4	6.2	5.9	—

^aThe samples were obtained from K. Poma.

the wet-ashing procedure. The method is restricted, however, to biological materials with arsenic contents of at least $0.3 \mu\text{g g}^{-1}$ (dry weight) if a 500-ml combustion flask is used. This limit of detection is not good enough for the determination of normal values of arsenic in many biological materials, although it suffices for much routine work (toxicology, food analysis, etc.). The method was applied with success for the determination of the arsenic content of organs and tissues of mice, which were fed arsenic to study certain toxicological mechanisms [13]. Some typical results are given in Table 3; a non-parametric statistical test showed that the results obtained by the combustion–extraction method and by neutron activation analysis (n.a.a.) were not significantly different. If determinations at a lower concentration level are necessary, the wet-ashing procedure described or a larger oxygen flask could be used.

The authors thank the FGWO for financial support and F. De Corte for the irradiation facilities made available at the Thetis reactor, Gent.

REFERENCES

- 1 J. Stary, *The Solvent Extraction of Metal Chelates*, Pergamon Press, Oxford, 1964, p. 21.
- 2 F. Puttemans and D. L. Massart, *Anal. Chim. Acta*, 141 (1982) 225.
- 3 A. K. De, S. M. Khopar and R. A. Chalmers, *Solvent Extraction of Metals*, Van Nostrand-Reinhold, London, 1970, p. 6.
- 4 A. R. Byrne, *Anal. Chim. Acta*, 59 (1972) 91.
- 5 M. Ishizaki, *Bunseki Kagaku*, 26 (1977) 667.
- 6 M. Ishizaki and F. Kataoka, *Jpn. J. Ind. Health*, 19 (1977) 136.
- 7 M. Ishizaki, M. Fujiki and S. Yamaguchi, *Jpn. J. Ind. Health*, 21 (1979) 234.
- 8 W. Schöninger, *Mikrochim. Acta*, (1955) 123.
- 9 W. Schöninger, *Mikrochim. Acta*, (1956) 869.
- 10 T. T. Gorsuch, *Analyst*, 85 (1960) 629.
- 11 P. Van den Winkel, *De bepaling van sporenelementen in biologisch materiaal door neutronenaktiverings analyse — Verhandeling Koninklijke Vlaamse Akademie v.d. Wetenschappen, België, Jaargang XXXII, 1970, Nr. 114.*
- 12 W. H. Gutenmann, L. E. Saint-John, D. L. Barry, E. D. Jones and D. J. Lisk, *J. Agric. Food Chem.*, 9 (1961) 50.
- 13 K. Poma and F. Puttemans, unpublished results.

DETERMINATION OF BARIUM AT ng ml^{-1} LEVELS BY FLAME EMISSION SPECTROMETRY AFTER ION-EXCHANGE SEPARATION FROM 1000-FOLD AMOUNTS OF CALCIUM

KEITH E. JOHNSON*, F. WAYNE YERHOFF, JOHN ROBINSON, and
CHRISTINE DEHM

Department of Chemistry, University of Regina, Regina S4S 0A2 (Canada)

(Received 27th July 1982)

SUMMARY

Atomic spectrometric techniques for the determination of ng ml^{-1} levels of barium in the presence of calcium are examined. Flame atomic absorption spectrometry appears to be free of interferences, but is subject to error from instrumental variations or high noise levels. Flame atomic emission spectrometry has an easily accessible detection limit of 5 ng ml^{-1} , but is subject to serious interference by calcium. This is solved by an efficient ion-exchange separation of barium from 1000-fold amounts of calcium in an all-plastic apparatus.

Many utilities require extremely pure water for the generation of steam and have had recourse to reverse osmosis for the last stage of purification. It has been found that barium, calcium and sulphate ions at concentrations below those required for precipitation can lead to the formation of a hard barium/calcium sulphate crust within the reverse osmosis membrane, which is eventually destroyed. One answer to this problem is pre-treatment of the water to remove barium. Such a process requires a method for determination of barium at concentrations down to a few ng ml^{-1} in order to monitor the pre-treatment process. Although such monitoring must be done on an ongoing basis, the number of samples is generally far too small to justify a major capital investment in new analytical equipment.

Various techniques for determining barium at the ng ml^{-1} level have been reported, primarily in the field of atomic spectrometry. The best results from flame atomic absorption spectrometry include a detection limit of 5 ng ml^{-1} for an air–acetylene flame after lead chromate co-precipitation and ion-exchange chromatography [1], and 8 ng ml^{-1} for a nitrous oxide–acetylene flame [2]. Detection limits claimed for inductively-coupled plasma emission range from 0.3 to 2 ng ml^{-1} [2–5], while nitrous oxide–acetylene flame emission values are reported in the range 2 – 3 ng ml^{-1} [6–8]. Graphite-furnace atomic absorption detection limits are in the region of 0.15 to 4 ng ml^{-1} [2, 9–11], while graphite-furnace emission gives a reported value of 0.4 ng ml^{-1} [12, 13].

An evaluation of these methods for use in monitoring reverse osmosis or similar systems must consider the presence in the samples of potentially interfering ions, especially calcium and alkali metals at up to 2000-fold and sulphate at up to 5000-fold concentration levels. The method should be easily and inexpensively used on generally available equipment by chemists or chemical technologists with no specialized analytical skills. An evaluation of methods and a procedure for determining ng ml^{-1} concentrations of barium based upon these criteria are reported below.

EXPERIMENTAL

Solutions and instrumentation

Barium stock solutions were made from Fisher Certified ACS barium chloride. Solutions for interference studies were made from the following salts: Fisher Certified ACS calcium chloride (0.002% Ba) or calcium nitrate (0.002% Ba), Fisher Certified lanthanum chloride (suitable for atomic absorption spectrometry of alkaline earths), Baker Analyzed Reagent sodium sulphate, and Fisher Certified ACS potassium dihydrogenphosphate. Ionization suppressors used were Baker Analyzed Reagent potassium chloride (<0.001% Ba) or Matheson, Coleman and Bell cesium chloride. A 1% solution of potassium chloride used for ionization suppression gave a total blank emission intensity equivalent to between 11 and 15 ng Ba ml^{-1} , depending on the spectrometer used.

Flame and furnace atomic absorption measurements were done on a Varian—Techtron AA-120 spectrometer with nitrous oxide—acetylene flame or a Varian Model 61 Mini-Massman graphite-rod furnace. Flame atomic emission measurements were made on the above instrument, and also on Perkin-Elmer 360, 380, and 603 spectrometers. The minimum slit-width setting available was used in all cases. The fuel—oxidant ratio and detector wavelength settings (553.6 nm) were optimized with barium standards immediately before sample runs and checked during runs. Detection limits were defined as the concentration equivalent of the peak-to-peak background noise observed under the operating conditions.

Ion-exchange separation and spectrometry

The ion-exchange apparatus consisted of an all-plastic column and pressurized air system as shown in Fig. 1. The column consisted of two 50-ml polypropylene graduated cylinders, a polypropylene funnel and a teflon stopcock welded together by using a plastic welding rod and a hot-air gun. An inverted 250-ml polypropylene bottle with bottom removed was welded to the top of the column to act as a solvent reservoir. The system was pressurized to allow optimum flow rate control. An aquarium pump served as the pressure source, with a bleed screw inserted in the line to control the pressure and an automotive fuel pump gauge included as a monitor. The pressure line entered the column through a well-seated rubber stopper that held a second, larger solvent reservoir which could also be pressurized.

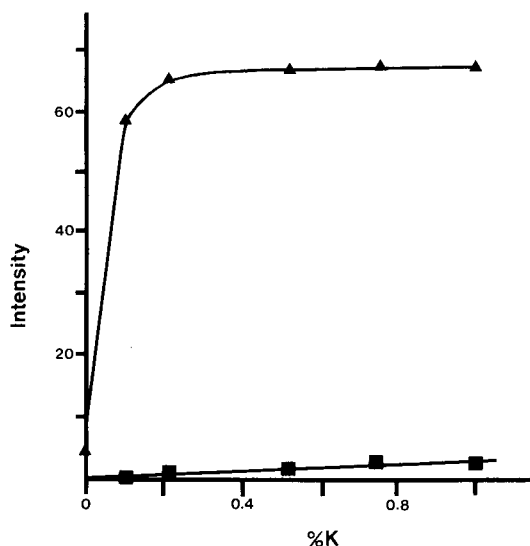
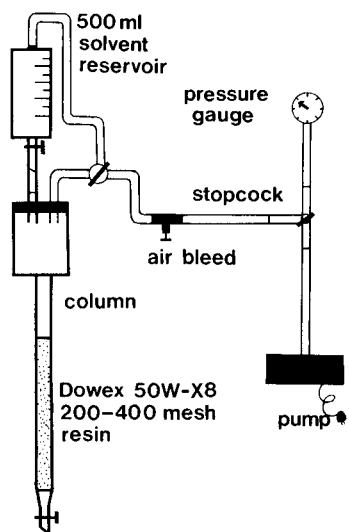


Fig. 1. Ion-exchange apparatus with pressurized flow system.

Fig. 2. Effect of potassium ion concentration on flame emission intensity for (■) 0; (▲) $0.5 \mu\text{g Ba ml}^{-1}$.

The ion-exchange resin was supported on a bed of shredded plastic made by grinding plastic welding rod in a coal grinder, then washing with 3 M hydrochloric acid and 3 M nitric acid. A suspension of Dowex 50W-X8 cation-exchange resin (200–400 mesh; Baker Analyzed Reagent) in 3 M hydrochloric acid was added slowly and allowed to settle to give a 10–15 cm column of resin. This column was washed at 3 ml min^{-1} with 300 ml of 3 M hydrochloric acid, and then with water until the effluent was neutral.

In a typical run, the water sample (25–50 ml) was added at the top of the resin column and run through at $2.5 \pm 0.4 \text{ ml min}^{-1}$. The column was eluted with 400–500 ml of 3 M hydrochloric acid/20% ethanol at 2.5 ml min^{-1} to remove most cations. The column was then eluted with 50–100 ml of water, followed by 3 M hydrochloric acid at 2.5 ml min^{-1} . The eluate was collected in 50-ml polypropylene volumetric flasks containing enough potassium chloride to give a 1% solution. Barium in the fractions was then measured by atomic emission spectrometry with a nitrous oxide–acetylene flame at 553.6 nm, using suitable standards containing 1% potassium chloride and a potassium chloride blank. All of the detectable barium was generally eluted in the first 6–8 fractions (usually in fractions 4–6). An additional 100–200 ml of 3 M hydrochloric acid was passed through to regenerate the column, which was washed to neutrality with distilled water.

RESULTS AND DISCUSSION

Evaluation of methods

The substantial ionization of barium in the nitrous oxide—acetylene flame leads to greatly decreased analytical sensitivity by absorption and emission methods, and there is interference by alkali and alkaline earth metals. This problem is generally eliminated by the addition of potassium or cesium salts as ionization suppressors. Although a 1 mg ml^{-1} concentration of either metal is often used, 5 mg of potassium has been recommended as the optimum concentration [8]. A study of the emission intensity of $0.5 \text{ } \mu\text{g Ba ml}^{-1}$ at various concentrations of potassium (Fig. 2) showed that 1 mg K ml^{-1} is insufficient; $\geq 3 \text{ mg ml}^{-1}$ is required to give an emission intensity which is insensitive to the presence of additional alkali metal. Further studies showed no significant difference between equal concentrations of potassium and cesium as ionization suppressors.

A CaOH absorption/emission band at 554 nm produces a well-known spectral interference at the most sensitive analytical wavelength (553.6 nm) of barium. In the case of atomic absorption spectrometry, the apparent interferences observed have been attributed solely to saturation of the detector by CaOH emission [14], thus making the problem an artifact of the individual spectrometer used. With the Varian AA-120, no change was found in the absorbance of $2 \text{ } \mu\text{g Ba ml}^{-1}$ at calcium concentrations up to 1 mg ml^{-1} . There was, however, a substantial increase in the noise level of readings at high calcium concentrations.

The detection limit observed for measurements on the AA-120 was 380 ng ml^{-1} , without undue effort to correct for flame instability and wavelength drift. With careful optimization of conditions, much better detection limits have been reported on other equipment. The absence of any real calcium interference makes atomic absorption spectrometry the method of choice for higher concentrations of barium in mixed systems. However, the large increase in noise resulting from high calcium concentrations appears to preclude the precise determination of barium in the presence of 1000-fold amounts of calcium at barium concentrations below ca. $0.5 \text{ } \mu\text{g per ml}$.

Calcium interference is a problem in flame atomic emission spectrometric determination of barium. The emission intensity obtained for $200 \text{ ng Ba ml}^{-1}$ (+1% potassium chloride) at 553.6 nm increases linearly with increasing calcium concentration. The emission intensity ratio of equal weights of barium and calcium under these circumstances was typically 400:1. By careful optimization of the fuel—oxidant ratio and burner height to maximize this ratio (not barium sensitivity), and by using $500 \text{ } \mu\text{g Ca ml}^{-1}$ with and without $0.2 \text{ } \mu\text{g Ba ml}^{-1}$, it was possible only to double (approximately) this value. It thus appears unlikely that barium can be accurately determined by flame emission spectrometry in the presence of a 1000-fold amount of calcium.

Phosphate is the major chemical interference reported for spectrometric

determination of the alkaline earths. Lanthanum salts are normally recommended to suppress this interference. It was found that the addition of a 100-fold excess of phosphate caused no change in barium emission intensity, but that an increase in intensity occurred on subsequent addition of lanthanum. Figure 3 shows the emission intensity relative to lanthanum concentration with and without added barium. High concentrations of sulphate were also found to give a small emission enhancement (Fig. 3), as well as an increased noise level.

A flame emission detection limit for barium of 4.5–6.5 ng ml⁻¹ was found on three different spectrometers after routine optimization of fuel–oxidant ratio and burner height. Results from several spectrometers suggested that the detection limits for barium obtained by flame emission spectrometry were much less sensitive to equipment condition and precise optimization of all parameters than those for atomic absorption spectrometry.

Electrothermal atomic absorption determination of barium was also attempted; a relatively inexpensive graphite furnace available for the Varian AA-120 was used. The reproducibility of results for both barium and copper was found to be poor, and very dependent on the skill of the operator. The detection limit for barium was about an order of magnitude higher than reported values.

Of the techniques examined, flame emission spectrometry appears most appropriate for the occasional determination of ng ml⁻¹ levels of barium, on the grounds of simplicity and sensitivity. Several reports leave no doubt that

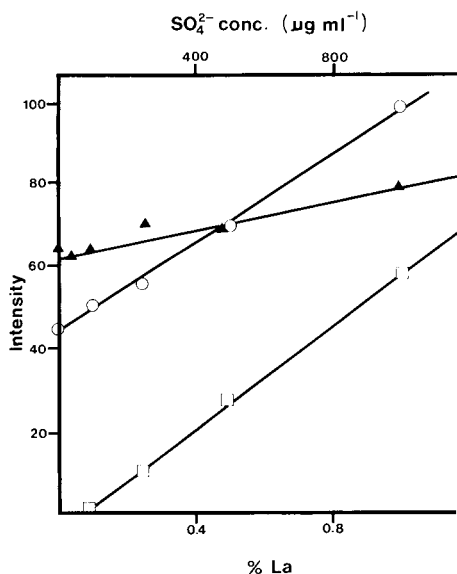


Fig. 3. Effect of phosphate, lanthanum and sulphate ions on the emission intensity of barium: (□) 1% KCl + 0.035% PO₄³⁻ vs. % La; (○) 3 µg Ba ml⁻¹ + 1% KCl + 0.035% PO₄³⁻ vs. % La; (▲) 0.2 µg Ba ml⁻¹ + 1% KCl vs. µg SO₄²⁻ ml⁻¹.

atomic absorption spectrometry using modern graphite-furnace systems with automated sample injectors can give precise and accurate values for barium down to a few ng ml^{-1} . However, the cost of these systems and the observations of calcium interferences in this type of measurement [9, 11, 12] make it appear less suitable for infrequent analyses. The major drawback to flame emission is that the removal of large amounts of calcium (and preferably sulphate) is required, but this can be done efficiently by ion-exchange chromatography.

Ion-exchange separation of calcium and barium

The procedure used was adapted from the method of Frache and Mazzucotelli [15] for the determination of barium in silicate rocks. These authors demonstrated that while 3 M hydrochloric acid/20% ethanol elutes most cations from a sulphonated cation-exchange resin, barium and some lanthanides are retained, and may be eluted separately with 3 M hydrochloric acid. The original apparatus described for this procedure used a glass column with a glass wool-resin support. Our initial attempts to separate solutions containing less than $5 \mu\text{g Ba ml}^{-1}$ using this apparatus resulted in the loss of up to 40% of the barium through adsorption on the glass. The addition of 1% nitric acid to the eluting agents greatly improved total barium recovery, but resulted in the elution of some barium with the calcium in the 3 M acid/20% ethanol. This apparatus was therefore replaced with an all-plastic column. A pressure system was also added to give faster flow rates where desirable. Separation results for solutions containing various concentrations of calcium and barium are shown in Table 1. The distribution curve for the 500:4 Ca:Ba sample is depicted in Fig. 4. With a solution containing $50 \mu\text{g Ca ml}^{-1}$ and 50 ng Ba ml^{-1} , 88% of the total barium was detected in three 50-ml fractions of the 3 M acid eluant (17, 23 and 4 ng ml^{-1} in fractions from 150 to 300 ml). Most of the barium was usually recovered in 2 or 3 fractions, although the distribution was shown to be affected by the initial

TABLE 1

Ion-exchange separation of calcium and barium

Vol. of Ba eluate ^a (ml)	Ca taken ($\mu\text{g ml}^{-1}$)	Ba taken ($\mu\text{g ml}^{-1}$)	Recovery (%)	
			Ca	Ba
550	500	5	98	—
500	500	4	102	97
550	500	3	—	89
500	500	2	88	90
500	50	0.05	—	88

^aCalcium was eluted with 500 ml of 3 M HCl/20% ethanol and then barium was eluted with 3 M HCl.

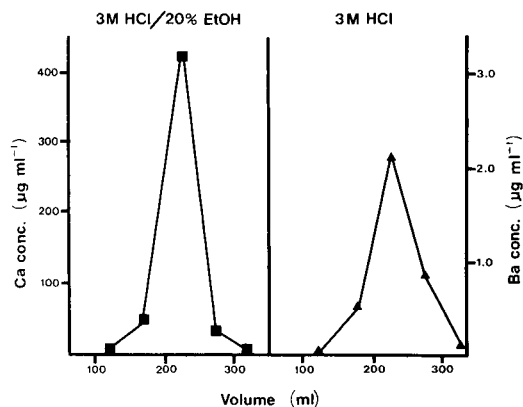


Fig. 4. Ion-exchange distribution curve for: (■) 500 µg Ca ml⁻¹; (▲) 4 µg Ba ml⁻¹.

sample volume. A 25-ml sample was sufficient for barium concentrations greater than 50 ng ml⁻¹.

This work was supported by the R and D area of Saskatchewan Power Corporation. We appreciate discussions with M. Barabas, P. Champagne and W. Gardener of SPC. We thank SPC and the Geochemistry Laboratory, University of Regina, for the use of equipment.

REFERENCES

- 1 V. Sixta, M. Miksovsky and Z. Sulcek, *Fresenius Z. Anal. Chem.*, 273 (1975) 193.
- 2 R. Ediger and G. Wallace, *Can. Res.*, May, 1981, p. 25.
- 3 N. R. McQuaker, P. D. Kluckner and G. N. Chang, *Anal. Chem.*, 51 (1979) 888.
- 4 G. F. Larson, R. T. Goodpasture and R. W. Morrow, *Proc. Conf. Appl. Plasma Emiss. Spectrochem.*, Heyden, Phil. (1979), p. 46.
- 5 J. R. Garbarien and H. E. Taylor, *Appl. Spectrosc.*, 33 (1979) 220.
- 6 E. E. Pickett and S. R. Koirtiyohann, *Spectrochim. Acta, Part B*, 23 (1968) 235.
- 7 F. D. Pierce and H. B. Brown, *Anal. Lett.*, 10 (1977) 685.
- 8 M. Pistekova, J. Jambor, V. Otruba and L. Sommer, *Collect. Czech. Chem. Commun.*, 44 (1979) 69.
- 9 R. Cioni, A. Mazzucotelli and G. Ottonello, *Anal. Chim. Acta*, 82 (1976) 415.
- 10 M. S. Epstein and A. T. Zander, *Anal. Chem.*, 51 (1979) 915.
- 11 K. C. Thompson and R. G. Godden, *Analyst*, 100 (1975) 198.
- 12 R. C. Hutton, J. M. Ottaway, T. C. Rains and M. S. Epstein, *Analyst*, 102 (1977) 429.
- 13 L. Ebdon, R. C. Hutton and J. M. Ottaway, *Anal. Chim. Acta*, 96 (1978) 63.
- 14 R. C. Rooney and J. F. Wooley, *Analyst*, 103 (1978) 1100.
- 15 R. Frache and A. Mazzucotelli, *Talanta*, 23 (1976) 389.

THE DIRECT AND INDIRECT DETERMINATION OF TRACES OF COPPER, LEAD AND CADMIUM IN MERCURY BY VOLTAMMETRY AT THE HANGING MERCURY DROP ELECTRODE

STEFAN GŁODOWSKI and ZENON KUBLIK*

Department of Chemistry, University of Warsaw, Pasteura 1, Warsaw 02093 (Poland)

(Received 13th October 1982)

SUMMARY

Direct and indirect methods of determining traces of copper, lead and cadmium in mercury are proposed. In the direct method, a small portion of the mercury under test is introduced into the hanging drop electrode, the anodic voltammogram is recorded, and the concentrations of the contaminants in the mercury phase are determined from the heights of the anodic peaks. The detection limits for this method are 2×10^{-7} mol dm⁻³ for lead and cadmium and 4×10^{-7} mol dm⁻³ for copper. The use of the pulse technique gives a fivefold improvement in the detection limits for lead and cadmium. In the indirect method, the contaminating metals are oxidized from mercury to an appropriate supporting electrolyte, and the determination is completed in the same electrolytic cell by anodic stripping voltammetry at a hanging mercury drop electrode. The detection limits for this procedure are 1×10^{-6} and 2×10^{-9} mol dm⁻³ for the voltammetric and differential pulse techniques respectively; the time required is 30–40 min.

The purity of mercury metal has essential significance for many branches of science and technology. The literature illustrates a marked interest in the development of new methods of mercury purification [1], yet there have been few attempts to develop simple and more sensitive methods of analysis of mercury for trace metals. In most of the methods proposed for the determination of impurities in mercury, a preliminary separation step is recommended [2–6], which makes the analysis cumbersome. The essential advantage of electrochemical methods is the possibility of direct analysis without prior separation. The exploitation of polarography for such a direct determination was proposed by Heyrovsky and Kalousek [7] many years ago. However, the detection limits attained by polarography are inadequate for true trace analysis.

The aim of the present work was to evaluate the use of the hanging mercury drop electrode (HMDE) for the direct determination of electroactive contaminants of mercury. The HMDE has not previously been used successfully in the analysis of mercury for trace metals. A mercury pool electrode was applied for such determinations by Neyman et al. [8] who stressed its usefulness. Some comparative results are given below.

EXPERIMENTAL

Equipment and reagents

Voltammograms were recorded with a Radelkis OH-105 polarograph or with a Unitra PP04 pulse polarograph connected with a KABID-PRESS 6801A X-Y recorder. Two kinds of indicating electrodes were used: a HMDE of the type described by Kemula and Kublik [9] and a mercury pool electrode prepared by pouring mercury into a small glass cup equipped with a sealed platinum contact. The approximate surface area of the latter electrode was 0.8 cm^2 . The counter electrode was a platinum foil with a surface area of ca. 2 cm^2 . As reference electrodes, two saturated calomel electrodes were used. The small electrode, with a surface area of about 7 cm^2 , was used in experiments with the HMDE, whereas the large electrode, with a surface area of about 100 cm^2 , was used in experiments with the mercury pool electrode.

The solutions were prepared from reagent-grade chemicals and water purified as described elsewhere [10]. Commercially available mercury was additionally purified, first by shaking with a 1 mol dm^{-3} nitric acid solution containing 1% mercury(I) nitrate and then by a two-stage distillation under reduced pressure. Amalgams of copper, lead and cadmium, at concentrations of $10^{-3}\text{ mol dm}^{-3}$, were prepared by the addition of an appropriate sample of weighed metal into pure mercury. The more dilute amalgams were prepared by dilution of the stock amalgams.

Procedures

For direct determinations, the HMDE or the pool electrode was filled with the amalgam under test. In experiments exploiting the selective oxidation of contaminants from mercury, the electrolytic cell was filled successfully with 12 cm^3 of pure water, the weighed sample of the mercury under test (about 80 g) and 0.12 cm^3 of concentrated perchloric acid solution. After addition of each constituent, the solution was deaerated. In principle, the oxygen dissolved in such solutions should accelerate the oxidation of impurities from mercury but in the presence of much oxygen, some mercury was also oxidized. The presence of these mercury ions led to a marked increase in the residual current and thus to worse detection limits. The investigated metals were oxidized from mercury to the supporting electrolyte either at appropriate potentials or at open electrical circuit. During this oxidation step, mercury and solution were stirred vigorously. After the oxidation step, the stirring was switched off and after several seconds of quiescence, the concentrations of the metal ions in solution were measured by the conventional anodic stripping procedure.

RESULTS

Preliminary experiments on the stability of the copper, lead and cadmium amalgams

It is well known that amalgams of many metals are unstable in the presence of oxidants [1]. In order to establish the conditions of stability of the amalgams used in the present study, two series of experiments were done. In the first series, samples of about 1×10^{-3} mol dm $^{-3}$ amalgams of copper, lead and cadmium, introduced into small test tubes, were left in contact with air or with 0.1 mol dm $^{-3}$ perchloric acid. After various periods of time, small portions of these amalgams were introduced to the container of the HMDE and the anodic voltammograms were recorded; a solution of very pure perchloric acid served as the supporting electrolyte. The variations in the height of the anodic peaks as a function of the time of contact of the amalgam with the air or solution provided information on the stability of the amalgams. The results obtained in experiments of this type are presented in Fig. 1.

It is evident that amalgams left in contact with acidic solutions are less stable than amalgams left in contact with air. It is probable that the layer of oxide formed on the dry amalgam diminishes the rate of the oxidation of the amalgam. The stability of more dilute amalgams was studied by holding the amalgam in the container of the HMDE. The drop of amalgam extruded

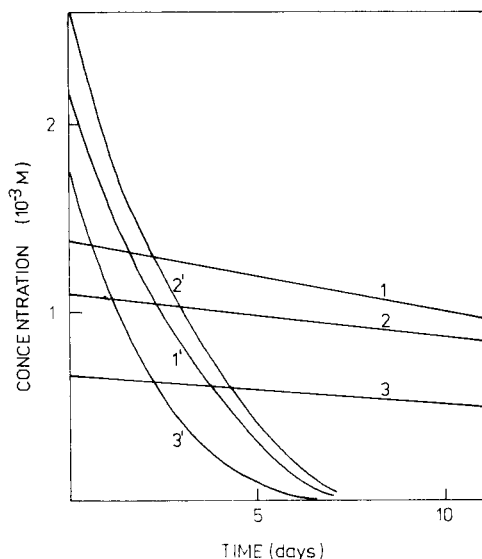


Fig. 1. The dependence of the concentrations of copper, lead and cadmium in mercury on the time of contact of the amalgam with air (curves 1–3) or with 0.1 mol dm $^{-3}$ perchloric acid (curves 1'–3'). Concentration of cadmium: (1) 1.4×10^{-3} ; (1') 2.2×10^{-3} mol dm $^{-3}$. Concentration of lead: (2) 1.2×10^{-3} ; (2') 2.6×10^{-3} mol dm $^{-3}$. Concentration of copper: (3) 0.65×10^{-3} ; (3') 1.8×10^{-3} mol dm $^{-3}$.

from the container of the HMDE remained in contact with deaerated solution for various periods of time at open electrical circuit and then the anodic voltammograms were recorded. Experiments of this type for mercury containing $5 \times 10^{-5} \text{ mol dm}^{-3}$ lead showed that the height of the anodic peak decreased to 5% of the initial value after a 3-min contact of the drop with a quiet, deaerated solution. In stirred solution, a similar decrease was observed after 30 s. In solutions containing much dissolved oxygen, the decrease in peak height was faster; this supports the opinion that traces of oxygen are responsible for oxidation of metal from the amalgam. Similar experiments for copper amalgam showed that a dilute amalgam of copper is markedly more stable than the diluted lead amalgam.

Direct determination of copper, lead and cadmium in mercury

Figure 2 shows the anodic voltammograms (curves 1–3) obtained at the HMDE for dilute amalgams of copper, lead and cadmium. The anodic peaks obtained for small amounts of cadmium and lead are well separated from the residual current and the reproducibility of the height of these peaks was quite good. In contrast, the peak corresponding to the oxidation of copper occurs in the potential range where the residual current shows a small increase, caused probably by the change in the capacity of the electrical double layer. The reproducibility of the height of the small copper peaks was therefore worse than the reproducibility of the peaks obtained for lead and cadmium.

The poor stability of the dilute amalgams created serious problems in the preparation of the calibration plots. Therefore, the concentrations of the metals in the samples of mercury were determined not from calibration plots but by using the theoretical relation between the magnitude of the analytical signal and the concentration of the metal in the mercury phase. Such a relation valid for voltammetry at the HMDE was given by Nicholson and Shain [11]. The values of the diffusion coefficients of the investigated metals in mercury, necessary for exploitation of the mentioned equation, were taken from the review given by Galus [12]. The detection limits estimated for lead and cadmium were equal to $2 \times 10^{-7} \text{ mol dm}^{-3}$. The detection limit estimated for the determination of copper was slightly higher ($4 \times 10^{-7} \text{ mol dm}^{-3}$).

A comparison of curves 2 and 5 in Fig. 2 shows distinctly that the use of the differential pulse technique offers a marked improvement in the signals obtained for lead and cadmium. Under these conditions, the concentrations of cadmium and lead in the mercury phase were determined on the basis of the theoretical relation given by Parry and Osteryoung [13]. The application of the differential pulse technique reduced the detection limits for lead and cadmium to $4 \times 10^{-8} \text{ mol dm}^{-3}$. A comparison of the quantitative results obtained for the same mercury sample by the d.c. and differential pulse techniques gave very good agreement for lead and cadmium. In contrast to the behaviour of lead and cadmium, the determination of copper by the differential pulse technique was very difficult; in the potential range where

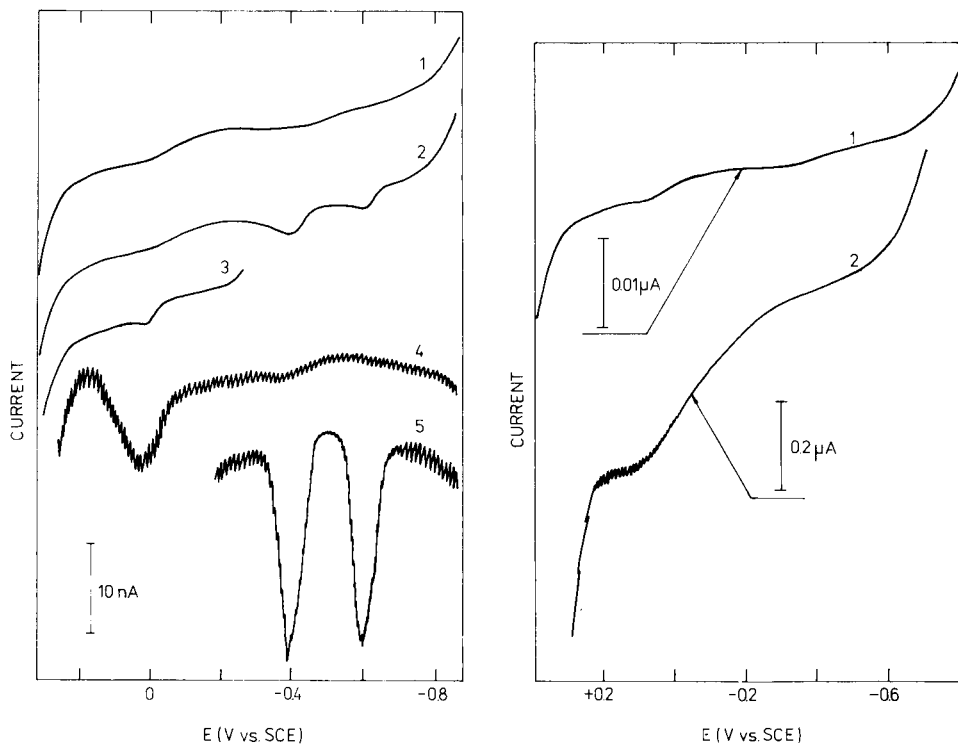


Fig. 2. Anodic voltammograms (1–3) and anodic differential pulse voltammograms (4, 5) obtained in 0.02 mol dm^{-3} perchloric acid solution for: (1, 4) very pure mercury; (2, 5) mercury containing $5 \times 10^{-7} \text{ mol dm}^{-3}$ lead and $4.5 \times 10^{-7} \text{ mol dm}^{-3}$ cadmium; (3) mercury containing $4 \times 10^{-7} \text{ mol dm}^{-3}$ copper. Surface area of the mercury drop, 3.8 mm^2 . Voltage scan rate 0.4 V min^{-1} . Conditions for the pulse voltammograms: 20-ms delay time, 20-ms sampling time, 50-mV amplitude.

Fig. 3. The influence of different surface areas of the electrode on the shape of the residual currents obtained in 0.02 mol dm^{-3} perchloric acid. Surface areas: (1) 3.8 mm^2 HMDE; (2) 78.5 mm^2 mercury pool. Scan rate 0.4 V min^{-1} .

copper is oxidized, the blank test (curve 4) showed an irregular anodic peak, caused probably by desorption of traces of surface-active agents.

Attempts to use the mercury pool electrode for the direct determination of traces of metals in mercury

The fact that diffusion currents are proportional to the surface area of the electrode is well established. Taking into account this general statement, some authors [8] assumed that an increase in the area of the electrode should lead to improved detection limits. However, such an opinion seems to be invalid when very small concentrations of electroactive substances are reduced or oxidized. The detection limit is defined not by the magnitude of the surface area of the electrode but by the ratio of the electrolytic current

to the capacity current. Both these currents are strictly proportional to the electrode surface area and, therefore, the ratio of the magnitude of the analytical signal to the magnitude of the capacity current should be independent of variations in the surface area of the electrode.

Experiments at electrodes with different surface areas showed that increased surface area led to increased steepness of the curve. Measurements of the height of the required signals on such steep curves became difficult. In order to improve the measurements it was necessary to decrease the sensitivity of the recorder. Figure 3 shows a comparison of the curves of the blank test obtained at electrodes with the surface area ratio close to 1:20 and with the sensitivity ratio also equal to 1:20. The detection limits estimated for lead on the basis of curves 1 and 2 were 2×10^{-7} and 3×10^{-7} mol dm⁻³, respectively. An increase in the surface area did not give any significant improvement of the detection limit.

Determination of copper, lead and cadmium after selective oxidative separation

The advantage of this variation would be significant if the electroactive contaminants of mercury could be quantitatively transferred to solution in a short period of time. In order to check the completeness of oxidation of the investigated metals, the concentrations of the metal ions in solution were studied as a function of the intensity of stirring and as a function of the applied potential. In these experiments, it was found that effective and reproducible oxidation was attained even with an open electrical circuit. It is evident that the concentration of oxygen present even in deaerated solution suffices to achieve the oxidation of metals from the very dilute amalgams. The efficiency of oxidation depended significantly on the kind of stirring. When the stirring bar moved only on the surface of the mercury, the concentration of metal ions in solution did not become constant even after 60 min of stirring. But when the stirring was so vigorous that the mercury formed a large number of small droplets, stirring for 5 min was sufficient to attain quantitative oxidation of the contaminants. After the oxidation step, the mercury was left quiescent for 30 s and then the concentrations of Cu²⁺, Pb²⁺ and Cd²⁺ ions in solution were determined by anodic stripping voltammetry at the HMDE.

Figure 4 presents the curves obtained for the same sample of mercury when the direct and indirect methods were used. On curve 3, obtained by direct anodic voltammetry, there are no anodic peaks, whereas curve 2, obtained after selective oxidation, shows three well developed anodic peaks. In contrast to the low stability of dilute amalgams, dilute acidic solutions of the metal ions investigated are stable; accordingly, the concentrations of these ions in solution could be determined from calibration plots. The plots obtained after a preconcentration time of 5 min could be described over a wide concentration range by the relation $i = \alpha C$, where α was equal to 0.300, 0.285 and 0.298 for Cu²⁺, Pb²⁺ and Cd²⁺ ions, respectively; in this relation,

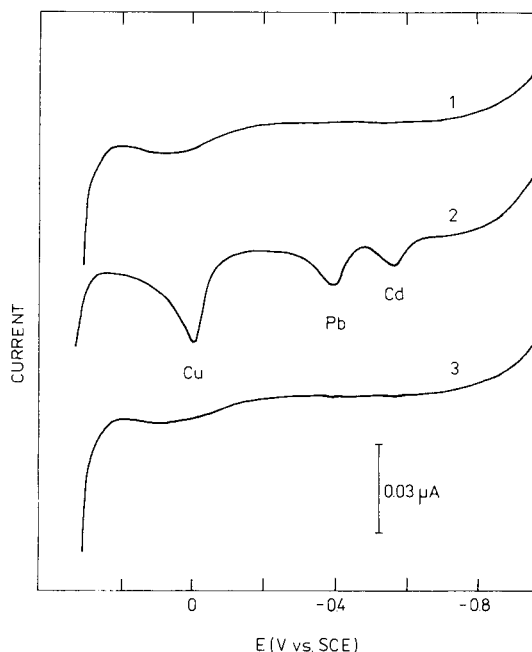


Fig. 4. Comparison of the sensitivity of the direct and indirect voltammetric methods. Concentrations of copper, lead and cadmium in mercury: 2.0×10^{-7} , 1.2×10^{-7} and 1.0×10^{-7} mol dm $^{-3}$, respectively. Concentration of perchloric acid in supporting electrolyte, 0.1 mol dm $^{-3}$. Curves: (3) direct anodic voltammogram at the HMDE; (2) anodic stripping voltammogram obtained after selective oxidation of contaminants followed by preconcentration of metals in the HMDE; (1) blank test for curve 2.

current is given in amperes and concentration in mol dm $^{-3}$. The measurement of the concentrations of Cu $^{2+}$, Pb $^{2+}$ and Cd $^{2+}$ ions in solution provided the concentrations of copper, lead and cadmium in mercury when the ratio of the volume of mercury to the volume of solution was known. The anodic peaks shown in Fig. 4 correspond to the following concentrations of metals in mercury: 2.0×10^{-7} mol dm $^{-3}$ copper, 1.2×10^{-7} mol dm $^{-3}$ lead and 1.0×10^{-7} mol dm $^{-3}$ cadmium. The detection limits obtained for this selective oxidation method, after preconcentration for 5 min, were 1×10^{-8} mol dm $^{-3}$ for lead and cadmium and 2×10^{-8} mol dm $^{-3}$ for copper. These detection limits could be lowered further by increasing the ratio of the mercury volume to the solution volume, or by increasing the purity of the supporting electrolyte, or by using the differential pulse technique. In the latter case, the blank curve again showed some irregularity in the potential range where copper is oxidized, so that the pulse technique is less convenient for the determination of copper than for determinations of lead and cadmium.

Determination of copper, lead and cadmium in real samples of mercury

The voltammetric curves obtained by the direct and selective oxidation procedures for "pure" mercury (POCH) did not show any signals corre-

sponding to copper, lead and cadmium, i.e., this sample of mercury appeared to be very pure. The analysis of mercury used for a long period of time in a vacuum diffusion pump showed the presence of copper, lead and cadmium at concentrations of 2.2×10^{-7} , 7.5×10^{-8} and 2×10^{-8} mol dm⁻³, respectively. Further analysis of the same mercury sample after four days showed a marked decrease in the concentrations of the three metals. The peaks of cadmium and lead were hardly seen, i.e., their concentrations were less than 1×10^{-8} mol dm⁻³. The concentration of copper decreased to 2×10^{-7} mol dm⁻³.

DISCUSSION

Few analytical techniques are available for the direct determination of metal contaminants in mercury. The detection limits offered by spectral analysis [14] or by classical polarography [7] are inadequate for real trace analysis. Neyman et al. [8] claimed that anodic voltammetry at a mercury pool electrode has very low detection limits, mainly because of the significant increase in the surface area of the electrode. However, the results obtained in the present work show clearly that increased surface area does not lead to a corresponding improvement of the detection limit. Under voltammetric conditions, the determination limit is defined by the ratio of the analytical signal to the capacity current and this ratio remains constant with an increase in the surface area of the electrode. The detection limits obtained in the present work at electrodes with surface areas of 0.038 and 0.8 cm² were nearly the same. Similar detection limits were obtained by Streuli and Cooke [15] at electrodes with surface areas of about 2.86 cm².

Literature data [16–19] indicate that amalgams of some metals are unstable when they are in contact with aqueous solutions containing even traces of atmospheric oxygen. Such instability was confirmed in the present study for the amalgams of copper, lead and cadmium. The low stability of dilute amalgams makes it difficult to prepare the calibration plots or appropriate standards. Therefore the concentrations of metals in amalgam were evaluated on the basis of theoretical relationships [11, 13]. The good agreement between the quantitative results obtained for the same sample of amalgam by the voltammetric and differential pulse techniques means that the exploitation of equations given by Nicholson and Shain [11] and by Parry and Osteryoung [13] is justified.

The selective oxidation method proposed above takes more time than the direct method, but the separation and measurement steps are done in the same vessel and the actual working time is not excessive.

A comparison of the characteristics of several methods for the determination of copper, lead and cadmium in mercury is presented in Table 1. This comparison suggests that the methods proposed here offer many advantages.

TABLE 1

Characteristic of methods for the determination of traces of copper, lead and cadmium in mercury

Separation technique	Measurement technique	Detection limit (% w/w)	Analysis time (h)	Weight of Hg sample (g)	Ref.
Extraction ^a	Stripping voltammetry at HMDE	5×10^{-6}	4	10	2
Precipitation of Hg by HCOOH ^a	Stripping voltammetry at HMDE	1×10^{-7}	2.5	100	3
Precipitation of Hg by HCOOH ^a	Stripping voltammetry at Hg film electrode	1×10^{-6}	2	0.5	5
Extraction ^a	Spectrophotometry	5×10^{-6}	4	10	2
Precipitation of Hg by HCOOH ^a	Spectrophotometry	1×10^{-7}	2.5	100	3
Extraction ^a	Spectrophotometry	1×10^{-7}	3	10	20
Precipitation of Hg by HCOOH ^a	Stripping voltammetry at Hg film electrode	1×10^{-6}	2	0.5	21
None	Anodic voltammetry at Hg pool electrode	1×10^{-6}	0.8	130	8
None	Anodic voltammetry at HMDE	1×10^{-7}	0.5	5	This work
None	Anodic pulse voltammetry at HMDE	2×10^{-6}	0.5	5	This work
Oxidation of contaminants by trace oxygen	Stripping voltammetry at HMDE	1×10^{-8}	0.6	80	This work
Oxidation of contaminants by trace oxygen	Pulse stripping voltammetry at HMDE	2×10^{-9}	0.6	80	This work

^a After dissolution of the mercury in nitric acid.

REFERENCES

- 1 P. P. Pugatchewitch, Rabota so Rtutju, Khimija, Moscow, 1972.
- 2 E. Jackwerth, Fresenius Z. Anal. Chem., 206 (1964) 269.
- 3 J. Meyer, Fresenius Z. Anal. Chem., 219 (1966) 147.
- 4 E. Jackwerth, Fresenius Z. Anal. Chem., 251 (1970) 353.
- 5 L. S. Anisimova, W. F. Sliptchenko, W. E. Katjukhin, A. A. Kaplin and K. M. Spektor, Zavod. Lab., 44 (1978) 1304.
- 6 A. A. Kaplin, I. P. Mamontova and A. G. Stromberg, Zavod. Lab., 45 (1979) 484.
- 7 J. Heyrovsky and M. Kalousek, Collect. Czech. Chem. Commun., 11 (1939) 464.
- 8 E. Ya. Neyman, E. D. Kuzniec and L. A. Belova, Zavod. Lab., 35 (1969) 277.
- 9 W. Kemula and Z. Kublik, Anal. Chim. Acta, 18 (1958) 104.
- 10 E. Bednarkiewicz, M. Donten and Z. Kublik, J. Electroanal. Chem., 127 (1981) 241.
- 11 R. S. Nicholson and I. Shain, Anal. Chem., 36 (1964) 706.
- 12 Z. Galus, CRC Crit. Rev. Anal. Chem., 4 (1975) 396.
- 13 E. P. Parry and R. A. Osteryoung, Anal. Chem., 37 (1965) 1634.
- 14 A. M. Gorbacheva and E. L. Grinzayd, Tr. Leningr. Politekh. Inst., 201 (1959) 77; quoted from [1].
- 15 C. A. Streuli and W. D. Cooke, Anal. Chem., 25 (1953) 1691.

- 16 F. Chao and M. Costa, *Bull. Soc. Chim. Fr.*, 54 (1968) 548.
- 17 M. Pelletier, J. Buffle and D. Monnier, *Chimia*, 25 (1971) 61.
- 18 J. Buffle, M. Pelletier and D. Monnier, *J. Electroanal. Chem.*, 43 (1979) 185.
- 19 A. Barański and Z. Galus, *J. Electroanal. Chem.*, 30 (1971) 219.
- 20 E. Jackwerth, *Fresenius Z. Anal. Chem.*, 202 (1964) 81.
- 21 A. I. Ziebreva, R. N. Matakova and R. B. Zholdybayeva, *Zh. Anal. Khim.*, 36 (1981) 405.

VOLTAMMETRY AT A TRIOCTYLPHOSPHINE OXIDE-COATED GLASSY CARBON ELECTRODE AND ITS USE FOR THE DETERMINATION OF TRACE URANYL IONS AFTER PRECONCENTRATION

KOSUKE IZUTSU*, TOSHIO NAKAMURA, RITSUO TAKIZAWA and HIROSHI HANAWA

Department of Chemistry, Faculty of Science, Shinshu University, Asahi, Matsumoto 390 (Japan)

(Received 1st September 1982)

SUMMARY

The voltammetric characteristics of a trioctylphosphine oxide (TOPO)-coated glassy carbon (GC) electrode and its use in the determination of trace uranyl ions are described. Among various substances examined, only uranyl ions were effectively concentrated into the TOPO layer on the GC electrode at 0 V vs. Ag/AgCl electrode and gave a reduction wave when the electrode potential was scanned in a negative direction. Some substances could reach the GC surface through the TOPO layer and reacted electrochemically, but others could not pass the TOPO layer. A method is given for the determination of uranyl ions in 0.5 M NaCl adjusted to pH 4 with acetate buffer after preconcentration; the detection limit is 2×10^{-9} M, and uranyl ions between 2×10^{-9} M and 2×10^{-7} M can be determined. The method is very selective for uranyl ions, suggesting possible application in the analysis of sea water. A preliminary investigation for artificial sea water showed that a simple pretreatment involving boiling at pH 2.5 (to remove dissolved carbon dioxide) made the determination possible.

Several kinds of modified electrodes have recently been proved useful as indicator electrodes for voltammetric determination of trace electroactive species [1–7]. Typically, electrodes are modified either by covalent attachment of functional groups or by irreversible adsorption of organic reagents or functional polymers, and voltammetric stripping is done after preconcentration.

In a previous paper, Izutsu et al. [3] reported briefly that a glassy carbon (GC) electrode coated with trioctylphosphine oxide (TOPO) could be used to determine trace uranyl ions after their preconcentration on the TOPO layer. This paper deals with the voltammetric characteristics of the TOPO-coated GC electrode and gives more details of its use in the determination of trace uranyl ions.

EXPERIMENTAL

Preparation and use of the TOPO-coated electrode

The TOPO-coated GC electrode was prepared by putting 5 μ l of ethanolic TOPO solution (5×10^{-3} M; $M = \text{mol dm}^{-3}$) on the surface of a GC disk electrode, evaporating the ethanol, and then heating the TOPO layer for 3 min under an infra-red lamp to melt and fix the TOPO to the GC surface (Fig. 1). The GC electrode, which was made from GC-30 (Tokai Carbon Co.), was 3 mm in diameter and was polished, once a day, with extremely fine silicon carbide powder for a few minutes. The TOPO layer was renewed after measurements in each solution: TOPO was removed by washing with acetone and 1 M hydrochloric acid and then the electrode was conditioned by ultrasonic washing in an ethanolic potassium hydroxide solution and in 5 M acetic acid, each for 5 min. After being rinsed in water, the electrode was coated again with TOPO.

A weighing bottle (80 mm tall, 30 mm diameter) served as the electrolytic cell, and an Ag/AgCl reference electrode and a platinum wire counter electrode were set through a teflon stopper. During preconcentration, the solution in the cell was stirred magnetically at 600 rpm.

Equipment and reagents

Voltammograms were measured by using a potentiostat (model 314; Fuso Seisakusho Co.), a function generator (model FG-101; Nikko Keisoku Co.),

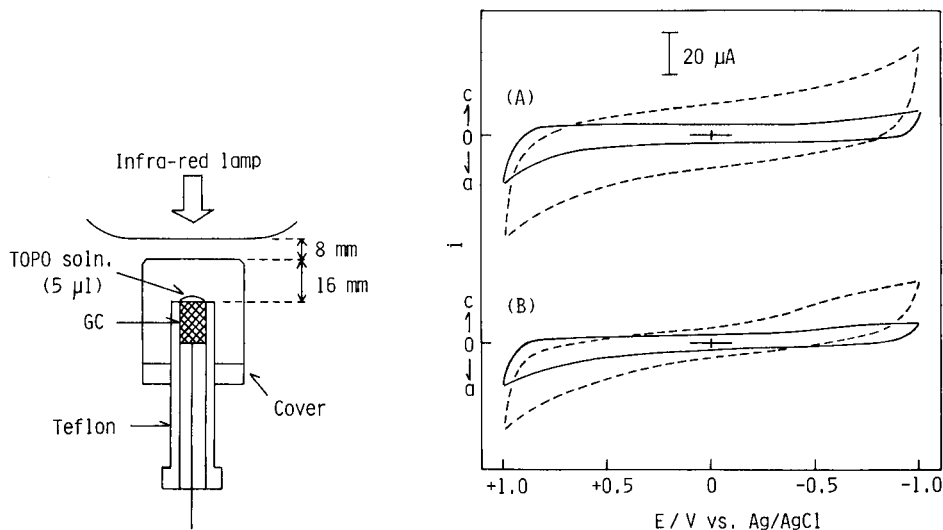


Fig. 1. Preparation of the TOPO-coated GC electrode.

Fig. 2. Cyclic voltammograms at the GC electrodes: (—) with TOPO coating; (-----) uncoated. (A) In 0.5 M NaCl; (B) in 0.1 M HCl. Scan rate 1 V s⁻¹. (a and c show the anodic and cathodic currents, respectively.)

and an x-y recorder (model RW-11; Rikadenki Kogyo Co.). For measurements at high potential scan rates, a personal computer (Sol-20; Processor Technology), equipped with 12-bit A/D and D/A converters was used in combination with the above instruments. Except where otherwise stated, all measurements were at 25°C.

The TOPO was a Dotite reagent (Dojindo Co.). Other reagents were of analytical-reagent grade (Wako Pure Chemicals Industries). They were used as received.

RESULTS AND DISCUSSION

Voltammetric characteristics of the TOPO-coated GC electrodes

Cyclic voltammograms at the GC electrodes with and without TOPO coating were compared in various supporting electrolytes. As shown in Fig. 2, the residual current was usually much smaller at the TOPO-coated electrode. The coated electrode also had a wider potential range; the hydrogen overpotential increased considerably in acidic solutions (Table 1). Though the TOPO layer seemed to be partially removed by dissolution, its characteristic properties were maintained for several hours, except in 0.1 M sodium hydroxide in which the layer was removed fairly easily.

The behavior of various chemical species at the TOPO-coated GC electrode was examined in 0.5 M NaCl solutions. The results are summarized in Table 2. Among the inorganic species examined, only uranyl ions were concentrated into the TOPO layer of the electrode kept at 0 V vs. Ag/AgCl electrode and were reduced when the electrode was scanned to negative potentials. Some species, though not concentrated at 0 V, could pass the TOPO layer fairly rapidly giving reduction waves approximately controlled by the diffusion in solution. For other species, the rate of passing the TOPO layer was slower or negligibly small. Lead and thallium ions, which gave reduction waves at uncoated GC electrodes could not pass the TOPO layer to any measurable extent, virtually being masked electrochemically [8, 9].

TABLE 1

Potential window available at GC electrodes with and without TOPO-coating (V vs. Ag/AgCl)

Supporting electrolyte	TOPO-coated	Uncoated
0.1 M HClO ₄	+1.2 ₅ to -1.2 ₄	+1.2 ₅ to -0.8 ₅
0.1 M HCl	+1.1 ₅ to -1.3 ₅	+1.1 ₅ to -1.1 ₅
0.5 M NaCl	+1.0 ₀ to -1.4 ₅	+1.0 ₃ to -1.3 ₀
0.1 M (C ₂ H ₅) ₄ NClO ₄	+1.2 ₃ to -1.6 ₈	+1.1 ₅ to -1.7 ₅
0.05 M KH ₂ PO ₄		
+ 0.05 M Na ₂ HPO ₄	+1.2 ₅ to -1.3 ₅	+1.0 ₅ to -1.3 ₅
0.1 M NaOH	+0.7 ₅ to -1.5 ₀	+0.6 ₅ to -1.5 ₀

TABLE 2

Behavior of chemical species at the TOPO-coated GC electrode

1. Concentrated at 0 V vs. Ag/AgCl, and produce a reduction wave on negative potential scan	UO_2^{2+} (and some organic species)
2. Not concentrated at 0 V, but can pass the TOPO layer rapidly and be reduced	Mo(VI) , O_2
3. Pass the TOPO layer slowly and reduced	Cu^{2+} , Hg^{2+} , Sn^{2+} , Bi^{3+} , Fe^{3+} , CrO_4^{2-}
4. Cannot pass the TOPO layer (electrochemically masked)	Pb^{2+} , Tl^+

The behavior of several organic species was also examined. Such organic reagents as eriochrome black T, 1-(2-pyridylazo)-2-naphthol and α -nitroso- β -naphthol were concentrated on the TOPO-coated GC electrode at 0 V and reduced on the negative potential scans. All of them showed more or less similar behavior even at the uncoated GC electrode, suggesting no special analytical merit of the TOPO-layer.

Use of the TOPO-coated GC electrode in the determination of trace uranyl ions

As described above, uranyl ions (UO_2^{2+}) are concentrated onto the TOPO-coated GC electrode and give a reduction wave. Curve 1 in Fig. 3 was obtained for 10^{-7} M uranyl after preconcentration for 10 min at 0 V from a 0.5 M NaCl solution adjusted to pH 4.0. Just before the preconcentration, the electrode potential was cyclically scanned ten times between 0 V and -1.4 V to remove uranyl ion which had previously been deposited on the electrode. Curve 2 in Fig. 3 was obtained in the absence of uranyl ion after the electrode had been held for 10 min at 0 V. A small current (blank current) was observed at the potential corresponding to the peak in curve 1.

Conditions for the determination of the uranyl ion were investigated in detail as follows.

Supporting electrolyte and pH of the solution. Sodium chloride between 0.1 M and 1 M was satisfactory as the supporting electrolyte. Sodium sulfate and potassium nitrate could also be used. As the intention was to apply the electrode in the determination of the uranyl ion in sea water, 0.5 M NaCl was used throughout.

The pH of the solution had a significant effect on the peak current, maximum current being obtained at pH between 3.7 and 4.5 when 10^{-3} M acetate buffer was used for pH adjustment (Fig. 4). In this work, the pH was usually adjusted to 4.0. Concentration changes of the acetate buffer between 4×10^{-4} M and 4×10^{-2} M did not affect the peak current to a measurable extent.

Potential of preconcentration. The effect of the preconcentration potential is shown in Fig. 5. The peak current increased with the positive shift of the potential up to ca. +0.3 V, but 0 V was usually selected for preconcentration because the blank current increased at more positive potentials.

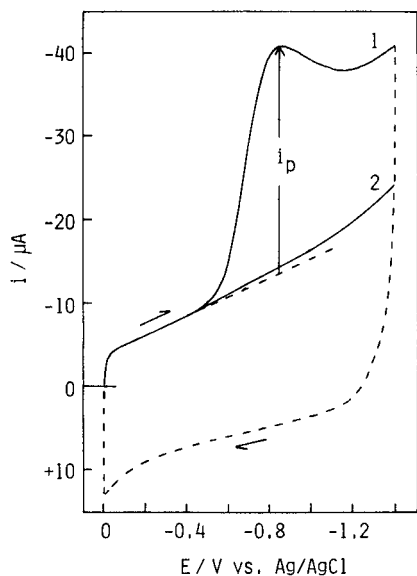


Fig. 3. Voltammograms at the TOPO-coated GC electrode in 0.5 M NaCl (pH 4.0) after polarization at 0 V for 10 min: (1) in the presence of 1×10^{-7} M UO_2^{2+} ; (2) in the absence of UO_2^{2+} . Scan rate 10 V s^{-1} .

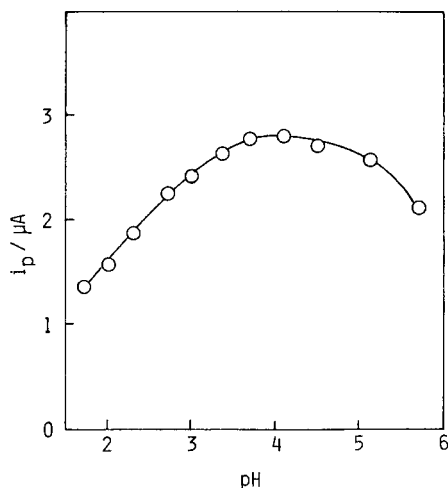


Fig. 4. Effect of pH of the solution on the peak current of 1×10^{-7} M UO_2^{2+} in 0.5 M NaCl with 10^{-3} M acetate buffer. Preconcentration for 10 min; scan rate 1 V s^{-1} .

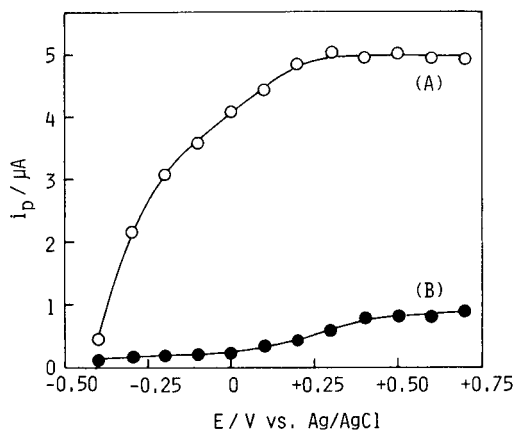


Fig. 5. Effect of the potential of preconcentration: (A) i_p for 2×10^{-7} M UO_2^{2+} ; (B) blank current. Preconcentration for 5 min; scan rate 1 V s^{-1} .

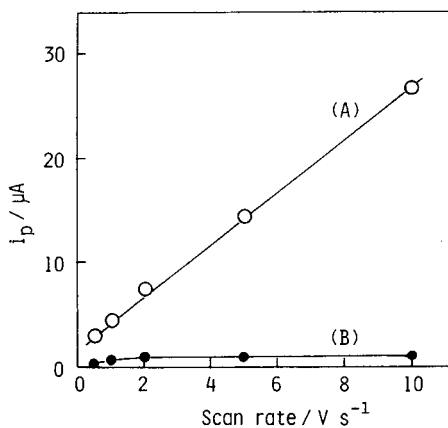


Fig. 6. Effect of the potential scan rate: (A) i_p for 1×10^{-7} M UO_2^{2+} ; (B) blank current. Preconcentration for 10 min.

Effect of potential scan rate. The effects of the scan rate on the peak current for the uranyl ion and on the blank current are shown in Fig. 6. The peak current increased approximately linearly with the scan rate, but the blank current did not increase to the same extent. Figure 7 shows the voltammograms obtained in the absence of uranyl ion after the electrode had been held at 0 V for 10 min. A definite wave appeared at a scan rate of 1 V s^{-1} , but it virtually disappeared at 10 V s^{-1} . From the results, the blank current seems to be due to some slow process, probably at the GC electrode surface. Although the peak potential for the uranyl ion was shifted from ca. -0.75 V to ca. -0.85 V by the increase in scan rate from 1 V s^{-1} to 10 V s^{-1} , the effect of the blank current was much smaller at 10 V s^{-1} .

Thickness of the TOPO layer. The effect of the thickness of the TOPO layer was examined by coating the GC electrode with $5 \mu\text{l}$ of various concentrations of TOPO solution. As shown in Fig. 8, an electrode coated with TOPO solution between $1 \times 10^{-3} \text{ M}$ and $5 \times 10^{-3} \text{ M}$ gave a maximum peak current which was approximately independent of the TOPO concentrations. In this work $5 \times 10^{-3} \text{ M}$ TOPO was used for coating, because the residual current was smaller at the electrode with the thicker TOPO layer. Though the TOPO layer, which seems to be 10^3 molecular layers thick by rough estimation, may be dissolved partly during repeated measurements, this does not affect the peak current, as can be understood from the result in Fig. 8.

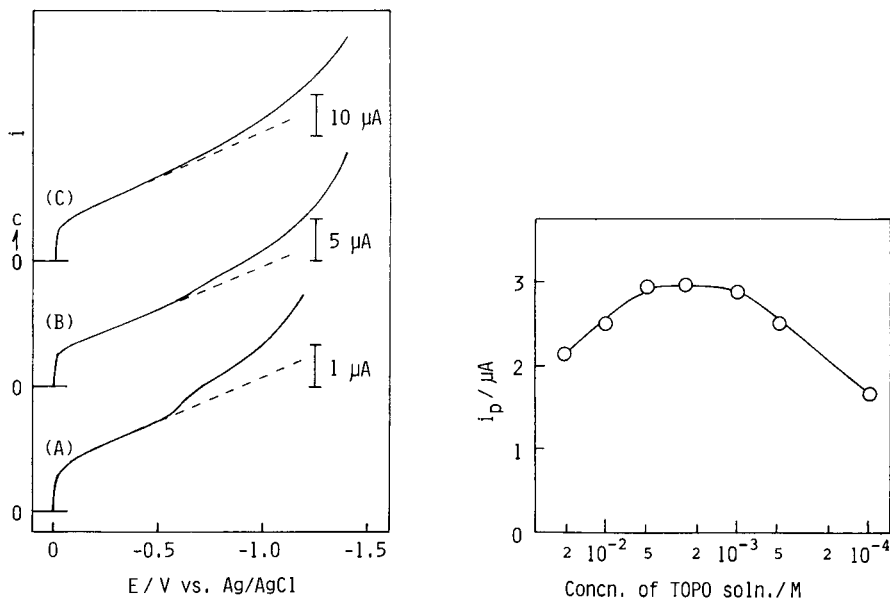


Fig. 7. Effect of the potential scan rate on the blank current at the TOPO-coated GC electrode. Scan rate: (A) 1 V s^{-1} ; (B) 5 V s^{-1} ; (C) 10 V s^{-1} . Recorded after polarization at 0 V for 10 min in 0.5 M NaCl (pH 4.0).

Fig. 8. Effect of the thickness of the TOPO coating (see text).

Effect of temperature. The peak current increased approximately linearly with temperature between 10°C and 45°C. The coefficient was 4.4% deg⁻¹, which is somewhat larger than that expected for diffusion-controlled processes. Optimum temperature was between 25°C and 35°C because the TOPO layer became less stable and the blank current increased at higher temperatures.

Calibration graphs and reproducibility. The peak current increased with the preconcentration time but tended to saturate. Calibration graphs for uranyl ion between 0 and 2×10^{-7} M and between 0 and 2×10^{-8} M were obtained with preconcentration times of 10 and 30 min, respectively, which were considered to be appropriate. Voltammograms were measured with the aid of the personal computer at a scan rate of 10 V s⁻¹. Line A in Fig. 9 shows the results for the uranyl ion between 0 and 2×10^{-7} M. Though deviations occurred at higher concentrations, a good linear relation was obtained below 1.4×10^{-7} M, with an intercept of 1.0 μ A, a slope of 2.30 μ A/ 10^{-8} M, and a correlation coefficient of 0.998. The coefficient of variation of the peak current for 1×10^{-7} M uranyl ion was 1.8% when ten measurements were done successively in the same solution without renewal of the TOPO layer, but this coefficient increased to about 5% when the TOPO layer was renewed after each measurement. Polishing the GC electrode gently with extremely fine silicon carbide powder did not affect the peak currents, but the peak currents varied by more than 20% when the electrode was polished vigorously with emery papers.

Line B in Fig. 9, obtained for up to 2×10^{-8} M uranyl ion, shows a good linear relation with an intercept of 1.2 μ A, a slope of 0.65 μ A/ 10^{-9} M, and a

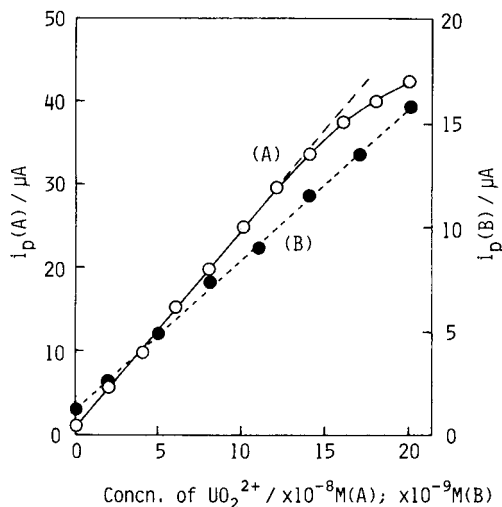


Fig. 9. Calibration graphs for uranyl ion: (A) for 0– 2×10^{-7} M UO_2^{2+} after preconcentration for 10 min; (B) for 0– 2×10^{-8} M UO_2^{2+} after preconcentration for 30 min at 0 V. Scan rate 10 V s⁻¹.

correlation coefficient of 0.995. Because the blank current (intercept) forms a significant part of the peak current, it must be kept at a small constant value. Complete elimination of dissolved oxygen and carbon dioxide, reproducible pretreatment of the electrode, and rapid potential scanning in the voltammetric measurement are essential for this purpose. To achieve best results, it is recommended that the blank current of the supporting electrolyte be measured before the sample solution is measured with the same electrode.

Effect of diverse ions. The effect of diverse ions on the peak current of 10^{-7} M uranyl ion was examined by the standard addition method. Species which affected the current more than 5% are shown in Table 3. Only citrate ions interfered at the 2×10^{-6} M level, and Hg^{2+} , Sn^{2+} , and chromate ions at 10^{-5} M concentrations: Ti^{+} , Cd^{2+} , Pb^{2+} , Zn^{2+} , Mo(VI) , W(VI) , V(V) , NO_3^- , tartrate were tolerated up to 10^{-4} M, and carbonate was tolerated up to 2×10^{-3} M at pH 4.0. Thus the proposed method seems to be very selective for the uranyl ion, because no other species was concentrated in the TOPO-coated GC electrode to give a reduction wave on the negative potential sweep.

Preliminary study in artificial sea water

Sea water usually contains about 1.4×10^{-8} M uranium(VI) and the present method seems to be sensitive enough to determine it. Moreover, from the above results, trace components in sea water would not seem to interfere with its determination. A preliminary study for the determination of uranyl ion in sea water was made by using the artificial sea-water recipe of Lyman and Fleming [10]. When the artificial sea water, free from uranyl ion, was adjusted to pH 4.0 with hydrochloric acid and acetate buffer (10^{-3} M) and a voltammogram was measured in it after the TOPO-coated electrode had been polarized for 10 min at 0 V, a small wave appeared at ca. -0.7 V, increasing the blank current significantly. The wave was shown to be due to the dissolved carbon dioxide, and was removed by boiling the artificial sea water for 5 min at pH 2.5. Fluoride ions, which interfered in 0.5 M NaCl, did not interfere in the artificial sea water, probably because they were masked, e.g., by calcium

TABLE 3

Effect of diverse ions on the peak current of 1×10^{-7} M uranyl ion

Ions	Error (%) ^a caused by			Ions	Error (%) ^a caused by		
	2×10^{-6} M	1×10^{-5} M	1×10^{-4} M		2×10^{-6} M	1×10^{-5} M	1×10^{-4} M
Bi^{3+}	—	—	**b	F^-	—	—	—27 ^d
Cu^{2+}	—	—	+65	I^-	—	—	+34
Fe^{3+}	—	—	+69	CrO_4^{2-}	—	—46	**
Hg^{2+}	—	+40	+79	EDTA	—	—	—14
Sn^{2+}	—	+26 ^c	+67	Citrate	—14	—29	—42

^aDashes indicate that effects are less than $\pm 5\%$. ^bWave height not measurable. ^cEffect removed by 10^{-5} M EDTA. ^dEffect removed by 10^{-4} M Al^{3+} .

ion. A calibration graph for uranyl ion obtained in the decarbonated artificial sea water (pH 4.0), showed a linear relation up to 2×10^{-8} M with a slope about two-thirds of that of line B, Fig. 9. Though the sensitivity in this case is somewhat less than that in 0.5 M NaCl, it is apparent that the method is very promising for the analysis of sea water. A study on this application is now in progress.

Conclusion

The TOPO-coated GC electrode provides a sensitive and selective voltammetric method for uranyl ions in chloride solutions. The mechanism of the preconcentration seems to be the extraction of UO_2^{2+} into TOPO. As shown in Fig. 3, the reduction of the uranyl ion is completely irreversible. Though the mechanism of the electrode process has not been elucidated so far, the reduction product seems to be eliminated rapidly from the electrode, thus making the TOPO layer applicable for repeated measurements. Further investigation is also in progress to eliminate the blank current more effectively.

This work was supported by a Grant-in-Aid for Scientific Research from the Ministry of Education of Japan (No. 421707).

REFERENCES

- 1 G. T. Cheek and R. F. Nelson, *Anal. Lett.*, **A11** (1978) 393.
- 2 T. Yao and S. Musha, *Anal. Chim. Acta*, **110** (1979) 203.
- 3 K. Izutsu, T. Nakamura and T. Oku, *Nippon Kagaku Kaishi*, (1980) 1656.
- 4 J. A. Cox and M. Majda, *Anal. Chim. Acta*, **118** (1980) 861.
- 5 J. F. Price and R. P. Baldwin, *Anal. Chem.*, **52** (1980) 1940.
- 6 M. Karayama and S. Suzuki, *Nippon Kagaku Kaishi*, (1982) 61, 66.
- 7 N. Oyama and F. C. Anson, *J. Am. Chem. Soc.*, **101** (1979) 3450.
- 8 C. N. Reilley, W. G. Scribner and C. Temple, *Anal. Chem.*, **28** (1956) 450.
- 9 T. Fujinaga and K. Izutsu, *Bunseki Kagaku (Jpn. Anal.)*, **10** (1961) 63.
- 10 S. Musha (Ed.), *Bunseki Kagaku Jiten (Dictionary of Analytical Chemistry)*, Kyoritsu, Tokyo, 1972, p. 941.

QUANTITATIVE MEASUREMENT OF TRIBUTYLTIN OXIDE IN SEA WATER BY DIFFERENTIAL PULSE ANODIC STRIPPING VOLTAMMETRY

PAUL KENIS* and ALBERTO ZIRINO

Marine Environment Branch, Code 5132, Naval Ocean Systems Center, San Diego, CA 92152 (U.S.A.)

(Received 7th July 1982)

SUMMARY

Bis(tri-n-butyltin) oxide (TBTO) was measured directly in sea water at $\mu\text{g l}^{-1}$ levels at a hanging drop mercury electrode (HDME) and at a mercury-film rotating-disc glassy carbon electrode (MFE) by differential pulse anodic stripping voltammetry. The HDME responded to TBTO additions in sea water purged either with nitrogen (pH 8.2) or carbon dioxide (pH 4.8) with two distinct stripping peaks. The MFE produced stripping peaks for TBTO at pH 8.2 and no response at pH 4.8. Peak potentials and peak heights varied depending upon the history of the water sample, suggesting an influence by dissolved organic materials. The limit of detection for TBTO in sea water on the HMDE was approximately $5 \mu\text{g l}^{-1}$. The HMDE responded to additions of inorganic tin in sea water at both pH 4.8 and 8.2, whereas the MFE did not respond at either pH.

Organotin compounds are often used in place of copper compounds as antifouling coatings on ship hulls. They are believed to leach from surfaces of ships at a dependable rate, thereby optimizing the control of biological fouling of the surfaces. Organotin compounds are thought to degrade in sea water to harmless inorganic tin, thereby posing few long-term environmental problems. However, the rate of this degradation under natural conditions has not been measured. Recently, evidence has been obtained for the microbial methylation of tin by a *Pseudomonas*-type bacterium isolated from the sediments of Chesapeake Bay [1], suggesting that organotin may pose a continuing hazard to estuarine and freshwater environments. The correct assessment of that water hazard is dependent on the availability of accurate and reliable methods to quantify the organotin species in fresh and salt waters. Because of its inherent simplicity and high sensitivity, differential pulse anodic stripping voltammetry (d.p.a.s.v.) has been widely used for quantifying the micro-constituents of sea water [2–4]. However, to our knowledge, the quantitation of organotin compounds in sea water by a.s.v. has not been reported. The purpose of this work is to evaluate the method of direct d.p.a.s.v. in sea water for a single compound, bis(tri-n-butyltin) oxide (TBTO), a major component of tin-based antifouling paints.

EXPERIMENTAL

Instrumentation

All current-voltage measurements were made with a Princeton Applied Research Corporation (PAR) Model 174A polarographic system in conjunction with either a Hewlett-Packard Model 7034A or a PAR Model RE0073 recorder. A PAR Model 315 automated electroanalysis controller was used to automate the Model 174A. A Corning 476055 combination microelectrode connected to a Corning Model 130 pH meter was used to measure pH.

The electrochemical cell consisted of the appropriate electrode (see below) mounted in a PAR K66 polarographic cell top. A PAR K60 borosilicate glass cell bottom completed the cell. Stirring was effected with a 1.1-cm teflon-covered stirring bar coupled to a Sargent-Welch 600-rpm synchronous-speed magnetic stirrer. A PAR K0077 calomel electrode (SCE) was placed in a PAR K0065 reference electrode bridge tube with vycor tip to form a double-junction reference electrode. Sea water filled the outer junction. The auxiliary electrode was a bare platinum wire. All experiments were done at room temperature.

Electrodes

Many determinations were done with a hanging mercury drop electrode (HMDE; K20, PAR). This electrode, no longer supplied by PAR, is manufactured by Metrohm (Herisau, Switzerland). A mercury drop was extruded from the capillary by turning the micrometer screw four divisions. Measurements with the HMDE were done with a 5-min plating time at a deposition potential of -1.45 V and a $1\text{-}\mu\text{A}$ current range output to the recorder.

Other determinations were done with a Beckman rotating-disc glassy carbon electrode (RDGCE) obtained from Beckman Instruments (Irvine, CA) connected to a Beckman variable-speed controller. The glassy carbon disc was 5 mm in diameter and was rotated at 2,000 rpm for all experiments. Initially, the surface of the glassy carbon was polished to a metallic luster by pressing the rotating disc to a polishing pad embedded with $5\text{-}\mu\text{m}$ diamond polishing compound suspended in olive oil. Final polishing was with aluminum oxide suspended in water. The electrode was then rinsed with deionized water (Milli-Q, Millipore Corp., Bedford, MA) and wiped with a cloth wet with dichloroethane. Measurements were done in the electrolysis cell on a sample to which mercury(II) nitrate had been added to produce a concentration of 2×10^{-5} M. The procedure used was that described by Florence [5]. Measurements with this electrode were done with a 5-min plating time at a deposition potential of -1.35 V and a $10\text{-}\mu\text{A}$ current range output to the recorder.

Solutions and samples

The TBTO standard was made by adding an excess of TBTO to sea water and agitating gently for 24 h. The sea water saturated with TBTO was then

decanted, leaving the undissolved TBTO on the bottom of the container, and filtered through Whatman 14 filter paper to remove a visible surface film which was sometimes present. The amount of TBTO in the saturated sea water was determined by extraction with methyl isobutyl ketone and measurement of tin on a Perkin-Elmer Model 5000 atomic absorption spectrometer. Values presented in this report represent concentrations as $\mu\text{g l}^{-1}$ (ppb) TBTO computed from the tin values obtained by atomic absorption spectrometry.

Inorganic tin was obtained from a 1,000-ppm atomic absorption tin standard in 1% nitric acid.

Most sea water samples were collected by hand in a precleaned polyethylene bottle from the tide pool area adjoining the laboratory on Point Loma, San Diego. Other samples were obtained from the tide pool area adjoining the Naval Ocean Systems Center laboratory at Kailua, Hawaii. Samples were filtered through $0.45\text{-}\mu\text{m}$ filters to remove particulates. "Organic-free" sea water was produced by placing the filtered sea water in a high-energy photolysis chamber [6].

RESULTS

Experiments with the HMDE

Additions of the TBTO standard in sea water to a sample of Point Loma sea water at pH 8.2 produced no peaks at the 5-ppb level ($8.4 \times 10^{-9} \text{ M}$), one small peak when TBTO was increased to 10 ppb, and two distinct peaks at higher concentrations (Fig. 1). These peaks occurred at approximately -0.75 V and -0.90 V (all potentials are given vs. the SCE). The first of these, designated as Peak I (-0.75 V), increased linearly with increasing TBTO concentrations to 30 ppb and then increased nonlinearly to 90 ppb, the highest level tested. The peak potential also showed a positive potential shift, going from -0.75 V at 10 ppb to -0.68 V at 90 ppb. The second peak (Peak II, -0.90 V)

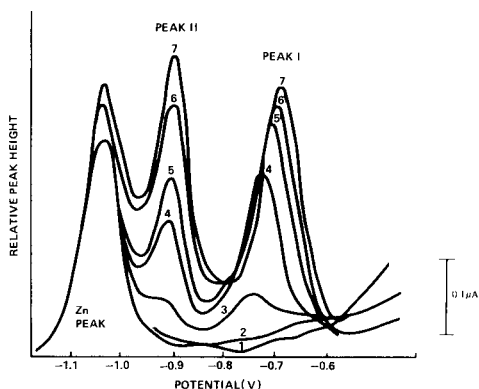


Fig. 1. Response of the hanging drop mercury electrode to additions of TBTO to Point Loma sea water at pH 8.2. TBTO (ppb): (1) 0; (2) 5; (3) 10; (4) 30; (5) 50; (6) 70; (7) 90.

emerged on the shoulder of the "natural" zinc peak and increased linearly with TBTO additions to 90 ppb. Peak II did not exhibit a significant potential shift with concentration. Peaks I and II were also observed to increase nonlinearly with electrolysis time to a maximum of 900 s, a reasonable practical limit for this type of quantitation.

A repetition of the above experiment with a similar sample of Point Loma sea water purged with carbon dioxide (pH 4.8) yielded only one major peak at approximately -0.80 V and at least two minor peaks at -0.63 and -0.56 V (Fig. 2). The peak at -0.80 V (Peak I) showed the greatest response to TBTO and increased linearly with standard additions to 180 ppb, the highest concentration tested. Over this range, the peak potential shifted from -0.82 V at 5 ppb to -0.74 V at 180 ppb. Figure 2 shows only concentrations to 60 ppb because higher values were recorded on another scale. Because Peak I showed excellent linearity with standard additions, other tests were conducted in carbon dioxide-saturated media with the purpose of maximizing the signal.

Varying the deposition potential of a sample containing 10 ppb TBTO showed that a maximum peak height occurred at -1.45 V and decreased sharply at both higher and lower values (Fig. 3). Adding EDTA at the 10^{-5} M level eliminated the zinc peak and greatly suppressed the cadmium and lead peaks, but did not affect the TBTO peak significantly (Fig. 4).

Over a 6-month period, additions of TBTO were made to several samples of sea water collected at various times from Point Loma, a sample from Kailua, Hawaii, and a Scripps Pier (La Jolla, CA) sample from which organic matter had been removed by ultraviolet photolysis. The results of these tests are shown in Table 1. One of the Point Loma samples showed a predominant TBTO peak at -0.83 V (similar to that of the sample shown in

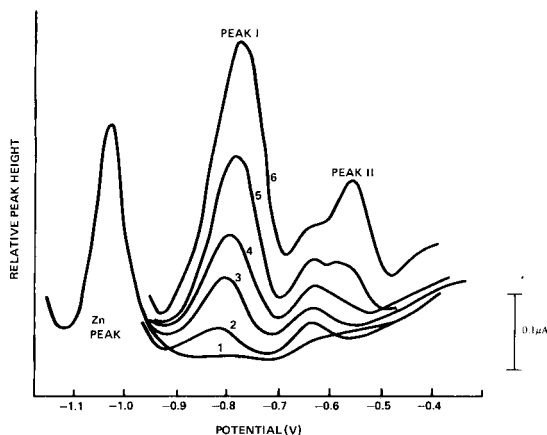


Fig. 2. Response of the hanging drop mercury electrode to additions of TBTO to Point Loma sea water at pH 4.8. TBTO (ppb): (1) 0; (2) 5; (3) 10; (4) 20; (5) 40; (6) 60.

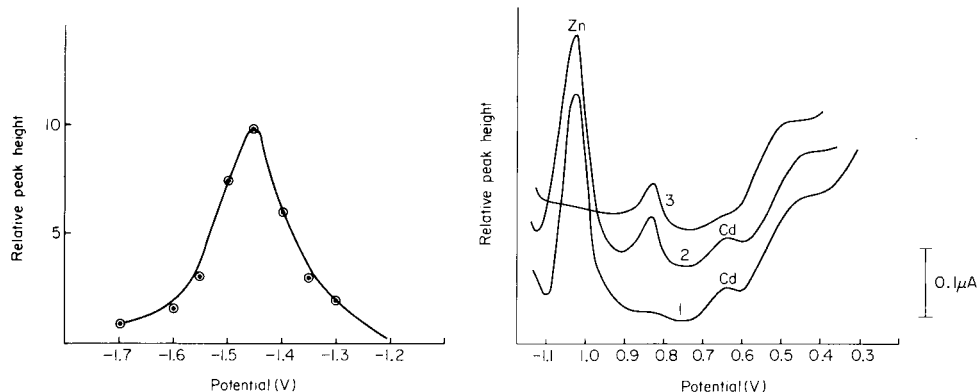


Fig. 3. Effect of deposition potential on TBTO peak height on the hanging drop mercury electrode at pH 4.8. TBTO at 5 ppb in Point Loma sea water was plated for 5 min at various deposition potentials.

Fig. 4. Effects of EDTA at 10^{-5} M on the zinc, cadmium and TBTO peak heights with the hanging drop mercury electrode at pH 4.8: (1) Point Loma sea water only; (2) + 16 ppb TBTO; (3) + EDTA.

Fig. 2) but collected several months earlier. A different Point Loma sample, however, produced the main TBTO peak between -0.92 V and -0.89 V, and it was broader and less well shaped. Sensitivity to TBTO was diminished, and the auxiliary peak between -0.70 and -0.65 V was poorly formed.

The Hawaii sample showed a response similar to the Point Loma sample but the primary peak occurred more positively and appeared to be a combination of two peaks. The sample of organic-free Scripps sea water showed one predominant peak for TBTO, but it was much more positive than for the previous samples, occurring at -0.65 V. All predominant peaks for all water samples were found to increase linearly with added TBTO; however, the slopes, i.e., the change in peak height per ppb TBTO added, varied with each sea water sample.

TABLE 1

Stripping potentials for TBTO peaks I and II and relative response of peak I

Sea water	Peak I potential for most responsive peak (V)	Peak II potential for second most re- sponsive peak (V)	Relative response of peak I (nA/ppb TBTO)
Point Loma (A)	-0.92 to -0.89	-0.70 to -0.65	12.5
Point Loma (B)	-0.83	-0.65 to -0.61	7.0
Hawaii	-0.80 to -0.76	-0.61 to -0.57	18.0
Organic-free	-0.65	-0.77 to -0.75	23.7

Point Loma sea water spiked with inorganic tin, presumably tin(IV) (atomic absorption standard), exhibited stripping peaks that varied with the purging agent: nitrogen purge (pH 8.2), carbon dioxide purge (pH 4.8). The greatest response to low inorganic tin levels occurred at pH 8.2 (Fig. 5) with the stripping peak at -0.67 V. Inorganic tin at 2 ppb was detected, and a linear relationship between concentration and peak height occurred up to 15 ppb, the highest concentration tested. The response to inorganic tin with a carbon dioxide purge produced a peak at -0.55 V with a secondary peak emerging at -0.65 V (Fig. 6). The potential at which the characteristic inorganic tin stripping peaks occurred could be changed reversibly by changing from a nitrogen to a carbon dioxide purge and then back to nitrogen.

The inorganic tin peak at pH 8.2 coincided with the cadmium peak (-0.65 V), while the primary inorganic tin peak at pH 4.8, which occurs at -0.55 V, is between the cadmium and lead peaks. When TBTO was added to sea-water samples, it produced a primary peak between -0.75 and -0.95 V, which is between the zinc and cadmium peaks.

Experiments with the mercury-film rotating-disc glassy carbon electrode

Determinations of TBTO in sea water were done with the mercury film electrode in a manner similar to that of the determination with the HMDE. Initially, the dependence of peak height on solution pH was determined (Fig. 7). The pH of a sea-water sample containing 5 ppb TBTO was decreased after each measurement by increasing the partial pressure of carbon dioxide in the nitrogen. This caused the solution pH to vary in discrete steps between pH 4.8 and 8.4. An initial electrolysis potential of -1.35 V vs. SCE was maintained and Point Loma sea water was used. A marked pH dependency

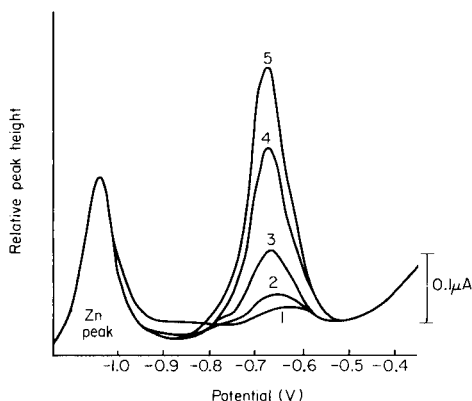


Fig. 5. Response of the hanging drop mercury electrode to additions of inorganic tin to Point Loma sea water at pH 8.2. Tin added (ppb): (1) 0; (2) 2; (3) 5; (4) 10; (5) 15.

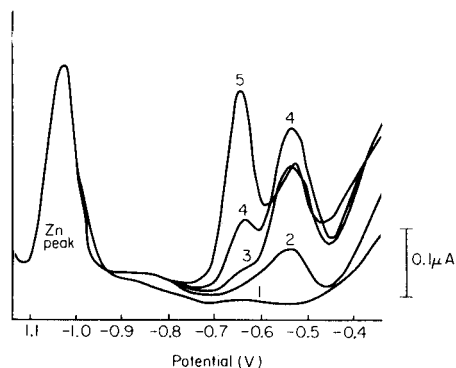


Fig. 6. Response of the hanging drop mercury electrode to additions of inorganic tin to Point Loma sea water at pH 4.8. Tin added (ppb): (1) 0; (2) 10; (3) 30; (4) 50; (5) 70.

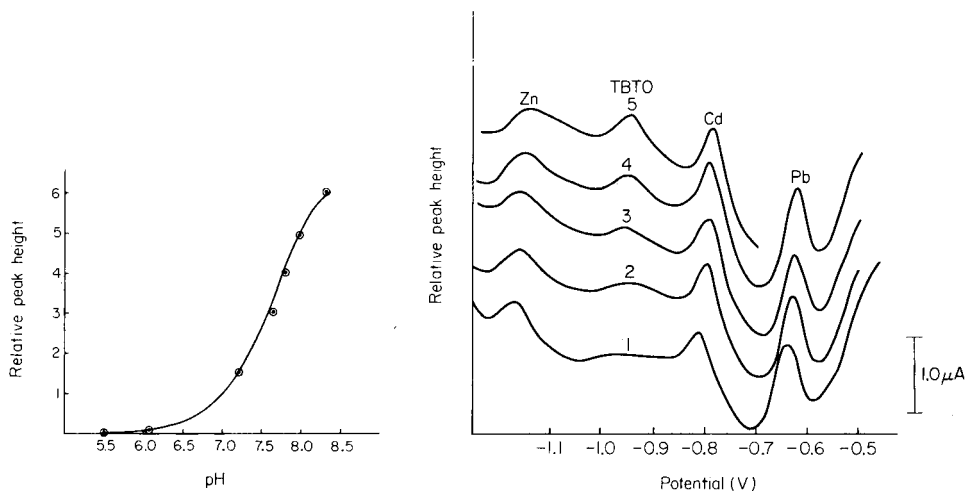


Fig. 7. Effect of pH on the response of the mercury film electrode to 5 ppb TBTO in Point Loma sea water.

Fig. 8. Response of the mercury film electrode to additions of TBTO to Point Loma sea water at pH 8.2: (1) sea water only; (2) + 0.6 ppb TBTO; (3) + 1.2 ppb TBTO; (4) + 1.8 ppb TBTO; (5) + 3.0 ppb TBTO.

was observed. Unlike the HMDE, which gave a sharper response with 100% carbon dioxide, the MFE produced the greatest peaks at the natural pH of sea water and no peaks at all below pH 6. Thus, all subsequent tests were done with 300 ppm carbon dioxide in the nitrogen purging gas. This mixture, which contains only slightly less carbon dioxide than the atmosphere, maintains sea-water samples at a pH only slightly higher (0.1 pH units) than is the case under natural conditions.

It was observed that the MFE produced a well-defined TBTO peak at -0.94 V in sea-water media (Fig. 8). This peak was highly dependent on the electrolysis potential, reaching a maximum at a potential of -1.35 V and declining sharply at either more positive or more negative potentials. Under optimum conditions, electrode response was 10–20 fold greater than found for the HMDE. Accordingly, smaller concentrations could be quantified. For the sample shown in Fig. 8, concentrations of TBTO as small as 0.6 ppb could be resolved; Zn^{2+} , Cd^{2+} , and Pb^{2+} naturally present in the sample did not interfere.

Unlike the HMDE, there was no response to inorganic tin at the MFE at pH 8.2 or 4.8 at concentrations up to 100 ppb.

The procedure described above was used to quantify "unknown" quantities of TBTO in aquarium samples. Sea-water samples from a bioassay study conducted at the Kailua laboratory were used. Panels coated with TBTO-antifouling paint were placed in a flow-through sea-water aquarium to assess the toxicity of the dissolved organotin paint. After 6 months of contact

with the panels in the flow-through aquarium, samples of the aquarium water were sent to San Diego for measurement of TBTO. Initially, sea water from a control tank was examined for TBTO. This was to verify that there was no TBTO contamination and no carryover of TBTO from the cell and electrode surfaces. The control sample was then followed with a sample from the treatment tank.

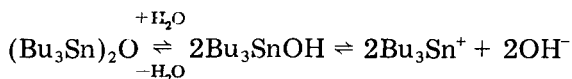
Samples spiked with TBTO were also checked for precision and yield. The method of standard additions was applied to four replicates each of samples containing 0.75 and 7.5 ppb TBTO. At the 0.75 ppb level, the values ranged from 0.60 ppb to 0.75 ppb with a mean of 0.70 and a standard deviation (1σ) of ± 0.07 ppb. At the 7.5 ppb level, the values ranged from 5.0 ppb to 10.0 ppb with a mean of 7.0 and a standard deviation of ± 2.16 ppb.

The results presented here describe the optimum performance of the MFE. Unfortunately, the performance declined with time and often could not be completely restored even after re-polishing. A deteriorating electrode showed less sensitivity to standard additions and low response at all concentrations. Another problem was a baseline shift, which obscured the TBTO peak at high TBTO concentrations, making standard additions difficult.

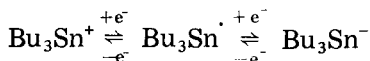
DISCUSSION

Several of the observations made above indicate that the stripping voltammetry of TBTO in sea water yields currents attributable to the oxidation of TBTO and its various forms adsorbed on the mercury or mercury film electrode rather than to the formation of inorganic tin either in the reduction or oxidation step. These observations include the formation of multiple peaks, nonlinearity of peak height with electrolysis time, nonlinearity of peak height at higher concentrations, and lack of a diffusion plateau in stripping polarograms [7]. The criteria usually associated with the d.p.a.s.v. of diffusion-controlled metal ions in sea water are not met [8].

This conclusion is given circumstantial support by the work of Fleet and Fouzder [9], who investigated the voltammetric behavior of TBTO in 50% (v/v) ethanol solutions. They suggested that TBTO undergoes reduction at the dropping mercury electrode (DME) as follows. Initially, TBTO hydrolyzes to yield the tributyltin cation:



The cation is then reduced directly to give, initially, the radical $\text{Bu}_3\text{Sn}^\cdot$:



In turn, the radical and the anion may dimerize and hydrate, respectively, to form the hexalkyl and tri-substituted hydride. Direct-current and differential pulse polarography experiments showed four distinct "waves." Two were

shown to be diffusion-controlled and two were due to adsorption on the DME. Listed in order of cathodically increasing potential, the second and fourth corresponded to normal reduction waves attributable to the formation of the free radical and anion, respectively. The first and third waves were attributed to the adsorption of the free radical and other unspecified electrolysis products.

Cyclic voltammograms showed all four peaks during both the forward (cathodic) and reverse (anodic) sweeps. Thus, the adsorption of TBTO and its electrolysis products yields currents suitable for stripping analysis. In fact, Booth and Fleet [10] had earlier demonstrated that triphenyltin could be quantified by a.s.v. to 10^{-8} M using a mercury-coated platinum wire. They suggested that the triphenyltin radical is stabilized by adsorption onto the mercury film and that multiple peaks were due to removal of the surface and bulk monolayers. Our observations of the behavior of TBTO in sea water suggest agreement with the mechanisms proposed by Booth and Fleet [10].

Table 1 shows that peak current yields per unit TBTO and peak potentials vary with the history and presumed organic content of the water. Organic-free sea water produced the greatest current per unit concentration, followed by oligotrophic Hawaii coastal water, and finally by Point Loma coastal water, generally considered nutrient-rich and organic-rich because of the local kelp beds. This information suggests that "naturally"-occurring organic materials compete with TBTO for adsorption onto mercury [11].

Inorganic tin should not interfere with the quantitative measurement of TBTO at the HMDE under carbon dioxide conditions because its peak occurred more positively in relation to the TBTO peak for all the sea-water samples tested. Inorganic tin peaks in ultraviolet-treated sea water coincided with those of TBTO, causing interference. However, ultraviolet-treated sea water is not a common medium. No inorganic tin peaks were obtained with the mercury film electrode.

Overall, the direct stripping method of determining TBTO in sea water is feasible but problematic. Although the MFE is more sensitive, it is also more susceptible to interferences than the HMDE. The poorer response of the HMDE may make it unsuitable for quantifying low levels (<5 – 10 ppb), but its reproducible surface makes the HMDE more appropriate for routine studies.

REFERENCES

- 1 J. A. Jackson, W. R. Blair, F. E. Brinckman and W. P. Iverson, *Environ. Sci. Technol.*, **16** (1982) 111.
- 2 A. Zirino, in M. Whitfield and D. Jagner (Eds.), *Marine Electrochemistry*, Wiley, New York, 1981, pp. 421–503.
- 3 W. Davison and J. Whitfield, *J. Electroanal. Chem.*, **75** (1977) 763.
- 4 M. Whitfield, in J. P. Riley and G. Skirrow (Eds.), *Chemical Oceanography*, 2nd edn., Academic Press, London, 1975, pp. 1–154.
- 5 T. M. Florence, *J. Electroanal. Chem.*, **27** (1970) 273.
- 6 F. A. Armstrong, P. M. Williams and J. D. H. Strickland, *Nature*, **211** (1966) 481.

- 7 A. Zirino and S. P. Kounaves, *Anal. Chim. Acta*, 113 (1980) 79.
- 8 W. Lund and D. Onshus, *Anal. Chim. Acta*, 86 (1976) 109.
- 9 B. Fleet and N. B. Fouzder, *J. Electroanal. Chem.*, 63 (1975) 59.
- 10 M. D. Booth and B. Fleet, *Anal. Chem.*, 42 (1970) 825.
- 11 P. Sagberg and W. Lund, *Talanta*, 29 (1982) 457.

CONTROLLED-POTENTIAL COULOMETRIC DETERMINATION OF PLUTONIUM WITH CONCURRENT CORRECTION FOR A SECOND REVERSIBLE COUPLE

Application to Solutions containing Plutonium and Iron or Neptunium

MICHAEL K. HOLLAND* and KENNETH LEWIS

New Brunswick Laboratory, U.S. Department of Energy, 9800 South Cass Avenue, Argonne, IL 60439 (U.S.A.)

(Received 4th November 1982)

SUMMARY

The controlled-potential coulometric determination of plutonium with a concurrent measurement of an interfering reversible couple is described. Sample electrolysis over two different potential spans is used. The Nernst equation is utilized to determine the fraction electrolyzed for the plutonium and the interfering reversible couple for each potential span. Two linear equations, in two variables, each containing the appropriate data from one of the sample electrolyses are solved simultaneously for the quantities of plutonium and interfering reversible couple present. Appropriate background current corrections are discussed. This concurrent measurement technique has been applied to the determination of plutonium in solutions containing either plutonium and iron or plutonium and neptunium with a reliability of better than 0.1% for plutonium.

Relatively accurate and precise results have been obtained at a number of laboratories in the nuclear community using various modifications of the controlled-potential coulometric determination of plutonium [1–4]. Experience at the New Brunswick Laboratory which handles a wide variety of plutonium-bearing samples resulted in the adoption of a procedure based on separation of the plutonium by anion exchange prior to measurement by controlled-potential coulometry [5]. Reliability of better than 0.05% has been achieved by using this procedure. The only elements not separated from the plutonium are gold, iridium, neptunium, palladium, platinum and thorium. Samples received for plutonium assay do not generally contain gold, iridium, palladium or platinum; although thorium is not unusual in samples, it is electrochemically inactive and does not directly interfere in the coulometric determination. However, the occurrence of significant amounts of neptunium in samples received at the laboratory resulted in the need for a method for determining the plutonium in the presence of this element.

Initial attempts to use a different separation procedure [6, 7] consisting of an anion-exchange column in the chloride form, hydrochloric acid medium,

and ammonium iodide or iron(II) sulfamate to reduce the plutonium selectively showed that this system was incompatible with the large quantities of salts used in the bisulfate fusion necessary to effect sample dissolution. An alternative approach was then considered based on information in the literature [8–10] that the neptunium(V)/(VI) couple acted reversibly whereas the neptunium(IV)/(V) couple was highly irreversible, because of the formation and breakage of metal–oxygen bonds. A procedure had been previously developed and used for the simultaneous coulometric determination of the two reversible couples, plutonium(III)/(IV) and iron(II)/(III) [11]. It was thought that this procedure might be applicable to solutions containing plutonium and neptunium if suitable conditions were attained. The successful application of this procedure, the basis for the method, and the procedural details are described here.

THEORY

Determination of plutonium

The basic theory of the controlled-potential coulometric determination of plutonium in which the plutonium(III)/(IV) couple is treated as a reversible couple has been given previously [12]. Also a complete discussion was given of corrections for the fraction of the plutonium electrolyzed and the use of appropriate background corrections. The use of a procedural modification referred to as the control-potential adjustment technique (including the theoretical basis for the use of this technique) was also described [12]. This technique allowed a decrease in the time needed for coulometry without loss in precision or accuracy. The equation used for calculating the quantity of plutonium is

$$M_{\text{Pu}} = (M_{\text{T}} - M_{\text{E}})/f_{\text{Pu}} \quad (1)$$

where M_{Pu} is the milliequivalents of plutonium present, M_{T} is the total milliequivalents of material electrolyzed, M_{E} is the milliequivalents of supporting electrolyte electrolyzed (corrected for the solution redox potential span of the sample measurement), and f_{Pu} is the fraction of the plutonium electrolyzed over the redox potential span used [12].

Determination of plutonium in the presence of iron

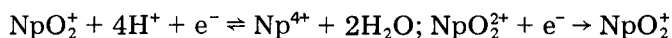
Iron is a common interference in the determination of plutonium and several approaches have been used to correct for its presence [1, 13, 14]. Both the plutonium(III)/(IV) and iron(II)/(III) couples are reversible. This behavior has been used advantageously [11] by electrolyzing a solution containing plutonium and iron over two different potential spans and solving the set of simultaneous equations for the plutonium and iron content. The equations have the form

$$M_{\text{T}} - M_{\text{E}} = M_{\text{Pu}} f_{\text{Pu}} + M_{\text{Fe}} f_{\text{Fe}} \quad (2)$$

where M_T , M_E , M_{Pu} and f_{Pu} are as defined above, M_{Fe} is the milliequivalents of iron present, and f_{Fe} is the fraction of iron electrolyzed (calculated from an equation of the form of Eqn. 5 [12] using the formal potential of the iron(II)/(III) couple).

Determination of plutonium in the presence of neptunium

The application of the concurrent measurement technique to solutions containing plutonium and neptunium requires the consideration of some specific aspects of the chemistry and electrochemistry of neptunium. Solutions of neptunium can contain a mixture of the oxidation states neptunium(IV), neptunium(V), and neptunium(VI). The neptunium couples of interest involving these oxidation states are



Because the neptunium(V)/(VI) couple is reversible whereas the neptunium(IV)/(V) couple is highly irreversible, coulometric electrolyses are possible at potentials involving the reversible plutonium(III)/(IV) and neptunium(V)/(VI) couples without complications from any neptunium(IV) in the solution. Electrolysis over two different potential spans in a solution containing plutonium and neptunium results in a set of simultaneous equations of the same form as Eqn. (2) with appropriate changes for neptunium in place of iron; solution of these equations leads to the determination of the plutonium content and the quantity of neptunium that was in the solution as neptunium(V) or neptunium(VI). If the total neptunium content were required, a prior oxidation of the solution would be needed to convert any neptunium(IV) to neptunium(V) or neptunium(VI) before the concurrent measurement technique was applied.

EXPERIMENTAL

Apparatus and instrumentation

The cell, composed of a gold working electrode, platinum counter electrode, saturated calomel reference electrode, NBL-designed stirring assembly, and other specialized apparatus, has been described in detail [5]. The determination of plutonium [5, 12] was improved by incorporating instrumentation of superior quality and related procedural changes to facilitate automation [15, 16].

Preparation of samples

Preparation of the plutonium/iron standard material. Aliquots containing plutonium and iron at a mole ratio of approximately 70:1 were prepared by weight using standard solutions prepared from National Bureau of Standards SRM-949f plutonium metal and Johnson-Matthey high-purity iron. The resulting solutions were then evaporated to dryness in sulfuric acid.

Preparation of the plutonium/neptunium sample material. A sample con-

taining plutonium and neptunium at a mole ratio of approximately 100:1 and typical levels of other metallic impurities was dissolved by 8 M nitric acid—0.01 M hydrofluoric acid digestion followed by sodium bisulfate fusion of the insoluble residue and recombination with the acid digestion product. Aliquots were taken by weight and evaporated to dryness in sulfuric acid. Several of these aliquots were taken for the controlled-potential coulometry, mass spectrometric determination of the atomic weight, and for the determination of plutonium by isotope-dilution mass spectrometry. Four aliquots, taken for controlled-potential coulometry, were treated to adjust all plutonium to plutonium(IV), purified by anion exchange, and evaporated to dryness in sulfuric acid. Iron, sodium, and any other commonly encountered impurities (as well as their associated sulfate anions from the fuming step) were removed, thereby permitting measurement on the plutonium/neptunium sample without additional complications. Two of the four aliquots taken were then spiked with an aliquot from a pure plutonium assay standard solution to obtain a standard addition comparison of the proposed method. The plutonium content of the four aliquots was quantified by the proposed method.

Determination of plutonium in the presence of iron or neptunium

The supporting electrolyte blank is determined in exactly the same way as in the determination of pure plutonium. Two measurements are made on the sample containing plutonium and either iron or neptunium; each measurement is made in a manner analogous to that of pure plutonium except for changes in the potential spans used. In solutions containing iron, the potential spans used were 0.40–0.85 V vs. SCE and 0.51–0.85 V vs. SCE. The first potential span is achieved by starting the reduction and oxidation at 0.33 V and 0.91 V respectively, and making the control-potential adjustment at 75 μ A for both the reduction and oxidation. The second potential span is achieved by starting the reduction and oxidation at 0.49 V and 0.91 V vs. SCE, respectively, and again making the control-potential adjustment at 75 μ A for the reduction and oxidation.

In solutions containing neptunium, the potential spans used were 0.48–0.82 V vs. SCE and 0.48–0.94 V vs. SCE. The first potential span is achieved by starting the reduction and oxidation at 0.40 V and 0.84 V vs. SCE, respectively, and making the control-potential adjustment at 75 μ A for both the reduction and oxidation. The second potential span is achieved by starting the reduction and oxidation at 0.40 V and 1.0 V vs. SCE, respectively, and again making the control-potential adjustment at 75 μ A. Other combinations of control-potential at which the electrolyses are initiated and current magnitudes at which the control-potential adjustments are made, could have been used to achieve the desired potential spans.

After each day of measurements on solutions containing neptunium, the platinum counter electrode was flamed to white heat and quenched in 8 M nitric acid. This flaming was required to obtain the proper electrode condi-

tion and prevent measurement bias on subsequent days. The reason for the counter electrode fouling and associated measurement errors is not understood, because the flaming is not required after measurements in solutions containing plutonium alone or plutonium and iron. However, this same effect was also observed in the measurement of plutonium in the presence of thorium which is not electroactive in this system. The problem of counter electrode fouling by thorium has also been reported by others (private communication) using significantly different measurement techniques.

RESULTS AND DISCUSSION

Determination of plutonium in the presence of iron

Plutonium was quantified in the presence of iron in the present work by using improved instrumentation and a standard solution prepared from known quantities of both plutonium and iron. Results shown in Table 1 illustrate that the technique gives results for plutonium comparable to those obtained in solutions containing plutonium alone [11]. Recoveries for iron are included in Table 1 as supplemental information. The significant difference between the reliabilities for plutonium and iron is due partly to the relative quantities of each element present and partly to the deliberate attempt to optimize the concurrent measurement technique for plutonium.

Determination of plutonium in the presence of neptunium

Table 2 presents results obtained for a mixture of plutonium and neptunium. Results for replicate aliquots of plutonium are seen to agree very well. The estimated precision for plutonium is better than 0.05% RSD. The significant difference in the precision for plutonium and neptunium is again due partly to differences in the relative quantities of each element present and the deliberate attempt to optimize the reliability for plutonium. Additionally, because only neptunium(V) and neptunium(VI) are quantified, there is a further contribution to the uncertainty for neptunium because the

TABLE 1

Recoveries of plutonium and iron from a standard solution by the concurrent measurement technique

Aliquot	Plutonium			Iron		
	Taken ^a (mg)	Found (mg)	Recovery (%)	Taken ^b (mg)	Found (mg)	Recovery (%)
1	8.3181	8.3150	99.96	0.0274	0.0281	102
2	8.9017	8.8966	99.94	0.0287	0.0353	123

^aPrepared value calculated from NBS certified weight and purity according to certificate instructions. ^bPrepared value calculated from manufacturer's certified value; this value was previously verified at NBL by controlled-potential coulometry.

TABLE 2

Measurement of plutonium and neptunium by using the concurrent technique directly and after standard addition

	Direct sample		Standard addition	
Sample aliquot	1	2	3	4
Weight % Pu	84.19	84.19	84.20	84.17
Weight % Np ^a	0.71	0.80	0.76	1.20

^aNeptunium(IV) is not quantified. Weight % neptunium is the total of neptunium(V) and neptunium(VI) as noted in the text.

fraction of neptunium in these measurable oxidation states may vary from aliquot to aliquot.

Because these plutonium determinations were made on a single sample, two further measurements were done to confirm the result. The procedure was applied to a solution spiked with a known amount of plutonium, and the original plutonium content was quantified by the method of standard additions. An independent result was obtained by isotope-dilution mass spectrometry (i.d.m.s.). The plutonium results (Table 2) are in excellent agreement with those obtained by the direct determination. A value of 84.23% plutonium was obtained by i.d.m.s. which agrees to within 0.05% with the coulometric determinations. The estimated uncertainty of the i.d.m.s. measurement is of the order of 0.1–0.2%.

Alternative potential spans can be chosen for the electrolyses. The primary reasons for selecting the spans used were to obtain a significant change in the fraction of neptunium electrolyzed, only a minimal change in the fraction of plutonium electrolyzed, and a sufficient difference in potential from the respective formal potentials of the two couples to minimize errors in the calculated fractions electrolyzed. The potential spans must also be chosen to avoid potential regions in which the working electrode may undergo changes.

The instrumentation used in this work has several significant features that were important to the successful application of the concurrent measurement technique. First, the instrumentation is calibrated by using an electrical standard certified to 0.0015%. Secondly, the plutonium procedure is based on the electrical calibration value, not on a chemical reference material. Thirdly, the gold working electrode and nitric acid supporting electrolyte yield a low constant background current and a reproducible blank on the order of 0.2% of the sample measurement; the blank value is a linear function of the potential span, thus allowing blank corrections for any potential span used. Finally, the control-potential adjustment technique results in accurate potential measurements at particular stages of electrolysis leading to an accurate calculation of the fraction electrolyzed over each potential span. The accurate determination of the fraction of each species electro-

lyzed, and the linear relation between the blank value and electrolysis potential span are critical to the concurrent measurements described above.

The authors gratefully acknowledge the technical assistance of Charles E. Pietri, D. Dennis Wilkey, Dorothy B. Stuit, and Jon R. Weiss, and thank Margaret A. Legel, David W. Crawford, and Colleen G. Cacic for their contributions to the mass spectrometry and i.d.m.s. measurements.

REFERENCES

- 1 W. D. Shults, *Talanta*, 10 (1963) 833.
- 2 F. A. Scott and R. M. Peekema, U.S. Atomic Energy Commission Report, HW-58491, 1958.
- 3 G. C. Goode and J. Herrington, *Anal. Chim. Acta*, 33 (1965) 413.
- 4 D. D. Jackson, R. M. Hollen, F. R. Roensch and J. E. Rein, *Anal. Chim. Acta*, 117 (1980) 205.
- 5 M. K. Holland, J. R. Weiss and C. E. Pietri, U.S. Dept. of Energy Report, NBL-299, 1981.
- 6 F. Nelson, D. C. Michelson and J. H. Holloway, *J. Chromatogr.*, 14 (1964) 258.
- 7 N. Jackson and J. F. Short, British Report, AERE-M-444, 1959.
- 8 R. W. Stromatt, U.S. Atomic Energy Commission Report, HW-59447, 1959.
- 9 R. W. Stromatt, *Anal. Chem.*, 32 (1960) 134.
- 10 S. Casadio and F. Orlandini, *J. Electroanal. Chem.*, 33 (1971) 212.
- 11 M. K. Holland and J. R. Weiss, U.S. Dept. of Energy Report, NBL-292 (1979) 28.
- 12 M. K. Holland, J. R. Weiss and C. E. Pietri, *Anal. Chem.*, 50 (1978) 236.
- 13 W. D. Shults, *Anal. Chem.*, 33 (1961) 15.
- 14 J. R. Stokely, Jr. and W. D. Shults, *Anal. Chem.*, 43 (1971) 603.
- 15 M. K. Holland, T. L. Frazzini, J. R. Weiss and C. E. Pietri, U.S. Dept. of Commerce Report, NBS SP-582 (1980) 164.
- 16 T. L. Frazzini, M. K. Holland, J. R. Weiss and C. E. Pietri, *Anal. Chim. Acta*, 129 (1981) 125.

POLAROGRAPHIC REDUCTION AND DETERMINATION OF NALIDIXIC ACID

W. J. VAN OORT*, R. H. A. SOREL, D. BRUSSEE, S. G. SCHULMAN^a, P. ZUMAN^b
and J. DEN HARTIGH

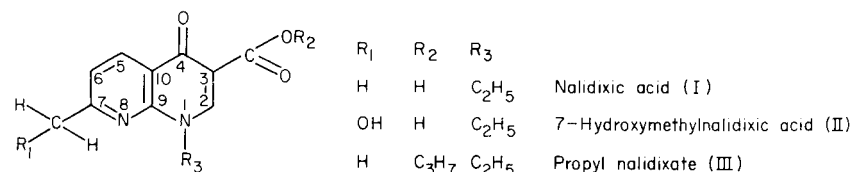
Department of Analytical Pharmacy, Faculty of Pharmacy, State University of Utrecht, Catharijnesingel 60, 3511 GH Utrecht (The Netherlands)

(Received 24th November 1982)

SUMMARY

Protonated and uncharged forms of nalidixic acid (1-ethyl-1,4-dihydro-7-methyl-4-oxo-1,8-naphthyridine-3-carboxylic acid) and its 7-hydroxymethyl derivative are reduced at the dropping mercury electrode in two one-electron waves, whereas their anions are reduced in a single one-electron wave. Reduction of nalidixic acid results in hydrogenation of the ethylenic bond in the azinone ring. Protonated and uncharged forms of the propyl ester of the nalidixic acid are reduced in a single one-electron wave. In acidic media, the C–O bond in the 7-hydroxymethylnalidixic acid is also reduced. Structural effects on the properties of the acid–base equilibria are discussed. Based on these studies, a differential pulse polarographic method for the determination of 10^{-5} – 10^{-6} M nalidixic acid and its metabolite, the 7-hydroxymethyl derivative, in urine was developed; only a simple extraction is needed.

Nalidixic acid (I; 1-ethyl-1,4-dihydro-7-methyl-4-oxo-1,8-naphthyridine-3-carboxylic acid) is an antibacterial agent which has been used extensively in the treatment of gram-negative urinary tract infections for over 15 years [1]. Its physico-chemical properties and assays have been reviewed by Grubb [2].



It is heat-stable but sensitive to photodecomposition, soluble in polar organic solvents, and sparingly soluble in water. The major metabolite of nalidixic acid is the 7-hydroxymethyl analogue (II) which exhibits at least in vitro anti-bacterial activity nearly identical in spectrum and potency to that of the

^aPermanent address: College of Pharmacy, University of Florida, Gainesville, FL 32610, U.S.A.

^bPermanent address: Department of Chemistry, Clarkson College of Technology, Potsdam, NY 13676, U.S.A.

parent compound [3]. Recently, chromatographic methods have been published for the determination of nalidixic acid and its active metabolite in biological fluids [4–7]. The g.l.c. method is based on extraction followed by a pre-column butylation, and the h.p.l.c. method either on derivatization by methylation or on a dynamic anion-exchange system with a cetrimide solution as the eluent.

To investigate the possibilities of electroanalytical assays and to broaden knowledge about the physico-chemical properties of these compounds, the reduction patterns of nalidixic and hydroxynalidixic acids were investigated. Some preliminary information on the d.c. polarographic reduction and preparative electrolysis of the compounds has been reported [8]. Based on limited data, a mechanism was proposed which turned out to be inadequate. A more detailed study is presented in this paper. To distinguish the roles of individual acidic groups, the study was extended to the ester, propyl nalidixate (III). The polarographic behaviour of this compound, which is a monobasic acid, is simpler than that of the parent compound (I). The understanding of the processes occurring during the electroreduction of III was a key to elucidating the mechanism of reduction of compounds I and II. This understanding of the processes involved in polarographic reduction of nalidixic acid enabled a procedure for the determination of this acid in urine to be developed.

EXPERIMENTAL

Apparatus

The polarographic curves were recorded on a Bruker E310 modular electrochemical system, equipped with a drop-timer and a Houston 2000 x-y recorder, and on a Metrohm Polarecord E506 equipped with a polarographic stand E505. A water-jacketed 10-ml polarographic cell (Metrohm EA880T-5) with a dropping mercury electrode, a Metrohm EA436 Ag/AgCl/saturated KCl reference electrode and a platinum wire auxiliary electrode was maintained at $20 \pm 0.5^\circ\text{C}$. The dropping mercury electrode used had a flow rate (m) of 2.1 mg s^{-1} and a drop-time t_1 of 2 s at mercury height of 70 cm (at 0.0 V vs. SCE).

Controlled-potential electrolysis with a hanging mercury drop electrode (HMDE) was done with a PAR-364 polarograph as potential source. The current changes were recorded on a Houston 2000 x-y recorder. The HMDE was obtained from a PAR-303 electrode stand (large drop mode). Controlled-potential electrolysis with a mercury pool electrode was done with a Bruker E44s polarograph as potentiostat. Stirring was done by passing nitrogen. The current was recorded with a Kipp and Zonen BD-7 x-t recorder. The mercury pool electrode (Metrohm EA996-20) had a surface area of about 7.1 cm^2 .

The pH values were measured with a Radiometer PHM-64 research pH meter, equipped with an Ingold LOT-401 combined glass/reference electrode. Spectra were recorded with a double-beam Shimadzu UV-200 spectrophotometer with a 1-cm silica cell.

Chemicals and solutions

Nalidixic acid (I) and 7-hydroxymethylnalidixic acid (II), both from Sterling-Winthrop, were used as received. Propyl nalidixate was prepared as previously described [4]. Methanol (Nanograde, Malinckrodt and "zur Analyse" Merck) and dimethylformamide (Spectrar, Malinckrodt) were used as received. Chemicals used for the preparation of buffers and other supporting electrolytes were of analytical-reagent grade (Merck).

Stock solutions (0.01 M) of nalidixic acid and its derivatives were prepared freshly by dissolving in dimethylformamide. The composition of the aqueous buffers used was the same as reported previously [9]. To characterize the activity of hydrogen ions in strongly acidic media, values of the acidity function H_0 [10] in solutions of sulphuric acid were taken as an arbitrary acidity scale, even when the condition of similarity of structure of the indicators used and compounds studied was not strictly followed.

General procedures

The buffer or another supporting electrolyte (10 ml) was deaerated by a stream of nitrogen for about 10 min and the current-voltage curve of this solution was recorded. To this solution, 100 μ l of a freshly prepared 0.01 M stock solution of the compound studied in dimethylformamide was added. The polarographic curve of the resulting solution, containing 9.9×10^{-5} M of the compound studied and about 1% dimethylformamide, was then recorded, after additional deaeration for 1 min. A controlled drop-time of 2 s and a scan-rate of 2 mV s⁻¹ were used throughout this study.

Controlled-potential electrolysis of the nalidixic acid (I) was examined at the mercury pool electrode and at the HMDE. The electrolyzed solution (20 ml) was 1×10^{-3} M in nalidixic acid in 90% methanol and contained phosphate buffer pH 5.6. The solution was stirred vigorously by bubbling nitrogen during electrolysis, which was continued for about 5 h. For the electrolysis at the HMDE, 2.5 ml of the same solution as above was stirred in a small cell by a small magnetic stirrer; the potential was controlled manually and electrolysis was continued for about 3 h.

Determination of nalidixic acid in urine

A portion (5 ml) of spiked urine or urine of volunteers under treatment with nalidixic acid was mixed with 0.5 ml of an acetate buffer pH 5.0 prepared from 1.5 M acetic acid and 1.0 M sodium acetate. To a 2.0-ml aliquot of this buffered urine sample, 3.0 ml of chloroform was added, the mixture was vortexed for 1 min, and the layers were separated by centrifugation for 2 min at 2500g. Most of the aqueous layer was removed by a Pasteur pipette and the remaining mixture was separated by a phase-separating filter (Whatman IPS). The residue on the filter was rinsed with 1.0 ml of chloroform. From the combined chloroform solutions the solvent was distilled off at 70°C by a stream of nitrogen gas. The residue was dissolved in 1.0 ml of methanol with ultrasonic vibration for 15 min. The blank solution, consisting of 5 ml

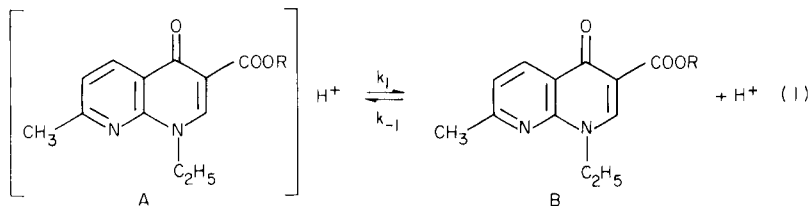
of a phosphate buffer pH 3 containing 50% (v/v) methanol, was deaerated by purging with nitrogen and a differential pulse polarographic (d.p.p.) curve was recorded. Then 100 μ l of the methanolic sample solution was added to the blank and after deaeration for 1 min the d.p.p. curve was recorded again. To the same mixture, 100 μ l of a standard solution of an appropriate concentration of nalidixic acid was added and another d.p.p. curve was recorded. The concentration of nalidixic acid in the sample was estimated from the usual relationship for the standard addition procedure after all curves had been corrected for the blank.

RESULTS AND DISCUSSION

Propyl nalidixate (III)

The polarographic reduction of the propyl ester **III** follows the simplest pattern among the three compounds studied and will therefore be discussed first. Reduction, investigated from $H_0 = -1$ to pH 13, occurs in three waves (Figs. 1 and 2, Table 1). The most positive pre-wave i_a is governed by adsorption, as proved by its independence of the concentration of ester **III** at $C > 2 \times 10^{-4}$ M and by the linear dependence of its height on the height of mercury column.

The reduction occurs in a one-electron step and is accompanied by an acid-base equilibrium (see below), which results in changes of polarographic curves with pH [11, 12]. The transfer of a single electron was confirmed by comparison of the waves of compound **III** with those of equimolar solutions of acetophenone, benzophenone and methylene blue. The one-electron wave i_3 observed at pH > 8 corresponds to a reduction of a species (B) which predominates in the solution in this pH range. This can be deduced from the pH independence of the half-wave potentials of this wave between pH 8 and 10 (Fig. 2A, Table 1). The one-electron wave i_1 observed at $H_0 = -1$ to pH 9 corresponds to the reduction of the conjugate acid (A). The acid form A is formed over the whole pH range where it is observed, by protonation of species B (predominating in the bulk of the solution) which occurs at the surface of the electrode with rate constant k_{-1} . The role of pre-protonation is shown by the dependence of the half-wave potential of wave i_1 on pH with a reciprocal slope of $-dE_{1/2}/dpH = 0.076$ V/pH. The reactions are as follows:



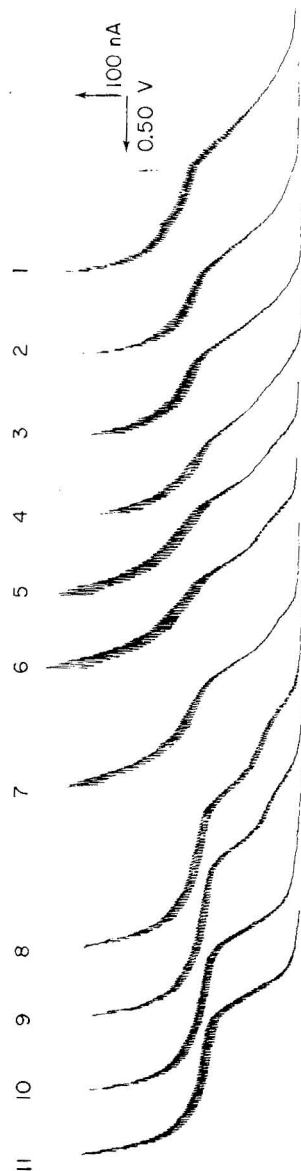


Fig. 1. D.c. polarographic curves of 10^{-4} M propyl ester of naldixic acid in buffer solutions of pH: (1) 2.0; (2) 3.1; (3) 4.75; (4) 5.3; (5) 6.4; (6) 6.7; (7) 7.4; (8) 8.15; (9) 9.1; (10) 10.2; (11) 14.0. Starting potentials for the curves: (1, 2) -0.6 V; (3, 4) -0.8 V; (5-8) -1.0 V; (9, 10) -1.2 V; (11) -1.4 V.

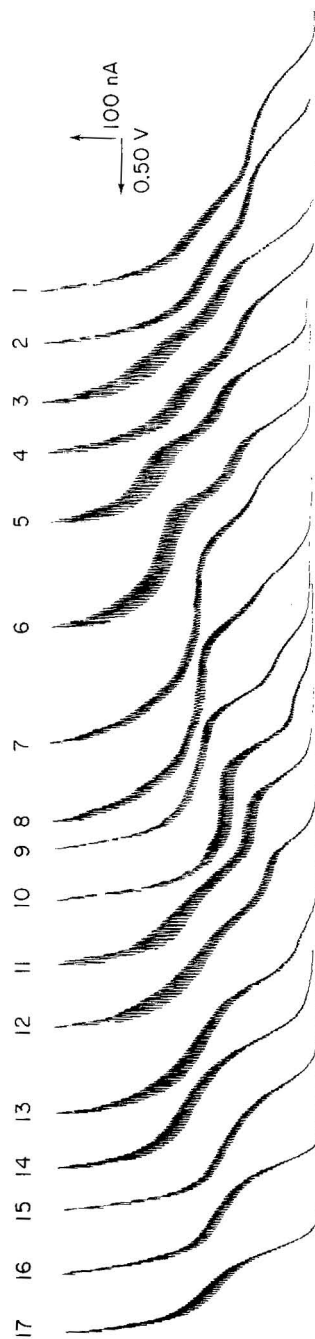
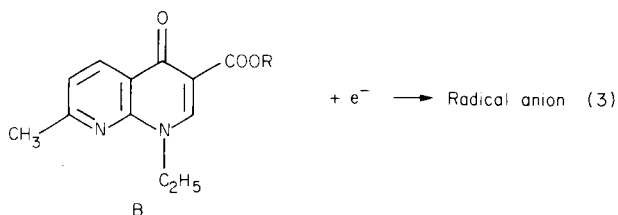
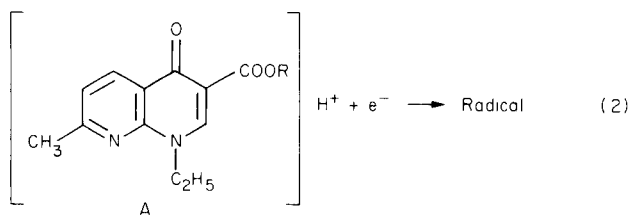


Fig. 3. D.c. polarographic curves of 10^{-4} M naldixic acid in buffer solutions of pH: (1) -0.3 ; (2) 0.0 ; (3) 1.5 ; (4) 3.1 ; (5) 4.2 ; (6) 5.7 ; (7) 6.4 ; (8) 7.1 ; (9) 7.9 ; (10) 8.1 ; (11) 8.6 ; (12) 9.1 ; (13) 9.7 ; (14) 10.2 ; (15) 11.5 ; (16) 12.5 ; (17) 14.0 . Starting potentials for the curves: (1) -0.5 V; (2, 3) -0.6 V; (4-6) -0.8 V; (7-10) -1.0 V; (11-13) -1.2 V; (14-17) -1.4 V.



Decrease in the rate of protonation with rate constant k_{-1} at pH greater than about 7 results in a decrease in the height of wave i_1 in the shape of a dissociation curve (Fig. 2B) with an inflection point at pH about 8.5. This leads to a replacement of wave i_1 by wave i_3 (reaction 3). The available experimental data are inadequate to distinguish whether compound A is predominantly protonated on the pyridine or azinone ring at equilibrium in the bulk of solution. Nevertheless, in the dynamic process involved in

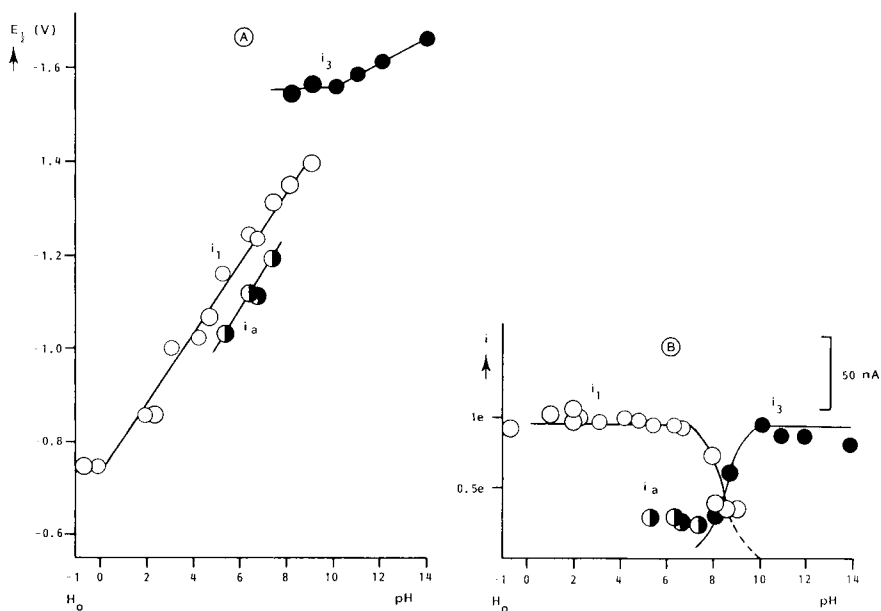


Fig. 2. Dependence on pH of the d.c. polarographic half-wave potentials (A) and d.c. limiting currents (B) of 10^{-4} M propyl ester of nalidixic acid in aqueous buffers, sulphuric acid (from $H_0 = -1$ to pH 1) and sodium hydroxide solutions (from pH 12 to pH 14): (○) wave i_1 ; (●) wave i_3 ; (◐) adsorption pre-wave.

TABLE 1

Polarographic characteristic data for propyl nalidixate (III) and nalidixic acid (I)

(Current i in μA , $E_{1/2}$ in V vs. SCE; 1×10^{-4} M compound I and III in buffers, sulphuric acid and sodium hydroxide solutions containing 1% DMF)

Propyl nalidixate					Nalidixic acid											
pH/ H_0	i_a	$E_{1/2}^a$	i_1^b	$E_{1/2}^1$	i_3	$E_{1/2}^3$	i_1	$E_{1/2}^1$	$i_1 + i_2$	$E_{1/2}^2$	i_3	$E_{1/2}^3$	i_4	$E_{1/2}^4$	$i_4 + i_5$	$E_{1/2}^5$
-0.70	—	—	0.09 _s	-0.75	—	—	0.08	-0.64 _s	0.17 _s	—	—	—	—	—	—	—
0.00	—	—	0.10	-0.74 _s	—	—	0.09	-0.69	0.17 _s	-0.91	—	—	—	—	—	—
1.00	—	—	0.11	-0.81 _s	—	—	0.10	-0.76 _s	0.17 _s	-0.97	—	—	—	—	—	—
3.10	—	—	0.10	-1.01	—	—	0.09 _s	-0.88	0.17	-1.07 _s	—	—	—	—	—	—
4.20	—	—	0.10 _s	-1.04	—	—	0.10	-0.95	0.18	-1.12	—	—	—	—	—	—
5.30	0.03	-1.03 _s	0.10	-1.17	—	—	0.09	-0.99	0.17	-1.18	—	—	—	—	—	—
6.40	0.03	-1.12 _s	0.10	-1.26	—	—	0.05 _s	-1.11	0.14	-1.27	—	—	0.06	-1.08	0.14	-1.26
6.70	0.03	-1.12	0.09 _s	-1.25	—	—	—	—	—	—	—	—	0.05	-1.20	0.13	-1.36
7.40	0.03	-1.20	—	-1.32	—	—	—	—	—	—	—	—	0.04	-1.23	0.12	-1.39
7.90	—	—	—	—	—	—	—	—	—	—	—	—	0.01	- ^c	0.09	-1.39
8.00	—	—	0.08	-1.36	0.03	-1.55	—	—	—	—	0.06 _s	-1.60	—	—	0.06	-1.41
8.20	—	—	—	—	—	—	—	—	—	—	—	—	—	—	—	—
8.50	—	—	0.04	-1.41	0.06	-1.57	—	—	—	—	0.08 _s	-1.58	—	—	0.02 _s	-1.43
8.70	—	—	—	—	—	—	—	—	—	—	0.09	-1.59	—	—	0.02	- ^c
9.00	—	—	—	—	—	—	—	—	—	—	0.11 _s	-1.58	—	—	—	—
9.40	—	—	—	—	0.10	-1.57	—	—	—	—	0.18	-1.59	—	—	—	—
10.20	—	—	—	—	0.09	-1.60	—	—	—	—	0.11	-1.63	—	—	—	—
12.00	—	—	—	—	0.09	-1.62 _s	—	—	—	—	0.11	-1.68	—	—	—	—
13.50	—	—	—	—	—	—	—	—	—	—	—	—	—	—	—	—

^aCurrent and half-wave potential of adsorption pre-wave. ^bThe height of wave i_1 includes the height of wave i_a in strongly alkaline and strongly acidic media, the measured current was corrected by a multiplication factor $(\eta/\eta_0)^{1/2}$, where η is the viscosity of the medium and η_0 is the viscosity of water. ^cBadly developed wave, $E_{1/2}$ not measurable.

electrolysis, the protonation is more likely to occur on the ethylenic bond which is reduced (for proof, see below). The fate of the radical formed in wave i_1 or the radical anion generated in wave i_3 was not further investigated. It may participate in one of the possible dimerizations or disproportionations or be deactivated by reaction with the solvent. The shift in the half-wave potential of wave i_3 at $\text{pH} \geq 11$ is due to an increase in sodium ion concentration in the supporting electrolyte. The half-wave potential is shifted by about $-dE_{1/2}/dp\text{Na} = 0.07 \text{ V/log} [\text{Na}^+]$.

Nalidixic acid (I)

The polarographic reduction of nalidixic acid (Figs. 3, 4; Table 1) resembles that of the ester (III) with two notable exceptions. First, in addition to waves i_1 and i_3 in acidic and alkaline media, respectively, another one-electron wave i_4 is observed at pH 6–10. The height of this wave increases with increasing pH at $\text{pH} \geq 5.5$ and decreases at about $\text{pH} > 7$ (Figs. 3, 4B). Secondly, waves i_1 and i_4 are accompanied at more negative potentials by waves i_2 and i_5 , which are of practically the same height as i_1 and i_4 . This indicates that in both processes (corresponding to i_1 and i_4) the reduction of the product of the one-electron transfer occurs for acid I within the accessible range of potentials, whereas for ester III the uptake of the second electron may occur only outside this range.

Both these differences result from a replacement of the grouping COOR by COOH or COO^- . The presence of the additional waves i_4 and i_5 can be attributed to the possibility of dissociation of the carboxyl group, for which $\text{p}K_{\text{COOH}}$ values varying between 6.02 and 6.11 have been reported [13–15]. To decide whether the decrease in wave i_1 or i_4 with pH corresponds to dissociation of the carboxyl group, the shapes of the i – pH plots and the value of $\text{p}K_{\text{COOH}}$ were compared. Wave i_1 decreases with increasing pH in the shape of a dissociation curve with an inflection point at about pH 6.7 ($\text{p}K'_{i_1}$), whereas wave i_4 shows the inflection point at about pH 8.5 ($\text{p}K'_{i_4}$) (Fig. 4B). Attribution of the decrease of wave i_1 to the dissociation of the carboxyl group would involve $\text{p}K'_{i_1} \approx \text{p}K_{\text{COOH}}$. Such agreement implies an acid–base equilibrium established slowly when compared with the time-window of a polarographic measurement (3 s). Such slow protonation of the carboxylate ion seems rather improbable. Attribution of the decrease of wave i_4 to dissociation of the carboxyl group results in $\text{p}K'_{i_4} > \text{p}K_{\text{COOH}}$. Because of recombination of anions with proton donors [16, 17] in the vicinity of the electrode, the inflection points of polarographic dissociation curves ($\text{p}K'$) for reducible acids are shifted to higher pH values than the thermodynamic $\text{p}K$ value.

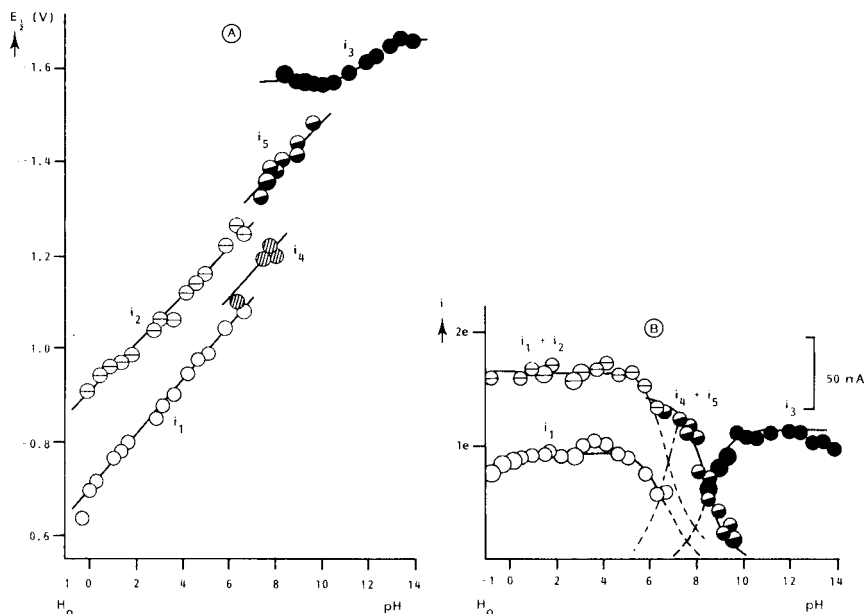
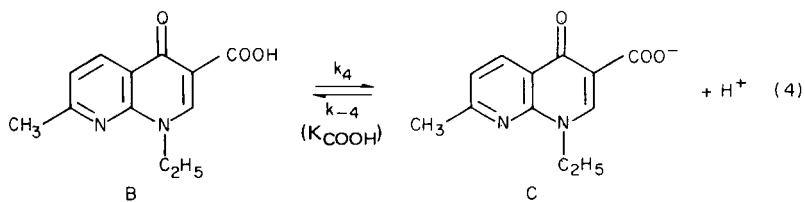
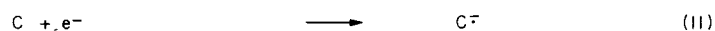
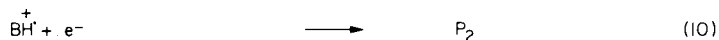


Fig. 4. Dependence on pH of the d.c. polarographic half-wave potentials (A) and d.c. limiting currents (B) of 10^{-4} M nalidixic acid in aqueous buffers, sulphuric acid (from $H_0 = -1$ to pH 1) and sodium hydroxide solutions (from pH 12 to pH 14): (○) wave i_1 ; (◐) total height of waves i_1 and i_2 ; (●) total height of waves i_4 and i_5 ; (●) wave i_3 . The height of wave i_4 was not plotted to simplify the plot.

Thus the decrease of waves i_4 and i_5 with increasing pH at about pH 8 can be attributed to the dissociation of the carboxyl group.

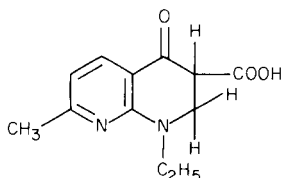
The reaction scheme can be described by the acid-base equilibrium between species A and B given by reaction (1) (for $R = H$), followed by reactions (4–11):





(symbols A, B, C, A[·], AH^{·+}, etc. do not try to indicate the actual unit charge of the individual species).

Waves i_1 – i_5 are considered to be due to reactions (5), (7), (11), (8) and (10), respectively. A decrease in the rate of protonation of the species B in reaction (1) with rate constant k_{-1} causes a decrease in wave i_1 at pH > 5 (Fig. 4B). Controlled-potential electrolysis of the limiting current of wave i_2 resulted in formation of a dihydroderivative (P_1). This was proved by the



presence of an absorption band corresponding to a carbonyl group conjugated with an aromatic system in the u.v. spectra obtained after electrolysis, as well as by the retention of both carbonyl bands at 1710 and 1615 cm⁻¹ together with disappearance of the ethylenic bands at 975 and 700 cm⁻¹ in the i.r. spectra. As a saturated ketone rather than an unsaturated alcohol is the product of the two-electron reduction, it can be concluded that protonation of species B preceding electro-reduction in wave i_1 occurs on the ethylenic band. Protonation of B resulting in formation of A is responsible for the shift of -61 mV/pH of the half-wave potential of wave i_1 (Fig. 4A) over the entire range of its existence. The shift of the half-wave potentials of wave i_2 indicates the presence of a proton transfer (reaction 6) between the first and second electron uptake.

Wave i_4 , which replaces wave i_1 at pH > 6, corresponds to reduction of species B (reaction 8). Decrease in the rate of protonation with rate constant k_{-4} results in a decrease in the height of wave i_4 at pH > 7 (Fig. 4B). On the assumption that reaction (4) is homogeneous and so unaffected by adsorption, it is possible [17] to write

$$\log k_{-4} = 2 \text{p}K'_{i_4} - \text{p}K_{\text{COOH}} - 2 \log 0.886 - \log t_1 \quad (12)$$

Values for $\text{p}K'_{i_4} = 8.5$ and $\text{p}K_{\text{COOH}} = 6.1$ yield a $\log K_{-4}$ value of about 10.5, which is within the range of rates of protonation of other carboxylic acids [18]. Shifts of half-wave potentials of wave i_4 of $-dE_{1/2}/\text{dpH} = 0.063 \text{ V}$ indicate protonation of the anion C (which in this pH range predominates in the bulk of the solution) in reaction (4) preceding the first electron uptake (reaction 8). Wave i_5 (which at pH 7–9.5 overlaps wave i_4) corresponds to a one-electron reduction of the product of reduction of species B. The shift of the half-wave potentials of wave i_5 by -0.054 V/pH indicates

another proton transfer (reaction 9) occurring between the first and second electron transfer (reactions 8 and 10).

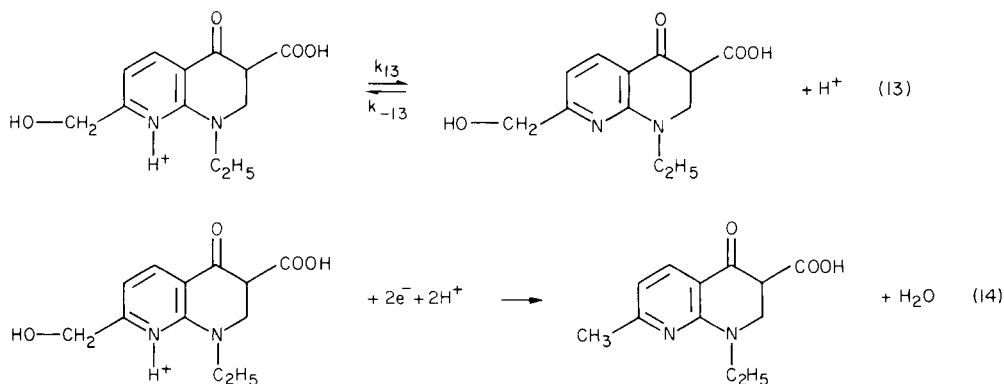
Wave i_3 , similarly as for the ester **III**, corresponds to a one-electron reduction (reaction 11) of the least protonated species (C). As the form C is the predominant species in solution, the half-wave potential of wave i_3 is pH-independent in principle. The shift observed at pH > 11 is due to an increase in sodium ion concentration and corresponds to $-dE_{1/2}/dpNa = 0.07 \text{ V/log [Na}^+]$.

The decrease in the limiting current of wave i_1 between pH 1 and 6 reported earlier for nalidixic acid [8] could not be confirmed. The role of incomplete solubilization in this pH range between two known pK values of -0.9 [13] and about 6.1 [13–15] should be considered.

The most marked difference between the behaviour of the acid **I** and the ester **III** is the appearance of waves i_2 and i_5 for the former. The absence of these waves on the curves obtained for the ester **III** can be caused either by fast deactivation of the radical A^{\cdot} (by dimerization, disproportionation or reaction with the solvent) or by a shift of the half-wave potentials to potentials more negative than those of the final rise of current. The difference between the polar effects of COOR and COOH cannot be responsible for such a shift of several hundred millivolts. A surface orientation of the radical of the acid which permits further protonation and reduction that is not possible for the ester might be a plausible explanation.

1-Hydroxymethylnalidixic acid (**II**)

The general reduction pattern of the 7-hydroxymethyl derivative **II** (Figs. 5 and 6, Table 2) resembles that of the parent acid **I** (Figs. 3 and 4) and shows waves i_1 and i_2 in acidic media, i_4 and i_5 in the medium pH range and a wave i_3 in alkaline solutions. The only additional feature is the appearance of wave i_6 in acidic media. This wave is attributed to the reduction of the C—O bond in the side-chain in the *N*-protonated reduced form of **II**:



Similar reactions have been observed for pyridoxal [19] and other 4- and 2-hydroxymethylpyridines [20].

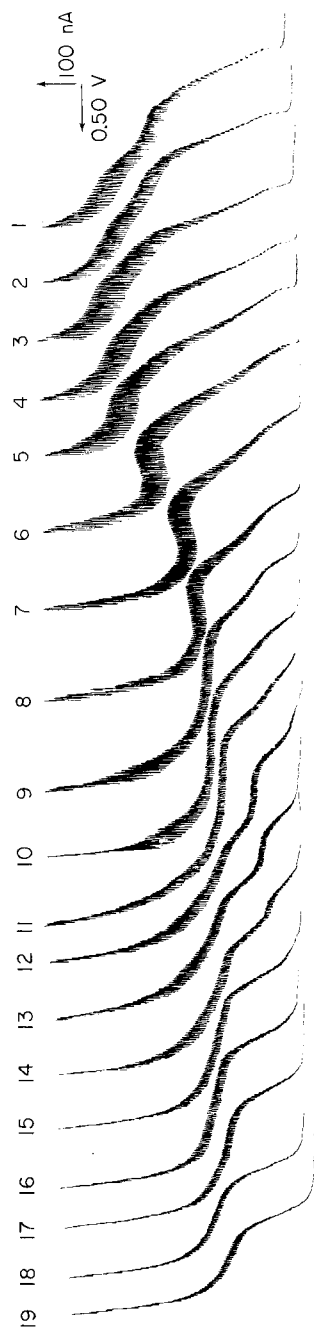


Fig. 5. D.c. polarographic curves of 10^{-4} M 7-hydroxymethylinalidixic acid in buffer solutions: (1) -0.3 ; (2) 0.0 ; (3) 1.0 ; (4) 2.0 ; (5) 3.1 ; (6) 4.2 ; (7) 4.8 ; (8) 5.2 ; (9) 5.9 ; (10) 6.7 ; (11) 7.9 ; (12) 8.2 ; (13) 8.6 ; (14) 9.1 ; (15) 9.7 ; (16) 10.2 ; (17) 11.5 ; (18) 13.0 ; (19) 14.0 . Starting potentials for the curves: (1-3) -0.6 V; (4-7) -0.8 V; (8-10) -1.0 V; (11-14) -1.2 V; (15-19) -1.4 V.

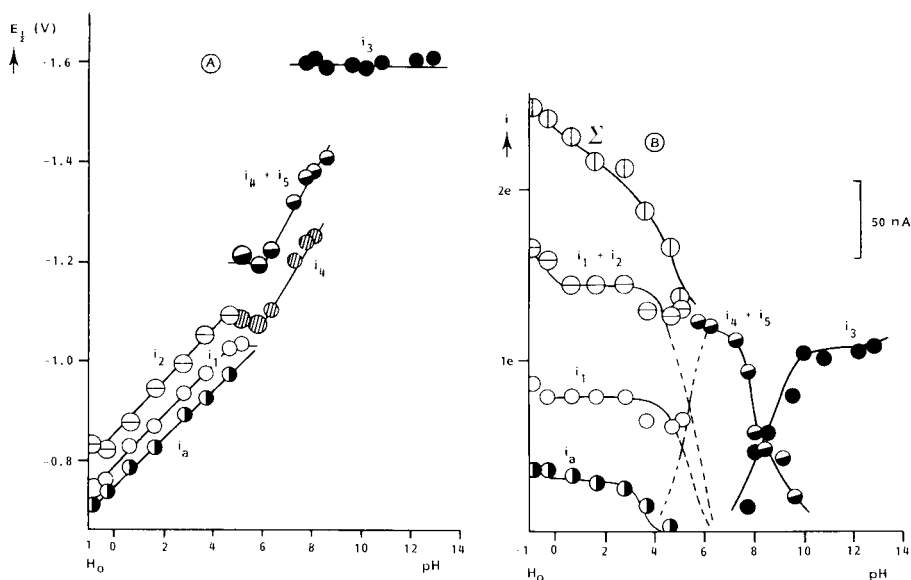


Fig. 6. Dependence on pH of the d.c. polarographic half-wave potentials (A) and d.c. limiting currents (B) of 10^{-4} M 7-hydroxymethylnalidixic acid in aqueous buffers, sulphuric acid (from $H_0 = -1$ to pH 1) and sodium hydroxide solutions (from pH 12 to pH 14): (\circ) wave i_1 ; (\ominus) total height of waves i_1 and i_2 ; (\oplus) sum of the heights of waves i_1 , i_2 and i_6 (Σ); (\bullet) total height of waves i_4 and i_5 ; (\bullet) wave i_3 ; (\circ) adsorption pre-wave. The height of wave i_4 was not included to simplify the plot.

The pH at the inflection point of the decrease (Fig. 6B) of currents i_1 and ($i_1 + i_2$), $pK'_1 = 5.5$, corresponds to protonation in reaction (1). This value decreases (Table 3) in the sequence $\text{III} > \text{I} > \text{II}$. This decrease is affected both by the value of the thermodynamic dissociation constant K_1 of reaction (1) and by the rate of protonation with the rate constant k_{-1} . It seems, nevertheless, that the rate of surface protonation is fastest for the ester, and slowest for the hydroxymethyl derivative. This sequence seems to parallel the hydrophobicity of the reacting species, which in turn governs the adsorbability. Hence it seems probable that the rate of protonation increases with surface concentration of the species.

The pH of the inflection point of the increase in the height of wave i_3 ($pK'_4 = 8.5$) (Fig. 6B), which corresponds to the protonation of the carboxylate, is practically equal to the value found for pK'_4 for nalidixic acid (Table 3). Thus substitution by a hydroxy group in the side-chain in position 7 has predictably little effect on the rate of protonation of the carboxylate group in position 3. The decrease in wave i_6 at pH > 2.5 with an inflection point at pH 4.25 (Fig. 6B) corresponds to reaction (13), indicating a decrease in the rate of surface protonation with rate constant k_{-13} .

The slopes of the plots of $E_{1/2}$ vs. pH (Fig. 6A, Table 3) for the 7-hydroxymethyl derivative (II) are similar to those for the parent acid (I). Yet the differences in the slopes of the pH dependences for individual compounds

TABLE 2

Polarographic characteristic data for 7-hydroxymethylalidixic acid (II)

(Current i in μA , $E_{1/2}$ in V vs. SCE, 1×10^{-4} M compound II in buffers, sulphuric acid and sodium hydroxide solutions containing 1% DMF)

pH/ H_0	i_a	$E_{1/2}^a$	i_1^b	$E_{1/2}^c$	$i_1 + i_2$	$E_{1/2}^d$	i_3	$E_{1/2}^e$	i_4	$E_{1/2}^f$	$i_4 + i_5$	$E_{1/2}^g$	i_5^h	i_6^i	$E_{1/2}^j$	Σ
-0.85	0.05	-0.70	0.12	-0.73	0.23	-0.82	—	—	—	—	—	—	0.12	0.12	-1.07	0.34
-0.25	0.05	-0.73	0.11	-0.75	0.22	-0.81	—	—	—	—	—	—	0.11	0.11	-1.06	0.33
0.70	0.04 _s	-0.78	0.11	-0.82	0.20	-0.87	—	—	—	—	—	—	0.11 _s	0.11 _s	-1.05	0.32
1.70	0.04	-0.82	0.11	-0.86	0.20	-0.94	—	—	—	—	—	—	0.10	0.10	-1.06	0.30
2.88	0.03 _s	-0.88	0.11	-0.93	0.20	-0.99	—	—	—	—	—	—	0.09	0.09	-1.07	-1.12 (i_a) 0.29 _s
3.77	0.02	-0.92	0.09	-0.97	0.18	-1.05	—	—	—	—	—	—	0.08	0.08	-1.07	-1.17 (i_a) 0.26 _s
4.75	0.00 _s	-0.97	0.08 _s	-1.02	0.17 _s	-1.09	—	—	—	—	—	—	0.04 _s	0.04 _s	e	0.23
5.20	—	—	0.09 _d	-1.03 _d	0.18 _d	(-1.16) _d	—	—	—	-1.08	—	-1.21	0.00 _s	0.00 _s	e	0.19
5.90	—	—	—	—	—	—	—	—	0.08	-1.07	0.17	-1.20	—	—	—	—
6.40	—	—	—	—	—	—	—	0.07 _s	-1.10	0.16 _s	—	-1.23	—	—	—	—
7.41	—	—	—	—	—	—	—	0.08	-1.20	0.15 _s	—	-1.32	—	—	—	—
7.86	—	—	—	—	—	—	0.02	-1.60	0.06	-1.24	0.13	-1.37	—	—	—	—
8.15	—	—	—	—	—	—	0.06	-1.61	—	-1.25	0.08	-1.38	—	—	—	—
8.64	—	—	—	—	—	—	0.07 _s	-1.59	—	—	0.06 _s	-1.41	—	—	—	—
9.70	—	—	—	—	—	—	0.11	-1.60	—	—	0.02 _s	—	—	—	—	—
10.20	—	—	—	—	—	—	0.14 _s	-1.59	—	—	—	—	—	—	—	—
11.00	—	—	—	—	—	—	0.14	-1.62	—	—	—	—	—	—	—	—
12.30	—	—	—	—	—	—	0.14 _s	-1.62 _s	—	—	—	—	—	—	—	—
13.00	—	—	—	—	—	—	0.15	-1.63	—	—	—	—	—	—	—	—

^aCurrent and half-wave potential of adsorption pre-wave. ^bThe height of wave i_1 includes the height of wave i_a ; in strongly alkaline and strongly acidic media the measured current was corrected by a multiplication factor $(\eta/\eta_0)^{1/2}$ where η is the viscosity of the medium and η_0 is the viscosity of water. ^cWave includes an ill-separated adsorption pre-wave. ^dSum of waves $i_1 + i_4$ or $i_2 + i_3$. ^eBadly developed wave, $E_{1/2}$ was not measurable.

TABLE 3

Comparison of polarographic data related to acid-base reactions for nalidixic acid and its derivatives

Compound	$-dE_{1/2}/dpH$ (mV pH ⁻¹)					pK'_1	pK'_4	$E^3_{1/2}$
	i_1	i_2	i_3	i_4	i_5			
I	61	54	0	63	54	6.7	8.5	-1.60
II	55	55	0	75	77	5.5	8.5	-1.60
III	76	—	0	—	—	8.5	8.5	-1.57

(Table 3) and the effect of additional acid-base equilibria involving the carboxyl group prevent meaningful comparison of the half-wave potentials of waves i_1 . Comparison is possible for the pH-independent half-wave potentials of wave i_3 , corresponding to the reduction of the least protonated species. This half-wave potential is -1.60 V for both compounds I and II and -1.57 V for the ester III. This indicates a significant change in substituent effect when the group COO^- is replaced by $COOR$, in agreement with the change in the values of $\sigma_{m-COO^-} = 0.09$ and $\sigma_{m-COOR} = 0.37$ [21]. Such an effect is understandable, as the substituent is located on the ethylenic bond which is the electro-active centre.

Determination of nalidixic acid and its 7-hydroxymethyl derivative in urine

The above study indicates that best developed waves for nalidixic acid and its 7-hydroxymethyl derivative are obtained at pH 2–5 or pH 10–12. The limited solubility of nalidixic acid in aqueous solutions led to a choice of a supporting electrolyte consisting of equal volumes of methanol and an aqueous solution of phosphate buffer pH 3.0. In this medium, the changes in half-wave potentials and limiting currents with pH followed similar patterns as in the aqueous solutions discussed above. Furthermore, the presence of the organic solvent suppressed adsorption phenomena. In the above supporting electrolyte, the heights of peaks obtained by differential pulse polarography (Fig. 7) were a linear function of concentration of compounds I and II between 4×10^{-7} M and 1×10^{-4} M.

Nalidixic acid can be extracted from aqueous solutions by chloroform, toluene and ethyl acetate as well as a 3:1 mixture of chloroform and 2-propanol [22]. For reasons of purity, chloroform was chosen [6], but because it yields polarographic reduction waves, the solvent must be evaporated off and the residue dissolved in methanol. The mean recovery of nalidixic acid and 7-hydroxymethylnalidixic acid was 99%; the relative standard deviation for 6 repetitive determinations was 11%. Attempts to determine both nalidixic acid and its 7-hydroxymethyl derivative in mixtures were unsuccessful. Even when the separation of half-wave potentials was about 100 mV, neither d.c. nor differential pulse polarography yielded satisfactory separation because of the drawn-out character of the waves. Results

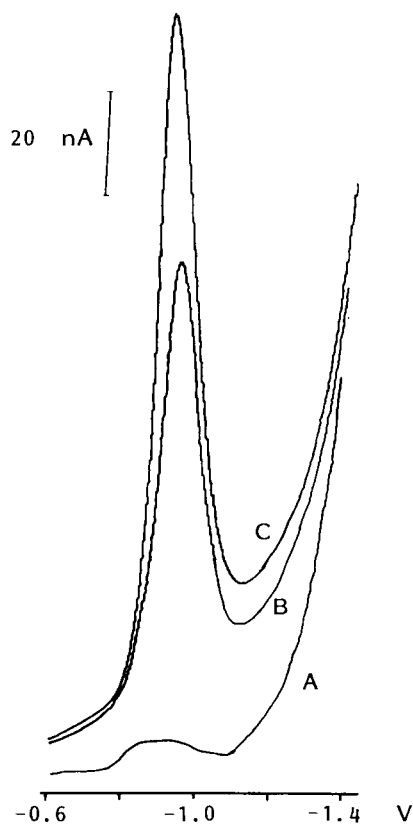


Fig. 7. Differential pulse polarographic curves: (A) blank polarographic solution, consisting of a 1:1 mixture of methanol and phosphate buffer pH 4; (B) sample solution; (C) sample solution with added standard solution of nalidixic acid so that its concentration increased by 4×10^{-6} M.

enabled the concentration of nalidixic acid (I) and its metabolite (II) to be estimated with standard deviations of 20–40%. Nevertheless, the sum of both nalidixic acid and 7-hydroxymethylnalidixic acid in urine of volunteers to whom nalidixic acid had been administered could be determined at levels between 10^{-5} and 10^{-6} M.

This work was supported in part by Z. W. O. (Nederlandse organisatie voor Zuiver Wetenschappelijk Onderzoek) by means of a visiting scientist appointment (P. Z.), which is gratefully acknowledged. The work is part of the Ph.D. thesis (1982) of R. H. A. Sorel.

REFERENCES

- 1 R. Gleckman, S. Alvarez, D. W. Joubert and S. J. Mathews, *Am. J. Hosp. Pharm.*, **36** (1979) 1071.
- 2 P. E. Grubb, in K. Florey (Ed.), *Analytical Profiles of Drug Substances*, Vol. 8, Academic Press, New York, 1979, p. 371.
- 3 E. W. McChesney, E. J. Froelich, G. Y. Leshner, A. V. R. Crain and D. Rosi, *Toxicol. Appl. Pharmacol.*, **6** (1964) 292.
- 4 R. H. A. Sorel and H. Roseboom, *J. Chromatogr.*, **162** (1979) 461.
- 5 H. Roseboom, R. H. A. Sorel, H. Lingeman and R. Bouwman, *J. Chromatogr.*, **163** (1979) 92.
- 6 R. H. A. Sorel, A. Hulshoff and C. Snelleman, *J. Chromatogr.*, **221** (1980) 129.
- 7 G. Cuisinaud, N. Ferry, M. Seccia, N. Bernard and J. Sassard, *J. Chromatogr.*, **181** (1980) 399.
- 8 R. Starościk, I. Prochowska and J. Sulkowska, *Pharmazie*, **29** (1974) 387.
- 9 H. S. de Boer, W. J. van Oort and P. Zuman, *Anal. Chim. Acta*, **130** (1981) 111.
- 10 R. H. Boyd, in J. F. Coetzee and C. D. Ritchie (Eds.), *Solute—Solvent Interactions*, Dekker, New York, 1969, p. 97ff.
- 11 P. Zuman, in P. Zuman, L. Meites and P. Kolthoff (Eds.), *Progress in Polarography*, Vol. III, Wiley-Interscience, New York, 1972, p. 73 ff.
- 12 M. Heyrovský and S. Vavříčka, *J. Electroanal. Chem.*, **36** (1972) 202, 222.
- 13 R. Starościk and J. Sulkowska, *Acta Polon. Pharm.*, **28** (1971) 603.
- 14 K. Timmers and R. Sternglanz, *Bioinorg. Chem.*, **9** (1978) 145.
- 15 W. R. Vincent, S. G. Schulman, J. M. Midgley, W. J. van Oort and R. H. A. Sorel, *Int. J. Pharm.*, **9** (1981) 191.
- 16 R. Brdička, *Collect. Czech. Chem. Commun.*, **12** (1947) 212.
- 17 J. Koutecký, *Collect. Czech. Chem. Commun.*, **18** (1953) 597.
- 18 R. Brdička, *Collect. Czech. Chem. Commun.*, **19** (1945) S 41.
- 19 O. Manoušek and P. Zuman, *Collect. Czech. Chem. Commun.*, **29** (1964) 1432.
- 20 J. Rusling, Ph.D. Thesis, Clarkson College of Technology, Potsdam, NY 13676, U.S.A.
- 21 D. Exner, in N. B. Chapman and J. Shorter (Eds.), *Correlation Analysis in Chemistry*, Plenum Press, New York, 1978, p. 439 ff.
- 22 H. Roseboom and A. Hulshoff, *J. Chromatogr.*, **173** (1979) 65.

KINETIC ASSAY OF ENZYMES WITH AN AMMONIA GAS-SENSING ELECTRODE

Part 1. Dynamic Responses of the Sensor

MASAKATSU HATO*, TOSHIO MASUOKA and YUKIO SHIMURA

Research Institute for Polymers and Textiles, Yatabehigashi, 1-1-4, Tsukubagun, Ibaraki-305 (Japan)

(Received 20th July 1982)

SUMMARY

The input-response relationship of an ammonia gas-sensing electrode was studied with special emphasis on its potential application to kinetic assay of enzyme activity. The transfer function of the electrode was determined from stepwise changes in sample ammonia concentration. A mathematical expression for the electrode response to a linear increase in ammonia concentration (a simulated signal for an enzyme reaction under zero-order conditions) was derived. This expression showed reasonable agreement with experimental results. Optimal conditions for enzyme activity determinations are discussed.

Ammonia gas-sensing electrodes (ammonia sensors) have been used for a variety of analytical measurements, mostly equilibrium measurements in thermodynamically stable systems [1]. Investigations of the dynamic response and applications of the ammonia sensor to kinetic measurements have been few. However, such applications will include enzyme-catalyzed reactions which involve ammonia production [2], because assays of such enzymes require kinetic rather than equilibrium measurements [3]. Other methods for quantifying ammonia are not useful for in situ monitoring of enzymatic reactions.

The ammonia sensor is composed of a glass pH-sensing electrode behind a gas-permeable membrane holding a thin film of electrolyte against the glass membrane. Ammonia diffuses through the permeable membrane until equilibrium is established in the electrolyte film. At equilibrium, the pH of the electrolyte film is established by the reaction $\text{NH}_4^+ \xrightleftharpoons{K_a} \text{NH}_3 + \text{H}^+$, with $\bar{C}(\text{H}^+) = K_a \bar{C}(\text{NH}_4^+)/\bar{C}$, where K_a is the equilibrium constant, and $\bar{C}(\text{H}^+)$, $\bar{C}(\text{NH}_4^+)$ and \bar{C} are the concentrations of hydrogen ion, ammonium ion and ammonia in the electrolyte film, respectively. Activity is assumed to be equal to concentration. The electrolyte film contains ammonium chloride at a sufficiently high level so that the $\bar{C}(\text{NH}_4^+)$ can be considered constant, and the potential response E is expressed as $E = \text{const.} - (RT/F)\ln \bar{C}$. At equilibrium, the ammonia concentrations in the sample solution C and in the electrolyte film \bar{C} are equal.

Thus the potential response of the sensor to ammonia is Nernstian and is a direct measure of the ammonia level in the sample solution.

The electrode response rate becomes important when the ammonia sensor is used to monitor the rates of enzyme-catalyzed reactions in situ. The dynamic response of the ammonia sensor has been discussed [4–6]. Larsen et al. [4] described the application of the air-gap electrode to an enzyme assay, but no explicit account of the response rate was taken. Ross et al. [5] developed a theoretical model describing the electrode response to a stepwise change in sample ammonia concentration as a function of such variables as electrode geometry, membrane properties, electrolyte film composition. Although the response characteristics depend in a complex manner on these variables, they were found to be in good agreement with theoretical predictions. Bailey and Riley [6] discussed various parameters which affect the response rate of the sensor. For the kinetic assay of enzymes, however, a continuous change in ammonia concentration has to be monitored. It is thus desirable to extend the model of Ross et al. and to develop a method of predicting the electrode response to such a continuous change in ammonia concentration. This would provide a useful means of examining the relative importance of various factors which affect the measurements, establishing optimal experimental conditions, and estimating the errors involved. For this purpose, it is convenient to determine the transfer function of the ammonia sensor [7].

The aim of the present paper is to elucidate the input-response relationship of the ammonia sensor with special emphasis on its application to in situ monitoring of enzymatic reactions.

EXPERIMENTAL

Materials and apparatus

All chemical substances were of extra pure grade and were used as received. Water was doubly distilled in an all-glass apparatus.

An Orion ammonia sensor model 95-10 was used with 0.1 M ammonium chloride as the internal electrolyte. The measuring cell consisted of the sensor dipped in a sample solution (50 ml) which was stirred magnetically. The cell was kept at constant temperature by circulating thermostated water through a glass jacket. Samples were injected through a hole in the beaker lid which also held the sensor in position.

Procedures

The response to a stepwise change in sample ammonia concentration was determined as follows. The solution containing C_0 ammonia was adjusted to the desired pH (>12) by adding 10 M sodium hydroxide [5], and an equilibrium potential E_0 was recorded. At time $t = 0$, an aliquot of concentrated ammonia solution (pH also adjusted by adding 10 M sodium hydroxide) was injected through the small hole in the lid to raise the ammonia concentration from C_0 to C_1 , and the electrode potential approaching a new equilibrium

value was recorded as a function of time by an Orion model 801 mV meter with a Yokogawa type 3047 strip chart recorder. Figure 1A shows a typical mV vs. time curve in which the ammonia concentration was increased at time $t = 0$ (indicated by an arrow) from 1.0 mM to 2.0 mM at 37°C. This curve was converted to an ammonia concentration vs. time curve by means of a conventional calibration graph obtained from measurements at equilibrium.

To simulate a real enzymatic reaction under zero-order conditions, the response of the sensor to a linear increase in ammonia concentration was studied in 50 mM phosphate buffer at pH 7.5 and 37°C. The sensor was pre-equilibrated with the sample solution (total ammoniacal concentration $[C + C(\text{NH}_4^+)]_0$). The total ammoniacal concentration was then increased at a constant rate α by injecting a concentrated ammonium chloride buffer by means of a microfeeder (Furue Science Co., Tokyo, Japan) and the electrode response was recorded as a function of time. The mV vs. time curves thus obtained were converted to total ammoniacal concentration vs. time curves by means of appropriate calibration graphs. The injection rate of the microfeeder ($85 \mu\text{l min}^{-1}$) was so chosen that the volume increase in the sample solution was not more than 1% of the original volume. The desired α value was obtained by adjusting the concentration of the injected solution. Preliminary experiments showed that when the stirring rate exceeded 700 rpm, it did not affect the response of the sensor, and a stirring rate of 800 rpm was used in all later work.

THEORY

The response of the ammonia sensor to a stepwise change in sample ammonia concentration

In order to facilitate subsequent discussion, the theory of Ross et al. [5] is summarized first. If the sensor is equilibrated with a sample solution

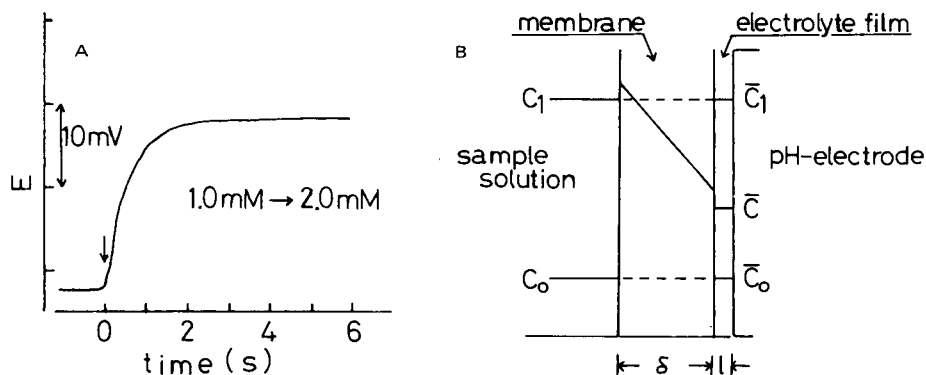


Fig. 1. A, Typical response rate curve for the sensor. B, Concentration profile at the sensing end of an ammonia sensor (for terms, see text).

having an ammonia concentration of C_0 , and the ammonia concentration is then changed from C_0 to C_1 at time $t = 0$, the input function $I(t)$ will have the form $I(t) = C - C_0 = C_1 - C_0$ ($t \geq 0$), where C is the sample ammonia concentration at time t . The concentration profile of ammonia around the permeable membrane of the sensor is shown in Fig. 1B. Initially at equilibrium, the concentration of ammonia in the electrolyte film (thickness l) \bar{C}_0 is equal to C_0 . The ammonia concentration in the membrane (thickness δ) C^m is given by $C^m = KC$, where K is the partition coefficient of ammonia between the aqueous phase (sample solution and electrolyte film) and the membrane phase. At time $t = 0$, assuming an immediate partition equilibrium at the membrane/sample solution interface, C^m is changed from $C_0^m [= KC_0]$ to a new value $C_1^m [= KC_1]$. The concentration gradient of ammonia thus established leads to a net flux across the membrane. As a result, the ammonia concentration in the electrolyte film starts to change towards a new equilibrium value $\bar{C}_1 [= C_1]$. According to the model proposed by Ross et al., the ammonia concentration in the electrolyte film (\bar{C}) at time t is given by

$$d \ln [(\bar{C}_1 - \bar{C})/\bar{C}_1] = - (1/T) dt \quad (1)$$

where $T = -(l\delta/DK\epsilon)[1 + (d\bar{C}(\text{NH}_4^+)/d\bar{C})]$, D is the diffusion constant of ammonia in the membrane and ϵ is the area fraction of the pore region in the membrane through which ammonia can diffuse. Equation (1) indicates that the response of the ammonia sensor is characterized by the term T . From the definition of symbols, $l\delta$ reflects the effects of electrode geometry and $DK\epsilon$ reflects the effects of membrane characteristics. Hence, the term $l\delta/DK\epsilon$ can be considered as a constant which depends on the sensor configuration and temperature. The term $[1 + (d\bar{C}(\text{NH}_4^+)/d\bar{C})]$ reflects the effects of the electrolyte film composition. By using the electroneutrality condition in the electrolyte film, $\bar{C}(\text{NH}_4^+) + \bar{C}(\text{H}^+) = \bar{C}(\text{Cl}^-) + \bar{C}(\text{OH}^-)$, $d\bar{C}/d\bar{C}(\text{NH}_4^+)$ (abbreviated to G) is expressed [5, 8] as

$$G = (K_a/\bar{C}(\text{H}^+)) [1 + \bar{C}(\text{NH}_4^+)/(\bar{C}(\text{H}^+) + \bar{C}(\text{OH}^-))] \quad (2)$$

Figure 2 shows the calculated values of G^{-1} as a function of the ammonia concentration in the electrolyte film at various ammonium chloride concentrations at 37°C. A K_a value of 1.29×10^{-9} M is obtained from the interpolation of the literature values [9].

Figure 2 indicates that G^{-1} values tend to increase rapidly as the ammonia concentration in the electrolyte film \bar{C} decreases. With 0.1 M ammonium chloride as the film electrolyte, G^{-1} exceeds 80 at about 2×10^{-6} M ammonia. With an increase in \bar{C} , the G^{-1} values decrease rapidly and approach zero asymptotically. At ca. 3×10^{-5} M ammonia concentrations, G^{-1} becomes <0.1 . With 0.01 M ammonium chloride as the film electrolyte, the curve shifts to a lower concentration range without a change in the general shape. As large T values mean a slow electrode response, employment of the ammonia sensor at low \bar{C} level (or at low C level) is unfavourable for moni-

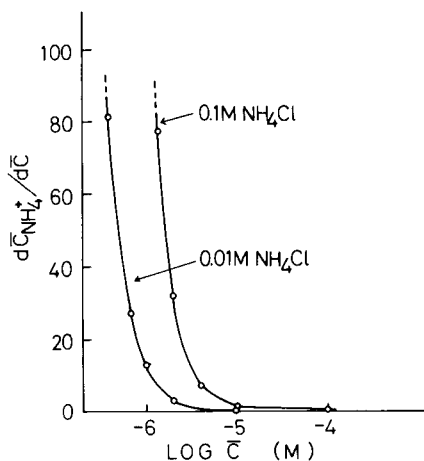


Fig. 2. $(d\bar{C}(\text{NH}_4^+)/d\bar{C}) (= G^{-1})$ values as a function of ammonia concentration \bar{C} in the electrolyte film (37°C).

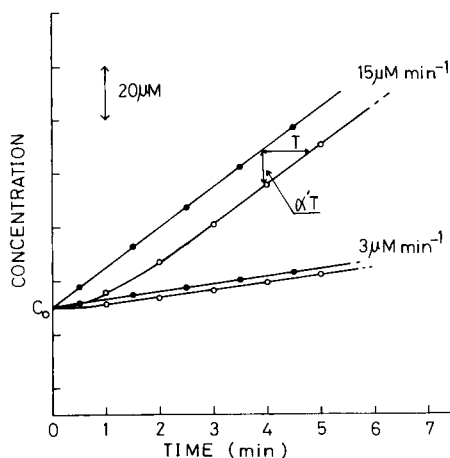


Fig. 3. Theoretical input vs. response relationship of an ammonia sensor: (●) input $I(t)$; (○) output $R(t)$ electrode response, calculated from Eqn. (4).

toring of enzymatic reactions. Moreover, changes in T with \bar{C} complicate the interpretation of the electrode response. Therefore, the ammonia sensor must be used under conditions in which either $G^{-1} \ll 1$ so that $T = l\delta/DK\epsilon$ or the concentration range to be measured is sufficiently small that the G^{-1} is constant.

Under these restrictions, integration of Eqn. (1) gives

$$\bar{C} - C_0 = (C_1 - C_0) [1 - \exp(-t/T)]$$

This equation has the usual form of an exponential approach to a new equilibrium value.

The transfer function of the ammonia sensor

It is more convenient to rewrite Eqn. (1) in terms of the electrode response $R(t)$ and the input $I(t)$. $R(t) = \bar{C} - \bar{C}_0 = \bar{C} - C_0$. Substituting this equation into Eqn. (1) under the restriction $G^{-1} \ll 1$ or constant G^{-1} , gives

$$T[dR(t)/dt] + R(t) = C_1 - C_0 = I(t)$$

Laplace transformation of this equation gives

$$TsR(s) + R(s) = I(s)$$

$$I(s) = (C_1 - C_0)/s$$

where $R(s)$ and $I(s)$ are defined [7] as

$$R(s) = L[R(t)] = \int_0^\infty \exp(-st)R(t) dt \text{ and } I(s) = L[I(t)] = \int_0^\infty \exp(-st)I(t) dt.$$

From these equations, the transfer function $F(s)$ of the ammonia sensor,

which is defined as $R(s)/I(s)$, is obtained as $1/(Ts + 1)$. The electrode responses, $R(t)$, to various input signals are now derived by taking the inverse Laplace transformation of $F(s)$

$$R(t) = L^{-1} [1/(Ts + 1) \cdot I(s)] \quad (3)$$

The response of the ammonia sensor to a linear increase in ammonia concentration

In enzyme activity determinations, the enzymatic reaction is usually monitored under conditions of zero-order conditions [3], i.e., the ammonia concentration in the reaction mixture increases linearly with time. If the ammonia sensor is initially equilibrated with a substrate buffer having an ammonia concentration of C_0 , and if at time $t = 0$, an aliquot of the enzyme solution (e.g., serum) is added to the substrate buffer so that the enzymatic reaction occurs, then the input function $I(t)$ to the sensor during ammonia production has the form $C - C_0 = \alpha' t$ ($t \geq 0$), where α' is the rate of ammonia production and is related to the enzyme activity. Substituting $I(s)$ ($= \alpha'/s^2$) into Eqn. (3), the response $R(t)$ is derived for $t \geq 0$:

$$R(t) = \alpha' [T \exp(-t/T) + t - T] \quad (4)$$

At time $t \gg T$, $R(t)$ is expressed as

$$[R(t)]_{t \gg T} = \alpha'(t - T) = I(t - T)$$

The response error, $[I(t) - R(t)]$, is expressed as

$$[I(t) - R(t)]_{t \gg T} = \alpha T \quad (5)$$

These results indicate that at time $t \gg T$, $R(t)$ and $I(t)$ are identical in functional form (identical slope) except that $R(t)$ is delayed from $I(t)$ by a time T and $R(t)$ contains an error of $\alpha'T$. Taking a value for T of 60 s the relationship between $I(t)$ and $R(t)$ was calculated by using Eqn. (4) and plotted in Fig. 3 for α' values of 15 and $3 \mu\text{M min}^{-1}$. It is clear from Fig. 3 that $R(t)$ changes in parallel to $I(t)$ at time $t \gg T$ and the response error decreases with a decrease in the α' value as is expected from Eqn. (5). If T is sufficiently small with respect to the time scale of the abscissa of Fig. 3 and α' is sufficiently small that $\alpha'T$ can be considered negligible, then $R(t)$ coincides with $I(t)$. Under such conditions, α' values can be obtained from the slope of $R(t)$.

RESULTS AND DISCUSSION

The $l\delta/DK\epsilon$ value of the ammonia sensor

The $l\delta/DK\epsilon$ value was determined from the electrode response to a step-wise change in ammonia concentration. When C_0 and C_1 are sufficiently high so that $T = l\delta/DK\epsilon$, the integrated form of Eqn. (1) becomes

$$t = 2.303(l\delta/DK\epsilon) [\log(C_1 - C_0)/C_1 - \log p] \quad (6)$$

where $p = (C_1 - \bar{C})/C_1$. If the integrated form of Eqn. (1) is a good approximation to the electrode response, a plot of $\log p$ against t will give a straight line with slope $-2.303 (l\delta/DK\epsilon)$. Figure 4 shows typical examples of plots where the sample ammonia concentration was increased from 1.0 to 2.6 mM (25°C) and from 1.0 to 2.0 mM (37°C). The plots are linear. The $l\delta/DK\epsilon$ values obtained from the slopes of the plots with various combinations of C_0 and C_1 at 37°C were 0.75 s ($C_0 = 0.1$ mM, $C_1 = 0.2$ mM), 0.7 s ($C_0 = 1.0$ mM, $C_1 = 2.0$ mM), 0.9 s ($C_0 = 2.0$ mM, $C_1 = 3.0$ mM) and 0.6 s ($C_0 = 9.0$ mM, $C_1 = 18$ mM). The $l\delta/DK\epsilon$ values at 25°C were 1.15 s ($C_0 = 1.0$ mM, $C_1 = 2.6$ mM), 1.05 s ($C_0 = 2.8$ mM, $C_1 = 4.7$ mM) and 1.20 s ($C_0 = 10$ mM, $C_1 = 20$ mM). Though the experimental procedures were only preliminary, the $l\delta/DK\epsilon$ values were found to be nearly constant over a wide concentration range, in accord with theory. The average $l\delta/DK\epsilon$ value at 37°C was 0.74 s and at 25°C was 1.13 s.

It is interesting to evaluate the order of magnitude of the DK value. The value for ϵ is roughly estimated as 0.2 through a scanning electron microscopic observation of the membrane. Taking values for l , δ and $l\delta/DK\epsilon$ of 10^{-3} cm, 10^{-2} cm and 0.7 s, respectively, a value of about 10^{-4} $\text{cm}^2 \text{s}^{-1}$ is obtained for DK . Considering the experimental errors involved, this value is in fair agreement with the reported value of 5×10^{-4} $\text{cm}^2 \text{s}^{-1}$ [5].

Response to a linear increase in ammonia concentration

Figure 5 shows typical examples of the electrode response to a linear increase in total ammoniacal concentration. The ammonia concentration at pH 7.5 calculated from the K_a value is plotted as the ordinate on the right hand side. The input and response plots are in good agreement with that of theoretical prediction (Fig. 3).

Figure 5A shows the responses when the total ammoniacal concentration was increased from 1.12 mM at two different rates. It is clear that the response and input plots agree with each other within experimental error. As

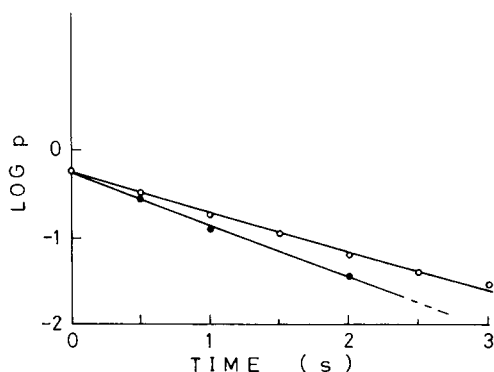


Fig. 4. Typical examples of plots of Eqn. (6): (○) $C_0 = 1.0$ mM to $C_1 = 2.6$ mM (25°C); (●) $C_0 = 1.0$ mM to $C_1 = 2.0$ mM (37°C).

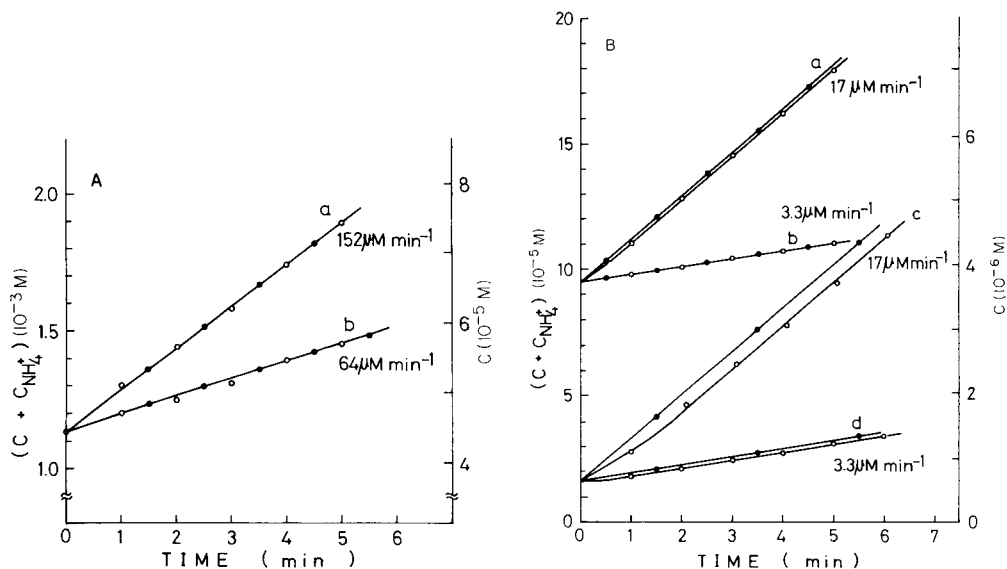


Fig. 5. Responses to a linear increase in total ammoniacal concentration in the sample (pH 7.5, 37°C): (●) input (total ammoniacal conc.); (○) output (response). See text for further explanation.

the condition $G^{-1} \ll 1$ holds at this concentration level, $T = 0.74$ s (Fig. 2, Eqn. (1)). The response errors calculated from Eqn. (2) were $0.8 \mu\text{M}$ and $1.9 \mu\text{M}$ for curves b and a, respectively, well below the experimental error. Figure 5B shows the responses at lower total ammonia levels. The condition $G^{-1} \ll 1$ no longer holds at these low concentrations. However, the concentration range to be measured was not large so G^{-1} was considered to be constant. For the curves indicated by $\alpha = 17 \mu\text{M min}^{-1}$, the experimental T value and the response error were found to be 5 s and $1.5 \mu\text{M}$, respectively, whereas the theoretical T and response error values were in reasonable agreement at about 4 s and $1.1 \mu\text{M}$, respectively. For $\alpha = 3.3 \mu\text{M min}^{-1}$ (curve b), the theoretical response error was $0.2 \mu\text{M}$ which was less than the experimental error, indicating that the response curve should coincide with the input curve, as was found experimentally.

When the initial total ammoniacal concentration was decreased to $17 \mu\text{M}$ (Figure 5B, curves c and d), the experimental T value increased to 30 s and the response errors increased to $8 \mu\text{M}$ (curve c) and $1.7 \mu\text{M}$ (curve d). These results qualitatively agree with the theory that the response of the sensor becomes slower with a decrease in ammonia concentration. It is noted, however, that theoretical T values obtained from Fig. 2 for curves c and d, were more than 200 s, hence the response errors were expected to be $>57 \mu\text{M}$ (curve c) and $>11 \mu\text{M}$ (curve d). These values are considerably larger than those observed experimentally. These discrepancies are possibly due to the effects of interchange of ammonia between the electrolyte film

and the bulk of the internal electrolyte [10, 11]. At very low ammonia concentration levels, the effect of interchange of ammonia becomes significant, therefore the ammonia concentration in the electrolyte film is no longer equal to sample ammonia concentration, but is determined by a dynamic equilibrium between the ammonia diffusing into the electrolyte film from the bulk electrolyte (which contains ammonia of the order of $6\text{ }\mu\text{M}$ for 0.1 M ammonium chloride solution [10]) and the ammonia diffusing out of the electrolyte film through the gas permeable membrane into a sample solution. The real ammonia concentration in the electrolyte film, \bar{C} , is larger than the value expected from the simple equilibrium partition of ammonia between the electrolyte film and a sample solution. Similar effects have also been indicated for the pCO_2 electrode [12].

It can be concluded from the foregoing results that the theory shows good agreement with the experimental results. As the response errors can be evaluated from the product of α and T values, one can readily establish optimal experimental conditions. Provided that the order of magnitude of α is known, T should be as low as possible. Figure 2 and Eqn. (1) indicate that the T value can be reduced to a minimum (say 0.7 s at 37°C) at a high total ammoniacal concentration, which can be adjusted to a desired value by adding ammonium chloride to a sample solution in advance. However, the use of such a high concentration leads to difficulties in monitoring enzymatic reaction, when α values for enzyme reactions are not so large (e.g., several $\mu\text{M min}^{-1}$) that the presence of excess of ammonia in the buffer conceals the ammonia produced by the enzymatic reaction. A low total ammoniacal concentration, however, though favourable for monitoring such reactions, leads to a slow response of the sensor. Therefore, it is important to choose the optimal total ammoniacal concentration. Figure 2 suggests that a reduction of the film electrolyte concentration is also effective for enhancing the response rate.

Provided that the value of α is of the order of $5\text{ }\mu\text{M min}^{-1}$, and the allowable error is $0.5\text{ }\mu\text{M}$, T should be less than 6 s . Hence for 0.1 M ammonium chloride as electrolyte film, the optimal total ammoniacal concentration is estimated to be $\sim 100\text{ }\mu\text{M}$ at $\text{pH } 7.5$ and 37°C , while for 0.01 M ammonium chloride, the optimal value is estimated to be about $40\text{ }\mu\text{M}$.

In the following paper, the kinetic assay of serum leucine aminopeptidase with the ammonia sensor will be described.

We thank Miss. H. Nakayama for excellent technical assistance.

REFERENCES

- 1 See, e.g., N. Lakshminarayanaiah, *Membrane Electrodes*, Academic Press, New York, 1976, p. 315; G. E. Baiulescu and V. V. Cosofret, *Applications of Ion-Selective Membrane Electrode in Organic Analysis*, Ellis Horwood, Chichester, 1977, p. 156.
- 2 M. Dixon and E. C. Webb, *The Enzymes*, 3rd edn., Longmans, London, 1979, p. 684.

- 3 I.U.P.A.C. and I.F.C.C., *Pure and Appl. Chem.*, 37 (1974) 519.
- 4 N. R. Larsen, E. H. Hansen and G. G. Guilbault, *Anal. Chim. Acta*, 79 (1975) 9.
- 5 J. W. Ross, J. H. Rieseman and J. A. Kreuger, *Pure Appl. Chem.*, 36 (1973) 473.
- 6 P. L. Bailey and M. Riley, *Analyst*, 100 (1975) 145.
- 7 J. H. Seinfeld and L. Lapidus, *Mathematical Methods in Chemical Engineering*, Vol. 3, Prentice-Hall, Englewood Cliffs, NJ, 1974, p. 46.
- 8 F. Van Der Pol, *Anal. Chim. Acta*, 97 (1978) 245.
- 9 R. G. Bates and G. D. Pinching, *J. Am. Chem. Soc.*, 72 (1950) 393.
- 10 P. L. Bailey and M. Riley, *Analyst*, 102 (1977) 213.
- 11 M. Mascini and C. Cremisini, *Anal. Chim. Acta*, 97 (1978) 237.
- 12 M. A. Jensen and G. A. Rechnitz, *Anal. Chem.*, 51 (1979) 1972.

KINETIC ASSAY OF ENZYMES WITH AN AMMONIA GAS-SENSING ELECTRODE

Part 2. In situ monitoring of serum leucine aminopeptidase

MASAKATSU HATO*, HIROKO NAKAYAMA and YUKIO SHIMURA

Research Institute for Polymers and Textiles, Yatabehigashi-1-1-4, Tsukubagun, Ibaraki-305 (Japan)

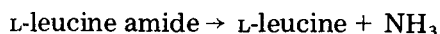
(Received 20th July 1982)

SUMMARY

A kinetic assay for serum leucine aminopeptidase with an ammonia gas sensor is described. The time course of ammonia formation in the reaction, L-leucine amide \rightarrow L-leucine + NH_3 , is directly monitored by the sensor under zero-order kinetic conditions. The initial total ammoniacal concentration in the sample was adjusted to $50 \mu\text{M}$ to keep the response at a sufficiently high level for accurate monitoring. The reaction rates determined agreed with those found by a conventional method to within 6%.

A mathematical expression for the response of an ammonia gas-sensing electrode (ammonia sensor) to a linear increase in total ammoniacal concentration (a simulated signal for an enzymatic reaction under zero-order kinetic conditions) was derived in the preceding paper [1]. The expression showed reasonable agreement with experimental results. The study suggested that the sensor could be applied to a kinetic enzyme assay if the ammonia level in the sample were adjusted appropriately. At sufficiently high ammonia levels, the time constant of the sensor, T , can be reduced to as little as 1 s at 25°C . It was also established that the electrode response error can be expressed by the product of T and a reaction rate α , i.e., αT . Therefore, if α and T are sufficiently small, so that αT may be considered to be negligible, the response of the sensor can be considered as an accurate measure of the time course of the reaction. Hence, it is interesting to check the theory for a real enzyme reaction. In this paper, the use of the ammonia sensor in a kinetic assay for serum leucine aminopeptidase (LAP) is studied as an example.

Serum LAP levels are of clinical significance; elevated levels have been found in a number of conditions of the liver, pancreas and biliary tract, including acute pancreatitis, viral hepatitis and carcinoma of the pancreas [2]. LAP catalyzes the reaction



Several methods with L-leucine amide as substrate have been described for the assay of LAP [3–7]. Mitz and Schlueter [3] measured the LAP activity

spectrophotometrically at 238 nm (disappearance of L-leucine amide). Ono and Eto [4] and Fujii et al. [5, 6] determined the LAP activity by measuring the increase in ammonia concentration spectrophotometrically. Sugiura [7] measured the LAP activity by employing L-amino acid oxidase and measuring the L-leucine formed by a spectrophotometric procedure. However, these procedures appear to suffer from difficulties when applied to routine enzyme assays, and a simpler method is required.

The ammonia sensor enables ammonia concentrations to be determined accurately and selectively [8]. Therefore, it should be useful for the assay of LAP if it can be used for in situ monitoring of ammonia formed in the enzymatic reaction. This approach has several advantages over conventional spectrophotometric methods based on synthetic substrates such as L-leucyl- β -naphthylamide or L-leucyl-*p*-nitroanilide [9–11] as well as the above-mentioned methods. The need for long incubation and color development time can be eliminated. Moreover, there is no need to stop the reaction by adding strong acids or bases. Further, there is no interference from coloured species and further enzymes are not required. Larsen et al. [12] have described a kinetic assay of urease and arginase with the air-gap electrode, but their study was limited to the reaction of purified enzymes. The reaction rates studied were more than 200 times larger than those observed in the serum LAP reaction (see below). Therefore, adjustment of the sample ammonia level would be needed in order to measure the serum LAP reaction. A conventional ammonia sensor seemed to be more practical for this purpose. The present paper illustrates the effectiveness of a conventional ammonia sensor for the kinetic assay of serum LAP.

EXPERIMENTAL

Materials

L-Leucine amide (Nakarai Chem., Co., Kyoto) and other chemical substances were of extra pure grade and were used as received. Water was doubly distilled in an all-glass apparatus. Serum was obtained from a male rabbit. The buffer was 0.2 M Tris-HCl at pH 8.5.

Apparatus and procedures

The apparatus used has been described [1]. An Orion model 95-10 ammonia gas-sensing electrode (with 0.1 M ammonium chloride as the internal electrolyte) was dipped into the substrate-buffer (5 ml) stirred magnetically. The whole system was kept at $25 \pm 0.1^\circ\text{C}$ by circulating thermostatted water through the glass jacket; 20 mM L-leucine amide in 0.2 M Tris-HCl at pH 8.5 was used as the substrate-buffer ($K_m = 4.5 \text{ mM}$). The total ammoniacal concentration in the buffer was adjusted to $50 \mu\text{M}$ by adding the required amount of ammonium chloride in advance. At this concentration level, the condition $d\bar{C}(\text{NH}_4^+)/d\bar{C} \ll 1$ holds, so that the time constant of the ammonia sensor becomes the minimum value of 1 s [1].

The enzymatic reaction was followed directly with the ammonia sensor which was preequilibrated in the substrate—buffer. At time $t = 0$, male rabbit serum was added to the substrate buffer through the vessel inlet and mV readings were recorded as a function of time by an Orion model 801 mV meter and a Yokogawa type 3047 strip-chart recorder. The pH of the reaction mixture was constant throughout the reaction. The mV—time curves thus obtained were converted into concentration—time curves via a mV—log (concentration) graph. The lower limit for proportionality between the electrode response and log (concentration) was $7 \mu\text{M}$.

The procedures used to examine the electrode response to simulated signals for enzymatic reaction under zero-order kinetic conditions were essentially the same as in the previous paper [1]. The total ammoniacal concentration was increased linearly from $50 \mu\text{M}$ at a constant rate by injecting a concentrated ammonium chloride buffer from a micro feeder (Furue Science Co., Tokyo).

RESULTS AND DISCUSSION

Electrode response to the LAP reaction

Figure 1 shows typical mV—time curves as a function of serum volume at pH 8.5. The millivolt values rose steeply for the first 3 min, and then less steeply. The initial steep rise mainly resulted from the electrode response to serum ammonia, which reached a steady value in 2–3 min after serum addition. Figure 2 shows the time course of the LAP reaction as a function of serum volume, converted from the mV—time curves shown in Fig. 1. The plots for the first 3 min are omitted, because of the response to serum ammonia during that time. It is clear from Fig. 2 that the reaction proceeds linearly with time for at least 20 min. At the highest reaction rate, 0.3% of the substrate was converted into L-leucine and ammonia in 20 min. The reaction rates obtained from Fig. 2 increase linearly with serum volume (ca. $4.5 \mu\text{M min}^{-1} \text{ ml}^{-1}$) so that the method is effective for serum LAP determination.

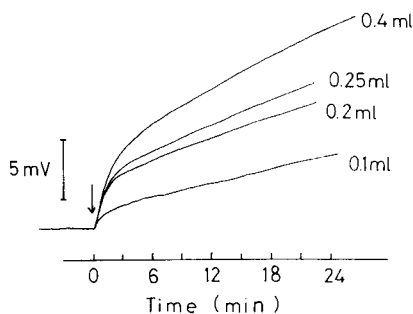


Fig. 1. Typical mV—time curves as a function of rabbit serum volume added to 5 ml of substrate buffer at 25°C . (Serum addition indicated by arrow.)

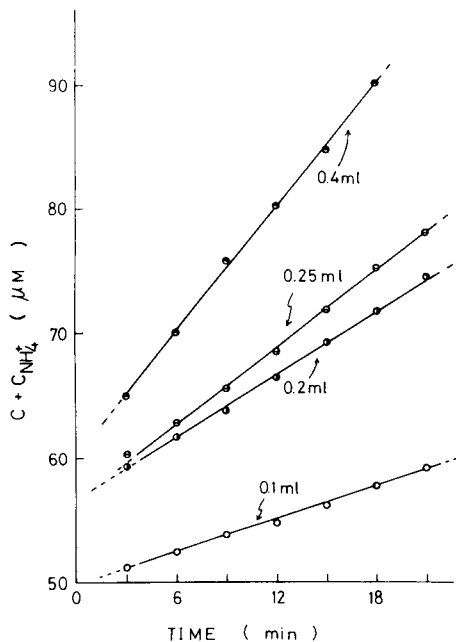


Fig. 2. Time course of the LAP reaction as a function of serum volume (converted from Fig. 1). C and $C_{\text{NH}_4^+}$ denote the concentration of ammonia and ammonium ion in the reaction mixture.

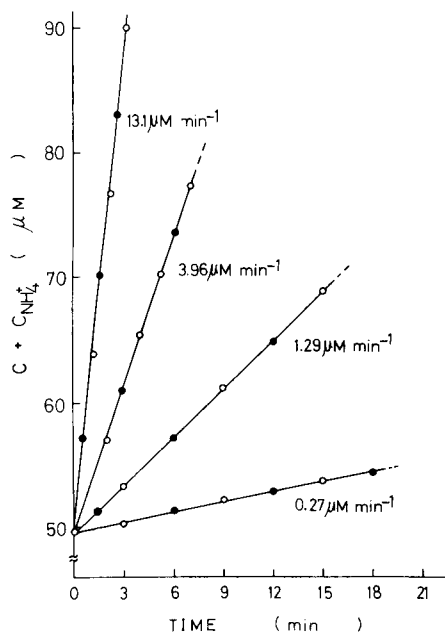


Fig. 3. Typical electrode response to simulated signals for the enzyme reaction (25°C, 0.2 M Tris-HCl pH 8.5: (●) input signals; (○) response signals).

Accuracy and stability of the response

It is important to estimate the possible response error, i.e., the difference between input and corresponding electrode response. At total ammoniacal concentration levels of 50 μM , the T value is estimated to be 1 s [1]. With a typical value for the reaction rate of 1 $\mu\text{M min}^{-1}$, the response error is calculated to be about 0.02 μM . This value is considered to be negligible and is well below the experimental error, indicating that the sensor can monitor accurately the time course of the LAP-catalyzed reaction.

Figure 3 shows typical examples of the electrode response to simulated signals where the total ammoniacal concentration was increased linearly from 50 μM at varying rates from 0.27 to 13.1 $\mu\text{M min}^{-1}$. It is clear that the response and input plots are completely coincident for all reaction rates studied, indicating that the response rate of the ammonia sensor under the present experimental conditions can be considered to be sufficiently rapid for the in situ monitoring of the LAP reaction. The slope of the response curve is a direct measure of the reaction rate. These results agree well with those obtained from the above calculation.

In order to check the accuracy of the method further, the reaction rate

was also determined by a method similar to that of Hjemsdahl-Monsen et al. [13], i.e., removing an aliquot of the reaction mixture at fixed time intervals and quickly transferring it to a second vessel containing the required amount of 10 M sodium hydroxide to terminate the reaction and to raise the pH to >12 . The total ammoniacal concentration each time was determined by a second ammonia sensor. For each run, 0.2 ml of serum was added to the substrate—buffer (in this experiment, 10 ml of substrate—buffer was used) and 4-ml aliquots were removed 3 min and 12 min after serum addition. At pH >12 , the mV readings showed a slight but continuous upward drift ($0.5\text{--}1\text{ mV min}^{-1}$); this was probably due to an increase in ammoniacal concentration caused by alkaline decomposition of the substrate and/or serum components. In order to compensate for the drift, mV readings were recorded for 10 min to obtain a concentration—time curve. The concentration—time curves thus obtained for the removed reaction mixture at 3 and 12 min were parallel straight lines. Therefore, the concentration difference between the two lines was taken as the total ammoniacal concentration increase during the time interval.

The reaction rates thus determined for various serum samples were 0.44, 1.19, 1.36 and $3.14\text{ }\mu\text{M min}^{-1}$, while the reaction rates determined from the slopes of the response curves were 0.43, 1.14, 1.41 and $2.95\text{ }\mu\text{M min}^{-1}$, respectively (average of 3 measurements). For three identical measurements, the relative standard deviation was 5%. This indicates that the reaction rates determined by the present method are in good agreement with those determined by the established method (within 6%). Thus, it can be concluded that the ammonia sensor can be used for the kinetic assay of serum LAP.

Practical difficulties accompanying the use of an ammonia sensor have often been pointed out, e.g., clogging of the gas-permeable membrane in biological fluids such as serum [13, 14]. In kinetic applications, membrane clogging can severely limit the usefulness of the sensor, because this will lead to a slow or irregular response. It was found, however, that the response in the buffered serum showed no appreciable change, and was stable for at least 3 weeks (5–10 assays/day). Therefore, the ammonia sensor seems to have no serious practical limitations when employed in moderately diluted serum samples.

REFERENCES

- 1 M. Hato, T. Masuoka and Y. Shimura, *Anal. Chim. Acta*, **149** (1983) 193.
- 2 G. G. Guilbault, *Handbook of Enzymatic Methods of Analysis*, Dekker, New York, 1976, p. 137.
- 3 M. Mitz and R. Schlueter, *Biochim. Biophys. Acta*, **27** (1958) 168.
- 4 T. Ono and K. Eto, *Med. Biol.*, **88** (1974) 225.
- 5 S. Fujii and H. Okuda, *Tokushima J. Exptl. Med.*, **22** (1975) 1.
- 6 S. Ito, T. Tanaka, S. Kishi, H. Okuda and S. Fujii, *Tokushima J. Exptl. Med.*, **24** (1977) 33.
- 7 M. Sugiura, *Japan Kokai*, 78 65787.
- 8 See, e.g., N. Lakshminarayanaiah, *Membrane Electrodes*, Academic Press, New York, 1976, p. 315; G. E. Baiulescu and V. V. Cosofret, *Applications of Ion-Selective Membrane Electrode in Organic Analysis*, Ellis Horwood, Chichester, 1977, p. 156.

- 9 J. Goldberg, E. Pineda and A. Rutenberg, *Am. J. Clin. Pathol.*, 32 (1959) 571.
- 10 E. Wachsmuth, I. Fritze and G. Pfeiderer, *Biochemistry*, 5 (1966) 169, 175.
- 11 E. Wachsmuth, *Biochem. Z.*, 344 (1966) 361.
- 12 N. R. Larsen, E. H. Hansen and G. G. Guilbault, *Anal. Chim. Acta*, 79 (1975) 9.
- 13 C. E. Hjemdahl-Monsen, D. S. Papastathopoulos and G. A. Rechnitz, *Anal. Chim. Acta*, 88 (1977) 253.
- 14 L. D. Bowers and P. W. Carr, *Anal. Chem.*, 48 (1976) 544A.

THE PERFORMANCE OF A CADMIUM ION-SELECTIVE ELECTRODE IN METAL BUFFER SOLUTIONS AND THE DETERMINATION OF THE STABILITY CONSTANTS OF CADMIUM COMPLEXES

AKIO YUCHI, HIROKO WADA and GENKICHI NAKAGAWA*

Laboratory of Analytical Chemistry, Nagoya Institute of Technology, Gokiso-cho, Showa-ku, Nagoya 466 (Japan)

(Received 4th August 1982)

SUMMARY

The potential response of a cadmium ion-selective electrode was examined in twelve metal buffer solutions. In the absence of ligands, Nernstian response down to 10^{-6} mol dm⁻³ was obtained between pH 4 and 8. In metal buffer solutions much lower concentrations could be measured, depending on the ligand and pH. The stability constants were determined successfully for cadmium complexes with various ligands: acetic acid, ammonia, glycine, iminodiacetic acid, ethylenediamine-*N,N'*-diacetic acid, nitrilotriacetic acid, *N*-hydroxyethylethylenediamine-*N,N'*-triacetic acid (H₃HEDTA), ethyleneglycol-bis(2-aminoethylether)-*N,N,N',N'*-tetraacetic acid (H₄EGTA), 1,3-diaminopropan-2-ol-*N,N,N',N'*-tetraacetic acid (H₄DPTA), 2,2'-bipyridine, and 1,10-phenanthroline. In the cases of H₃HEDTA, H₄EGTA, H₄DPTA, and H₄EDTA(ethylenediamine-*N,N,N',N'*-tetraacetic acid), the ion-selective electrode behaved abnormally under certain conditions. Critical conditions for the normal response of the ion-selective electrode are discussed.

The response of ion-selective electrodes in metal buffer solutions has been studied by several authors [1–10]. Usually in unbuffered metal ion solutions, ion-selective electrodes give Nernstian response down to about 10^{-6} mol dm⁻³, whereas in metal buffer solutions they may show potentials corresponding to much lower free metal ion concentration. So long as the electrode potential gives the activity of the free metal ion in the metal buffer solution, the stability constants of the complexes formed in the solution can be obtained. In the case of H₄EDTA, however, the response is very slow and the potential obtained is abnormally high. Some reasons for the abnormalities with H₄EDTA have been discussed [1–5, 8–10].

In previous work, the response of copper(II) and lead ion-selective electrodes was examined in various metal buffer solutions [4, 5]. To complete this work, the responses of a cadmium ion-selective electrode are described in the present paper. Special attention is given to the conditions essential for normal responses in metal buffer solutions.

EXPERIMENTAL

Reagents

Cadmium nitrate tetrahydrate was recrystallized twice and dissolved to give a 10^{-2} mol dm $^{-3}$ stock solution, which was standardized against 0.01 mol dm $^{-3}$ Na $_2$ H $_2$ EDTA solution with use of eriochrome black T as indicator. All the ligands were of analytical-reagent grade and were used as received. Potassium nitrate was recrystallized twice. Carbonate-free potassium hydroxide was prepared as described previously [11].

Measurements

All solutions for measurement were placed in an air bath thermostated at $25 \pm 0.1^\circ\text{C}$. The ionic strength was maintained at 0.10 mol dm $^{-3}$ with potassium nitrate. The cell arrangement used for measuring the cadmium ion concentration was:

Cd ion-selective electrode	Test solution	0.1 mol dm $^{-3}$ KNO $_3$	3.33 mol dm $^{-3}$ KCl calomel electrode
-------------------------------	---------------	--------------------------------	--

The cadmium ion-selective electrode (Denki Kagaku Keiki Co.; DKK type 7120) was conditioned as described elsewhere [4, 5]. The e.m.f. was read with a DKK ion-meter IOC-10, to 0.1 mV. Hydrogen ion concentration was determined with a Radiometer PHM-64 pH meter equipped with a Radiometer glass electrode (G202C) and a calomel electrode (K401). A 1.00×10^{-2} mol dm $^{-3}$ nitric acid solution of ionic strength 0.1 mol dm $^{-3}$ (KNO $_3$) was used as the standard for hydrogen ion concentration and the change in liquid-junction potential was taken into account as a linear function of hydrogen ion concentration. The test solution was stirred at constant speed (300 rpm) and the geometrical arrangement of the electrodes in the cell was kept constant. Nitrogen was bubbled through the test solution during measurements.

Cadmium ion concentration was monitored as a function of hydrogen ion concentration by titrating the test solution with a potassium hydroxide solution. The total concentrations of cadmium and the ligand were kept constant during the titrations. In the cases of 1,10-phenanthroline (phen) and 2,2'-bipyridine (bipy) the total concentration of cadmium was decreased because of the low solubilities of their tris complexes.

RESULTS

Potential response in unbuffered solutions

The response of the cadmium ion-selective electrode was examined in solutions containing 10^{-3} – 10^{-6} mol dm $^{-3}$ cadmium ion in the pH range 3–10. 2-(*N*-Morpholino)ethanesulfonic acid (MES; $\log K_{\text{HA}} = 6.2$) was used as a pH buffer, because it is hardly capable of complexing with cadmium. Cadmium hydroxide having a larger solubility product than copper(II) or

lead hydroxide [$\text{Cd}(\text{OH})_2$, $10^{-13.2}$; $\text{Cu}(\text{OH})_2$, $10^{-18.2}$; $\text{Pb}(\text{OH})_2$, $10^{-15.7}$], constant potentials were observed over a wider pH range (Fig. 1). Nernstian response with a 29-mV slope was obtained down to 10^{-6} mol dm^{-3} in the pH range 4–8.

The electrode potential in a solution containing no cadmium ion is also shown (curve 5, Fig. 1). The lower limit of the electrode response is determined by this value, which is much higher than that expected from the simple calculation based on the solubility product of the electroactive material, CdS (see Discussion).

Potential response in cadmium buffer solutions

The potential response of the cadmium ion-selective electrode was examined in the twelve cadmium buffer solutions listed in Table 1. In the cases of ammonia, acetic acid, glycine, iminodiacetic acid (H_2IDA), ethylenediamine- N,N' -diacetic acid (H_2EDDA), nitrilotriacetic acid (H_3NTA), 2,2'-bipyridine (bipy) and 1,10-phenanthroline (phen), the response was rapid over all the pH region measured. In contrast, with aminopolycarboxylates that form cadmium complexes with larger stability constants, a very slow increase in the potential after the rapid decrease was observed above certain pH values, i.e., pH 7 for 1,3-diaminopropan-2-ol- N,N,N',N' -tetraacetic acid (H_4DPTA), pH 5 for ethyleneglycol-bis(2-aminoethylether)- N,N,N',N' -tetraacetic acid (H_4EGTA), pH 4 for N -hydroxyethylethylenediamine- N,N',N' -triacetic acid (H_3HEDTA), and pH 2 for H_4EDTA .

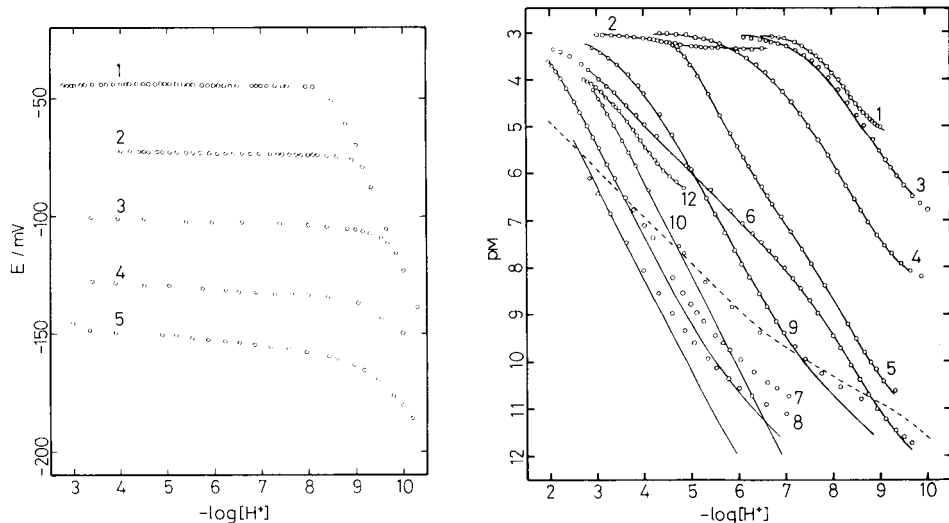


Fig. 1. Potential response of the DKK-7120 cadmium ion-selective electrode at 25°C and at $\mu = 0.1$ mol dm^{-3} KNO_3 . Cadmium concentration (mol dm^{-3}): (1) 10^{-3} ; (2) 10^{-4} ; (3) 10^{-5} ; (4) 10^{-6} ; (5) detection limit.

Fig. 2. Electrode response in cadmium buffer solutions. See Table 1 for identification of curves and experimental conditions. Solid lines: curves calculated from the constants obtained, and for H_4EDTA from constants in the literature. Broken lines: curves calculated according to refs. [1–3]. The data for bipy have been omitted for clarity.

TABLE 1

Experimental conditions, protonation constants of ligands, and the stability constants of Cd complexes

No.	Ligand	C_{Cd} (mol dm ⁻³)	C_L (mol dm ⁻³)	Logarithmic protonation constants used ^a				Logarithmic stability constants					
				K_{HL}	K_{H_2L}	K_{H_3L}	K_{H_4L}	obtained			literature ^a		
								K_1	K_2	K^b	K_1	K_2	K^b
1	NH ₃	9.875 × 10 ⁻⁴	1.000 × 10 ⁻¹	9.29				2.82	2.22		2.60	2.05	
2	CH ₃ COOH		3.217 × 10 ⁻²	4.53				1.52			1.5		
3	Glycine		1.012 × 10 ⁻²	9.63	2.41			4.53	3.58		4.65	3.36	
4	H ₂ IDA		5.199 × 10 ⁻³	9.40	2.50			5.96	4.49		5.73	4.46	
	H ₂ IDA ^c	Varied	Varied					{ 5.49	4.55 }		—	—	
	H ₂ IDA ^{c,d}	Varied	Varied	9.27	2.58	1.80		{ 5.49	4.43 }				
5	H ₂ EDDA	9.875 × 10 ⁻⁴	4.795 × 10 ⁻³	9.62	6.55			9.17	4.72		9.40	—	
6	H ₃ NTA		4.939 × 10 ⁻³	9.58	2.88	2.0		9.98	4.46		10.0	4.6	
7	H ₃ HEDTA		2.990 × 10 ⁻³	9.81	5.41	2.72		14.27		2.81	{ 13.0 ^f		—
											{ 13.6 }		
8	H ₄ EDTA		3.009 × 10 ⁻³	10.34	6.24	2.75	2.07	—		—	16.5		2.9
9	H ₄ DPTA		3.000 × 10 ⁻³	9.49	6.96	2.60	1.6	11.97		4.28	12.1		4.12
10	H ₄ EGTA		3.016 × 10 ⁻³					{ 16.32		3.06	{ 16.1 }		3.5
	H ₄ EGTA ^e	Varied	Varied	9.54	8.93	2.73	2.08	{ 16.4		3.2	{ 16.7 }		
11	Bipy	1.975 × 10 ⁻⁴	2.077 × 10 ⁻³	4.44				4.35	3.75		4.28	3.51	
12	Phen		9.686 × 10 ⁻⁴	4.92				5.65	4.84		5.63	5.04	

^aFrom [12, 13]. ^b $K = [CdLH]/[CdL][H]$. ^cIonic strength 1.0 mol dm⁻³ KNO₃. ^dAmalgam method. ^eHg electrode. ^fFrom [14, 15].

The $pM(-\log[Cd^{2+}])$ value was calculated from the equilibrated potential by means of the Nernst equation and plotted against $-\log[H^+]$ in Fig. 2. Each system gave the characteristic curve depending on the formation of the cadmium complexes and the protonation of the ligand.

The potential responses in solutions containing a ligand but no cadmium ion were also studied as described previously [4, 5]. These potentials determine the lower limit of detection in the metal buffer solutions. The potentials are depressed to a large extent in the presence of strong complexing agents and at high pH values; they should be lower than the potential in the metal buffer solution at the same pH. This was actually the case for most of the ligands examined, but with H_3HEDTA , H_4EDTA , and H_4EGTA , the same or higher potential was observed above certain pH values. In these cases, the potential does not reflect the cadmium ion concentration in the metal buffer solution (see Discussion). This type of check is always needed to measure the free metal ion concentration in metal buffer solutions [4, 5].

Determination of the stability constants

So long as the electrode potential reflects the free cadmium ion concentration in the bulk solution, evaluation of the plots of pM against $-\log[H^+]$ will provide the stability constants of the complexes. The overall stability constant of the cadmium complex, CdL_n , is expressed as (charges are omitted) $\beta_n = [CdL_n]/[Cd][L]^n$. The free cadmium ion concentration being extremely low, $C_{Cd} = [CdL_n]$, if only CdL_n is formed. If the consumption of the ligand for the formation of the complex is neglected as a first approximation, then $C_L = \alpha_{L(H)}[L]$, where $\alpha_{L(H)}$ is the side-reaction coefficient taking into account the protonation of L (Table 1). Thus the concentration of the free cadmium ion is given by

$$pM = -n pL + (\log \beta_n - \log C_{Cd}) \quad (1)$$

A plot of pCd against $pL (-\log[L])$ will give a straight line with a slope of $-n$. From the intercept and $\log C_{Cd}$, $\log \beta_n$ can be obtained.

The results are shown in Fig. 3, where a large pL value corresponds to a low pH value in each system. Each line generally starts with a portion of zero slope at high pL . With decreasing pL , cadmium begins to form complexes and the pM value increases. Distinct linear portions with a slope of -1 or -2 were observed for H_2EDDA (curve 5) and H_3NTA (curve 6). The lines for ammonia (curve 1), acetic acid (curve 2), glycine (curve 3), H_2IDA (curve 4), bipy (curve 11) and phen (curve 12) curve gradually, which reflects the successive formation of complexes having only slightly different stabilities.

In contrast, aminopolycarboxylates such as H_3HEDTA (curve 7), H_4EDTA (curve 8), and H_4EGTA form the complexes even at low pH, i.e. large pL , so that no portion of the curve with zero slope was observed. The rounded curve to slope -1 is explained by the formation of the protonated metal complex with these ligands. After reaching a slope of -1 , the curves become variable below certain pL values, which nearly coincide with the range of abnormal potential response described above. In these cases, the stability

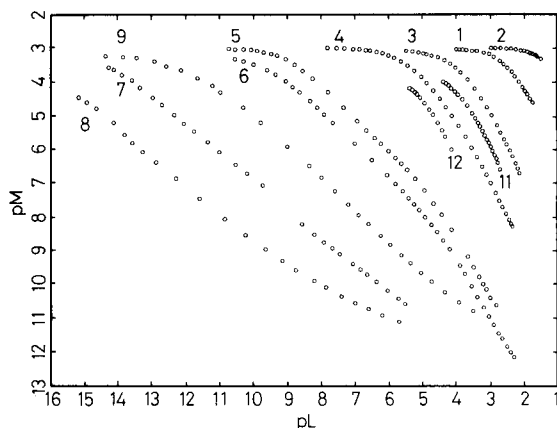


Fig. 3. Plots of pM vs. pL. See Table for identification of curves and experimental conditions. The data for H_4EGTA coincided with those for H_4EDTA (curve 8) and have been omitted for clarity.

constants were obtained by omitting these data, but in the case of H_4EDTA there was no pH range of normal potential response under the present experimental conditions. Although the stability constant of the H_4EGTA complex with cadmium ion is comparable to that of H_4EDTA , it could be obtained successfully because of the low conditional stability constant of the $Cd-EGTA$ complex.

From the intercept of the tangent with a slope of $-n$, the approximate stability constant β_n was estimated. Taking into account all the equilibria and the mass balances, these constants were refined to give the least square sum of errors about pM, $U = \sum (pM_{obs.} - pM_{calc.})^2$, with an electronic computer. The constants obtained are summarized in Table 1 together with those reported in the literature. The calculated curves (solid lines in Fig. 2) based on the constants obtained are in good agreement with the data except in the range of abnormal response. The curve for H_4EDTA was calculated with literature values.

DISCUSSION

For the membrane ion-selective electrodes based on mixed sulfides, the lower limit of electrode response in metal buffer solutions has been discussed by several authors. Hansen, Ružička and Lamm [1–3] calculated the detection limit, assuming that it was fixed only by the solubility of the electrode material and not by the ligand (dotted line in Fig. 2). But much lower potentials than this value were actually obtained for some ligands in the present work. Other workers [8–10] considered the limit to be fixed by the excess of ligand alone. The abnormal potential response in some aminopolycarboxylates (H_4EDTA and H_3NTA) was ascribed to the

enhanced dissolution of metal sulfides by preferential attack of the electrode surface by negatively charged ligands. In the present study, however, the electrode behaved normally in the metal buffer solutions containing the same ligand in small excess or at low pH. Moreover, the copper(II) ion-selective electrode from DKK acted normally in H_3NTA , whereas that from Orion behaved abnormally [4, 5]. Thus the normal potential response of ion-selective electrodes depends not only on the type of ligand but also on many other factors.

As a first approximation, the mixed sulfide membrane electrodes are electrodes of the third kind, responding to silver ion in equilibrium with the metal ion through the sulfide ion: $M(Cu, Pb, Cd)S \rightleftharpoons M^{2+} + S^{2-}$; $Ag_2S \rightleftharpoons 2Ag^+ + S^{2-}$. Generally these silver and sulfide ions derive from dissolution of the electrode material. The fact that the limit of detection in solutions containing no cadmium ion is much higher than that expected from the solubility of cadmium sulfide suggests a high activity of cadmium ion at the membrane surface.

The ligands which gave normal potential responses, form stable complexes with both cadmium and silver ions and so the detection limit was reduced. Thus, in the metal buffer solution, very low concentrations of free metal ion could be measured correctly. Jyo et al. [16] found that when the potential was plotted against the total concentration of the metal ion in various metal buffer solutions, linear response was obtained down to about 10^{-6} mol dm $^{-3}$. This result together with the detection limit in unbuffered solution suggests the presence of cadmium ion at around 10^{-6} mol dm $^{-3}$.

When the aminopolycarboxylate forms a cadmium complex with a fairly large stability constant, pCd becomes large even at low pH, and this will cause more dissolution of cadmium sulfide. As the stability of the silver complex with such ligands is much less than that of the cadmium complex, the activity of silver ion becomes unfavorably large at the surface of the electrode. Thus the potential of the electrode is determined by the concentration of silver ion and no longer reflects that of cadmium ion in the solution. These abnormalities seem to be easily affected by small changes in factors such as the type and the concentration of the ligand, pH and the electrode used.

Conclusion

The stability constants determined in this study are generally in good agreement with those reported in the literature, those determined with a cadmium amalgam electrode for H_2IDA , and those determined with a mercury electrode for H_4EGTA (see Table 1).

Neither of the stability constants for the $Cd-H_3HEDTA$ complex reported in the literature (13.0 [14] and 13.6 [15]), agrees with the present value (14.27), even when the differences in experimental conditions are considered. The present value agrees well with that found by using a metal-

exchange reaction with ion-selective electrodes. With this value, the difference between the logarithmic stability constants for the H_4EDTA and H_3HEDTA complexes lies in the range 1.5–2.5, which is generally found for many metal ions.

From these results, it can be concluded that ion-selective electrodes are effective in the determination of the stability constants of the metal complexes, if attention is given to the detection limit of the electrodes.

The authors gratefully acknowledge a Grant-in-Aid for Scientific Research (No. 57740289) from the Ministry of Education, Science and Culture.

REFERENCES

- 1 E. H. Hansen, C. G. Lamm and J. Růžička, *Anal. Chim. Acta*, 59 (1972) 403.
- 2 J. Růžička and E. H. Hansen, *Anal. Chim. Acta*, 63 (1973) 115.
- 3 E. H. Hansen and J. Růžička, *Anal. Chim. Acta*, 72 (1974) 365.
- 4 G. Nakagawa, H. Wada and T. Hayakawa, *Bull. Chem. Soc. Jpn.*, 48 (1975) 424.
- 5 G. Nakagawa, H. Wada and T. Sako, *Bull. Chem. Soc. Jpn.*, 53 (1980) 1303.
- 6 P. Kivalo, R. Virtanen, K. Wickström, M. Wilson, E. Pungor, K. Tóth and G. Sundholm, *Anal. Chim. Acta*, 87 (1976) 387.
- 7 P. Kivalo, R. Virtanen, K. Wickström, M. Wilson, E. Pungor, G. Horvai and K. Tóth, *Anal. Chim. Acta*, 87 (1976) 401.
- 8 G. J. M. Heijne and W. E. van der Linden, *Anal. Chim. Acta*, 96 (1978) 13.
- 9 G. J. M. Heijne, W. E. van der Linden and G. den Boef, *Anal. Chim. Acta*, 100 (1978) 193.
- 10 W. E. van der Linden and R. Oostervink, *Anal. Chim. Acta*, 108 (1979) 169.
- 11 J. E. Powell and M. A. Hiller, *J. Chem. Educ.*, 34 (1957) 330.
- 12 L. G. Sillen and A. E. Martell, *Stability Constants of Metal-ion Complexes*, and Supplement No. 1, The Chemical Society, London, 1964 and 1971.
- 13 D. D. Perrin, *Stability Constants of Metal-Ion Complexes Part B*, IUPAC, Pergamon, Oxford, 1979.
- 14 S. Chaberek, Jr. and A. E. Martell, *J. Am. Chem. Soc.*, 77 (1955) 1477.
- 15 Y. Koike and H. Hamaguchi, *J. Inorg. Nucl. Chem.*, 29 (1967) 473.
- 16 A. Jyo, T. Hashizume and N. Ishibashi, *Anal. Chem.*, 49 (1977) 1868.

COATED-WIRE ORGANIC ION-SELECTIVE ELECTRODES IN TITRATIONS BASED ON ION-PAIR FORMATION

Part 4. Determination of Some Acidic Anthraquinone Dyestuffs^c

K. VYTRÁS*, J. SYMERSKÝ, C. DOŽRU^a and A. ONUR^b

Department of Analytical Chemistry, College of Chemical Technology, 532 10 Pardubice (Czechoslovakia)

(Received 5th October 1982)

SUMMARY

1-(Ethoxycarbonyl)pentadecyltrimethylammonium bromide (Septonex) is recommended as a titrant for the determination of singly-charged acidic anthraquinone dyestuffs. Other cationic titrants such as cetylpyridinium bromide or cetyltrimethylammonium bromide can be used for titrations of dilute aqueous solutions (about 10^{-4} M) or in the presence of additional solvent (5% n-propanol). An aluminium wire electrode coated with a PVC membrane plasticized with 2-nitrophenyl alkyl ether (where alkyl is either n-octyl or 2-ethylhexyl) is used for end-point indication. Characteristic data for the potentiometric titration curves and a statistical evaluation of results are reported.

Acidic anthraquinone dyestuffs are a group of relatively simple anthraquinone derivatives containing one or more sulphonic acid groups. They have clear brilliant shades and excellent stabilities against light, soaps and detergents, so that they are widely used in the textile industry despite their high price. Nevertheless, reliable analytical methods for the determination of these dyes are few, because the dyes always contain undefined impurities, particularly inorganic salts such as sodium sulphate. The present paper is concerned with a simple and rapid determination of the dye content in commercial products. The method is based on titration of the acidic dyestuff with an oppositely charged titrant. If such a titration is followed with an organic ion-selective electrode, the potentiometric titration curve is easily used for the determination required.

Similar procedures for the determination of acidic anthraquinone dyestuffs have not been described previously. Probably the first papers dealing with the titrimetric determination of other anionic dyes with ion-selective indicator electrodes were presented by Fogg et al. [2, 3], who used electrodes with natural rubber disc membranes soaked in a solution of the relevant ion-pair with crystal violet in 1,2-dichlorobenzene. More recently, Fogg and Yoo [4]

^aPermanent address: University of Istanbul, Turkey.

^bPermanent address: Technical University of Istanbul, Turkey.

^cPart 3 is ref. 1.

used poly(vinyl chloride) membrane electrodes in which similar ion-pairs were dissolved in a mixture of 2-nitrophenyl-n-butyrate and diisooctylphthalate. In both cases, a crystal violet solution was used as titrant. Selig [5] proposed cetyltrimethylammonium bromide as a titrant for organic anionic compounds, including two sulphonaphthalein dyes, the end-point being monitored with commercial electrodes. In the work reported here, quaternary ammonium salts were also preferred as titrants because their pure preparations are generally more accessible than pure crystal violet. The titrations were followed with simple coated-wire electrodes based on an aluminium conductor [6].

EXPERIMENTAL

Solutions

Cetylpyridinium bromide (CPB) solution (10^{-3} M) was prepared by dissolving 0.40247 g of the substance (p.a., Lachema) in about 100 ml of warm water, cooling to room temperature, and diluting the solution to 1 l. The solution was standardized potentiometrically against 10^{-3} M lauryl sulphate [7]. 1-(Ethoxycarbonyl)pentadecyltrimethylammonium bromide solution (10^{-2} M) was prepared by dissolving 4.2251 g of Septonex (purum, Slovako-farma) in 1 l of water; this was standardized potentiometrically against 10^{-3} M sodium tetraphenylborate, which had been standardized against a thallium(I) nitrate solution. More concentrated solutions (10^{-2} M) of CPB and cetyltrimethylammonium bromide (CTAB) prepared in n-propanol-water mixtures containing 5–20% (v/v) of alcohol were not standardized.

Stock solutions of the acidic anthraquinone dyestuffs were prepared in concentrations of about 10^{-3} mol l⁻¹. The specimens used are listed with their Colour Index numbers in Table 1. The presence of coloured impurities in the dye samples was tested by using paper chromatography [8]; all the dyes showed one colour spot only.

Equipment and procedure

A digital pH meter (OP-208, Radelkis) was used for potentiometric measurements. The potential changes were monitored by a coated-wire electrode with a double-junction saturated calomel reference electrode (10^{-2} M sodium nitrate salt bridge). Indicator electrodes of the coated-wire type were prepared by using an aluminium conductor [6, 9] from tetrahydrofuran solutions of poly(vinyl chloride) (28.3 mg ml⁻¹) and 2-nitrophenyl alkyl ether (6.3% v/v), the alkyl being either 2-ethylhexyl (electrode working code 878C) or n-octyl (180A). Electrodes were pre-conditioned by titration of thallium(I) with sodium tetraphenylborate, but sometimes by the relevant ion-pair titration.

Titrations were made in unbuffered solutions at room temperature in 100-ml beakers. The solution titrated (initial volume 50 ml) was stirred magnetically, the titrant being added from a 10-ml automatic burette.

TABLE 1

List of dyestuffs investigated

Common name	Colour index number and name	Substituents on the 9,10-anthraquinone skeleton	Molecular mass
Bromoamine acid	— ^a	1-NH ₂ , 2-SO ₃ Na, 4-Br	404.17
Bromoacyl acid	— ^a	1-NH ₂ , 2-SO ₃ Na, 4-Br, 5-NHCOCH ₃	461.22
Alizarin red SW	58005	1,2-dioH, 3-SO ₃ Na(+H ₂ O)	360.28
Alizarin violanol R	Mordant Red 3		
	60730	1-OH, 4-NHC ₆ H ₃ (2'-SO ₃ Na, 4'-CH ₃)	431.40
Alizarin brilliant green	Acid Violet 43		
G Extra	61570	1,4-diNHC ₆ H ₃ (2'-SO ₃ Na, 4'-CH ₃)	622.57
Alizarin pure blue B	Acid Green 25		
	62105	1-NH ₂ , 2-Br, 4-NHC ₆ H ₃ (2'-SO ₃ Na, 4'-CH ₃)	509.31
Alizarin azurol A2G	Acid Blue 78		
	62125	1-NH ₂ , 2-SO ₃ Na, 4-NHC ₆ H ₄ (4'-NHCOCH ₃)	473.44
Alizarin azurol B	Acid Blue 40		
	63010	1,5-diNH ₂ , 3,7-diSO ₃ Na, 4,8-dioH	446.33
Alizarin azurol SW	Acid Blue 45		
	63610	1,8-dioH, 2,7-diSO ₃ Na, 4,5-diNH ₂	446.33
Alizarin brilliant pure blue G	Acid Blue 69		
	64005	1-NH ₂ , 2-SO ₃ Na, 4-NHC ₆ H ₃ (CH ₂) ₄ CH ₂ , 5-NHCOCH ₃	479.48
Isomer of alizarin direct blue 6G	Acid Blue 124		
	— ^b	1-NH ₂ , 2-SO ₃ Na, 4-NHC ₆ H ₄ (4'-NHCOCH ₃), 8-NHCOCH ₃	530.49

^a Intermediate product. ^b Alizarin direct blue 6G, C.I. 64010, is a 5-acetoamido derivative instead of 8-acetoamido derivative.

End-points of the recorded potentiometric titration curves were evaluated by Tubbs' method [10].

RESULTS

Titration of dilute solutions

A 10^{-3} M CPB solution was used for titrations of dilute dye solutions, containing about $5\text{ }\mu\text{mol}$ of the dye in 50 ml. Titration curves with good potential breaks and well-defined end-points were usually obtained (Fig. 1). Initially, the equilibrium potential of the pre-conditioned electrodes was established quickly after each addition of titrant, but a longer time (ca. 2 min) was needed to establish the potential near the inflection point. Titrations of alizarin red SW (C.I. 58005) were poorly reproducible. Titration curves could not be recorded for either alizarin azurol B or alizarin azurol SW, both of which have two $-\text{SO}_3\text{H}$ and $-\text{OH}$ groups bonded directly to the anthraquinone skeleton. In contrast, useful titration curves were obtained in titrations of alizarin brilliant green G Extra, which contains the $-\text{SO}_3\text{H}$ groups outside the main ring structure.

Titration of more concentrated solutions

For solutions containing about $50\text{ }\mu\text{mol}$ of the dye in 50 ml, 10^{-2} M Sep-tonex was used as titrant. The rate of potential establishment, and thus the titration rate, was similar to those observed in titrations of the more dilute solutions with CPB. When the potential break is sufficiently large, the end-point reading is not significantly influenced by the time needed for complete attainment of the equilibrium potential. As shown in Table 2, the curves recorded with the two kinds of indicator electrodes are practically identical (cf. Fig. 2).

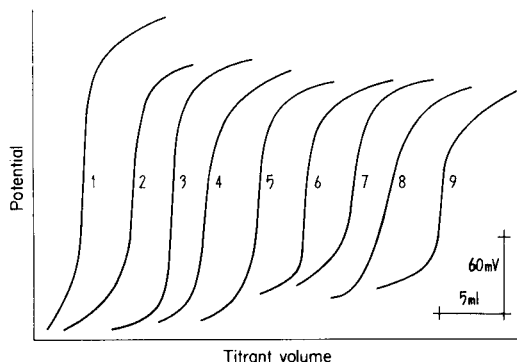


Fig. 1. Potentiometric titration curves for acidic anthraquinone dyes (about $5\text{ }\mu\text{mol}$ in 50 ml of the solution titrated) with 10^{-3} M cetylpyridinium bromide: (1) C.I. 62105; (2) C.I. 60730; (3) C.I. 64005; (4) C.I. 62125; (5) bromoamine acid; (6) isomer of C.I. 64010; (7) bromoacyl acid; (8) C.I. 58005; (9) C.I. 61570. Potentiometric cell consisted of the 878C coated-wire electrode vs. SCE with a 10^{-2} M NaNO_3 salt bridge.

TABLE 2

Titrations of acidic anthraquinone dyestuffs in aqueous solutions

Sample ^a	Conc. ($\mu\text{mol}/$ 50 ml)	Titrant	Electrode	Titration curve		Assay ^b (%)
				Overall potential break (mV)	Steepness near the end-point (mV/0.1 ml)	
Bromoamine acid	5	CPB ^c	878C	180–190	13–16	See Table 4
	50	Sept. ^d		220–230	35–40	
			180A	210–240	30–42	
Bromoacyl acid	5	CPB	878C	160–170	7–9	84.0 \pm 1.4
	50	Sept.		180–210	27–35	83.6 \pm 1.3
			180A	180–215	20–30	
58005	5	CPB	878C	140–160	3–5	56.3 \pm 5.0
	50	Sept.		130–150	6–10	55.1 \pm 2.5
			180A	135–145	4–8	
60730	5	CPB	878C	200–220	15–17	54.2 \pm 2.7
	50	Sept.	180A	200–240	33–40	53.9 \pm 0.4
61570	5	CPB	878C	140–160	12–15	46.4 \pm 3.9
	50	Sept.	180A	110–140	25–45	46.2 \pm 0.5
62105	5	CPB	878C	235–255	15–19	42.5 \pm 3.5
	50	Sept.	180A	250–270	25–35	41.7 \pm 0.2
62125	5	CPB	878C	180–200	12–18	28.4 \pm 4.4
	50	Sept.	180A	100–115	7–9	26.4 \pm 0.1
64005	5	CPB	878C	210–240	23–30	85.6 \pm 3.0
	50	Sept.	180A	250–275	65–95	83.1 \pm 0.7
64010 isomer	5	CPB	878C	150–170	12–14	68.6 \pm 1.9
	50	Sept.	180A	190–210	15–25	70.7 \pm 2.6

^aFor C.I. numbers, see Table 1. ^bExpressed as reliability interval $\bar{x} \pm u_0 R$ for significance level 0.05 (95% probability), calculated from 3 titrations. ^cCetylpyridinium bromide, $10^{-3} \text{ mol l}^{-1}$. ^dSeptonex, $10^{-2} \text{ mol l}^{-1}$.

The potentiometric titration curves recorded for these more concentrated solutions of acidic anthraquinone dyestuffs are better developed. When the titrant is not very soluble in water (as with CPB or CTAB), a small amount of some other solvent must be added to increase the reagent solubility [11, 12]. Although this addition of another solvent is beneficial for the titrant solubility, it can worsen both the steepness and the overall potential break of the titration curve because of the solubility of the ion-pair formed; eventually, the extractability of the ion-pair into the membrane solvent (plasti-

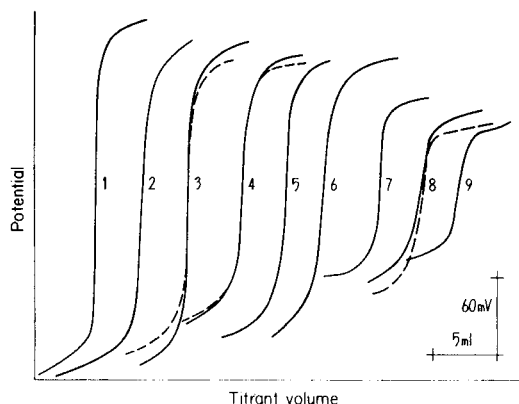


Fig. 2. Potentiometric titration curves for acidic anthraquinone dyes (about 50 μ mol in 50 ml of the solution titrated) with 10^{-2} M Septonex: (1) C.I. 64005; (2) C.I. 62105; (3) bromoamine acid; (4) bromoacetyl acid; (5) C.I. 60730; (6) isomer of C.I. 64010; (7) C.I. 61570; (8) C.I. 58005; (9) C.I. 62125. The sensor was a 180A (full lines), or a 878C (dashed lines) electrode; measured vs. SCE with a 10^{-2} M NaNO_3 salt bridge.

cizer) is also affected. To evaluate this effect, the same amounts of n-propanol were added to the titrant and to the solution to be titrated. As shown in Fig. 3A, the addition had to be as small as was necessary just to dissolve the titrant. At high concentrations of propanol, the potential break was scarcely measurable and the electrode lifetime became shorter because the plasticizer was dissolved from the membrane. Some data are given in Table 3. For practical purposes, however, the addition of propanol is needed only for the titrant solution; in such cases, the titration curve is not significantly influenced (Fig. 3B) because the final concentration of propanol at the end-point is quite low.

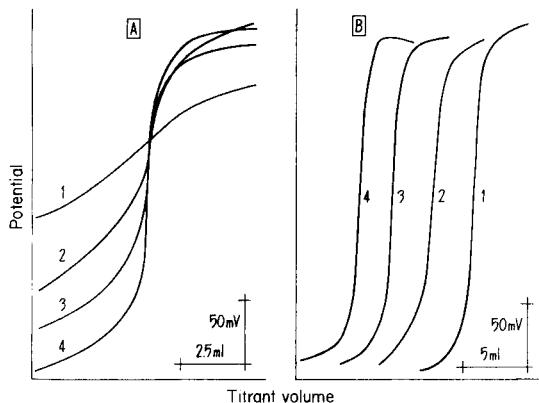


Fig. 3. Influence of additional solvent on the shape of the titration curves for bromoamine acid (50 μ mol in 50 ml): A, titration with 10^{-2} M CTAB; B, titration with 10^{-2} M CPB. Both the titrated solution and the titrant (A), or the titrant only (B), contained n-propanol as follows: (1) 20; (2) 15; (3) 10; (4) 5% (v/v). Recorded with a 180A electrode vs. SCE.

TABLE 3

Influence of n-propanol on the potentiometric titration curves for some acidic anthraquinone dyes with 10^{-2} M cetyltrimethylammonium bromide (CTAB) and a 180A coated-wire indicator electrode

Sample ^a	Concentration of n-propanol (% v/v)	Titration curve	
		Overall potential break (mV)	Steepness near the end-point (mV/0.1 ml)
C.I. 60730	5	170	16–20
	10	165	11–15
	15	145	5–7
	20	70	1–2
C.I. 61570	5	165	9–13
	10	135	7–10
	15	90	4–5
C.I. 62105	5	250	30–34
	10	220	30–32
	15	140	23–27

^aFor C.I. constitution numbers, see Table 1.

DISCUSSION

Evaluation of the accuracy and precision of these titrations is complicated, in that commercial dye specimens usually contain many impurities and adequate standard samples are not available. Only two standard samples of bromoamine acid were available; their nominal concentrations were based on determination of the amino group (titrimetrically with sodium nitrite) or bromine (by Schöniger's method). These samples were used to estimate the accuracy. The results obtained by the proposed titrations agree reasonably well with the nominal contents (Table 4). Table 2 shows results obtained for some other samples. The results with the two titrants are in good agreement, and titrations of more concentrated solutions are more precise, as expected.

Possible sources of systematic error must be considered. One such source is in the preparation of anthraquinone dye stock solutions. Solutions more concentrated than 10^{-3} M may contain solid residues from the sample. If this happens, the reproducibility of results will obviously be poor. Only the bromoamine acid solutions could be prepared at a 10^{-2} M concentration. For other samples, the preparation of 10^{-2} M stock solutions by adding another solvent cannot always be recommended, because some of the dyestuffs are not fully dissolved even in 40% (v/v) n-propanol, and the effect of this solvent on the ion-pair formation must be considered. When the aqueous 10^{-3} M stock solutions were prepared, all the finely suspended particles of the dye samples were perfectly dissolved after standing overnight at most.

TABLE 4

Titrations of standard bromoamine acid samples

Sample code	Bromoamine acid content (%)		Experimental conditions
	Nominal	Found ^a	
431/291	86.1 ^b 84.0 ^c	86.6 ± 3.1 (3)	Septonex ^d
431/293	88.7 ^b 86.4 ^c	87.0 ± 0.2 (3)	Septonex ^d
431/293	88.7 ^b 86.4 ^c	85.5 ± 0.7 (4)	Septonex ^e
431/293	88.7 ^b 86.4 ^c	85.6 ± 4.4 (3)	CPB ^e

^aExpressed as reliability interval $\bar{x} \pm u_0 R$ for number of measurements given in parentheses and significance level 0.05 (95% probability). ^{b,c}The percentage declaration is based on the determination of (b) NH_2 group or (c) bromine content. ^{d,e} Titrated with either 10^{-2} M Septonex or 10^{-3} M cetylpyridinium bromide and (d) 180A or (e) 878C indicator electrodes.

The last, not fully solved, question is the titration stoichiometry. In agreement with analogous determinations of similar ionic organic compounds, a 1:1 stoichiometric ratio would be expected for an ion-pair formed by a univalent anion with a univalent cation. This was finally corroborated by analysis of the bromoamine acid standard samples. The interaction between such an acidic anthraquinone dye and a cationic surfactant has been studied spectrophotometrically [13]; it was shown that the insoluble ion-pair contains equimolar amounts of cation and anion. However, alizarin brilliant green G (C.I. 61570) has two sulphonic acid groups. To calculate the dye content in the sample, a stoichiometric ratio of 1:2 (dye:titrant) was assumed; if a 1:1 ion-pair were assumed, the calculated dye content would be higher than 92% which is very improbable. Finally, it should be stated that suitable conditions for the determination of the dyestuffs with two sulphonic acid groups bound directly to the anthraquinone skeleton (C.I. 63010 and C.I. 63610) could not be established.

REFERENCES

- 1 K. Vytřas and M. Dajková, *Anal. Chim. Acta*, 141 (1982) 377.
- 2 A. G. Fogg and K. S. Yoo, in E. Pungor and I. Buzás (Eds.), *Ion-Selective Electrodes* (Conf., Budapest, 1977), Elsevier, Amsterdam, and Akadémiai Kiadó, Budapest, 1978, p. 369.
- 3 A. G. Fogg, A. A. Al-Sibaai and K. S. Yoo, *Anal. Lett.*, 10 (1977) 173.
- 4 A. G. Fogg and K. S. Yoo, *Anal. Chim. Acta*, 113 (1980) 165.
- 5 W. Selig, *Mikrochim. Acta*, (1979/II) 437.

- 6 K. Vytřas, M. Dajková and M. Remeš, *Cesk. Farm.*, 30 (1981) 61.
- 7 K. Vytřas, M. Dajková and V. Mach, *Anal. Chim. Acta*, 127 (1981) 165.
- 8 I. Gemzová and J. Gasparič, *Collect. Czech. Chem. Commun.*, 34 (1969) 3075.
- 9 K. Vytřas, M. Remeš and H. Kubešová-Svobodová, *Anal. Chim. Acta*, 124 (1981) 91.
- 10 C. T. Tubbs, *Anal. Chem.*, 26 (1954) 1670.
- 11 N. Ciocan and D. Anghel, *Tenside Deterg.*, 13 (1976) 4.
- 12 D. F. Anghel, G. Popescu and N. Ciocan, *Mikrochim. Acta*, (1977/II) 639.
- 13 Y. Miyashita and S. Hayano, *Yakugaku*, 30 (1981) 573; *Chem. Abstr.* 96: 21627g.

DIFFERENTIAL ELECTROLYTIC POTENTIOMETRY WITH ION-SELECTIVE ELECTRODES FOR END-POINT DETECTION IN COMPLEXIMETRIC TITRATIONS OF MERCURY(II), COPPER(II), NICKEL(II) AND BISMUTH(III)

G. A. EAST* and I. A. DA SILVA

Departamento de Química, Universidade de Brasília, 70.910 Brasília, DF (Brazil)

(Received 12th August 1982)

SUMMARY

Electrodes prepared by activating hydrophobized spectrographic graphite rods with various mercury(II) chalcogenides, alone or mixed with silver(I) chalcogenides or mercury itself, were used successfully in differential electrolytic potentiometry (d.e.p.) to locate end-points in compleximetric titrations of mercury(II) solutions with EDTA. Several materials gave useful d.e.p. peaks at the expected end-points, showing that these electrodes can replace the commoner mercury and amalgamated gold electrodes. To demonstrate the usefulness of the sensors in EDTA titrations of metal ions other than mercury(II), titrations of copper(II) were performed. The electrode response takes place via reaction of the ion with sulphide or selenide in the electroactive layer. Electrodes activated by copper(II), bismuth(III), and nickel(II) chalcogenides were also studied; those sensors that produced good ion-selective electrodes were also useful in d.e.p. titrations.

In a previous paper [1], the disadvantages associated with the use of mercury and amalgamated gold as indicating electrodes were discussed and graphite-supported ion-selective electrodes similar to those described by Ružička et al. [2] were described as substitutes. These electrodes proved to be useful in direct potentiometry and zero-current potentiometric titrations of mercury(II) with EDTA. This paper reports the evaluation of several such electrodes for titrations based on differential electrolytic potentiometric (d.e.p.) detection of end-points. The d.e.p. technique affords a very precise method of end-point location in volumetric and coulometric titrations [3–6], and is judged superior to zero-current potentiometry. In the work reported here, electrodes activated by several precipitates or mixtures of precipitates were tested for end-point detection in compleximetric titrations of mercury(II), copper(II), nickel(II), and bismuth(III) with EDTA. Applications of d.e.p. to compleximetry have been few [6–12] and in all previous cases mercury or amalgamated gold has been used.

EXPERIMENTAL

Reagents and apparatus

All reagents were of analytical grade and were used as received. Construction of the electrodes and preparation of mercury(II) standard solutions and mercury(II) chalcogenides and their admixtures with Ag_2S or Ag_2Se were described earlier [1]. Materials prepared by known methods were CuS [13], Cu_2S [14], and NiSe , CuSe , and Bi_2Se_3 [15]. Nickel(II) sulphide was prepared as follows: to a hot nickel(II) nitrate solution were added ammonium chloride, excess of ammonia solution and ammonium sulphide solution to give a 20% excess of sulphide with respect to nickel(II); after boiling for 10 min, the precipitate of nickel sulphide was filtered, washed several times with water, and finally washed with acetone and dried in an oven at 60°C . Bismuth(III) sulphide was prepared in the same manner from bismuth(III) nitrate.

A spinning system for twin electrodes for precise d.e.p. titrations was designed as shown in Fig. 1(a); Fig. 1(b) shows the complete assembly. The electrode body was made of acrylic resin moulded into a piece of glass tubing of appropriate width. External electric contact of the graphite was made with two brass rings, C. The final electric contact with the constant current source was provided by the carbon brushes, F, glued to the brass

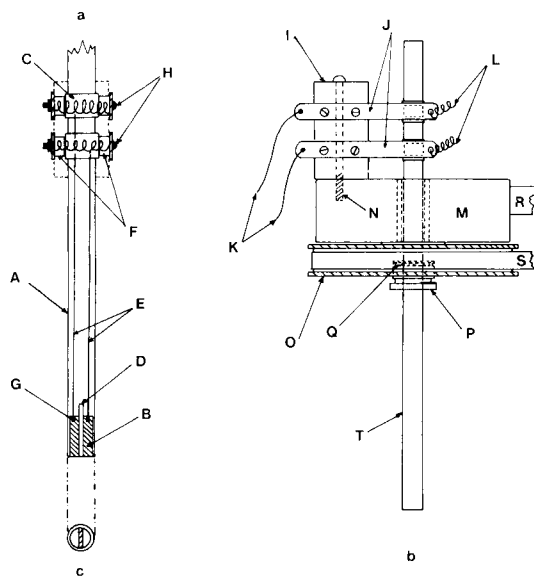


Fig. 1. Twin rotating electrodes for d.e.p. (a) Front view of the electrode and external electric contacts: A, polyester resin electrode body; B, treated and hydrophobized graphite; C, brass rings; D, acrylic separator; E, copper wires; F, carbon brushes; G, solder; H, screws. (b) Side view of the assembly: I, acrylic resin holder; J, brass strips; K, copper wires to source; L, springs; M, aluminium body; N, screw; O, grooved rotating wheel; P, brass nut; Q, silicone rubber washer; R, assembly support; S, driving belt to motor; T, twin electrodes. (c) Bottom electrode cross-section.

strips, J. The springs, L, ensure good contact between brushes and brass rings. The driving unit was a turn-table motor (Mamco Corp., WI, U.S.A.) capable of driving the electrode at constant speeds of up to 1,200 rpm.

The direct current (d.c.) d.e.p. circuitry permitting polarizing currents between 1.4 nA and 14 μ A was that described by Hartshorn and Bishop [16] and was constructed with operational amplifiers from a MP-System 1000 (McKee-Pedersen Instruments). A Corning Model 12 research pH-meter was used to measure potentials. A saturated calomel electrode (Corning) was used as the reference electrode. All the d.e.p. titrations were done with a 2.500-ml Radiometer auto-burette (Type ABU 1c).

Titration procedure

Titrations were done by taking 1.00 ml of a 1.00×10^{-2} M standard solution of the analyte in a 50-ml beaker, adding 4 ml of the appropriate buffer solution (acetate, pH 4.75 for Hg(II)) and diluting with water to a final volume of about 35 ml. The 1.0×10^{-2} M EDTA titrant was delivered from the auto-burette with fast stirring until ca. 0.1 ml before the end-point. Then increments of 0.002 ml of titrant were added until the end-point was passed, when the increments were increased to 0.3 ml. After each increment, potentials were measured with the aid of a switch box in the order: indicating electrode—SCE, anode—SCE, cathode—SCE, and differential potential ΔE . The potentials were read when the potential drift became less than 1 mV min⁻¹.

Current density, another important parameter in d.e.p., was studied in order to establish the value giving the sharpest peaks at the end-point. A current density of 2 μ A cm⁻² gave suitable results and was therefore utilized throughout this work.

RESULTS AND DISCUSSION

Mercury(II) titrations

Electroactive materials studied were HgS(black)/Ag₂S coprecipitated, HgS(black)/Hg obtained by disproportionation of mercury(I) sulphide, HgS(black), HgS(red), HgSe, and mechanical mixtures of HgSe with Ag₂S or Ag₂Se. The use of silicone grease mixed with the activating precipitate, that enhanced the electrode performance in direct potentiometry of mercury(II) [1], caused distorted d.e.p. curves (Fig. 2) and so was abandoned. Conditioning in the way described previously [1] improved the quality of the end-point detection by means of d.e.p. In addition, electrodes left for some time in the titrated solution performed even better and therefore this method of conditioning was adopted for electrodes employed in d.e.p.; the effect is illustrated in Fig. 2. Electrodes prepared and conditioned as above were used for up to 15 titrations without any noticeable deterioration in the d.e.p. peaks (Figs. 3 and 4). All the electroactive materials tested except the mixture of HgSe and Ag₂Se, yielded useful sensors for end-point detection in the

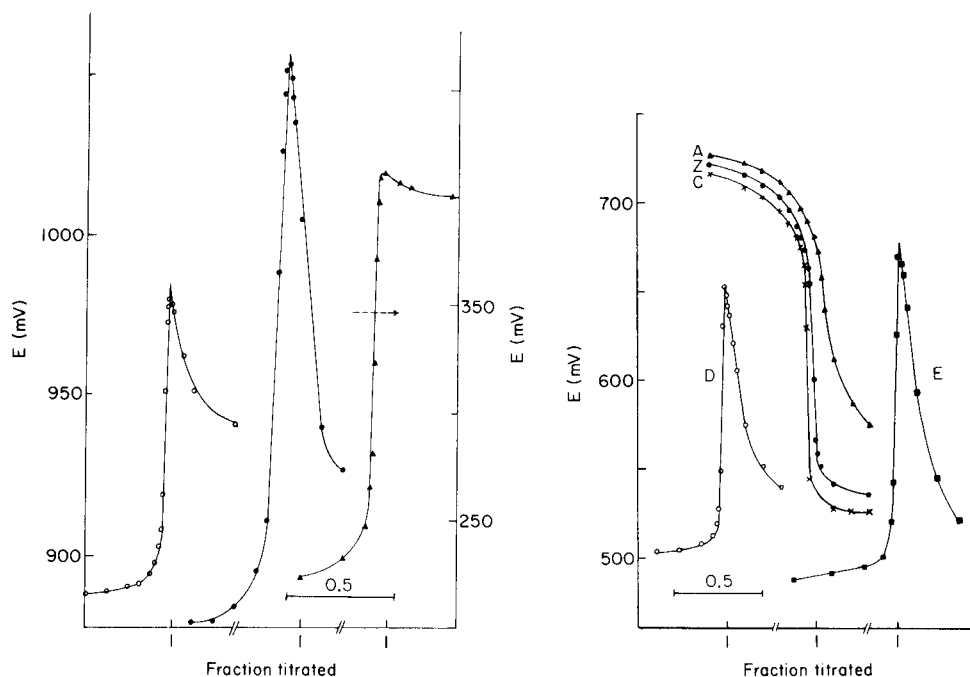


Fig. 2. Direct current d.e.p. curves with HgS(black)/Hg electrodes, showing the effect of conditioning and silicone grease: (○) freshly activated electrode; (●) after 15 h in the titrated solution; (▲) activating precipitate mixed with silicone grease. Initial Hg(II) concentration, 2.9×10^{-4} M; pH 4.8 (acetate buffer); current density $2 \mu\text{A cm}^{-2}$.

Fig. 3. Individual electrode behaviour and d.c. d.e.p. curves with HgS(black)/Ag₂S electrodes: A, anode potential; C, cathode potential; Z, zero-current indicator potential; D and E, d.e.p. curves. Initial Hg(II) concentration, 2.9×10^{-4} M; pH 4.8 (acetate buffer); current density $2 \mu\text{A cm}^{-2}$. Curve E was obtained after 15 titrations of mercury(II).

titration of mercury(II) with EDTA. However, those activated with HgS(black)/Ag₂S gave the sharpest peaks, probably because of the presence of Ag₂S with its well-known conducting properties (Fig. 3); those activated with HgS(black)/Hg were second best (Fig. 2). Sensors activated with HgS(black) and HgSe produced reasonably good peaks, whereas those activated with HgS(red) and HgSe + Ag₂S, respectively, still yielded useful d.e.p. peaks but they were broader and the precision was thus diminished (Fig. 4). Table 1 shows some results obtained with those sensors.

To study the behaviour of the individual electrodes, a third indicator electrode was introduced and used in a zero-current mode, along with a reference electrode (SCE), in order to compare the zero-current behaviour with that of the cathode and anode. Bishop [4] found that in oxidation–reduction titrimetry the anode leads and the cathode lags with respect to the zero-current indicator electrode; therefore the difference in potential of the two polarized electrodes follows the first derivative of the zero-current potenti-

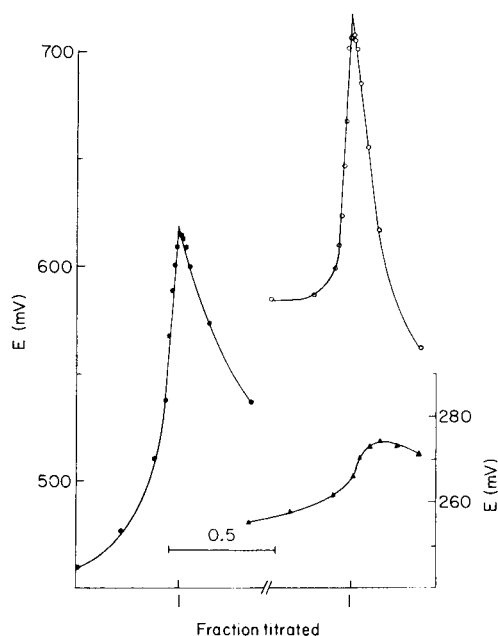


Fig. 4. Direct current d.e.p. with HgSe-based electrode. (○) HgSe electrodes after 11 titrations and in the absence of oxygen; (●) HgSe/Ag₂S electrodes; (▲) HgSe/Ag₂Se electrodes. Initial Hg(II) concentration, 2.9×10^{-4} M; pH 4.8 (acetate buffer); current density $2 \mu\text{A cm}^{-2}$.

metric curve, giving rise to a sharp peak at the end-point, with the shape and height governed by current density, reaction equilibrium constant, and analyte concentration. Figure 3 illustrates the individual behaviour of graphite electrodes activated with HgS(black)/Ag₂S when used as sensors in the titration of mercury(II) with EDTA. As in redox titrimetry, the anode potential, curve A, leads and the cathode, curve C, lags behind the zero-current indicator electrode potential, curve Z. The resulting differential, curve D, shows a positive going peak starting at about 500 mV vs. SCE, showing that the potential-determining reaction takes place with a high

TABLE 1

Results of the titration of mercury(II) solutions with EDTA and d.e.p. end-point location

Activating material	Mean conc. ^a (10^{-3} M)	Activating material	Mean conc. ^a (10^{-3} M)
HgS(black)/Ag ₂ S	9.96 ± 0.04	HgSe	9.77 ± 0.09
HgS(black)/Hg	9.89 ± 0.05	HgS(red)	9.73 ± 0.10
HgS(black)	9.81 ± 0.04		

^aMean with 95% confidence limits based on 5 titrations.

charge-transfer overpotential. The potential then increases sharply to a peak at the end-point and finally decreases at a modest rate to a steady potential of about 540 mV vs. SCE. It does not reach zero and the rate-determining reaction after the end-point occurs with a high charge-transfer overpotential. Curve D presents the same general pattern found in other compleximetric d.e.p. titrations with EDTA when mercury or amalgamated gold polarized electrodes are used [12]; this shows that the processes at the cathode and anode before and after the end-point are of the same nature in both cases. When mercury is absent, as in the present case, except for electrodes activated by HgS(black)/Hg, the anodic process before and after the end-point must be either oxidation of the metal chalcogenide (HgS, HgSe, Ag₂S, or Ag₂Se) or oxidation of free sulphur or selenium that may be present at the electrode surface, depending on which process takes place with the lowest charge-transfer overpotential. Whatever the electrode reaction may be, it must proceed with a higher overpotential than mercury oxidation and therefore the initial potential observed is high. The easiest cathodic reaction before the end-point is reduction of Hg(II) to Hg(I) or Hg, but, after the end-point, when all Hg(II) has been complexed by EDTA, there are three likely reactions: reduction of HgEDTA²⁻, oxygen or sulphur (selenium). The presence of dissolved oxygen is essential for obtaining sharp peaks in compleximetric titrations when mercury or amalgamated gold electrodes are used for d.e.p. [9, 12]. This finding has been ascribed to the high charge-transfer overpotential at which HgEDTA²⁻ is reduced at the mercury cathode; consequently reduction of oxygen, which proceeds with a much lower overpotential at the same cathode, will be preferentially reduced. The effect of oxygen on the quality of the d.e.p. peaks obtained with graphite activated by mercury(II) chalcogenides or their admixtures was studied; there was no practical difference whether oxygen was present or not. This finding indicates that another electrode reaction proceeds with lower overpotential than oxygen reduction or perhaps that the oxygen overpotential on the activated graphite surface is high and thus the faster electrode process is reduction of HgEDTA²⁻ or sulphur (selenium).

Mercury or amalgamated gold electrodes have been used extensively as third-kind electrodes to determine ions forming weaker complexes with EDTA than mercury(II) by adding a few drops of HgEDTA²⁻ to the analyte solution with zero-current [7, 17] or d.e.p. [12] end-point location. To illustrate the usefulness of graphite electrodes activated by mercury(II) chalcogenides or their mixtures with silver(I) chalcogenides as pM indicators in d.e.p., copper(II) was titrated, using electrodes activated by HgS(black)/Ag₂S. For comparison purposes, titrations of copper(II) with EDTA were done in the presence and in the absence of HgEDTA²⁻. The d.e.p. curves so obtained were slightly different from those in Fig. 3, but quite similar to each other, showing that addition of HgEDTA²⁻ is unnecessary when the activating material incorporates a chalcogenide, sulphide or selenide, that forms an insoluble compound (CuSe or CuS) with the ion to be titrated. This

should also be valid for other metal ions forming sparingly soluble compounds with the chalcogenide of the electroactive material. Consequently, titration of many other ions by compleximetry with EDTA using these sensors in d.e.p. is promising.

Copper(II), nickel(II) and bismuth(III) chalcogenide electrodes for d.e.p.

The above findings should not be restricted to graphite electrodes activated by mercury(II) chalcogenides or their admixtures with silver(I) chalcogenides. Other sensors of similar nature that are good ion-selective electrodes should also produce good d.e.p. indication. To corroborate this, some copper(II), nickel(II), and bismuth(III) chalcogenides and their mixtures with Ag_2S or Ag_2Se were tested as the electroactive material in indicating electrodes for compleximetric titrations of copper(II), nickel(II) and bismuth(III) solutions, respectively, with d.e.p. end-point detection. Precipitates and mixtures of precipitates studied were CuS , $\text{Cu}_2\text{S}/\text{Ag}_2\text{S}$, $\text{CuS}/\text{Ag}_2\text{S}$, NiS , NiSe , $\text{NiS}/\text{Ag}_2\text{S}$, $\text{NiSe}/\text{Ag}_2\text{S}$, Bi_2S_3 , $\text{Bi}_2\text{S}_3/\text{Ag}_2\text{S}$, and $\text{Bi}_2\text{Se}_3/\text{Ag}_2\text{Se}$. As expected, electrodes activated with CuS or Cu_2S mixed with Ag_2S , in particular those activated with $\text{Cu}_2\text{S}/\text{Ag}_2\text{S}$, produced the best sensors. Curve A in Fig. 5 shows a sharp peak coinciding with the estimated end-point. Next best were those activated by $\text{Bi}_2\text{S}_3/\text{Ag}_2\text{S}$ (curve B, Fig. 5). Unfortunately, electrodes activated with nickel(II) chalcogenides, alone or mixed with Ag_2S or

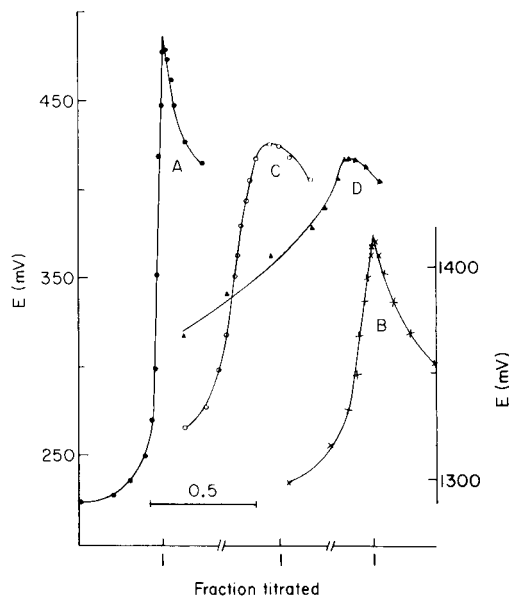


Fig. 5. Direct current d.e.p. with $\text{Cu}_2\text{S}/\text{Ag}_2\text{S}$, $\text{Bi}_2\text{S}_3/\text{Ag}_2\text{S}$ and NiSe , $\text{NiSe}/\text{Ag}_2\text{S}$ electrodes. A, Cu(II) titration with $\text{Cu}_2\text{S}/\text{Ag}_2\text{S}$ electrodes; B, Bi(III) titration with $\text{Bi}_2\text{S}_3/\text{Ag}_2\text{S}$ electrodes; C and D, Ni(II) titration with NiSe and $\text{NiSe}/\text{Ag}_2\text{S}$ electrodes, respectively. Initial analyte concentration 2.9×10^{-4} M. For Cu(II) and Ni(II) determinations, pH 4.8 (acetate buffer); for Bi(III) , pH 2 with nitric acid; current density $2 \mu\text{A cm}^{-2}$.

Ag₂Se, showed poor performance, producing rounded d.e.p. peaks or S-shaped curves (curves C and D). These results are consistent with the fact that copper(II) or copper(I) chalcogenides with silver sulphide as matrix yield very good ion-selective electrodes, whereas bismuth and nickel chalcogenides produce unsatisfactory sensors [18], no matter what matrix is used.

REFERENCES

- 1 G. A. East and I. A. da Silva, *Anal. Chim. Acta*, 148 (1983) 41.
- 2 J. Růžička, C. G. Lamm and Chr. Tjell, *Anal. Chim. Acta*, 62 (1972) 45.
- 3 E. Bishop, *Mikrochim. Acta*, (1956) 619.
- 4 E. Bishop, *Analyst*, 83 (1958) 212.
- 5 E. Bishop and T. J. N. Webber, *Analyst*, 98 (1973) 697.
- 6 L. G. Hartshorn, Ph.D. Thesis, University of Exeter, 1972.
- 7 A. E. Martin and C. N. Reilley, *Anal. Chem.*, 31 (1959) 992.
- 8 G. C. Goode and W. T. Jones, *Anal. Chim. Acta*, 38 (1967) 363.
- 9 R. G. Monk and K. C. Steed, *Anal. Chim. Acta*, 26 (1962) 305.
- 10 C. O. Huber and D. R. Tallant, *J. Electroanal. Chem.*, 18 (1968) 421.
- 11 G. Kraft and H. Dosch, *Fresenius Z. Anal. Chem.*, 260 (1972) 261.
- 12 G. A. East, Ph.D. Thesis, University of Exeter, 1975.
- 13 E. H. Hansen, C. G. Lamm and J. Růžička, *Anal. Chim. Acta*, 59 (1972) 403.
- 14 H. Hirata and K. Date, *Talanta*, 17 (1970) 883.
- 15 G. E. Cranton and R. D. Heyding, *Can. J. Chem.*, 43 (1955) 2029.
- 16 L. G. Hartshorn and E. Bishop, *Analyst*, 96 (1971) 885.
- 17 C. N. Reilley and R. W. Schmid, *Anal. Chem.*, 30 (1958) 947.
- 18 I. Sekerka and J. F. Lechner, *Anal. Lett.*, 9 (1966) 1099.

LIQUID—LIQUID EXTRACTION OF METAL IONS WITH SULFONAMIDE CHELATING AGENTS

SHUNSUKE IDE

Department of Chemistry, Faculty of Liberal Arts, Kitakyushu Technical College, 140 Shii, Kokura-minami-ku, Kitakyushu 803 (Japan)

TSUKASA YOSHIDA, SHUGO MATSUNO, MAKOTO TAKAGI and KEIHEI UENO*

Department of Organic Synthesis, Faculty of Engineering, Kyushu University, Higashi-ku, Fukuoka 812 (Japan)

(Received 19th November 1982)

SUMMARY

The liquid—liquid extraction of divalent metal ions (Co, Cu, Zn, Cd, Pb, Hg) with 8-octanesulfonamidoquinoline (I; HL), 1,2-bis(octanesulfonamido)benzene (II; H₂L), 1,8-bis(octanesulfonamido)naphthalene (III; H₂L), 2-octanesulfonamidophenol (IV; H₂L), and some other related sulfonamide chelating agents was studied between aqueous and aromatic solvents. Compound I extracted divalent metals by forming ML₂-type complexes; copper(II) was extracted at by far the lowest pH region except for mercury(II). Compounds II–IV formed ML complexes with divalent metals, which were extracted in the organic solution in the presence of lipophilic uncharged ligands (A) such as 4-benzylpyridine and 1,2-bis(alkylthio)ethane through the formation of MLA_m-type complexes. Copper(II) was again the most readily extracted, but the extraction selectivity among the metals was less than that with compound I. Compounds II and III extracted divalent metals in the presence of lipophilic quaternary ammonium salt (trioctylmethylammonium chloride, Aliquat-336S, Q⁺Cl⁻); a mechanism including the formation of an anionic complex of the type ML₂⁻ or MLCl_nⁿ⁻ followed by an ion-pair extraction with Q⁺ is suggested. The sulfonamides I–IV showed by far the highest extraction ability for mercury among the divalent metal ions. An especially strong affinity was shown by compound I, with which mercury was extracted completely even at pH 1. Several other sulfonamide homologues of I–IV were also synthesized and the metal complexes which relate to those formed in the extraction were isolated.

The importance of organic reagents in analyses for metallic elements has somewhat diminished because of the substantial development of physical methods based on atomic spectra. The use of organic reagents seems to be shifting to the separation part of an analysis or to the separation itself as in the use of liquid—liquid extraction of metals in hydrometallurgical processes.

Sulfonamides derived from primary amines have an amide proton of comparable acidity to phenols, and the conjugate bases therefrom can form stable coordination compounds with various metal ions when the sulfonamide group is part of the coordinating site of the chelating agent. This type of chelating agent was first introduced by Billman and Chernin in the early

1960s, providing selective gravimetric and colorimetric reagents for some transition metal ions, particularly copper(II) [1–3]. In the following decade, over ten publications appeared, some of which dealt with similar aspects of the reagent [4–7], and some with applications to the fluorimetric determination of zinc and cadmium [8–13]. Formation constants of the complexes were also estimated [14, 15]. However, they seem to have failed to find any particular advantages in using this family of reagents in analytical and separation chemistry over traditional reagents such as phenols and β -diketones. The compounds treated in these studies were the sulfonamides derived from 8-aminoquinolines, *o*-phenylenediamine (mono-sulfonamide), and 2-alkylthioanilines.

In the surge of increasing industrial utilization of hydrometallurgical liquid–liquid extraction processes, however, sulfonamide chelating agents were reviewed in the late 1970s, and several reports appeared, dealing with the synthesis of highly lipophilic sulfonamide chelating agents and their application to hydrometallurgical metal extraction [16–20]. These sulfonamides included 8-(4-dodecylbenzenesulfonamido)quinoline (LIX 34) [16–18], 2-arenesulfonamidophenols [19], and sulfonamide-oximes derived from aromatic and aliphatic aminoketones [20]. High extraction selectivity to copper(II) and the lack of interfering effect from iron(III) were claimed for the 8-sulfonamidoquinoline type reagent [16, 17].

Independently, a variety of sulfonamide chelating agents has also been synthesized in this laboratory, and their potential utility for separating and concentrating metals by liquid–liquid extraction has been described [21]. Steric bulkiness of sulfonamide anion on coordination to metal ions was suggested for the low affinity toward iron(III), aluminum(III), and alkaline earth metal ions, which is in a sharp contrast with its reasonably high affinity toward copper(II) and some of the transition and post-transition metals [22].

The evidence collected in these recent papers clearly indicates that these sulfonamides are versatile chelating agents, whose metal selectivity and utility in metal extraction processes have not been covered by traditional chelating agents. In view of the less than two dozen scattered reports published in this field, it seems highly desirable to make a systematic and broader study on the nature of this class of chelating agents. In the study reported here, the liquid–liquid extraction of metal ions with 8-octanesulfonamidoquinoline (I; HL), 1,2-bis(octanesulfonamido)benzene (II; H_2L), 1,8-bis(octanesulfonamido)naphthalene (III; H_2L), and 2-octanesulfonamidophenol (IV; H_2L), and some other related sulfonamide chelating agents, was examined, in a continuation of earlier work [21].

EXPERIMENTAL

Compound I and related sulfonamides

Compound I. 8-Aminoquinoline (8.57 g, 59 mmol) was dissolved in dry pyridine (40 ml) in a flask protected from moisture. 1-Octanesulfonyl

chloride (13.9 g, 65 mmol) dissolved in benzene (15 ml) was then added dropwise under stirring at below 20°C. The mixture was stirred for 1 h, then gradually heated to 60°C, and kept at this temperature for 1 h. Water (4 ml) was added and the mixture was kept stirred for a further 0.5 h. The reaction mixture was concentrated under reduced pressure, and the residue was shaken with chloroform (100 ml) and water (60 ml, pH 2–3). The chloroform layer was separated and washed with acidified water (pH 2–3, sulfuric acid), then with aqueous sodium carbonate solution (5%). The viscous residue obtained by concentrating the chloroform solution was taken into ether (30 ml) and treated with perchloric acid (60%, 20 ml). The perchlorate salt of compound I separated as slightly brownish crystals, which were collected on a filter, washed with ether, and dried. In order to recover the free base of I from the salt, the crystals were treated with a mixture of benzene and aqueous sodium hydroxide. The benzene layer was separated, dried, concentrated under reduced pressure, and finally distilled to give a pale yellow viscous oil. [B.p. 190–205°C (bath temperature) at 0.05 Pa; yield 14.4 g (75%). ¹H-n.m.r. (CDCl₃; δ ppm from internal TMS): δ = 0.83–2.23 (15 H, m, (CH₂)₆CH₃), 3.18 (2 H, t, *J* = 7.5 Hz, –SO₂CH₂–), 7.30–8.29 (6 H, m, aromatic H), 8.6–9.2 (1 H, broad, NH; D exchange with D₂O). I.r. (neat): 3270 (NH), 1335, 1152 cm⁻¹ (SO₂). Found: 63.5%C, 7.45%H, 8.7%N. Calcd. for C₁₇H₂₄N₂O₂S: 63.7%C, 7.55%H, 8.8%N.] The highly pure perchlorate salt of I was prepared by crystallization from an ethereal solution of distilled I with perchloric acid. [White crystals, m.p. 148–150°C.]

8-Butanesulfonamido (V), 8-ethanesulfonamido- (VI), and 8-methanesulfonamido- (VII) quinolines. These were prepared in a similar manner to I. Compound V was purified by distillation (bath temperature, 170–195°C at 0.7 Pa), and VI and VII were purified by recrystallization (mp: VI, 72–73.5°C; VII, 148–149°C). These preparations gave satisfactory analytical data.

Compound II and related sulfonamides

Compound II. *o*-Phenylenediamine (5.80 g, 54 mmol), pyridine (20 ml), 1-octanesulfonyl chloride (25.7 g, 121 mmol) and benzene (15 ml) were mixed and treated in a manner similar to that described for I. The reaction mixture was concentrated and the residue was taken into benzene (40 ml) and washed with acidified water (sulfuric acid, pH 2), and then with aqueous sodium carbonate solution (5%). The benzene solution was dried, passed through a small column of silica gel, and concentrated to dryness. The residue was recrystallized from cyclohexane (100 ml) to give white crystals. [M.p. 70.5–71°C; yield 13 g (86%). ¹H-n.m.r. (CDCl₃): δ = 0.77–2.13 (30 H, m, (CH₂)₆CH₃ × 2), 3.10 (4 H, t, *J* = 7.5 Hz, SO₂CH₂ × 2), 7.10 (s, NH × 2), 7.05–7.49 (m, aromatic H) (6 H for protons at δ = 7.10 and 7.05–7.49 ppm). I.r. (nujol): 3260 (NH), 1326, 1152 cm⁻¹ (SO₂). Found: 57.4%C, 8.7%H, 6.1%N. Calcd. for C₂₂H₄₀N₂O₄S₂: 57.4%C, 8.75%H, 6.1%N.]

1,2-Bis(butanesulfonamido)benzene (VIII) and 1,2-bis(methanesulfonamido)benzene (IX). Compound VIII was prepared in a similar manner to that described for II. The recrystallization was done from ether at -10°C . Compound IX precipitated on adding excess of water to the reaction mixture. The crystalline solid was recrystallized from methanol. The product was further purified by first dissolving the crude IX in aqueous sodium hydroxide, treating the solution with activated charcoal, and finally acidifying the filtrate with mineral acid. M.p. $217\text{--}217.5^{\circ}\text{C}$. The preparations of both VIII and IX were analytically pure.

Compound III

1,8-Naphthalenediamine (11.4 g, 72 mmol), pyridine (100 ml), 1-octanesulfonyl chloride (35.2 g, 165 mmol), and benzene (20 ml) were mixed and treated in a manner similar to that described for I. The reaction mixture was concentrated, and the residue was taken up in a mixture of chloroform (150 ml) and water (70 ml, pH 2). The chloroform solution was washed successively with acidified water and aqueous sodium hydrogencarbonate solution, dried, and finally filtered through a small column of silica gel. The filtrate was concentrated to dryness, and the residue was repeatedly recrystallized from methanol and cyclohexane. The column filtration and recrystallization were necessary to remove the trace of brownish coloration. [White crystals, m.p. $77\text{--}78^{\circ}\text{C}$; yield 9.6 g (26%). ^1H -n.m.r. (CDCl_3): $\delta = 0.85\text{--}1.85$ (30 H, m, $(\text{CH}_2)_6\text{CH}_3 \times 2$), 3.30 (4 H, t, $J = 7.5$ Hz, $\text{SO}_2\text{CH}_2 \times 2$), 7.19–7.68 (6 H, m, aromatic H), 9.05 (2 H, s, $\text{NH} \times 2$). I.r. (nujol): 3250 (NH), 1340, 1139 cm^{-1} (SO_2). Found: 61.1%C, 8.3%H, 5.6%N. Calcd. for $\text{C}_{26}\text{H}_{42}\text{N}_2\text{O}_4\text{S}_2$: 61.1%C, 8.3%H, 5.5%N.]

Compound IV and related sulfonamides

Compound IV. *o*-Aminophenol (5.31 g, 49 mmol), pyridine (40 ml), 1-octanesulfonyl chloride (10.1 g, 48 mmol), and benzene (15 ml) were mixed and treated in a manner similar to that described for I. After the reaction, aqueous sodium hydroxide solution (2.0 g of sodium hydroxide in 4 ml of water) was added and the mixture was concentrated to dryness under reduced pressure. The residue was taken up in warm chloroform (170 ml) and filtered through a small column of silica gel (kept at $45\text{--}50^{\circ}\text{C}$). On cooling the filtrate, crystals were obtained, which were dissolved in methanol and treated with activated charcoal. The evaporation of the methanol solution and the recrystallization of the residue from cyclohexane gave white crystals. [m.p. $88\text{--}88.5^{\circ}\text{C}$; yield 6.1 g (45%). ^1H -n.m.r. (CDCl_3): $\delta = 0.59\text{--}1.85$ (15 H, m, $(\text{CH}_2)_6\text{CH}_3$), 3.09 (2 H, t, $J = 7.5$ Hz, SO_2CH_2), 6.58 (2 H, s, broad, NH and OH), 6.79–7.30 (4 H, m, aromatic H). I.r. (nujol): 3460 (OH), 3266 (NH), 1322, 1125 cm^{-1} (SO_2). Found: 58.8%C, 8.15%H, 4.8%N. Calcd. for $\text{C}_{14}\text{H}_{23}\text{NO}_3\text{S}$: 58.9%C, 8.1%H, 4.9%N.]

1-Octanesulfonamido-2-naphthol (X). 1-Amino-2-naphthol hydrochloride (85% purity, 10.4 g, 45 mmol), pyridine (40 ml), and triethylamine (20 ml)

were mixed in a moisture-protected flask, and to the mixture was added dropwise a solution of 1-octanesulfonyl chloride (11.9 g, 49 mmol) in benzene (10 ml). The mixture was then heated to 60–80°C for 3 h, treated with water (3 ml), and finally concentrated under reduced pressure. The residue was taken into chloroform, washed with acidified water (sulfuric acid, pH 2), dried, treated with silica gel, and finally recrystallized from cyclohexane followed by methanol. [Pale brownish crystals, m.p. 71.5–72.5°C; yield 6.1 g (40%). ¹H-n.m.r. (CDCl₃): δ = 0.88–2.00 (15 H, m, (CH₂)₆CH₃), 3.35 (2 H, t, *J* = 7.5 Hz, –SO₂CH₂–), 3.88 (2 H, s, OH, NH), 7.18–7.68 (6 H, m, aromatic H). I.r. (nujol): 3480 (OH), 3385 (NH), 1354, 1149 cm^{–1} (SO₂).]

o-Methanesulfonamidophenol (XI). The compound was synthesized in a manner similar to that described for IV, and recrystallized from water followed by chloroform. [White crystals, m.p. 116–118°C (115–116°C [23]).]

Other sulfonamides

1-Butylthio-2-butanefulfonamidobenzene (XII). *o*-Butylthioaniline was allowed to react with butanesulfonyl chloride in a manner similar to that described for I. The product was distilled under reduced pressure to give a colorless oil. [B.p. 120–130°C (bath temperature) at 0.02 Pa; yield 61%.]

2-Octanesulfonamidoaniline (XIII). Equimolar amounts of *o*-phenylenediamine and 1-octanesulfonyl chloride were treated in a manner similar to that described for II. The concentrated reaction mixture was taken into chloroform, and washed with dilute acid (sulfuric acid, pH 4) followed by aqueous sodium carbonate. The crude product was distilled (bath temperature, 188–205°C at 0.08 Pa), and finally recrystallized from methanol–water. [White crystals, m.p. 58–60°C; yield 61%.]

The other sulfonamides were prepared in a similar manner from the corresponding primary amines and sulfonyl chlorides. All the preparations gave satisfactory analytical results.

Other reagents

Triethylmethylammonium chloride (Aliquat-336S; General Mills) was used as received. 4-Benzylpyridine perchlorate was obtained by neutralizing freshly-distilled 4-benzylpyridine with perchloric acid in methanol, and recrystallized from methanol.

1,2-Bis(hexylthio)ethane was prepared as follows. Potassium hydroxide (4.9 g, 87 mmol) was dissolved in methanol (50 ml) under nitrogen, and 1-hexanethiol (10.1 g, 85 mmol) was added with ice-cooling, followed by a solution of 1,2-dibromoethane (6.64 g, 35 mmol) in methanol (15 ml) from a dropping funnel. After stirring for 1 h, the temperature was raised to room temperature and kept for 4 h. The reaction mixture was concentrated, extracted with benzene, and distilled to give a clear liquid. [B.p. 169°C/700 Pa, yield 6.0 g (65%); the product was analytically pure (g.c., ¹H-n.m.r.).]

The other chemicals were of analytical grade and were used as received.

Liquid-liquid extraction of metal ions

The organic and aqueous solutions (10 ml each) were placed in a 50-ml glass-stoppered centrifuge tube and equilibrated on a mechanical shaker. The aqueous solution contained $7.2\text{--}8.5 \times 10^{-5}$ M (1 M = 1 mol dm⁻³) metal salts, 0.1 M potassium nitrate, and 0.01–0.005 M pH-buffering agents. Hydrochloric and acetic acids were used to control the pH below 6, and, at pH above 6, Good Buffers were used. The organic solution (usually chlorobenzene) contained ordinarily $1.6\text{--}2.0 \times 10^{-2}$ M sulfonamide reagent and other auxiliary reagents where needed. A shaking time of 30 min was usually enough to attain equilibrium in the present extraction study. The mixture was centrifuged, and the pH of the aqueous solution was measured. The metal concentration in the aqueous solution was determined by atomic absorption spectrometry. The amount of metal ion extracted was calculated from the difference of the concentrations before and after the extraction; care was taken to ensure that there was no turbidity in either the aqueous or the organic phase or at the interface. The sulfonamide reagents I–IV and their metal complexes were soluble in organic solvents and insoluble in water.

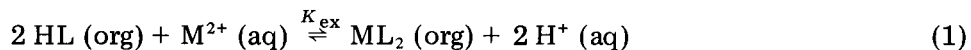
Acidity constant

The acidity constant of 4-benzylpyridinium (perchlorate salt) in aqueous solution (0.1 M KCl) was determined potentiometrically at $25.0 \pm 0.1^\circ\text{C}$ in a standard manner [24]. The potentiometric measurement in aqueous–organic heterogeneous system was done in essentially the same way except for the presence of organic phase. In a typical run, 50 ml of chlorobenzene solution 0.01 M in compound II and 0.04 M in Aliquat-336S, and 50 ml of aqueous solution 0.10 M in potassium chloride, were placed in a water-jacketed titration vessel. The mixture was titrated with standard 0.1 M sodium hydroxide. After each addition of the base, the mixture was stirred and allowed to settle, and the pH of the aqueous phase was measured in the usual manner.

RESULTS

Extraction of metal ions

The extraction of divalent metal ions with compound I (HL) into toluene follows the reaction [21]



$$K_{\text{ex}} = [\text{ML}_2]_{\text{o}} [\text{H}^+]_{\text{w}}^2 / [\text{HL}]_{\text{o}}^2 [\text{M}^{2+}]_{\text{w}} \quad (2)$$

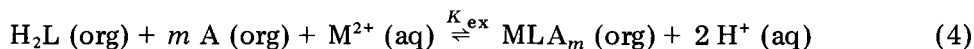
where subscripts o and w indicate the organic and aqueous phases, respectively. When only the ML_2 complex is formed and extracted, the distribution ratio D , which can be experimentally determined, is expressed in terms of K_{ex} , $[\text{H}^+]$, and $[\text{HL}]_{\text{o}}$:

$$\log D = \log [\text{ML}_2]_{\text{o}} / [\text{M}^{2+}]_{\text{w}} = \log K_{\text{ex}} + 2 \log [\text{HL}]_{\text{o}} + 2 \text{pH} \quad (3)$$

Divalent metal ions were extracted by using an excess molar amount of compound I, and the metal distribution ratio was determined as a function of pH. The plot of $\log D$ values against pH gave a straight line, and the slope and the intercept were calculated by the least-squares method. The results are summarized in Table 1. The extraction of nickel took an unusually long time to reach equilibrium, and the extraction reaction also seemed different from Eqn. (1). The results will be the topic of a separate publication.

In contrast to compound I, sulfonamides XII and XIII showed much less extraction ability toward metal ions. Only copper was extracted. The extraction constant and the half-extraction pH in toluene under conditions similar to those in Table 1 were as follows: XII, $\log K_{\text{ex}} = -9.4$, $\text{pH}_{1/2} = 6.5$; XIII, $\log K_{\text{ex}} = -4.6$, $\text{pH}_{1/2} = 4.0$. The slopes of the $\log D - \text{pH}$ plots were 1.3 for XII and 1.7 for XIII. The former value (1.3) deviated considerably from the theoretical slope of 2 in Eqn. (3). This is most probably due to partial hydrolysis of copper ion under the extraction conditions.

The sulfonamides II–IV (H_2L) have two amide protons in neighboring positions, and the conjugate bases (dianions) behave as bidentate ligands to form five- or six-membered chelate complexes with divalent metal ions [21]. Though the complexes are electrically neutral, they are usually not lipophilic enough to be extracted, because the coordination sites of the divalent metals are not filled with a single bidentate ligand. However, by replacing the water in the rest of the coordination sphere with lipophilic neutral ligands, the complexes could be made extractable. The reaction is described by



$$K_{\text{ex}} = [\text{MLA}_m]_{\text{o}} [\text{H}^+]_{\text{w}}^2 / [\text{H}_2\text{L}]_{\text{o}} [\text{A}]_{\text{o}}^m [\text{M}^{2+}]_{\text{w}} \quad (5)$$

TABLE 1

Linear relation between $\log D$ and pH in the extraction of divalent metals into chloro-benzene with compound I ($\log D = \alpha \text{pH} + \beta$)^a

M^{2+}	n	α	β	S.d.	$\text{pH}_{1/2}$ ^b	$\log K_{\text{ex}}$ ^c	$\log K_{\text{ex}}$ ^d
Cu	4	2.2	-5.5	0.105	2.3	-1.0	-0.1
Zn	4	2.1	-11.4	0.038	5.4	-7.2	-6.8
Co	4	2.1	-13.6	0.058	6.6	-9.6	-9.0
Cd	5	2.0	-11.5	0.179	5.9	-8.2	-9.2
Pb	5	1.7	-10.9	0.021	6.3	-9.0	—

^a $[\text{M}^{2+}]_{\text{w}} = 7.2\text{--}8.5 \times 10^{-5} \text{ M}$ and $[\text{HL}]_{\text{o}} = 1.6 \times 10^{-2} \text{ M}$ before extraction; 0.10 M KNO_3 , 25°C. The number of data points is indicated by n ; s.d. means standard deviation. ^b Half-extraction pH ($\log D = 0$). ^c $\log K_{\text{ex}} = -2 \log [\text{HL}]_{\text{o}} - 2 \text{pH}_{1/2}$. ^d Extraction into kerosene [21].

where A denotes a neutral ligand such as 4-benzylpyridine or 1,2-bis(hexylthio)ethane. When a large molar excess of sulfonamide reagent and auxiliary neutral ligand are used, the extraction of metal ions can be described by

$$\log D = \log K_{\text{ex}} + \log [\text{H}_2\text{L}]_0 + m \log [\text{A}]_0 + 2 \text{ pH} \quad (6)$$

where $[\text{H}_2\text{L}]_0$ and $[\text{A}]_0$ are practically constant, and $\log D$ varies linearly with the pH of the medium giving a slope of 2. Tables 2–4 summarize the experimental results.

Some extractions listed in Tables 2–4 were done in appreciably acidic pH regions. As 4-benzylpyridine is basic, its distribution into the aqueous phase in its conjugate acid form had to be considered under such conditions. The perchlorate salt of 4-benzylpyridinium ($\text{AH}^+ \cdot \text{ClO}_4$) was titrated potentiometrically, and the acidity constant was found to be $\text{p}K_a = 5.70 \pm 0.05$ ($\mu = 0.10$ KCl, $25.0 \pm 0.1^\circ\text{C}$). The distribution constant ($[\text{A}]_w/[\text{A}]_o$) between aqueous 0.10 M KCl and chlorobenzene was found to be 1.1×10^{-3} . Calculation showed that the distribution of 4-benzylpyridine from chlorobenzene to aqueous solution was less than 6% at pH 4. Thus, the acidity of the medium could affect the linearity of the $\log D$ vs. pH plots only for copper and only to a negligible extent. The cation (AH^+) was quite hydrophilic and did not distribute to organic solution as trioctylmethylammonium did (see below).

In order to evaluate the m value in Eqn. (6), the extraction of the metal into chlorobenzene was measured at varying concentrations of 4-benzylpyridine while the pH was kept constant. At concentrations of 1.6×10^{-2} M II, 7.2 – 8.5×10^{-5} M metal salt and 0.10 M potassium nitrate, the concentra-

TABLE 2

Linear relationship between $\log D$ and pH in the extraction of divalent metals with compound II and 4-benzylpyridine ($\log D = \alpha \text{ pH} + \beta$)

M^{2+}	Solvent	n^a	α	β	S.d.	$\text{pH}_{1/2}$	$\log K_{\text{ex}}^b$
Cu	$\text{C}_6\text{H}_5\text{Cl}^c$	5	2.1	-9.2	0.143	4.5	-4.8
Zn	$\text{C}_6\text{H}_5\text{Cl}^c$	4	1.9	-9.8	0.181	5.2	-6.2
Co	$\text{C}_6\text{H}_5\text{Cl}^c$	5	1.9	-11.7	0.079	6.2	-8.2
Cd	$\text{C}_6\text{H}_5\text{Cl}^c$	6	1.9	-14.1	0.055	7.5	-10.8
Pb	$\text{C}_6\text{H}_5\text{Cl}^c$	5	2.1	-11.5	0.030	5.4	-6.6
Cu	$\text{C}_6\text{H}_5\text{CH}_3^d$	7	1.8	-7.7	0.015	4.3	-4.7
Cu	$\text{C}_6\text{H}_5\text{CH}_3^e$	4	1.8	-9.7	0.018	5.5	-7.6
Zn	$\text{C}_6\text{H}_5\text{CH}_3^d$	7	2.0	-10.2	0.013	5.0	-6.1
Co	$\text{C}_6\text{H}_5\text{CH}_3^d$	6	1.8	-10.7	0.009	6.1	-8.3
Cd	$\text{C}_6\text{H}_5\text{CH}_3^d$	4	1.7	-11.6	0.021	7.1	-10

^aFor the meaning of n , s.d., and $\text{pH}_{1/2}$, see Table 1. ^b $\log K_{\text{ex}} = -\log [\text{H}_2\text{L}]_0 - m \log [\text{A}]_0 - 2 \text{ pH}_{1/2}$; $m = 2$ for 4-benzylpyridine and $m = 1$ for 1,2-bis(hexylthio)ethane.

^c $[\text{M}^{2+}]_w = 7.2$ – 8.5×10^{-5} M, $[\text{H}_2\text{L}]_0 = 1.6 \times 10^{-2}$ M, and $[\text{4-benzylpyridine}]_0 = 6.4 \times 10^{-2}$ M in chlorobenzene; 0.10 M KNO_3 , 25°C . ^d $[\text{M}^{2+}]_w = 1 \times 10^{-4}$ M, $[\text{H}_2\text{L}]_0 = 2 \times 10^{-2}$ M, and $[\text{4-benzylpyridine}]_0 = 8 \times 10^{-2}$ M in toluene; 0.10 M KNO_3 , 25°C . ^e $[\text{H}_2\text{L}]_0 = 2 \times 10^{-2}$ M and $[\text{1,2-bis(hexylthio)ethane}]_0 = 2 \times 10^{-2}$ M in toluene; 0.10 M KNO_3 , 25°C .

TABLE 3

Linear relation between $\log D$ and pH in the extraction of divalent metals with compound III and 4-benzylpyridine ($\log D = \alpha \text{ pH} + \beta$)^a

M ²⁺	Solvent	<i>n</i>	α	β	S.d.	pH _{1/2}	$\log K_{\text{ex}}$
Cu	C ₆ H ₅ Cl	6	1.7	-7.2	0.034	4.3	-4.4
Zn	C ₆ H ₅ Cl	5	1.8	-11.3	0.109	6.4	-8.6
Co	C ₆ H ₅ Cl	4	1.8	-13.5	0.097	7.3	-10.4
Cd	C ₆ H ₅ Cl	4	1.7	-11.9	0.034	7.2	-10.2
Cu	C ₆ H ₅ CH ₃	6	1.7	-7.4	0.035	4.3	-4.7
Zn	C ₆ H ₅ CH ₃	6	2.1	-12.4	0.019	6.0	-8.1

^aRefer to Table 2 for the conditions and data treatment; no extraction of Pb.

tion of 4-benzylpyridine was varied from 10⁻¹ to 10⁻⁴ M, and the distribution ratio of the metal was measured. The *m* values were obtained from the slope of the plots $\log D - \log [4\text{-benzylpyridine}]_0$ with the following results: metal ion, *m* value (pH at which the measurements were made); Cu, 1.3 (5.8); Zn, 1.4 (6.7); Co, 1.5 (7.8); Cd, 1.2 (8.2); Pb, 0.9 (5.4). The plots were rather scattered with the standard deviation in the range 0.109–0.353. There is also some uncertainty about the association or acid-base neutralization reaction between compound II and 4-benzylpyridine in the organic solution, because II is appreciably acidic as is discussed later. In consideration also of the composition of the isolated complexes (see below), it is deemed reasonable that the *m* value is two.

The H₂L-type sulfonamides also proved to extract divalent metals in a different manner from Eqn. (4). The extraction behavior was studied in a manner similar to the above, i.e., by using an excess of both sulfonamide and auxiliary reagent (trioctylmethylammonium chloride, Aliquat-336S Q⁺Cl⁻). The distribution ratio of the metals was analyzed as a function of pH, and the results are summarized in Table 5. The plots of $\log D$ vs. pH gave fairly good straight lines with slopes ranging from 2.0 to 3.9, suggesting that under

TABLE 4

Linear relation between $\log D$ and pH in the extraction of divalent metals into chlorobenzene with compound IV and 4-benzylpyridine ($\log D = \alpha \text{ pH} + \beta$)^a

M ²⁺	<i>n</i>	α	β	S.d.	pH _{1/2}
Cu	14	1.2	-5.6	0.165	4.8
Zn	8	1.8	-12.5	0.042	7.0
Co	8	1.3	-10.8	0.082	(8.3) ^b

^aRefer to Table 2 for the conditions; no extraction of Cd and Pb. 1-Octanesulfonamido-2-naphthol (X) did not extract any metals. ^b52% extraction at pH 8.3. The extraction leveled off above this pH.

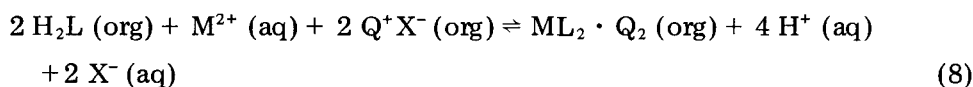
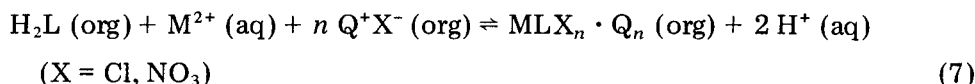
TABLE 5

Linear relation between $\log D$ and pH in the extraction of divalent metals with diprotonated bidentate sulfonamide reagents in the presence of trioctylmethylammonium chloride (Aliquat 336S) ($\log D = \alpha \text{ pH} + \beta$)^{a,b}

H ₂ L	M ²⁺	Solvent	<i>n</i>	α	β	S.d.	pH _{1/2}
II	Zn	C ₆ H ₅ Cl	22	2.5	-13.2	0.240	5.3
II	Cu	C ₆ H ₅ CH ₃	4	3.1	-14.5	0.058	4.7
II	Zn	C ₆ H ₅ CH ₃	5	3.9	-19.9	0.044	5.1
III	Cu	C ₆ H ₅ CH ₃	2	2.5	-16.5	—	6.5
IV	Cu	C ₆ H ₅ Cl	17	3.3	-15.2	0.190	4.7
IV	Zn	C ₆ H ₅ Cl	14	2.2	-13.6	0.184	6.1
IV	Co	C ₆ H ₅ Cl	9	2.2	-15.9	0.060	7.1
IV	Pb	C ₆ H ₅ Cl	10	2.0	-9.8	0.036	4.9

^a[M²⁺]_w = 7.2–8.5 × 10⁻⁵ M, [H₂L]_o = 1.6 × 10⁻² M, and [Aliquat]_o = 6.2 × 10⁻² M in chlorobenzene; [M²⁺]_w = 1 × 10⁻⁴ M, [H₂L]_o = 2 × 10⁻² M, and [Aliquat]_o = 1 × 10⁻² M in toluene; 0.10 M KNO₃, 25 °C. ^bFor the meaning of *n*, s.d., and pH_{1/2}, see Table 1.

the extraction conditions, the reactions were



Some metals were extracted even in the absence of Aliquat-336S. In the extraction of copper into toluene, the extraction was straightforward without Aliquat-336S (Table 6). However, in the extraction of zinc into toluene, distinct, white precipitates were formed in the aqueous phase at pH above 6.2; on standing, these coagulated onto the aqueous–organic interface. The precipitates were not the metal hydroxide and were solubilized into toluene

TABLE 6

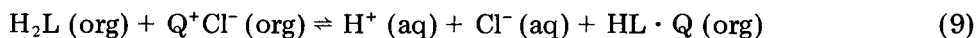
Linear relation between $\log D$ and pH in the extraction of divalent metals with compound II in the absence of auxiliary reagent ($\log D = \alpha \text{ pH} + \beta$)^a

M ²⁺	Solvent	Conc. of II (M)	<i>n</i>	α	β	S.d.	pH _{1/2}
Cu	C ₆ H ₅ CH ₃	0.02	4	4.2	-25.5	0.190	6.0
Zn	C ₆ H ₅ Cl	0.01	36	2.7	-21.7	0.287	8.0
Zn	C ₆ H ₅ Cl	0.03	38	3.1	-23.8	0.290	7.7
Zn	C ₆ H ₅ Cl	0.10	24	3.1	-22.8	0.210	7.4

^a[Cu²⁺]_w = 1 × 10⁻⁴ M, [Zn²⁺]_w = 0.8 × 10⁻⁴ M; 0.10 M KNO₃, 25 °C.

by the addition of Aliquat-336S. When chlorobenzene was used as the extraction solvent, the behavior was somewhat different from the above result. Copper was extracted only in the presence of Aliquat-336S, while zinc was extracted both in the absence and in the presence of Aliquat-336S. Interestingly, zinc formed white precipitates at pH above 6 (in the absence of Aliquat-336S), but they disappeared on the addition of potassium nitrate (0.10 M for ionic strength adjustment), helping to complete the extraction of zinc. No evidence is available at present for the structure of the precipitates, but the hydrated zinc complex of II, $\text{ZnL}(\text{H}_2\text{O})_n$, is a possibility. The effect of potassium nitrate may include the extraction of a $\text{ZnL}_2 \cdot \text{K}_2$ type complex which is similar to $\text{ML}_2 \cdot \text{Q}_2$ in Eqn. (8) but the ammonium ion is replaced by potassium. The extraction of metals by compound II without auxiliary reagents is summarized in Table 6.

In the system involving the reaction (7) or (8), one should consider the presence of HL^- or $\text{HL} \cdot \text{Q}$ species in appreciable concentration in the organic phase in the presence of Aliquat-336S. Dibasic sulfonamides II and IV were thus titrated with a standard aqueous base in a water-chlorobenzene heterogeneous mixture in order to evaluate the extent of acid dissociation:



$$K_a = [\text{H}^+]_w [\text{Cl}^-]_w [\text{HL} \cdot \text{Q}]_o / [\text{H}_2\text{L}]_o [\text{Q}^+\text{Cl}^-]_o \quad (10)$$

The titration data indicated that in the absence of Aliquat-336s the sulfonamide H_2L did not behave as an acid at all. In the presence of Aliquat-336s, however, the sulfonamide behaved as a monobasic acid of medium strength, giving a distinct dissociation constant defined by Eqn. (10). No further proton dissociation from HL^- was experimentally indicated. The constants determined for the water-chlorobenzene system at $\mu = 0.10$ (KCl), $[\text{Aliquat}]_o = 0.04$ M, and $25.0 \pm 0.1^\circ\text{C}$ were 5.40 ± 0.05 for compound II and 8.70 ± 0.05 for compound IV in $\text{p}K_a$ unit. An increase (decrease) in the Aliquat-336S concentration led, as expected, to an enhanced (suppressed) acid dissociation in the pH-titration curve. However, the acidity constant was not constant, suggesting that the constant calculated from Eqn. (10) was conditional. A complexity in the association-dissociation equilibria of ion-pairs in the organic phase could be responsible.

The extraction of mercury(II) was especially easy with the sulfonamide reagents, as is summarized in Table 7. The half-extraction pH with compound I could not be experimentally determined because the extraction into chlorobenzene was complete even at pH 1. Auxiliary reagents were not required for the extraction with compounds II-IV, and the $\log D$ vs. pH relation gave lines with unit slopes. The effect of anionic species in the extraction system was not studied. The concentration of chloride ion varied between 10^{-2} and 10^{-4} M around the half-extraction pH in Table 7.

TABLE 7

Extraction of mercury(II) into chlorobenzene with sulfonamide reagents ($\log D = \alpha \text{ pH} + \beta$)^a

Reagent	<i>n</i>	α	β	S.d.	pH _{1/2}
I					<1
II	13	1.2	-3.4	0.187	2.9
III	24	0.9	-2.4	0.247	2.7
IV	17	0.9	-3.1	0.213	3.4

^a[Hg²⁺]_w = 5×10^{-7} M, [H₂L]_o = 1.6×10^{-2} M, μ = 0.10 (KNO₃-HCl), 25°C.

Separation of metal ions by using sulfonamide reagent

The mutual separation of copper and zinc in a liquid membrane separation device was achieved by using compound I as a mobile metal carrier. The experimental set-up was similar to those described elsewhere [25, 26]. A glass cell with two compartments separated by a micro-porous polypropylene film (Duragard 2500; Polyplastics) was used, and a kerosene solution containing 2×10^{-2} M I was applied onto the membrane. A pH-controlled aqueous solution containing copper nitrate and zinc nitrate both at 1×10^{-3} M concentration was placed in one compartment of the cell, and a dilute nitric acid (pH 1) was placed in the other. The solutions were stirred magnetically, and the transport of metal ions through the membrane was measured at 25°C at appropriate time intervals. Table 8 summarizes the results in terms of the initial flux of metal ions through the membrane. A period of 10 h was required for the transport of over 90% of copper from one compartment to the other. It is seen that the flux of copper was high even at pH 4, while the flux of zinc remained zero. Thus, the extraction selectivity of compound I was adequately reflected in the membrane separation device, in which I served as a selective carrier for copper.

A selective extraction of copper from an aqueous solution containing 100-fold amounts of iron was studied. A 2×10^{-4} M copper nitrate solution

TABLE 8

Flux of metal transport through kerosene liquid membrane by using compound I as carrier^a

pH	Flux ($\mu\text{g cm}^{-2} \text{ min}^{-1}$)	
	Cu	Zn
4.0	1.05	0.00
4.5	1.10	0.05
4.9	1.05	0.16

^aInitial flux, 0.5–1 h after the initiation of transport; see text for detailed conditions. Flux is expressed as μg of metal/cm² of membrane/min.

(10 ml) containing 2×10^{-2} M iron(III) nitrate was shaken with 5 ml of benzene solution containing 2×10^{-2} M 8-(*p*-toluenesulfonamido)-quinoline for 0.5–1 h. The pH of the aqueous solution was adjusted to 1–2 by adding nitric acid. The aqueous solution was separated by centrifugation and copper and iron were measured. The fractions of copper extracted were 0.44 (pH 1.4), 0.77 (1.7), 0.89 (1.9), and 0.93 (2.0), while no extraction of iron took place. Similar results were obtained by using compound I, but I behaved slightly differently from the *p*-toluenesulfonamido derivative, extracting iron at pH above 3 in somewhat irregular manner. The phenomena will be discussed separately elsewhere.

Isolation of metal complexes

The metal complexes were obtained by allowing the sulfonamides and, when necessary, other complexing agents to react with metal salts in the presence of a suitable base. Water, methanol, acetone, dioxane or a mixture thereof was used as the reaction medium. Complexes usually separated out from the reaction mixture as crystalline solids, which were often analytically pure without further treatment. Those derived from monoprotonated, bidentate ligands like I were recrystallizable from an appropriate solvent. Complexes were characterized and identified by elemental analysis, and infrared and ^1H -n.m.r. spectroscopy.

Various sulfonamide derivatives (methane-, ethane-, butane-, and *p*-toluenesulfonamides) were prepared besides compound I from 8-aminoquinoline, and they all produced the corresponding divalent metal (Co, Ni, Cu, Zn) complexes readily on reaction with the acetate salt of the metals or with another salt in acetate-buffered medium. Except for nickel, the metal chelates separated from the reaction mixture either without inclusion of crystal water or with inclusion of crystal water which was readily lost on standing. Nickel complexes, which were usually obtained as greenish crystalline solids (octahedral complexes), kept crystal water (or coordination water) rather strongly, and were not soluble in non-polar organic solvents. This partially accounted for the fact that nickel was very slowly extracted by compound I. Heating the isolated green complexes often removed the coordination water, and the brownish complexes (tetragonal complexes) then obtained were soluble in non-polar organic solvents. For the lower family of 8-alkanesulfonamido-quinolines, the isolated metal complexes decomposed on heating without melting, but compound I formed a copper complex which showed a definite melting point at 157–160°C. Iron(III) reacted with 8-alkane-sulfonamido-quinolines in acetate-buffered media, but gave no well-defined complexes. There was no indication for complex formation with alkaline earth metals or aluminum.

Only copper complexes were obtained from the sulfonamides (HL; methane-, butane-, and *p*-toluenesulfonamides) of *o*-methylthioaniline. The sulfonamide and a copper salt reacted in a stoichiometric ratio in ammoniacal methanol. The precipitates formed were collected and dried in vacuo to give dark blue crystalline solids which showed the composition CuL_2 .

The sulfonamides IX and XI (H_2L) formed MLA_n -type complexes with divalent metals, where A denotes uncharged, uni- or bi-dentate ligands. The complexes isolated and fully identified are summarized in Table 9. The preparation of metal complexes from XI was not worked through in detail because the complexes were very soluble in the reaction medium, which made their isolation difficult.

DISCUSSION

For use in large-scale hydrometallurgical applications, metal extraction agents should have a high lipophilicity or a high solubility in hydrocarbon solvents. In the present type of sulfonamide reagents, the lipophilicity is readily afforded by using long-chain alkane- or arene-sulfonyl functional groups such as 4-dodecylbenzenesulfonyl [16–19, 21]. However, the preparation of such compounds suffers inevitably from impurities originating in the preparative reactions, because satisfactory methods are not available for purifying such large molecular-weight compounds, solid or oil, with high lipophilicity and low crystallinity, which are contaminated with impurities of similar nature. The reagents synthesized in the present study are endowed with sufficient lipophilicity, can be obtained in high purity, and are well suited to basic studies on the metal extraction behavior of sulfonamide chelating agents.

A strong affinity of compound I for copper in the metal extraction was indicated in Table 1 and adequately verified in the separation experiments. A similar behavior was suggested for compounds XII and XIII but not

TABLE 9

Divalent metal complexes of diprotonated bidentate sulfonamides^a

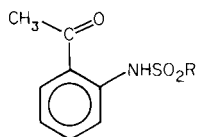
Sulfonamide H_2L	Metal complex, MLA_n		
	M	A_n	Color
IX	Cu	phen · 0.5 H_2O	blue
	Zn	1.5 phen · 0.5 H_2O ^b	yellow
	Ni	2 phen · 0.5 H_2O	yellow-brown
	Co	2 phen	red-brown
	Cu	2 NH_3	violet
	Zn	2 NH_3	white
	Ni	2.5 NH_3 · H_2O	violet
	Cu	en	dark-brown
	Zn	en	white
	Ni	en · 1/3 H_2O · 1/3 NH_3	violet
XI	Zn	2 NH_3	white

^aIdentified by elemental analysis, i.r., and 1H -n.m.r.; phen, 1,10-phenanthroline; en, ethylenediamine. ^bA fraction (0.5) of phen molecules is not coordinated in solution (1H -n.m.r.).

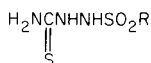
verified quantitatively, because the half-extraction pH of copper was very high and extraction of other metals could not be observed. In a search for other sulfonamide reagents, compounds XIV and XV were prepared and tested for metal extraction.

Sulfonamide XIV could not extract copper or other divalent metal ions. In fact, XIV ($R = \text{CH}_3$) formed crystalline complexes with copper, nickel, and zinc only in the presence of ammonia, where the carbonyl group in XIV was converted to an imino group in the reaction mixture [21]. The conversion of XIV to its imino homologue gives no profit in metal extraction, because the imino group is hydrophilic and tends to hydrolyze under the extraction conditions. Sulfonamide XV formed stable complexes with nickel and zinc, but not with copper because of some unidentified redox reaction between the metal and the ligand. Moreover, XV was highly crystalline ($R = p\text{-CH}_3\text{C}_6\text{H}_5$, m.p. $211\text{--}212^\circ\text{C}$; $R = n\text{-C}_8\text{H}_{17}$, m.p. $192\text{--}194^\circ\text{C}$) and sparingly soluble in non-polar solvents, and was not suitable for extraction studies.

In contrast to the high metal extraction ability and selectivity exemplified by compound I, sulfonamides II–IV showed only a moderate extraction

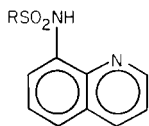


XIV ($R = n\text{-C}_8\text{H}_{17}$)

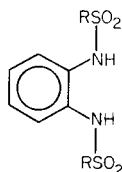


XV ($R = n\text{-C}_8\text{H}_{17}, p\text{-CH}_3\text{C}_6\text{H}_5$)

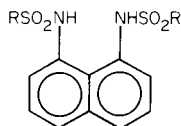
ability and selectivity among divalent metals. The exact reason for the lower metal selectivity is not clear at present, nor is the reason for the high selectivity of compound I toward copper. There are few N, N' - or N', N' -coordinating ligands with known complex stability constants, which makes it difficult to discuss and understand the extraction data on a firm basis. The stability constants of a structurally related chelating agent, 2-methanesulfonamido-methylpyridine (HL) in water were observed as follows [22]: metal ion, $\log ([\text{ML}_2]/[\text{M}^{2+}][\text{L}^-]^2)$; Cu, 17.7; Hg, 17.6; Pb, 12.3; Zn, 12.2; Ni, 12.1; Co, 11.1; Cd, 10.2. The trend of the stability is essentially in line with the extraction data of the present study (Tables 1 and 7). It is possible that the selectivity for copper and mercury is inherent to the N, N' -coordinating ligands. However, a somewhat different trend in the stability of divalent



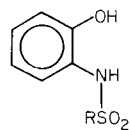
I



II



III



IV

$R = n\text{-C}_8\text{H}_{17}$

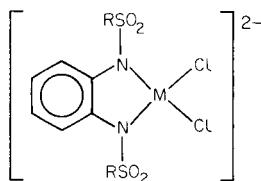
metal complexes has been reported for 2-(*p*-toluenesulfonamido)aniline [15], which had the stability constants in 50% (v/v) water-dioxane: Cu, 19.1; Ni, 18.9; Co, 18.7; Zn, 18.2. Thus, this chelating agent is characterized by a complete lack of metal selectivity.

The nature of reaction in which mercury is extracted by compounds II–IV is not clear. Though the plots of $\log D$ vs. pH were rather scattered, the observed slope of 0.9–1.2 strongly suggests that anionic species other than that of the sulfonamide are involved in the extraction. A possibility that the sulfonamide behaved as a singly-charged anion cannot be excluded. The high affinity of sulfonamides for mercury is no doubt related to the somewhat soft character of the N[−] donor atom, but the large ionic size of mercury must also be considered, because it relieves any inter-ligand steric hindrance in the coordination of the bulky sulfonamide anion to the metal.

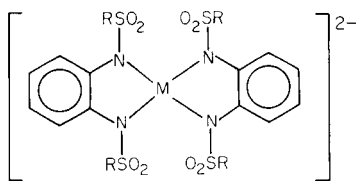
The divalent metal extraction by compounds II–IV in the presence of Aliquat-336S (Table 5) seems to proceed essentially by reactions (7) and (8). This yields slopes of 2 and 4 in the $\log D$ vs. pH plots for reactions (7) and (8), respectively. Here, however, it must be pointed out that the proton dissociation reaction (9) can be a complicating factor. However, a simple calculation shows that, around the pH region well below the pK_a values of the extraction agent (Eqn. 10), the change in reagent concentration, $[H_2L]_o$, caused by pH variation is small and does not seriously affect the observed slope of the $\log D$ vs. pH plots. The extraction of copper by compound II into toluene gave a slope of 3.1 and a $pH_{1/2}$ value of 4.7. Similarly, the extraction of copper by compound IV into chlorobenzene gave the values 3.3 and 4.7 for the slope and the $pH_{1/2}$, respectively. This means that more than two but less than four protons are released on extraction of one copper ion. The overlapping reactions (7) and (8) should result in such a behavior.

The extraction behavior in the presence of Aliquat-336S in the pH region near the pK_a values is difficult to treat in the quantitative manner. The proton dissociation (9) is expected, at least, to cause a decrease in the observed slope of the $\log D$ vs. pH plots because of the decrease in the proportion of H_2L species in the organic phase. From this angle, it is notable that all the observed slopes exceeded 2 (Table 5); this certainly reflects the contribution of reaction (8). It should be noted in passing that Aliquat-336S is known to extract some divalent metal ions itself by forming the corresponding chlorocomplexes. In that case, the $\log D$ vs. pH plots should give a zero slope, and in fact, the observed slope for the extraction of cadmium with compound II was around 0.03–0.10, indicating a negligible contribution of reactions (7) and (8).

As to the structure of the complexes extracted by reactions (7) and (8), formulae XVI and XVII, respectively, are postulated, though direct evidence has yet to be collected. In formula XVI, a four-coordinate model around the metal is assumed, but six-coordination cannot be excluded from the available data. A coordination structure of type XVII is quite popular in complexation with catechol and related phenolic chelating agents.



XVI



XVII

No conclusive comments can be made on the nature of the extraction with compound II in the absence of Aliquat-336S. The hydrolysis of metal ions must be considered, though precipitates of metal hydroxides were not detected under the extraction conditions. However, the extraction is real and reproducible as is shown in Table 6, and the slope of the log D vs. pH plot is definitely larger than 2. An extraction reaction similar to (8) may be suggested, in which the role of the quaternary ammonium ion is assumed by potassium ion in the aqueous phase.

The authors are grateful for a Grant-in-Aid for Scientific Research from the Ministry of Education, Science, and Culture of Japan (Project No. 543020).

REFERENCES

- 1 J. H. Billman, N. S. Janetos and R. Chernin, *Anal. Chem.*, **32** (1960) 1342.
- 2 J. H. Billman and R. Chernin, *Anal. Chem.*, **34** (1962) 408.
- 3 J. H. Billman and R. Chernin, *Anal. Chem.*, **36** (1964) 552.
- 4 D. T. Haworth and J. H. Muntoe, *Anal. Chem.*, **41** (1969) 529.
- 5 *Jpn. Pat.*, 25 (1965) 253; *Chem. Abstr.*, **64** (1966) 9640e.
- 6 V. M. Dziornko, *Sb. Statei, Vses. Nauchno-Issled. Inst. Khim. Reaktivov i Osobo Chistyykh Khim. Veshchestv*, No. 24 (1961) 9; *Chem. Abstr.*, **57** (1962) 4002e.
- 7 M. Katyal, G. Sharma and R. P. Singh, *J. Inst. Chem. (India)*, **40** (1968) 207; *Chem. Abstr.*, **70** (1969) 73863p.
- 8 E. A. Bozhevol'nov and G. V. Serebryakova, *Sb. Statei, Vses. Nauchno-Issled. Inst. Khim. Reaktivov i Osobo Chistyykh Khim. Veshchestv*, No. 24 (1961) 36; *Chem. Abstr.*, **57** (1962) 24b.
- 9 D. P. Shcherbov and V. V. Kolmogorova, *Metody Analiza Khim. Reaktivov i Preparatov*, Gos. Kom. Sov. Min. SSSR po Khim. No. 4 (1962) 125; *Chem. Abstr.*, **61** (1964) 2480d.
- 10 E. A. Bozhevol'nov, G. V. Serebryakova, V. M. Yanishevckava and S. U. Kreingol'd, *Acta Chim. Acad. Sci. Hung.*, **32** (1962) 199.
- 11 E. A. Bozhevol'nov and G. V. Serebryakova, *Metody Analiza Khim. Reaktivov i Preparatov*, Gos. Kom. Sov. Min. SSSR po Khim. No. 4 (1962) 120; *Chem. Abstr.*, **61** (1964) 3690c.
- 12 E. A. Bozhevol'nov, *Oesterr. Chem.-Ztg.*, **66** (1965) 74; *Chem. Abstr.*, **65** (1966) 7989.
- 13 G. V. Serebryakova, I. A. Krasavin, E. A. Bozhevol'nov and V. M. Dziomko, *Tr. Vses. Nauchno-Issled. Inst. Khim. Reaktivov Osobo Chist. Khim. Veshchestv*, **26** (1964) 97; *Chem. Abstr.*, **66** (1967) 72198f.
- 14 S. U. Kreingol'd, E. A. Bozhevol'nov and G. V. Serebryakova, *Tr. Vses. Nauchno-Issled. Inst. Khim. Reaktivov*, **25** (1963) 422; *Chem. Abstr.*, **61** (1964) 82a.
- 15 D. Betteridge and R. Rangaswamy, *Anal. Chim. Acta*, **42** (1968) 293.

- 16 G. A. Kordosky, K. D. MacKay and M. J. Virnig, *Trans. Soc. Min. Eng. AIME*, 262 (1977) 36.
- 17 M. J. Virnig, *International Solvent Extraction Conference, Toronto, Canada, 1977; Canadian Institute of Mining and Metallurgy, Special Volume*, 21 (1979) 535.
- 18 G. Barthel, *Tech. Mitt. Krupp, Werksber.*, 35 (1977) 73; *Chem. Abstr.*, 88 (1978) 92870b.
- 19 K. D. MacKay, *U.S. Pat.* 4239699; *Chem. Abstr.*, 94 (1981) 160463x.
- 20 M. J. Virnig and K. D. MacKay, *U. S. Pat.* 4160807; *Chem. Abstr.*, 91 (1979) 161021b.
- 21 M. Takagi, T. Omori, S. Matsuo, S. Matsuno, K. Ueno and S. Ide, *Chem. Lett.*, (1980) 387.
- 22 Y. Moriguchi, T. Yoshimatsu, M. Takagi and K. Ueno, *Bunseki Kagaku*, 31 (1982) 318.
- 23 B. S. Portnaya and I. I. Levkoev, *Zh. Organ. Khim.*, 1 (1965) 2202; *Chem. Abstr.*, 64 (1966) 12845d.
- 24 Y. Murakami and M. Takagi, *Bull. Chem. Soc. Jpn.*, 38 (1965) 828.
- 25 A. Ohki, M. Takagi and K. Ueno, *Chem. Lett.*, (1980) 1591.
- 26 S. Matsuno, A. Ohki, M. Takagi and K. Ueno, *Chem. Lett.*, (1981) 1543.

THE SUBSTITUENT EFFECT ON THE SYNERGIC EXTRACTION OF EUROPIUM AND SCANDIUM WITH 1-PHENYL-3-METHYL-4-ACYLPYRAZOL-5-ONE AND TRI-*n*-OCTYLPHOSPHINE OXIDE

KAZUE SASAYAMA, SHIGEO UMETANI and MASAKAZU MATSUI*

The Institute for Chemical Research, Kyoto University, Uji, Kyoto 611 (Japan)

(Received 9th August 1982)

SUMMARY

The substituent effect of several 1-phenyl-3-methyl-4-acylpyrazol-5-ones on the adduct formation between their europium and scandium chelates and tri-*n*-octylphosphine oxide (TOPO) in benzene was studied by liquid–liquid extraction. The europium acylpyrazolonates react with TOPO to form an adduct of the EuR_3L type for an aliphatic group and the EuR_3L_2 type for aromatic and trifluoromethyl groups. The stability of the adducts increases in the order aliphatic < aromatic < trifluoromethyl. A steric effect of the terminal group on adduct formation was observed for 2-, 3- and 4-methyl-substituted benzoylpyrazolonates of europium and especially scandium.

In the liquid–liquid extraction of metal β -diketonates, it is well known that the presence of a Lewis base such as TOPO enhances the extractability, because of adduct formation between the metal chelates and Lewis bases. Such synergism has been widely investigated, but steric hindrance by the terminal groups in the β -diketones has hardly been recognized [1]. It has been shown [2] that the extracted species of strontium with 4-acylpyrazol-5-ones and tri-*n*-octylphosphine oxide (TOPO) are $\text{SrR}_2(\text{TOPO})_2$ for 1-phenyl-3-methyl-4-benzoylpyrazol-5-one and $\text{SrR}_2(\text{TOPO})_3$ for 1-phenyl-3-methyl-4-trifluoroacetylpyrazol-5-one. This difference in adduct formation may be caused by the steric effect of the terminal group of the 4-acylpyrazol-5-ones. The present study is directed towards evaluation of the substituent effect, especially steric hindrance, on the synergic extraction of europium and scandium with 4-acylpyrazol-5-one derivatives.

EXPERIMENTAL

Materials

All the 4-acyl derivatives of 1-phenyl-3-methylpyrazol-5-one were prepared by the method of Jensen [3] from 1-phenyl-3-methylpyrazol-5-one and the corresponding acid chloride or anhydride. The compounds were recrystallized; their analytical data have been given in previous papers [4, 5]. Tri-*n*-octylphosphine oxide (TOPO; Dojindo Co.) was sufficiently pure to be used as

received. All other reagents were of reagent grade. Radioactive tracers $^{152,154}\text{Eu}$ and ^{46}Sc were obtained from the Radiochemical Centre, Amersham. Carrier solutions of europium and scandium were prepared by dissolving their oxides in hydrochloric acid.

Procedures

Extraction experiments were done in a thermostated room at $25 \pm 1^\circ\text{C}$. The organic solution (benzene) containing 4-acylpyrazol-5-one (0.01 or 0.02 M) and TOPO was placed in a stoppered 30-ml glass centrifuge tube with the aqueous solution containing the metal ion with the radioactive tracer, sodium perchlorate (0.1 M), sodium hydroxide or perchloric acid, and acetic acid—sodium acetate (0.02 M) buffer. The initial volume of each phase was 10 ml in all cases and the initial metal concentration was about 10^{-6} M. The two phases were shaken mechanically for 1 h; preliminary experiments indicated that a shaking time of 10 min was sufficient to attain the distribution equilibrium. After centrifugation, 2 ml of each phase was pipetted into test tubes, and the γ -radioactivities were measured with a NaI(Tl) well-type scintillation counter. The pH value of the aqueous phase was checked after extraction.

The extraction constants of the metal chelates, K_{ex} , and the stability constants of the metal chelate adducts, β_n , can be calculated by the following equations [6]:

$$K_{\text{ex}} = [\text{MR}_3]_{\text{o}} [\text{H}^+]^3 / [\text{M}^{3+}] [\text{HR}]_{\text{o}}^3 \quad (1)$$

$$\log K_{\text{ex}} = \log D - 3\log[\text{HR}]_{\text{o}} - 3\text{pH} \quad (2)$$

$$\beta_n = [\text{MR}_3\text{L}_n]_{\text{o}} / [\text{MR}_3]_{\text{o}} [\text{L}]_{\text{o}}^n \quad (3)$$

$$\log D^*/D = \log \left(1 + \sum_{n=1}^n \beta_n [\text{L}]_{\text{o}}^n \right) \quad (4)$$

where D and D^* are the distribution ratios in the absence and in the presence of TOPO; M stands for trivalent metal, HR for 4-acylpyrazol-5-one, and L for TOPO. Subscript o designates the concentration of the chemical species in the organic phase.

RESULTS AND DISCUSSION

Synergic extraction of europium

Extraction of europium with a 4-acylpyrazolone alone was reported previously [4, 5]; there was a linear relationship between the extraction constants of 4-acylpyrazolone, $\log K_{\text{ex}}$, and the dissociation constants of the extractant, $\text{p}K_{\text{a}}$, i.e., $\log K_{\text{ex}}$ decreased linearly as $\text{p}K_{\text{a}}$ increased [4], and the extraction of europium was enhanced when octanol was used as a solvent instead of benzene [5].

Synergic extraction of europium with 4-acylpyrazolones in the presence

of TOPO as a Lewis base was investigated here, in order to obtain detailed information on the effect of the terminal group of the extractants on the adduct formation between the europium chelates and TOPO. Typical $\log D$ (and $\log D^*$) vs. pH plots in the presence and absence of TOPO are illustrated in Fig. 1. Enhanced extraction was observed in the presence of 10^{-3} M TOPO.

Figure 2 shows typical plots of $\log D^*/D$ vs. $\log [\text{TOPO}]_0$, from which the stability constant of the adducts, β_n , can be calculated. Table 1 gives the values of β_n together with $\text{p}K_a$, $\text{pH}_{1/2}$, and $\log K_{\text{ex}}$. As shown in this Table, one molecule of the europium chelate binds only one molecule of TOPO for 4-aliphatic-substituted extractants, whereas it binds two molecules of TOPO for the 4-trifluoromethyl-substituted extractant. In the typical

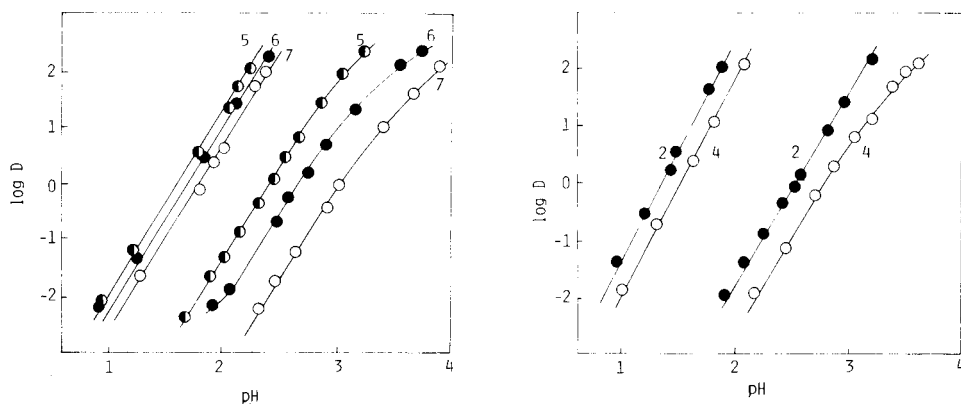


Fig. 1. Typical plots of $\log D$ vs. pH for europium(III). The numerals correspond to the reagent numbers in Table 1. Reagent: 2×10^{-2} M in benzene. Plots for reagents 2 and 4 are separated from the rest for clarity. In each block, the group of plots to the right was obtained in the absence of TOPO, and the plots to the left in the presence of 10^{-3} M TOPO.

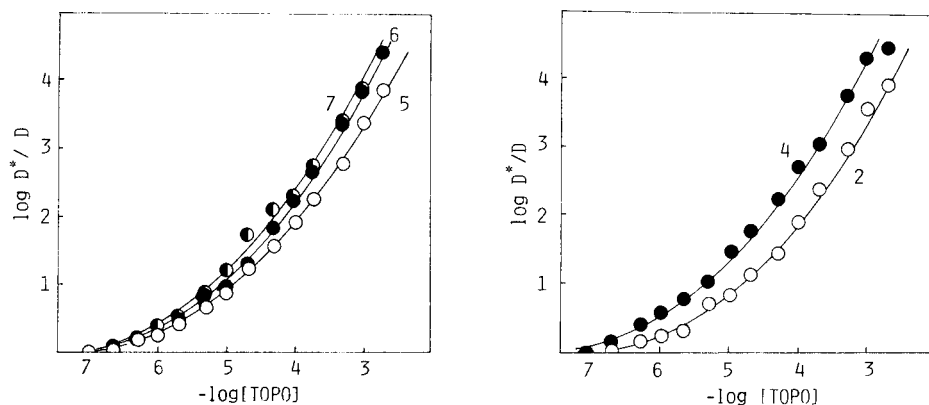


Fig. 2. Variation of the distribution ratio of europium(III) as a function of TOPO concentration. Reagent: 2×10^{-2} M in benzene.

TABLE 1

The extraction constants of europium 4-acylpyrazolonates and the stability constants of the adducts with TOPO

No.	R	pK_a	$pH_{1/2}$	$\log K_{ex}$	$\log \beta_1$	$\log \beta_2$
1	Phenyl	4.02 ^a	3.20	-4.50	6.10	10.40
2	2-Chlorophenyl	3.43 ^a	2.55	-2.55	5.65	10.05
3	2,4-Dichlorophenyl	3.24 ^a	2.46	-2.28	5.75	10.15
4	4-Chlorophenyl	3.75	2.85	-3.45	6.30	10.40
5	2-Methylphenyl	3.70 ^a	2.74	-3.12	5.80	9.30
6	3-Methylphenyl	4.08 ^a	3.00	-3.90	5.95	9.60
7	4-Methylphenyl	4.13 ^a	3.14	-4.32	6.00	10.10
8	2-Naphthyl	4.00 ^a	2.95	-3.75	6.00	10.30
9	Cyclohexyl	4.19 ^a	3.70	-6.00	6.20	—
10	n-Heptyl	3.99	3.70	-6.00	5.90	—
11	Methyl	4.10 ^b	3.74	-6.12	6.20	—
12	Trifluoromethyl	2.70 ^b	2.57	-2.61	7.05	12.70

^aAcidity constants from ref. 4. ^bAcidity constants from ref. 5.

β -diketonate system, the stability of the adducts formed increases in the following order: aliphatic groups (e.g., acetylacetone, dipivaloylmethane) < aromatic groups (e.g., benzoylacetone, dibenzoylmethane) < trifluoromethyl groups (e.g., trifluoroacetylacetone, thenoyltrifluoroacetone) [1]. Similarly, the adducts formed with unfluorinated 4-aliphatic-substituted pyrazolones are expected to be less stable than those formed with 4-aryl- or 4-trifluoromethyl-substituted pyrazolones. This is reflected by the reaction of one mole of TOPO with one mole of the europium chelate to form an EuR_3L adduct for the aliphatic-substituted pyrazolone system.

The general trend that the synergic effect increases in the order described above [1, 7] can also apply to the present system, i.e., a trifluoromethyl group strongly withdraws electrons between the metal ion and the acylpyrazolone, whereas an aromatic group gives a resonance effect to π -electrons of the chelate ring. Accordingly, when an alkyl group replaces an aromatic or trifluoromethyl group, the interaction between the metal and the ligand may weaken, and the residual coordinating power of the metal may increase. Such a situation would be favorable for adduct formation.

In β -diketonate systems, the extraction constant of the metal chelate, $\log K_{ex}$, was found to increase approximately linearly with an increase in the stability constant of the adduct formation, $\log \beta_1$ [1]. This implies that there is no steric hindrance by terminal groups on the adduct formation. However, similar trends could not be found in the relationship between $\log K_{ex}$ and $\log \beta_n$ in the acylpyrazolone adduct systems, as indicated in Table 1. In the set of methyl-substituted benzoylpyrazolone adducts, the $\log K_{ex}$ values decrease in the order 2-methylbenzoyl > 3-methylbenzoyl > 4-methylbenzoyl, but the order of the adduct stability, $\log \beta_1$ and $\log \beta_2$,

is the reverse. This unusual behavior may be caused by steric hindrance arising from the terminal group; rotation around the 4-substitution axis of pyrazolone is probably restrained by the interaction between the 3-methyl group of pyrazolone and the *o*- or *m*-methyl group of 4-benzoylpyrazolone. A similar effect is observed in 2- and 4-chlorobenzoylpyrazolones.

Synergic extraction of scandium

It is interesting to compare scandium with europium with regard to the terminal group effect on adduct formation, especially from the standpoint of the steric hindrance, because scandium has a considerably smaller ionic radius than europium. The steric effect of the *o*-, *m*-, and *p*-methyl-substituted benzoylpyrazolones on adduct formation between the scandium chelates and TOPO was therefore examined. Figure 3 shows the plots of $\log D$ (or $\log D^*$) vs. pH and the plots of $\log D^*/D$ vs. $-\log [\text{TOPO}]_0$ in the extraction of scandium. The values of $\log \beta_n$ were obtained graphically and are listed in Table 2. As shown, the terminal group effect on the adduct formation

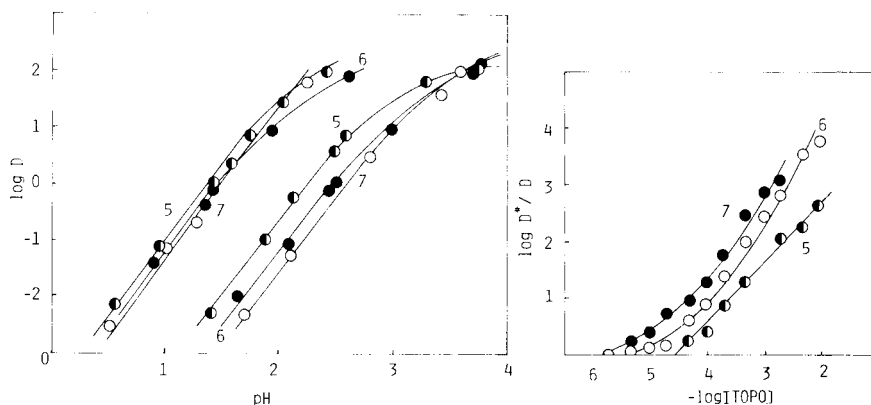


Fig. 3. Logarithm of the distribution ratio of scandium as (A) a function of pH and (B) a function of TOPO concentration for reagents 5–7 (2×10^{-4} M in benzene). In (A), the three plots to the right were obtained in the absence of TOPO, and the plots to the left in the presence of 10^{-3} M TOPO.

TABLE 2

The extraction constants of scandium 4-acylpyrazolonates and the stability constants of the adducts with TOPO

No.	R	pK_a	$pH_{1/2}$	$\log K_{ex}$	$\log \beta_1$	$\log \beta_2$
5	2-Methylphenyl	3.70	2.28	-4.26	4.50	—
6	3-Methylphenyl	4.08	2.52	-3.54	4.55	8.45
7	4-Methylphenyl	4.13	2.66	-3.12	5.10	8.75

between the scandium chelate and TOPO is unusual: the values of $\log \beta_n$ decrease as the methyl group bound to the 4-benzoyl ring gets nearer the coordinating bond between scandium and the ligand, and for the *o*-derivative only one mole of TOPO combines with one mole of the scandium chelate, though two moles of TOPO combine with one mole of the chelate for the other pyrazolones.

REFERENCES

- 1 T. Honjyo, Bull. Chem. Soc. Jpn., 42 (1969) 995.
- 2 S. Umetani, K. Sasayama and M. Matsui, Anal. Chim. Acta, 134 (1982) 327.
- 3 B. Jensen, Acta Chem. Scand., 13 (1959) 1668.
- 4 S. Umetani, M. Matsui, J. Tōei and T. Shigematsu, Anal. Chim. Acta, 113 (1980) 315.
- 5 M. Matsui, J. Tōei, S. Umetani and T. Shigematsu, Bull. Inst. Chem. Res., Kyoto Univ., 57 (1979) 337.
- 6 T. Shigematsu, M. Tabushi, M. Matsui and T. Honjyo, Bull. Chem. Soc. Jpn., 39 (1966) 165; 40 (1967) 2807.
- 7 K. Batzer, D. E. Goldbery and L. Newman, J. Inorg. Nucl. Chem., 29 (1967) 1511.

EXTRACTION OF TIN(IV) WITH SUBSTITUTED 8-QUINOLINOLS

A. M. GUTIERREZ*, R. GALLEG0 and A. SANZ-MEDEL^a

Departamento de Química Analítica, Facultad de Ciencias Químicas, Universidad Complutense, Madrid-3 (Spain)

(Received 30th July 1982)

SUMMARY

The extraction equilibria of tin(IV) between aqueous solutions and chloroform solutions of 8-quinolinol or its 5,7-dichloro and 2-methyl-5,7-dichloro derivatives, in the absence or presence of chloride are considered. The identity of the binary and ternary complexes responsible for the extraction of tin(IV) is established and, when possible, extraction and adduct formation constants in the organic phase are reported. These complexes were isolated in the solid state, and their u.v.–visible, i.r. and proton n.m.r. spectra are reported.

Although 8-quinolinol had been used for the extractive–spectrophotometric determination of tin(IV) [1, 2], contradictory conclusions have been reported, as several authors have claimed that this extraction is not possible [3–5]. Precipitation procedures have also been proposed [6]. The 5,7-dibromo-8-quinolinol derivative has also been used for the extractive–spectrophotometric determination of tin(IV) [3, 7], and a method has been proposed for the determination of tin(IV) with 5,7-dichloro-8-quinolinol [8]. However, as neither the extraction processes nor the nature of the complexes involved in the extraction of tin(IV) with 8-quinolinol and its halogen derivatives are yet well known, a detailed study of these areas was considered worthwhile.

The present paper is concerned with the equilibrium extraction of tin(IV) into chloroform solutions containing either 8-quinolinol (HQ), 5,7-dichloro-8-quinolinol (HCQ) or 2-methyl-5,7-dichloro-8-quinolinol (HMQ), alone or with chloride ions. The nature of the complexes responsible for the extraction of tin(IV) was established, some of the complexes were isolated in the solid state and their visible, i.r. and proton n.m.r. spectra were obtained. The metal distribution coefficients and the relative stabilities of the different complexes are reported and conflicting results found in the literature concerning tin(IV)-8-quinolinol extraction are clarified.

^aPresent address: Departamento de Química Analítica, Facultad de Ciencias, Universidad de Oviedo, Oviedo (Spain).

EXPERIMENTAL

Reagents and equipment

Standard tin(IV) solutions were freshly prepared by dilution of an 8.4×10^{-3} M stock solution obtained from tin metal and sulphuric acid. The tin content was checked gravimetrically. The reagents 5,7-dichloro and 2-methyl-5,7-dichloro-8-quinolinol were recrystallized from hot ethanol and dissolved in chloroform just prior to use. Sodium monochloroacetate (0.1 M), sodium acetate (0.5 M), and hexamethylenetetramine (2.5 M)—perchloric acid (0.2 M) buffers were used in the pH ranges 3–4, 4–6 and 6–8, respectively. The visible absorption spectra of the complexes obtained in the presence and absence of buffers, in any of the tested conditions, were identical in absorbance and wavelength of maximum absorption, indicating that any possible formation of different ternary complexes involving buffer ions was negligible. Other chemicals were of analytical grade and were used as received.

Hydrogen ion concentration was determined by a Metrohm pH meter, (model E-516) with a glass—calomel electrode pair (Metrohm UX-120). Visible and u.v. spectra were recorded with a Beckman DK-2A spectrophotometer and absorbances were measured with a Beckman DU spectrophotometer, using 10-mm cells. Infrared and proton n.m.r. spectra were recorded with a Perkin-Elmer 125 spectrometer and a Bruker HX-90 pulse spectrometer, respectively. A Perkin-Elmer 303 atomic absorption spectrometer, with an electrodeless-discharge lamp, was used for the determination of tin.

Extraction procedure

All complexes were extracted as follows: 10 ml of a 1% (w/v) solution of one of the chelating agents in chloroform was added to about 1 ml of the standard tin(IV) solutions contained in a 100-ml separating funnel. After gentle shaking, the halide solution was added, when required, to reach a final concentration of 0.2 M and the pH was adjusted by addition of ammonia and the appropriate buffer solution; the aqueous phase was then diluted to 10 ml (resulting in a maximum tin concentration of 8.4×10^{-5} M). Finally, the extraction was done by vigorous manual shaking of the funnel for 4–10 min, depending on the experiment. After phase separation, atomic absorption spectrometry was used to determine the tin content of the organic phase by evaporation of the organic solvent or by back-extraction into an aqueous 0.1 M sodium fluoride solution.

Preparation of solid complexes

Bischloro-bis(8-quinolinato)tin(IV) $[\text{Cl}_2\text{SnQ}_2]$ was prepared by precipitation following the method of Hamaguchi and Ikeda [6]. (Found 45.2% C, 2.8% H, 5.9% N, 13.2% Cl, 25.1% Sn; calculated 45.2% C, 2.5% H, 5.9% N, 14.8% Cl, 24.8% Sn.)

Bischloro-bis(5,7-dichloro-8-quinolinato)tin(IV) $[\text{Cl}_2\text{Sn}(\text{CQ})_2]$ was obtained as follows: a 4.2×10^{-3} M tin(IV) solution, 0.04 M in ammonium

chloride and 1.7 M in sulphuric acid, was mixed with a 6.2×10^{-2} M solution of 5,7-dichloro-8-quinolinol in 1.7 M sulphuric acid. The mixture was maintained at 100°C for 2 h. The solid obtained was filtered off, washed with 3.5 M sulphuric acid and water, and finally dried and recrystallized from methanol. (Found 34.7% C, 1.35% H, 4.7% N, 34.4% Cl, 19.8% Sn; calculated 35.1% C, 1.29% H, 4.5% N, 34.6% Cl, 19.3% Sn.)

Bischloro-bis(2-methyl-5,7-dichloro-8-quinolinato)tin(IV) $[\text{Cl}_2\text{Sn}(\text{MQ})_2]$ was obtained by a precipitation procedure analogous to the preceding one. (Found 36.8% C, 1.85% H, 4.3% N, 32.2% Cl, 19.1% Sn; calculated 37.3% C, 1.9% H, 4.35% N, 33.1% Cl, 18.4% Sn.)

A mixture of oxobis(5,7-dichloro-8-quinolinato)tin(IV) $[\text{SnO}(\text{CQ})_2]$ and its self-adduct $[\text{SnO}(\text{CQ})_2 \cdot \text{HCQ}]$ was obtained when the extraction procedure described above was applied to an 8.4×10^{-3} M tin(IV) solution at pH 2 and the chloroform was evaporated. These complexes are termed I and II, respectively. The yellow solid was purified by washing with hot methanol and dried at 60°C . (Found 39.3% C, 1.6% H, 5.3% N, 25.6% Cl; calculated for I, 38.5% C, 1.4% H, 5.0% N, 25.3% Cl; calculated for II, 41.8% C, 1.7% H, 5.4% N, 27.5% Cl).

Establishment of stoichiometry

The stoichiometry of highly dissociated complexes cannot be obtained by the usual spectrophotometric methods, e.g., continuous variations, mole ratio and slope ratio methods. The methods of Asmus [9] and Edmonds and Birnbaum [10] were applied to obtain the stoichiometry of all the complexes studied. Slope analysis [11, 12] was also used, which was decisive for establishing reliable stoichiometries. In this method, the extraction data were used to obtain plots of $\log D$ (distribution ratio of tin(IV)) against the logarithm of the concentration of one of the species, chelating agent, halide, or H^+ , whilst the other two were kept constant.

RESULTS AND DISCUSSION

Tin(IV)—8-quinolinol binary complex

The visible spectrum of this complex is shown in Fig. 1 (curve I). The range of pH that corresponds to maximum absorption was found to be 2.5–5.5. This agrees well with the results of Gentry and Sherrington [1] who, in contrast to Ruf [3], affirmed that extraction is possible in this range. This discrepancy is connected with the order of addition of reactants, which was found here to play an important role in the extraction. In fact, if the pH of the aqueous phase is adjusted before the addition of the complexing agent, no extraction is achieved. Hydrolysis of tin(IV), occurring at $\text{pH} > 0.5$ is likely to be the reason.

A ternary complex with chloride is extractable at lower pH values [2] with improved selectivity of extraction. Therefore, the main trend of this investigation was directed towards ternary complexes.

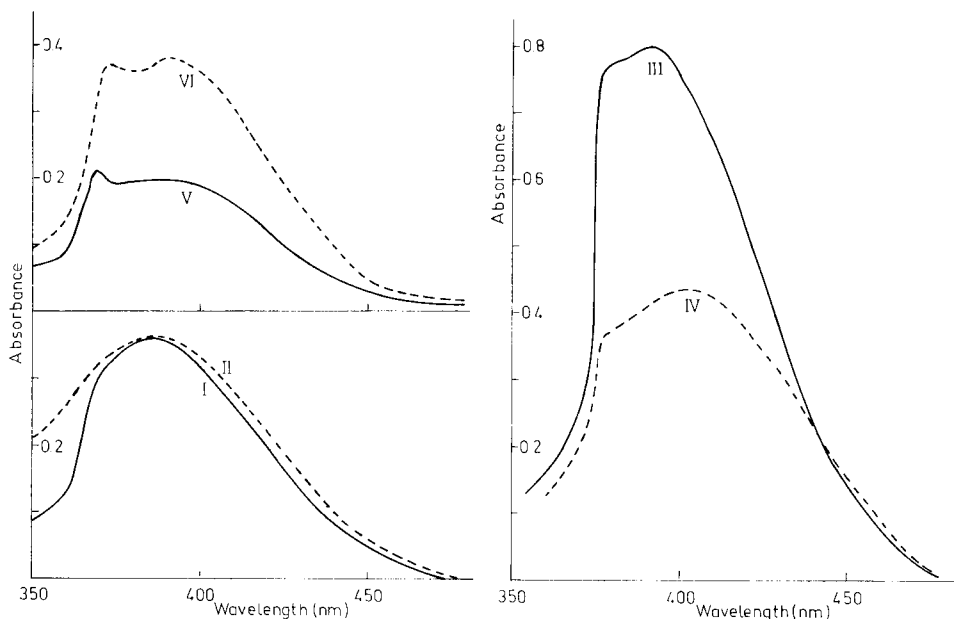


Fig. 1. Visible absorption spectra of the tin(IV) complexes extracted with the following reagents: (I) HQ; (II) HQ and Cl^- ; (III) HCQ; (IV) HCQ and Cl^- ; (V) HMQ; (VI) HMQ and Cl^- . The corresponding values of λ_{max} (nm) and ϵ ($10^3 \text{ l mol}^{-1} \text{ cm}^{-1}$) are 385, 385, 390, 403, 390, 390 and 4.6, 4.6, 12, 4.7, 2.5, 5.3, respectively.

Tin(IV)—8-quinolinol—chloride ternary complex

The visible spectrum, pH range of maximum extraction and apparent molar absorptivity of the species extracted in the presence of chloride ions were reported previously [2]. Nevertheless, a clear distinction between different extractable binary and ternary complexes has not been made. Figure 1 shows that the visible spectra of both complexes have a different shape. For the ternary complex the pH range of maximum absorbance is 0.65–1.5 (above pH 1.5 only the binary complex is extracted, as deduced from the shape of the spectra).

The stoichiometry obtained by the above-mentioned methods [9, 10] gave a consistent metal to ligand ratio of 1:2. Slope analysis, involving plots of $\log D$ vs. $\log [\text{HQ}]_0$ at constant pH and chloride concentration, yielded a straight line of slope 2, confirming the ratio obtained above.

The infrared spectrum of the solid species, the so-called SnQ_2Cl_2 shows an absorption band at 1100 cm^{-1} characteristic of metal chelates with 8-quinolinol [13]. The bands assignable to OH bending vibrations at 705 and 1280 cm^{-1} had disappeared in the complex indicating that this group is involved in the coordination (Fig. 2-I). In the proton n.m.r. spectrum at -40°C , the appearance of tin satellite lines proves that a tin complex has been formed. Lines are also shifted downfield compared with their positions in the free 8-quinolinol spectrum. The absence of free 8-quinolinol in the purified complex is proved by the absence of the corresponding lines in the proton

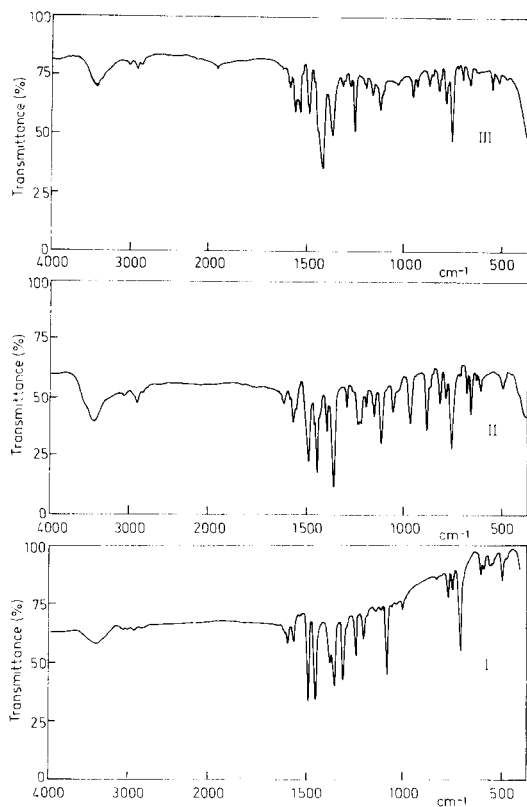
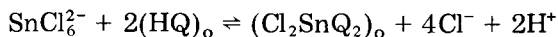


Fig. 2. Infrared spectra of the solid tin(IV) complexes: (I) Cl_2SnQ_2 ; (II) $\text{Cl}_2\text{Sn}(\text{CQ})_2$; (III) $\text{Cl}_2\text{Sn}(\text{MQ})_2$.

n.m.r. spectrum. (A complete analysis of the n.m.r. spectra of these complexes will be published elsewhere). The visible absorption spectrum and the molar absorptivity of this solid when dissolved into chloroform are identical to the ones obtained for the extracted species in the presence of chloride ions. This proves that both complexes are the same. The empirical formula (that agrees with tentative results reported by Eberle and Lerner [2]) obtained by elemental analysis of the solid complex corresponds to Cl_2SnQ_2 .

From these data, and because the predominant initial tin species under the conditions used is SnCl_6^{2-} [14], the following extraction equilibrium may be proposed:

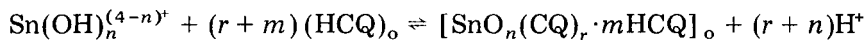


where subscript o indicates the organic phase. The conditional equilibrium constant obtained from the slope analysis experiments was $\log K_{\text{ex}} = 2.5 \pm 0.2$.

Tin(IV)—5,7-dichloro-8-quinolinol binary complex

Evidence for the formation of this complex at $\text{pH} > 1$ has been reported previously [8]. Its spectrum is given in Fig. 1 (curve III). The metal/ligand

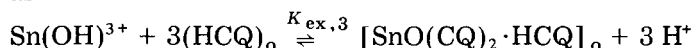
ratio, obtained by the first two above-mentioned methods was 1:2. When the slope analysis method was applied, the results shown in Fig. 3(a) were obtained. It can be seen that the slope was 2 at low ligand concentrations but increases with increasing reagent concentration, reaching a final value of about 3. This can be assigned to the formation of a self-adduct [15] at higher ligand concentrations. The extraction stoichiometry can be expressed in this case as



The distribution ratio, D , is given by

$$D = [\text{Sn}]_o / [\text{Sn}] = K_{\text{ex}} [\text{HCQ}]_o^{r+m} / [\text{H}^+]^{r+n}$$

The measured values for r and $r+m$ were 2 and 3, respectively, so that m and n are both 1. Hence, the tin complex can be represented by the formula $\text{SnO}(\text{CQ})_2 \cdot \text{HCQ}$, and the extraction equilibrium can be formulated as



From the data shown in Fig. 3(a) and from the above equation for D , it is possible to calculate values of $K_{\text{ex},3} = \beta_{1,0} K_{\text{DC}} \beta_2 K_a^2 / K_{\text{DR}}^2$, where $\beta_{1,0} = [\text{SnO}(\text{CQ})_2 \cdot \text{HCQ}]_o / [\text{SnO}(\text{CQ})_2]_o [\text{HCQ}]_o$ (see below), $K_{\text{DC}} = [\text{SnO}(\text{CQ})_2]_o / [\text{SnO}(\text{CQ})_2]$, $\beta_2 = [\text{SnO}(\text{CQ})_2] [\text{H}^+] / [\text{Sn}(\text{OH})] [\text{CQ}]^2$, and K_a and K_{DR} are the acid dissociation and distribution constants of the ligand, [16] respectively. This gives $\log K_{\text{ex},3} = 1.6 \pm 0.1$. At very low ligand concentrations, the extraction equilibrium can be formulated as

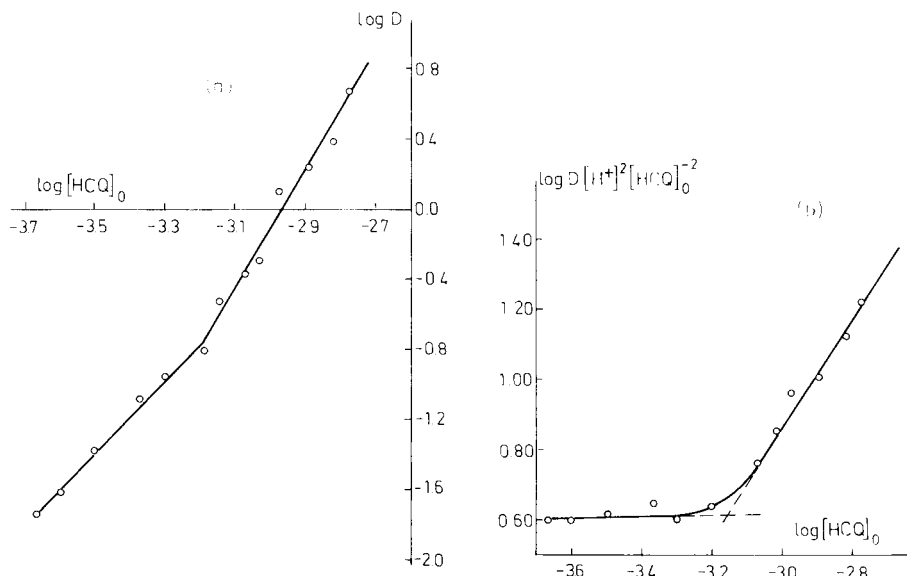
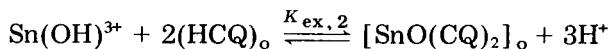
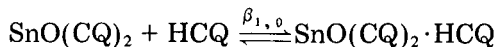


Fig. 3. $\text{Sn}(\text{IV})$ —5,7-dichloro-8-quinolinol—chloroform system: (a) distribution coefficient of tin(IV) as a function of $[\text{HCQ}]_o$; (b) extraction constant as a function of $[\text{HCQ}]_o$.



This gives $\log K_{\text{ex},2} = -2.5 \pm 0.1$ from the experimental data.

Both tin complexes are extractable and they should be in equilibrium in the organic phase:



The value of $m = 1$, the number of neutral HCQ adduct molecules, can be confirmed by plotting $\log D - 2 \text{ pH} - 2 \log [\text{HCQ}]_o$ vs. $\log [\text{HCQ}]_o$ [17]. The resulting slope (see Fig. 3(b)) was about 1. Thus, the formation constant for the self-adduct formed in the organic phase, obtained from this plot, was $\log \beta_{1,0} = 3.1 \pm 0.1$.

Attempts to isolate the self-adduct in the solid state by the extraction technique given in the experimental section yielded a mixture of the two complexes (I) and (II). On washing with hot methanol, complex (II) loses HCQ to give mainly complex (I), as demonstrated by the results of elemental analysis. Such a methanol-washed, dried solid was dissolved into chloroform and its visible absorption spectrum was recorded as a function of time (Fig. 4). It is evident (curves 1–5) that the absorption maxima at 325 nm and 340 nm (typical of the free reagent) increase with time, while the maximum at 395 nm decreases. However, if the solid is dissolved into chloroform containing 1%(w/v) HCQ, the maximum moves slightly towards longer wavelength ($\lambda_{\text{max}} = 390$ nm), and the absorbance first doubles, then remains

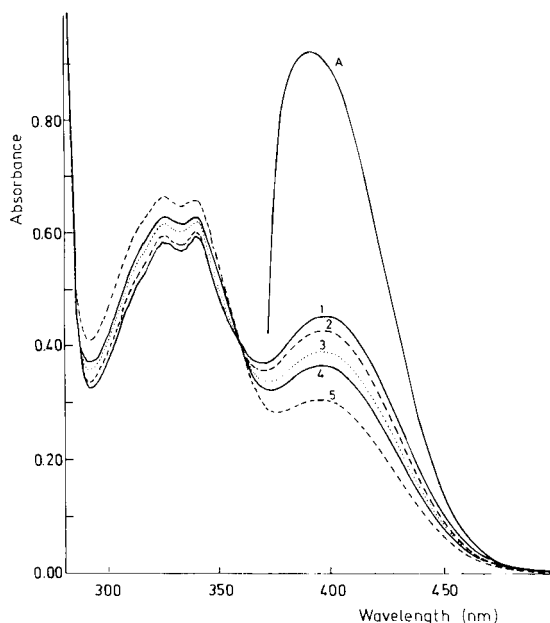


Fig. 4. Absorption spectra of chloroform solutions of $\text{SnO}(\text{CQ})_2$ and its self-adduct. Variation with time when dissolved in pure chloroform (curves 1–5) and chloroform that contains 1% w/v HCQ (curve A). Time: (1) 0; (2) 0.2; (3) 0.6; (4) 1.5; (5) 16 h.

constant for at least 70 h (Fig. 4, curve A). This indicates that an additional HCQ molecule has been added to the complex, and that the self-adduct effectively exists only in the presence of a large excess of HCQ.

However, the i.r. spectrum of this mixture, in addition to the absorption band at 1100 cm^{-1} characteristic of 8-quinolinol chelates, showed another band at 870 cm^{-1} assignable to $\text{M}=\text{O}$ bonds [13] which supports the proposed formula where tin(IV) is extracted as a SnO^{2+} entity at the pH of extraction.

Tin(IV)—5,7-dichloro-8-quinolinol—chloride ternary complex

A mixed ternary complex of tin(IV) with HCQ and chloride is extracted from strongly acidic media (0.3–2 M sulphuric acid) in the presence of ammonium chloride [8]. The metal:HCQ ratio for this complex was 1:1.5 when studied by the slope method. This fractional value may be attributed to the formation at such acidity of significant amounts of tin(IV)—CQ complexes, soluble in the aqueous phase. In fact, the distribution coefficient measured for this complex was the lowest measured, 15% of tin remaining in the aqueous phase after extraction. The tin(IV):chloride ratio obtained by classical spectrophotometric methods was 1:2.

The solid complex obtained by precipitation, $\text{Cl}_2\text{Sn}(\text{CQ})_2$, and the extracted complex are the same, as deduced from their identical spectral features (Fig. 1, curve IV). Again the information obtained from the i.r. spectrum is the disappearance of the OH band and the appearance of the band at 1100 cm^{-1} characteristic of metal—quinolinates (Fig. 2, curve II). The absence of impurities of free quinolinol was confirmed from the proton n.m.r. spectrum at low temperature, that also showed evidence of the formation of a complex by the appearance of tin satellite lines. In the light of all these data, the mixed ternary complex may be assigned the formula $\text{Cl}_2\text{Sn}(\text{CQ})_2$.

Tin(IV)—2-methyl-5,7-dichloro-8-quinolinol complexes

A binary complex of HMQ with tin(IV) can be extracted in the pH range 4.2–5.2 by the general extraction procedure, the half-extraction pH being 3.5. The apparent molar absorptivity is the lowest among all the complexes studied (Fig. 1, curve V). Because of this low molar absorptivity and also the reduced pH range of extraction, this complex is of little interest for the determination of tin(IV), and a detailed study was not made.

A ternary complex with chloride can be extracted at pH 0.8–2.2, the half-extraction pH being 0.45. Its absorption spectrum was similar to that of the binary complex, but its apparent molar absorptivity was higher (Fig. 1, curve VI). The shaking time required to reach maximum Sn(IV) extraction was 10 min, longer than the shaking time required for the other complexes studied here; thus the complex forms only slowly. In addition, the ligand/metal ratio required for extraction is also the highest, indicating that this complex is unstable and cannot be formed unless a large excess of HMQ is

TABLE 1

Extracted complexes of tin(IV) by 8-quinolinols

Reagent	Proposed formula	pH _{1/2} ^a	Sn(IV) extracted (%)	log K _{ex}
8-Quinolinol (HQ)	Cl ₂ SnQ ₂	0.2	100	2.5 ± 0.2
5,7-Dichloro-8-quinolinol (HCQ)	SnO(CQ) ₂	—	—	—2.5 ± 0.1
	SnO(CQ) ₂ · HCQ	0.1	95	1.6 ± 0.1
	Cl ₂ Sn(CQ) ₂	—1.0 ^b	85	—
2-Methyl-5,7-dichloro-8-quinolinol (HMQ)	Cl ₂ Sn(MQ) ₂	0.45	95	—

^apH of 50% extraction. ^bHammett acidity function H₀.

present. Attempts were made to determine the metal/ligand ratio by using extraction—spectrophotometric methods, but conclusive results were not obtained.

This ternary complex was obtained in the solid state by a precipitation procedure. When redissolved into chloroform, it showed a u.v.—visible absorption spectrum identical to that of the extracted complex and its i.r. spectrum shows the 1100 cm⁻¹ band characteristic of 8-quinolinol chelates (see Fig. 2, curve III). In the low-temperature proton n.m.r. spectrum, the complex lines appeared at frequencies higher than those of the free ligand, which in this case cannot be removed completely because the complex partially decomposes when dissolved. The low solubility causes a poor signal-to-noise ratio in the spectrum and tin satellite lines could not be observed.

It is worth noting that self-adduct formation was observed only in the absence of chloride. This could be attributed to the bigger residual Lewis acidity [18] of SnO²⁺ compared with SnCl₂²⁺ after chelation with HCQ (although hydrogen bonding through the oxygen of SnO²⁺ could also be responsible for self-adduct formation).

Table 1 provides a resumé of the proposed formulae of the different species studied along with some extraction data.

The authors thank J. L. Nieto for obtaining the proton n.m.r. spectra and for his helpful comments regarding the original manuscript, and C. Pérez-Conde for many helpful suggestions.

REFERENCES

- 1 C. H. R. Gentry and L. G. Sherrington, *Analyst*, 75 (1950) 17.
- 2 A. R. Eberle and M. W. Lerner, *Anal. Chem.*, 34 (1962) 627.
- 3 E. Ruf, *Fresenius Z. Anal. Chem.*, 162 (1958) 9.
- 4 R. Berg, *Die analytische Verwendung von 8-Oxychinolin und Seiner Derivate*, F. Enke-Verlag, Stuttgart, 1938, p. 3.

- 5 W. Prodinger, *Organische Fällungsmittel in der quantitativen Analyse*, F. Enke-Verlag, Stuttgart, 1954, p. 99.
- 6 H. Hamaguchi and N. Ikeda, *Bull. Chem. Soc. Jpn.*, 32 (1959) 656.
- 7 T. Matsuo and K. Funayama, *J. Chem. Soc. Jpn., Pure Chem. Sect.*, 87 (1966) 433.
- 8 A. Sanz-Medel and A. M. Gutierrez Carreras, *Analyst*, 103 (1978) 1037.
- 9 E. Asmus, *Fresenius Z. Anal. Chem.*, 178 (1960) 104.
- 10 S. M. Edmonds and N. Birnbaum, *J. Am. Chem. Soc.*, 63 (1941) 1471.
- 11 T. Sekine and D. Dyrssen, *J. Inorg. Nucl. Chem.*, 26 (1964) 1727.
- 12 T. Sekine and Y. Hasegawa, *Solvent Extraction Chemistry*, M. Dekker, New York, 1977, p. 156.
- 13 J. P. Phillips and J. F. Deye, *Anal. Chim. Acta*, 17 (1957) 233.
- 14 J. Kragten, *Talanta*, 22 (1975) 505.
- 15 O. Tochiyama and H. Freiser, *Anal. Chem.*, 53 (1981) 874.
- 16 J. Stary and H. Freiser, *IUPAC Equilibrium Constants of Liquid-Liquid Distribution Reactions, Part IV: Chelating Extractants*, Pergamon, Oxford, 1978, p. 82.
- 17 M. Kawashima and H. Freiser, *Anal. Chem.*, 53 (1981) 284.
- 18 F. Chou and H. Freiser, *Anal. Chem.*, 40 (1968) 34.

SYNTHESIS OF *N*-SULFOALKYL DERIVATIVES OF 2-(2-PYRIDYLAZO)-5-AMINOPHENOL AND THE SPECTROPHOTOMETRIC DETERMINATION OF URANIUM(VI)

K. OHSHITA

Laboratory of Chemistry, Daido Institute of Technology, Minami-ku, Nagoya (Japan)

H. WADA* and G. NAKAGAWA

Laboratory of Analytical Chemistry, Nagoya Institute of Technology, Showa-ku, Nagoya (Japan)

(Received 10th August 1982)

SUMMARY

Six *N*-sulfoalkyl derivatives of 2-(2-pyridylazo)-5-aminophenol were synthesized. The acidity constants of the reagents and the stability constants of several of their metal complexes were determined. Their application to the spectrophotometric determination of metals in aqueous solution was studied. 2-(3,5-Dibromo-2-pyridylazo)-5-[*N*-ethyl-*N*-(3-sulfopropyl)amino]phenol was found to be a highly sensitive reagent for some metal ions. The molar absorptivities ($\text{l mol}^{-1} \text{ cm}^{-1}$) of metal complexes at λ_{max} (nm) are 66 000 (592 nm) for uranium(VI), 138 000 (560 nm) for zinc, 70 000 (558 nm) for copper(II) and 88 000 (568 nm) for iron(II). The effects of various masking agents were examined. The determination of uranium(VI) is described in detail.

For the last 30 years, various highly sensitive heterocyclic azophenols have been synthesized and examined as spectrophotometric reagents for various metal ions. Of these compounds, pyridylazophenols which have an alkylamino group in the *p*-position to the azo group in the phenol ring are the most sensitive, but most of them are sparingly soluble in water.

In an earlier study on water-soluble reagents [1], several sulfonated 1-(2-pyridylazo)-2-naphthol (PAN) and α -PAN derivatives were synthesized, and the properties of these reagents and the determination of nickel with 1-(2-pyridylazo)-2-naphthol-6-sulfonic acid (PAN-6S) were described. In these cases, the position of the substituted sulfonic acid group affected the reactivities with metal ions because of changes in the basicities of donor atoms and the steric effect of the reagents.

In the present study, sulfoalkyl groups were introduced into the amino groups of 2-(2-pyridylazo)-5-aminophenols. The introduction of the sulfoalkyl groups made these reagents extremely soluble in water and more sensitive than 2-(2-pyridylazo)-5-aminophenol. Of the reagents synthesized, 2-(3,5-dibromo-2-pyridylazo)-5-[*N*-ethyl-*N*-(3-sulfopropyl)amino]phenol (3,5-diBr-PAESPAP) is the best because it provides high sensitivity and is

easily prepared. The application of 3,5-diBr-PAESPAP to the spectrophotometric determinations of uranium(VI), zinc, copper(II) and iron(II) was examined, and the determination of uranium was found to be attractive.

EXPERIMENTAL

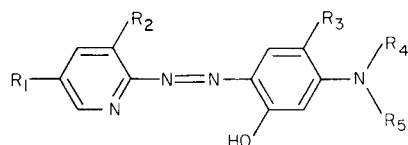
Preparation of azo compounds

The dyes synthesized are listed in Table 1. These azo compounds were synthesized by almost the same procedure. The mono- or di-brominated 2-aminopyridine was diazotized as described previously [2]. The diazonium compound was added to an ethanolic solution of the appropriate *N*-alkyl-*N*-sulfoalkylaminophenol with stirring, and the mixture was stirred overnight at room temperature. Carbon dioxide was bubbled through for 2 h, and then the mixture was allowed to stand overnight. The precipitate was filtered and recrystallized from ethanol containing a small amount of water. Recrystallization was repeated until the absorption spectra of the reagents at different pH values and the copper(II) chelate at different copper(II) concentrations showed distinct isosbestic points. The preparation and purification of 3,5-diBr-PAESPAP were the easiest and the yield was the largest.

Coupling components were synthesized as follows. *N*-(3-Sulfopropyl)-*m*-aminophenol was prepared by Zeid and Ismail's method [3]. *N*-Ethyl-*N*-(3-sulfopropyl)-*m*-aminophenol and 5-[*N*-ethyl-*N*-(3-sulfopropyl)amino]-*p*-cresol were synthesized by heating a mixture of propanesulfonamide and *N*-ethyl-*m*-aminophenol or 3-ethylamino-4-methylphenol according to Zeid and Ismail's procedure for the preparation of *N*-sulfopropylamino benzoic acid [3]. *N*-(2-Sulfoethyl)-*m*-aminophenol was prepared by the reaction of 2-bromo-

TABLE 1

Azo compounds synthesized



Compound	Acronym	R ₁	R ₂	R ₃	R ₄	R ₅
2-(3,5-Dibromo-2-pyridylazo)-5-[<i>N</i> -(3-sulfopropyl)amino]phenol	3,5-diBr-PASPAP	Br	Br	H	H	CH ₂ CH ₂ CH ₂ SO ₃ H
2-(5-Bromo-2-pyridylazo)-5-[<i>N</i> -(3-sulfopropyl)amino]phenol	5-Br-PASPAP	Br	H	H	H	CH ₂ CH ₂ CH ₂ SO ₃ H
2-(3,5-Dibromo-2-pyridylazo)-5-[<i>N</i> -(2-sulfoethyl)amino]phenol	3,5-diBr-PASEAP	Br	Br	H	H	CH ₂ CH ₂ SO ₃ H
2-(3,5-Dibromo-2-pyridylazo)-5-[<i>N</i> -ethyl- <i>N</i> -(3-sulfopropyl)amino]phenol	3,5-diBr-PAESPAP	Br	Br	H	CH ₂ CH ₃	CH ₂ CH ₂ CH ₂ SO ₃ H
2-(5-Bromo-2-pyridylazo)-5-[<i>N</i> -ethyl- <i>N</i> -(3-sulfopropyl)amino]cresol	5-Br-PAESPAC	Br	H	CH ₃	CH ₂ CH ₃	CH ₂ CH ₂ CH ₂ SO ₃ H
2-(5-Bromo-2-pyridylazo)-5-[<i>N</i> -ethyl- <i>N</i> -(3-sulfopropyl)amino]phenol	5-Br-PAESPAP	Br	H	H	CH ₂ CH ₃	CH ₂ CH ₂ CH ₂ SO ₃ H

ethanesulfonic acid and *m*-aminophenol on a steam bath. A concentrated sodium hydroxide solution was added dropwise with stirring, maintaining the pH between 7 and 8. After about 3 h, the pH of the solution did not change further. The reaction mixture was then acidified to pH 2 with hydrochloric acid, and cooled. To the reaction mixture, a large excess of ethanol was added with stirring, and then the *N*-(2-sulfoethyl)-*m*-aminophenol precipitated. The precipitate was filtered and washed with ethanol.

The results of elemental analysis for 3,5-diBr-PAESPAP were as follows: calcd. for $C_{16}H_{17}N_4O_4SBr_2Na \cdot 3H_2O$, 32.1% C, 3.9% H, 9.4% N, 26.7% Br; found 32.7% C, 3.9% H, 9.7% N, 26.0% Br. For the other reagents, the elemental analyses were not done because of the hygroscopic properties of their sodium salts.

Reagents and apparatus

Each azo compound was dissolved in water.

Metal ion solutions. The standard solutions of nickel, copper(II) and cobalt(II) were prepared as previously [2]. Zinc, uranium(VI) and iron(III) solutions were prepared from zinc sulfate, uranyl nitrate hexahydrate and iron(III) ammonium sulphate dodecahydrate, respectively; all three solutions were standardized by EDTA titration. Other metal ion solutions were prepared by dissolving the metal with nitric acid or from the appropriate nitrate, sulfate or chloride. All these salts were of analytical-reagent grade. All masking agents were of reagent grade.

Buffer solutions. Acetic acid—sodium acetate (2M, pH 3–6), potassium dihydrogenphosphate—sodium hydroxide (2M, pH 6–8), ammonia—ammonium chloride (2M, pH 8–10), and triethanolamine—hydrochloric acid (1M, pH 8–10) were used.

All water used had been redistilled from a hard-glass vessel.

A Shimadzu Model UV-200 spectrophotometer and a Hitachi-Horiba pH meter Model F-7 were used.

Recommended procedure for the determination of uranium(VI)

To the sample solution (in a 25-ml volumetric flask) containing 0–120 μg of uranium(VI), add 2 ml of 0.5 M sodium fluoride and 1 ml of 10^{-2} M CyDTA. Then add 2 ml of 10^{-3} M 3,5-diBr-PAESPAP solution and 1.5 ml of 1 M triethanolamine—hydrochloric acid buffer solution (pH 8.5). Dilute the mixture to the mark with water and stand for 40 min. Measure the absorbance at 590 nm against the reagent blank.

RESULTS AND DISCUSSION

Acidity constants of the reagents

All the reagents were highly soluble in water and were yellow in acidic and neutral solutions but pink in alkaline solutions. Absorption maxima of the reagents and their molar absorptivities are shown in Table 2. The absorption

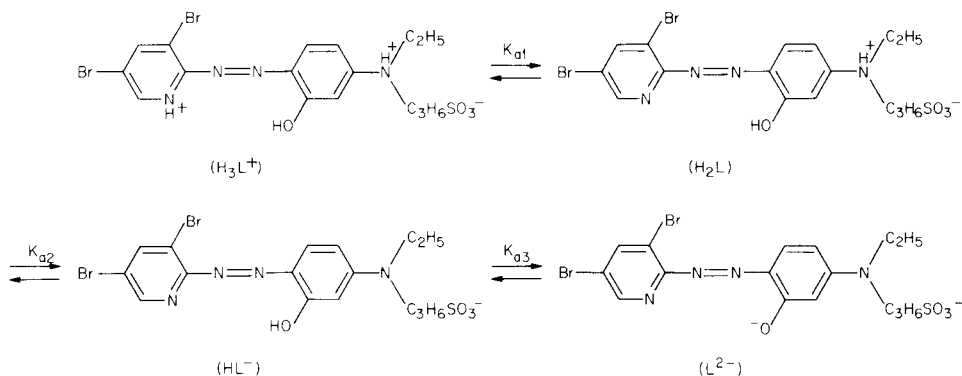
TABLE 2

Absorption maxima and molar absorptivities of the compounds^a

Compound	pH 1		pH 6		pH 12	
	λ_{\max}	ϵ	λ_{\max}	ϵ	λ_{\max}	ϵ
3,5-diBr-PASPAP	446	4.7	438	4.7	514	4.8
5-Br-PASPAP	440	4.4	433	5.0	500	4.4
3,5-diBr-PASEAP	462	4.7	456	5.1	520	4.6
3,5-diBr-PAESPAP	467	5.2	452	5.0	525	5.7
5-Br-PAESPAC	—	—	460	4.7	510	2.8
5-Br-PAESPAP	464	4.8	446	5.2	508	5.3

^a λ_{\max} is given in nm. All molar absorptivities are given as $10^4 \text{ l mol}^{-1} \text{ cm}^{-1}$.

spectra of 3,5-diBr-PAESPAP are shown in Fig. 1. The dissociation equilibria of these reagents can be written as follows, 3,5-diBr-PAESPAP being taken as example



The three successive acidity constants are then defined by $K_{a1} = a_{H^+}[H_2L]/[H_3L^+]$, $K_{a2} = a_{H^+}[HL^-]/[H_2L]$, and $K_{a3} = a_{H^+}[L^{2-}]/[HL^-]$. Being less than 1, the K_{a1} values of all the reagents were not determined. The K_{a2} and K_{a3} values were determined by Hildebrand and Reilley's method [4]. The results are shown in Table 3. The values of pK_{a2} for the dibromo derivatives are smaller than those for the monobromo derivatives, whereas the pK_{a3} values are similar for all the compounds except 5-Br-PAESPAC.

Reaction with metal ions

All the reagents react with many metal ions as do other pyridylazo-phenols. Most of the metal chelates, like the reagents, were highly soluble in water. The absorption maxima and the molar absorptivities of some of the metal chelates with these reagents are shown in Table 4. These results indicate that: (1) *N*-alkyl-*N*-sulfoalkyl derivatives are more sensitive than *NH*-sulfoalkyl derivatives; (2) monobromo derivatives are slightly more

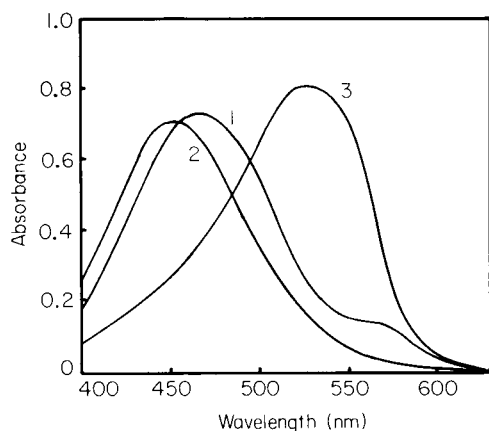


Fig. 1. Absorption spectra of 3,5-diBr-PAESPAP (1.5×10^{-5} M) at different pH values: (1) 1; (2) 6; (3) 13. $\mu = 0.1$, 25°C .

TABLE 3

Acidity constants of the compounds at $\mu = 0.1$ and 25°C in aqueous solution

Compound	$\text{p}K_{\text{a}2}^{\text{a}}$	$\text{p}K_{\text{a}3}$
3,5-diBr-PASPAP	2.05	11.25
5-Br-PASPAP	2.70	10.80
3,5-diBr-PASEAP	2	10.75
3,5-diBr-PAESPAP	1.80	11.20
5-Br-PAESPAC	3.60	9.60
5-Br-PAESPAP	2.90	10.85

^a $\text{p}K_{\text{a}1} < 1$.

TABLE 4

Absorption maxima and molar absorptivities of metal complexes^a

	Cu(II)		Ni(II)		Co(III)		Zn(II)		U(VI)	
	λ_{max}	ϵ	λ_{max}	ϵ	λ_{max}	ϵ	λ_{max}	ϵ	λ_{max}	ϵ
3,5-diBr-PASPAP	544	5.9	546–554	10.0	590	5.7	550	10.0	575	5.4
5-Br-PASPAP	537	6.1	546	10.5	580	6.0	582–588	11.2	562	5.5
3,5-diBr-PASEAP	556	6.3	568	11.5	600	8.6	562	12.3	578	6.3
3,5-diBr-PAESPAP	558	7.0	566	14.2	596	10.3	560	13.8	592	6.6
5-Br-PAESPAC	560	5.8	566	9.5	560–590	8.4	560	11.1	585	4.8
5-Br-PAESPAP	553	7.1	556	15.2	586	10.6	551	14.8	578	6.9

^a λ_{max} (nm) is given with ϵ expressed as $10^4 \text{ l mol}^{-1} \text{ cm}^{-1}$.

sensitive than dibromo ones; (3) a methyl group at the *o*-position of the dialkylamino group reduces the sensitivity.

Among these reagents 5-Br-PAESPAP provides the best sensitivity, but the preparation and purification of this compound was troublesome because of its great solubility in water. From the viewpoints of high sensitivity and ease of preparation, 3,5-diBr-PAESPAP was the best as a realistic spectrophotometric reagent for some metal ions.

Metal chelates with 3,5-diBr-PAESPAP

The absorption spectra of the metal chelates with 3,5-diBr-PAESPAP are shown in Fig. 2. Iron(II) chelate shows two absorption maxima; one at 748 nm ($\epsilon = 39\,000$) may be useful for the determination of iron without interferences by other metal ions.

The formation of 3,5-diBr-PAESPAP chelates with copper(II), nickel, zinc, cobalt(III), uranium(VI), iron(II), gallium(III), indium(III), vanadium(V) was examined. The effects of pH on the absorbance of those metal chelates are shown in Fig. 3. The absorption maxima, molar absorptivities, the pH range where the absorbances of the chelates are constant, and the compositions of the chelates are summarized in Table 5.

The stability constants (K_{ML} and β_{ML}) of the copper(II), nickel, zinc or cadmium chelates with 3,5-diBr-PAESPAP were determined in aqueous solution by spectrophotometry as described previously [2]. These stability constants are given in Table 6 together with those of chelates formed with other reagents synthesized. The stability constants of these chelates, taking into account the basicity of the reagent, are comparable with those of other pyridylazophenols. Thus the properties of the reagents for the formation of the chelates were not affected by the introduction of a sulfoalkyl group, while the sensitivity and the solubility in water were much improved.

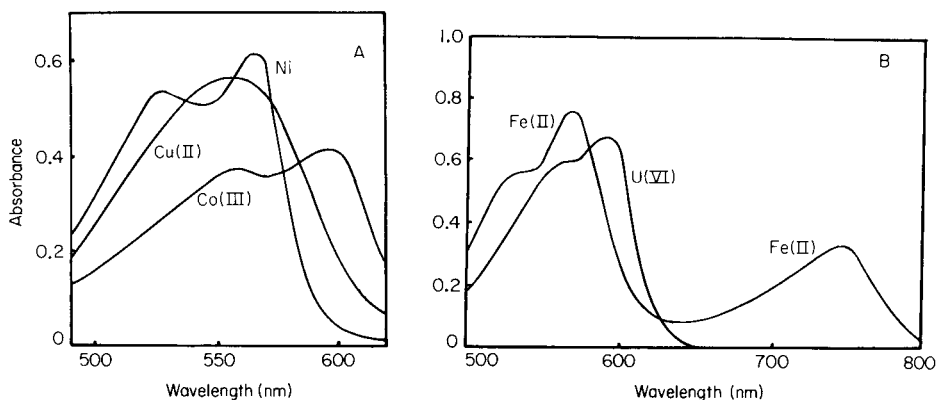


Fig. 2. Absorption spectra of metal chelates with 3,5-diBr-PAESPAP (2×10^{-5} M). A, Cu(II) (8×10^{-6} M), Co(III) (4×10^{-6} M) and Ni(II) (4×10^{-6} M). B, U(VI) (1×10^{-5} M) and Fe(II) (8×10^{-6} M) (in the presence of ascorbic acid).

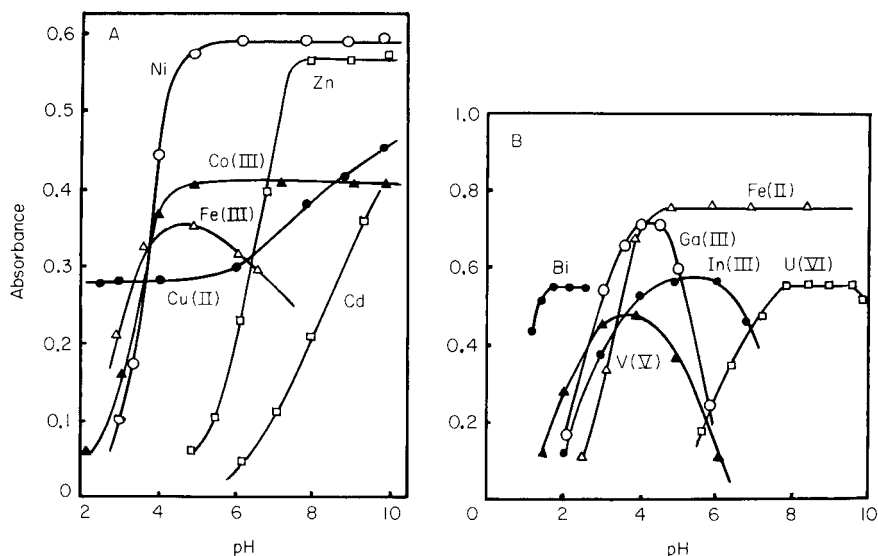


Fig. 3. Effect of pH on the absorbance of metal-3,5-diBr-PAESPAP chelates in aqueous solution. A, 4×10^{-6} M metal ion with 2×10^{-5} M 3,5-diBr-PAESPAP; B, 8×10^{-6} M metal ion with 2×10^{-5} M 3,5-diBr-PAESPAP.

Effect of masking agents on the formation of 3,5-diBr-PAESPAP chelates

To evaluate the applicability of 3,5-diBr-PAESPAP to the determination of some metal ions in practical samples, the effects of various masking agents which are usually used for interfering metal ions were studied. To a 25-ml

TABLE 5

Absorption maxima and molar absorptivities of metal-3,5-diBr-PAESPAP complexes

	λ_{\max} (nm)	ϵ (10^4 l mol $^{-1}$ cm $^{-1}$)	pH	Mole ratio (M:L)
Cu(II)	558	7.0	2-5	1:1 ^a
Ni(II)	566	14.2	5.5-10	1:2
Zn(II)	560	13.8	8-10	1:2
Co(III)	596	10.3	5-10	1:2
Fe(III)	596	8.5	3.5-4.5	1:2
Fe(II)	568	8.8		
	748	3.9	5-9	1:2
Ga(III)	570	8.0	4.0-4.5	1:1
In(III)	575	6.8	5.0-6.0	1:1
V(V)	595	6.0	3.5-4.0	1:1
Bi(III)	600	6.7	1.8-2.5	1:1
U(VI)	592	6.6	7.8-9.5	1:1

^aAt pH >6 the absorbance increased because of the formation of the 1:2 chelate.

TABLE 6

Logarithmic stability constants of metal chelates at $\mu = 0.1$ and 25°C in aqueous solution^a

	Cu	Ni		Zn		Cd
	K_{ML}	K_{ML}	β_{ML_2}	K_{ML}	β_{ML_2}	K_{ML}
3,5-diBr-PASPAP	13.6	11.6	24.2	9.6	19.3	8.4
5-Br-PASPAP	13.3	10.0	22.6	8.7	18.0	8.0
3,5-diBr-PASEAP	—	11.6	23.9	9.4	19.0	8.3
3,5-diBr-PAESPAP	16	11.9	24.9	9.8	19.6	8.7
5-Br-PAESPAC	12.7	9.5	21.2	8.3	16.8	7.3
5-Br-PAESPAP	13.8	10.9	23.7	9.3	19.0	8.1

^a $K_{\text{ML}} = [\text{ML}]/[\text{M}][\text{L}]$, $\beta_{\text{ML}_2} = [\text{ML}_2]/[\text{M}][\text{L}]^2$.

volumetric flask were added 0.2 ml of 10^{-3} M metal ion solution, the masking agent (final concentrations are shown in Table 7) and 1.0 ml of 10^{-3} M 3,5-diBr-PAESPAP solution; then the pH of the mixture was adjusted to 6 or 8.5 with 1 ml of the appropriate buffer solution, and the absorbance of the metal chelate was measured. The results are shown in Table 7. From these results, CyDTA and fluoride appear to be versatile masking agents for the determination of uranium(VI), and DTCS for the determination of zinc or iron(II). For the determination of copper(II), suitable masking agents could not be found, but copper(II) can be determined at pH 2 where a few metal ions react with the reagent.

These results show that 3,5-diBr-PAESPAP is a highly sensitive reagent that can be made selective by masking, for the determination of uranium(VI), copper(II), zinc or iron(II). In the present paper, the detailed results of the study on the spectrophotometric determination of uranium(VI) are described.

Experimental conditions for the determination of uranium(VI)

As has been seen in Fig. 3B, the maximum absorbance of the uranium(VI) chelate was observed in the pH range 8–9. Triethanolamine solution adjusted to pH 8.5 by the addition of hydrochloric acid was used as a buffer solution. For the determination of 20–120 μg of uranium(VI), 2 ml of 10^{-3} M 3,5-diBr-PAESPAP was sufficient. Because the rate of reaction was slow, especially when V(V), Zr(III) and Cr(III) were present, the optimum standing time was 40 min. Under these conditions, Beer's law was obeyed up to 120 μg of uranium(VI) in the final 25-ml volume; the Sandell sensitivity was $0.0036 \mu\text{g cm}^{-2}$.

In a paper on the determination of uranium(VI) with 2-(5-bromo-2-pyridylazo)-5-diethylaminophenol (Br-PADAP), Johnson and Florence [5] reported that a uranium(VI)–Br-PADAP–fluoride mixed ligand complex is formed in the presence of fluoride. But in our case, the absorption maximum of the uranium complex was only slightly shifted (2 nm) to longer

TABLE 7

The decrease (in percent) in the absorbances of metal chelates on addition of masking agents^a

[At pH 6]												
	Cu(II)	Zn(II)	Co(II)	Ni(II)	Fe(III)	Pb(II)	V(V)	Hg(II)	U(VI)	Pd(II)	Th(IV)	Ti(IV)
NTA	20	100	0	65	70	100	90	48	20	15	100	85
IDA	0	15	0	0	0	0	0	0	15	65	0	0
EDTA	100	100	100	100	100	100	100	100	75	45	100	100
CyDTA	100	100	100	100	100	100	35	100	0	100	100	100
EGTA	95	100	0	65	87	100	32	100	50	100	100	0
Phen	100	100	100	100	75	100	85	100	0	100	100	0
Tartrate	0	75	0	0	60	82	72	0	100	0	100	100
SSA	0	0	0	0	40	0	30	0	0	0	55	0
F ⁻	0	0	0	0	10	0	20	0	0	0	100	0
I ⁻	0	10	0	0	0 ^b	0	18	100	0	67	0	20
DTCS	100	70	100	100	0 ^b	100	77	100	100	100	80	20
[At pH 8.5]												
	Cu(II)	Zn(II)	Co(II)	Ni(II)	Fe(III)	Cd(II)	Mn(II)	Pb(II)	U(VI)	Pd(II)	Th(IV)	Ti(IV)
NTA	20	83	12	50	25	100	100	100	15	100	100	100
IDA	0	0	0	0	0	0	0	10	10	80	50	0
EDTA	100	100	100	100	100	100	100	100	5	93	30	100
CyDTA	100	100	100	100	100	100	100	100	0	100	83	100
EGTA	100	100	5	83	0	100	100	100	35	100	100	0
Phen	83	100	95	100	30	83	50	10	20	100	0	0
Tartrate	0	0	0	0	27	0	28	37	90	83	100	100
SSA	0	0	0	0	0	0	0	0	0	15	0	0
F ⁻	0	0	0	0	0	0	0	5	0	0	100	62
I ⁻	0	0	0	0	0 ^b	20	0	0	18	83	32	0
DTCS	100	0	100	50	0 ^b	97	0	100	0	100	100	50
β -DTCPA	90	0	95	0	0 ^b	82	0	95	0	100	32	0

TABLE 7 (continued)

	Cu(II)	Zn(II)	Co(II)	Ni(II)	Fe(III)	Cd(II)	Mn(II)	Pb(II)	U(VI)	Pd(II)	Th(IV)	In(III)	Ti(IV)
P ₂ O ₇ ⁴⁻	0	67	0	0	97	92	100	100	100	100	100	100	100
TEA	0	0	20	0	0	38	0	70	0	100	95	70	80
S ₂ O ₃ ²⁻	15	0	0	0	0 ^b	22	0	0	0	100	92	60	45
CN ⁻	100	100	100	100	100	100	100	8	0	100	100	60	100
DDC	—	—	—	—	90	—	0	—	0	—	100	—	100

^a Abbreviations: NTA, nitrilotriacetic acid (10^{-4} M); IDA, iminodiacetic acid (10^{-4} M); EDTA, ethylenediaminetetraacetic acid (10^{-4} M); CyDTA, cyclohexane-1,2-diaminetetraacetic acid (10^{-4} M); EGTA, ethyleneglycolbis(2-aminoethyl ether)tetraacetic acid (10^{-4} M); Phen, 1,10-phenanthroline (4×10^{-4} M); SSA, sulfosalicylic acid (4×10^{-3} M); DTCS, *N*-(dithiocarbamino)sarcosine (4×10^{-4} M); β -DTCPA, β -dithiocarbaminopropionic acid (4×10^{-4} M); TEA, triethanolamine (4×10^{-2} M); DDC, diethyldithiocarbamate (4×10^{-4} M). Tartrate: 2×10^{-2} M, F⁻: 4×10^{-3} M, I⁻: 5×10^{-2} M, P₂O₇⁴⁻, S₂O₃²⁻ and CN⁻: 10^{-2} M.

^b Fe(III) was reduced to Fe(II).

TABLE 8

Tolerable amounts of diverse metal ions in the determination of uranium(VI)

Ion	Maximum permissible amount (mg)	Ion	Maximum permissible amount (mg)
Al(III)	2	Mo(VI)	5
Bi(III)	1.6	Ni(II)	0.6
Cd(II)	1.2	Pb(II)	2.5
Co(II)	0.6	Th(IV)	7
Cr(III)	0.5	Ti(IV)	0.5
Cu(II)	1.2	V(V)	2.5
Fe(III)	1	W(VI)	9
Ga(III)	1.5	Zn(II)	3
In(III)	2	Zr(IV)	0.2
Mn(II)	0.6		

wavelength by the addition of fluoride, thus the formation of any ternary complex of uranium(VI) with 3,5-diBr-PAESPAP and fluoride could not be recognized clearly.

Effect of other ions. As has been seen, many metal ions react with 3,5-diBr-PAESPAP in the pH range 8–9. CyDTA (1.0 ml of 10^{-2} M) and sodium fluoride (2.0 ml of 0.5 M) are very effective for masking a number of interfering metal ions, but masking for copper(II) and chromium(III) was incomplete. Copper(II) could be masked by β -mercaptopropionic acid, and chromium(III) by boiling for 10 min after the addition of CyDTA. The tolerable amounts of diverse metal ions when the procedure given under Experimental is used, are shown in Table 8.

From these results, it is clear that this method is very useful because of its high sensitivity and the high solubility of the reagent and the uranium(VI) chelate. In these aspects, the method compares favorably with various procedures in the literature [6–8].

REFERENCES

- 1 K. Ohshita, H. Wada and G. Nakagawa, *Anal. Chim. Acta*, 140 (1982) 291.
- 2 K. Ohshita, H. Wada and G. Nakagawa, *Anal. Chim. Acta*, 124 (1981) 193.
- 3 I. Zeid and I. Ismail, *Justus Liebigs Ann. Chem.*, (1974) 667.
- 4 G. H. Hildebrand and C. N. Reilley, *Anal. Chem.*, 29 (1957) 258.
- 5 D. A. Johnson and T. M. Florence, *Talanta*, 22 (1975) 253.
- 6 K. L. Cheng, *Anal. Chem.*, 30 (1958) 1027.
- 7 D. A. Johnson and T. M. Florence, *Anal. Chim. Acta*, 53 (1971) 73.
- 8 L. Sommer and V. M. Ivanov, *Talanta*, 14 (1967) 171.

DETERMINATION OF OXIDIZED KETONE BODIES IN MILK BY FLOW INJECTION ANALYSIS

PETER MARSTORP

Department of Analytical and Marine Chemistry, Chalmers University of Technology and University of Gothenburg, Fack, S-412 96 Göteborg (Sweden)

TORBJÖRN ANFÄLT

Tecator AB, Bifok/Optilab Division, Box 124, S-191 22 Sollentuna (Sweden)

LENNART ANDERSSON*

Experimental Station, Veterinary Institute, Box 234, S-532 00 Skara (Sweden)

(Received 29th October 1982)

SUMMARY

A flow injection method is described for the determination of oxidized ketone bodies in milk. Acetoacetate is decarboxylated to acetone at 100°C. Acetone is separated from the sample by gas diffusion through a teflon membrane and measured spectrophotometrically. The detection limit is 0.1 mM. Accuracy and reproducibility are good up to 5 mM. The sample capacity is up to 100 samples/h.

Changes of circulating ketone bodies reflect deviations in the energy metabolism. Dairy cows in peak lactation are very sensitive to changes in the energy balance. Undernutrition often leads to increased blood levels and increased excretion of ketone bodies via the lungs and kidneys and also via the mammary gland. High levels of ketone bodies are connected with the clinical disease ketosis. Lower but still increased levels often exist without clinical signs (subclinical ketosis) and may be regarded as indicators of energy imbalance in the diet. It is therefore of great importance to detect ketone bodies as a basis for correction of diet even in apparently healthy cows.

The term ketone bodies normally includes 3-hydroxybutyric acid, acetoacetic acid and acetone. The sum of acetoacetic acid and acetone is called oxidized ketone bodies. Oxidized ketone bodies in milk are accurate indicators of subclinical ketosis, as the correlations to the concentrations in blood are high [1].

Acetoacetate in blood can be determined enzymatically by using 3-hydroxybutyrate dehydrogenase with nicotinamide adenine dinucleotide (NADH) as coenzyme. Either the ultraviolet absorption of NADH [2, 3] or its fluorescence [4, 5] can be monitored. These methods are not easily applicable to milk because of severe matrix problems. A rapid semiquantitative method is

based on commercially available paper strips impregnated with disodium pentacyanonitrosylferrate(II) but it does not provide acceptable selectivity and sensitivity except as a screening test. Acetoacetic acid is easily decarboxylated to acetone which can be determined with many colorimetric reagents [6–12]. The milk matrix makes direct colorimetric measurement impossible, thus separation of acetone from the sample by distillation [7, 9], extraction [6, 10] or diffusion [8, 12] is necessary. Other possibilities are chromatographic procedures [13–18]. These techniques give accurate results but are time-consuming.

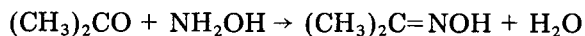
The aim of the present work was to obtain a rapid and accurate method for oxidized ketone bodies in milk based on flow injection analysis (f.i.a.), which allows a large number of samples per time unit to be processed automatically.

THEORY

Oxidized ketone bodies can be estimated by determination of acetone after decarboxylation of acetoacetic acid to acetone. High temperature and low pH increase the decarboxylation rate. As acetone is volatile, it is easily separated from a complex matrix by diffusion into another medium. Gas diffusion is normally slow so that it is unfavourable to let the diffusion go to steady state. A flow-injection technique [19] gives the constant conditions needed to use separation by gas diffusion without reaching steady state while good accuracy and precision are maintained.

In the f.i.a. technique, a sample introduced into a stream of reagent is dispersed and thus mixed with the reagent. The mixing is controlled by the length and diameter of tube coils. The solutions are propelled by a peristaltic pump to a flow-through detector, which gives peak-shaped response curves on a strip-chart recorder. Gas diffusion in f.i.a. is achieved by injecting a sample into a carrier stream, which is separated from a stream of reagent by a gas-diffusible membrane [19]. Acetone in milk samples injected into the carrier stream diffuses through the membrane and can be detected in the reagent stream.

In the reagent stream, acetone reacts with hydroxylamine to form acetoxime



thus changing the hydroxylammonium–hydroxylamine equilibrium, $\text{NH}_3\text{OH}^+ \rightleftharpoons \text{NH}_2\text{OH} + \text{H}^+$. The shift in pH can be monitored by an acid–base indicator [20–22]. A pH around 4 in the reagent solution ensures a suitable degree of dissociation of the hydroxylammonium ions. A suitable indicator is methyl orange, which has a transition pH interval of 3.0–4.4. The unprotonated indicator is yellow and the acid form pink, absorbing light at 520 nm.

EXPERIMENTAL

Apparatus

All experiments were done with a Flow Injection Analyzer (FIA-05, Tecator, Sweden) consisting of a single-channel injection valve with variable sample size and a thermostatted water bath, in which a modular block system with tube coils and connectors is placed. The gas diffusion module consists of two parts, each containing a cavity 2 mm wide, 80 mm long and 0.2 mm deep. They are separated from each other by a 0.07-mm thick teflon membrane. The sample carrier stream is pumped through one of the cavities and the reagent stream through the other. An eight-channel peristaltic pump FIA-08 (Bifok) and a flow-through colorimeter FIA-06 (Bifok) with a 520-nm filter were used. A computer system (Apple II) was used for data retrieval and evaluation.

A Bruker 4410 gas chromatograph with a glass column (2 m, 1/8 in. diameter) filled with Porapak QS was used for the reference determination of acetone.

Flow injection manifold. The flow injection manifold is described in Fig. 1. All tubes (PTFE) were 0.5 mm i.d., 1.6 mm o.d. A 30-cm coil was included in the manifold after the diffusion cell in order to give sufficient time for the reaction between acetone and the reagent. The injected sample size was 100 μ l.

Reagents

A stock solution (0.288 M) of hydroxylammonium chloride was prepared by dissolving 20 g of the compound in 1 l of distilled water. The stock solution of indicator (7.6×10^{-4} M) contained 0.25 g of methyl orange and 2 ml of 1 M sodium hydroxide per litre of distilled water. The reagent solution was prepared by mixing 10 ml of the indicator stock solution and

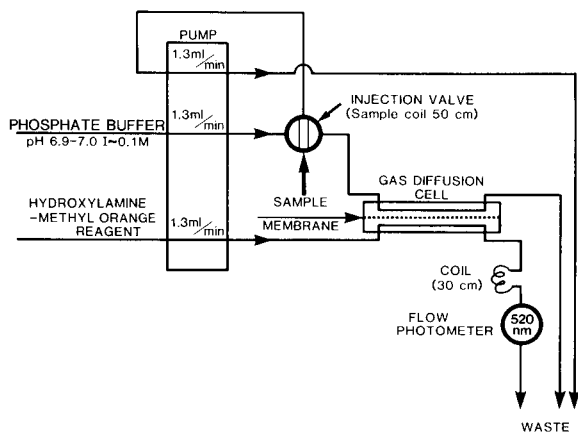


Fig. 1. The flow injection manifold.

15 ml of the hydroxylammonium chloride solution and diluting to 100 ml with distilled water. The gradual decomposition of hydroxylammonium chloride makes it essential to renew this stock solution and the reagent solution each week. The phosphate buffer solution (0.1 M) was at pH 6.9–7.0.

Acetone standards were prepared by diluting a 10 mM stock solution of acetone. They were renewed each week. The stock standard could be kept one month. For preparation of acetoacetate standards, lithium acetoacetate was used. Milk samples were treated with 0.02% (w/v) bronopol (2-bromo-2-nitropropane-1,3-diol) as a preservative, and a little methylene blue as a marker.

Procedures

Flow injection analysis. Milk samples with bronopol–methylene blue in closed bottles were kept in a water bath at 100°C for 35 min. The samples were run through a homogenizer, placed in 2-ml cups in an automatic sampler and fed into the FIA-05 unit. Standards were run before every 40th injection. Evaluation was done by means of a standard graph. Because the plot was slightly curved, it was evaluated by Lagrange interpolation.

Gas chromatography. A chromatographic method was used for comparison with the f.i.a. method. The milk protein was precipitated with perchloric acid. Sulphuric acid was added to the supernatant liquid and the acetone was separated by steam distillation. The acetone was measured by gas chromatography with ethanol as internal standard. Helium was used as carrier gas at a flow rate of 30 ml min⁻¹.

RESULTS AND DISCUSSION

Sample pretreatment

When only acetone was determined, the milk samples could be injected without pretreatment. There was, however, a risk that fat particles might block the tubings of the system.

For determination of total oxidized ketone bodies in preserved milk, the acetoacetate must be converted to acetone. When perchloric acid was used at 100°C, the decomposition of added acetoacetate was complete within 15 min, but the denatured protein caused blocking of the tubing. Therefore decomposition simply by heating at 100°C was examined. The acetoacetate (1 mM) was completely decomposed to acetone after 35 min, but the high temperature caused changes in the fat structure. Fat particles accumulated on the diffusion membrane, changing its diffusive character. This fat problem was solved by mechanical homogenization (particle size 2 µm) after heating and cooling of the samples. At temperatures below 65°C, the decomposition of acetoacetate was too slow to be of practical interest. As a result of these investigations, decomposition at 100°C for 35 min followed by mechanical homogenization was used for all milk samples in the following experiments.

Reagent composition

Figure 2 shows peaks from injections of acetone standards (0–8 mM) and some milk samples with the recommended manifold. Several factors affected the peak height. In order to establish a suitable reagent composition, varying concentrations of hydroxylammonium chloride and methyl orange and different pH values were examined. Reagent solutions (pH 3.4–4.4) with four hydroxylammonium chloride concentrations (0.022 M, 0.043 M, 0.086 M, and 0.130 M) and constant indicator concentration (7.6×10^{-5} M) were used to measure a 1 mM acetone standard. Figure 3 shows that a concentration of 0.043 M hydroxylammonium chloride and a pH around 3.7 gave the highest sensitivity.

Figure 4 shows the response when different acetone concentrations (0.25–

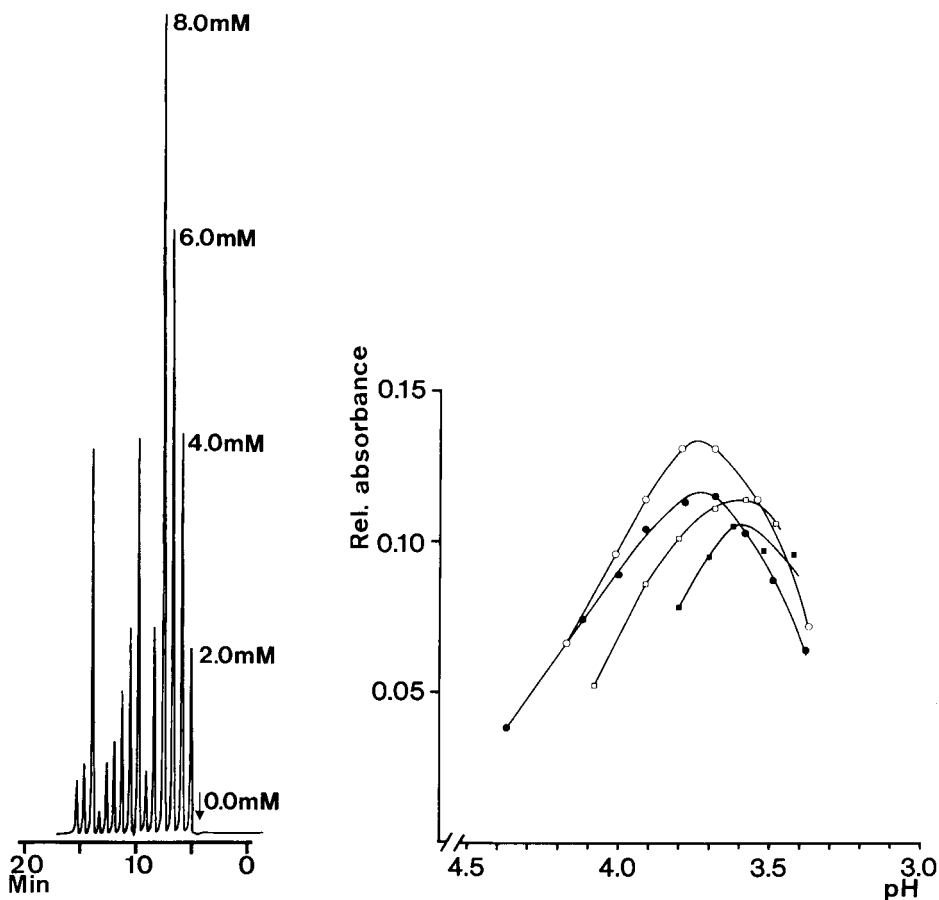


Fig. 2. Responses for different acetone standards and milk samples.

Fig. 3. The response as a function of pH to injections of 1 mM acetone standard at different hydroxylammonium chloride concentrations: (●) 0.022 M; (○) 0.043 M; (□) 0.086 M; (■) 0.130 M.

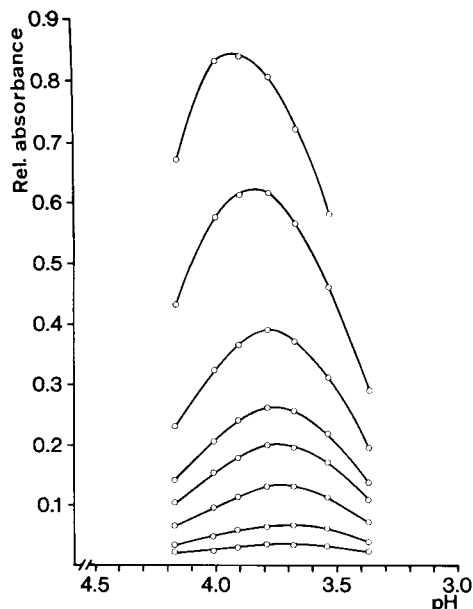


Fig. 4. The response as a function of pH at a hydroxylammonium chloride concentration of 0.043 M for injections of different acetone standards (from bottom 0.25, 0.5, 1.0, 1.5, 2.0, 3.0, 5.0 and 7.0 mM).

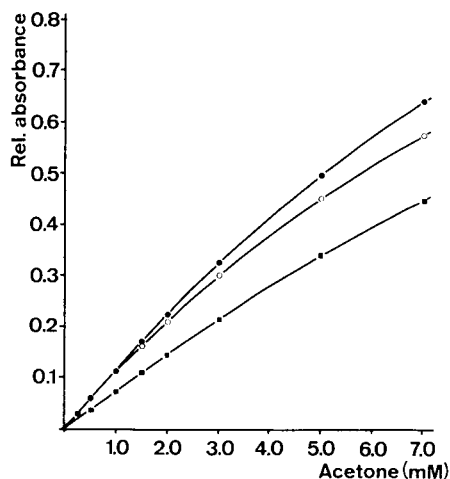


Fig. 5. The response as a function of injected acetone standards for three indicator concentrations: (■) 3.8×10^{-5} M; (●) 7.6×10^{-5} M; (○) 11.4×10^{-5} M.

7.0 mM) were injected at a hydroxylammonium chloride concentration of 0.043 M. There seems to be an increasing pH optimum with increasing acetone concentration. The effect of varying indicator concentration (3.8×10^{-5} M, 7.6×10^{-5} M, 11.4×10^{-5} M) at constant hydroxylammonium chloride concentration (0.086 M) and pH (3.6) is shown in Fig. 5. The 7.6×10^{-5} M solution gave the highest response. Indicator concentrations around 7×10^{-5} M are therefore recommended, particularly because higher concentrations of indicator caused increased background absorbance, which affected the precision of results.

Temperature dependence and diffusion rate

The gas diffusion rate is greatly enhanced by increased temperature. In order to study this enhancement, the diffusion module was placed in a thermostatted water bath at 47°C. The peaks became approximately 45% higher. It is, however, not possible to increase the temperature very much, because dissolved gases in the reagent could be released, thus causing problems in the flow-through cell. Because of this, diffusion was done at room temperature.

In order to measure the diffusion rate through the membrane, the carrier stream was replaced by a 1 mM acetone standard solution, pumped through the diffusion cell at a flow rate of 1.0 ml min⁻¹. The acetone standard was collected after passing the diffusion module and the remaining acetone was determined. It was found that 19% of the acetone had diffused through the membrane. The diffusion increased at lower flow rates through the diffusion cell.

Interferences

There are interfering substances (formaldehyde, methyl ethyl ketone, ammonia) which diffuse and may affect the pH in the reagent stream. A 1 mM formaldehyde solution gave no measurable response. A 10 mM solution caused a peak about 6% of a 1 mM acetone peak. A solution of 1 mM methyl ethyl ketone gave a peak which was 77% of a 1 mM acetone peak. At pH 7.3 a 2 mM solution of ammonia gave a negative signal about 5% the size of a 1 mM acetone response. However, these interferences are of no interest in the analysis of milk samples. The bronopol-methylene blue preservative did not interfere.

Limit of detection, accuracy and precision

The detection limit was established as four times the noise level. This corresponded to 0.1 mM acetone when the optimal reagent concentrations were used at flow rates of 1.3 ml min⁻¹.

The accuracy was evaluated by using milk boiled until all oxidized ketone bodies were lost. The milk was divided into seven portions. Six of them were spiked with acetone and acetoacetate (1:1) at total concentrations of 0.2–5.0 mM. Table 1 shows the good agreement between the f.i.a. and g.c. methods. The results obtained by the f.i.a. and g.c. methods were further compared by analyzing 66 milk samples by both methods. The regression

TABLE 1

Results obtained for boiled milk spiked with acetone and acetoacetate by f.i.a. and gas chromatography (g.c.)

Total conc. acetone + acetoacetate (1:1) (mM)	Total conc. found (mM)	
	F.i.a.	G.c.
0	0.02	0.05
0.20	0.20	0.23
0.40	0.42	0.41
0.70	0.74	0.65
1.00	1.05	1.10
2.00	2.10	2.11
5.00	5.12	5.10

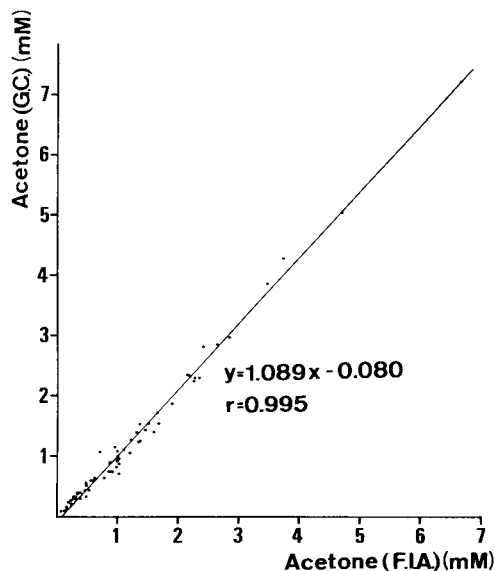


Fig. 6. Comparison between the f.i.a. and g.c. procedures for milk samples.

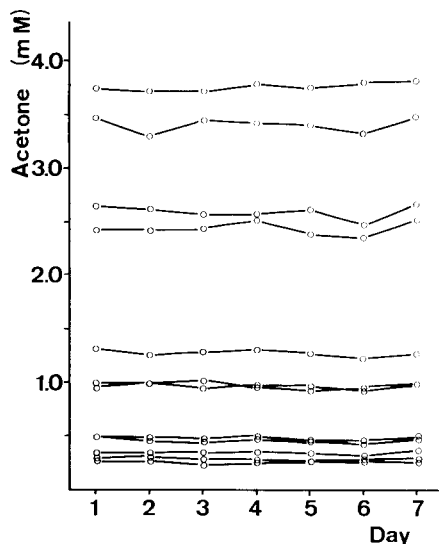


Fig. 7. Reproducibility. The acetone concentrations in 12 milk samples were determined once daily for seven days.

coefficient was 1.089 and the correlation coefficient 0.995 ($p \leq 0.001$) (Fig. 6).

To check the repeatability, ten complete determinations on one milk sample gave a mean value of 1.01 mM acetone with a relative standard deviation of 2.0%. One sample was heated at 100°C for 35 min, cooled, homogenized and then injected 10 times. The mean value was 1.01 mM and the relative standard deviation was 0.5%.

To check reproducibility, 12 samples were run once a day for seven days (Fig. 7). The relative standard deviations for single samples varied from 1.0% for that with the highest concentration of oxidized ketone bodies to 6.3% for that with the lowest. This reproducibility is entirely acceptable.

This investigation was financially supported by the Association for Swedish Livestock Breeding and Production (SHS).

REFERENCES

- 1 H. Steger, H. Girschewski, B. Piatkowski and J. Voigt, *Arch. Tierernähr.*, 22 (1972) 157.
- 2 D. H. Williamson, J. Mellanby and H. A. Krebs, *Biochem. J.*, 82 (1962) 90.
- 3 K. G. M. M. Alberti and T. D. R. Hockaday, *Br. Med. J.*, 2 (1972) 565.
- 4 C. Olsen, *Clin. Chim. Acta*, 33 (1971) 293.

- 5 P. T. Ozand, R. L. Hawkins, R. M. Collins, Jr., J. T. Tildon and M. Cornblath, *Biochem. Med.*, 14 (1975) 170.
- 6 H. Göshke, *Clin. Chim. Acta*, 28 (1970) 359.
- 7 H. G. Schuster and G. Baasch, *Z. Med. Labortech.*, 12 (1971) 312.
- 8 C. Thin and A. Robertson, *Biochem. J.*, 51 (1952) 218.
- 9 E. Mehnert, *Arch. Exp. Veterinärmed.*, 24 (1970) 1269.
- 10 A. D. Woolhouse, *N.Z. J. Med. Lab. Technol.*, 25 (1971) 82.
- 11 V. H. Peden, *J. Lab. Clin. Med.*, 63 (1964) 332.
- 12 H. Steger and J. Voigt, *Arch. Tierernähr.*, 20 (1970) 631.
- 13 P. Hradechý and P. Jagos, *J. Chromatogr.*, 46 (1978) 327.
- 14 C. J. P. Eriksson, *Anal. Biochem.*, 47 (1972) 235.
- 15 L. Siegel, N. J. Robin and L. J. McDonald, *Clin. Chem.*, 23 (1977) 46.
- 16 G. J. van Stekelenburg and J. W. de Bruyn, *Clin. Chim. Acta*, 28 (1970) 233.
- 17 M. D. Trotter, M. J. Sulway and E. Trotter, *Clin. Chim. Acta*, 35 (1971) 137.
- 18 I. A. McDonald, L. P. Hackett and L. J. Dusci, *Clin. Chim. Acta*, 63 (1975) 235.
- 19 G. Svensson and T. Anfält, *Clin. Chim. Acta*, 119 (1982) 7.
- 20 M. H. Hashmi, *Anal. Chim. Acta*, 17 (1957) 383.
- 21 C. O. Haughton, *Ind. Eng. Chem., Anal. Ed.*, 9 (1937) 167.
- 22 M. Marasco, *Ind. Eng. Chem.*, 18 (1926) 701.

SPECTROPHOTOMETRIC DETERMINATION OF MAGNESIUM BY FLOW INJECTION ANALYSIS WITH A LIGAND BUFFER FOR MASKING CALCIUM

HIROKO WADA*, AKIO YUCHI and GENKICHI NAKAGAWA

Laboratory of Analytical Chemistry, Nagoya Institute of Technology, Showa-ku, Nagoya (Japan)

(Received 4th October 1982)

SUMMARY

1-(2-Hydroxy-3-sulfo-5-chloro-1-phenylazo)-2-naphthol-3,6-disulfonic acid is used in a spectrophotometric flow-injection system for the determination of magnesium ($0.2\text{--}2.4\text{ mg l}^{-1}$) at a sampling rate of 80 h^{-1} . Interference of calcium is eliminated by using a barium-(II)—EGTA ligand buffer. Iron(III), aluminum(III), copper(II), zinc(II), manganese(II) and cadmium(II) are masked by cyanide and triethanolamine. The method is suitable for application to tap and pond waters.

Xylidyl blue-I [sodium 1-azo-2-hydroxy-3-(2,4-dimethylcarboxanilido)-naphthalene-1'-(2-hydroxybenzene-5-sulfonate)] has been recommended for the spectrophotometric determination of magnesium because of its sensitivity and selectivity [1, 2]. However, this reagent is not very satisfactory because of the low solubilities of the reagent and its magnesium chelate and also the very large reagent blank.

In a previous study [3], several *o, o'*-dihydroxyazo compounds were synthesized and employed as metallochromic indicators for the EDTA titration of calcium. These reagents also form more stable chelates with magnesium than with calcium. Of the reagents examined, 1-(2-hydroxy-3-sulfo-5-chloro-1-phenylazo)-2-naphthol-3,6-disulfonic acid (CPR) forms a very stable magnesium chelate around pH 10, and the reagent and the magnesium chelate are stable in alkaline solution on standing. This paper describes the spectrophotometric determination of magnesium with CPR by flow injection analysis. Satisfactory results were obtained in the determination of magnesium in freshwater samples.

EXPERIMENTAL

Reagents

The CPR reagent was synthesized and purified as described previously [3]; it was dissolved in water to give a $7.5 \times 10^{-5}\text{ M}$ solution. The solution was stable for three months in a refrigerator. A standard magnesium solution

(0.24 mg ml⁻¹) was prepared from magnesium chloride and standardized against EDTA. Solutions of other metal ions were prepared from the chloride, nitrate or sulfate salts, and also standardized against EDTA.

The ligand buffer masking solution was prepared from barium nitrate and ethylene glycol-bis(β -aminoethyl ether)-*N, N, N', N'*-tetraacetic acid (EGTA). The EGTA was dissolved in the calculated amount of 1 M sodium hydroxide and diluted with water to give a 10⁻² M solution which was standardized by titration with a standard cadmium solution in presence of eriochrome black T indicator. A barium nitrate solution (about 5 \times 10⁻² M) in water was standardized by EDTA titration in presence of Mg-EDTA and eriochrome black T indicator. The ligand buffer solution containing masking reagents was then prepared by mixing 108 ml of 10⁻² M barium nitrate, 100 ml of 10⁻² M EGTA, 1.3 g of potassium cyanide and 3 g of triethanolamine with 500 ml of 0.2 M ammonia-ammonium chloride buffer solution (pH 10), and diluting to 1 l. This mixture gives an 8% excess of barium ions, 2 \times 10⁻² M cyanide and 2 \times 10⁻² M triethanolamine. It should be prepared weekly.

Water was redistilled from hard-glass apparatus. All salts used were of analytical-reagent grade.

Apparatus

A flow diagram of the home-made flow-injection apparatus is shown in Fig. 1. A Gilson Minipuls HP-4 peristaltic pump was used. A Kyowa-Seimitsu rotary valve to which a loop with a given volume was attached was employed for sample injection. A JASCO (Japan Spectroscopic Co.) UVIDEK 100-II W spectrophotometer (Model UVIDEK 100-II W) equipped with a flow cell (optical path 10 mm, volume 8 μ l) and a Hitachi Model 056 recorder were used. A Denki-Kagaku-Keiki Flow Injection Analyzer (FICS) was also used.

RESULTS AND DISCUSSION

The absorption spectra of the magnesium-CPR chelate and CPR solutions at pH 10 are shown in Fig. 2. The absorption maxima of the magnesium-CPR chelate and of CPR appear at 527 nm and 600 nm, respectively. The difference of the absorbances between CPR and its magnesium chelate was large around 520 and 600 nm. Because measurements of the decrease in absorbance at

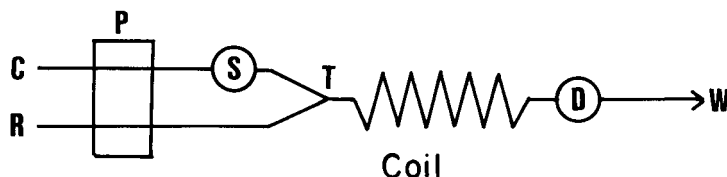


Fig. 1. Flow diagram for magnesium determination. P, pump; S, sample injector (40 μ l); T, confluence point; Coil, teflon reaction coil (0.5 mm i.d., 200 cm long); D, detector (510 nm, sensitivity 0.16 absorbance full scale); W, waste; C, ligand buffer masking solution; R, 7.5 \times 10⁻⁵ M CPR solution. Flow rates, 0.73 ml min⁻¹ in each channel.

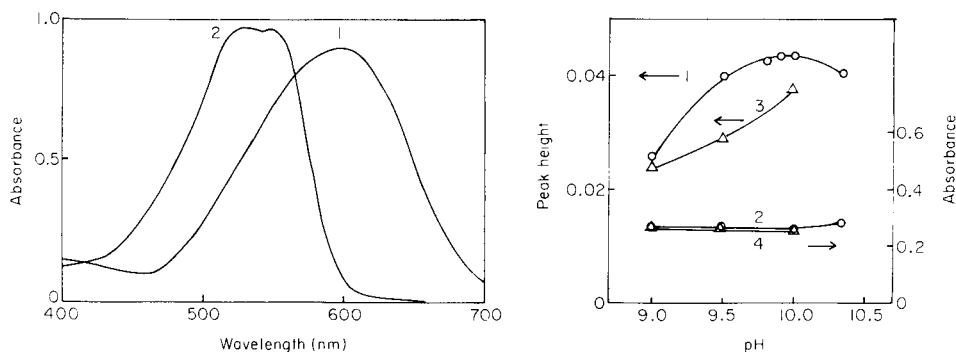


Fig. 2. Absorption spectra of CPR and the Mg-CPR chelate in 0.1 M $\text{NH}_3\text{--NH}_4\text{Cl}$ buffer solution (pH 10): (1) 4×10^{-5} M CPR; (2) 4×10^{-5} M CPR with 8×10^{-4} M Mg^{2+} .

Fig. 3. Effect of pH on the peak height for Mg-CPR and the absorbance of CPR: (1) peak height for 1.44 mg l^{-1} Mg in 0.1 M $\text{NH}_3\text{--NH}_4\text{Cl}$ buffer; (2) reagent blank for (1); (3) peak height for 1.44 mg l^{-1} Mg in 0.05 M $\text{Na}_2\text{B}_4\text{O}_7\text{--NaOH}$ buffer; (4) reagent blank for (3).

600 nm by the formation of the magnesium chelate were not reproducible in the flow-injection system, measurements at 500, 510 and 520 nm were examined. The signals for 1.44 ppm Mg and for the reagent blank increased as the wavelength of measurement was increased, but at 520 nm the reagent blank absorbance (almost 0.4) was too large to be cancelled, and the reproducibility was poor. All measurements were therefore done at 510 nm.

Optimal reaction conditions

As seen in Fig. 3, the peak height was largest at pH 9.8–10.1 in ammonia–ammonium chloride buffer; the tetraborate buffer system provided less sensitivity. Although increasing the CPR concentration gave larger peaks and increased the amount of magnesium that could be measured, the reagent blank became excessive. Therefore, a 7.5×10^{-5} M CPR solution was employed for the determination of magnesium in the range $0.2\text{--}2.4 \text{ mg l}^{-1}$.

When the mixing coil in the flow system (Fig. 1) was only 1 m long, dispersion and reaction were inadequate and reproducibility was poor. A 2-m coil was therefore used, although the peak height was then lower because of increased dispersion. There was no significant difference in peak heights when the coil length was increased to 3 m.

The flow rates used were the same for the buffer and the CPR solutions. Changes in the flow rates from 0.28 to 1.34 ml min^{-1} in each channel had little effect on peak heights, but at flow rates higher than 1 ml min^{-1} , reproducibility was poor. By considering the sampling rate, a flow rate of $0.7\text{--}0.75 \text{ ml min}^{-1}$ was preferred for each solution. Under these conditions, the residence time was 45 s. On the home-made apparatus, the best sample volume was $40 \mu\text{l}$. The dispersion (C_0/C_{max}) in this system was about 5.4.

As shown in Fig. 4, the calibration graph was linear for 0.2–2.4 mg l⁻¹ magnesium. The relative standard deviation was 0.66% ($n = 10$) when 0.97 mg l⁻¹ magnesium was determined.

This method was also examined with the commercial FICS analyzer which was used previously [4]. A 1-m mixing coil was used, but the solution concentrations and the flow rates were the same as above. Sample injections of 50 μ l were required for adequate peaks. Under these conditions, the calibration graph for magnesium was linear for the range 0.2–1.5 mg l⁻¹, and the dispersion of the sample was about 32.

Effects of interfering ions

Elimination of interference from calcium. Usually calcium interferes with the spectrophotometric determination of magnesium. However, the magnesium–CPR chelate is more stable than the calcium chelate [3] and the calcium–EGTA complex ($\log K_{(\text{CaY})} = 11.0$) is much more stable than the magnesium complex ($\log K_{(\text{MgY})} = 5.2$) [5]. Therefore, calcium may be masked readily with EGTA. In practice, calcium was completely masked by injecting samples into a stream of 0.1 M ammonia–ammonium chloride containing EGTA (10^{-3} M), but at the same time the peak height of magnesium–CPR chelate diminished. Then a ligand buffer [6] containing EGTA and a small excess of strontium or barium was examined. The stability constants of the strontium and barium complexes with EGTA ($\log K_{(\text{SrY})} = 8.5$, $\log K_{(\text{BaY})} = 8.4$ [5]) are between those of the calcium and magnesium complexes. When these ligand buffer systems were used, calcium was completely masked without any decrease in the peak height for magnesium. In the case of the strontium–EGTA system, however, the reagent blank was raised by the formation of a colored strontium–CPR chelate. In the barium–EGTA system, a 1–50% excess of barium did not affect the reagent blank. A 10^{-3} M barium–EGTA buffer containing an 8% excess of barium could mask the interference of calcium up to 35 mg l⁻¹. The calibration recording for magnesium in the presence of 14 mg l⁻¹ calcium is shown in Fig. 4.

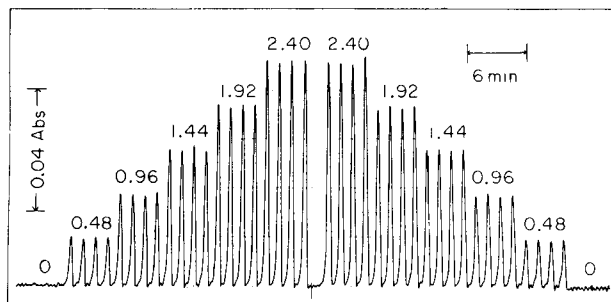


Fig. 4. Calibration graph for magnesium in the absence (right) and in the presence (left) of calcium (14 mg l⁻¹). The numbers on the peaks are mg l⁻¹ magnesium.

TABLE 1

Effects of various ions on the determination of magnesium (0.97 mg l^{-1})

Cation	Added (mg l^{-1})	Mg found (mg l^{-1})	Anion	Added (M)	Mg found (mg l^{-1})
Fe^{3+}	5.6	0.97	PO_4^{3-}	10^{-5}	0.97
	56	1.01		4×10^{-5}	0.95
Al^{3+}	1.4	0.97		10^{-4}	0.94
	2.7	1.05		10^{-3}	0.90
Cu^{2+}	7.6	0.97	CO_3^{2-}	10^{-5}	0.97
Zn^{2+}	25.4	0.97		10^{-4}	1.00
Cd^{2+}	112.4	0.97		10^{-3}	0.99
Mn^{2+}	0.54	0.97			
	2.7	0.99			
			SO_4^{2-}	10^{-5}	0.97
Ca^{2+}	14			10^{-4}	0.98
Fe^{3+}	2.8			10^{-3}	0.97
Al^{3+}	1.1	0.97			
Cu^{2+}	0.76				
Mn^{2+}	0.97				

Effects of other ions. Iron(III), aluminum(III), copper(II), zinc(II), cadmium(II) and manganese(II) interfered with this method. The barium-EGTA ligand buffer completely masked cadmium ions but iron(III), aluminum, copper(II), zinc and manganese(II) were only partly masked. When the ligand buffer solution also contained potassium cyanide ($2 \times 10^{-2} \text{ M}$) and triethanolamine ($2 \times 10^{-2} \text{ M}$), these interferences were completely eliminated (Table 1).

The effects of phosphate, carbonate and sulfate are also given in Table 1. Phosphate (10^{-3} M) decreased the peak height significantly whereas the effect of carbonate was slight.

TABLE 2

Determination of magnesium in water samples

Sample	Mg found (mg l^{-1})	EDTA titration (mg l^{-1})	
		Mg	Ca
Pond water (1)	3.59, 3.55 ^a	3.5	9.4
Pond water (2)	2.12, 2.06 ^a	2.0	6.5
Pond water (3)	2.00, 1.92 ^a	1.9	6.0
Pond water (4)	2.87, 2.84 ^a	2.7	7.4
Tap water (1)	3.71	3.7	8.1
Tap water (2)	0.78	0.8	6.5

^a After removal of carbonate.

Application to water samples

The method was applied to the determination of magnesium in four pond-water samples and two tap-water samples. The results are given in Table 2 together with those obtained by EDTA titration. When any interference from carbonate was eliminated by boiling an aliquot of the water with hydrochloric acid, the differences between the results were not significant.

In conclusion, the flow-injection system enables a color-forming reagent which is unsuitable for conventional spectrophotometry because of its high reagent blank, to be used successfully. This should also be useful for the determination of magnesium in sera and plants.

REFERENCES

- 1 C. K. Mann and J. H. Yoe, *Anal. Chem.*, 28 (1956) 202.
- 2 H. Watanabe and H. Tanaka, *Bunseki Kagaku*, 26 (1977) 635.
- 3 H. Wada and G. Nakagawa, *Anal. Chim. Acta*, 121 (1980) 265.
- 4 G. Nakagawa, H. Wada and C. Wei, *Anal. Chim. Acta*, 145 (1983) 135.
- 5 A. Ringbom, *Complexation in Analytical Chemistry*, John Wiley, New York, 1963.
- 6 M. Tanaka, *Anal. Chim. Acta*, 29 (1963) 193.

SPECTROFLUORIMETRIC DETERMINATION OF CATECHOLAMINES WITH 2-CYANOACETAMIDE

SUSUMU HONDA*, YOKO ARAKI, MASAYE TAKAHASHI and KAZUAKI KAKEHI

Faculty of Pharmaceutical Sciences, Kinki University, 3-4-1 Kowakae, Higashi-osaka (Japan)

(Received 20th September 1982)

SUMMARY

A simple and sensitive spectrofluorimetric method is described for the determination of catecholamines, based on their reaction with 2-cyanoacetamide. This method is highly selective for compounds having a vicinal diphenolic group, and allows reproducible determination of 1×10^{-8} – 1×10^{-5} M epinephrine and norepinephrine, and 5×10^{-8} – 5×10^{-5} M dopamine. Reducing carbohydrates interfere but polysaccharides (amylose and glycogen) do not; amino acids, carboxylic acids (fumaric, citric acid, etc.), pyrimidine and purine bases, nucleic acids and proteins do not interfere.

The amounts of catecholamines in body tissues and fluids are very small, thus sensitive methods are required for their determination. Although numerous fluorimetric methods are available for this purpose, most are modifications of either the method of Lund [1] based on oxidation to fluorescent trihydroxyindole derivatives or that of Natelson et al. [2] based on reaction with 1,2-diaminoethane to give fluorescent condensates. The trihydroxyindole method has a high sensitivity to epinephrine and norepinephrine but its sensitivity to dopamine is lower by two orders of magnitude. The 1,2-diaminoethane method has relatively uniform sensitivity to all catecholamines, but it is less sensitive to epinephrine and norepinephrine than the trihydroxyindole method. In addition the reagent must be purified by redistillation before use.

Recently, it was found that 2-cyanoacetamide reacts with reducing carbohydrates to form intensely fluorescent products [3], and this reaction was applied to monitoring carbohydrates separated by high-performance liquid chromatography [4]. Further examination showed that catecholamines also fluoresced intensely with this reagent. This paper thus proposes a new method for the spectrofluorimetric determination of catecholamines with use of 2-cyanoacetamide.

EXPERIMENTAL

Materials and apparatus

2-Cyanoacetamide (Kanto Chemical Company, Nihonbashi, Chuo-ku, Tokyo) was used as received. The samples of epinephrine and norepinephrine

were obtained as their bitartrates, whereas those of dopamine, DL-metanephrine, DL-normetanephrine, DL-synephrine and DL-octopamine were obtained as their hydrochlorides. Other amines were the free bases. All these samples and chemicals were of the highest grade commercially available.

Fluorescence spectra and intensities were recorded on a Shimadzu RF-500 spectrofluorimeter by using a 1 cm × 1 cm quartz cell.

Procedures

Optimization studies. In every experiment, an aqueous solution (1 ml) of catecholamine, an aqueous solution (1 ml) of 2-cyanoacetamide and a buffer (2 ml) were mixed, and the mixture was heated in a thermostated water bath. The reaction mixture was cooled to room temperature, and the fluorescence intensity was measured.

Determination of catecholamines. An aqueous solution (1 ml) of a catecholamine sample was pipetted into a 10-ml screw-capped tube, and an aqueous 1% solution (1 ml) of 2-cyanoacetamide and a 0.3 M borate buffer (2 ml) were added. The tube was heated for 10 min in a boiling water bath, then cooled immediately in tap water. The fluorescence intensity was measured and the concentration of the catecholamine was measured from a calibration graph obtained from standards treated under identical conditions. The pH of the buffer and the detection wavelengths to be used for each catecholamine are given in Table 1.

RESULTS AND DISCUSSION

Fluorescence reaction and spectra

2-Cyanoacetamide was first used for fluorimetric determination of reducing carbohydrates [3]. Catecholamines and reducing carbohydrates have tautomeric enediol and α -hydroxycarbonyl groups, respectively. Thus the fluorescence reactions of these two groups of compounds should be essentially of the same type, namely producing *N*-heterocyclic compounds by dehydrative cyclization of the condensates. Figure 1 shows the fluorescence spectra of the reaction products of catecholamines with 2-cyanoacetamide. The wavelengths of the excitation and emission maxima were different for each catecholamine species, and are given in Table 1. Dopamine gave the greatest emission intensity.

TABLE 1

pH Values and detection wavelengths for determination of catecholamines

Catecholamine	pH	Wavelength (nm)	
		Excitation	Emission
Epinephrine	12.0	380	483
Norepinephrine	10.0	361	460
Dopamine	11.0	362	435

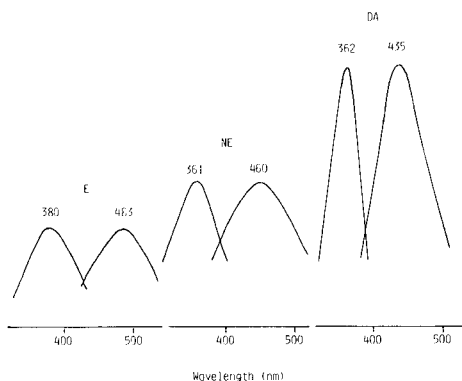


Fig. 1. Fluorescence excitation and emission spectra of equimolar concentrations of (E) epinephrine; (NE) norepinephrine; (DA) dopamine, after reaction with 2-cyanoacetamide under the recommended conditions.

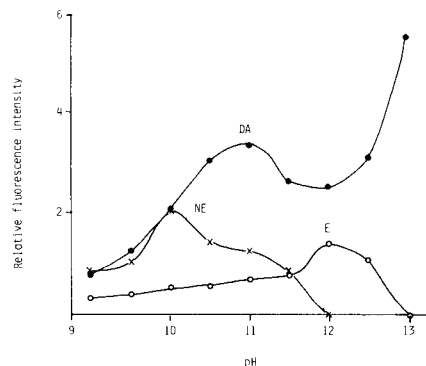


Fig. 2. pH dependence of fluorescence intensity for the compounds in Fig. 1 (1×10^{-6} M) under the recommended conditions.

Optimization

Figure 2 shows the pH dependence of fluorescence intensity. Epinephrine and norepinephrine gave single maxima at pH 12 and 10, respectively. Dopamine gave a maximum at pH 11, but higher intensity was observed above pH 12.

Figure 3 summarizes the results of optimization studies for other reaction parameters. Among the various kinds of buffer examined, including carbonate, phosphate, glycine, and borate buffers, the last gave the highest intensity.

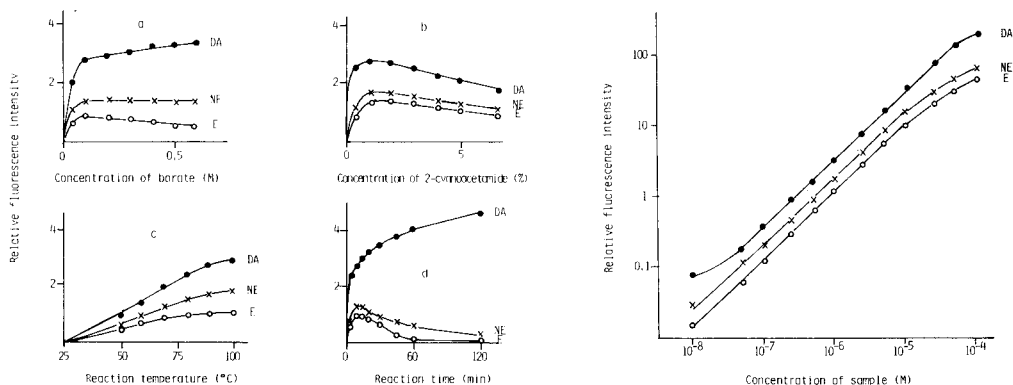


Fig. 3. Optimization of fluorescence reaction for 1×10^{-6} M samples. (a) Effect of buffer concentration for 1% reagent, 100°C , 10 min reaction time. (b) Effect of reagent concentration for 0.3 M buffer, 100°C , 10 min reaction time. (c) Effect of reaction temperature for 0.3 M buffer, 1% reagent, 10 min reaction. (d) Reaction time with 0.3 M buffer, 1% reagent, 100°C .

Fig. 4. Calibration graphs for catecholamines.

In borate buffer, an intensity plateau was reached at 0.1 M buffer for each catecholamine. The effect of reagent concentration was similar, giving maximum intensities at 1% reagent for all the catecholamines. Fluorescence intensity continued to increase as reaction temperature rose up to 100°C, and reached a maximum value at reaction times of ca. 10 min for the epinephrines, after which it gradually decreased. The fluorescence of dopamine continued to increase for at least 120 min. The recommended procedure was established on the basis of these results.

Calibration and reproducibility

As seen in Fig. 4, the log-log calibration graphs are linear over the range 1×10^{-8} – 1×10^{-5} M for the epinephrines, and 5×10^{-8} – 5×10^{-5} M for dopamine, with a slope of 1.0. Table 2 gives precision data for the determination of catecholamines at the lowest and highest limits of the linear range, as well as at intermediate concentrations. Table 3 lists the relative intensities of the fluorescences from equimolar amounts of catecholamines.

Effect of other compounds

The fluorescence intensities and wavelengths for related compounds are also given in Table 3. The most important observation is that all compounds having hydroxyl groups at adjacent positions in the benzene ring fluoresced intensely, with the exception of pyrogallol. It is notable that a few components of the metabolic pathway of tyrosine, such as L-dopa, 3,4-dihydroxyphenylacetic acid and 3,4-dihydroxymandelic acid, also fluoresced strongly. Pyrogallol has an additional aromatic hydroxyl group which might hinder tautomerization to the α -hydroxycarbonyl group, which is presumably the reactive form. In contrast, no compounds without adjacent hydroxyl groups fluoresced.

Reducing carbohydrates interfered with the determination of catecholamines. The relative molar intensities for D-arabinose, D-glucose and L-fucose with respect to dopamine were 0.033, 0.035, and 0.017, respectively. D-Glucos-

TABLE 2

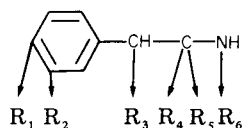
Reproducibility of determination of catecholamines

Concentration (M)	Coefficient of variation (%) ^a		
	Epinephrine	Norepinephrine	Dopamine
1×10^{-6}	6.1	3.3	—
5×10^{-6}	—	—	6.5
5×10^{-7}	4.7	2.6	—
1×10^{-6}	—	—	3.0
1×10^{-5}	2.1	2.6	—
5×10^{-5}	—	—	1.9

^a10 determinations.

TABLE 3

Comparison of fluorescence intensities and wavelengths for catecholamines and related compounds^a



Compound	R ₁	R ₂	R ₃	R ₄	R ₅	R ₆	λ_{\max} (nm) excitation/ emission	Fluorescence intensity ^b
Dopamine	OH	OH	H	H	H	H	362/435	30.1
Norepinephrine	OH	OH	OH	H	H	H	361/460	17.0
Epinephrine	OH	OH	OH	H	H	Me	380/483	10.5
Isoproterenol	OH	OH	OH	H	H	CMe ₂	334/496 382/485	6.6 6.6
Tyramine	OH	H	H	H	H	H	—	nil
DL-Normetanephrine	OH	OMe	OH	H	H	H	—	nil
DL-Metanephrine	OH	OMe	OH	H	H	Me	—	nil
DL-Octopamine	OH	H	OH	H	H	H	—	nil
DL-Synephrine	OH	H	OH	H	H	Me	—	nil
L-Dopa	OH	OH	H	H	COOH	H	363/445	16.6
3,4-Dihydroxy-phenylacetic acid	OH	OH	H	=O	OH	—	380/467	12.8
3,4-Dihydroxy-mandelic acid	OH	OH	OH	=O	OH	—	380/470	21.8
3,4-Dihydroxy-benzoic acid	OH	OH	—	—	—	—	367/453	11.1
3-Methoxy-4-hydroxy-mandelic acid	OH	OMe	OH	=O	OH	—	—	nil
3-Hydroxy-phenylacetic acid	H	OH	H	=O	OH	—	—	nil
Pyrocatechol	OH	OH	—	—	—	—	420/483	13.2
Resorcinol	OH	H	—	—	—	—	—	nil
p-Hydroquinone	OH	H	—	—	—	—	—	nil
Pyrogallol	OH	OH	—	—	—	—	—	nil

^a 1×10^{-5} M at pH 11.0.

^b Relative to that for 1×10^{-8} M quinine sulfate in 0.1 M sulfuric acid at its maximum wavelengths.

amine (0.169) and D-glucuronic acid (0.107) gave higher values, but non-reducing carbohydrates, such as D-glucitol, D-gluconic acid, N-acetylneuraminic acid, and myoinositol did not give any fluorescence. The production of fluorescence from polysaccharides such as amylose and glycogen was negligible. Other compounds examined included amino acids (L-glycine, L-alanine, L-leucine, L-phenylalanine, L-cysteine, L-methionine, L-threonine, L-aspartic acid, L-glutamic acid, L-asparagine, L-lysine, L-histidine, L-tryptophan, and β -alanine), carboxylates in the tricarboxylic acid cycle

(malic acid, fumaric acid, citric acid and succinic acid), pyrimidine and purine bases (adenosine, guanosine, thymidine, uridine, AMP, ADP and ATP), as well as nucleic acids (salmon sperm DNA and yeast RNA), proteins (ovalbumin, human serum globulin and human serum transferrin), and inorganic salts found in body fluids (sodium chloride, sodium sulfate and ammonium chloride). The fluorescence intensities for all these compounds were less than 1% of that of dopamine at the same concentration.

Comparison with conventional methods

Table 4 compares the fluorescence intensities of 10^{-7} M catecholamines obtained by the present method with those obtained by the trihydroxyindole [5] and 1,2-diaminoethane [6] methods. It is apparent that the trihydroxyindole method had a lower sensitivity for dopamine than for the epinephrines. In contrast, the intensities for the epinephrines by the present method were slightly lower than those obtained by the trihydroxyindole method, but the intensity for dopamine was more than thirty times higher than that obtained by the trihydroxyindole method. The 1,2-diaminoethane method was much less sensitive; catecholamines were not measurable at 10^{-7} M.

The simplicity of the present method should be pointed out. It requires only one reagent compared to four (potassium hexacyanoferrate(III), zinc sulfate, ascorbic acid and sodium hydroxide) in the trihydroxyindole method. It uses directly a sample of commercial reagent, while the 1,2-diaminoethane method requires purification of the commercial reagent by distillation. It is also superior to the 1,2-diaminoethane method because of its much higher sensitivity, and has a more uniform sensitivity for all catecholamines than the trihydroxyindole method. Because reducing carbohydrates interfere, prior separation of catecholamines by appropriate means, such as fractionation on columns of aluminium oxide and ion-exchange resins, is necessary for some biological samples. Separation by high-performance liquid chromatography will be valuable for this purpose, and a study of monitoring catecholamines in high-performance liquid chromatography will be reported elsewhere.

TABLE 4

Comparison of the 2-cyanoacetamide method with the trihydroxyindole and 1,2-diaminoethane methods

Catecholamine ^a	2-Cyanoacetamide		Trihydroxyindole		1,2-Diaminoethane
	R.I. ^b	$\lambda_{\text{ex}}/\lambda_{\text{em}}$ (nm)	R.I. ^b	$\lambda_{\text{ex}}/\lambda_{\text{em}}$ (nm)	R.I. ^b
Epinephrine	1.87	380/483	3.64	408/508	ND ^c
Norepinephrine	2.09	361/460	2.70	389/500	ND
Dopamine	3.09	362/435	0.09	392/458	ND

^a 10^{-7} M sample. ^bFluorescence intensity relative to 1×10^{-9} M quinine sulfate in 0.1 M sulfuric acid at its maximum wavelength. ^cNot detected.

REFERENCES

- 1 A. Lund, *Acta Pharmacol. Toxicol.*, 5 (1949) 231.
- 2 S. Natelson, J. K. Lugovoy and J. B. Pincus, *Arch. Biochem.*, 23 (1949) 157.
- 3 S. Honda, Y. Matsuda, M. Takahashi, K. Kakehi and S. Ganno, *Anal. Chem.*, 52 (1980) 1079.
- 4 S. Honda, M. Takahashi, K. Kakehi and S. Ganno, *Anal. Biochem.*, 113 (1981) 130.
- 5 A. H. Anton and D. F. Sayre, *J. Pharmacol. Exptl. Ther.*, 138 (1962) 360.
- 6 H. Weil-Malherbe and A. D. Bone, *Biochem. J.*, 51 (1952) 311.

REACTION OF AMINES OF BIOLOGICAL IMPORTANCE WITH 4-FLUORO-7-NITROBENZO-2-OXA-1,3-DIAZOLE

TOSHIMASA TOYO'OKA, YOSHIHIKO WATANABE and KAZUHIRO IMAI*

Department of Analytical Chemistry, Faculty of Pharmaceutical Sciences, University of Tokyo, Hongo 7-3-1, Bunkyo-ku, Tokyo 113 (Japan)

(Received 7th October 1982)

SUMMARY

The reaction of amines, amino acids and imino acids with 4-fluoro-7-nitrobenzo-2-oxa-1,3-diazole (NBD-F) were investigated by high-performance liquid chromatography (h.p.l.c.) with fluorimetric detection. All the amino compounds tested, except tryptophan, gave fluorescent derivatives at 524—541 nm with excitation at 467—472 nm. The reaction rates for secondary amines, imino acid, primary amine and amino acid decreased in this order. The NBD derivatives of synephrine were separated on h.p.l.c., and fractions were collected and subjected to chemical-ionization mass spectrometry. It is shown that the *N*-mono-NBD derivative of synephrine, $(M + H)^+ = 331$, is formed rapidly and disappears gradually while the *N,O*-di-NBD derivative, $(M + H)^+ = 494$, forms. The h.p.l.c. of putrescine, spermidine and spermine is described; the detection limits are 76 fmol, 0.43 pmol and 1.20 pmol, respectively.

Among the fluorogenic reagents for amines, fluorescamine [1] and *o*-phthalaldehyde (OPA) [2] are known to react with primary amines to give the corresponding fluorophores. Dansyl chloride [3] reacts with both primary and secondary amines to yield fluorescence. 4-Chloro-7-nitrobenzo-2-oxa-1,3-diazole (NBD-Cl), introduced by Ghosh and Whitehouse [4] as a fluorogenic reagent for both primary and secondary amines, has been favorably used for the determination of proline and hydroxyproline [5] in biological fluids. Ahnoff et al. [6] have shown that the reactivity of NBD-Cl with amino acids was much lower than that with imino acids such as proline and hydroxyproline.

In previous papers [7, 8], the 4-fluoro analog of NBD-Cl, 4-fluoro-7-nitrobenzo-2-oxa-1,3-diazole (NBD-F), was shown to react 10 times faster than NBD-Cl, with both amino and imino acids. Pre-column labelling of amino and imino acids with NBD-F and the high-performance liquid chromatography at picomolar levels were achieved [8, 9].

In this paper, the reactivities of amines, amino and imino acids with NBD-F are studied by the separation and measurement of the resultant fluorophores by high-performance liquid chromatography (h.p.l.c.). The applicability of the pre-column labelling of catecholamines and polyamines with the reagent is also discussed.

EXPERIMENTAL

Materials

Amino and imino acids (Ajinomoto Co., Tokyo) were used as received. All other chemicals were of reagent grade. NBD-F, and its glycine and hydroxyl derivatives were synthesized by the methods of Nunno et al. [10], Ghosh [11] and Dal Monte et al. [12], respectively. Water was deionized and distilled just prior to use.

Synthesis of proline derivative of NBD. To a solution of proline (575 mg) in 5% (w/v) sodium acetate solution (100 ml) was added a solution of NBD-Cl (1.0 g) in ethanol (50 ml). The reaction mixture was refluxed for 10 min, acidified with 4 M HCl to pH 1.5 and evaporated to dryness. The powder was dissolved in water and extracted with ethyl acetate. The organic layer was evaporated to dryness. Recrystallization from benzene-ethyl acetate yielded the proline derivative (0.3 g) as orange needles (m.p. 156–157°C; calculated for $C_{11}H_{15}N_4O_4 \cdot H_2O$, 44.6% C, 4.1% H, 18.9% N; found, 44.3% C, 3.8% H, 18.75% N).

Reaction of amines, amino acids and imino acids with NBD-F

The amine or amino or imino acid (about 0.3 μ mol) in 2 ml of phosphate buffer (pH 7.0, prepared with 0.066 M potassium dihydrogenphosphate and disodium hydrogenphosphate) in a 10-ml stoppered test tube was treated with 2 ml of a freshly prepared ethanolic solution of NBD-F (about 3.0 μ mol). Immediately after the reagent addition, the tube was tightly capped, covered with an aluminum foil, and heated at 50°C. At certain time intervals, a 0.2-ml portion of the mixture was removed to a small test tube, cooled in ice water, and mixed with 25 μ l of 0.5 M HCl to stop the further reaction. Aliquots of the final solution were subjected to h.p.l.c. to establish the time course of the reactions.

In the case of polyamines, 45–67.5 pmol of the amine dissolved in 0.1 ml of the phosphate buffer (pH 7.0) was treated with 0.1 ml of NBD-F (60 nmol) in ethanol at 50°C for 1 min. After the addition of 25 μ l of 0.5 M HCl, 10 μ l of the mixture was injected for h.p.l.c.

Conditions for h.p.l.c.

A column of TSK LS-160 (polyethyleneglycol dimethacrylate gel, 5 μ m, 125 mm long, 8 mm i.d.; Toyo Soda Manufacturing Co., Tokyo) was used to separate the NBD derivatives. The column was maintained at 50°C. The eluting solvents, pumped with a Milton-Roy minipump, were: (A) methanol-acetonitrile (7:3); (B) methanol-acetonitrile-35% HCl (70:30:0.9); or (C) methanol-0.066 M phosphate buffer, pH 6.0, (95:5). The flow rate was 0.4 or 0.6 ml min⁻¹ for all the derivatives. For detection, a Schoeffel FS-970 spectrofluorimeter was equipped with a 5- μ l flow cell and a cut-off filter at 490 nm (excitation at 470 nm), or a Hitachi fluorescence spectrophotometer 650-10S was equipped with an 18- μ l flow cell (excitation at 470 \pm 5 nm and emission at 530 \pm 5 nm).

Fluorescence characteristics and chemical ionization mass spectrometry of the resultant fluorophors

A portion (20 μ l) of the reaction mixture (after 5 min) described above was injected onto the h.p.l.c. column. The fraction corresponding to each NBD derivative was collected and diluted with methanol–acetonitrile (7:3). The excitation and emission spectra of this solution were measured with the Hitachi spectrofluorimeter (slit width about 10 nm). The fractions corresponding to NBD derivatives of synephrine were dried in vacuo and the residues (100–500 μ g) were subjected to chemical ionization mass spectrometry (c.i.m.s.) in a gas chromatograph/double focusing mass spectrometer M-80 (Hitachi Seisakusho Co., Tokyo). The conditions were as follows: reactant gas, isobutane; chamber temperature, 200°C; chamber voltage, 70 eV; total current, 80 μ A; ion accelerator, 3 kV.

RESULTS AND DISCUSSION

All the NBD derivatives of amino and imino acids exhibited similar excitation and emission maxima at wavelengths in the ranges 467–472 and 524–541 nm, respectively (Table 1): some of these agree with data reported by Fager et al. for NBC-Cl [13]. The fluorescence intensities of the chromatographic peaks were therefore measured with a Toshiba Y-49 cut-off filter (490 nm) and excitation at 470 nm.

Most of the reaction mixtures examined (amine, amino acid or imino acid) gave only one peak accompanying a peak corresponding to the hydrolyzed product of NBD-F [12], on the chromatogram. Exceptions were catecholamines, synephrine and octopamine, which gave two peaks on the chromatogram, and tryptophan which gave no identifiable peaks. In earlier work [13],

TABLE 1

Excitation and emission maxima^a of some NBD derivatives

Compound	λ_{ex} (nm)	λ_{em} (nm)	Compound	λ_{ex} (nm)	λ_{em} (nm)
HPEA ^b	470	537	Alanine	468	529
MHPEA ^c	471	539	Methionine	468	537
Putrescine	470	530	Aspartic acid	468	532
Spermidine	468	539	Lysine	469	529
Spermine	467	541	Arginine	468	528
Octopamine	468	535	Histidine	468	537
Synephrine	471	530	Tyrosine	467	524
Norepinephrine	470	535	Proline	472	525
Epinephrine	471	539	Leu-Gly	468	525
Glycine	468	535	NBD-OH	469	546

^aSolvent system, methanol–acetonitrile (7:3); uncorrected values. ^b β -Hydroxyphenylethylamine. ^cN-Methyl- β -hydroxyphenylethylamine.

the tryptophan derivative of NBD-Cl, which has the same R_F value as the hydrolyzed product (chloroform—methanol, 7:3; $R_F = 0.53$), was claimed to fluoresce. However, in the present work, the tryptophan derivative with NBD-F was easily prepared but did not fluoresce. The structure of the product is being studied.

Reaction of phenylalkylamines, amino and imino acids

N-Methyl- β -hydroxyphenylethylamine (MHPEA), a secondary amine, reacted more quickly with NBD-F to reach its maximum value than β -hydroxyphenylethylamine (HPEA), a primary amine (Fig. 1). The same trend was observed for proline versus glycine, alanine, lysine, leucylglycine and tyrosine; the data for glycine and pyroline are shown in Fig. 1. However, formation of the aspartic acid derivative proceeded more slowly than for the other amino or imino acids listed. The fraction corresponding to the MHPEA derivative was collected, evaporated to dryness in vacuo and subjected to c.i.m.s. (isobutane). The molecular ion peak $((M + H)^+ = 315)$ was obtained without any other notable fragment ions.

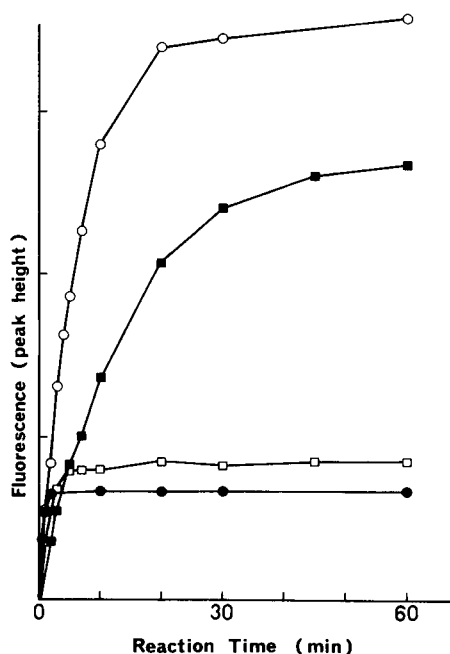


Fig. 1. Time courses of the reaction of amines, glycine and proline (0.15 mM) with NBD-F (1.5 mM) at 50°C and pH 7.0: (○) β -hydroxyphenylethylamine (HPEA); (●) *N*-methyl- β -hydroxyphenylethylamine (MHPEA); (■) glycine; (□) proline. Eluent for h.p.l.c. (0.4 ml mm^{-1}): methanol—acetonitrile (7:3) for HPEA or MHPEA, methanol—0.066 M phosphate buffer, pH 6.0 (95:5) for glycine or proline.

Reaction rate constants of amines, amino and imino acids with NBD-F

In order to compare the reactivity of the amines, and amino and imino acids quantitatively, the reaction rate constants were measured. Authentic samples of the glycine, proline and hydroxyl products were available by chemical synthesis, and the rate constants for these compounds were obtained as the absolute values. Authentic specimens of the derivatives of other amines or amino acids with NBD-F were not available. However, glycine, a model primary amino acid, reacted quantitatively with an excess of NBD-F (60:1 mole ratio) on treatment at 50°C and pH 7.0 for 90 min. The rate constants for the other derivatives were calculated on the basis of the fluorescence intensity of each amine or amino acid treated with NBD-F (100:1 mole ratio) at 50°C and pH 7.0 for 90 min.

All the amines, amino acids and imino acids tested reacted with NBD-F in a pseudo-first order reaction when the reagent was present in excess. Hydrolysis of the reagent was also a pseudo-first order reaction. As expected from the reaction time curves in Fig. 1, reaction of the secondary amines or imino acids was 10 times faster than that of primary amines or amino acids (Table 2). The reaction of the secondary amine, MHPEA, was slightly faster than that of the imino acids, proline; the primary amine, HPEA, reacted more quickly than the amino acid, glycine. The rate of hydrolysis of the reagent was of the same order as the reaction of amino acids. The reaction rate constants obtained agree well with those obtained previously by u.v. spectrophotometry, in which much less reagent (10 μ M) was used and the fluorophores were not separated [8].

Reactions of hydroxyphenylethylamines and catecholamines

Although, under the conditions given in the Experimental part, only one peak appeared on a chromatogram obtained from the reaction of synephrine or octopamine with NBD-F, the reactions of amines having a hydroxyphenyl group with the reagent might be somewhat different from those of aliphatic amines, amino acids or imino acids because the phenolic hydroxyl might react as it does with NBD-Cl [4]. Figure 2 shows that synephrine reacted with equal quantities of NBD-F (0.15 mM) to give three peaks on the chro-

TABLE 2

Reaction rate constants for amines, amino acids or imino acids with NBD-F^a

Compound	k_{obs} (min ⁻¹)	Compound	k_{obs} (min ⁻¹)
HPEA	1.10×10^{-1}	Aspartic acid	7.67×10^{-3}
MHPEA	1.96	Proline	4.35×10^{-1}
Glycine	3.66×10^{-2}	NBD-F \rightarrow NBD-OH	3.03×10^{-2}
Lysine	2.56×10^{-2}		

^aIn phosphate buffer (pH 7.0), 50°C.

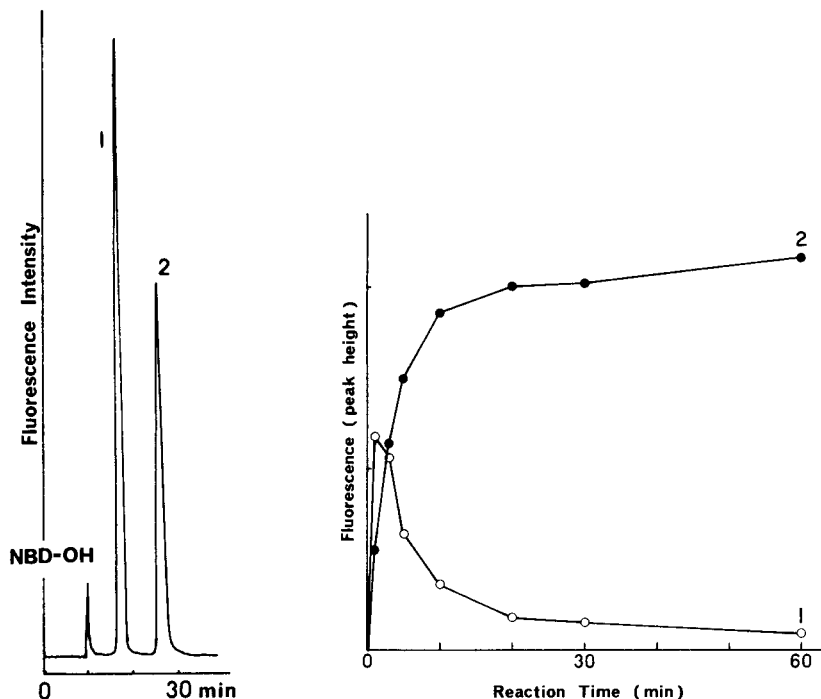


Fig. 2. Chromatogram obtained from the reaction of synephrine with an equimolar amount (0.15 mM) of NBD-F at 25°C and pH 7.0. Peaks: (1) *N*-NBD-synephrine; (2) *N,O*-di-NBD-synephrine. Conditions as for Fig. 1 with methanol–acetonitrile (7:3) eluent.

Fig. 3. Time courses for the formation of (1) *N*-NBD-synephrine and (2) *N,O*-di-NBD-synephrine. Reaction and h.p.l.c. conditions as for Fig. 2.

matogram. The peak with the smallest capacity factor corresponded to the hydrolyzed product. Peak 1 appeared at an early stage of the reaction and decreased slowly as the reaction proceeded; peak 2 increased to a maximum as peak 1 decreased (Fig. 3). The reaction curves suggested that peak 1 might be the *N*-NBD derivative and peak 2 the *N,O*-di-NBD derivative. In order to confirm this, the compound corresponding to peak 1 was collected and subjected to c.i.m.s.; the spectrum (Fig. 4A) showed the structure to be the *N*-NBD-synephrine derivative, with $(M + H)^+ = 331$. The compound corresponding to peak 2 was identified as the *N,O*-di-NBD-synephrine derivative, with $(M + H)^+ = 494$ (Fig. 4B). There might be another peak of the *O*-NBD derivative, but this would not be detected by the present fluorimetric system because its fluorescence intensity can be assumed to be 100 times less than that of the *N*-NBD derivative [4].

With regard to these c.i.m. spectra, the molecular ion peaks are easily obtained. The $\text{CH}_2\text{--N}$ bond is more stable than the CH(OH)--CH_2 bond of $\text{CH(OH)--CH}_2\text{--N(CH}_3\text{)--NBD}$ and forms $((\text{CH}_2\text{--N(CH}_3\text{)--NBD}) + \text{H})^+ = 208$ (Fig. 4A). The phenyl-*O*-NBD bond was cleaved in the case of the

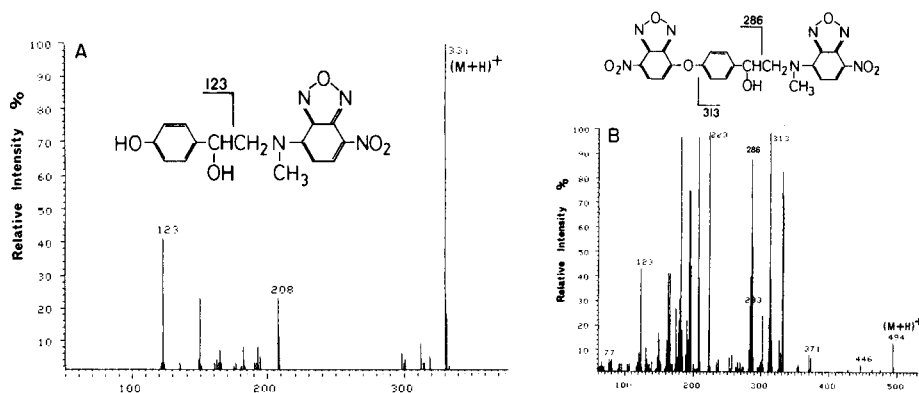


Fig. 4. C.i.m. spectra (iso-butane): (A) *N*-NBD-synephrine; (B) *N,O*-di-NBD-synephrine.

N,O-di-NBD compound to give $(M - (O\text{-NBD}))^+ = 313$ (Fig. 4B). This technique of derivatization of amines with NBD-F, isolation of the derivatives by h.p.l.c., and c.i.m.s. might be useful for obtaining the molecular weight of unknown substances in biological fields.

When catecholamines (epinephrine and norepinephrine) were treated with

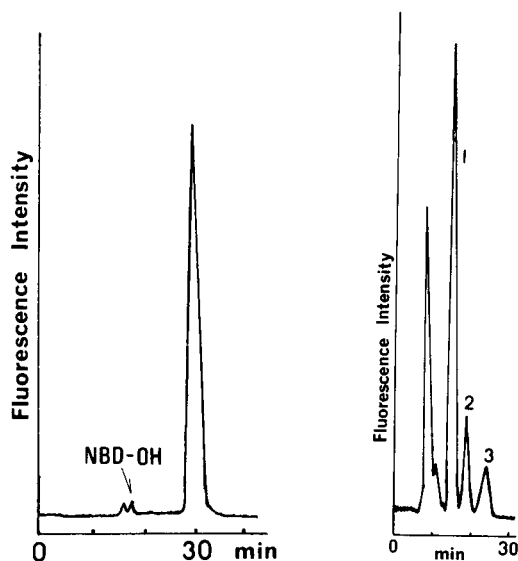


Fig. 5. Chromatogram obtained from the reaction of norepinephrine (0.15 mM) with NBD-F (1.5 mM) at 50°C and pH 7.0 for 30 min. Conditions for h.p.l.c. as for Fig. 2.

Fig. 6. Chromatogram obtained from the reaction of polyamines (50 μ M) with NBD-F (50 mM) at 50°C and pH 7.0 for 1 min. Peaks: (1) putrescine, 2.0 pmol; (2) spermidine, 2.4 pmol; (3) spermine, 3.0 pmol. Conditions: eluent, methanol-acetonitrile-35% HCl (70:30:0.9); flow rate, 0.6 ml min⁻¹.

a >20-fold molar excess of the reagent at 50°C and pH 7.0 for 120 min, four peaks, including the ever-present NBD-OH, appeared on the chromatogram. The peak with the second smallest capacity factor, which appeared soon after the reaction, decreased slowly with time while the third peak increased. By analogy with the data for synephrine, this third peak is probably the *N,O*-di-NBD derivative. However, under the selected conditions (see Experimental) only the third peak was obtained (Fig. 5).

Reaction and h.p.l.c. of polyamines

The above data suggest that amines, amino acids and imino acids (except tryptophan) react with NBD-F to yield fluorescent derivatives. Polyamines having primary and secondary amino groups in the skeleton reacted with NBD-F almost as quickly as primary amines such as HPEA, to give the *N,N*-di-NBD derivative for putrescine, the *N,N,N*-tri-NBD derivative for spermidine, and the *N,N,N,N*-tetra-NBD derivative for spermine. The labeling with NBD was suitable for quantifying these polyamines; reaction for 1 min at 50°C and pH 7.0 (phosphate buffer) sufficed (Fig. 6). Putrescine, spermidine and spermine were detected in amounts as low as 76 fmol, 0.43 pmol and 1.20 pmol (signal:noise = 3), respectively. These limits are rather better than those reported previously [14].

The authors thank Prof. Z. Tamura, University of Tokyo, for his interest and support; Dr. Y. Shida, Tokyo College of Pharmacy, for the c.i.m.s.; and Dr. H. Watanabe, Toyo Soda Manufacturing Co., for his generous gift of column packings.

REFERENCES

- 1 S. Udenfriend, S. Stein, P. Bohlen, W. Dairman, W. Leimgruber and M. Weigle, *Science*, 178 (1972) 871.
- 2 M. Roth, *Anal. Chem.*, 43 (1971) 880.
- 3 W. R. Gray, *Methods in Enzymology*, Vol. 11, Academic Press, New York, 1967, p. 137.
- 4 P. B. Ghosh and M. W. Whitehouse, *Biochem. J.*, 108 (1968) 155.
- 5 M. Roth, *Clin. Chim. Acta*, 83 (1978) 273.
- 6 M. Ahnoff, I. Grundavik, A. Arfwidsson, J. Fonselius and B. Persson, *Anal. Chem.*, 53 (1981) 485.
- 7 K. Imai and Y. Watanabe, *Anal. Chim. Acta*, 130 (1981) 377.
- 8 Y. Watanabe and K. Imai, *Anal. Biochem.*, 116 (1981) 471.
- 9 Y. Watanabe and K. Imai, *J. Chromatogr.*, 239 (1982) 723.
- 10 L. D. Nunno, S. Florio and P. E. Todesco, *J. Chem. Soc., Section C*, (1970) 1433.
- 11 P. B. Ghosh, *J. Chem. Soc., Section B*, (1968) 334.
- 12 D. Dal Monte, E. Sandri and P. Mazzaracchio, *Boll. Sci. Fac. Chim. Ind. Bologna*, 26 (1968) 165.
- 13 R. S. Fager, C. B. Kutina and E. W. Abrahamson, *Anal. Biochem.*, 53 (1973) 290.
- 14 J-K. Lin and C-C. Lai, *J. Chromatogr.*, 227 (1982) 369.

DOSAGE DU NOMBRE DE CHAINONS OXYETHYLENES DE QUELQUES AGENTS TENSIOACTIFS NON IONIQUES PAR OXYDATION AU VANADIUM(V)

C. DAUPHIN, C. BAHSOUN et M. HAMON*

*Laboratoire de Chimie Analytique, Faculté des Sciences Pharmaceutiques et Biologiques,
Rue J.B. Clément, F-92290 Chatenay-Malabry (France)*

J. LIKFORMAN

*Laboratoire de Physique Appliquée aux Médicaments, Faculté des Sciences
Pharmaceutiques et Biologiques, Rue J.B. Clément, F-92290 Chatenay-Malabry (France)*

(Reçu le 21 mai 1982)

SUMMARY

(Determination of the number of oxyethylene groups in nonionic surfactants by oxidation with vanadium(V).)

Oxidation with vanadate in 5 M sulfuric acid at boiling point, allows the determination of the number of oxyethylene groups in various surface-active agents on a few centigrams of substance. After the oxidation, which requires 6–10 h, the excess of vanadate is titrated potentiometrically with iron(II) solution. This oxidizing method was compared with proton magnetic resonance; the results were found to agree well. The precision of the titrimetric method is about 3%.

RESUME

L'oxydation par le vanadium(V), en milieu sulfurique 5 M et à l'ébullition, de différents agents tensioactifs polyoxyéthylénés permet la détermination du nombre de chaînons oxyéthylénés de ces produits sur quelques centigrammes de substance. Une comparaison a été réalisée entre cette méthode et la résonance magnétique nucléaire; les résultats concordants prouvent la validité de la méthode oxydante dont la précision est de l'ordre de 2–3%.

Le contrôle des agents de surface non ioniques dont la partie hydrophile est constituée par une ou plusieurs chaînes polyéthylénées, fait appel actuellement à des techniques peu spécifiques. C'est ainsi que la Pharmacopée Européenne préconise la détermination de la densité relative, de la viscosité et d'un certain nombre d'indices: indices d'acide, d'hydroxyle, d'iode, de saponification; elle mentionne également la détermination de la teneur en eau et des cendres sulfuriques, la recherche d'impuretés réductrices et de métaux lourds. Seule, la fiche AFNOR NFT 73/203 indique une méthode iodimétrique de dosage des groupements oxyéthylénés [1]. D'autres méthodes ont été mentionnées dans la littérature, telles que la gravimétrie [2], la chromatographie sur couche mince directe [3], ou après décomposi-

tion thermique (thermofractographie) [4], spectrométrie infrarouge et surtout de résonance magnétique nucléaire [3, 5].

Pour notre part, poursuivant nos travaux sur l'oxydation au vanadium(V) qui nous ont déjà permis de mettre au point une technique de dosage et d'estimation des poids moléculaires des polyéthylèneglycols [6], nous proposons une méthode de dosage fondée sur le même principe, et vérifiée par une étude parallèle en résonance magnétique nucléaire du proton.

Tous les agents tensioactifs comportent deux pôles, hydrophile et hydrophobe. Dans le cas des produits étudiés ici, le pôle hydrophobe est constitué par la longue chaîne aliphatique d'un acide ou d'un alcool gras; la liaison avec le pôle hydrophile est réalisée par un groupement ester ou étheroxyde selon les cas. Cette partie hydrophile peut être constituée simplement par une chaîne polyoxyéthylénée, ou, comme dans les polysorbates inscrits à la Pharmacopée Européenne, comporter une ou plusieurs chaînes polyoxyéthylénées fixées sur un produit de déshydratation du sorbitol: le sorbitanne. Ce produit est utilisé sans aucune éthérification par des polyoxyéthylèneglycols pour former des esters d'acide gras ayant aussi un caractère tensioactif et qui, compte-tenu de la parenté étroite avec les précédents, ont également été inclus dans cette étude. Les principaux produits étudiés sont indiqués dans les Tableaux 1 et 2.

PARTIE EXPERIMENTALE

Technique proposée

Dans une fiole jaugée de 100 cm³, introduire une prise d'essai exactement pesée, correspondant environ à 0,3 chaînon oxyéthyléné (donc variable suivant le produit étudié) puis 50 cm³ d'acide sulfurique 8 M, 20 cm³ exactement mesurés d'une solution de pentoxyde de vanadium 0,1 M (soit 0,2 M en VO₂⁺) et de l'acide sulfurique 5 M jusqu'à 100 cm³.

Après agitation, transvaser dans un ballon de 250 cm³, en y ajoutant quelques morceaux de pierre ponce, adapter un réfrigérant à reflux et porter ce mélange à ébullition dans un chauffe-ballon. L'ébullition doit être régulière durant toute l'oxydation. Pour les alcools ou acides gras polyoxyéthylénés à 25 chaînons ou moins, la réaction est totale en 6 h. Pour le polysorbate 80 et les dérivés à plus grand nombre de chaînons, il est nécessaire de poursuivre l'oxydation pendant au moins 10 h.

Après refroidissement, ajuster à nouveau le volume à 100 cm³ et prélever 10 cm³ du mélange homogène, titrer l'excès de pentoxyde de vanadium par la solution de fer(II) 0,1 M (solution de sulfate de fer(II) et d'ammonium dans l'acide sulfurique à 10% p/v) en utilisant une indication potentiométrique. L'électrode de mesure est en platine, et l'électrode de référence est au calomel.

Calculs

Le nombre de millimoles d'oxydant réduit par la prise d'essai est donné par la relation $x = 20 t - 10 nt'$, ou t = le titre exact de la solution de pent-

TABLEAU 1

Principaux esters d'acides gras simples ou polyoxyéthylènes et éthers polyoxyéthylènes [7]

Nature chimique	Nombre de chaînons oxyéthylènes	Exemples de noms déposés
Monolaurate de sorbitanne	0	Span, Montane, Arlacell 20
Monopalmitate de sorbitanne	0	Span, Montane, Arlacell 40
Monostéarate de sorbitanne	0	Span, Montane, Arlacell 60
Monooléate de sorbitanne	0	Span, Montane, Arlacell 80
Monolaurate de sorbitanne polyoxyéthyléné ^a	20	Tween, Montanox 20
Monopalmitate de sorbitanne polyoxyéthyléné ^a	20	Tween, Montanox 40
Monostéarate de sorbitanne polyoxyéthyléné ^a	20	Tween, Montanox 60
Monooléate de sorbitanne polyoxyéthyléné ^a	20	Tween, Montanox 80
Lauryl PEG	4	Brij 30, Simulsol P 4
Lauryl PEG	23	Brij 34, Simulsol P 23
Cetyl PEG	2	Brij 52, Simulsol 52
Cetyl PEG	10	Brij 56, Simulsol 56
Cetyl PEG	20	Brij 58, Simulsol 58
Stéaryl PEG	2	Brij 72, Simulsol 72
Stéaryl PEG	10	Brij 76, Simulsol 76
Stéaryl PEG	20	Brij 78, Simulsol 78
Oleyl PEG	2	Brij 92, 93, Simulsol 92
Oleyl PEG	10	Brij 96, 97, Simulsol 96
Oleyl PEG	20	Brij 98, 99, Simulsol 98
Nonylphenol PEG	10	Simulsol 1030 NP, Nonoxynol

^aPolysorbate.

TABLEAU 2

Acides stéarique polyoxyéthylène [7]

8 OE	Myrj 45, Simulsol M 45
20 OE	Myrj 49, Simulsol M 49
40 OE	Myrj 52, Simulsol M 52
100 OE	Myrj 59, Simulsol M 59

oxyde de vanadium, exprimé en mole de VO_2^+ par litre, t' = le titre de la solution de fer(II), et n = le volume de solution fer(II) consommée.

Sachant que l'oxydation de chaque chaînon consomme 6 mol de VO_2^+ , le nombre de chaînons est $N = xPM/6 P_e$, soient PM = le poids moléculaire, P_e = la prise d'essai (en mg), et x = le nombre de millimoles consommés par la prise d'essai.

Dans le cas particulier des polysorbates, il convient de retrancher la con-

somation de la molécule d'ester de sorbitanne en millimoles d'oxydant de celle de son homologue polyoxyéthyléné et seulement ensuite de diviser par six afin de déterminer le nombre de chaînons.

Détermination des conditions opératoires optimales

Le nombre de chaînons oxyéthylénés par molécule diffère de façon très importante selon les produits étudiés, puisqu'il varie de 2 à 100. Des essais préliminaires ont montré que, pour une bonne reproductibilité, la quantité d'oxydant mise en oeuvre (soit 4 mmol) doit être au moins double de celle nécessaire à l'oxydation. Ceci correspond à environ 0,3 chaînon par prise d'essai. Si N' est le nombre de chaînons théorique contenu dans la molécule: $Pe \text{ (mg)} = 0,3 PM/N'$.

Ayant déterminé la température d'ébullition du mélange comme température optimale, lors de l'étude de l'oxydation de l'éthylèneglycol et des polyoxyéthylèneglycols [6], nous nous sommes placés dans les mêmes conditions pour l'oxydation de ces produits de condensation avec l'oxyde d'éthylène.

RESULTATS

Tout d'abord, nous avons effectué l'oxydation du propylèneglycol seul, trouvant une consommation de $5,94 \text{ mol mol}^{-1}$ qui est analogue à celle d'un chaînon $-\text{CH}_2-\text{CH}_2-\text{O}$. Le stéarate de propylène glycol condensé avec 25 molécules d'oxyde d'éthylène se comporte donc comme comprenant $25 + 1 = 26$ chaînons; il consomme 160 mol mol^{-1} , ce qui donne 26,6 chaînons par molécule. Les résultats concernant les alcools et acides gras oxyéthylénés sont consignés dans le Tableau 3.

Nous avons effectué l'oxydation des esters de sorbitanne simples, puis celle des esters polyoxyéthylénés. La différence de consommation entre ces deux dérivés étant due à la présence des chaînons oxyéthylénés, nous

TABLEAU 3

Détermination du nombre de chaînons oxyéthylènes de différents alcools et acides gras oxyéthylènes

Nature chimique	Nombre de chaînons theorique	Mol VO_2^+ / mol	Nombre de chaînons déterminé
Alcool laurique	4	21	3,5
	23	141	23,5
Alcool cétylique	2	11,4	1,89
	10	63	10,5
	20	96	16
Acide stéarique	8	55	9,2
	20	119	19,8
	40	242	40,3
	100	628	104,6

avons retranché la consommation de l'ester de sorbitanne de celle de son homologue polyoxyéthyléné. Les résultats sont regroupés dans le Tableau 4.

TABLEAU 4

Détermination du nombre de chaînons oxyéthylènes des polysorbates

Nature chimique	Mol VO_2^+ / mol	Nombre de chaînons déterminé ^a
Monolaurate de sorbitanne	17	—
Monostéarate de sorbitanne	17	—
Monooleate de sorbitanne	30	—
Monopalmitate de sorbitanne	17	—
Polysorbate 60	122 105	17,5
Polysorbate 80	135,6 105,6	17,6
Polysorbate 40	137 120	20
Polysorbate 20	130 113	18,8

^aNombre théorique: 20.

L'oxydation du nonylphénol ordinaire conduit à une consommation de 18 mol mol⁻¹ et celle du nonylphénol polyoxyéthyléné à 78,7 mol mol⁻¹ donc à 60,6 mol par les chaînons oxyde d'éthylène. Le nombre expérimental était 10,1 chaînons.

Les déterminations du nombre de chaînons ont été effectuées sur six échantillons de quelques produits. Les résultats sont résumés dans le Tableau 5 où figurent également les limites de confiance.

TABLEAU 5

Réproductibilité des résultats obtenus

Nature chimique	Nombre théorique de chaînons	Nombre de chaînons expérimental $\bar{x} \pm s^a$
Cetyl PEG	2	1,89 \pm 0,19
Polysorbate 80	20	17,60 \pm 0,29
Lauryl PEG	23	23,50 \pm 1,26
Ester stéarique de PEG	40	40,30 \pm 0,71
	100	104,60 \pm 1,29

^aMoyenne et l'écart type, $n = 6$.

Comparaison avec la r.m.n.

Les résultats obtenus par le dosage proposé n'étant pas toujours conformes à la théorie, nous avons vérifié le nombre de chaînons oxyéthylénés par résonance magnétique nucléaire (r.m.n.) du proton d'un certain nombre de produits tensioactifs précédemment étudiés. Les analyses sont effectuées

TABLEAU 6

Comparaison des résultats obtenus

Esters de sorbitanne polyoxyéthyléné	Nombre de chaînons		
	Théorique	Par r.m.n.	Par oxydation
Ester laurique	20	20 \pm 1	18,8
Ester stéarique	20	17,8 \pm 1	17,5 \pm 0,33
Ester oléique	20	16,6 \pm 1	17,6 \pm 0,29
Alcool laurique polyoxyéthylène	23	23,9 \pm 1	23,5 \pm 1,26

il devient 2,52 ce qui donne respectivement 16,4 ou 16,8 chaînons oxyéthylénés.

Pour l'alcool laurique polyoxyéthyléné (23 OE), on retrouve sur le spectre le pic du méthyle à 0,87 ppm, et les chaînons méthyléniques non oxygénés à 1,23 ppm. Les protons de chaînons oxyéthylénés forment un pic important à 3,63 ppm, ainsi qu'un massif à 4,43 ppm et un pic à 4,47 ppm. Le rapport théorique est 4,13 ppm. Les intégrations entre 0,1 et 2,5 ppm et 2,5–4,5 ppm conduisent à un rapport moyen de 4,16, soit la présence de 23,9 chaînons oxyéthylénés.

Nous pouvons établir une comparaison entre les résultats obtenus par r.m.n. et par oxydation avec le vanadium(V) (Tableau 6) sachant que la précision de 2% de l'intégration électronique en r.m.n. ne permet le décompte du nombre de chaînons, dans la zone de 20 chaînons, qu'à une unité près.

Conclusion

L'oxydation par le pentoxyde de vanadium, comme le montre le Tableau 5, permet tout d'abord une estimation de nombre de chaînons oxyéthylénés dans les échantillons d'agents tensio-actifs polyoxyéthylénés. Cette détermination paraît au moins aussi précise que celle qui est réalisée par résonance magnétique nucléaire.

Dans le cas où la structure, et notamment le nombre de chaînons oxyéthylénés, sont connus, la méthode permet également un dosage simple de ces produits.

BIBLIOGRAPHIE

- 1 Norme Française Homologuée NFT 73/203 (avril 1972).
- 2 C. F. Smullin, *J. Assoc. Off. Anal. Chem.*, 61 (1978) 506.
- 3 J. R. Bergueiro, M. Bao et J. J. Casores, *Ing. Quim.*, 115 (1978) 275.
- 4 E. Stahl et F. Werndorff, *Parfüm. Kosmet.*, 58 (1977) 321.
- 5 1st Cong. Int. Technol. Pharm., Paris, A.P.G.I., 1977, p. 17.
- 6 C. Dauphin, A. Dauphin et M. Hamon, *Analysis*, 7 (1979) 73.
- 7 M. J. Rosen et H. A. Goldsmith, *Systematic Analysis of Surface-Active Agents*, 2nd edn., Wiley-Interscience, New York, 1972.

APPARATUS FOR WET ASHING OF ORGANIC MATERIALS WITH NITRIC AND SULPHURIC ACIDS

SIXTO BAJO*, URSULA SUTER and BEAT AESCHLIMAN

Swiss Federal Institute for Reactor Research, 5303 Würenlingen (Switzerland)

(Received 6th October 1982)

SUMMARY

A simple apparatus is described for the wet ashing of organic materials (fats, charcoal, plastics, foodstuffs) with nitric and sulphuric acids at atmospheric pressure. The ashing may be run automatically without supervision. Quantitative recovery of added elements (As, Au, Hg, Se and Tc) was demonstrated by using radioactive tracers.

Wet ashing of organic matter for trace element determinations is covered by a large bibliography [1–9]. Nevertheless, at present there is no generally applicable wet-ashing method for the total destruction of organic materials; such a method should be applicable to such materials as fats, plastics, and those with covalent chlorine, and the elements sought (including As, Hg, and Se) must be retained quantitatively in solution. The nitric acid/sulphuric acid mixture was chosen in the present search for a simple wet-ashing method which would avoid perchloric acid. Nitric acid has strong oxidizing powers even at room temperature, whereas hot concentrated sulphuric acid destroys most organic compounds primarily by charring; the oxidizing power of nitric acid is enhanced by addition to hot concentrated sulphuric acid.

In the proposed equipment, organic material is wet-ashed at atmospheric pressure in easily made vessels. No manipulations are required during the process, and the method is applicable to sample sizes of at least 1 g. Novel aspects of the method include the repeated sequential, self-feeding of small amounts of nitric acid to the reaction mixture maintained at the high temperature (about 300°C) of fuming sulphuric acid, and the trapping in nitric acid solution of nearly all species vaporized after (i.e., at a higher temperature than) nitric acid. Many different types of samples were examined. The recovery of added elements was studied by using inorganic radioactive tracers. Advantages and disadvantages of this technique have been thoroughly discussed [2]; endogenously labeled samples were not examined.

EXPERIMENTAL

Reagents

The acids used were nitric acid (65% and 100%) and sulphuric acid (95–97%). The following radioactive tracers were employed: ^{76}As as arsenic(III) sulphate in 3 M H_2SO_4 , ^{198}Au as gold(III) chloride in 1 M HCl , ^{82}Br as ammonium bromide in water, $^{115\text{m}}\text{Cd}$ as cadmium(II) chloride in 0.1 M HCl , ^{59}Fe as iron(III) chloride in 0.1 M HCl , ^{203}Hg as mercury(II) chloride in 0.1 M HNO_3 , ^{125}Sb as antimony(V) chloride in 4 M HCl , ^{75}Se as selenious acid in 0.1 M HNO_3 , and $^{99\text{m}}\text{Tc}$ as sodium pertechnetate in 0.1 M ammonia solution.

Apparatus

The wet-ashing apparatus is shown in Fig. 1. It consists of a reaction vessel (D or E), a stopper with capillary (C), and an air condenser containing a diffusion funnel (B) and four cylindrical plugs (A). The plugs are used as filling material. The stopper, funnel and plugs are made of teflon. No clamps are necessary and the components fit together with minimum pressure, like ground-glass laboratory apparatus.

For wet ashing, reaction vessel D (Fig. 1) was used on a hot-plate (380 × 180 mm; 1400 W at full power); eight such apparatus could be heated simultaneously. Reaction vessel E was used with a temperature-programmable aluminium heating block with cavities 27 mm diameter and 120 mm deep (type RNS2HR4, Gebr. Liebig, Bielefeld, German Federal Republic). A small pad of steel wool was placed in the bottom of each cavity to avoid cracking of the quartz reaction vessels. Nine apparatus could be located simultaneously in the heating block.

The vessel used in measurements of the recovery of added radioactive tracers was described previously [10]. Counting was done with a well-type NaI(Tl) crystal linked to a single-channel γ -spectrometer.

Wet-ashing procedures

The organic materials, 2-mm glass balls, radioactive tracer (100 μl , containing 0.2–20 μg of the element except for technetium, which was carrier-free), water (only in some experiments), nitric acid, and sulphuric acid were added, in that order, to the reaction vessel. More details are given below for the volumetric flask procedure with reaction vessel D (Fig. 1) and the quartz vessel procedure with reaction vessel E (Fig. 1).

No violent reaction was observed when nitric acid was added to the organic material, with the single exception of olive oil and 100% nitric acid. In this case, vigorous evolution of nitrogen oxides took place, with risk of solution losses. To prevent this, both the olive oil and the nitric acid were cooled in an ice bath before mixing. The teflon stopper and the air condenser were connected as shown in Fig. 1. The cooled nitric acid was added through the condenser, followed by sulphuric acid. The acids pass slowly into the reaction vessel and a yellow homogeneous solution is obtained. This method was also used for lard and butter.

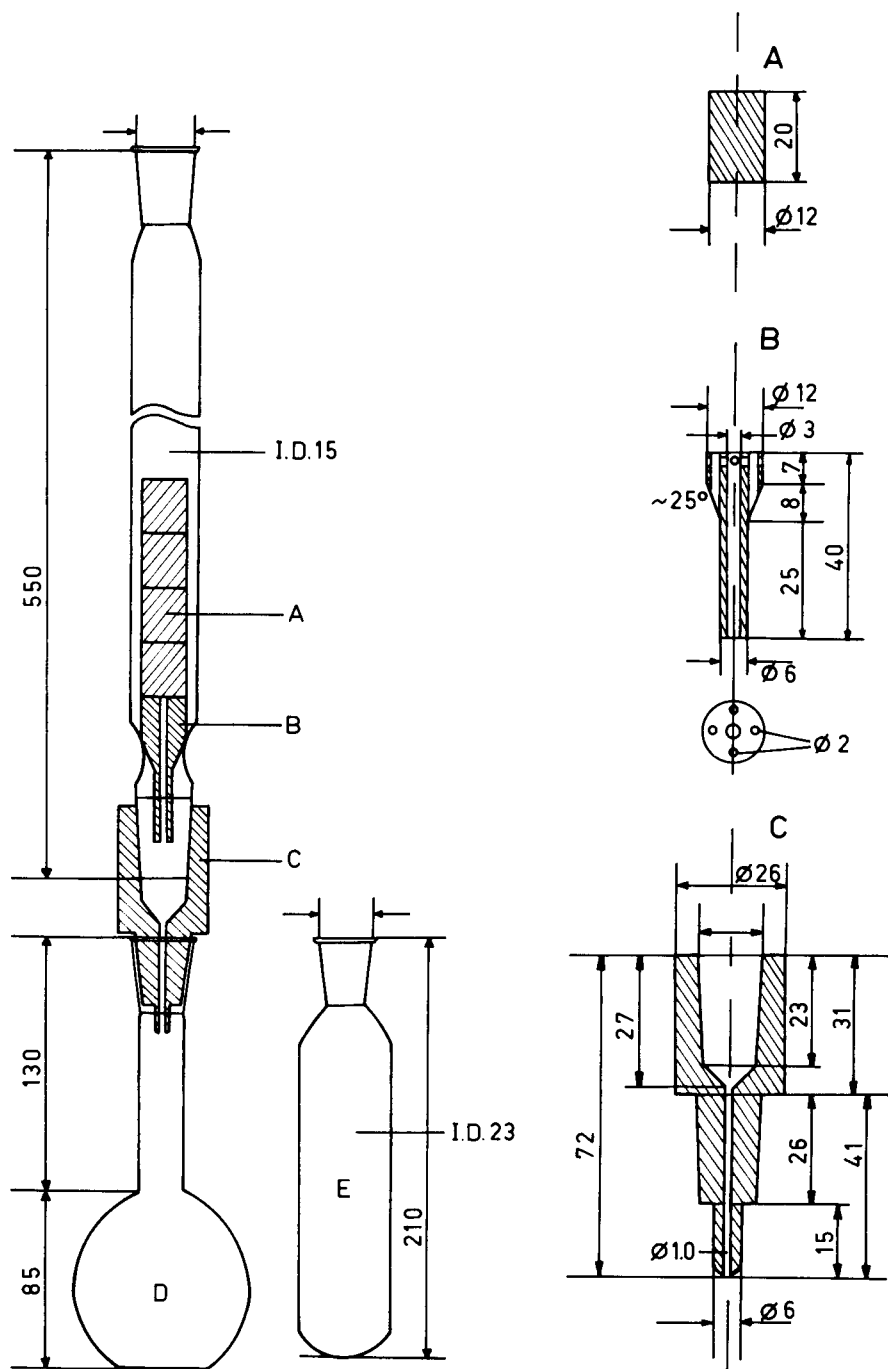


Fig. 1. Wet-ashing apparatus. (A) Teflon cylindrical plugs; (B) teflon diffusion funnel; (C) teflon stopper with capillary; (D) 250-ml Duran volumetric flask; (E) 70-ml quartz vessel (wall, 1.5 mm thick). All joints (glass, quartz, and teflon) are 14.5/23. All dimensions in mm. Detailed dimensions of the teflon components A, B, and C are given on the right.

Volumetric flask procedure. A heavy lead ring (about 0.7 kg) was placed as ballast around the neck of the volumetric flask, and the teflon stopper and the air condenser were connected as in Fig. 1. The apparatus was placed on the hot-plate at room temperature in a fume hood. An aluminium shield near the hot-plate prevented excessive convective cooling of the flask body by the fume hood air flow. The hot-plate was switched on at full power (see heating programme in Fig. 2). Heating was continued for about 30 min after the formation of a clear yellow solution, the total heating time being at least 60 min.

The following stages were observed during the wet ashing: (1) reaction between the nitric acid and the sample (e.g., sugar) or no reaction (e.g., polyethylene); (2) distillation of the excess of nitric acid with collection in the air condenser; (3) charring of the sample with sulphuric acid and further distillation of the reaction products; (4) reflux of the distillate; (5) periodic refluxes of the distillate with progressive oxidation of the charred material; (6) formation of a clear yellow solution, which remained unchanged even when the heating was continued for some hours.

After the first heating cycle of at least an hour, it was necessary to allow all the distillate to return to the reaction vessel. This was easily done by switching off the heating or by removing the apparatus from the hot-plate. For certain samples it was necessary to apply several consecutive heating cycles.

Quartz vessel procedure. The quartz vessel was introduced into its location

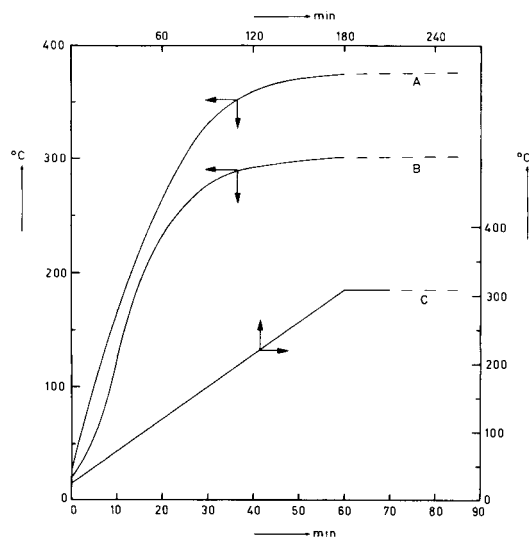


Fig. 2. Heating programmes. (A) Temperature measured on the hot plate surface; (B) temperature measured with 30 ml of sulphuric acid in the volumetric flask; (C) temperature measured in the quartz vessel containing sulphuric acid and at the cavity surface.

in the aluminium heating block, the teflon stopper and the air condenser were connected, and the heating programme (Fig. 2) was switched on. The heating time was at least 210 min, although this was longer than necessary to obtain a clear yellow solution in most cases. After the heating had been switched off, the ashing apparatus normally remained in the block; 6 h was the time needed to bring the block back to room temperature. Most experiments were done overnight.

Compared with the volumetric flask procedure, the quartz vessel method is smoother. The slower heating rate allows a longer initial reaction time with nitric acid. Refluxing begins before charring. As in the volumetric flask procedure, multiple heating cycles were needed in some cases. After the initial cycle of at least 210 min, time was allowed to bring down the distillate. Heating was then switched on again at full power to reach 310°C. Heating the block from 20°C to 310°C took 50 min. This temperature was maintained till the end of second cycle. Further cycles were identical to the second.

Handling of the solution after wet ashing

The apparatus was removed from the heating source and set aside to cool. About 10 ml of water was then added through the air condenser. The teflon stopper/reaction vessel connection was loosened to allow the wash water to drain into the reaction vessel. Washing was repeated and the reaction vessel was removed from the apparatus. It then contained the sample solution which served several different purposes.

Radioactive tracer recovery. Recovery was measured as described previously [10] either directly in the above sample solution (method A) or after pre-treatment as follows. In method B, the sample solution was boiled for 5 min in the volumetric flask used or in a covered 150-ml glass beaker after transference from the quartz vessel. In method C, the sample solution in the volumetric flask used was evaporated to continuous fumes of sulphur trioxide, then cooled, diluted with 5 ml of water, evaporated again to fumes, diluted with 20 ml of water and boiled for 5 min. In method D, the solution was treated as in method C, but after the second heating to sulphur trioxide fumes, the solution was cooled and diluted successively with 5 ml of water, 2 ml of 12 M HCl, and 0.50 ml of 30% hydrogen peroxide; the flask was then stoppered, shaken, and set aside for 5 min, after which the solution was diluted with 20 ml of water and boiled for 5 min.

The justification for these different treatments is given below.

Acid consumption in the wet ashing. The sample solution was diluted to 100 ml with water. Aliquots were taken for the determination of the total acidity by titration with sodium hydroxide. Sulphate was determined nephelometrically with barium chloride, and nitrate photometrically with β -methylumbelliferone [11].

Efficiency of wet ashing. The sample solution was taken rapidly to dryness. If the residue was black, no oxidation or only partial oxidation had taken place. If the residue was white or absent, the oxidation was assumed to be

complete. A thorough study of this aspect [7] was beyond the scope of this work.

RESULTS AND DISCUSSION

The essential feature of the wet-ashing apparatus (Fig. 1) is the teflon stopper with capillary. This material is unbreakable, easily machined, highly resistant to chemical attack and swells slightly upon heating to provide an excellent seal. It also serves as a thermal insulator, maintaining the distillate (nitric acid) at a temperature far below boiling. The narrow capillary serves to detain the distillate in the condenser so long as sufficient positive pressure exists in the heated flask. Limiting the maximum temperature of the hot-plate prevents taking the flask to dryness and the natural small fluctuations in temperature cause small amounts of distillate to reflux. Cost, maintenance and operation can be compared advantageously with existing methods [12–16]. If necessary, the system can be scaled down for microchemical work. The method can be adapted to existing apparatus [14, 15]. The need for pumping the reagents during the ashings and the use of special perchloric acid hoods is thus eliminated. The ashing is done automatically, and may be left overnight using a time-controlled hot-plate.

At the beginning of the wet ashing, the nitric acid not consumed in the first oxidation stage distills to the air condenser. All the gases produced during the charring stage (i.e., under reducing conditions in the reaction vessel) are scrubbed through the oxidizing solution (aqueous nitric acid) in the air condenser. When the reflux begins, the high temperature of the sulphuric acid and the suspended carbonaceous matter enhance the oxidizing power of the nitric acid. The small volumes of each reflux avoids excessive dilution of the sulphuric acid. Elements volatilized from the reaction vessel are retained in the distillate because of its moderate temperature ($<100^{\circ}\text{C}$) and/or by reaction with the nitric acid.

The quantities of acids needed for efficient ashing depend on the nature of the sample, its weight, and the concentration of the acids used. White fumes in the reaction vessel during refluxing of the distillate indicate lack of nitric acid; if a few milliliters of nitric acid are added through the condenser, brown fumes appear. A dry, charred residue means a shortage of sulphuric acid. Because of the smoother oxidizing conditions (slower heating rate), the quartz vessel procedure needs less acid than the volumetric flask procedure. Less nitric acid is needed for non-volatile elements, because of the lower concentrations required in the distillate. Another factor to be considered is the shape of the reaction vessel; the bottom must be covered with a layer of sulphuric acid so that the charred material can be oxidized readily with the nitric acid refluxes. In general, 15 ml of 100% nitric acid and 5 ml of sulphuric can be recommended as an acid mixture applicable to most 1-g samples.

The two wet-ashing systems are essentially similar. However, the volu-

metric flask procedure is faster whereas the quartz vessel procedure is slower, gentler and better for conserving both the acids and any volatile species.

The volumetric flask procedure

Time for wet ashing. The times needed for ashing different materials are presented in Table 1. The yellow colour of the final sample solution is due to nitrogen oxides dissolved in the acid mixture. It disappears on shaking, boiling, or on oxidation with some drops of a permanganate solution, or hydrogen peroxide. This was the case for all the samples tested in Table 1, which gave perfectly clear, colourless solutions. A persistent yellow or green indicates residual organic matter. The ashing of materials with moderate fat content (e.g., cheese, cocoa, egg yolk, peanuts and soup) with 65% nitric acid produces slightly turbid colourless solutions on dilution with water; this turbidity indicates the presence of undestroyed fat. If 100% nitric acid is employed instead of the 65% acid, no fat can be seen in the sample solution. With pure fat materials like butter, lard and olive oil, no turbidity was observed when 100% nitric acid was used, but the solution sometimes became yellow on dilution with water. In such cases, three consecutive wet-ashing cycles, (three 60-min heating cycles separated by 60 min without

TABLE 1

Wet-ashing times for different materials by the volumetric flask procedure

Acid mixture ^a	Time ^b (min)	Samples ashed ^c
10 ml 65% HNO ₃	20–30	Rice, sugar, wheat
	30–40	Cheese, corn, egg yolk (hard boiled), fish (freeze-dried), milk (dry, skimmed), soup (concentrated, solid), tobacco
	40–50	Cocoa, Dowex 50-X8, peanuts, polycarbonate (0.5)
	50–70	Charcoal (0.5), Dowex 1-X8, plexiglas (0.5), polypropylene (0.5), PVC
	70–100	Lampblack (0.5), neoprene, polyethylene (0.5), soot (0.5)
15 ml 65% HNO ₃	100–200	Graphite (0.2)
10 ml 100% HNO ₃	70–90	Charcoal
	10–20	Cheese
	20–30	Peanuts, wheat
15 ml 100% HNO ₃	30–40	Cocoa, corn, milk (dry, skimmed), rice, sugar
	20–30	Soup (concentrated, solid), sugar
	30–50	Charcoal (0.5), butter, lard, olive oil, peanuts

^aAll with 5 ml of sulphuric acid present. ^bTime needed to obtain a clear yellow solution.

^cSamples of 1 g unless otherwise stated (weight in g between brackets).

heating), produced perfectly clear, colourless solutions. Two cycles may prove to be sufficient. The total destruction of fats eliminates the need for a filtration stage after ashing.

The essential advantage of 100% nitric acid over the 65% acid is that the former reacts with the fat. With liquid fat, an exothermal reaction occurs immediately when the sample is mixed with the acid at room temperature. Nitration and oxidation occur simultaneously and the reaction products are soluble in the excess of acid. A yellow solution is obtained in some minutes. With the 65% acid, there is no visible reaction and two phases remain after some hours at room temperature. Attempts at wet-ashing olive oil with 65% nitric acid were unsuccessful; the oil distilled partially into the condenser and floated over the nitric acid distillate without reaction. For materials without fat, the use of 100% instead of 65% nitric acid has no effect on the ashing time.

Plastics do not react with nitric acid in the first stage of the wet ashing, and the acid distils into the condenser. They are charred by sulphuric acid and the carbon formed is then oxidized by the refluxing nitric acid. With other materials, charring is less intense because of the previous partial oxidation with nitric acid. Ashing is even possible when the acid mixture is diluted with water, but a longer time is needed; about 1.4 times longer for 1 g of milk, PVC or sugar when ashed with 20 ml of water, 10 ml of 65% HNO_3 and 5 ml of sulphuric acid. This is because a larger volume must be distilled. Yet, the time from the beginning of the charring to the production of the clear yellow solution remains constant. This is advantageous for the direct ashing of solutions or wet samples without prior drying.

In the development stage of the apparatus, teflons stoppers (C, Fig. 1) with capillaries having diameters of 1.0, 1.5, 2.0, and 3.0 mm were tried. Diameters of 1.0 and 1.5 mm were the best and that with 1.0 mm was finally adopted; with the larger diameters, the distillate was not retained in the air condenser. Later, the performance of the stoppers was compared by ashing identical samples with the same acid mixture. The results are shown in Table 2. Butter and olive oil show the largest difference. Wet-ashing times depend on the volume of the refluxes, which are bigger for the 1.5 mm than for the 1.0 mm capillaries. However, large refluxes can propel the charred material from the reaction vessel to the condenser, especially when fine carbon materials (e.g., lampblack) are digested.

Acid consumed. The consumption of nitric acid in experiments without organic matter is shown in Fig. 3. With organic materials, the consumption of nitric acid decreases significantly if the acid mixture is diluted with water. Thus, ashing 1 g of sugar with 10 ml of 65% nitric acid and 5 ml of sulphuric acid (total heating time, 60 min) consumes 66% of the nitric acid, but only 27% when 20 ml of water is added to the acid mixture. Total recovery of sulphuric acid was obtained in all cases; the sulphur trioxide vapours condense in the distillate, and any sulphur dioxide formed in the charring stage is reoxidized to sulphuric acid by the nitric acid in the distillate.

TABLE 2

Influence of the capillary diameter on wet-ashing time by the volumetric flask procedure

Sample ^a	HNO ₃ added ^b (ml, %)	Capillary diameter (mm)	
		1.0	1.5
		Time for clear yellow solution (min)	
Butter	15 (100)	45	25
Milk (dry, skimmed)	10 (65)	32	26
Olive oil	15 (100)	43	25
PVC	10 (65)	51	42
PVC	10 (65) ^c	68	57
Sugar	10 (65)	30	25
Sugar	10 (65) ^c	43	35

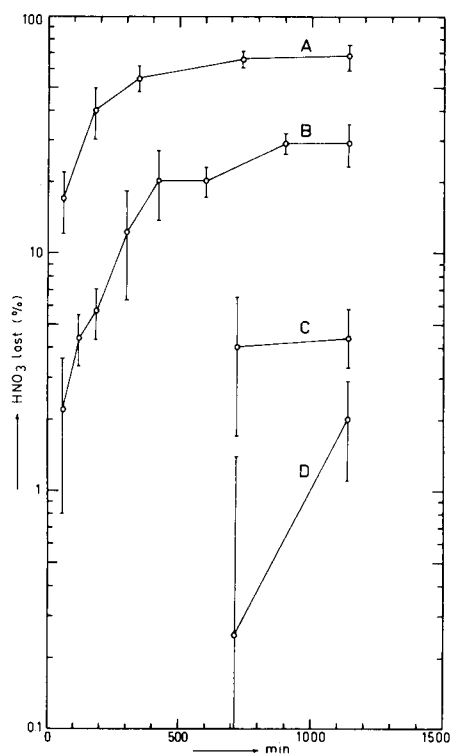
^a 1-g sample. ^b 5 ml of sulphuric acid was always added. ^c 20 ml of water added.

Fig. 3. Losses of nitric acid in the volumetric flask procedure vs. heating time. Conditions: no organic matter, 10 ml of 65% HNO₃, 5 ml of H₂SO₄ and *x* ml of H₂O (A, *x* = 0 ml; B, 5 ml; C, 10 ml; D, 20 ml). Mean of 4 replicates \pm 1 standard deviation.

Losses of nitric acid in the absence of organic material are produced by the thermal decomposition of the acid ($2 \text{HNO}_3 \rightarrow 2 \text{NO}_2 + 1/2 \text{O}_2 + \text{H}_2\text{O}$) in the refluxing stage, as evidenced by the brown fumes produced. Dilution with water minimizes such losses; decomposition of nitric acid apparently does not occur below a certain concentration.

Ashing efficiency. Heating 1-g samples of egg yolk, fish, milk, sugar or wheat with 10 ml of 65% nitric acid and 5 ml of sulphuric acid for 60 min produced pure white residues when taken to dryness. The same was true for Dowex 1-X8 and PVC (1-g sample, 10 ml of 65% HNO_3 , 5 ml of sulphuric acid, 90-min heating time) and milk and sugar (1-g sample, 10 ml of 65% HNO_3 , 5 ml of sulphuric acid, 20 ml of water, 60-min heating time).

The enhanced oxidizing power of nitric acid with the present apparatus is demonstrated by the wet ashing of natural graphite (Table 1), which was reported to be totally resistant to nitric/sulphuric acid mixtures [17]. 1,10-Phenanthroline chloride monohydrate ($\text{C}_{12}\text{H}_9\text{ClN}_2 \cdot \text{H}_2\text{O}$), a very resistant compound [7], was successfully ashed (1-g sample, 15 ml of 100% HNO_3 , 5 ml of sulphuric acid, 180-min heating time); no charring was observed. In general, any failure to ash a sample can be overcome by increasing the reaction time and /or the nitric acid volume and concentration.

Tracer recovery. The recoveries of added radioactive tracers are shown in Table 3. Three of the four different methods employed between the ashing and the recovery measurements (methods B, C and D) follow normal analytical practice. With method B it is possible to eliminate the nitrogen oxides, which may interfere if a liquid-liquid extraction with dithizone or diethyldithiocarbamate follows the ashing. The elimination of nitric acid is possible by applying method C. With method D, elements such as gold, which could be easily reduced by the fuming sulphuric acid step, are dissolved by the chlorine produced in the general reaction. Boiling the solution of sulphuric acid after dilution with water (methods C and D) rehydrates the sulphates of trivalent transition elements.

Arsenic, Cd, Fe, Sb, and Tc were always quantitatively recovered. Mercury was lost in the ashing of plant materials (e.g., corn, rice, sugar, and wheat); the losses depended on the weight of the sample (Table 4) and occurred between the beginning of the distillation and the first reflux. This was demonstrated in one experiment by scrubbing the gases leaving the air condenser through 65% nitric acid, in which mercury was quantitatively retained. Total recovery was obtained by using 100% instead of 65% nitric acid with these materials. The influence of 100% nitric acid in the total recovery of mercury can be explained by its higher oxidizing power and its lower boiling point (b.p. 65% HNO_3 , 122°C ; b.p. 100% HNO_3 , 84°C). Addition of water to the acid mixture also caused low mercury recoveries, as can be seen with milk and PVC in Table 3. Quantitative mercury recoveries were obtained with all other materials with both 65% and 100% nitric acid.

Selenium losses occurred with all the materials tested, but not in the absence of organic material, when 65% nitric acid was used. With 100%

TABLE 3

Tracer recovery after wet ashing by the volumetric flask procedure (A, B, C, and D denote the treatment applied to the sample solutions after the wet ashing)

Sample ^a	HNO ₃ added ^b (ml, %)	Quantitative recovery ^c		Other recoveries
		As	Hg	
Charcoal	15 (65)			Au(A,100%)
	15 (100)		B	
Cheese	10 (100)		B	
Corn	10 (65)			Hg(A,96%)
	10 (100)		A	
Egg yolk (hard boiled)	10 (65)	A	A ^d	
Fish (freeze-dried)	10 (65)	A	A	
Lard	15 (100)	C	A ^e	
Milk (dry, skimmed)	10 (65)	A	B ^e	Sb(A,100%), Se(A,50%)
	10 (65) ^f			Hg(A,95%)
	15 (100)			Se(A,93%)
None ^g	10 (65)		B	Se(A,100%), Tc(A,100%)
	10 (65) ^f		A	
	15 (100)		A	Se(A,100%)
Olive oil	15 (100)	C	A ^{e,h}	Au(A,100%)
PVC	10 (65)	A	B ^e	Au(D,100%), Cd(C,100%)
				Fe(C,100%), Se(A,80%)
				Tc(A,100%)
	10 (65) ^f	A		Hg(A,92%)
	10 (100)			Se(A,100%)
Rice	10 (65)			Hg(A,92%)
	10 (100)		A	
Sugar	10 (65)	A		Au(D,100%), Cd(C,100%)
				Hg(A, 84%), Se(A,30%)
				Tc(A,100%)
	15 (100)		B	Se(A,83%)
Wheat	10 (65)	A		Hg(A, 87%)
	10 (100)		A	Se(A,96%)

^a1-g sample unless otherwise stated. ^b5 ml of sulphuric acid added in all cases. ^cQuantitative recovery is defined as a mean recovery of 100 ± 2% for at least four replicates.

^dQuantitative recovery was obtained with the following samples: Dowex 1-X8, Dowex 50-X8, gelatine, graphite (0.5 g), lampblack (0.5 g), neoprene, plexiglas, polycarbonate (0.5 g), polyethylene (0.5 g), polypropylene (0.5 g), soot (0.5 g), soup (concentrated, solid), and tobacco. ^eThree heating cycles of 60 min separated by 60 min without heating.

^f20 ml of water added. ^gHeating time of 60 min. ^hThe same result was also obtained with butter, cocoa, and peanuts.

TABLE 4

Influence of the sample weight and the nitric acid concentration on the recovery of mercury by the volumetric flask procedure (Method A)

Sample	Weight (g)	HNO ₃ added ^a (ml, %)	Recovery ^b (%)
Sugar	2.0	10 (65) ^c	39 ± 9
	1.0	10 (65)	84 ± 6
	0.75	10 (65)	92 ± 2
	0.50	10 (65)	98 ± 2
	0.25	10 (65)	101 ± 2
	1.0	10 (100)	96 ± 1
	1.0	15 (100)	101 ± 1
Wheat	1.0	10 (65)	87 ± 3
	0.50	10 (65)	98 ± 1
	0.25	10 (65)	102 ± 1
	1.0	10 (100)	101 ± 2

^a5 ml of sulphuric acid was always added. ^bHg added, 20 µg; mean ± 1 standard deviation of at least four replicates. ^cLack of nitric acid; 5 ml extra added through the condenser during the ashing.

nitric acid, losses were much smaller or completely absent in some cases (e.g., PVC). Losses are due to volatilization of selenium during the charring stage. In one experiment, selenium was recovered by scrubbing the gases leaving the air condenser through a permanganate solution in diluted sulphuric acid. Only a high nitric acid concentration in the air condenser during the charring stage can retain the selenium.

Gold is fixed on the walls of the flask with method C. The other methods allow quantitative recovery of this element. It must be always borne in mind that gold may be fixed on the walls of the reaction vessel. Method D, or any other including a final step with hydrochloric acid and a strong oxidizing agent, is highly recommended.

Bromine is lost to a great extent. Recovery was always ≤ 20% (Method A). Elimination of ⁸²Br is of particular interest in radiochemical neutron activation analysis. To eliminate it completely, it is necessary to heat the sample solution to fumes of sulphur trioxide (Method C). The losses seem to be similar with one or three heating cycles and with either 65% or 100% nitric acid.

Quantitative recovery of volatile elements (As, Au, Hg, and Tc) is a clear advantage over previously described methods [12, 15, 18, 19]. Although not tested here, total recovery would be expected for rhenium, ruthenium and osmium (from analogy with technetium), and germanium and lead (by analogy with arsenic and mercury) [6].

The quartz vessel procedure

In general, the comments applicable to the volumetric flask procedure are also valid here. The slower heating rate (Fig. 2) allows a longer reaction time with nitric acid before charring starts. In general, all the steps proceed more smoothly than in the volumetric flask method. A clear yellow solution is obtained after 90 min if 1 g of sugar, milk or rice is ashed with 10 ml of 100% nitric acid and 5 ml of sulphuric acid. Resistant materials (e.g., butter, lard and PVC) need longer times; the clear yellow solution appearing after 180–250 min. To utilize fully the oxidizing power of the acid mixture, the minimum heating time used was 210 min.

The recoveries of the radioactive tracers added are shown in Table 5. Heating times were always much longer than necessary to ash the samples. These extended heating times did not affect the tracer recoveries, which were at least as good as with the volumetric flask procedure. With some samples, 100% nitric acid must again be employed for quantitative recovery of mercury and selenium. The volume of sulphuric acid can safely be reduced to 2 ml (or even entirely omitted) with samples of sugar, wheat and similar materials. Total recovery is expected for tellurium and polonium, from analogy with selenium [6].

Safety

All the materials listed in Tables 1–5 were ashed safely. More than one thousand ashings were done smoothly by both procedures. An explosion occurred in the ashing of 1-nitroso-2-naphthol when the volumetric flask procedure was used with 1 g of sample, 10 ml of 65% nitric acid and 5 ml of sulphuric acid; this happened only in one of a series of four identical ashings, some minutes after the beginning of the charring stage. After cooling, a white crystalline product was observed at the neck of all four volumetric flasks and all four capillaries were obstructed. A second explosion happened in the ashing of 3 g of sugar with the same procedure by using 20 ml of water, 10 ml of 65% nitric acid and 5 ml of sulphuric acid. The explosion again occurred after the beginning of the charring stage. In both cases, the hood was sprayed with acid. The explosion caused no damage to property or operator. It is therefore recommended that ashings should always be done behind a protective screen. Doubtful materials must be first tested by taking small samples. The wetting of dry fine powdered materials with some drops of diluted nitric acid prior to the addition of 100% nitric acid is a safe practice. An extraction system for the nitrogen oxides may be placed over the tops of the columns.

The authors express their gratitude to A. Ernst for the glass and quartz components, K. Jakob for the teflon machining, R. Keil for the nitrate and sulphate determinations, and E. Rössler for the drawings. The authors are also grateful for the critical reviews provided by P. Baertschi, L. Smith and A. Wytttenbach.

TABLE 5

Tracer recovery after wet ashing by the quartz vessel procedure (A and B denote the treatment applied to the sample solutions after the wet ashing)

Sample ^a	Acid mixture ^b	Heating time (min)	Quantitative recovery ^c		Other recoveries
			Hg	Se	
Butter	15 (100) + 5	3 cycles ^d	B	B	
	15 (100) + 2	3 cycles	B		
Charcoal	15 (100) + 5	390		B	
	15 (100) + 5	3 cycles			Au(A,100%)
	15 (100) + 2	3 cycles	B	B	
Milk (dry, skimmed)	10 (65) + 5	210	A		Se(A,39%)
	10 (100) + 5	210		A	
Olive oil	10 (100) + 5	300	A		
	10 (100) + 5	3 cycles	A		Se(B,60%)
	15 (100) + 5	3 cycles		B	Au(A,100%)
	15 (100) + 2	3 cycles	B		
Polyethylene ^e	10 (100) + 5	300		B ^f	
PVC	10 (65) + 5	210	A		Au(A,100%), Se(A,92%)
	10 (100) + 5	240		B	
	10 (65) + 2	300	A		
	10 (65) + 2	3 cycles	B		
	15 (100) + 2	3 cycles		B	Au(A,100%)
	10 (65) + 5	210			Au(A,100%), Hg(A,90%), Se(A,46%) Se(A,97%)
Sugar	10 (100) + 5	240	A		
	15 (100) + 5	240		B	
	10 (100) + 2	300	A		
	10 (65) + 5	210			Hg(A,93%)
	10 (100) + 5	210	A	B	
	10 (100) + 2	3 cycles	B		
Wheat	10 (100) + 5	240			
	10 (100) + 2	300	A		
	10 (65) + 5	210			
	10 (100) + 5	210	A	B	
	10 (100) + 2	3 cycles	B		

^a 1-g sample unless otherwise stated. ^b ml HNO₃ (%) + ml H₂SO₄. ^c Quantitative recovery is defined as in Table 3. ^d 210 min of heating, 180 min without heating, 90 min with heating, 180 min without heating, and 90 min with heating. ^e 0.50-g sample. ^f The same result was obtained with lard, polypropylene (0.5 g), rice, and soot (0.5 g).

REFERENCES

- 1 T. T. Gorsuch, in I. M. Kolthoff and P. J. Elving (Eds.), *Treatise on Analytical Chemistry*, Interscience, New York, 1965, Part II, Vol. 12, pp. 295-372.
- 2 T. T. Gorsuch, *The Destruction of Organic Matter*, Pergamon, Oxford, 1970.
- 3 R. Bock, *Aufschlussmethoden der anorganischen und organischen Chemie*, Verlag Chemie, Weinheim, 1972.
- 4 G. Tölg, *Talanta*, 19 (1972) 1489.
- 5 O. G. Koch and G. A. Koch-Dedic, *Handbuch der Spurenanalyse*, Springer-Verlag, Berlin, 1974.

- 6 T. T. Gorsuch, in P. D. LaFleur (Ed.), *Accuracy in Trace Analysis: Sampling, Sampling, Sample Handling, Analysis*, U.S. Government Printing Office, Washington DC, 1976, Vol. 1, NBS Spec. Publ. No. 422.
- 7 G. D. Martinie and A. A. Schilt, *Anal. Chem.*, 48 (1976) 70.
- 8 E. B. Sandell and H. Onishi, *Photometric Determination of Traces of Metals (General Aspects)*, Wiley, New York, 1978.
- 9 B. Sansoni and V. Iyengar, *Sampling and Sample Preparation Methods for the Analysis of Trace Elements in Biological Material*, Kernforschungsanlage Jülich, Report Jül-Spez-13, Jülich, 1978.
- 10 S. Bajo, *Anal. Chem.*, 50 (1978) 649.
- 11 R. Keil, *Fresenius Z. Anal. Chem.*, 271 (1974) 359.
- 12 J. L. Down and T. T. Gorsuch, *Analyst*, 92 (1967) 398.
- 13 C. Feldman, *Anal. Chem.*, 46 (1974) 1606.
- 14 G. Knapp, *Fresenius Z. Anal. Chem.*, 274 (1975) 271.
- 15 B. Schreiber and H. R. Linder, *Fresenius Z. Anal. Chem.*, 298 (1979) 404.
- 16 M. M. Schachter and K. W. Boyer, *Anal. Chem.*, 52 (1980) 360.
- 17 R. Bock, *Aufschlussmethoden der anorganischen und organischen Chemie*, Verlag Chemie, Weinheim, 1972, p. 146.
- 18 G. Knapp, B. Sadjadi and H. Spitzzy, *Fresenius Z. Anal. Chem.*, 274 (1975) 275.
- 19 K. W. Budna and G. Knapp, *Fresenius Z. Anal. Chem.*, 294 (1979) 122.

Short Communication

APPLICATION OF UNCOATED PIEZOELECTRIC CRYSTALS FOR THE DETECTION OF AN ORGANIC PHOSPHONATE

JANOS KRISTOFF and GEORGE G. GUILBAULT*

Department of Chemistry, University of New Orleans, New Orleans, LA 70148 (U.S.A.)

(Received 4th November 1982)

Summary. Uncoated piezoelectric crystals with gold, silver and nickel electrodes give linear calibration graphs for diisopropylmethylphosphonate in the $\mu\text{g l}^{-1}$ range. The sensitivity increases and the selectivity decreases in the order: gold, silver, nickel. The response and recovery times for the gold-plated crystal are 0.12 and 2 min, respectively. Increasing temperatures (30–50°C) decrease the sensitivity. Interferences are few.

Piezoelectric crystals as air pollution detectors generally work in the ppm and ppb range. Recently, small sized detectors have been developed for portable use [1]. The theory and the application possibilities of piezoelectric crystal detectors have already been discussed in detail [2, 3].

Because of their high toxicity, the detection of organophosphorus compounds in air is of great importance. In recent years, there have been several studies on the piezoelectric detection of organophosphorus compounds in air. The cobalt complex of isonitrilobenzoylacetate [4] and the iron(III) chloride complex of pesticides [5] were first used as coatings. The iron(III) complex showed a very slow response and lacked the desired sensitivity. The application of the former coating was limited by its very short lifetime.

A ternary mixture of 1-n-dodecyl-3-hydroximinomethylpyridinium iodide (3-PAD), Triton X-100 and sodium hydroxide was reported by Tomita and Guilbault [6] for the detection of organophosphonates such as diisopropylmethylphosphonate. Advantages of faster response, longer lifetime and sensitivity in the $\mu\text{g l}^{-1}$ range were obtained. L-Histidine hydrochloride was also suggested [6] for the detection of organophosphorus compounds such as malathion. Copper complexes showing fast, reversible and weak complexation toward organophosphorus compounds at room temperature were evaluated by Guilbault et al. [7]. Higher sensitivity and shorter response and recovery times can be achieved by using polymer-bonded copper chelates as coatings [8].

In this study, uncoated piezoelectric crystals with different metal electrodes were investigated for the detection of diisopropylmethylphosphonate (DIMP) used as a model compound.

Experimental

A schematic diagram of the apparatus used is shown in Fig. 1. Nitrogen carrier gas flows through a vessel filled with phosphorus(V) oxide. The gas flow is divided into three parts, F_1 for desorption, F_2 for dilution and F_3 for generation; $F_1 = F_2 + F_3$ in all cases. The required concentration of DIMP in the gas flow can be adjusted by changing the F_2/F_3 ratio. The flow rate through the cell was $100 \text{ cm}^3 \text{ min}^{-1}$.

There are two possible modes for conducting measurements, monitoring and batch modes. In the batch mode, gas containing DIMP is injected through a septum (11 in Fig. 1); dilutions are made with ambient air to the desired level by using gaseous diffusion in the gas syringe. In the monitoring mode, the sample is introduced in a continuous flow of carrier gas (nitrogen or ambient air) which intermittently contains the organophosphonate to be determined. Most of the assays described in this work were done in the monitoring mode. The nitrogen carrier gas in F_3 was bubbled through liquid DIMP using a small pore-size sintered glass frit. The vapor concentration at 7 in Fig. 1 is known from the vapor pressure of DIMP. The concentration at the exit to the cell (12 in Fig. 1) can be calculated by collecting a sample of the gas and analyzing it either directly by gas chromatography or enzyme inhibition [9]. The DIMP content in the gas flow can be adjusted by varying either the temperature of the water bath or the gas flow. In this investigation, the temperature was maintained constant and the gas flow was varied.

A four-part valve was used to make a selection between pure nitrogen and the carrier gas containing DIMP. An injection port was inserted into the pure nitrogen stream for selectivity studies. For temperature studies the cell with the crystal was immersed in a water bath. The gas, before entering the cell, was passed through a gas-chromatographic column, also immersed in the water bath. The temperature inside the cell was monitored by a thermocouple.

Two crystals, both 9 MHz, were used, one as a reference to give a balanced response close to 0 Hz. Crystal placement and position in the detector cell were done with an HC 25/U socket (International Crystal Mfg. Co.). The

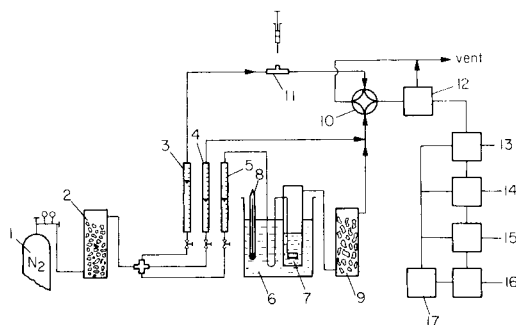


Fig. 1. Experimental arrangement: (1) gas cylinder, (2) P_2O_5 dryer, (3) F_1 flowmeter, (4) F_2 flowmeter, (5) F_3 flowmeter, (6) water bath, (7) DIMP generator, (8) thermometer, (9) glass wool, (10) four-port valve, (11) injection port, (12) cell, (13) oscillator, (14) frequency counter, (15) A/D converter, (16) recorder, (17) power supply.

instrumentation consisted of a low-frequency transistor oscillator (International Crystal Mfg. Co.) powered with a regulated power supply (Model IP-28, Heath-Schlumberger, Benton Harbor, MI 49022). The applied voltage was regulated to 6 V d.c. for all measurements. The oscillator output frequency (crystal vibrating frequency) was monitored using a frequency counter (digital display) with a 0.1-Hz resolution capacity (Heath-Schlumberger Model SM-4100). A permanent record of the frequency changes was generated by adapting a digital-to-analog converter circuit to the difference output of the frequency counter to provide a voltage output directly proportional to a change in crystal frequency; the output was connected to a potentiometric recorder.

Results and discussion

The results obtained for the crystals plated with gold, silver and nickel are summarized in Table 1. The calibration graphs are shown in Fig. 2. The frequency changes and reaches a new steady frequency in a time known as the response time (generally 5 s for the gold crystal and several minutes for the silver or nickel crystal). The recovery time is the time required for the frequency to return to the baseline after exposure to DIMP. This time is generally 1–4 min for the gold electrode.

The calibration graphs (Fig. 2) do not pass through the origin because there is a 5–30 Hz difference in frequency between the measuring and reference crystals. The smallest weight of compound detected at $10 \mu\text{g l}^{-1}$ (Fig. 2) is about 0.5 ng. The value can be compared to the theoretical limit of detection of a 9-MHz crystal which is 1 pg. The nickel-plated crystal shows the highest sensitivity to DIMP, but the reproducibility is poor, and the response and recovery times are too long. Better results were obtained for the silver-plated crystal but the recovery times are still high and nitrogen dioxide can irreversibly adsorb on the crystal. From practical considerations, the gold-plated crystal is recommended. The effect of temperature on the

TABLE 1

Experimental data obtained for gold-, silver- and nickel-plated crystals

DIMP concentration ($\mu\text{g l}^{-1}$)	Mean ΔF^a (Hz)			Response time (min)			Recovery time (min)		
	Au	Ag	Ni						
				Au	Ag	Ni	Au	Ag	Ni
8.9	18 ± 1	33 ± 1	48 ± 4	0.12	1	1	2	7	6
15.1	27	51 ± 3	70 ± 2	0.12	1	3	2	12	10
20.9	34 ± 1	62 ± 1	87 ± 3	0.3	1	3	2	13	16
25.9	39	74 ± 2	101 ± 8	0.3	2	5	2	8	12
30.0	45	85 ± 4	113 ± 10	0.4	2	6	3	9	20
36.5	53	98 ± 1	—	0.8	2	—	3	10	—
41.1	56 ± 2	109 ± 1	—	1	2	—	3	10	—
45.6	63 ± 1	120 ± 2	—	1.2	2	—	4	12	—

^a Average of 3 measurements \pm average deviation from mean.

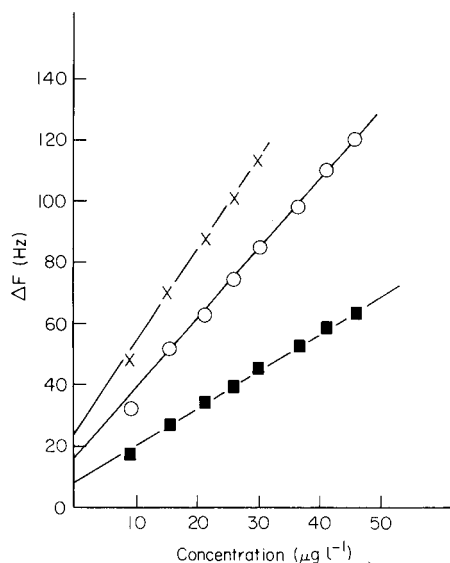


Fig. 2. Calibration graphs for DIMP obtained with various electrodes: (x) Ni; (o) Ag; (■) gold.

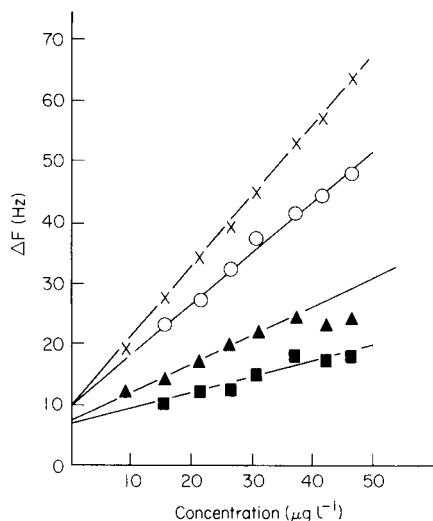


Fig. 3. Calibration graphs obtained with gold-plated crystals at different temperatures: (x) 20°C; (o) 30°C; (▲) 40°C; (■) 50°C.

response of the gold-plated crystal was examined at four different temperatures for the same concentrations of DIMP. Linear calibration graphs were observed in all instances (Fig. 3) but the sensitivity decreased with increasing temperature.

The results for selectivity testing, by the injection method, are listed in Table 2. Nitrogen dioxide is a serious interference when the silver-plated crystal is used, but the gold-plated crystal is almost interference-free. Water vapor is not a serious interference, even at 50% relative humidity. The effect

TABLE 2

Effect of other compounds

Compound	Concentration (mg l ⁻¹)	ΔF (Hz)		Compound	Concentration (mg l ⁻¹)	ΔF (Hz)	
		Au	Ag			Au	Ag
HCl	1000	2	2	Benzene	100	0	2
NH ₃	1000	0	2	Toluene	100	0	3
NO ₂	1000	2	25 ^a	Chloroform	100	0	1
SO ₂	1000	0	2	Car exhaust gas	1:10	1	1
CO	1000	0	0	H ₂ O	50% RH ^b	1	3
H ₂ S	1000	0	2				

^a Irreversible response. ^b Relative humidity.

of the contaminants at the same concentrations was also tested in the presence of $50 \mu\text{g l}^{-1}$ DIMP using the gold-plated crystal. Results similar to those in Table 2 were obtained, except for water vapor where a slightly enhanced response was observed ($\Delta F = 50$ Hz for DIMP and 55 Hz for DIMP + water vapor).

REFERENCES

- 1 E. P. Scheide and R. B. Warnar, *J. Am. Hyg. Assoc. J.*, 39 (1978) 745.
- 2 W. H. King, Jr., *Res./Dev.*, 20(5) (1969) 28.
- 3 J. Hlavay and G. G. Guilbault, *Anal. Chem.*, 49 (1977) 1890.
- 4 W. M. Shackelford and G. G. Guilbault, *Anal. Chim. Acta*, 73 (1974) 383.
- 5 E. P. Scheide and G. G. Guilbault, *Anal. Chem.*, 44 (1972) 1764.
- 6 Y. Tomita and G. G. Guilbault, *Anal. Chem.*, 52 (1980) 1484.
- 7 G. G. Guilbault, J. Affolter, Y. Tomita and E. S. Kolesar, Jr., *Anal. Chem.*, 53 (1981) 2057.
- 8 J. Kristoff and G. G. Guilbault, USAF Report SAM-TR-82-14, 1982.
- 9 G. G. Guilbault, J. Affolter, Y. Tomita and E. S. Kolesar, USAF Report SAM-TR-81-6, May 1981.

Short Communication

THE DETERMINATION OF SALICYLIC ACID AND ITS METABOLITES IN BLOOD PLASMA BY HIGH-PERFORMANCE LIQUID CHROMATOGRAPHY WITH AMPEROMETRIC DETECTION

KRZYSZTOF SELINGER and WILLIAM C. PURDY*

Department of Chemistry, McGill University, 801 Sherbrooke St. W., Montreal, Quebec H3A 2K6 (Canada)

(Received 21st September 1982)

Summary. The separation of salicylic acid and its main metabolites, salicyluric and gentisic acids, by reversed-phase liquid chromatography is followed by electrochemical oxidation in a thin-layer detection cell with a low-temperature isotropic carbon working electrode. The limits of detection for salicylic and gentisic acids are in the subnanogram range with linear responses of 0.5–150 ng, 2–250 ng and 0.2–200 ng for salicylic acid, salicyluric acid, and gentisic acid, respectively. The method makes it possible to quantify salicylates simultaneously in human blood plasma.

Continuing interest in determinations of salicylic acid and its metabolites is undoubtedly due to the high consumption of these drugs. Also, their therapeutic action and toxicity still remain the subjects of continuing research. Several chromatographic methods have been developed for the determination of salicylic acid in pharmaceutical formulations [1–6] and biological fluids [7–16]. Those methods which employ liquid chromatography use either ultraviolet [1, 2, 5, 6, 9, 11–13, 15, 16] or fluorescent [2, 10, 15] detection. To date there are no reports of the use of amperometric detection for these species. The present communication deals with a reversed-phase liquid chromatographic separation of salicylic acid and its main metabolites, salicyluric acid and gentisic acid, followed by detection in a thin-layer amperometric cell.

Experimental

Reagents. Salicylic acid, gentisic acid and salicyluric acid (Aldrich Chemical Company) were used to prepare ca. 1 mg ml⁻¹ stock solutions in spectrograde methanol (BDH Chemicals); these solutions were stored in a refrigerator at 4°C. Working standards were prepared as needed and diluted in methanol or in pooled plasma found to have no detectable salicylates by the present method. Water was deionized and distilled. All other reagents were of analytical-reagent grade.

Apparatus. The liquid chromatographic system consisted of a piston minipump (Milton Roy Corp.) used isocratically at a flow rate of 1.5 ml min⁻¹.

The mobile phase was continually degassed by a laboratory-designed helium-purge system. A Waters U6K injection valve was used to introduce samples to the chromatographic stream. The Waters column (0.46×15 cm) was packed with Spherisorb ODS ($5 \mu\text{m}$) and preceded by a guard column loosely packed with Pell ODS ($30\text{--}38 \mu\text{m}$, Whatman).

The amperometric cell was a thin-layer electrochemical detector designed in this laboratory [17]. Some minor changes were made with respect to the cell volume and the placement of the auxiliary electrode. Amperometric measurements were made with a PAR-174A polarographic analyzer (Princeton Applied Research). All chromatograms were recorded on a strip-chart recorder (Heath-Schlumberger, SR-204).

Mobile phase. Two different mobile phases were used. Mobile phase A consisted of an 18:82 volume ratio of methanol to 0.1% phosphoric acid solution which was 0.04 M in sodium perchlorate and 0.012 M in potassium dihydrogenphosphate at pH 2.2. Mobile phase B consisted of a 30:70 volume ratio of methanol to 0.1% phosphoric acid solution, 0.05 M in potassium dihydrogenphosphate at pH 3.40.

Procedure. A small volume ($5\text{--}20 \mu\text{l}$) of standard or "spiked" plasma was injected into the liquid chromatograph and peak heights were measured. No internal standard was used.

Results and discussion

Hydrodynamic voltammograms were run on the three compounds in mobile phases A and B. There were only slight differences in the responses of these compounds in the two mobile phases. Gentisic acid is the most easily oxidized of the acids with a wave occurring about 0.5 V less positive than those for salicylic acid or salicyluric acid. The data from these voltammograms were used to choose the potential of the working electrode, after consideration of the sensitivity and selectivity of the detector toward these compounds.

Calibration graphs for the three compounds were prepared with different combinations of mobile phase and working-electrode potential. Results of these studies are shown in Table 1. The final choice of mobile phase and working-electrode potential depended on the purpose of the analysis. If the three acids were to be determined simultaneously, then the potential of the working electrode was set at 1.4 V and mobile phase A was used (see Fig. 1). If salicylic acid were the only compound of interest and 17.5 min were too long for the separation/measurement step, then mobile phase B with a working electrode potential of 1.4 V was used. These conditions provide a shorter retention time for salicylic acid (7.2 min) but do not permit separation of the other two acids from other substances usually present in blood plasma (Fig. 2A). Finally, if only gentisic acid is to be determined, mobile phase A is used and the potential of the working electrode is set at 0.8 V, a potential where salicylic and salicyluric acids are not oxidized in mobile phase A (Fig. 2B).

TABLE 1

Calibration graphs for salicylic acid, salicyluric acid and gentisic acid prepared under differing conditions

Acid	Mobile phase	E^a (V)	Calibration graph ^b				Retention time (min)
			Range (ng)	S.d. (ng)	Slope \pm s.e. (nA ng ⁻¹)	Intercept \pm s.e. (nA)	
Gentisic	A	1.4	0.2–200	1.1	2.42 ± 0.013	0.7 ± 0.5	6.5
Salicyluric	A	1.4	2–250	1.2	0.65 ± 0.006	0.4 ± 0.5	9.8
Salicylic	A	1.4	0.5–150	1.9	1.02 ± 0.014	0.2 ± 0.8	17.5
Salicylic	B	1.4	0.5–150	2.0	1.05 ± 0.015	0.4 ± 0.8	7.2
Gentisic	A	0.8	0.05–200	1.0	2.36 ± 0.012	0.5 ± 0.4	6.5

^aPotential applied to working electrode. ^bLinear range, standard deviation, slope and intercept with standard errors, from 7–8 points for each graph.

Over a period of several months, numerous calibration graphs were obtained. The relationships between peak height and the acid concentration in plasma were linear for the concentration ranges shown in Table 1 for the three compounds. The correlation coefficient for the linear regression calculation was always better than 0.998 for the three compounds tested; other relevant statistics are included in Table 1. Similar electrochemical

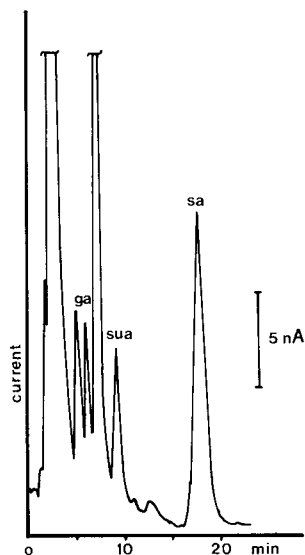


Fig. 1. Chromatogram of salicylic acid (26.44 ng), salicyluric acid (41.49 ng) and gentisic acid (7.98 ng) in plasma using mobile phase A. Voltage applied to the working electrode is 1.4 V.

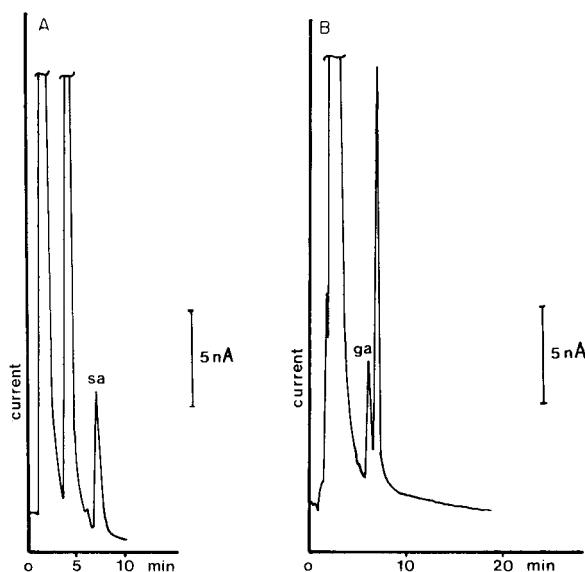


Fig. 2. Chromatograms for blood plasma. A, Separation of salicylic acid (36.4 ng) with mobile phase B at an applied potential of 1.4 V. B, Separation of gentisic acid (7.98 ng) with mobile phase A at an applied potential of 0.8 V.

behavior was observed throughout the range 10–30% (v/v) methanol content in the mobile phase.

Recovery studies indicated that the mobile phase is not a critical parameter (see Table 2). It was found that the relative standard deviation was generally

TABLE 2

Recovery studies on the assay of salicylic, salicyluric and gentisic acids

Acid	Injected (ng)	Found (ng)	S.d. (ng)	Confidence limit (95%, ng)	Recovery (%)
<i>A. Within-run (n = 7)</i>					
Gentisic	7.98	7.7	0.4	7.7 ± 0.54	97 ± 7
Salicyluric	41.49	43.0	1.4	43.0 ± 1.60	104 ± 1
Salicylic	26.44	27.6	0.6	27.6 ± 0.73	104 ± 3
<i>B. Day-to-day (n = 10)</i>					
Gentisic	125.4	121	5	121 ± 3	96 ± 2
Salicyluric	96.0	96	5	96 ± 3	100 ± 3
Salicylic	87.2	87	5	87 ± 3	99 ± 4
Gentisic	12.5	12.0	0.96	12.0 ± 0.56	96 ± 5
Salicyluric	9.6	9.4	1.01	9.4 ± 0.58	98 ± 6
Salicylic	8.7	9.1	0.86	9.1 ± 0.50	105 ± 6

between 5 and 10% for all three compounds below the 10-ng level and less than 5% in the range 10–100 ng. In water, the relative standard deviations were about half those obtained in plasma.

Attractive features of the proposed method are that the plasma sample is injected directly into the chromatographic system without prior treatment or clean-up, no internal standard is needed. Several compounds with suitable transition times (*o*-nitrophenol, *o*-nitroaniline, picric acid) were tested as possible internal standards but none gave a significant improvement in precision or accuracy.

The detection limit (defined as the amount of compound which would produce a signal twice that of the peak-to-peak noise) determined for salicylic acid (5 ng) by the present method is comparable to that for the other most sensitive methods [8, 14, 16]. For gentisic acid the detection limit is better (0.2 ng vs. 3 μ g [12] while for salicyluric acid it is worse (0.5 vs. 0.05 ng [16]). The precision of the present method for all three compounds is slightly worse than that of existing methods below the 10-ng level and about the same above that level.

Because its hydroxyl group is acetylated, it is not possible to detect aspirin, the most frequently used of the salicylates, by this method. However, aspirin has a very short half-life in man and its metabolites are rapidly excreted. For this reason, salicylic acid must be considered as the active compound. Furthermore, the determination of salicylic acid as an impurity in aspirin is necessary because its presence is limited to 0.05–3% in various pharmacopoeiae. The liquid chromatographic method with the amperometric detector seems to be specially suitable for this purpose.

The authors are indebted to the Natural Sciences and Engineering Research Council of Canada for support of this research.

REFERENCES

- 1 V. Das Gupta, *J. Pharm. Sci.*, **69** (1980) 110.
- 2 R. D. Kirchhoeffer and W. E. Juhl, *J. Pharm. Sci.*, **69** (1980) 548.
- 3 R. G. Baum and F. F. Cantwell, *J. Pharm. Sci.*, **67** (1978) 1066.
- 4 S. L. Ali, *J. Chromatogr.*, **126** (1976) 651.
- 5 P. P. Ascione and G. P. Chrekian, *J. Pharm. Sci.*, **64** (1975) 1029.
- 6 R. A. Henry and J. A. Schmit, *Chromatographia*, **3** (1970) 116.
- 7 L. I. Morrison, M. L. Funk and R. E. Ober, *J. Pharm. Sci.*, **69** (1980) 1271.
- 8 G. W. Peng, M. A. F. Gadalla, V. Smith, A. Peng and W. L. Chiou, *J. Pharm. Sci.*, **67** (1978) 710.
- 9 D. L. Maulding and J. F. Young, *J. Pharm. Sci.*, **69** (1980) 1224.
- 10 I. Bekersby, H. G. Boxenbaum, M. H. Whitson, C. V. Puglisi, R. Pocelinko and S. A. Kaplan, *Anal. Lett.*, **10** (1977) 539.
- 11 C. P. Terweij-Groen, T. Vahlkamp and J. C. Kraak, *J. Chromatogr.*, **145** (1978) 115.
- 12 B. E. Cham, D. Johns, F. Bochner, D. M. Imhoff and M. Rowland, *Clin. Chem.*, **25** (1979) 1420.
- 13 C. P. Terweij-Groen, S. Heemstra and J. C. Kraak, *J. Chromatogr.*, **181** (1980) 385.
- 14 L. Y. Lo and A. Bye, *J. Chromatogr.*, **181** (1980) 473.
- 15 E. N. Amick and W. D. Mason, *Anal. Lett.*, **12** (1979) 629.
- 16 J. N. Buskin, R. A. Upton and R. L. Williams, *Clin. Chem.*, **28** (1982) 1200.
- 17 B. R. Hepler, S. G. Weber and W. C. Purdy, *Anal. Chim. Acta*, **113** (1980) 269.

Short Communication

THE BEHAVIOUR OF BINUCLEAR ALKYNE—CARBONYL IRON DERIVATIVES IN REVERSED-PHASE HIGH-PERFORMANCE LIQUID CHROMATOGRAPHY

A. MANGIA* and G. PREDIERI

Istituto di Chimica Generale ed Inorganica, Università di Parma, Via M. D'Azeglio 85, 43100 Parma (Italy)

E. SAPPA

Istituto di Chimica Generale ed Inorganica, Università di Torino, C. so M. D'Azeglio 48, 10125 Torino (Italy)

(Received 16th November 1982)

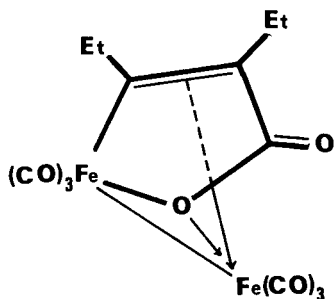
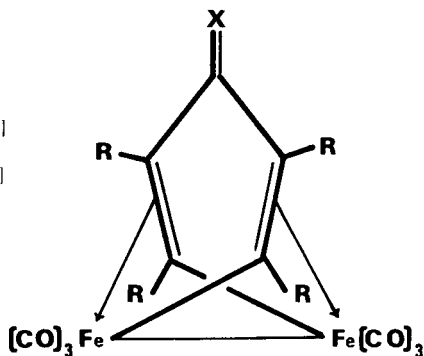
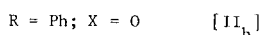
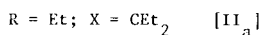
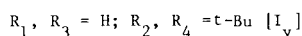
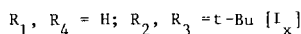
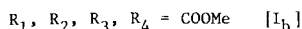
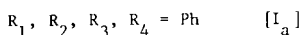
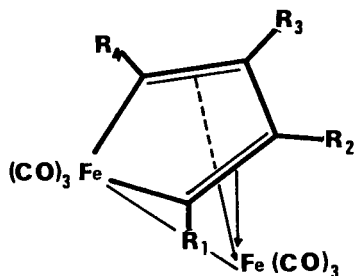
Summary. Mixtures of binuclear alkyne—carbonyl iron derivatives are considered. Geometrical isomers and compounds having similar structures but different substituents on the alkyne moiety can be separated on a RP-18 column by using methanol—acetonitrile mixtures as mobile phases. The order of elution is related to the different polarity of the compounds, deriving from the nature and the position of the substituents on the alkyne chain.

The separation and purification of mixtures of transition organometallic derivatives are fundamental steps in preparative procedures for these compounds. Chromatographic techniques are widely used for these purposes. Classical column chromatography permits separation of only a relatively small number of derivatives. Thin-layer chromatography (t.l.c.) has been used for both analytical and preparative purposes [1, 2]; in some cases mixtures of geometrical isomers have been separated with notable efficiency [3]. However, t.l.c. allows the separation of only small amounts of substances, and is time-consuming as well as unsuitable for direct quantitative measurements. New, fast and reliable techniques of separation and determination are required for organometallic compounds, and particularly for polynuclear clusters, because of the ever-increasing number of studies on this class of compound.

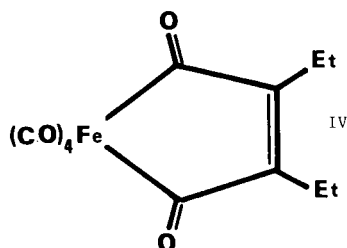
Within the framework of a program of research on the high-performance liquid chromatography (h.p.l.c.) of metal complexes [4–7], the potentialities of h.p.l.c. were examined for the separation and determination of polynuclear iron carbonyl derivatives. Some examples of the use of h.p.l.c. for the separation of mononuclear metal carbonyl derivatives have been reported [8, 9], but there seems to be only one application to polynuclear carbonyl compounds, namely, the separation of tri- and tetra-ruthenium carbonyl clusters [10].

As a first approach to this problem, some alkyne—carbonyl iron derivatives

were selected; these compounds are easily obtained by treating iron carbonyls with the appropriate acetylenes [11]. The selected compounds are derivatives of $\text{Fe}_2(\text{CO})_6(\text{RC}_2\text{R}')_2$ [11, 12], $\text{Fe}_2(\text{CO})_6(\text{C}_2\text{Et}_2)_3$ [13, 14], $\text{Fe}_2(\text{CO})_6(\text{C}_2\text{Ph}_2)_2\text{-CO}$ [15, 16], $\text{Fe}_2(\text{CO})_6(\text{C}_2\text{Et}_2)(\text{CO}_2)$ [17], and $\text{Fe}(\text{CO})_4(\text{C}_2\text{Et}_2)(\text{CO})_2$ [18]. Their structures are shown below. All these compounds, except IV, have the same basic $\text{Fe}_2(\text{CO})_6$ unit and contain different metallacyclic systems, built up by varying the number and the nature of the substituents on the alkyne moiety. Their behaviour in reversed-phase h.p.l.c. was studied with the aim



III



IV

of verifying the influence of the steric and electronic effects and of establishing conditions for analytical and preparative separations of polynuclear carbonyl derivatives.

Experimental

Complexes I–IV were prepared as described in the literature [11–18]. After crystallization, the identity and the purity of the complexes were checked by means of i.r. and mass spectrometry; the isomerism of I_x and I_y was confirmed by $^1\text{H-n.m.r.}$

TABLE 1

Electronic absorption maxima, λ_{\max} (nm), with their molar absorptivity coefficients, ϵ ($\text{l mol}^{-1} \text{cm}^{-1}$), for complexes I–IV in acetonitrile–methanol

	I _a	I _b	I _x	I _y	II _a	II _b	III	IV
λ_{\max}	408, 320	420, 290	445, 325	395, 270	455, 325	415, 320	290	300
ϵ	3220, 7470	2740, 5640	1780, 9080	4210, 8970	2330, 3880	6440, 8250	4890	1730

The h.p.l.c. system consisted of a Perkin-Elmer series 3B chromatograph, a Rheodyne 7105 injector and a LC-75 variable-wavelength u.v.–visible detector. A stainless steel column (25 cm \times 0.4 cm i.d.) containing LiChrosorb RP-18 (Merck; mean particle size 10 μm) was used. Solvents were h.p.l.c. grade (LiChrosolv, Merck).

Acetonitrile solutions of the compounds (5 μl) were injected; the content of metal in the samples ranged between 50 ng and 1 μg . Isocratic elutions were done at a flow rate of 1 $\text{cm}^3 \text{min}^{-1}$. The iron content of the column eluates was checked by using a Perkin-Elmer model 303 atomic absorption spectrometer, equipped with a HGA-72 atomizer.

Results and discussion

As spectrometric detection was used in the chromatographic system, the u.v.–visible spectra of complexes I–IV in acetonitrile–methanol were run

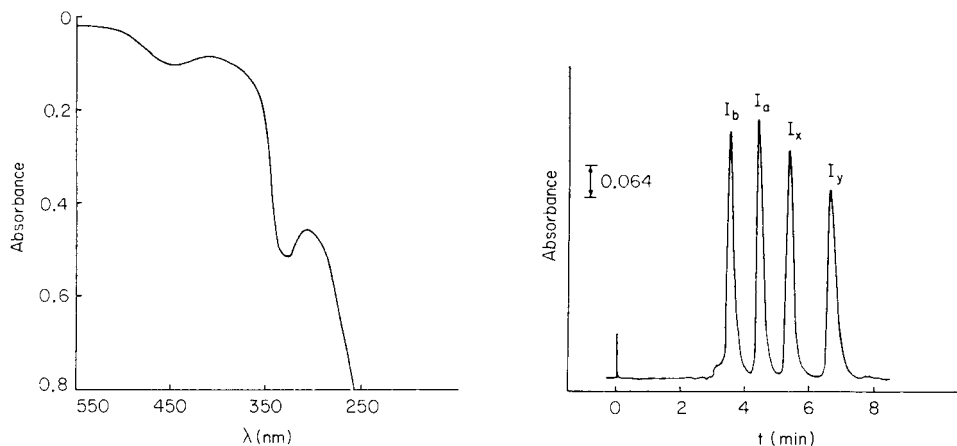


Fig. 1. Electronic spectrum of a 10^{-4} M solution of $\text{Fe}_2(\text{CO})_6(\text{HC}_2\text{Bu}^t)_2$ [I_x] in 1:1 acetonitrile–methanol.

Fig. 2. Separation of $\text{Fe}_2(\text{CO})_6(\text{PhC}_2\text{Ph})$ [I_a], $\text{Fe}_2(\text{CO})_6(\text{COOMeC}_2\text{COOMe})_2$ [I_b], $\text{Fe}(\text{CO})_5(\text{HC}_2\text{Bu}^t)_2$ [I_x] (isomer ii), $\text{Fe}_2(\text{CO})_6(\text{HC}_2\text{Bu}^t)_2$ [I_y] (isomer ie). LiChrosorb RP-18 column, $\lambda = 420 \text{ nm}$, $\text{CH}_3\text{CN}-\text{MeOH}$ 80:20 mobile phase, flow rate 1 $\text{cm}^3 \text{min}^{-1}$.

in the range 250–550 nm. The spectral data for the absorption maxima are listed in Table 1. A typical u.v.–visible spectrum is shown in Fig. 1.

On the basis of the solubility of these compounds in solvents of different polarity, a reversed-phase chromatographic system was chosen. Mixtures of acetonitrile and methanol were used as mobile phases on a C₁₈ column. The elution of the compounds was monitored at different wavelengths in successive injections. For all complexes, the values of the absorbance at different wavelengths measured with the u.v. detector were in agreement with the spectra of the single compounds dissolved in the same solvent. The presence of iron in the fractions of column eluates corresponding to peaks was checked by electrothermal a.a.s., other fractions of the mobile phase serving as a blank. Attempts to use water in the mobile phase resulted in peak broadening, probably owing to partial decomposition.

Figure 2 shows the isocratic separation of the set of compounds I, obtained by using an 80:20 (v/v) acetonitrile–methanol mixture and detection at 420 nm. Chromatographic data are quoted in Table 2. These compounds are structurally related, with a dimeric (CO)₃Fe–Fe(CO)₃ system and an alkyne unit. Complexes I_a, I_b, I_x, I_y differ by the presence of substituents with different electron-donating power on the ferra-cyclopentadienyl moiety. In I_x and I_y, the same substituent (*t*-butyl) occupies different positions on the ferra-alkyne ring. The elution order appears to be related to Taft's σ_I of the substituents: the retention volume increases as the σ_I decreases ($\sigma_{\text{COOMe}} > \sigma_{\text{Ph}} > \sigma_{\text{H}} > \sigma_{\text{But}}$) [19].

Of particular interest is the separation of the two positional isomers I_x and I_y; the “internal–internal” isomer I_x (where both hydrogen atoms are in the ferra-alkyne ring close to the iron atom) shows a shorter retention time. A reasonable explanation is that in the “internal–external” isomer the effects of the substituents in non-adjacent positions of the ring compensate for each other, whereas in the “ii” isomer a dipole is formed.

Figure 3A shows the separation of the pair of compounds II_a and II_b, obtained with a 50:50 acetonitrile–methanol mixture. The two compounds have similar structural skeletons and the elution order is in agreement with the more polar character of the substituents on the alkyne chain of compound II_b. The separation of complexes III and IV, obtained under the same conditions (Fig. 3B) is reported even though compound IV has a monomeric

TABLE 2

Capacity factor, k' , and resolution factor, R_s , for the separation of the set of compounds I, under the conditions of Fig. 2

	I _b	I _a	I _x	I _y ^a
k'	0.25	0.35	0.93	1.40
R_s	2.25	2.20	2.40	

^a Number of theoretical plates for I_y is 1990.

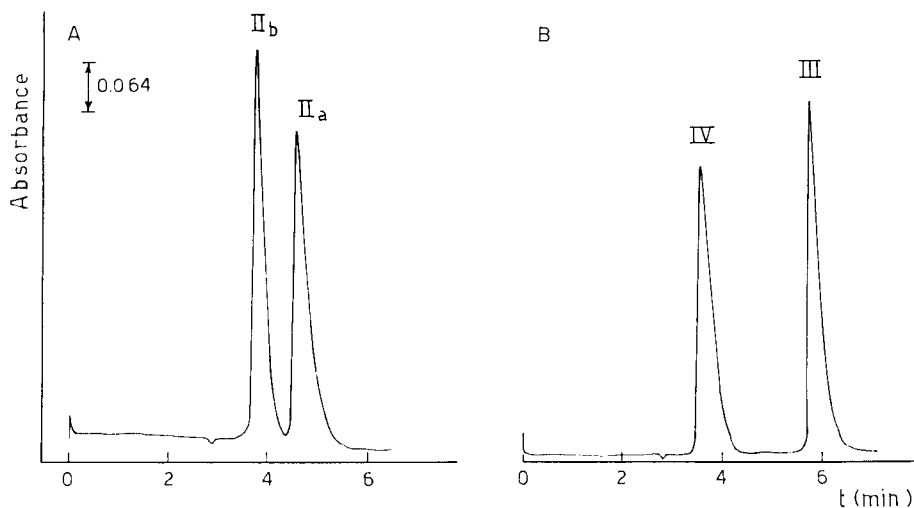


Fig. 3. A, Separation of $\text{Fe}_2(\text{CO})_6(\text{C}_2\text{Et}_2)_3$ [II_a] and $\text{Fe}_2(\text{CO})_6(\text{C}_2\text{Ph}_2)_2\text{CO}$ [II_b]; $R_s = 1.60$; LiChrosorb RP-18 column, $\lambda = 420$ nm, $\text{CH}_3\text{CN}-\text{MeOH}$ 50:50 mobile phase, flow rate $1 \text{ cm}^3 \text{ min}^{-1}$. B, Separation of $\text{Fe}_2(\text{CO})_6(\text{C}_2\text{Et}_2)(\text{CO}_2)$ [III] and $\text{Fe}(\text{CO})_4(\text{C}_2\text{Et}_2)(\text{CO})_2$ [IV]; $R_s = 4.20$; same conditions as for A.

structure. These products derive from the same class of reaction [17, 18] involving iron carbonyls and hex-3-yne, therefore their separation could be useful from a preparative point of view.

In the light of the results obtained, it is possible to state that h.p.l.c. is effective for the separation of binuclear iron carbonyl derivatives for both analytical and preparative purposes. Studies on the behaviour of simple and substituted tri- and tetra-metallic carbonyl clusters are in progress.

This work was supported by C. N. R. (Rome), Grant No. 81.01664.03.

REFERENCES

- 1 G. Cetini, O. Gambino, R. Rossetti and E. Sappa, *J. Organomet. Chem.*, **8** (1967) 149.
- 2 E. Sappa, A. Tiripicchio and M. Tiripicchio Camellini, *J. Chem. Soc. Dalton Trans.*, (1978) 419.
- 3 D. Osella, E. Sappa, A. Tiripicchio and M. Tiripicchio Camellini, *Inorg. Chim. Acta*, **42** (1980) 183.
- 4 E. Gaetani, C. F. Laureri, A. Mangia and G. Parolari, *Anal. Chem.*, **48** (1976) 1725.
- 5 A. Mangia, G. Parolari, E. Gaetani and C. F. Laureri, *Anal. Chim. Acta*, **92** (1977) 111.
- 6 A. Mangia, E. Gaetani and C. F. Laureri, *Ann. Chim. (Rome)*, **69** (1979) 181.
- 7 A. Mangia, P. L. Messori, C. Pelizzi and G. Predieri, *Inorg. Chim. Acta*, **68** (1982) 137.
- 8 H. Veening and R. B. Willeford, *Rev. Inorg. Chem.*, **1** (1979) 281 and references therein.
- 9 D. Sellmann, E. Jonk, H. J. Reinecke and T. Würminghausen, *Fresenius Z. Anal. Chem.*, **294** (1979) 372.
- 10 C. T. Enos, G. L. Geoffroy and T. H. Risby, *J. Chromatogr. Sci.*, **15** (1977) 83.
- 11 W. Hübel, in I. Wender and P. Pino (Eds.), *Organic Syntheses via Metal Carbonyls*, Wiley-Interscience, New York, 1968, Vol. 1, p. 273.

- 12 S. Aime, L. Milone and E. Sappa, *J. Chem. Soc. Dalton Trans.*, (1976) 838.
- 13 E. Sappa, M. L. Nanni Marchino and V. Raverdino, *Ann. Chim. (Rome)*, 68 (1978) 349.
- 14 J. Meunier Piret, P. Piret and M. Van Meersche, *Acta Crystallogr.*, 19 (1965) 85.
- 15 V. Raverdino and E. Sappa, *Ann. Chim. (Rome)*, 67 (1977) 423.
- 16 F. A. Cotton, D. L. Hunter and J. M. Troup, *Inorg. Chem.*, 15 (1976) 63.
- 17 S. Aime, L. Milone, E. Sappa, A. Tiripicchio and M. Tiripicchio Camellini, *J. Chem. Soc. Dalton Trans.*, (1979) 1155.
- 18 S. Aime, L. Milone, E. Sappa, A. Tiripicchio and A. M. Manotti Lanfredi, *J. Chem. Soc. Dalton Trans.*, (1979) 1664.
- 19 R. W. Taft, Jr., in M. S. Newman (Ed.), *Steric Effects in Organic Chemistry*, Ch. 13, Wiley, New York, 1956.

Short Communication

AUTOMATED DETERMINATION OF BROMIDE IN WATERS BY ION CHROMATOGRAPHY WITH AN AMPEROMETRIC DETECTOR

G. S. PYEN* and D. E. ERDMANN

U.S. Geological Survey, National Water Quality Laboratory, 6481-H Peachtree Industrial Blvd., Doraville, GA 30340 (U.S.A.)

(Received 20th October 1982)

Summary. An automated ion chromatograph, including a program controller, an automatic sampler, an integrator, and an amperometric detector, was used to develop a procedure for the determination of bromide in rain water and many ground waters. Approximately 10 min is required to obtain a chromatogram. The detection limit for bromide is 0.01 mg l^{-1} and the relative standard deviation is $<5\%$ for bromide concentrations between 0.05 and 0.5 mg l^{-1} . Chloride interferes if the chloride-to-bromide ratio is greater than $1000:1$ for a range of 0.01 – 0.1 mg l^{-1} bromide; similarly, chloride interferes in the 0.1 – 1.0 mg l^{-1} range if the ratio is greater than $5000:1$. In the latter case, a maximum of 2000 mg l^{-1} of chloride can be tolerated. Recoveries of known concentrations of bromide added to several samples, ranged from 97 to 110%.

At present, an indirect spectrophotometric technique [1, 2] is used in U.S. Geological Survey laboratories to determine the bromide concentration in water. This method, based on the catalytic effect of bromide on the oxidation of iodine to iodate by potassium permanganate in sulfuric acid solution, can determine 0.01 – 0.10 mg l^{-1} bromide. A skilled operator is required because reaction temperature and time for each reaction step are critical. Also, a hazardous situation exists because the operator must continuously handle carbon tetrachloride.

An ion-chromatographic method for determining selected anions in water has been described [3] in which the minimum detection limit for bromide is 0.10 mg l^{-1} when conductimetric detection is used. Applications of simultaneous detection in ion chromatography have been reported [4].

In this communication, an automated ion-chromatographic method with an amperometric detector is described for the determination of bromide. The sample stream from the column flows through an electrochemical cell, where a fixed potential is applied to the cell. Any electroactive species having an oxidation/reduction potential near the applied potential will generate a current that is directly proportional to the concentration of the electroactive species.

Experimental

Apparatus. A Dionex Model 12 ion chromatograph was used with a 200- μ l sample loop, an eluent flow rate of 2.3 ml min⁻¹ (30% of full capacity), and a sample pump flow rate of 3.8 ml min⁻¹ (50% of full capacity). A pulse damper was installed just before the injection valve to reduce flow pulsation. A Dionex amperometric detector consisting of cell and potentiostat was used. The cell contains a silver working electrode, a platinum counter electrode, and an Ag/AgCl reference electrode. This cell is installed between separator and suppressor columns. The working silver electrode should be cleaned monthly by polishing the surface with a small amount of an abrasive toothpaste on a paper tissue to remove the grey tarnish and then rinsing with deionized water. An applied potential of 0.10 V and a detector output range of 100 nA V⁻¹ were used.

A Technicon autosampler-IV automatically delivered the sample to the ion chromatograph and a Spectra Physics SP-4100 integrator measured the peak heights.

Reagents. All reagent solutions were prepared in deionized water. Reagent-grade sodium bromide was used for the preparation of standards. The eluent mixture consisted of 0.003 M NaHCO₃ and 0.002 M Na₂CO₃. A Dionex 4 \times 50 mm fast-run anion precolumn and a 4 \times 250 mm separator column were used.

Procedure. It was necessary to allow eluent to flow for approximately 30 min to reach equilibrium. It took about 10 min to complete a chromatogram using a 200- μ l sample loop. The retention time of bromide was 5.4 min. Two calibration graphs were used, one for bromide concentrations of 0.10–1.0 mg l⁻¹ (with a 10 V input) using a quadratic fit, and another for bromide concentrations of 0.01–0.10 mg l⁻¹ (with a 1 V input) using single-point calibration with intercept of zero. A U.S. Geological Survey Standard reference water sample was used in every twentieth position of the tray.

Results and discussion

Ten replicates from each of six U.S. Geological Survey standard reference water samples were randomly placed in a sample tray and the bromide concentrations were determined over a period of one month. The average results for bromide ranged from 0.049 to 0.502 mg l⁻¹ and the relative standard deviations ranged from 1.6% to 4.1%.

The detection limit (defined as the concentration which gives a signal twice that of background noise) for bromide is 0.01 mg l⁻¹.

Samples containing large concentrations of chloride interfered with the recovery of bromide. When chloride passed through the detector, large currents were generated because of silver chloride formation on the surface of the silver working electrode. This was followed by the stream of eluent which removed silver chloride, thus generating a negative peak. The higher the chloride concentration, the longer it took for the system to return to baseline conditions. For a working calibration range 0.01–0.10 mg l⁻¹ bromide, the chloride interfered if the chloride-to-bromide ratio was greater

TABLE 1

Recovery of bromide in filtered water samples

Sample No.	Concentration (mg l ⁻¹)				
	Chloride	Bromide	Bromide added	Bromide found	Recovery (%)
1	31	0.59	0.5	1.13	108
2	263	0.49	0.5	1.03	108
3	63	0.33	0.3	0.65	107
4	56	0.30	0.3	0.61	103
5	2.28	0.22	0.3	0.51	97
6	5.95	0.040	0.05	0.089	98
7	4.59	0.037	0.05	0.086	98
8	4.78	0.031	0.03	0.062	103
9	4.89	0.029	0.01	0.039	100
10	5.05	0.031	0.03	0.064	110

than 1000:1. The allowable chloride for 100% "recovery" of bromide increased linearly with bromide concentration. A similar interference was present for the 0.10–1.0 mg l⁻¹ calibration range, when the chloride-to-bromide ratio exceeded 5000:1. Sulfite elutes at almost the same time as bromide. However, this does not affect the bromide results, because sulfite is readily oxidized to sulfate.

To determine recoveries, known concentrations of bromide were added to several natural water samples; recoveries ranged from 97 to 110%. Typical results are given in Table 1.

Conductimetric and amperometric detectors are commonly used simultaneously. Seven anions, namely F⁻, Cl⁻, NO₂⁻, PO₄³⁻, Br⁻, NO₃⁻, and SO₄²⁻ are determined by conductivity detection. At the same time, bromide concentrations less than 0.1 mg l⁻¹ are determined by amperometric detection. A typical chromatogram of these seven anions obtained with conductimetric and amperometric detection simultaneously is shown in Fig. 1. The concentration of the anions are as follows: fluoride 0.25, chloride 1.0, nitrite 0.5, phosphate 0.5, bromide 0.5, nitrate 0.5, and sulfate 3.0 mg l⁻¹. There is excellent agreement between the results obtained with these two detectors. The plot of these comparison data yielded a least-squares slope of 0.975 ± 0.021 , a y intercept of -0.0015 ± 0.014 , and a correlation coefficient of 0.998. If a sample contained a chloride concentration greater than 1000 mg l⁻¹, the bromide peak would be masked by the chloride peak with conductimetric detection. In contrast, the maximum chloride concentration allowable for amperometric detection is 2000 mg l⁻¹, as long as the chloride-to-bromide ratio is less than 5000:1.

A comparative study between the standard catalytic procedure and the ion-chromatographic procedure was conducted. An average recovery of 105% with a standard deviation of 2.6% was obtained by the ion-chromatographic method. An average recovery of 100% with a standard deviation of 34% was obtained with the catalytic procedure.

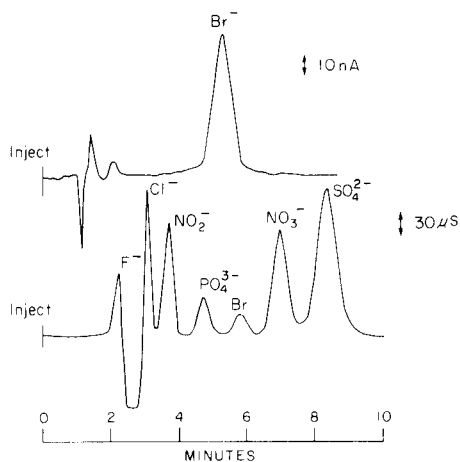


Fig. 1. Chromatograms for selected anions with conductimetric (lower curve) and amperometric (upper curve) detection.

REFERENCES

- 1 M. J. Fishman and M. W. Skougstad, *Anal. Chem.*, 35 (1963) 146.
- 2 M. W. Skougstad, M. J. Fishman, L. C. Friedman, D. E. Erdmann and S. S. Duncan, *Techniques of Water-Resources Investigations of the U.S. Geological Survey, Methods for the Determination of Inorganic Substances in Water and Fluvial Sediments, Book 5, Chapter A1*, 1979, p. 329.
- 3 M. J. Fishman and G. S. Pyen, *Water-Resources Investigations*, 1979, p. 79.
- 4 E. L. Johnson and E. Cathers, *International Symposium on Ion Chromatography, 23rd Rocky Mountain Conference*, 1981.

Short Communication

COMBINED USE OF TWO SURFACTANTS FOR FLOTATION OF METAL HYDROXIDE PRECIPITATES IN SEA WATER

N. J. SONAWANE^a, MASATAKA HIRAIDE and ATSUSHI MIZUIKE*

Faculty of Engineering, Nagoya University, Chikusa-ku, Nagoya 464 (Japan)

(Received 2nd December 1982)

Summary. Various surfactants are surveyed for the flotation of iron(III), aluminum and indium hydroxide collector precipitates for concentrating trace heavy metals in sea water. A 1:3 mixture of sodium oleate and sodium dodecyl sulfate is most recommended to obtain the complete flotation and stable foam-layer formation essential to this preconcentration technique.

Coprecipitation with metal hydroxides followed by flotation is a simple and rapid multi-element preconcentration technique for the determination of trace heavy metals [e.g., Cr(III), Mn(II), Fe(III), Co, Ni, Cu(II), Zn and Pb] in water samples [1, 2]. Single surfactant ions are conventionally used for rendering the precipitate surface hydrophobic. However, it has been shown that the combined use of two surfactants, sodium oleate and sodium dodecyl sulfate, is required for quantitative recovery of indium hydroxide precipitate at pH 9–9.5 from sea water [2]. With sodium oleate alone, re-dispersion of the floated precipitate occurred during collection, because a stable foam layer was not formed under the precipitate. With sodium dodecyl sulfate alone, the flotation was not achieved. In the present work, the roles of surfactants in the flotation of iron(III), aluminum and indium hydroxide precipitates in sea water are investigated in detail.

Experimental

Apparatus. The flotation cell consisted of a 40 mm i.d. × 250 mm long glass tube tapered at the lower end with a sintered-glass disk (No. 4; 5- to 10- μ m nominal porosity) near the lower end.

Reagents. Metal solutions (10 mg ml⁻¹) were prepared from iron(III) chloride, aluminum chloride and indium metal. Surfactant solutions (1 mg ml⁻¹) were prepared by dissolving in 70% (v/v) ethanol. Artificial sea water was prepared by the formula of Lyman and Fleming [3]. All reagents used were of reagent grade, except for surfactants (Extra Pure).

Procedure. To 200 ml of artificial sea water in a 300-ml beaker, 1 ml of

^aPresent address: Chemistry Department, K.T.H.M. College, University of Poona, Nasik-2, India.

metal solution was added. The pH was adjusted to 9 with aqueous 1M and 0.1 M ammonia, while stirring with a magnetic stirrer. Then 1–4 ml of single or mixed surfactant solution was added and the contents of the beaker were quantitatively transferred to a flotation cell. Nitrogen was passed at a flow rate of $1 \text{ ml cm}^{-2} \text{ min}^{-1}$ from the lower end of the cell for 30 s, to obtain complete mixing and flotation of the precipitates with the aid of numerous tiny bubbles (diameter below 0.5 mm). The completion of the flotation and the foam layer formation were inspected visually.

Results and discussion

Different anionic, cationic and nonionic surfactants were used singly, with the results shown in Table 1. The flotation behavior of iron(III),

TABLE 1

Flotation of metal hydroxide precipitates with a single surfactant in sea water at pH 9

Surfactant (1 mg)		Flotation ^a		
Name	Formula ^b	Fe(OH) ₃	Al(OH) ₃	In(OH) ₃
<i>Anionic</i>				
Na-caprate	C ₉ H ₁₉ COONa	P'	P'	P'
Na-laurate	C ₁₁ H ₂₃ COONa	P	P	P
Na-myristate	C ₁₃ H ₂₇ COONa	P'	—	—
Na-palmitate	C ₁₅ H ₃₁ COONa	P'	P'	P'
Na-stearate	C ₁₇ H ₃₅ COONa	P'	—	—
Na-oleate	C ₁₇ H ₃₃ COONa	P	P	P
Na-linoleate	C ₁₇ H ₃₁ COONa	P	—	—
Na-ricinoleate	C ₁₇ H ₃₂ (OH)COONa	P	P	P
Na-naphthenate	C ₁₄ H ₂₇ COONa etc.	P	—	—
Na-dodecyl sulfate	C ₁₂ H ₂₅ OSO ₃ Na	F + P'	F + P'	F + P'
Na-dodecylbenzene-sulfonate	C ₁₈ H ₂₉ SO ₃ Na	F + P'	F + P'	F + P'
<i>Cationic</i>				
Cetyltrimethyl-ammonium bromide	[CH ₃ (CH ₂) ₁₅ N(CH ₃) ₃]Br	F	F	F
Cetyldimethylammonium bromide	[CH ₃ (CH ₂) ₁₅ N(CH ₃) ₂ C ₂ H ₅]Br	F	—	—
Benzalkonium chloride	[RN(CH ₃) ₂ CH ₂ C ₆ H ₅]Cl	F	F	F
n-Dodecylamine	CH ₃ (CH ₂) ₁₁ NH ₂	F	—	—
n-Dodecylamine hydrochloride	CH ₃ (CH ₂) ₁₁ NH ₂ HCl	F	—	—
<i>Nonionic</i>				
Brij 35	C ₁₂ H ₂₅ (OCH ₂ CH ₂) ₂₃ OH	F	F	F

^aP: The precipitate is completely floated, but a foam layer is not formed;

P': The precipitate is partially floated and a foam layer is not formed;

F + P': A foam layer is formed and then part of the precipitate is floated;

F: Only a foam layer is formed.

^bR: Alkyl groups.

aluminum and indium hydroxides is similar. No single surfactant is suitable for the flotation followed by formation of a stable foam layer. For the flotation, sodium oleate was selected from five anionic surfactants (shown as P), because it is most economical. Flotation with sodium oleate was also less affected by the nitrogen flow rate than sodium laurate. Iron(III), aluminum and indium on the precipitate surface react with oleate ions rendering the surface hydrophobic, hence the precipitates are easily floated. This reaction was confirmed as follows: iron(III) hydroxide (10 mg Fe) was precipitated in 25 ml of sea water, 30 ml of sodium oleate solution was added, and then the solution was shaken with 25 ml of chloroform for 2 min. The precipitate was completely extracted into the organic phase. In the absence of sodium oleate (only 30 ml of 70% ethanol was added), the precipitate remained completely in the aqueous phase.

Sodium oleate, however, also reacts with magnesium present in sea water, and therefore a foam layer is not formed. When an excess of sodium oleate (8 g) is added to 200 ml of sea water (stoichiometrically 6.4 g), a large amount of white magnesium oleate precipitates. In this case, rapid flotation is not achieved and the foam layer contains magnesium which sometimes interferes with the determination of the desired trace elements. Changing the nitrogen flow rate or the bubbling time was useless for the formation of a stable foam layer.

A stable foam layer is necessary to support the floated precipitate for quantitative collection as well as to minimize the amount of accompanying mother liquor. Therefore, different anionic, cationic and nonionic surfac-

TABLE 2

Flotation of metal hydroxide precipitates with mixed surfactants in sea water at pH 9

Sodium oleate (1 mg) plus	Flotation ^a			
	1 mg ^b	3 mg ^b		
	Fe(OH) ₃	Fe(OH) ₃	Al(OH) ₃	In(OH) ₃
Na-dodecyl sulfate	P	P + F	P + F	P + F
Na-dodecylbenzenesulfonate	P	P + F	P + F	P + F
Cetyltrimethyl- ammonium bromide	F	—	—	—
Cetyldimethyl- ammonium bromide	F	—	—	—
Benzalkonium chloride	F	—	—	—
n-Dodecylamine	P'	—	—	—
n-Dodecylamine hydrochloride	F + P'	—	—	—
Brij 35	F + P'	—	—	—

^aP + F: The precipitate is floated and then a foam layer is formed supporting it; for other abbreviations, see Table 1.

^bQuantity of a combined surfactant.

tants were tested in combination with sodium oleate in attempts to obtain a stable foam layer. The results are shown in Table 2. When sodium oleate is combined with cationic and nonionic surfactants, flotation is suppressed. By combining 1 mg of sodium dodecyl sulfate or sodium dodecylbenzenesulfonate with sodium oleate, complete flotation is achieved, but a stable foam layer is not formed, although the precipitate layer is more stable than that with sodium oleate alone. With 3 mg of combined surfactant, 2 ml cm⁻² min⁻¹ of flow rate and 1 min of bubbling time, successful results (precipitate layer and foam layer) were obtained. Because of water pollution with sodium dodecylbenzenesulfonate, sodium dodecyl sulfate is recommended.

A 1:3 mixture of sodium oleate and sodium dodecyl sulfate can be successfully applied to the flotation of various metal hydroxide collector precipitates for concentrating trace heavy metals in sea water.

REFERENCES

- 1 M. Hiraide, Y. Yoshida and A. Mizuike, *Anal. Chim. Acta*, 81 (1976) 185.
- 2 M. Hiraide, T. Ito, M. Baba, H. Kawaguchi and A. Mizuike, *Anal. Chem.*, 52 (1980) 804.
- 3 H. U. Sverdrup, M. W. Johnson and R. H. Fleming, *The Oceans: Their Physics, Chemistry, and General Biology*, Prentice-Hall, Englewood Cliffs, N.J., U.S.A., 1942, p. 186.

Short Communication

RAPID MICRODIFFUSION—PHOTOMETRIC DETERMINATION OF NANOGRAM QUANTITIES OF AMMONIA

SUSUMU KAWAKUBO and TSUTOMU FUKASAWA*

Department of Applied Chemistry, Faculty of Engineering, Yamanashi University, Kofu 400 (Japan)

ATSUSHI MIZUIKE

Faculty of Engineering, Nagoya University, Chikusa-ku, Nagoya 464 (Japan)

(Received 15th July 1982)

Summary. In a new type of microdiffusion unit, 20–280 ng of ammonia is quantitatively transferred from about 100 μ l of alkaline sample solution to 60 μ l of 0.1 M hydrochloric acid at 50°C within 30 min. The color is developed and the absorbance is measured for the photometric determination of ammonia with hypochlorite and 1-naphthol in the unit. The method is simple, rapid and sensitive. It was successfully applied to the identification of crystalline particulates found on the stages of an Andersen air sampler.

The microdiffusion method [1, 2] is widely used for the separation and determination of small amounts of ammonia. However, more than an hour is generally required for diffusion and less than 0.1 μ g of ammonia cannot be determined because of poor sensitivity of the photometric Nessler method or the titrimetric method.

This communication describes a new type of microdiffusion unit capable of quantitative separation of ammonia at 50°C within 30 min. The color development and absorbance measurements for the photometric determination of ammonia by the sensitive method with hydrochlorite and 1-naphthol [3] are done in situ in the absorbent compartment of the unit. Ammonia, 20–280 ng, can be separated and measured by the proposed method within an hour.

Experimental

Reagents. All reagents were of reagent grade (Wako Pure Chemicals) except for sodium hypochlorite. Water was deionized and distilled. A standard ammonia solution (0.944 mg ml⁻¹) was prepared by dissolving ammonium chloride in water, and was diluted to appropriate concentrations immediately before use. A 5% (w/v) acetone solution of 1-naphthol was stable for at least one day at about 20°C. A hypochlorite solution containing 0.5% available chlorine was prepared by diluting 10% sodium hypochlorite solution (Wako Pure Chemicals; food additive) and standardized by iodometric titration.

Conway microdiffusion unit (Fig. 1A). In a conventional glass unit (Sibata Chemical App. Mfg. Co.), an acrylic resin microcup (8 mm i.d., 0.4 ml) is placed to accommodate a small volume of absorbing solution. Vaseline and a clamp are used to make the unit airtight.

Vial-type microdiffusion unit (Fig. 1B). An acrylic resin microcup (5 mm i.d., 0.15 ml) for the absorbing solution is fixed to the rubber liner of the vial cap with an adhesive. A polyethylene ring is used to minimize contamination from the rubber liner.

Microdiffusion—photometry unit (Fig. 2). The unit consists of a detachable sample compartment and an absorbent compartment, in which the color is developed and the absorbance is measured. A tee support is attached to the absorbent compartment to facilitate handling and proper alignment in the spectrophotometer.

Other apparatus used included a Hitachi model 100-10 spectrophotometer, a Narishige MN-100 micromanipulator with a glass needle, a microscope (100 \times), a Cahn 26 electrobalance (weighing error ± 0.1 μ g), and two Eppendorf 4700 micropipettes.

Recommended procedure for the microdiffusion—photometry unit. Less than 60 μ l of solution containing less than 280 ng of ammonia is placed in the sample compartment. After addition of 50 μ l of 6 M potassium carbonate, the compartment is immediately connected with the absorbent compartment containing 60 μ l of 0.1 M hydrochloric acid (absorbing solution) as shown in Fig. 2. The unit is immersed in a water bath maintained at 50°C for 30 min to diffuse ammonia. The sample compartment is then removed, and the unit is turned through 90° so that the opening of the absorbent compartment faces

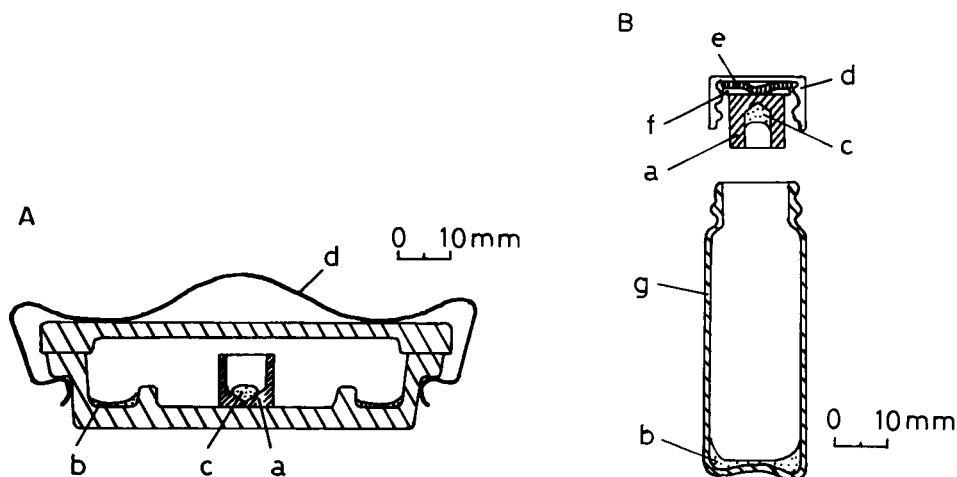


Fig. 1. A, Conway microdiffusion unit; B, vial-type microdiffusion unit. (a) Acrylic resin microcup; (b) sample solution; (c) absorbing solution; (d) clamp (A) or (d) plastic screw cap (B); (e) rubber liner; (f) polyethylene ring; (g) 10-ml glass vial.

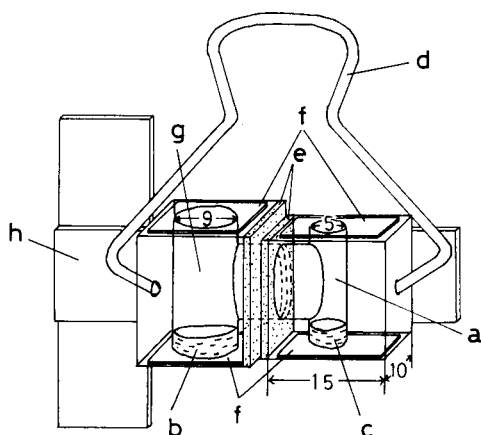


Fig. 2. Microdiffusion—photometry unit (dimensions in mm). (a) Acrylic resin absorbent compartment (i.d. 5 mm); (b) sample solution; (c) absorbing solution; (d) clamp; (e) soft polyvinyl chloride sheet; (f) acrylic resin window; (g) acrylic resin sample compartment (i.d. 9 mm); (h) polyvinyl chloride support.

upward. To the absorbing solution is added 60 μ l of 0.1 M sodium hydroxide followed by 20 μ l of ethanol to facilitate mixing. The solution is diluted to 240 μ l with water, and 20 μ l of hypochlorite solution (to form monochloramine), 100 μ l of 0.2 M sodium hydroxide, and 40 μ l of 1-naphthol solution (5% w/v in acetone) are added, the solution being well mixed by using a micropipette. The unit is placed in the spectrophotometer, and after 5 min, the absorbance of the solution is measured at 720 nm. A calibration curve is prepared by adding standard ammonia solutions into 60 μ l of 0.1 M hydrochloric acid and applying the photometric procedure.

Before re-use, the unit must be washed either with a (3 + 7) mixture of acetone and water or ethanol followed by water and air-dried, or it can be washed with 0.005 M potassium carbonate, to remove 1-naphthol and ammonia residues.

Results and discussion

First, a Conway-type microdiffusion unit with a microcup (Fig. 1A) was used to diffuse 76 ng of ammonia at 21°C from 1 ml of 3 M potassium carbonate to 60 μ l of 0.1 M hydrochloric acid. Ammonia was determined as described in the recommended procedure. The calibration graph was linear over the range 19–283 ng, with an error of about 4 ng. Figure 3A shows that the ammonia recovery was incomplete even after 90 min of diffusion. This unit was not usable at temperatures over 40°C because of leakage of ammonia.

The vial-type microdiffusion unit (Fig. 1B) was then constructed for the diffusion of ammonia at higher temperatures. To diffuse ammonia from 0.3 ml of 3 M potassium carbonate to 60 μ l of 0.1 M hydrochloric acid, the unit was completely immersed in a water bath maintained at 50°C. The

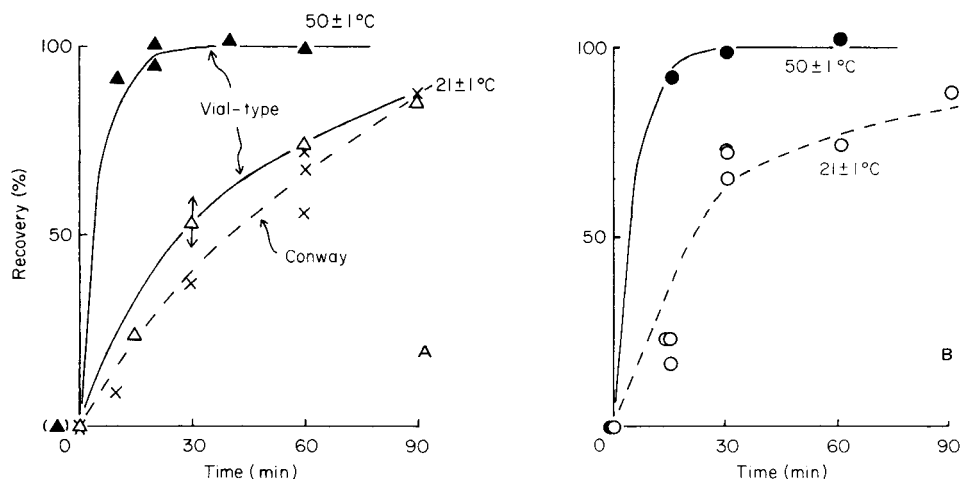


Fig. 3. Effects of diffusion time and temperature on the recovery of 76 ng of ammonia: (A) in a Conway or vial-type microdiffusion unit; (B) in a microdiffusion-photometry unit. The vertical arrows indicate the standard deviation of 6 determinations.

absorbed ammonia was determined as described above. Figure 3A shows that satisfactory recovery and reproducibility were obtained after 25 min of diffusion at 50°C in this unit. The effect of temperature is obvious.

Finally, a new type of microdiffusion unit was constructed, to provide a rapid and simple procedure. A feature of this unit is that the color development and absorbance measurements are done in the absorbent compartment of the unit, which minimizes time and effort, as well as loss and contamination of ammonia. The results obtained by the recommended procedure are shown in Fig. 3B; the curves were similar to those obtained with the vial-type unit (Fig. 3A). Table 1 shows that the recommended procedure gives satisfactory results for different amounts of ammonia.

Application

Transparent rectangular crystals, 100–300 μm long, were found on the stages of an Andersen air sampler after sampling of ambient air. They seemed to be ammonium sulfate from the results obtained by x-ray diffraction and microscopic refractive index measurements. Therefore, these crystalline particulates were analyzed for ammonia by the recommended procedure.

TABLE 1

Recovery of ammonia

Added (ng)	38	76	151	189	283
Found (ng)	37	75	152	181	276
Recovered (%)	97	99	101	96	98

TABLE 2

Analysis of ammonium sulfate crystals

Crystal size (μm)	Weight (μg)	Aliquot taken	NH ₃ found (ng)	NH ₃ in sample (%)
300 \times 180 \times 15 } + 110 \times 50 \times 10 }	1.5	1/5	79	26
250 \times 150 \times 30	2.5	1/5	96	19
	5.1	1/8	180	28
350 \times 220 \times 50	6.6	1/10	144	22
570 \times 310 \times 30	12.2	1/20	152	25
				Av. 24 \pm 4

TABLE 3

Analysis of unknown crystalline particulates collected on an Andersen air sampler

Crystal size (μm)	Weight (μg)	Aliquot taken	NH ₃ found (ng)	NH ₃ in sample (%)
310 \times 40 \times 30 } + 170 \times 70 \times 20 }	0.9	2/5	110	31
220 \times 60 \times 10 } + 190 \times 100 \times 20 }	1.3	1/5	76	29
140 \times 90 \times 20 } + 320 \times 100 \times 30 }	1.4	1/5	89	32
170 \times 110 \times 20 } + 260 \times 70 \times 30 }	3.1	1/5	133	21
				Av. 28 \pm 5

First, simulated particulates were prepared and analyzed. Large rectangular ammonium sulfate crystals were prepared by recrystallization and then crushed to rectangular crystals of length 0.1–1 mm. One or two crystals were dissolved in water and appropriate aliquots were treated by the recommended procedure. Table 2 shows that the results were in good agreement with the theoretical value (26%). The results for unknown crystalline particulates collected on the stages of an Andersen air sampler are shown in Table 3, which supports the results obtained by x-ray diffraction and microscopic refractive index measurements.

REFERENCES

- 1 P. L. Kirk, *Anal. Chem.*, **22** (1950) 354.
- 2 E. J. Conway, *Microdiffusion Analysis and Volumetric Error*, Crosby Lockwood, London, 1950.
- 3 Y. Morita and Y. Kogure, *J. Chem. Soc. Jpn., Pure Chem. Sect.*, **84** (1963) 816.

Short Communication

SYNERGIC EXTRACTION OF EUROPIUM(III) BY THENOYLTRIFLUOROACETONE IN THE PRESENCE OF QUINOLINES

M. S. BHATTI^a and G. DUYCKAERTS*

*Analytical Chemistry and Radiochemistry, University of Liège, Sart Tilman B-4000
Liège (Belgium)*

(Received 11th November 1982)

Summary. Synergic liquid–liquid extraction of europium(III) by thenoyltrifluoroacetone (HTTA) in the presence of several amines (B; quinoline, isoquinoline or 4-methylquinoline) into various solvents (cyclohexane, benzene, carbon tetrachloride or chloroform) has been investigated. Evaluation of the results for europium distribution shows that the synergic adduct complex in the organic phase is an ion-pair $\text{Eu}(\text{TTA})_4\text{HB}$. Values of the extraction and formation constants of the ion-pair complex are given.

The interpretation proposed by Sékine and Dyrssen [1] concerning the solvent extraction of Eu(III) with an organic solution of thenoyltrifluoroacetone (HTTA) and quinoline is based on the assumption of synergic adducts $\text{Eu}(\text{TTA})_3(\text{Quin})_m$ formation; m equals 1 for chloroform and 1 and 2 for carbon tetrachloride. Similar experiments carried out by Kuznik et al. [2] with HTTA and methylpyridine suggest the formation of an ion-pair $\text{Ln}(\text{TTA})_4(\text{HB})^+$. In fact, an ion-pair $\text{Nd}(\text{TTA})_4\text{HPy}$ (Py = pyridine) was isolated and confirmed by structural analysis [3]. Using trioctylamine (TOA) as neutral synergic extractant Newman and Klotz [4] suggested the formation of $\text{Ce}(\text{TTA})_3\text{HCl}\cdot\text{TOA}$, $\text{Ce}(\text{TTA})_3\text{HTTA}\cdot\text{HCl}$ and $\text{Ce}(\text{TTA})_3\cdot\text{HTTA}\cdot\text{TOA}$. Genov and Georgiev [5] reached the same conclusion but Genov and Dukov [6] later suggested the formation of the synergic adduct $\text{Ln}(\text{TTA})_3\cdot\text{TOA}$. Finally, aromatic heterocyclic amines such as 2,2'-bipyridine or 1,10-phenanthroline exhibit very strong synergism accounted for by Kassierer and Kertes [7] by adduct formation of $\text{Eu}(\text{TTA})_3\text{B}_n$ ($n = 1$ and 2) and by ourselves [8] on the basis of a 1:1 adduct formation. It seemed worthwhile therefore to re-investigate the synergic extraction of europium(III) with HTTA and various amines such as quinoline, isoquinoline and 4-methylquinoline.

Experimental

Materials. Thenoyltrifluoroacetone was vacuum-distilled and its melting point was checked; the various quinolines and the organic diluents were distilled and purity was checked spectroscopically. All other chemicals used were of reagent grade. The $^{152}\text{--}^{154}\text{Eu}$ was obtained from I.R.E. (Belgium).

^aPresent address: Nuclear Chemistry Division, Pakistan Institute of Nuclear Science and Technology, Pinstech, P.O. Nilore, Rawalpindi, Pakistan.

Procedure. The procedure was as described previously [8]. In some extraction experiments, the aqueous medium was the same as used before, i.e., 2 M NaClO₄—0.01 M sodium acetate buffer at pH 4.33. In other experiments, the aqueous phase was 0.05 M (Na,H)NO₃ in the pH range 3.0—3.7.

Mass action law and treatment of data. The formation constant $\beta_{n,m}$ of the organic synergic adduct MA_nB_m is given [8] by the following equation

$$\beta_{n,m} \equiv [\overline{\text{MA}_n\text{B}_m}] [\overline{\text{MA}_n}]^{-m} [\overline{\text{B}}]^{-n} = K_{\text{ex}}(\text{MA}_n\text{B}_m) K_{\text{ex}}^{-1}(\text{MA}_n) = (D_c^{1,2}/D_c)[\text{B}]^{-m} \quad (1)$$

K_{ex} and D_c being, respectively, the extraction constant and the distribution ratio with or without the organic adduct. Assuming ion-pair formation, one has to consider the equations



$$K_{\text{ex}}(\text{MA}_{n+m}(\text{HB})_m) = D_c^{1/2} Y [\text{H}^+]^n [\text{HA}]^{-(m+n)} [\text{B}]^{-m} \quad (3)$$

wherein $Y = 1 + \sum_1^n \alpha_i(\text{acetate})_i$ takes into account the acetate complexes of europium in the aqueous phase; $Y = 2.14$ in the experimental conditions used [8]. The formation constant $\beta_{n,m}$ of the ion-pair in the organic phase is given by the equations



$$\beta_{n,m} = K_{\text{ex}}(\text{MA}_{n+m}(\text{HB})_m) K_{\text{ex}}^{-1}(\text{MA}_n) = (D_c^{1/2}/D_c) [\text{HA}]^{-m} [\text{B}]^{-m} \quad (5)$$

The stoichiometric coefficients m and n are obtained by using the slope analysis method. In order to calculate the extraction and formation constants, it is necessary to know the concentrations of HTTA and B in the organic phase and this requires a knowledge of the $\text{p}K_a$ and the partition constants K_D of the reagents.

The values given in Table 1 were obtained by u.v. absorption spectro-

TABLE 1

Values of $\text{p}K_a$ and K_D for HTTA and the bases used ($T = 20^\circ\text{C}$)

Reagent	$\text{p}K_a$ ($T = 20^\circ\text{C}$)	K_D				Aqueous phase ^a
		C ₆ H ₁₂	C ₆ H ₆	CCl ₄	CHCl ₃	
HTTA	6.23	9.6	17	45.7 24.6	83	A ^b B
Quinoline	4.90	23.2 ± 0.1	109 ± 3	82 ± 0.6 56 ± 0.5	636 ± 8	A B
Isoquinoline	5.42			59 ± 1		B
4-Methylquinoline	5.67			133 ± 4		B

^aA, 2 M NaClO₄—0.01 M sodium acetate. B, 0.05 M (Na,H)NO₃. The $\text{p}K_a$ values quoted in the literature were used for both experiments in A and B aqueous solutions.

^bValues from Kassierer and Kertes [7].

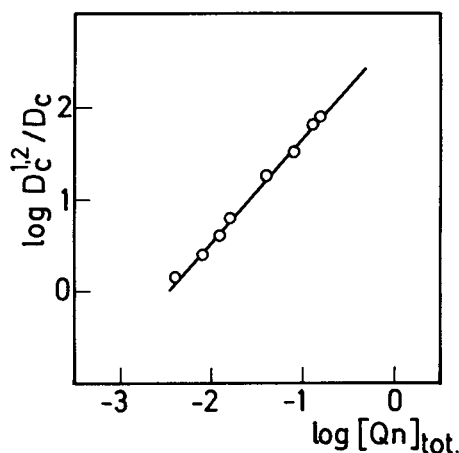


Fig. 1. Synergic extraction of Eu(III) by HTTA in the presence of quinoline in cyclohexane from an aqueous 2 M NaClO_4 —0.01 M sodium acetate buffer solution, pH 4.33, $T = 25^\circ\text{C}$, slope = 1.

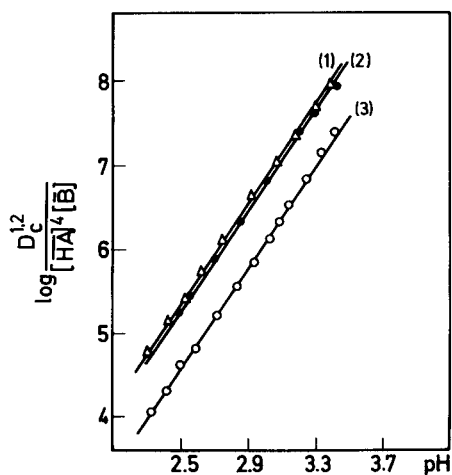
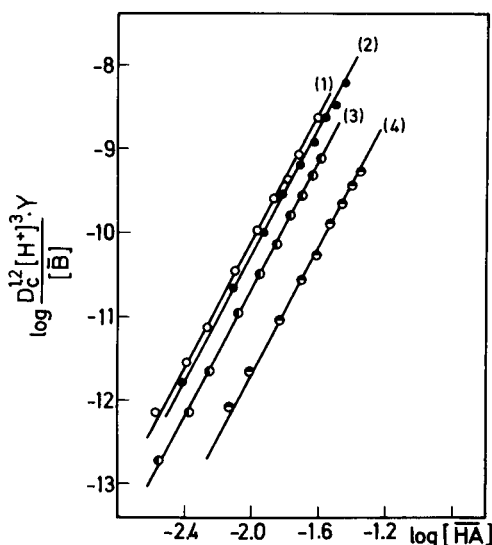


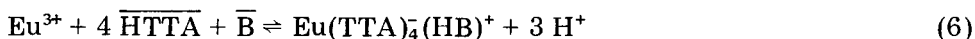
Fig. 2. Synergic extraction of Eu(III) by HTTA in the presence of quinoline in various solvents: (1) cyclohexane; (2) benzene; (3) carbon tetrachloride; (4) chloroform. Aqueous phase 2 M NaClO_4 —0.01 M sodium acetate buffer, pH 4.33, $T = 25^\circ\text{C}$. Slopes: (1) 3.67; (2) 3.61; (3) 3.80; (4) 3.61.

Fig. 3. Synergic extraction of Eu(III) by HTTA in the presence of quinoline (1), isoquinoline (2) and 4-methylquinoline (3) in carbon tetrachloride. Aqueous phase: 0.05 M $(\text{Na,H})\text{NO}_3$, $[\text{HTTA}]_t = 0.1 \text{ M}$, $[\text{B}]_t = 0.0125 \text{ M}$, $T = 25^\circ\text{C}$. Slopes: (1) 3.06; (2) 2.94; (3) 2.94.

photometry with a Cary 17. Ultraviolet spectrophotometry showed that there is no association between HTTA and the quinolines.

Results and discussion

The extraction of Eu(III) from a 2 M NaClO₄–0.01 M sodium acetate buffer at pH 4.33, as used elsewhere [8], with a mixture of HTTA and quinoline in cyclohexane is considered first. As shown in Fig. 1, the slope of $D_c^{1/2}/D_c$ as a function of $\log [\text{Quin}]_{\text{total}}$ equals one. For cyclohexane, benzene, carbon tetrachloride and chloroform solvents, however, $\log (D_c^{1/2} Y [H^+]^3/[B]^{-1})$ varies linearly with $\log [HA]$; as shown in Fig. 2, the slopes are respectively 3.67 ± 0.04 , 3.61 ± 0.07 , 3.80 ± 0.03 and 3.61 ± 0.03 . This indicates that under the given experimental conditions, the results are satisfactorily explained by assuming the synergic reaction



the adduct probably being an ion-pair.

A second series of extraction experiments for Eu(III) from a 0.05 M (H,Na)NO₃ aqueous phase at various values of pH into carbon tetrachloride with mixtures of HTTA and an amine (quinoline, isoquinoline or 4-methylquinoline) was done in order to confirm eqn. (6) under the experimental conditions used by Sékine and Dyrssen [1]. The variation of $\log (D_c^{1/2}/[HA]^4 [\overline{\text{B}}])$ as a function of pH is again linear with slopes respectively equal to 3.06 ± 0.03 , 2.94 ± 0.03 and 2.94 ± 0.02 (Fig. 3). Once more, the conclusion is the formation of an ion-pair $\text{Eu}(\text{TTA})_4(\text{HB})^+$ for the three quinolines.

Table 2 gives a summary of the extraction constants, K_{ex} , and formation constants, $\beta(4,1)$, of the organic ion-pair adduct. The extraction constants were obtained from Figs. 2 and 3 by adopting the $\text{Eu}(\text{TTA})_4\text{HB}$ composition. As expected, the stability of the adduct increases with the basicity of the neutral ligand.

TABLE 2

Extraction constants K_{ex} and formation constants $\beta(4,1)$ of $\text{Eu}(\text{TTA})_4\text{HB}$ ($T = 25^\circ\text{C}$)

Base	Diluent	$\log K_{\text{ex}}(\text{MA}_3)^a$	$\log K_{\text{ex}}(\text{MA}_4\text{HB})$	$\log \beta_{4,1}$	Aqueous phase
Quinoline	C ₆ H ₁₂	–(7.39 ± 0.09)	–(2.10 ± 0.1)	5.29 ± 0.13	2 M NaClO ₄ –0.01 M
	C ₆ H ₆	–(7.71 ± 0.08)	–(2.36 ± 0.14)	5.35 ± 0.16	
	CCl ₄	–(8.15 ± 0.02)	–(2.70 ± 0.07)	5.45 ± 0.07	Na acetate buffer pH 4.33
	CHCl ₃	–(8.22 ± 0.03)	–(3.76 ± 0.1)	4.46 ± 0.10	
Quinoline	CCl ₄	–(8.22 ± 0.03)	–(2.93 ± 0.02)	5.29 ± 0.035	0.05 M (Na,H)NO ₃
Isoquinoline	CCl ₄	–(8.22 ± 0.03)	–(2.25 ± 0.015)	5.97 ± 0.03	
4-methylquinoline	CCl ₄	–(8.22 ± 0.03)	–(2.19 ± 0.015)	6.03 ± 0.03	

^aComputed as described elsewhere [8] with standard deviation.

The conclusion of this work is that the synergism of the extraction of Eu(III) with HTTA by adding aromatic heterocyclic amines such as quino- lines, 2,2'-bipyridine or 1,10-phenanthroline is explained by the formation of the complex ion-pair $\text{Eu}(\text{TTA})_4^-(\text{HB})^+$.

This work was supported by the Belgian A.G.C.D. through a scholarship given to M.S.B., and by a grant from the Institut Interuniversitaire des Sciences Nucléaires.

REFERENCES

- 1 T. Sékine and D. Dyrssen, *J. Inorg. Nucl. Chem.*, 29 (1967) 1475.
- 2 B. Kuznik, L. Genov and G. Georgiev, *Monatsh. Chem.*, 105 (1974) 1190; 106 (1975) 1543.
- 3 J. G. Leipoldt, L. D. C. Boe, A. S. Basson, A. E. Laubscher and J. S. van Vollenhoven, *J. Inorg. Nucl. Chem.*, 39 (1977) 301.
- 4 L. Newman and P. Klotz, *Inorg. Chem.*, 5 (1966) 461; 11 (1972) 2150; *J. Phys. Chem.*, 67 (1963) 205.
- 5 L. Genov and G. Georgiev, *Monatsh. Chem.*, 100 (1969) 1892.
- 6 L. Genov and I. Dukov, *Monatsh. Chem.*, 104 (1973) 750; *Z. Chem.*, 14 (1974) 446.
- 7 E. F. Kassierer and A. S. Kertes, *J. Inorg. Nucl. Chem.*, 34 (1972) 3221.
- 8 M. S. Bhatti, J. F. Desreux and G. Duyckaerts, *J. Inorg. Nucl. Chem.*, 42 (1980) 767.

Short Communication

SEQUENTIAL SPECTROPHOTOMETRIC DETERMINATION OF CALCIUM AND MAGNESIUM IN FRESH WATERS WITH BERYLLON-II

QUI XING-CHU*

Agricultural Science Research Institute of Ganzhou Prefecture, Jiangxi (People's Republic of China)

ZHU YING-QUAN

P.O. Box 82, Chengdu (People's Republic of China)

(Received 10th September 1982)

Summary. Calcium and magnesium ions form 1:2 complexes with beryllon-II [2-(8-hydroxy-3,6-disulpho-1-naphthylazo)-1,8-dihydroxy-naphthalene-3,6-disulphonic acid] at pH 11.8. The apparent molar absorptivities at 605 nm are 3.0×10^3 and 8.4×10^3 l mol⁻¹ cm⁻¹ for the calcium and magnesium complexes, respectively. Calcium and magnesium can be determined sequentially by destroying the calcium complex by adding Pb-EGTA solution after the total has been measured. The method is applicable to river and well water.

Beryllon-II [2-(8-hydroxy-3,6-disulpho-1-naphthylazo)-1,8-dihydroxy-naphthalene-3,6-disulphonic acid] was first employed as a chromophoric reagent for beryllium [1] and has been used to determine beryllium in many materials [2–5]. Recently beryllon-II was shown to be a useful reagent for the spectrophotometric determination of magnesium [6]. In this communication, a new reaction with calcium ions and the possibility of sequential spectrophotometric determinations of calcium and magnesium in fresh water with beryllon-II are discussed.

Experimental

Apparatus. Spectra and absorbances were recorded with a Model 72 spectrophotometer (Shanghai Analytical Instruments Factory). A Model pH S-73 meter (Tianjin Analytical Instruments Factory) was used to measure pH.

Reagents. Beryllon-II (Shanghai Chemical Reagents) was used as an aqueous 0.2% (w/v) solution. The calcium and magnesium standard solutions (each 1 mg ml⁻¹) were prepared from calcium carbonate and magnesium sulphate heptahydrate, respectively, in the conventional manner. Working standard solutions were prepared from the stock solution by suitable dilution. A mixed standard solution, 40 µg Ca²⁺ ml⁻¹ and 10 µg Mg²⁺ ml⁻¹, was also used. For the EGTA-Pb solution, 1.9 g of ethylene-glycol-bis(2-aminoethylether)tetraacetic acid (EGTA) was dissolved in 45 ml of 0.1 M HCl, and 1.82 g of lead nitrate was added; the solution was stored in a dropping bottle.

Unless otherwise stated, all reagents used were of analytical-reagent grade, and distilled water was used throughout.

Sequential spectrophotometric determinations of calcium and magnesium in waters. Pipette a 10–30 ml sample of the water, containing less than 200 μg of calcium and 60 μg of magnesium into a 50-ml volumetric flask. Add 4 ml of triethanolamine solution (1 + 2), 6 ml of ammonia liquor (d. 0.88) and 4 ml of beryllon-II solution (0.2%). Dilute to the mark with water and mix well. Measure the absorbance at 605 nm in a 2.0-cm cell, against a reagent blank. This gives absorbance A_1 . To the remaining test solution, add 4 drops of the EGTA–Pb solution and mix well. Measure the absorbance of the Mg–beryllon-II complex in a 2.0-cm cell. This gives absorbance A_2 . Consequently, the absorbance of the calcium complex is $A_1 - A_2$. From the calibration graphs, calculate the amount of calcium or magnesium in the water sample.

For calibration, transfer to six 50-ml volumetric flasks 0–5.0 ml of mixed standard solution, and treat as described above. Plot absorbance against calcium or magnesium concentration.

Results and discussion

Spectral characteristics. Figure 1 shows the absorption spectra of beryllon-II and its complexes with calcium and magnesium ions at pH 11.8. The absorption maximum of the reagent appears at 540 nm. The wavelengths of maximum absorption of the calcium and magnesium complexes lie within the ranges 600–605 nm and 600–610 nm, respectively. The optimal wavelength for measurement is 605 nm.

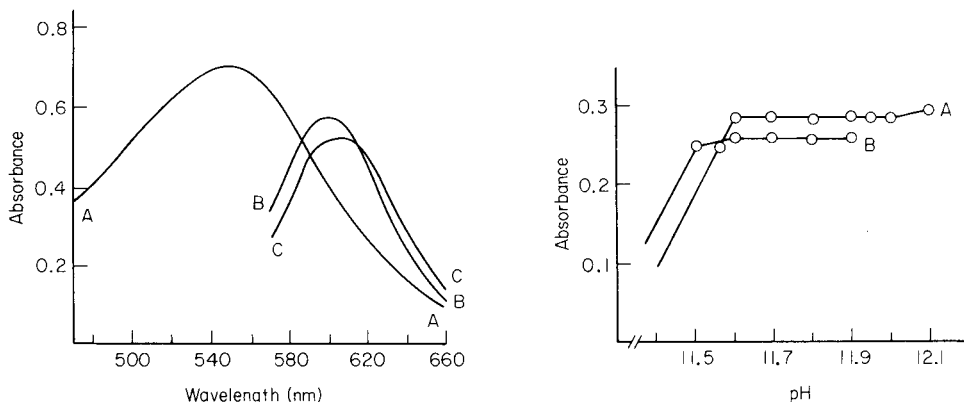


Fig. 1. Absorption spectra: A, beryllon-II (1.354×10^{-4} M) vs. water in a 0.5-cm cell; B, Ca-beryllon-II complex vs. reagent blank for 200 μg Ca^{2+} in a 2.0-cm cell; C, Mg-beryllon-II complex vs. reagent blank for 50 μg Mg^{2+} in a 2.0-cm cell.

Fig. 2. Effect of pH on the absorbances of beryllon-II complexes: A, calcium complex (200 μg Ca); B, magnesium complex (50 μg Mg). Both measured against a reagent blank in 1.0-cm cells.

TABLE 1

Effects of other ions on the determination of calcium (200 μg) or magnesium (40 μg)

Tolerance limit (μg)	Ion	Tolerance limit (μg)	Ion
1000	Fe^{3+}	50	Zn^{2+} , Mo(VI)
500	Al^{3+}	25	Mn^{2+} , Ni^{2+} , Co^{2+}
100	Cu^{2+} , Pb^{2+}		

Effects of experimental conditions. The effect of acidity on the absorbance of complex is shown in Fig. 2. It can be seen that the absorbances of the calcium and magnesium complexes remain constant over the pH ranges 11.6–12.0 and 11.6–11.9, respectively. Hence, pH 11.8 was chosen for the determination of calcium and magnesium. In 50-ml of solution, 3.0–5.0 ml of 0.2% beryllon-II solution gave maximum and constant absorbance with 200 μg of calcium and 60 μg of magnesium; 4 ml of this solution was therefore added for routine work. Under the conditions specified, the calcium and magnesium complexes were formed instantaneously and the absorbances remained stable for at least 10 h.

Stoichiometry of the complex. The stoichiometry of the calcium and magnesium complexes with beryllon-II was evaluated by the methods of Asmus [7] and Job [8]. The stoichiometry was found to be 1:2 metal–beryllon-II by both methods.

Conformance to Beer's law. Under the optimized conditions established, the calibration graph was linear for 0–200 μg of calcium in 50 ml of solution. The apparent molar absorptivity was $3.0 \times 10^3 \text{ l mol}^{-1} \text{ cm}^{-1}$ at 605 nm. Beer's law was obeyed for 0–60 μg of magnesium in 50 ml of solution. The effective molar absorptivity was calculated as $8.4 \times 10^3 \text{ l mol}^{-1} \text{ cm}^{-1}$.

TABLE 2

Recovery of calcium and magnesium added to freshwaters

Sample water	Calcium content (μg)			Recovery (%)	Magnesium content (μg)			Recovery (%)
	Initial	Added	Found		Initial	Added	Found	
River	98	20	112	94.9	20	5	24.2	96.8
		40	136	98.6		10	30.8	102.7
		60	150	94.9		15	35.8	102.3
Pond	88	20	111	102.8	20	5	24.6	98.4
		40	126	98.4		10	29.8	99.3
		60	144	97.3		15	35.8	102.3
Well	117	20	133	97.1	13.9	5	18.2	97.3
		40	156	99.4		10	22.5	94.9
		60	178	100.6		15	27.3	95.1

TABLE 3

Sequential determination of calcium and magnesium in freshwater

Sample water	Calcium content ^a (mg l ⁻¹)	Magnesium content ^a (mg l ⁻¹)
River	2.73 ± 0.047 (1.72)	0.545 ± 0.009 (1.71)
Pond	2.94 ± 0.016 (0.55)	0.794 ± 0.001 (1.72)
Well	0.382 ± 0.01 (2.57)	0.382 ± 0.01 (2.57)

^aMean for 6–8 samples with standard deviation; relative standard deviations (%) are in parentheses.

Tolerance limits for diverse ions. In the presence of triethanolamine, various ions can be tolerated at the levels given in Table 1. There was no effect from K⁺, Na⁺, nitrate, sulphate and chloride in larger amounts. Acetate interfered because it affected the pH adjustment.

Application. The proposed method was applied to the sequential determination of calcium and magnesium in fresh waters. The results are collected in Tables 2 and 3. It is evident that the accuracy and precision are good.

REFERENCES

- 1 A. M. Lukin and G. B. Zavarikina, Zh. Anal. Khim., 11 (1956) 393.
- 2 A. L. Markman and L. L. Galkina, Uzbek. Khim. Zhur., 4 (1962) 5.
- 3 N. A. Suvorovskaya, M. M. Voskresenskaya and T. A. Melnikova, Nauch Soob., Inst. Gorn. Dela Akad. Nauk. SSSR, 6 (1960) 63.
- 4 D. I. Ersitavi, F. I. Broucek and V. D. Eristavi, Trudy Gruz Politekh. Inst., 108 (1966) 41.
- 5 P. A. Rozenberg, Lab. Delo., 9 (1963) 11.
- 6 Zhu Ying-Quan and Zhang Lin, Analyst, 107 (1982) 957.
- 7 E. Asmus, Fresenius Z. Anal. Chem., 183 (1961) 321.
- 8 P. Job, Ann. Chim., 9 (1928) 113.

Short Communication

SPECTROPHOTOMETRIC DETERMINATION OF ALUMINIUM WITH ALIZARIN RED S SENSITIZED WITH POLYVINYLPIRROLIDONE

J. HERNÁNDEZ-MÉNDEZ*, R. CARABIAS-MARTÍNEZ, B. MORENO-CORDERO
and L. GUTIÉRREZ-DÁVILA

*Department of Analytical Chemistry, Faculty of Chemistry, University of Salamanca,
Salamanca (Spain)*

(Received 8th November 1982)

Summary. A molar absorptivity of $1.70 \times 10^4 \text{ l mol}^{-1} \text{ cm}^{-1}$ was obtained at 510 nm for acetate-buffered solutions at pH 4.75; this value was enhanced by ammonium and sulphate ions. Bismuth, copper and iron(III) are the most serious interferences.

The addition of surface-active species, ionic or non-ionic, is a common method of increasing the sensitivity and selectivity of spectrophotometric determinations. The introduction of a surface-active species or third component to a binary metal–ligand system may cause hyperchromic effects and/or bathochromic shifts in the absorption spectra. Such ternary systems have been applied to the spectrophotometric determination of trace elements [1, 2]. The interaction between binary complexes and ionic surfactants has been attributed to the formation of micelles or ion-associates [1, 3]. The exact nature of the effects observed with non-ionic surfactants is not clear. The present communication reports on the influence of polyvinylpyrrolidone on the aluminium–alizarin red S system in order to improve the method proposed by Parker and Goddard [4]. Cetyltrimethylammonium bromide (CTAB) and alkylbenzyltrimethyl chloride (ABDAC) were also tested.

Experimental

Reagents. A stock aluminium solution was prepared from aluminium nitrate nonahydrate and standardized with EDTA [5]. Aqueous solutions of alizarin red S ($4.5 \times 10^{-3} \text{ M}$), polyvinylpyrrolidone (PVP, K-90; 5.0%) and 0.5 M acetic acid–sodium acetate buffer were prepared.

Apparatus. A Varian-Techtron 635 spectrophotometer with a Radiometer Rec-61 recorder and 1.0-cm cuvettes was used. The pH values were measured with a Crison pH meter (model 501) equipped with a Metrohm 8100 combined electrode.

General procedure and calibration. To 10.0 ml of the buffer solution (optimal pH 4.75) was added 1.0 ml of alizarin red S solution. After mixing the solution, 4.0 ml of PVP K-90 was added together with various amounts

of aluminium, and the volume was made up to 25 ml. The absorbance was measured at 510 nm against a reagent blank after at least 10 min at 25°C.

Results and discussion

Absorption spectra. The addition of CTAB to the aluminium—alizarin red S system caused a slight shift in the wavelength of the absorption maximum. However, in its presence, the solutions needed at least 90 min to attain constant absorption. Furthermore, strong interaction between the alizarin red S and the surfactant was observed, producing a spectrum which was practically identical to that of the ternary system. In the presence of BDAC, colloidal solutions were obtained which were not suitable for measurement. The addition of PVP to the aluminium—alizarin red S system caused a bathochromic shift and a notable hyperchromic effect. Moreover, the spectrum of alizarin red S was hardly affected. Figure 1 shows the relevant absorption spectra.

It was observed that the order of addition of the reagents did not affect the absorbance of the aluminium—alizarin red S—PVP system, though it affected the time necessary to reach stable absorbance values. The order required to achieve maximum absorbance in minimum time was alizarin red S followed by PVP and then aluminium, which gave constant absorbance in 8 min, after which the absorbance remained stable for at least 72 h. In contrast, the absorbance of the binary system in the absence of PVP was stable only for 25 min.

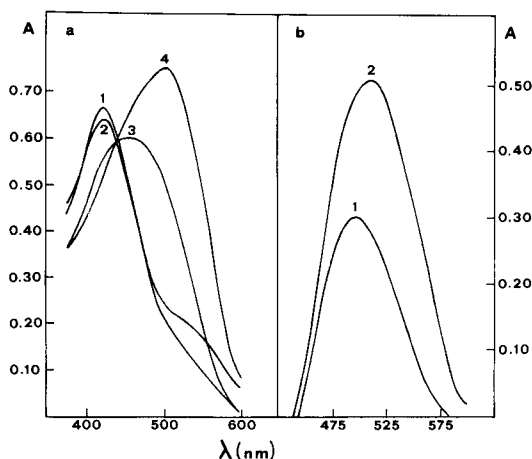


Fig. 1. Absorption spectra of the Al—alizarin red S system in 0.20 M acetate buffer, pH 4.75. (a) Absorption measured against water: (1) alizarin red S; (2) alizarin red S, 0.80% PVP; (3) alizarin red S, 3.0×10^{-5} M Al; (4) alizarin red S, 0.80% PVP, 3.0×10^{-5} M Al. (b) Absorption measured against reagent blanks: (1) alizarin red S, 3.0×10^{-5} M Al; (2) alizarin red S, 0.80% PVP, 3.0×10^{-5} M Al. In all cases, 1.8×10^{-4} M alizarin red S was present.

The aluminium—alizarin red S—PVP system. The absorbance increased with PVP concentration reaching a maximum at 0.40% PVP; above this concentration, the absorbance was constant. The absorption maximum of the aluminium—alizarin red S system at 485 nm, shifted progressively to 510 nm on increasing the concentration of PVP, again remaining constant above 0.40% PVP. Similar experiments carried out with PVP of lower molecular weight (K-25 and K-10) did not modify the results obtained with K-90.

The absorbance of the aluminium—alizarin red S system is markedly influenced by the pH and concentration of the buffer solution [4]. This was confirmed in the present work, the results being shown in Fig. 2. In the presence of PVP, the behaviour of the system was considerably modified and a pH zone close of 4.75 was found in which the absorbance was independent of the concentration of the buffer, though it was dependent on the concentration of alizarin red S. In experiments carried out with 6.0×10^{-4} M alizarin red S, the pH at which absorbance was independent of the buffer concentration was close to 4.3. For other ligand concentrations this pH was slightly different.

The mole ratio method was used to identify the composition of the complex. This gave an alizarin red S—aluminium ratio of 3.0 at a polymer concentration of 0.80%. This composition is different to that reported by Parker and Goddard [4] who described a 1:1 stoichiometry for the aluminium—alizarin red S system. Such differences might be due to changes

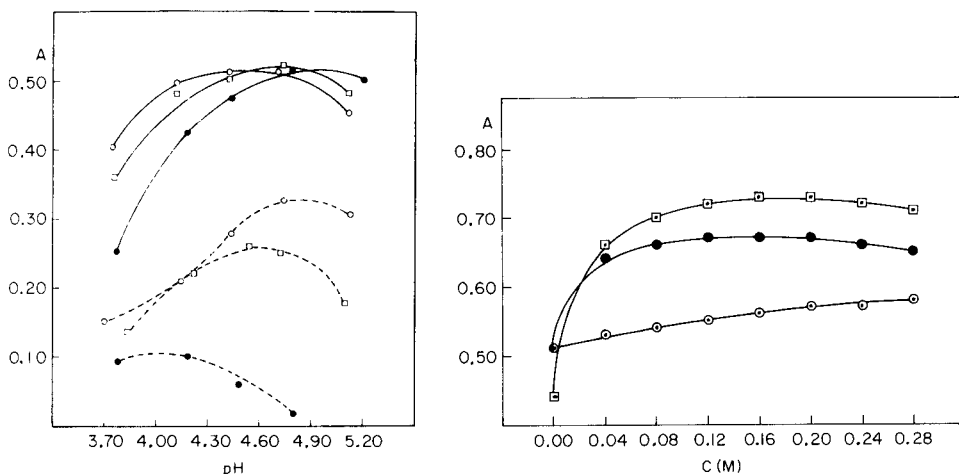


Fig. 2. Variations in absorbance with pH and concentration of the buffer for a solution of 1.8×10^{-4} M alizarin red S, 0.80% PVP, and 3.0×10^{-5} M Al: (●) 0.48 M acetate; (□) 0.12 M acetate; (○) 0.03 M acetate; (--) in absence of PVP; (—) in presence of PVP.

Fig. 3. Influence of sulphate concentration on the system containing 3.0×10^{-5} M Al, 1.8×10^{-4} M alizarin red S, and 0.20 M buffer, pH 4.75, 0.80% PVP: (●) $(\text{NH}_4)_2\text{SO}_4$ at 510 nm; (◐) $(\text{NH}_4)_2\text{SO}_4$ at 527 nm; (◑) Na_2SO_4 at 510 nm.

in the coordination sphere of the aluminium; for example, the PVP could produce a rearrangement of the water molecules surrounding the metal ion, thereby increasing its coordination capacity. Similar findings have been reported by other workers [2].

The system was found to obey Beer's law at 510 nm for less than $0.81 \mu\text{g Al ml}^{-1}$. The molar absorptivity was $1.70 \times 10^4 \text{ l mol}^{-1} \text{ cm}^{-1}$. Measurements on ten solutions containing $0.81 \mu\text{g Al ml}^{-1}$ gave a relative standard deviation of 0.5%.

Effect of salts. In the procedure proposed by Parker and Goddard [4], the presence of sodium or ammonium sulphate caused large losses in sensitivity, for which the authors were unable to account. This phenomenon prompted a study of the influence of such salts on the system in the presence of PVP, because avoidance of sulphate interference would be of great importance if the method were applied to samples treated with sulphuric acid. Figure 3 shows the effect of sodium and ammonium sulphate. In the presence of PVP, the addition of sodium sulphate did not cause a loss in sensitivity; rather the absorbance increased with increasing salt concentration, reaching a constant value above 0.20 M sodium sulphate. The addition of ammonium sulphate caused a greater increase in sensitivity, as well as a shift in the absorption maximum from 510 nm to 527 nm. In the presence of 0.20 M ammonium sulphate the system obeyed Beer's law at 527 nm up to $0.81 \mu\text{g Al ml}^{-1}$ giving a molar absorptivity of $2.40 \times 10^4 \text{ l mol}^{-1} \text{ cm}^{-1}$, which represents an increase in sensitivity of 40% over that obtained in the absence of ammonium sulphate.

Callahan and Cook [6] reported a systematic study of the effect of salts in sensitized spectrophotometric determinations. They found that the presence of such salts could alter the shape and intensity of the spectrum. They attributed this effect to ion exchange on the micelle surfaces. In order to find whether the above effect caused by the sulphates would also be induced by other indifferent salts, the study was broadened. The results in Table 1 show that only ammonium and sulphate ions gave rise to a major

TABLE 1

Effect of different salts on the molar absorptivity of the Al-alizarin red S-PVP system^a

Electrolyte added (0.20 M)	λ_{max} (nm)	Molar absorptivity ($10^4 \text{ l mol}^{-1} \text{ cm}^{-1}$)		Electrolyte added (0.20 M)	λ_{max} (nm)	Molar absorptivity ($10^4 \text{ l mol}^{-1} \text{ cm}^{-1}$)	
		At 510 nm	At λ_{max}			At 510 nm	At λ_{max}
None	510	1.70	1.70	LiCl	518	1.70	1.73
Na_2SO_4	515	1.90	2.03	NaCl	510	1.70	1.70
NaCl	515	1.70	1.70	KCl	510	1.63	1.63
NaNO_3	510	1.63	1.63	NH_4Cl	520	2.23	2.35
NaClO_4	510	1.73	1.73	$(\text{NH}_4)_2\text{SO}_4$	527	2.23	2.40

^a $3.0 \times 10^{-5} \text{ M Al}$, $1.8 \times 10^{-4} \text{ M alizarin red S}$, 0.8% PVP, pH 4.75.

TABLE 2

Effect of cations on the Al-alizarin red S-PVP system^a

Ion added	Error (%)			Ion added	Error (%)		
	Mole ratio to Al				Mole ratio to Al		
	1	10	100		1	10	100
Ca	1.5	14.0	36.5	Mn ²⁺	−3.9	−2.3	5.8
Sr	−0.6	9.6	11.9	Zn	−4.8	−1.9	9.2
Ba	7.7	8.3	9.4	Hg ²⁺	−3.5	−2.9	−7.7
Mg	0.4		−1.5	Fe ³⁺	32.1	23.5	
Cd	−1.9	3.5	10.6	Pb	3.1	14.6	
Ni	−0.6	3.3	23.5	Bi	36.5		
Co ²⁺		−0.4	11.2	Cu ²⁺	43.3		

^aConditions as outlined in footnote to Table 1 with a 30-min reaction time.

matrix effect and that this was more pronounced in the case of ammonium ion. The effect of several metal ions on the determination of aluminium was also studied (Table 2). The greatest interference was caused by iron(III), bismuth and copper. The presence of calcium ions produced an increase in the absorbance. This was a function of the calcium concentration and constant absorbance was achieved for a Ca:Al ratio greater than 60. The presence of calcium, as in the method proposed by Parker and Goddard, may thus increase the sensitivity of the determination, though in the presence of the polymer it is not necessary to heat to 60°C for 30 min to develop the colour.

REFERENCES

- 1 B. K. Chernova, J. Anal. Chem. U.S.S.R., 32 (1977) 1171.
- 2 S. B. Savvin, R. K. Chernova and L. M. Kudryavtsera, J. Anal. Chem. U.S.S.R., 34 (1979) 51.
- 3 B. W. Bailey, J. E. Chester, R. M. Dagnall and T. S. West, Talanta, 15 (1968) 1359.
- 4 C. A. Parker and A. P. Goddard, Anal. Chim. Acta, 4 (1950) 517.
- 5 E. Wanninen and A. Ringbom, Anal. Chim. Acta, 12 (1955) 308.
- 6 J. H. Callahan and K. D. Cook, Anal. Chem., 54 (1982) 59.

Short Communication

PRECONCENTRATION AND SPECIATION OF CHROMIUM IN WATERS BY COPRECIPITATION WITH LEAD SALTS AND NEUTRON ACTIVATION— γ -SPECTROMETRY

HAN-FEI ZHANG, JIRI HOLZBECHER and DOUGLAS E. RYAN*

Trace Analysis Research Centre, Department of Chemistry, Dalhousie University, Halifax, Nova Scotia B3H 4J1 (Canada)

(Received 9th December 1982)

Summary. Chromium species are preconcentrated from water samples by coprecipitation with lead salts and measured in situ after neutron activation. Both chromium(III) and chromium(VI) are coprecipitated with lead phosphate. If only chromium(VI) is collected in a separate sample with lead sulfate, the individual species can be quantified. The 320.1-keV γ -ray peak of ^{51}Cr ($t_{1/2} = 27.7$ d) is used for measurement. The procedure has a detection limit of $0.1 \mu\text{g l}^{-1}$ for chromium in sea water when 800-ml samples are used.

Chromium is a trace element present at the $\mu\text{g l}^{-1}$ (ppb) level in natural waters. Chromium(VI) is more toxic than chromium(III) and it is often desirable to quantify the species individually. Neutron activation has been used in quantifying chromium in waters after collection with insoluble precipitates [1], separation on ion-exchange resins [2, 3], adsorption on activated carbon [4], and extraction [5]. Chromium(VI) has been collected with lead sulfate and quantified by reflectance [6] or collected with barium sulfate and measured spectrophotometrically [7]. Chromium(III) has been preconcentrated by adding iron(III) chloride as coprecipitant [8]; by reducing Cr(VI) to Cr(III) in a separate sample, both species were quantified. Strontium phosphate has been recommended as a satisfactory collector for chromium [9]. Lead ions are attractive for preconcentration prior to activation and subsequent measurement because they give rise only to low activities on irradiation. A paper on the use of lead phosphate for this purpose has been published [10]. This communication describes the application of lead phosphate and lead sulfate to the determination of total chromium, chromium(VI) and chromium(III).

Experimental

Apparatus and chemicals. All samples were irradiated in the Dalhousie University SLOWPOKE Reactor at a neutron flux of $5 \times 10^{11} \text{ n cm}^{-2} \text{ s}^{-1}$. The samples were counted with a Princeton Gamma-Tech Ge(Li) detector having a 7.1% relative efficiency and 2.02-keV resolution at 1332 keV connected to a TN-1700 multichannel analyzer (Tracor Northern). Chromium was determined via its ^{51}Cr nuclide ($t_{1/2} = 27.7$ d, 320.1 keV).

Reagent-grade chemicals were used in preparation of all solutions for the coprecipitation procedure. Standard chromium(III) stock solution (1,000 ppm) was prepared by dissolving $\text{CrCl}_3 \cdot 6\text{H}_2\text{O}$ in deionized, distilled water. An atomic absorption standard solution of potassium dichromate (Alfa, 1,000 ppm Cr) was used for chromium(VI). Working chromium solutions were prepared as needed by dilution.

Coprecipitation of Cr(VI) with lead sulfate. Sodium sulfate (8 ml, 0.2 M) is added to an 800-ml aliquot of a water sample filtered through a $0.45\text{-}\mu\text{m}$ membrane filter. The pH of the solution is adjusted to 3 with dilute nitric acid and 8 ml of 0.2 M lead nitrate is added dropwise under stirring. The reaction mixture is stirred for about 5 min and allowed to stand for about 1 h. The precipitate is filtered by suction using a Nuclepore membrane filter (pore size $0.4\text{ }\mu\text{m}$) and washed with distilled water. The wet filter is folded into a 2/5-dram polyethylene vial and dried under an infrared lamp. The vial is sealed and irradiated for 16 h, and radioactivity is counted for 24 h after a two week delay. Standards are prepared by addition of known amounts of chromium to precipitates obtained by application of the above procedure to 800 ml of distilled water. Blanks are run concurrently.

The effect of pH on the coprecipitation of chromium with lead sulfate is shown in Fig. 1. Chromium(VI) ($10\text{ }\mu\text{g}$) is completely coprecipitated above pH 3 while Cr(III) ($100\text{ }\mu\text{g}$) is not collected below pH 4. The coprecipitation of Cr(VI) was, therefore, done at pH 3.

The effect of the mole ratio of sulfate to lead is shown in Fig. 2. The efficiency of chromate coprecipitation decreases with increasing mole ratio of sulfate to lead, probably because of competition for precipitate sites by the relatively large excess of strongly bonding sulfate ions. A mole ratio of about 1:1 is satisfactory.

Up to $100\text{ }\mu\text{g}$ of chromium(III) did not interfere with the collection of $10\text{ }\mu\text{g}$ of chromium(VI) at pH 3.

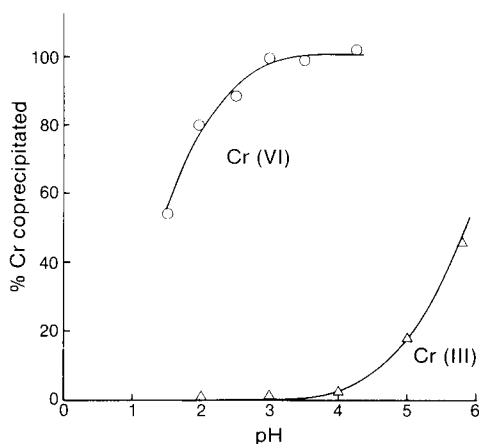


Fig. 1. Effect of pH on coprecipitation of Cr(III) and Cr(VI) with lead sulfate.

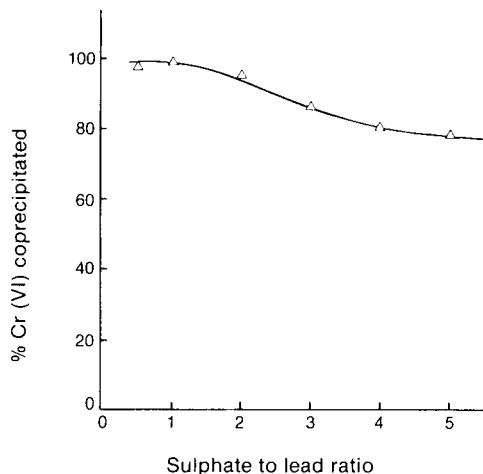


Fig. 2. Dependence of Cr(VI) recovery on the ratio of sulfate to lead.

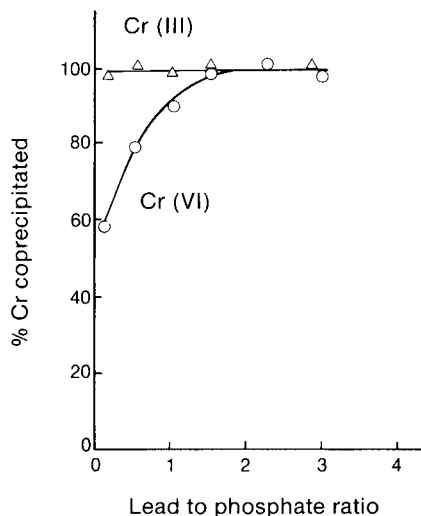


Fig. 3. Dependence of recovery of Cr(III) and Cr(VI) on the ratio of lead to phosphate.

Coprecipitation of total chromium with lead phosphate. An 800-ml water sample (filtered through a 0.45- μ m membrane filter) is acidified with 2 ml of (1+1) nitric acid; 3 ml of 0.2 M lead nitrate is added followed by 0.2 ml of 1 M ammonium dihydrogenphosphate and four drops of methyl red indicator; and (1 + 1) ammonia liquor is added dropwise with rapid stirring until the colour changes. The reaction mixture is allowed to stand for a few hours before filtration and the procedure is completed as in Cr(VI) collection.

Both Cr(III) and Cr(VI) were quantitatively coprecipitated at $\text{pH} \geq 6$.

The effect of the mole ratio of lead to phosphate is illustrated in Fig. 3. A large excess of phosphate was used in the previous study [10] to coprecipitate Cr(III) and other metal ions; to collect small amounts of Cr(VI), however, the lead ion should be in excess.

In the sea-water matrix, the ratio was kept at 3 to achieve a complete Cr(VI) collection. Chromium(III) is quantitatively coprecipitated over the range investigated.

Results and discussion

Spikes (10 μ g) of both Cr(III) and Cr(VI) were successfully recovered from 400-ml volumes of distilled water. The results for quadruplicate samples were 20.5 ± 1.3 μ g of total chromium and 10.2 ± 0.6 μ g of chromium(VI).

Local tap water, and sea water from the Northwest Arm, Halifax, Nova Scotia, taken from taps in the oceanography laboratory of the University, were also processed. Results for spiked samples (800 ml) are shown in Table 1. Recoveries of both Cr(III) and Cr(VI) were excellent for both sample

TABLE 1

Recovery of chromium by lead phosphate or lead sulfate

Sample	Cr(III) (μg)		Cr(VI) (μg)		Recovery (%)
	Added	Found	Added	Found	
<i>Coprecipitation with lead phosphate</i>					
Sea water	4.0	3.9	—	—	98
	6.0	6.3	—	—	105
	10.0	$10.5 \pm 0.7^{\text{a}}$	—	—	105
	—	—	4.0	3.8	95
	—	—	6.0	6.0	100
Tap water	—	—	10.0	$10.2 \pm 0.5^{\text{a}}$	102
	10.0	$10.3 \pm 0.5^{\text{a}}$	—	—	103
	—	—	10.0	$10.4 \pm 0.7^{\text{a}}$	104
<i>Coprecipitation with lead sulfate</i>					
Sea water	—	—	2.0	1.7	85
	—	—	6.0	5.2	87
	—	—	10.0	$8.7 \pm 0.4^{\text{a}}$	87
	100	0.3	—	—	0.3
Tap water	—	—	2.0	1.9	95
	—	—	6.0	5.9	98
	—	—	10.0	$9.7 \pm 0.7^{\text{a}}$	97
	100	0	—	—	0

^aMean \pm S.D. (4 samples).

types with lead phosphate. Chromium(VI) was quantitatively recovered by the lead sulfate procedure from tap water but its recovery from sea water was incomplete ($\approx 87\%$) because of the considerable amount of competing species, especially sulfate, present. Under the conditions used, the detection limit based on $2(\text{background})^{1/2}$ was $0.08 \mu\text{g Cr}$, i.e., $0.1 \text{ ng Cr ml}^{-1}$ for 800-ml samples.

A method of standard addition was applied to determine the chromium levels in sea water. To separate 800-ml aliquots were added 0, 2, 4, and $6 \mu\text{g}$ of chromium (both Cr(III) and (VI) in different series) and the chromium was coprecipitated with lead phosphate. Chromium(VI) was added in a third series and coprecipitated with lead sulfate. The results obtained by extrapolation from plotted data were $0.44 \pm 0.11 \text{ ng ml}^{-1}$ of total chromium and $0.38 \pm 0.12 \text{ ng ml}^{-1}$ of Cr(VI). The Cr(III) concentration was, therefore, less than 0.1 ng ml^{-1} and Cr(VI) was the dominant species. These findings are in good agreement with the literature data [11].

This work was supported by a grant from the Natural Science and Engineering Council of Canada.

REFERENCES

- 1 S. Nagatsuka and Y. Tanizaki, *Radioisotopes*, 25 (1976) 375.
- 2 F. W. Lima and C. M. Silva, *J. Radioanal. Chem.*, 1 (1968) 147.
- 3 E. Orvini, T. Zerlia, M. Gallorini and M. Speziali, *Radiochem. Radioanal. Lett.*, 43 (1980) 173.
- 4 H. A. Van Der Sloot, *J. Radioanal. Chem.*, 37 (1977) 727.
- 5 R. A. Kulmatov, A. A. Kist and I. I. Karimov, *Zh. Anal. Khim.*, 35 (1980) 254.
- 6 D. E. Ryan, J. Holzbecher and M. Granda, *Anal. Chim. Acta*, 77 (1975) 305.
- 7 H. Yamazahi, *Anal. Chim. Acta*, 113 (1980) 131.
- 8 H. Okusu, Y. Ueda, K. Ota and K. Kawano, *Kyushu Kogyo Daigaku Ken-kyu Hokoku, Kogaku*, 34 (1977) 19.
- 9 I. Bacic, N. Radakovic and P. Strohal, *Anal. Chim. Acta*, 54 (1971) 149.
- 10 J. Holzbecher and D. E. Ryan, *J. Radioanal. Chem.*, 74 (1982) 25.
- 11 T. M. Florence and G. E. Batley, *CRC Crit. Rev. Anal. Chem.*, 9 (1980) 219.

Short Communication

ELIMINATION OF NITRITE INTERFERENCE IN THE DETERMINATION OF SELENIUM BY HYDRIDE GENERATION

GREGORY A. CUTTER^a

*Center for Coastal Marine Studies, University of California, Santa Cruz, CA 95064
(U.S.A.)*

(Received 18th November 1982)

Summary. The levels of nitrite typically found in natural waters ($<3 \mu\text{M}$) can interfere significantly in the determination of selenium species by hydride generation. This interference was not found in the determination of arsenic and antimony by similar methods. Sulfanilamide reacts with nitrite to form a diazonium compound, which eliminates the interference.

The determination of selenium by hydride generation—atomic absorption spectrometry provides not only suitably low detection limits for the examination of natural waters, but also allows the determination of individual oxidation states of selenium [1, 2]. The method described by Cutter [1] involved the reduction of selenite to hydrogen selenide by sodium tetrahydroborate, trapping of the hydride at liquid nitrogen temperature, and quantitation by atomic absorption with an air/hydrogen flame and quartz tube burner. Inorganic interferences in the hydride method have been thoroughly studied by Pierce and Brown [3]. More recently, Roden and Tallman [4] have reported that organic interferences can be present in the determination of selenium in ground waters. In general, inorganic interferences are numerous, but it is important to note that the effects are observed only when the concentrations of interferents are much greater than those found in natural waters. Recent work in this laboratory has shown that nitrite, which was not previously examined, interferes seriously at environmental concentrations (i.e., $0.01\text{--}3.0 \mu\text{M}$). Nitrite is found in natural waters with high biological productivity and/or low dissolved oxygen concentrations ($<10 \mu\text{M}$). It is the purpose of this communication to describe the nitrite interference, and to show that it can be completely eliminated by an addition of sulfanilamide.

^aPresent address: Department of Oceanography, Old Dominion University, Norfolk, VA 23508, U.S.A.

Experimental

Apparatus. The apparatus has been previously described [1]. A Varian AA6 atomic absorption spectrometer fitted with a quartz-tube burner was also employed. Signals were recorded and processed on a Hewlett-Packard 3390A digital plotter/integrator.

Reagents and standards. Standard solutions of sodium selenite (1000 mg Se l^{-1}) and sodium nitrite (1000 μM) were utilized, and diluted working standards were prepared daily. A 4% (w/v) sodium tetrahydroborate solution (0.08 M in sodium hydroxide for stabilization) was used. A 2% (w/v) sulfanilamide solution was prepared daily with several drops of concentrated hydrochloric acid to facilitate dissolution.

Procedure to examine nitrite interference. The previous procedure [1] was followed exactly. The only exception was that in order to reduce selenate, Se(VI), to selenite, Se(IV), solutions containing selenate were acidified to 4 M HCl and boiled for 15 min. It was shown that the reduction of selenate to selenite is quantitative and relatively independent of time between 12 to 30 min of boiling.

Modified procedure. The following step is recommended in order to eliminate the potential nitrite interference. After the sample has been acidified to 4 M HCl, or after acidification and boiling, 1 ml of the sulfanilamide solution is added and allowed to react for 4 min prior to the addition of sodium tetrahydroborate (i.e., react while the solution is purged of air).

Discussion

Nitrite interference. Figure 1 shows the effect of low levels of nitrite on the recovery of selenite (as hydrogen selenide) by hydride generation. Two mechanisms might explain the nitrite interference: nitrite may compete with selenite for the reductant (typically, there is a thousand-fold excess of nitrite over selenite in natural waters), or nitrite may react with the generated hydride. In order to examine the first possibility, various combinations of selenite and tetrahydroborate concentrations in the presence of nitrite (1 μM) were examined for selenite recovery. It was found that increasing the amount of tetrahydroborate injected (2-fold) did not measurably increase the selenite recovery. So that the possible reaction of hydrogen selenide and nitrite in an acidic solution could be observed, the hydrogen selenide was generated in a solution without nitrite present, and then bubbled through helium-purged 4 M HCl solutions with and without nitrite added (3 μM). The selenide was collected by liquid nitrogen-cooled trapping of the gas from the second bubbler, and selenium was quantified as before. These experiments indicated that only 12% of the selenide was recovered when bubbled through the acidic nitrite-containing solution relative to that for the 4 M HCl control. Thus, it would appear that nitrite interferes by reacting with the hydrogen selenide.

Pierce and Brown [3] demonstrated that natural levels of nitrate do not interfere directly with the determination of selenite. However, nitrate can interfere indirectly with the determination of selenate; during the reduction of selenate to selenite, some nitrate is reduced to nitrite. Nitrate standards

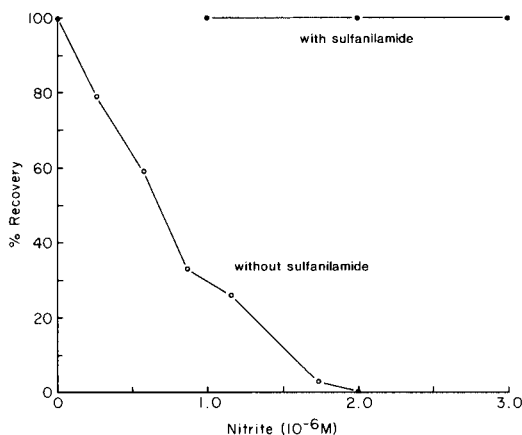


Fig. 1. Recovery of selenite (4.8 ng Se in 100 ml of sample) as a function of nitrite concentration with and without the addition of sulfanilamide (1 ml of a 2% w/v solution).

treated in the same manner as samples yielded a 1.7% recovery of nitrite ($n = 6$); this nitrite can then interfere as described above. At a typical nitrate level of $40 \mu M$, this would result in a 40% decrease in selenium recovery (see Fig. 1).

Elimination of interference. With low nitrite concentrations ($<0.2 \mu M$), the method of standard additions for each sample can correct for the observed nitrite interference. However, the interference becomes so severe at levels above $0.3 \mu M$ that it must be eliminated. Because one of the goals in studying selenium in natural waters is to measure the different species present, any method used to remove nitrite effects must not alter this speciation. With this in mind, reaction of nitrite with sulfanilamide was chosen. Sulfanilamide is used in the spectrophotometric determination of nitrite [5]; the diazotization reaction between nitrite and sulfanilamide is rapid (<1 min) and quantitative in acidic medium. The formation of the diazonium compound removes the interference (see Fig. 1), and a comparison of slopes of calibration graphs between nitrite/sulfanilamide solutions and control solutions showed them to be identical. The procedure can be used with samples containing either nitrite or nitrate.

Nitrite effect on arsenic and antimony determinations. The significant nitrite effects on the determination of selenium indicated that an examination of potential nitrite interference with two other hydride-forming elements, arsenic and antimony, was desirable. The hydride generation methods of Andreae [6] and Andreae et al. [7] were used for arsenic and antimony, respectively. There was no interference from nitrite at a concentration of $3 \mu M$. This may be due either to the low acidity used in the methods (pH 1–6), or the stability of arsine and stibine relative to hydrogen selenide.

TABLE 1

Uncorrected and corrected selenite data in sea water (18°N, 108°W^a)

Depth (m)	Nitrite (μ M)	Concentration (nM)	
		Apparent Se(IV)	Corrected Se(IV)
125	0.07	0.27	0.28
150	0.17	0.22	0.26
200	2.64	<0.01	0.23
350	0.96	<0.01	0.31
400	0.27	0.09	0.40
500	0.06	0.31	0.43
600	0.03	0.53	0.53

^aSamples taken aboard the R/V "Wecoma" in November 1981.*Conclusion*

The existence of nitrite interference in the determination of selenium by hydride generation, previously unreported, suggests that some past selenium studies employing this technique may be in error. In particular, aquatic environments with low dissolved oxygen concentrations typically contain elevated levels of nitrite. This could cause the apparent selenite concentration to decrease and display an oxidation/reduction type of behavior. The modified hydride procedure with addition of sulfanilamide alleviates this problem, and has been used successfully on sea-water samples containing nitrite (Table 1).

The author thanks R. Franks for manuscript review. This work was supported under the VERTEX program (NSF grant OCE 79 2332).

REFERENCES

- 1 G. A. Cutter, *Anal. Chim. Acta*, 98 (1978) 59.
- 2 G. A. Cutter, *Science*, 217 (1982) 829.
- 3 F. D. Pierce and H. R. Brown, *Anal. Chem.*, 49 (1977) 1417.
- 4 D. R. Roden and D. E. Tallman, *Anal. Chem.*, 54 (1982) 307.
- 5 K. Bendschneider and P. J. Robinson, *J. Mar. Res.*, 11 (1954) 87.
- 6 M. O. Andreae, *Anal. Chem.*, 49 (1977) 820.
- 7 M. O. Andreae, J. F. Asmode, P. Foster and L. Van't Dack, *Anal. Chem.*, 53 (1981) 1766.

Short Communication

DETERMINATION OF TRACE ELEMENTS IN COAL AND OTHER ENERGY-RELATED MATERIALS BY INDUCTIVELY-COUPLED PLASMA EMISSION SPECTROMETRY AFTER COLLECTION ON A POLY(DITHIOCARBAMATE) RESIN

HIMANSU S. MAHANTI^a and RAMON M. BARNES*

Department of Chemistry, GRC Towers, University of Massachusetts, Amherst, MA 01003-0035 (U.S.A.)

(Received 20th September 1982)

Summary. Trace elements in energy-related materials (coal, residual fuel oil, and shale oil) are quantified by inductively-coupled plasma atomic emission spectrometry after separation and preconcentration with a poly(dithiocarbamate) chelating resin. Trace elements were determined in coal (NBS 1632a), in a residual fuel oil (NBS 1634a), and in a shale oil (TOSCO). Detection limits ranged from a low of 2 ng ml⁻¹ for manganese to a high of 150 ng ml⁻¹ for lead. Relative standard deviations ranged from 1 to 5% and deviations from certified values (coal and residual fuel oil) were in the same range for fourteen elements. Recoveries of 1–5 µg of twelve elements added to the shale oil ranged from 96 to 99.5%.

The determination of the trace element content in coal and other energy-related materials is of major concern for many laboratories. Atomic emission spectrometry with an inductively-coupled plasma excitation source (i.c.p.e.s.) is one of the most useful methods for quantifying trace elements after appropriate pretreatment of sample [1–9]. For elements that occur below the limit of detection of i.c.p.e.s., a sample preconcentration step is required.

The poly(dithiocarbamate) resin retains more than fifty elements and is useful for concentrating and separating trace elements in complex matrices [10–15]. The purpose of the present investigation is the development of a procedure which combines i.c.p.e.s. and the poly(dithiocarbamate) chelating resin to extend the limit of detection for trace elements in coal and oil samples. In this work, coal is ashed prior to dissolution with aqua regia and hydrofluoric acid in a PTFE bomb. Residual fuel oil and shale oil samples are digested in a mixture of nitric and perchloric acids.

Experimental

Instrumentation. The instrumentation, operating conditions, and wavelengths used are listed in Table 1. The digestion bomb was fabricated accord-

^aOn leave from the National Institute of Foundry and Forge Technology, Hatia, Ranchi-834003, India.

TABLE 1

Instrumentation and operating conditions

A. Instrumentation

Generator	Plasma-Therm Model HFS-5000D, 40.68 MHz with 3-turn (1/8 in. copper) load coil.
Nebulizer	Babington with double-barrel glass spray chamber; sample uptake 1.2 ml min ⁻¹ .
Plasma torch	Conventional 18-mm i.d. quartz with 1.5-mm i.d. injector orifice.
Detection	Minuteman monochromator Model 310-SMP, 1-m Czerny-Turner with 1200 groove mm ⁻¹ grating. Slit widths 40–60 μ m, slit height 5 mm, 1:1 image formed by quartz lens (Oriel A-11-661-37). RCA-1P28 photomultiplier (–700 V), Keithley 411 picoammeter, Heath EU-201V log/linear recorder.

B. Operating conditions^a

Element	λ (nm)	Power (kW)	Element	λ (nm)	Power (kW)
Cu	324.754	0.8	Ni	341.48	0.5
Co	345.35	0.5	Pb	220.35	0.7
Ce	413.715	0.5	Th	283.73	0.7
Fe	259.94	0.8	Ti	334.94	0.7
La	408.67	0.5	U	385.958	0.7
Mn	257.61	0.7	V	292.40	0.7
Mo	202.03	0.7	Zn	213.856	0.7

^a Argon outer gas flow 16 l min⁻¹; aerosol gas flow 0.8 l min⁻¹ (24 psig back pressure) except for Ce and La (0.9 l min⁻¹); observation height 16 mm above induction coil except for Pb, Th, and U (14 mm).

ing to the design of Lechler and Leininger [16]. Operating conditions for each element were established by simplex optimization [17].

Reagents. Stock solutions were prepared from high-purity metals and reagent-grade chemicals. The poly(dithiocarbamate) chelating resin was synthesized as described earlier [10, 15]. Distilled, deionized water and high-purity acids were used throughout.

Reference solutions. Standards were prepared by serial dilution of stock solutions. Five reference solutions (0.1–10 μ g ml⁻¹) were prepared for each element, and the concentrations of elements in the digested resin solution were determined after calibration with acid-matched standard solutions.

Sample preparation. Coal (NBS-SRM 1632a) was dried for 2 h at 100°C. The two methods evaluated for sample preparation were digestion in a PTFE bomb with concentrated nitric acid and hydrofluoric acid, and ashing in a muffle furnace followed by dissolution in the PTFE bomb using a mixture of aqua regia and hydrofluoric acid. For wet ashing, 1 g of coal was weighed into a PTFE bomb, and 15 ml of concentrated nitric acid and 2 ml of hydrofluoric acid were added. The sealed bomb was heated at 150°C for 10 h. After cooling, the bomb was opened; black coal particles remaining indicated incomplete dissolution.

For dry ashing, 1 g of coal was placed in a quartz crucible and heated for 2 h at 275°C in a muffle furnace and then at 500°C for 4–5 h until a complete ash was apparent. The coal ash was then dissolved in 10 ml of aqua regia (HCl + HNO₃, 3:1) and 2 ml of hydrofluoric acid in a PTFE bomb at 110°C for 2 h. After cooling, the solution was diluted to 100 ml with distilled water.

About 0.1–2 g of residual fuel oil (NBS-SRM 1634a) or shale oil (TOSCO) was digested with 25 ml of concentrated nitric acid and 6 ml of perchloric acid on a hot plate at 200°C, and evaporated almost to dryness. The nitric and perchloric acid treatment was repeated for the residual fuel oil until the sample was digested completely. After cooling, 70 ml of distilled water was added.

Resin preconcentration. Previous studies of pH dependence of trace metal ion uptake [11–15] indicated that by selection of a suitable pH, most elements can be separated and preconcentrated. Based on this and current data, chelation of Cu, Fe, Mo, Ti, V, Ni, and Co was done at pH 5; U and Th at pH 6; Ce and La at pH 8; and Mn and Zn at pH 9; 10–100 ml of sample solution was used for each experiment. The resin column was prepared as described earlier [11] with 100 mg of poly(dithiocarbamate) resin (70–80 mesh). The coal sample solution (10–100 ml) was placed in a 250-ml PTFE beaker and heated on a hot plate at 100°C for 15–20 min. After cooling, 0.5 g of boric acid was added and the pH was increased to 5 or 6 by addition of 2 ml of acetic acid and ammonia solution. For experiments at pH 8 or 9, 5 ml of 10% tartaric acid was added prior to increasing the pH. The final solution volume was 120 ml before passing through the resin column. The flow rate was 1 ml min⁻¹. After all the sample had passed through the column, the resin was digested with hydrogen peroxide (30%) and concentrated nitric acid. The final volume of digested resin solution can be 2–10 ml for which concentration factors of 12–60 are achieved.

Samples of residual fuel oil or shale oil after wet digestion were placed in a PTFE beaker and the pH was increased to 5 or 6 by addition of ammonia solution. Then 5 ml of 10% tartaric acid was added prior to pH adjustment for the determination of Mn, Zn, Ce, and La. The volume before passing through the resin was 100 ml, and the final volume after resin digestion was 5 ml providing a concentration factor of 20.

Recovery studies. Because the concentrations of trace element in the shale oil were not known, recoveries of known element spikes to shale oil samples prior to acid digestion were established.

Results and discussion

Quantitative performance. Detection limit and background equivalent concentration (BEC) values for 14 elements determined in reference solutions containing nitric acid are given in Table 2. A simplex optimization procedure [17] was used to obtain the best signal-to-background value. These detection limits are similar to other i.c.p.e.s. detection limits for pneumatic

TABLE 2

Detection limits and background equivalent concentrations

Element	Detection limit ^a (ng ml ⁻¹)	BEC ^b (mg l ⁻¹)	Element	Detection limit ^a (ng ml ⁻¹)	BEC ^b (mg l ⁻¹)
Ce	50	1.7	Ni	10	0.33
Co	10	0.29	Pb	150	5
Cu	5	0.20	Ti	4	0.17
Fe	8	0.3	Th	50	1.4
La	8	0.3	U	100	2.9
Mn	2	0.08	V	8	0.28
Mo	8	0.45	Zn	9	0.34

^aConcentration giving a signal equal to 3 times the standard deviation of the background. Acid matrix was used. ^bBackground level expressed as analyte concentration equivalent.

nebulization [17–19]. Based on the concentration factor provided by the poly(dithiocarbamate) resin, a 12–60 times improvement in detection limit is obtained for coal, fuel oil, and shale oil.

Coal. High-temperature ashing of coal is the most commonly used procedure [20–23]; a concentration factor of 10 is obtained for the nonvolatile elements. Coal ash can be completely dissolved by treatment in PTFE bombs with aqua regia and hydrofluoric acid. Direct acid dissolution of the coal sample in a PTFE bomb was found to be unsatisfactory. A concentration enhancement of 12–60 was obtained with the poly(dithiocarbamate) chelating resin and the elements of interest were completely separated from alkali and alkaline earth elements. Fourteen elements were determined in the NBS-SRM coal sample by the proposed method; the results (Table 3) agree well with the NBS certified values. Recovery studies were done for molybdenum and lanthanum because no certified data for these elements are available; quantitative recovery was obtained. All the data reported in

TABLE 3

Results for elements in NBS-SRM 1632a coal

Element	Certified ^a ($\mu\text{g g}^{-1}$)	Found ^b ($\mu\text{g g}^{-1}$)	Element	Certified ^a ($\mu\text{g g}^{-1}$)	Found ^a ($\mu\text{g g}^{-1}$)
Ce	(30)	29.7 \pm 0.9	Ni	19.4 \pm 1	19.6 \pm 0.2
Co	(6.8)	6.7 \pm 0.1	Pb	12.4 \pm 0.6	11.8 \pm 0.2
Cu	16.5 \pm 1.0	16.3 \pm 0.2	Th	4.5 \pm 0.1	4.4 \pm 0.1
Fe	1.11 \pm 0.02%	1.10 \pm 0.02%	Ti	(0.18%)	0.170 \pm 0.005%
La	—	15.2 \pm 0.8	U	1.28 \pm 0.02	1.3 \pm 0.02
Mn	28 \pm 2	27.1 \pm 0.4	V	44 \pm 3	42 \pm 2
Mo	—	5.7 \pm 0.1	Zn	28 \pm 2	28 \pm 0.4

^a() Not certified. ^bMean of 3 replicates \pm standard deviation.

TABLE 4

Results for residual fuel oil (NBS-SRM 1634a) and shale oil

Element	Shale oil (TOSCO)	Residual fuel oil	
	Found ^a ($\mu\text{g g}^{-1}$)	Certified ^b ($\mu\text{g g}^{-1}$)	Found ^a ($\mu\text{g g}^{-1}$)
Ce	<LOD	—	<LOD
Co	0.1 ± 0.003	(0.3)	0.28 ± 0.006
Cu	0.61 ± 0.009	—	not determined
Fe	45.7 ± 0.8	(31)	30.8 ± 0.4
La	<LOD	—	<LOD
Mn	0.9 ± 0.02	0.19 ± 0.02	0.18 ± 0.004
Mo	0.58 ± 0.01	(0.12)	0.11 ± 0.003
Ni	0.63 ± 0.01	29 ± 1	29.2 ± 0.5
Pb	<LOD	2.8 ± 0.08	2.68 ± 0.03
Th	<LOD	—	<LOD
U	<LOD	—	<LOD
V	0.51 ± 0.01	56 ± 2	55.5 ± 1
Zn	8.06 ± 0.1	2.7 ± 0.2	2.54 ± 0.03

^aMean of 3 replicates \pm standard deviation; LOD is the limit of detection. ^bValues in parentheses not certified.

Table 3 are averages of 3–5 replicates; relative standard deviations ranged from 1% to 5%.

Residual fuel oil and shale oil. Table 4 presents results for trace elements in residual fuel oil and shale oil. The resin/i.c.p.e.s. values agree well with NBS certified values for the residual fuel oil (NBS-SRM 1634a). Because no data for the shale oil (TOSCO) sample were available for comparison, recoveries were examined by addition of standard amounts of each element. The

TABLE 5

Recovery of elements added to shale oil (TOSCO)

Element	Sample weight (g)	Weight of element (μg)			Recovery (%)
		Added	Expected	Found	
Ce	1	2	2	1.95 ± 0.05	97.5
Co	3	1	1.3	1.25 ± 0.02	96.2
Cu	2	1	2.22	2.20 ± 0.03	99.1
Fe	0.2	5	14.14	14.0 ± 0.2	99.0
La	1	2	2	1.96 ± 0.04	98.0
Mn	1	1	1.9	1.89 ± 0.03	99.5
Mo	1	1	1.58	1.53 ± 0.03	96.8
Ni	2	1	2.26	2.20 ± 0.04	97.3
Th	1	2	2	1.98 ± 0.04	99.0
U	1	2	2	1.95 ± 0.05	97.5
V	1	1	1.51	1.48 ± 0.03	96.8
Zn	1	4	12.06	12.0 ± 0.15	99.5

results (Table 5) indicate that essentially quantitative recovery was obtained at approximately the concentrations found in the shale oil. No Ce, La, U, or Th was found in either of the oil samples; however, amounts of these elements added to the sample were recovered quantitatively.

Extension of the resin/i.c.p.e.s. approach to other elements (e.g., W, Ag, Au, Cd, Sn, Bi, As, Sb, Se) [5] may depend on the volatility of the elements during ashing at elevated temperature. Hydride-forming elements are effectively determined in biological matrices by resin concentration followed by hydride/i.c.p.e.s. quantitation [13], and a similar procedure could be applied to residual fuel oil, shale oil, and similar materials after acid digestion.

This research was supported by Department of Energy Contract DE-AC02-77EV-0432.

REFERENCES

- 1 A. F. Ward and L. Marciello, *Jarrell-Ash Plasma Newsl.*, 1 (1978) 10.
- 2 R. A. Nadkarni, *Anal. Chem.*, 52 (1980) 929.
- 3 R. I. Botto, in R. M. Barnes (Ed.), *Developments in Atomic Plasma Spectrochemical Analysis*, Heyden, Philadelphia, 1981, p. 506.
- 4 M. A. Floyd, V. A. Fassel and A. P. D'Silva, *Anal. Chem.*, 52 (1980) 2168.
- 5 S. E. Church, *Geostand. Newsl.*, 5 (1981) 133.
- 6 S. S. Karacki and F. L. Corcoran, Jr., *Appl. Spectrosc.*, 27 (1973) 41.
- 7 M. M. McKown, D. L. Sgontz, M. P. Miller, J. E. Gebhart and A. L. Alford, in R. M. Barnes (Ed.), *Developments in Atomic Plasma Spectrochemical Analysis*, Heyden, Philadelphia, 1981, p. 523.
- 8 D. W. Hausler and L. T. Taylor, *Anal. Chem.*, 53 (1981) 1227.
- 9 D. W. Hausler, L. T. Taylor, J. Borst and W. B. Cooley, in R. M. Barnes (Ed.), *Developments in Atomic Plasma Spectrochemical Analysis*, Heyden, Philadelphia, 1981, p. 496.
- 10 D. S. Hackett and S. Siggia, in G. W. Ewing (Ed.), *Environmental Analysis*, Academic Press, New York, 1977, p. 253.
- 11 R. M. Barnes and J. S. Genna, *Anal. Chem.*, 51 (1979) 1065.
- 12 A. Miyasaki and R. M. Barnes, *Anal. Chem.*, 53 (1981) 299, 364.
- 13 P. Fodor and R. M. Barnes, *Spectrochim. Acta*, Part B, 38 (1983) in press.
- 14 M. Zhuang and R. M. Barnes, *Spectrochim. Acta*, Part B, 38 (1983) in press.
- 15 R. M. Barnes, P. Fodor, K. Inagaki and M. Fodor, *Spectrochim. Acta*, Part B, 38 (1983) in press.
- 16 P. J. Lechler and R. K. Leininger, *Jarrell-Ash Plasma Newsl.*, 2 (1979) 8.
- 17 M. Cave, R. M. Barnes and P. Denzer, 1982 International Winter Conference on Plasma Spectrochemistry, Orlando, FL, Paper No. 23 (1982).
- 18 R. L. Winge, V. J. Peterson and V. A. Fassel, *Appl. Spectrosc.*, 33 (1979) 206.
- 19 P. W. J. M. Boumans and R. M. Barnes, *ICP Inf. Newsl.*, 13 (1978) 445.
- 20 C. E. Capes, A. E. McIlhinney, D. S. Russell and A. F. Sirianni, *Environ. Sci. Technol.*, 8 (1974) 1107.
- 21 R. R. Ruch, H. J. Gluskoter and N. F. Shimp, III, *State Geol. Surv., Environ.-Geol. Notes*, 72 (1974).
- 22 R. J. Guidoboni, *Anal. Chem.*, 45 (1973) 1275.
- 23 E. N. Pollock, *ACS Div. Fuel Chem. Repr.*, 18 (1973) 92.

Short Communication

SEMI-AUTOMATIC END-POINT DETECTION IN THE DETERMINATION OF TOTAL HARDNESS IN WATER

ATHOS BELLOMO*, ALESSANDRO DE ROBERTIS and CARLO D'ARRIGO

Institute of Analytical Chemistry, University of Messina, Messina (Italy)

(Received 28th September 1982)

Summary. The simple semi-automatic apparatus functions by measuring electronically the change in absorbance during an EDTA titration when eriochrome black T is used as indicator. Relative standard deviations were better than 0.4% for titrations of standard calcium solutions and better than 0.8% for measurements of total hardness.

The most commonly measured quality of water is its total hardness (total calcium and magnesium content). Usually, this is measured in mg CaCO₃ l⁻¹ (ppm CaCO₃). The values for drinking water usually lie within the range 120–270 ppm CaCO₃, with the highest tolerable concentration being about 500 ppm [1]. Compleximetric titration at pH 10, with eriochrome black T (erio T) as indicator is normally used for measurements. Some titrimeters (e.g., Metrohm, Radiometer) have been proposed for this determination but these have the disadvantage of being both complex and costly. For continuous industrial monitoring of total water hardness, an apparatus with an automatic alarm (Hach) is available.

The present communication describes an instrument for the determination of total hardness that meets certain specifications, namely, ease of duplicating the apparatus, accuracy and precision within acceptable limits, ease of handling and maintenance, and low cost. It functions by measuring the change in absorbance during an EDTA titration, using Erio T as indicator.

Experimental

Apparatus [2]. Red radiation ($\lambda_{\max} = 630 \text{ nm}$) emitted by a LED (light-emitting diode) passes through the solution under examination, which is coloured red by the indicator, and impinges on a phototransistor placed on the other side of the titration vessel. At the end-point the solution becomes blue and thus absorbs the red radiation; under these conditions the phototransistor is de-energized. This transition is treated electronically to send a signal to stop the flow of titrant from an automatic burette (Amel model 232) adjusted to add equal increments of 0.01 ml. The use of the LED in place of a monochromator or optical filter is the innovative part of the system.

TABLE 1

Accuracy and precision of manual and automatic titrations of 0.0724 M calcium

Volume Ca soln. (ml)	Volume 0.050 M EDTA (ml)		
	Theor.	Found ^a	
		Manual	Automatic
3.00	4.34	4.34 ₄ ± 0.013	4.35 ₃ ± 0.016
7.00	10.14	10.14 ₆ ± 0.008	10.14 ₈ ± 0.014
10.00	14.48	14.48 ₅ ± 0.018	14.47 ₇ ± 0.020

^aMean ± standard deviation of 30 results.

The remainder of the apparatus consists essentially of a brass tube closed at the base and having at opposite points at the same level, two light-guide tubes also in brass, one of which contains the LED and the other the photo-transistor. A magnetic stirrer ensures the mixing of the solution.

Operational tests. To check both the accuracy and precision of the system, EDTA titrations of known quantities of a standard calcium solution were examined manually and automatically.

Fluka reagents were used to prepare the following solutions. Calcium (0.0724 M) was prepared from the nitrate and standardized with disodium-EDTA [3]. Disodium-EDTA (0.050 M) was prepared by dilution of a 0.1 M stock solution, previously standardized against pure zinc [4]. Erio T (20 mg) was dissolved in 25 ml of ethanol and made up to 100 ml with ethanolamine [3]. The pH 10 buffer solution was made by mixing ammonia and ammonium chloride [3].

For each control test, exactly 3.0, 7.0 and 10.0 ml of the calcium solution were taken and diluted to 100 ml with distilled water. To each was added 10 ml of buffer and 2.0 ± 0.3 ml of erio T solution. Each sample was titrated with the EDTA solution, manually and automatically. Before the tests for automatic titrations, the apparatus was adjusted so that when a beaker containing the blue solution at the end-point was inserted, the titrant flow was

TABLE 2

Values obtained by manual and automatic determination of total hardness in water

Sample no.	Volume 0.050 M EDTA (ml) ^a		Mean total hardness	
	Manual	Automatic	Manual	Automatic
1	1.65 ₆ ± 0.012	1.66 ₄ ± 0.014	82.8	83.2
2	5.03 ₂ ± 0.012	5.05 ₃ ± 0.018	251.6	252.8
3	6.42 ₈ ± 0.015	6.44 ₁ ± 0.019	321.4	322.1
4	6.99 ₀ ± 0.011	6.96 ₇ ± 0.020	349.5	348.4

^aMean ± standard deviation of 5 results.

stopped. The quantity and concentration of erio T required was previously established by a number of preliminary tests. Thirty manual measurements and an equal number of automatic measurements were made for each calcium concentration. The accuracies and precisions obtained are given in Table 1. Comparison with the manual method shows that the automatic system is sufficiently accurate and precise for use in routine water analysis.

Measurements of total hardness

A 100-ml portion of water was treated with 10 ml of buffer and 2.0 ± 0.3 ml of erio T solution, and titrated automatically as described above. The maximum time employed for an automatic titration was about 1 min. Because EDTA of exactly 0.050 M was used, and because 100 ml sample was taken, the total hardness in the water sample is given by $\text{ppm CaCO}_3 = \text{ml} \times 50$, in which ml is the volume of EDTA used. Various checks on the same samples, with manual and automatic titrations, were done. The resulting values of total hardness are reported in Table 2.

The apparatus described above was built specifically to measure total hardness in water. However, it can be used for any compleximetric titration for which a red/blue indicator change is available. Moreover, by simply changing the colour of the LED, it can be used for many other titrations.

The work was supported by Ministero della Pubblica Istruzione. The paper was presented at the IV Congresso Nazionale della Divisione di Chimica Analitica, Urbino, Italy, 1982.

REFERENCES

- 1 I. Melchiorre and U. Fortuna, *Igiene e Disinfezione della Acqua*, Il Campo Ed., Bologna, 1980.
- 2 C. D'Arrigo, A. De Robertis and A. Bellomo, Italian Pat. No. 18701/82 (pending); details can be obtained free of charge from the authors.
- 3 L. F. Hamilton and S. G. Simpson, *Quantitative Chemical Analysis*, Macmillan, New York, 1967.
- 4 H. A. Flaschka, *EDTA Titrations*, Pergamon, London, 1959.

AUTHOR INDEX

- Adams, M. J.
 —, Mitchell, M. C. and Ewen, G. J.
 A microcomputer system for processing data from a three-channel atomic absorption spectrometer 101
- Aeschliman, B., see Bajo, S. 321
- Andersson, L., see Marstorp, P. 281
- Anfält, T., see Marstorp, P. 281
- Araki, Y., see Honda, S. 297
- Arrigo, C. D', see Bellomo, A. 401
- Bahsoun, C., see Dauphin, C. 313
- Bajo, S.
 —, Suter, U. and Aeschliman, B.
 Apparatus for wet ashing of organic materials with nitric and sulphuric acids 321
- Barnes, R. M., see Mahanti, H. S. 395
- Barnett, N. W.
 —, Chen, L. S. and Kirkbright, G. F.
 Determination of trace concentrations of lead and nickel in freeze-dried human milk by atomic absorption spectrometry and inductively-coupled plasma emission spectrometry 115
- Bellomo, A.
 —, De Robertis, A. and D'Arrigo, C.
 Semi-automatic end-point detection in the determination of total hardness in water 401
- Bennekorn, W. P. van, see van der Lee, J. J. 29
- Berman, S. S., see Willie, S. N. 59
- Bhatti, M. S.
 — and Duyckaerts, G.
 Synergic extraction of europium(III) by thenoyltrifluoroacetone in the presence of quinolines 369
- Brezonik, P. L., see Tuschall, J. R., Jr. 47
- Brussee, D., see van Oort, W. J. 175
- Carabias-Martínez, R., see Hernández-Méndez, J. 379
- Chen, L. S., see Barnett, N. W. 115
- Cutter, G. A.
 Elimination of nitrite interference in the determination of selenium by hydride generation 391
- D'Arrigo, C., see Bellomo, A. 401
- Da Silva, I. A., see East, G. A. 227
- Dauphin, C.
 —, Bahsoun, C., Hamon, M. and Likforman, J.
 Dosage du nombre de chaînons oxyéthylénés de quelques agents tensioactifs non ioniques par oxydation au vanadium(V) 313
- Dehm, C., see Johnson, K. E. 129
- Demare, D., see Legret, M. 107
- den Hartigh, J., see van Oort, W. J. 175
- De Robertis, A., see Bellomo, A. 401
- Doğru, C., see Vytřas, K. 217
- Duyckaerts, G., see Bhatti, M. S. 369
- East, G. A.
 — and Da Silva, I. A.
 Differential electrolytic potentiometry with ion-selective electrodes for end-point detection in compleximetric titrations of mercury(II), copper(II), nickel(II) and bismuth(III) 227
- Ebdon, L., see Jones, P. 39
- Emma Sam, G., see Robinson, J. L. 11
- Erdmann, D. E., see Pyen, G. S. 355
- Ewen, G. J., see Adams, M. J. 101
- Fujinaga, T., see Nakata, R. 67
- Fukasawa, T., see Kawakubo, S. 363
- Gallego, R., see Gutiérrez, A. M. 259
- Gjøfs, N.
 —, Urdal, K., Ruyter, I. E. and Sjøvik, I. J.
 Identification of methacrylates and acrylates in dental materials by mass spectrometry 87
- Głodowski, S.
 — and Kublik, Z.
 The direct and indirect determination of traces of copper, lead and cadmium in mercury by voltammetry at the hanging mercury drop electrode 137
- Griffith, P. E., see Robinson, J. L. 11
- Guilbault, G. G., see Kristoff, J. 337

- Gutiérrez, A. M.
 —, Gallego, R. and Sanz-Medel, A.
 Extraction of tin(IV) with substituted
 8-quinolins 259
 Gutiérrez-Dávila, L., see Hernández-Méndez,
 J. 379
- Haas, H. F.
 — Krivan, V. and Ortner, H. M.
 Bestimmung von refraktärmetallen in
 pflanzlichem material durch röntgen-
 fluoreszenzanalyse nach anreicherung
 77
 Hamon, M., see Dauphin, C. 313
 Hanawa, H., see Izutsu, K. 147
 Hartigh, J. den, see van Oort, W. J. 175
 Hato, M.
 —, Masuoka, T. and Shimura, Y.
 Kinetic assay of enzymes with an am-
 monia gas-sensing electrode. Part 1.
 Dynamic responses of the sensor 193
 Hato, M.
 —, Nakayama, H. and Shimura, Y.
 Kinetic assay of enzymes with an am-
 monia gas-sensing electrode. Part 2. In
 situ monitoring of serum leucine amino-
 peptidase 203
 Hernández-Méndez, J.
 —, Carabias-Martínez, R., Moreno-Cordero,
 B. and Gutiérrez-Dávila, L.
 Spectrophotometric determination of
 aluminium with alizarin red S sensitized
 with polyvinylpyrrolidone 379
 Hiraide, M., see Sonawane, N. J. 359
 Hobbs, P. J., see Jones, P. 39
 Holland, M. K.
 — and Lewis, K.
 Controlled-potential coulometric deter-
 mination of plutonium with concurrent
 correction for a second reversible couple.
 Application to solutions containing plu-
 tonium and iron or neptunium 167
 Holzbecher, J., see Zhang, H.-F. 385
 Honda, S.
 —, Araki, Y., Takahashi, M. and Kakehi, K.
 Spectrofluorimetric determination of
 catecholamines with 2-cyanoacetamide
 297
 Hughes, S.
 — and Johnson, D. C.
 Triple-pulse amperometric detection of
 carbohydrates after chromatographic
 separation 1
- Ide, S.
 —, Yoshida, T., Matsuno, S., Takagi, M.
 and Ueno, K.
 Liquid-liquid extraction of metal ions
 with sulfonamide chelating agents 235
 Imai, K., see Toyo'oka, T. 305
 Izutsu, K.
 —, Nakamura, T., Takizawa, R. and
 Hanawa, H.
 Voltammetry at a trioctylphosphine
 oxide-coated glassy carbon electrode
 and its use for the determination of
 trace uranyl ions after preconcentration
 147
- Johnson, D. C., see Hughes, S. 1
 Johnson, K. E.
 —, Wayne Yerhoff, F., Robinson, J. and
 Dehm, C.
 Determination of barium at ng ml^{-1}
 levels by flame emission spectrometry
 after ion-exchange separation from
 1000-fold amounts of calcium 129
 Jones, P.
 —, Hobbs, P. J. and Ebdon, L.
 A dithizone post-column detector for
 the high-performance liquid chromato-
 graphic determination of trace metals
 39
- Kakehi, K., see Honda, S. 297
 Kawakubo, S.
 —, Fukasawa, T. and Mizuike, A.
 Rapid microdiffusion-photometric de-
 termination of nanogram quantities of
 ammonia 363
 Kenis, P.
 — and Zirino, A.
 Quantitative measurement of tributyltin
 oxide in sea water by differential pulse
 anodic stripping voltammetry 157
 Kirkbright, G. F., see Barnett, N. W. 115
 Kristoff, J.
 — and Guibault, G. G.
 Application of uncoated piezoelectric
 crystals for the detection of an organic
 phosphonate 337
 Krivan, V., see Haas, H. F. 77
 Kublik, Z., see Głodowski, S. 137
- Lee, J. J. van der, see van der Lee, J. J. 29
 Lee-Rijsbergen, H. B. J. van der, see van
 der Lee, J. J. 29

- Legret, M.
 —, Demare, D., Marchandise, P. et Robbe, D.
 Interférences des éléments majeurs sur la détermination de Pb, Cu, Cd, Cr et Ni dans les sédiments de cours d'eau et les boues de stations d'épuration par spectrométrie d'absorption atomique sans flamme 107
- Lewis, K., see Holland, M. K. 167
- Likforman, J., see Dauphin, C. 313
- Mahanti, H. S.
 — and Barnes, R. M.
 Determination of trace elements in coal and other energy-related materials by inductively-coupled plasma emission spectrometry after collection on a poly-(dithiocarbamate) resin 395
- Mangia, A.
 —, Predieri, G. and Sappa, E.
 The behaviour of binuclear alkyne-carbonyl iron derivatives in reversed-phase high-performance liquid chromatography 349
- Marchandise, P., see Legret, M. 107
- Marstorp, P.
 —, Anfält, T. and Andersson, L.
 Determination of oxidized ketone bodies in milk by flow injection analysis 281
- Massart, D. L., see Puttemans, F. 123
- Masuoka, T., see Hato, M. 193
- Matsui, M., see Sasayama, K. 253
- Matsuno, S., see Ide, S. 235
- Mitchell, M. C., see Adams, M. J. 101
- Mizuike, A., see Kawakubo, S. 363
- Mizuike, A., see Sonawane, N. J. 359
- Moreno-Cordero, B., see Hernández-Méndez, J. 379
- Nakagawa, G., see Ohshita, K. 269
- Nakagawa, G., see Wada, H. 291
- Nakagawa, G., see Yuchi, A. 209
- Nakamura, T., see Izutsu, K. 147
- Nakata, R.
 —, Okazaki, S., Hori, T. and Fujinaga, T.
 Collection of trace metals from sea water by column electrolysis for neutron activation- γ -spectrometry 67
- Nakayama, H., see Hato, M. 203
- Ohshita, K.
 —, Wada, H. and Nakagawa, G.
 Synthesis of *N*-sulfoalkyl derivatives of 2-(2-pyridylazo)-5-aminophenol and the spectrophotometric determination of uranium(VI) 269
- Okazaki, S., see Nakata, R. 67
- Onur, A., see Vytřas, K. 217
- Oort, W. J. van, see van Oort, W. J. 175
- Perlstein, P.
 The determination of light stabilisers in plastics by high-performance liquid chromatography 21
- Predieri, G., see Mangia, A. 349
- Purdy, W. C., see Selinger, K. 343
- Puttemans, F.
 —, van den Winkel, P. and Massart, D. L.
 The determination of arsenic by electrothermal atomic absorption spectrometry after liquid-liquid extraction 123
- Pyen, G. S.
 — and Erdmann, D. E.
 Automated determination of bromide in waters by ion chromatography with an amperometric detector 355
- Robbe, D., see Legret, M. 107
- Robertis, A. De, see Bellomo, A. 401
- Robinson, J., see Johnson, K. E. 129
- Robinson, J. L.
 —, Griffith, P. E., Salas, D. S. and Emma Sam, G.
 Separation of selected polynuclear aromatic hydrocarbons in mineral oil by liquid-solid chromatography on amberlite XAD-2 11
- Ruyter, I. E., see Gjøf, N. 87
- Ryan, D. E., see Zhang, H.-F. 385
- Salas, D. S., see Robinson, J. L. 11
- Sanz-Medel, A., see Gutiérrez, A. M. 259
- Sappa, E., see Mangia, A. 349
- Sasayama, K.
 —, Umetani, S. and Matsui, M.
 The substituent effect on the synergic extraction of europium and scandium with 1-phenyl-3-methyl-4-acylpyrazol-5-one and tri-*n*-octylphosphine oxide 253
- Schulman, S. G., see van Oort, W. J. 175
- Selinger, K.
 — and Purdy, W. C.
 The determination of salicylic acid and its metabolites in blood plasma by high-performance liquid chromatography with amperometric detection 343
- Shimura, Y., see Hato, M. 193
- Shimura, Y., see Hato, M. 203

- Silva, I. A. Da, see East, G. A. 227
 Sjøvik, I. J., see Gjøs, N. 87
 Sonawane, N. J.
 —, Hiraide, M. and Mizuike, A.
 Combined use of two surfactants for flotation of metal hydroxide precipitates in sea water 359
 Sorel, R. H. A., see van Oort, W. J. 175
 Sturgeon, R. E., see Willie, S. N. 59
 Suter, U., see Bajo, S. 321
 Symerský, J., see Vytřas, K. 217
 Takagi, M., see Ide, S. 235
 Takahashi, M., see Honda, S. 297
 Takizawa, R., see Izutsu, K. 147
 Tjaden, U. R., see van der Lee, J. J. 29
 Toyo'oka, T.
 —, Watanabe, Y. and Imai, K.
 Reaction of amines of biological importance with 4-fluoro-7-nitrobenzo-2-oxa-1,3-diazole 305
 Tuschall, J. R., Jr.
 — and Brezonik, P. L.
 Application of continuous-flow ultrafiltration and competing ligand/differential spectrophotometry for measurement of heavy metal complexation by dissolved organic matter 47
 Ueno, K., see Ide, S. 235
 Umetani, S., see Sasayama, K. 253
 Urdal, K., see Gjøs, N. 87
 van Bennekom, W. P., see van der Lee, J. J. 29
 van den Winkel, P., see Puttemans, F. 123
 van der Lee, J. J.
 —, van der Lee-Rijsbergen, H. B. J., Tjaden, U. R. and van Bennekom, W. P.
 A liquid chromatographic method for chloramphenicol and its nitro degradation products with reductive amperometric detection at a mercury electrode 29
 van der Lee-Rijsbergen, H. B. J., see van der Lee, J. J. 29
 van Oort, W. J.
 —, Sorel, R. H. A., Brussee, D., Schulman, S. G., Zuman, P. and den Hartigh, J.
 Polarographic reduction and determination of nalidixic acid 175
 Vytřas, K.
 —, Symerský, J., Doğru, C. and Onur, A.
 Coated-wire organic ion-selective electrodes in titrations based on ion-pair formation. Part 4. Determination of some acidic anthraquinone dyestuffs 217
 Wada, H., see Ohshita, K. 269
 Wada, H., see Yuchi, A. 209
 Wada, H.
 — Yuchi, A. and Nakagawa, G.
 Spectrophotometric determination of magnesium by flow injection analysis with a ligand buffer for masking calcium 291
 Watanabe, Y., see Toyo'oka, T. 305
 Wayne Yerhoff, F., see Johnson, K. E. 129
 Willie, S. N.
 —, Sturgeon, R. E. and Berman, S. S.
 Comparison of 8-quinolinol-bonded polymer supports for the preconcentration of trace metals from sea water 59
 Winkel, P. van den, see Puttemans, F. 123
 Xing-Chu, Q.
 — and Ying-Quan, Z.
 Sequential spectrophotometric determination of calcium and magnesium in fresh waters with beryllon-II 375
 Yerhoff, F. Wayne, see Johnson, K. E. 129
 Ying-Quan, Z., see Xing-Chu, Q. 375
 Yoshida, T., see Ide, S. 235
 Yuchi, A., see Wada, H. 291
 Yuchi, A.
 —, Wada, H. and Nakagawa, G.
 The performance of a cadmium ion-selective electrode in metal buffer solutions and the determination of the stability constants of cadmium complexes 209
 Zhang, H.-F.
 —, Holzbecher, J. and Ryan, D. E.
 Preconcentration and speciation of chromium in waters by coprecipitation with lead salts and neutron activation- γ -spectrometry 385
 Zirino, A., see Kenis, P. 157
 Zuman, P., see van Oort, W. J. 175

(continued from inside back cover)

Automated determination of bromide in waters by ion chromatography with an amperometric detector G. S. Pyen and D. E. Erdmann (Doraville, GA, U.S.A.)	355
Combined use of two surfactants for flotation of metal hydroxide precipitates in sea water N. J. Sonawane, M. Hiraide and A. Mizuike (Nagoya, Japan)	359
Rapid microdiffusion-photometric determination of nanogram quantities of ammonia S. Kawakubo, T. Fukasawa (Kofu, Japan) and A. Mizuike (Nagoya, Japan)	363
Synergic extraction of europium(III) by thenoyltrifluoroacetone in the presence of quinolines M. S. Bhatti and G. Duyckaerts (Liège, Belgium)	369
Sequential spectrophotometric determination of calcium and magnesium in fresh waters with beryllon-II Q. Xing-Chu (Jiangxi, People's Republic of China) and Z. Ying-Quan (Chengdu, People's Republic of China)	375
Spectrophotometric determination of aluminium with alizarin red S sensitized with polyvinylpyrrolidone J. Hernández-Méndez, R. Carabias-Martínez, B. Moreno-Cordero and L. Gutiérrez-Dávila (Salamanca, Spain)	379
Preconcentration and speciation of chromium in waters by coprecipitation with lead salts and neutron activation- γ -spectrometry H.-F. Zhang, J. Holzbecher and D. E. Ryan (Halifax, Nova Scotia, Canada)	385
Elimination of nitrite interference in the determination of selenium by hydride generation G. A. Cutter (Santa Cruz, CA, U.S.A.)	391
Determination of trace elements in coal and other energy-related materials by inductively-coupled plasma emission spectrometry after collection on a poly(dithiocarbamate) resin H. S. Mahanti and R. M. Barnes (Amherst, MA, U.S.A.)	395
Semi-automatic end-point detection in the determination of total hardness in water A. Bellomo, A. De Robertis and C. D'Arrigo (Messina, Italy)	401
Author Index	405

© Elsevier Science Publishers B.V., 1983

0003-2670/83/\$03.00

All rights reserved. No part of this publication may be reproduced, stored in a retrieval system or transmitted in any form or by any means, electronic, mechanical, photocopying, recording or otherwise, without the prior written permission of the publisher, Elsevier Science Publishers B.V., P.O. Box 330, 1000 AH Amsterdam, The Netherlands.

Submission of an article for publication implies the transfer of the copyright from the author(s) to the publisher and entails the author(s) irrevocable and exclusive authorization of the publisher to collect any sums or considerations for copying or reproduction payable by third parties (as mentioned in article 17 paragraph 2 of the Dutch Copyright Act of 1912 and in the Royal Decree of June 20, 1974 (S. 351) pursuant to article 16b of the Dutch Copyright Act of 1912) and/or to act in or out of Court in connection therewith.

Special regulations for readers in the U.S.A. — This journal has been registered with the Copyright Clearance Center, Inc. Consent is given for copying of articles for personal or internal use, or for the personal use of specific clients.

This consent is given on the condition that the copier pay through the Center the per-copy fee stated in the code on the first page of each article for copying beyond that permitted by Sections 107 or 108 of the U.S. Copyright Law. The appropriate fee should be forwarded with a copy of the first page of the article to the Copyright Clearance Center, Inc., 21 Congress Street, Salem, MA 01970, U.S.A. If no code appears in an article, the author has not given broad consent to copy and permission to copy must be obtained directly from the author. All articles published prior to 1980 may be copied for a per-copy fee of US \$2.25, also payable through the Center. This consent does not extend to other kinds of copying, such as for general distribution, resale, advertising and promotion purposes, or for creating new collective works. Special written permission must be obtained from the publisher for such copying.

Special regulations for authors in the U.S.A. — Upon acceptance of an article by the journal, the author(s) will be asked to transfer copyright of the article to the publisher. This transfer will ensure the widest possible dissemination of information under the U.S. Copyright Law.

Printed in The Netherlands.

continued from outside back cover)

controlled-potential coulometric determination of plutonium with concurrent correction for a second reversible couple. Application to solutions containing plutonium and iron or neptunium M. K. Holland and K. Lewis (Argonne, IL, U.S.A.)	167
clarographic reduction and determination of nalidixic acid W. J. van Oort, R. H. A. Sorel, D. Brussee, S. G. Schulman, P. Zuman and J. den Hartigh (Utrecht, The Netherlands)	175
netic assay of enzymes with an ammonia gas-sensing electrode. Part 1. Dynamic responses of the sensor M. Hato, T. Masuoka and Y. Shimura (Ibaraki, Japan)	193
netic assay of enzymes with an ammonia gas-sensing electrode. Part 2. In situ monitoring of serum leucine aminopeptidase M. Hato, H. Nakayama and Y. Shimura (Ibaraki, Japan)	203
ie performance of a cadmium ion-selective electrode in metal buffer solutions and the determination of the stability constants of cadmium complexes A. Yuchi, H. Wada and G. Nakagawa (Nagoya, Japan)	209
ated-wire organic ion-selective electrodes in titrations based on ion-pair formation. Part 4. Determination of some acidic anthraquinone dyestuffs K. Vytřas, J. Symerský, C. Dođru and A. Onur (Pardubice, Czechoslovakia)	217
fferential electrolytic potentiometry with ion-selective electrodes for end-point detection in compleximetric titrations of mercury(II), copper(II), nickel(II) and bismuth(III) G. A. East and I. A. Da Silva (Brasília, Brazil)	227
quid-liquid extraction of metal ions with sulfonamide chelating agents S. Ide (Kitakyushu, Japan), T. Yoshida, S. Matsuno, M. Takagi and K. Ueno (Fukuoka, Japan)	235
ie substituent effect on the synergic extraction of europium and scandium with 1-phenyl-3-methyl-4-acylpyrazol-5-one and tri-n-octylphosphine oxide K. Sasayama, S. Umetani and M. Matsui (Kyoto, Japan)	253
traction of tin(IV) with substituted 8-quinolinols A. M. Gutiérrez, R. Gallego and A. Sanz-Medel (Madrid, Spain)	259
nthesis of <i>N</i> -sulfoalkyl derivatives of 2-(2-pyridylazo)-5-aminophenol and the spectrophotometric determination of uranium(VI) K. Ohshita, H. Wada and G. Nakagawa (Nagoya, Japan)	269
stermination of oxidized ketone bodies in milk by flow injection analysis P. Marstorp (Göteborg, Sweden), T. Anfält (Sollentuna, Sweden) and L. Andersson (Skara, Sweden)	281
ectrophotometric determination of magnesium by flow injection analysis with a ligand buffer for masking calcium H. Wada, A. Yuchi and G. Nakagawa (Nagoya, Japan)	291
ectrofluorimetric determination of catecholamines with 2-cyanoacetamide S. Honda, Y. Araki, M. Takahashi and K. Kakehi (Kowakae, Japan)	297
raction of amines of biological importance with 4-fluoro-7-nitrobenzo-2-oxa-1,3-diazole T. Toyooka, Y. Watanabe and K. Imai (Tokyo, Japan)	305
usage du nombre de chaînons oxyéthylénés de quelques agents tensioactifs non ioniques par oxydation au vanadium(V) C. Dauphin, C. Bahsoun, M. Hamon et J. Likforman (Chatenay-Malabry, France)	313
paratus for wet ashing of organic materials with nitric and sulphuric acids S. Bajo, U. Suter and B. Aeschliman (Würenlingen, Switzerland)	321

Short Communications

application of uncoated piezoelectric crystals for the detection of an organic phosphonate J. Kristoff and G. G. Guilbault (New Orleans, LA, U.S.A.)	337
ie determination of salicylic acid and its metabolites in blood plasma by high-performance liquid chromatography with amperometric detection K. Selinger and W. C. Purdy (Montreal, Quebec, Canada)	343
ie behaviour of binuclear alkyne-carbonyl iron derivatives in reversed-phase high-performance liquid chromatography A. Mangia, G. Predieri (Parma, Italy) and E. Sappa (Torino, Italy)	349

(continued on p. 410)

CONTENTS

(Abstracted, Indexed in: Anal. Abstr.; Biol. Abstr.; Chem. Abstr.; Curr. Contents Phys. Chem. Earth Sci.; Life Sci.; Index Med.; Mass Spectrom. Bull.; Sci Citation Index; Excerpta Med.)

Triple-pulse amperometric detection of carbohydrates after chromatographic separation S. Hughes and D. C. Johnson (Ames, IA, U.S.A.)	1
Separation of selected polynuclear aromatic hydrocarbons in mineral oil by liquid-solid chromatography on amberlite XAD-2 J. L. Robinson, P. E. Griffith, D. S. Salas and G. Emma Sam (Durant, OK, U.S.A.)	11
The determination of light stabilisers in plastics by high-performance liquid chromatography P. Perlstein (Pretoria, Republic of South Africa)	21
A liquid chromatographic method for chloramphenicol and its nitro degradation products with reductive amperometric detection at a mercury electrode J. J. van der Lee, H. B. J. van der Lee-Rijsbergen, U. R. Tjaden and W. P. van Bennekom (Leiden, The Netherlands)	29
A dithizone post-column detector for the high-performance liquid chromatographic determination of trace metals P. Jones, P. J. Hobbs and L. Ebdon (Plymouth, Gt. Britain)	39
Application of continuous-flow ultrafiltration and competing ligand/differential spectrophotometry for measurement of heavy metal complexation by dissolved organic matter J. R. Tuschall, Jr. (Champaign, IL, U.S.A.) and P. L. Brezonik (Minneapolis, MN, U.S.A.)	47
Comparison of 8-quinolinol-bonded polymer supports for the preconcentration of trace metals from sea water S. N. Willie, R. E. Sturgeon and S. S. Berman (Ottawa, Ontario, Canada)	59
Collection of trace metals from sea water by column electrolysis for neutron activation- γ -spectrometry R. Nakata, S. Okazaki, T. Hori and T. Fujinaga (Kyoto, Japan)	67
Bestimmung von refraktärmetallen in pflanzlichem material durch röntgenfluoreszenzanalyse nach anreicherung H. F. Haas, V. Krivan (Ulm-Donau, B.R.D.) und H. M. Ortner (Reutte/Tirol, Österreich)	77
Identification of methacrylates and acrylates in dental materials by mass spectrometry N. Gjøs, K. Urdal, I. E. Ruyter and I. J. Sjøvik (Oslo, Norway)	87
A microcomputer system for processing data from a three-channel atomic absorption spectrometer M. J. Adams, M. C. Mitchell and G. J. Ewen (Aberdeen, Gt. Britain)	101
Intérférences des éléments majeurs sur la détermination de Pb, Cu, Cd, Cr et Ni dans les sédiments de cours d'eau et les boues de stations d'épuration par spectrométrie d'absorption atomique sans flamme M. Legret, D. Demare, P. Marchandise et D. Robbe (Bouguenais, France)	107
Determination of trace concentrations of lead and nickel in freeze-dried human milk by atomic absorption spectrometry and inductively-coupled plasma emission spectrometry N. W. Barnett, L. S. Chen and G. F. Kirkbright (Manchester, Gt. Britain)	115
The determination of arsenic by electrothermal atomic absorption spectrometry after liquid-liquid extraction F. Puttemans, P. van den Winkel and D. L. Massart (Brussels, Belgium)	123
Determination of barium at ng ml^{-1} levels by flame emission spectrometry after ion-exchange separation from 1000-fold amounts of calcium K. E. Johnson, F. Wayne Yerhoff, J. Robinson and C. Dehm (Regina, Canada)	129
The direct and indirect determination of traces of copper, lead and cadmium in mercury by voltammetry at the hanging mercury drop electrode S. Głódowski and Z. Kublik (Warsaw, Poland)	137
Voltammetry at a trioctylphosphine oxide-coated glassy carbon electrode and its use for the determination of trace uranyl ions after preconcentration K. Izutsu, T. Nakamura, R. Takizawa and H. Hanawa (Matsumoto, Japan)	147
Quantitative measurement of tributyltin oxide in sea water by differential pulse anodic stripping voltammetry P. Kenis and A. Zirino (San Diego, CA, U.S.A.)	157

(continued on inside back cover)